

**Design ungeladener Phosphor-, Kohlenstoff-
und Stickstoff-Superbasen**

Kumulative Dissertation

zur Erlangung des Doktorgrades der Naturwissenschaften (Dr. rer. nat.)
dem Fachbereich Chemie der Philipps-Universität Marburg
vorgelegt von

Sebastian Ullrich (M.Sc.)

aus Herford

Marburg 2019

Die vorliegende Arbeit wurde in der Zeit von November 2015 bis August 2019 unter der Leitung von Herrn Prof. Dr. Jörg Sundermeyer am Fachbereich Chemie der Philipps-Universität Marburg angefertigt.

Vom Fachbereich Chemie der Philipps-Universität Marburg (Hochschulkennziffer: 1180)
als Dissertation angenommen am: 15.10.2019

Erstgutachter: Prof. Dr. Jörg Sundermeyer

Zweitgutachter: Prof. Dr. Stefanie Dehnen

Tag der mündlichen Prüfung: 16.10.2019

Danksagung

An erster Stelle gilt mein Dank Prof. Dr. Jörg Sundermeyer für die Möglichkeit, diese Arbeit in seinem Arbeitskreis anfertigen und das interessante Thema nach eigenem Gutdünken bearbeiten zu dürfen.

Prof. Dr. Stefanie Dehnen danke ich für die Übernahme des Zweitgutachtens, Prof. Dr. Eric Meggers und Prof. Dr. Andreas Seubert für ihre Teilnahme an der Prüfungskommission.

Bei Dr. Danijela Barić und Dr. Borislav Kovačević bedanke ich mich für die fruchtbare Kooperation, die spannenden Diskussionen, die mein Wissen über die Chemie bereicherten, und die theoretische Unterstützung zu meinen Experimenten sowie für die tollen Tage in Zagreb und Umgebung.

Ich bedanke mich ganz herzlich bei allen aktuellen und ehemaligen Arbeitskreismitgliedern für die freundschaftliche Atmosphäre, die auch über die Arbeit hinausging. Besonders gilt dies für meine Boxpartnerin Jasmin sowie meine Skatpartner Susi, Alex und Marius H. Bei Marius Klein, Sebastian Wagner, Simon Werner, Greta Linden, Philipp Hofmann, Steffen Glöckner und Dr. Susanne Herritsch möchte ich mich für das kritische Korrekturlesen meiner Arbeit bedanken. Meinen Bachelorstudenten Andres Gonzalez, Björn Koch und Jens Braczek sowie allen Praktikumsstudenten gilt mein Dank für ihren Beitrag zu dieser Arbeit.

Den Serviceabteilungen für NMR-Spektroskopie, Massenspektrometrie und Elementanalytik, sowie der Röntgenstrukturanalyse des Fachbereichs danke ich für den reibungslosen Ablauf der Analytikexperimente und die schnelle Hilfe bei Problemen und Fragen. Besonderer Dank gilt dabei Dr. Xiulan Xie, die sich nicht zu schade war, zeitaufwendige Spektren auch mal am Wochenende zu messen.

Bei meinen Freunden und Kommilitonen Philipp, Steffen, Marius K., Greta, Tobi, Khang, Lukas, Eric, Andi, Timo und Willi möchte ich mich herzlich für die aufregende Studienzeit bedanken, ohne Euch wäre ich niemals an diesen Punkt gelangt. Meinen Eltern danke ich für ihre bedingungslose Unterstützung in allen Belangen. Zu guter Letzt möchte ich mich bei den beiden wichtigsten Menschen in meinem Leben bedanken, meiner Ehefrau Lara, die mich an guten wie an schlechten Tagen begleitet hat, und meinem Sohn Jonas dafür, dass er einfach da ist.

Publikationsliste

S. Ullrich, B. Kovačević, X. Xie, J. Sundermeyer, “Phosphazeryl Phosphines: The Most Electron-Rich Uncharged Phosphorus Brønsted and Lewis Bases”, *Angew. Chem. Int. Ed.* **2019**, *58*, 10335; *Angew. Chem.* **2019**, *131*, 10443.

S. Ullrich, B. Kovačević, B. Koch, K. Harms, J. Sundermeyer, “Design of Non-Ionic Carbon Superbases: Second Generation Carbodiphosphoranes”, *Chem. Sci.* **2019**, *10*, 9483.

S. Ullrich, D. Barić, X. Xie, B. Kovačević, J. Sundermeyer, “Basicity Enhancement by Multiple Intramolecular Hydrogen Bonding in Organic Superbase *N,N',N'',N'''*-Tetrakis(3-(dimethylamino)propyl)triaminophosphazene”, *Org. Lett.* **2019**, DOI: 10.1021/acs.orglett.9b03521.

J. Sundermeyer, S. Ullrich, “Phosphazeryl phosphines, Metal complexes of Phosphazeryl phosphines and their manufacturing and usage”, EP19171656.2, **2019**.

J. F. Kögel, B. Kovačević, S. Ullrich, X. Xie, J. Sundermeyer, “Chelating P₂-Bisphosphazenes with a (*R,R*)-1,2-Diaminocyclohexane Skeleton: Two New Chiral Superbases”, *Chem. Eur. J.* **2017**, *23*, 2591.

J. F. Kögel, S. Ullrich, B. Kovačević, J. Sundermeyer, “Phosphazeryl-Phosphanes (R₂N)₃P=N–P(NR₂)₂ – Strong P-Bases and Versatile Precursors for the Synthesis of Chelating Diphosphazene Superbases”, *in preparation*.

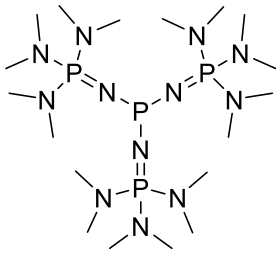
Abkürzungsverzeichnis

Ad	Adamantyl
ATR	abgeschwächte Totalreflexion
CDP	Carbodiphosphoran
cod	Cyclooctadien
CPI	Cyclopropenimin
Cym	<i>para</i> -Cymol
DABCO	1,4-Diazabicyclo[2.2.2]octan
DACN	1,8-Bis[bis(di- <i>iso</i> -propylamino)cyclopropeniminyl]naphthalin
DBU	1,8-Diazabicyclo[5.4.0]undec-7-en
DCM	Dichlormethan
DFT	Dichtefunktionaltheorie
DIPEA	Di- <i>iso</i> -propylethylamin
Dipp	2,6-Di- <i>iso</i> -propylphenyl
DMA	Dimethylamin
DMAN	1,8-Bis(dimethylamino)naphthalin
DMAP	Dimethylaminopyridin
DMSO	Dimethylsulfoxid
Dppm	Bis(diphenylphosphino)methan
ESI	<i>electrospray ionisation</i>
eq	Äquivalent
GB	Gasphasenbasizität
HMPN	1,8-Bis(hexamethyltriaminophosphazenyl)naphthalin
HRMS	<i>high resolution mass spectrometry</i>
HSAB	<i>Hard and Soft Acids and Bases</i>
HTFSI	Bis(trifluormethansulfonyl)imid
HMDS	Hexamethyldisilazan
IHB	Intramolekulare H-Brückenbindung
Ind	3-Phenyl-1H-inden-1-yliden
IR	Infrarot
LIFDI	<i>liquid injection field desorption ionisation</i>
Me ₃ tren	Tris(2- <i>N</i> -methylaminoethyl)amin
MeCN	Acetonitril
Mes	Mesityl

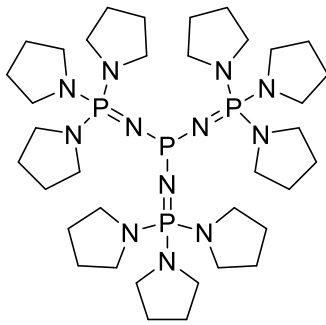
Abkürzungsverzeichnis

NHC	<i>N</i> -heterocyclisches Carben
NMR	<i>nuclear magnetic resonance</i>
PA	Protonenaffinität
PAP	Phosphazenyolphosphan
PMG	Pentamethylguanidin
Pyrr	Pyrrolidin
TDMPP	<i>N,N',N'',N'''</i> -tetrakis(3-dimethylaminopropyl)triaminophosphazen
THF	Tetrahydrofuran
THT	Tetrahydrothiophen
TMG	Tetramethylguanidin
TMGN	1,8-Bis(tetramethylguanidino)naphthalin
TMP	2,4,6-Trimethoxyphenyl
TMS	Trimethylsilyl
TPPN	1,8-Bis[tris(pyrrolidino)phosphazenylnaphthalin
TDMPG	<i>N,N',N''</i> -Tris(dimethylaminopropyl)guanidin
UV	Ultraviolett
Vis	<i>visible</i>
XRD	<i>single crystal X-ray diffraction</i>

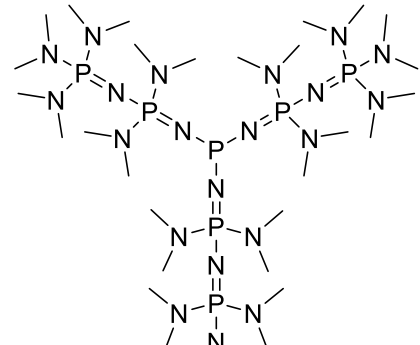
Strukturverzeichnis



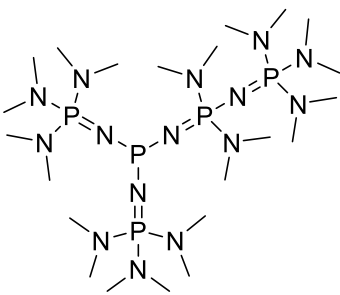
(dma) P_3P (**1a**)



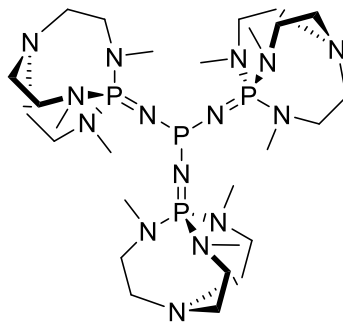
(pyrr) P_3P (**1b**)



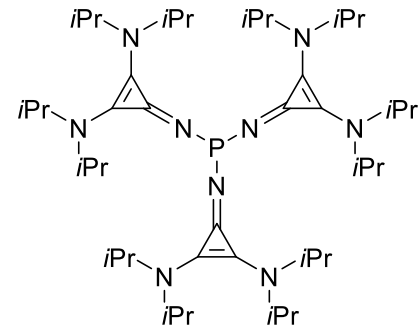
(dma) P_6P (**1c**)



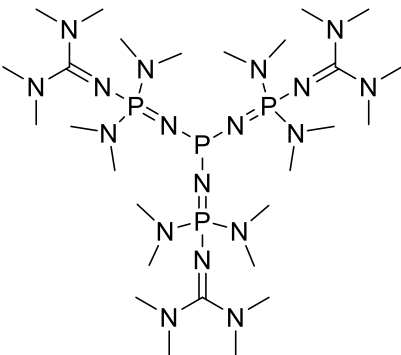
(dma) P_4P (**1d**)



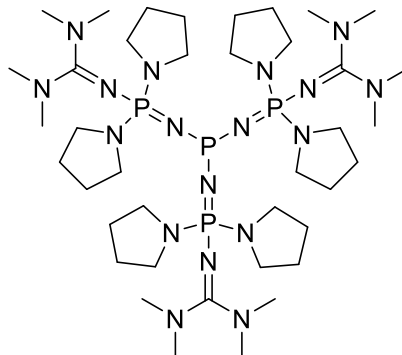
(Me₃tren) P_3P (**1e**)



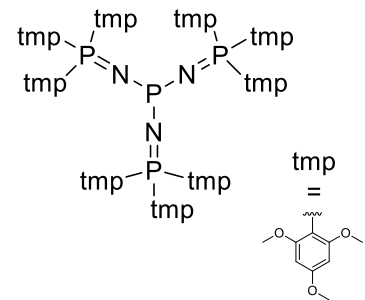
(cpi) $_3P$ (**1f**)



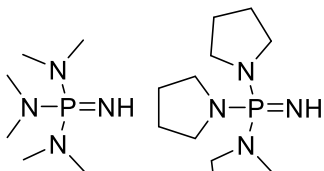
(tmg)(dma) $_2P_3P$ (**1g**)



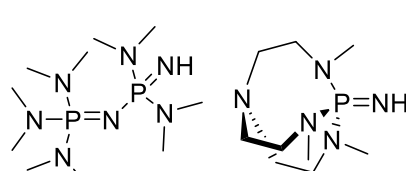
(tmg)(pyrr) $_2P_3P$ (**1h**)



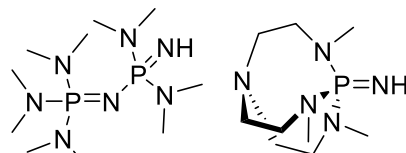
(tmp) P_3P (**1i**)



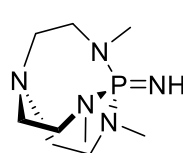
2a



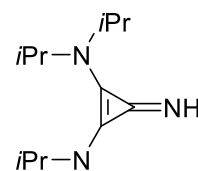
2b



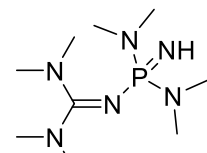
2c



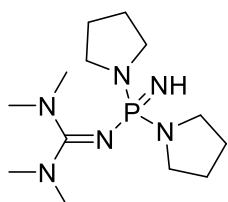
2e



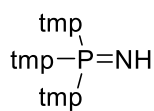
2f



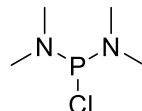
2g



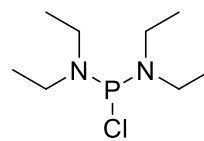
2h



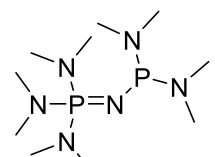
2i



3a

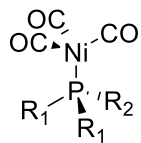


3b

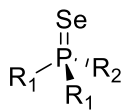


4

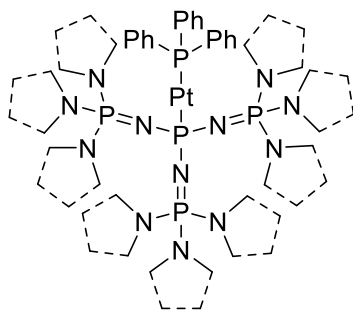
Strukturverzeichnis



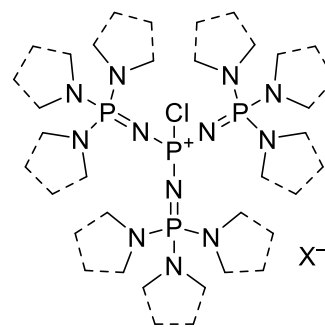
5a-e



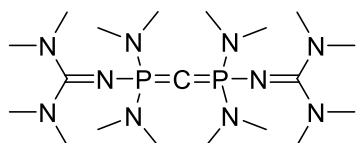
6a-e



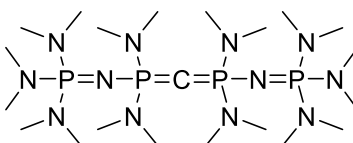
7a,b



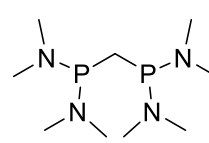
8aX, 8bX



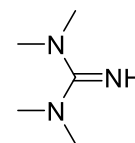
sym-(tmg)₂(dma)₄-CDP (9)



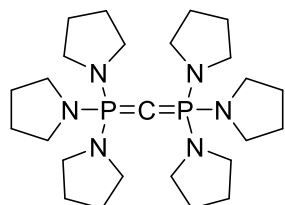
sym-(dmaP₁)₂(dma)₄-CDP (10)



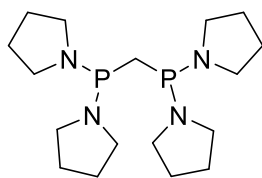
11



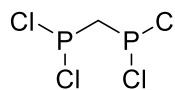
12



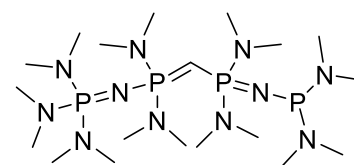
(pyrr)₆-CDP (13)



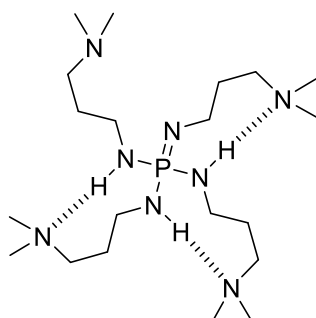
14



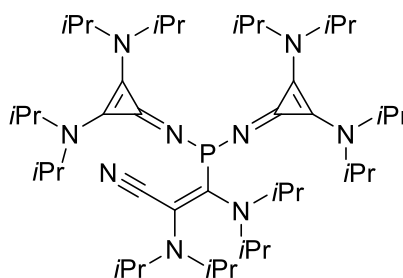
15



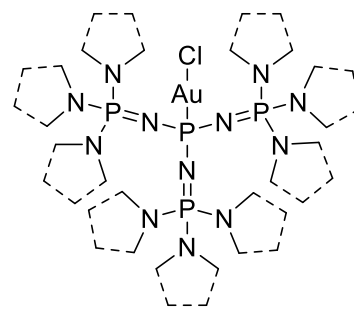
16



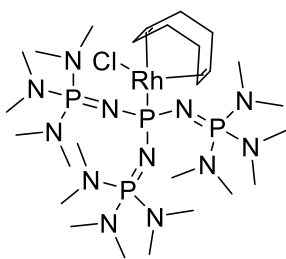
TDMPP (17)



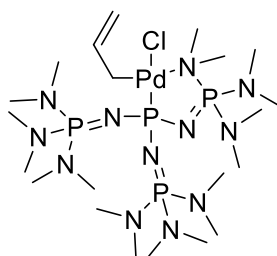
18



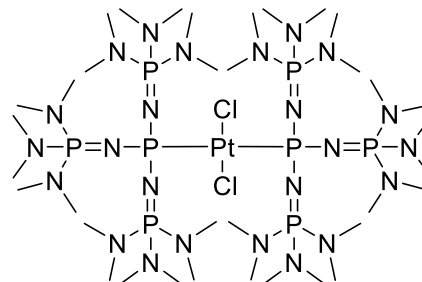
19a,b



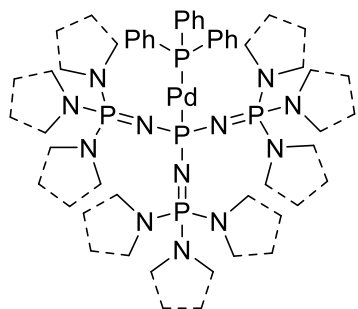
20



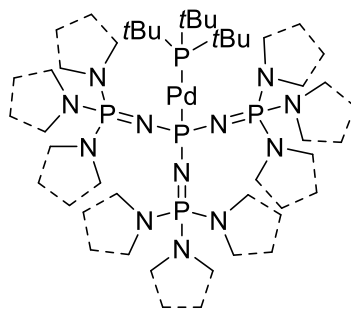
21



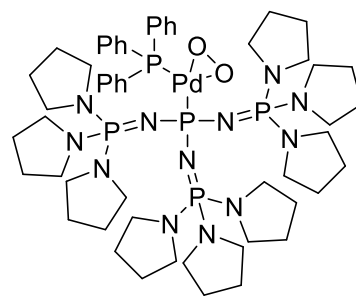
22



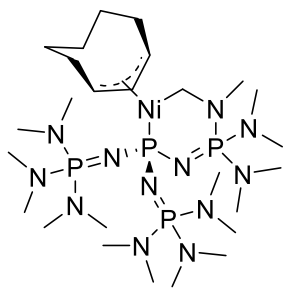
23a,b



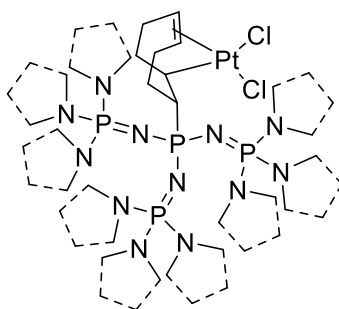
24a,b



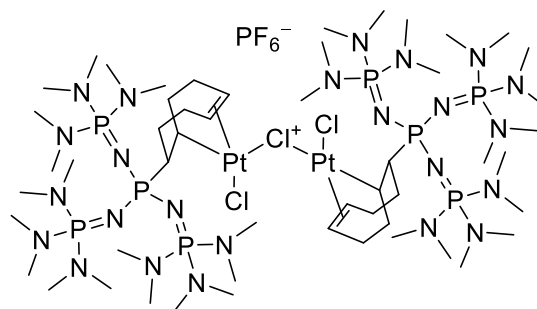
25



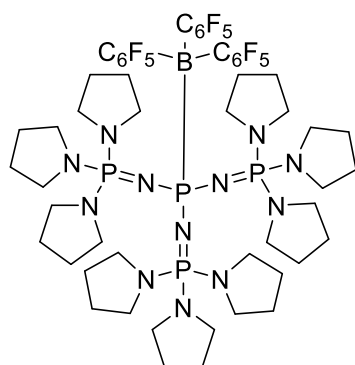
26



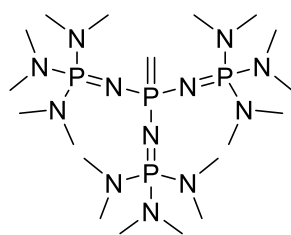
27a,b



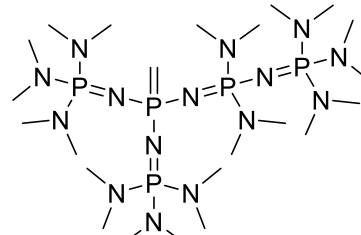
[27a]₂PF₆



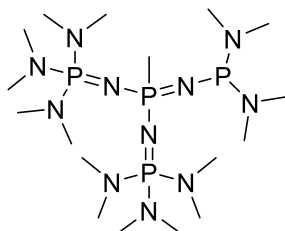
28



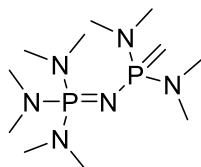
29



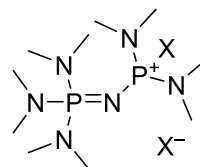
30



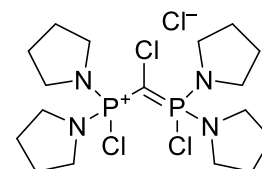
31



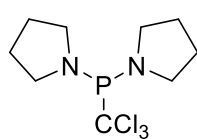
32



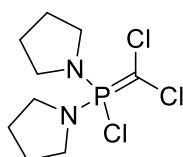
33X



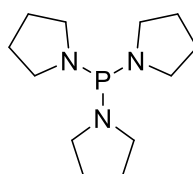
34



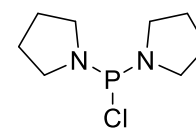
35



36



37



38

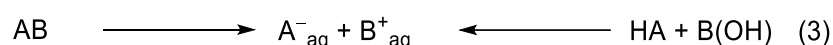
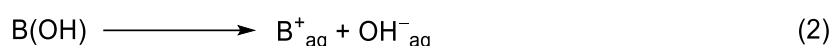
Inhaltsverzeichnis

1	Einleitung.....	1
1.1	Die Stärke von Superbasen	3
1.2	Stickstoffsuperbasen.....	6
1.3	Kohlenstoffsuperbasen	12
1.4	Phosphorsuperbasen	15
2	Aufgabenstellung	20
3	Kumulativer Teil.....	22
3.1	Phosphazenylyphosphane PAP: Die elektronenreichsten ungeladenen BRØNSTED- und LEWIS-Phosphor-Basen.....	22
3.2	Design nicht-ionischer Kohlenstoffsuperbasen: Carbodiphosphorane der zweiten Generation.....	24
3.3	Basizitätsverstärkung durch multiple intramolekulare Wasserstoff- brückenbindungen in der Organosuperbase <i>N,N',N'',N'''</i> -Tetrakis(3- dimethylaminopropyl)triaminophosphazen	25
4	Zusammenfassung	27
4.1	Beiträge zur Chemie superbasischer Phosphane	27
4.2	Design ungeladener Kohlenstoffsuperbasen	31
4.3	Eine Phosphazenebase mit Corona-Effekt.....	34
4.4	Fazit.....	35
5	Summary.....	36
5.1	Contributions to the Chemistry of Superbasic Phosphanes	36
5.2	Design of Uncharged Carbon Superbases	40
5.3	A Phosphazene Base with Corona Effect.....	43
5.4	Conclusion.....	44
6	Volltexte der Manuskripte	45
7	Appendix.....	110
7.1	Diskussion	110
7.2	Zusammenfassung.....	121
7.3	Experimenteller Teil.....	121
8	Kristallographischer Anhang	147
9	Literaturverzeichnis	170

1 Einleitung

Die Reaktion zwischen den antagonistischen Reaktionspartnern Säure und Base gehört, wie die zwischen den Paaren aus Reduktions- und Oxidationsmittel sowie Nukleo- und Elektrophil, zu den fundamentalsten Prozessen in der Chemie. Ihnen widmet jedes gängige Chemielehrbuch unabhängig davon, ob es sich um ein Lehrbuch zur anorganischen, organischen oder physikalischen Chemie handelt, ein eigenes Kapitel.^[1-3] Säuren und Basen kommen in vielen elementaren Reaktionsschritten, Namensreaktionen und industriellen Prozessen zum Einsatz, sie dienen dort als Aktivatoren, Puffer und Katalysatoren.^[4] Da viele Synthesen erst durch den Einsatz einer Säure bzw. Base ermöglicht werden, ist ein genaues Verständnis des Verhaltens dieser Reaktionspartner essentiell. Dazu wurden insbesondere seit Beginn des 19. Jahrhunderts verschiedene Konzepte und enger- oder weitergefasste Definitionen für Säuren und Basen entwickelt.

1887 beschrieb ARRHENIUS in seiner Abhandlung *Über die Dissociation der in Wasser gelösten Stoffe*,^[5] für die er 1903 mit dem Nobelpreis ausgezeichnet wurde, wie Elektrolyte bei der Auflösung in Wasser in positiv und negativ geladene Molekülteile zerfallen (Schema 1.1) und sortierte sie in drei Gruppen ein, die Säuren, die Basen und die Salze. Säuren dissoziieren in wässriger Lösung in Wasserstoffionen H^+ und einen anionischen Säurerest A^- (1), während Basen sich als ihr Gegenstück in wässriger Lösung in einen kationischen Basenrest B^+ und ein negativ geladenes Hydroxidion OH^- aufspalten (2). Salze schließlich bestehen aus einem Säure- und einem Basenrest und sind somit das Resultat einer Neutralisationsreaktion (3) der ersten beiden Gruppen.



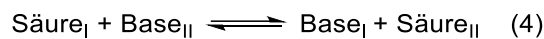
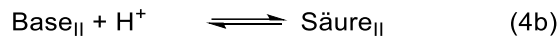
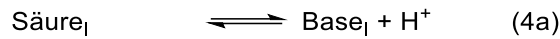
Schema 1.1: Definition für Säuren (1), Basen (2) und Salze (3) nach ARRHENIUS.

Dieses Modell ist auf Wasser als Lösungsmittel beschränkt und liefert keine Erklärung für die basische Reaktion von Verbindungen die keine Hydroxidionen enthalten, wie z. B. Ammoniak. BRØNSTED^[6] und LOWRY^[7] schrieben 1923 unabhängig voneinander dem Oxoniumion H_3O^+ , welches durch Abgabe eines Protons¹ einer Säure an ein Wassermolekül entsteht, die Säurewirkung zu. Analog dazu ist eine Base ein Stoff, der in wässriger Lösung Protonen aufnimmt und so Hydroxidionen generiert. Ursprünglich ebenfalls für wässrige Systeme

¹ In dieser Arbeit wird die in der Literatur übliche Bezeichnung Proton, für ein Wasserstoffkation ungeachtet seiner Kernmasse verwendet, obgleich diese laut IUPAC für das $^1H^+$ -Ion vorbehalten sein sollte und stattdessen die Bezeichnung Hydron empfohlen wird.^[8]

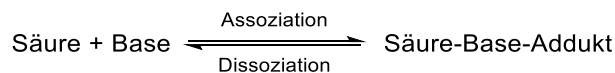
1 Einleitung

entwickelt ist dieses Modell jedoch auch auf wasserfreie Systeme anwendbar. Dies gilt, solange eine zweite Komponente vorhanden ist, welche anstelle des Wassermoleküls die Protonen einer Säure aufnimmt bzw. Protonen einer Base zur Verfügung stellt und somit selbst als Base bzw. Säure gemäß Schema 1.2 reagiert.^[1] Die nach dieser Definition benannten BRØNSTED-Säuren sind Protonendonoren, BRØNSTED-Basen sind Protonenakzeptoren. Sie können in Neutral-, Anion- und Kation-Säuren/-Basen eingeteilt werden.²



Schema 1.2: Säure-Base-Reaktion (4) zweier Substanzen, zusammengesetzt aus den Säure-Base-Halbreaktionen (4a und 4b) der einzelnen korrespondierenden Säure-Base-Paare.^[1]

Ebenfalls 1923 veröffentlichte LEWIS seine Abhandlung über Säuren als Elektronenpaar-akzeptoren und Basen als Elektronenpaardonoren und somit ein allgemeineres, da vom Protonenaustausch unabhängiges Konzept.^[9] Diesem zufolge lässt sich eine BRØNSTED-Säure HA als LEWIS-Säure-Base-Addukt der LEWIS-Säure H^+ und der LEWIS-Base A^- gemäß Schema 1.3 beschreiben, während BRØNSTED-Basen ein auf das Proton angewandter Spezialfall von LEWIS-Basen sind.



Schema 1.3: Säure-Base-Reaktion nach LEWIS.^[1]

1943 erfuhr dieses Konzept eine Erweiterung durch das HSAB-Prinzip (*hard and soft acids and bases*)^[10] von PEARSON. Dieses ermöglicht durch eine Einteilung in harte (wenig polarisierbare) und weiche (leicht polarisierbare) LEWIS-Säuren und -Basen eine qualitative Abschätzung der Stabilität von LEWIS-Säure-Base-Addukten. Demnach sind Kombinationen aus harter Säure und harter Base mit eher ionischem Bindungscharakter sowie aus weicher Säure und weicher Base mit eher kovalentem Bindungscharakter bevorzugt. Bei LEWIS-Säure-Base-Reaktionen werden immer dative Bindungen durch teilweisen Übergang eines Elektronenpaares der Base zur Säure gebildet. Sie unterscheiden sich demnach von Redoxreaktionen, bei denen ein vollständiger Übertrag eines oder mehrerer Elektronen vom Reduktions- zum Oxidationsmittel erfolgt. Im Grenzfall gehen beide Begriffe ineinander über, wobei starke Säuren auch starke Oxidationsmittel und starke Basen gute Reduktionsmittel sein können. USANOVICH generalisierte deshalb den Säure-Base-Begriff noch weiter und definiert Säuren als Stoffe, die

² Beispiele für BRØNSTED-Säuren: NH_4^+ , $\text{Al}(\text{OH}_2)_6^{3+}$ (kationisch); NH_3 , HF , H_2SO_4 (neutral); HSO_4^- , H_2PO_4^- (anionisch). Beispiele für BRØNSTED-Basen: $\text{Be}(\text{OH}_2)_3\text{OH}^+$, $\text{Cr}(\text{OH}_2)_5\text{OH}^{2+}$ (kationisch); NH_3 , NH_2OH (neutral); NH_2^- , MeO^- , HPO_4^{2-} (anionisch).

Kationen abspalten oder Anionen bzw. Elektronen aufnehmen können und Basen als Stoffe, die Anionen oder Elektronen abspalten bzw. Kationen aufnehmen können.^[11] Aufgrund dieser zu großen Allgemeingültigkeit, hat USANOVICHs Säure-Basen-Konzept, ebenso wie das auf Oxidionen in anorganischen Schmelzen fokussierte Konzept von LUX und FLOOD,^[12] nicht die Bekanntheit der Lehrbuchkonzepte von BRØNSTED oder LEWIS erlangt.

1.1 Die Stärke von Superbasen

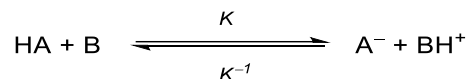
Die Stärke von BRØNSTED-Säuren wird über das protochemische Normalpotential, den pK_S -Wert, quantifiziert. Dieser ist über das protochemische Potential pH definiert als:

$$pH = pK_S + \log \frac{[A^-]}{[HA]} \quad (1.1)$$

Starke Säuren zeichnen sich durch einen möglichst niedrigen pK_S -Wert aus.³ Die Stärke von BRØNSTED-Basen wird über den pK_{BH^+} -Wert angegeben, dieser entspricht dem pK_S -Wert der konjugierten Säure und sollte demnach möglichst hoch sein. Eine eigene Basenkonstante K_B ist durch die Autoprotolysekonstante K_{auto} des Solvens gemäß Gleichung 1.2 obsolet:

$$pK_S + pK_B = pK_{\text{auto}} \quad (1.2)$$

Unbekannte Säurekonstanten können über Titration mit einer geeigneten Vergleichssäure/-base⁴ bestimmt werden. Bei der dabei auftretenden Konkurrenzreaktion zwischen zwei Säuren HA und BH^+ (Schema 1.4), ist die Gleichgewichtskonstante K über die Aktivität a der einzelnen Spezies gemäß Gleichung 1.3 definiert.⁵



Schema 1.4: Säure-Base-Reaktion zweier Komponenten mit der Gleichgewichtskonstante K .

$$K = \frac{a_{A^-} \cdot a_{BH^+}}{a_{HA} \cdot a_B} = \frac{[A^-] \cdot [BH^+]}{[HA] \cdot [B]} \quad (1.3)$$

Im Gleichgewicht haben sich die protochemischen Potentiale beider Reaktionspartner angeglichen; es gilt Gleichung 1.4 und folglich durch Einsetzen und Umformen Gleichung 1.5 und Gleichung 1.6.

$$pH_A = pH_B \quad (1.4)$$

$$pK_{S_A} + \log \frac{[A^-]}{[HA]} = pK_{S_B} + \log \frac{[B]}{[BH^+]} \quad (1.5)$$

$$\Delta pK_S = pK_{S_A} - pK_{S_B} = \log \frac{[B]}{[BH^+]} - \log \frac{[A^-]}{[HA]} = -\log \frac{[A^-] \cdot [BH^+]}{[HA] \cdot [B]} = -\log K \quad (1.6)$$

³ Beispiele für pK_S -Werte in wässrigem Medium: CF_3SO_3H (-14), $HClO_4$ (-10), HCl (-8), HNO_3 (-1.3), H_3PO_4 (2.1), CH_3COOH (4.8), H_2S (7.0), NH_4Cl (9.2), HCN (9.4), H_2O_2 (12), $tBuOH$ (17), NH_3 (38).^[13]

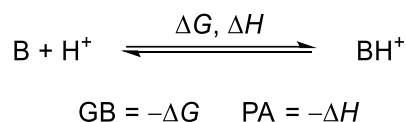
⁴ Der Unterschied der pK_S -Werte sollte maximal 1.5, bevorzugt nur 1.0 Größenordnungen betragen.^[14]

⁵ Bei genügend großer Verdünnung kann die Aktivität der Konzentration gleichgesetzt werden.^[1]

1 Einleitung

Die Lage des Gleichgewichts kann mittels NMR-Spektroskopie,^[15–17] Konduktometrie,^[18] Potentiometrie^[19,20] oder UV-Vis-Spektrophotometrie^[14,21–24] bestimmt werden. Mit dem bekannten pK_S -Wert der Vergleichsverbindung lässt sich mithilfe von Gleichung 1.6 die zu bestimmende Säurekonstante ermitteln.

In wässrigem Medium sind alle Säuren mit $pK_S \leq 0$ und alle Basen mit $pK_{BH^+} \geq 14$ wegen des nivellierenden Effekts des Wassers in ihrer Stärke nicht unterscheidbar. Zu diesem Zweck existieren selbstkonsistente pK_S -Skalen für andere Lösungsmittel wie 1,2-Dichlorethan,^[25] DMSO,^[26] Acetonitril^[21–23] und THF.^[14,27–29] Aufgrund unterschiedlicher stabilisierender Effekte wie Wasserstoffbrücken, Solvathüllen und Ionenpaarbildung in den verschiedenen Lösungsmitteln, sind diese jedoch nicht direkt⁶ miteinander vergleichbar.^[30] Deshalb wurde auch eine absolute pH-Skala bereits von KROSSING *et al.* diskutiert.^[31] Neben lösungsmittelabhängigen pK_{BH^+} -Werten wird die Basizität auch über die Gasphasenbasizität (GB) oder die Protonenaffinität (PA) quantifiziert. Letztere ist analog zur Elektronenaffinität definiert als Enthalpie (H), die bei der Annäherung eines Protons aus dem Unendlichen an die untersuchte Spezies in der Gasphase freigesetzt wird (Schema 1.5).^[32] Sie lässt sich leicht berechnen und wird deswegen in theoretischen Abhandlungen bevorzugt.^[33] Die GB berücksichtigt bei gleicher Reaktion die GIBBS-Energie (G), inkludiert also auch die Entropieänderung.⁷ Von ihr existiert, analog zu den pK_S -Skalen, auch eine experimentelle Skala.^[24,28,34]



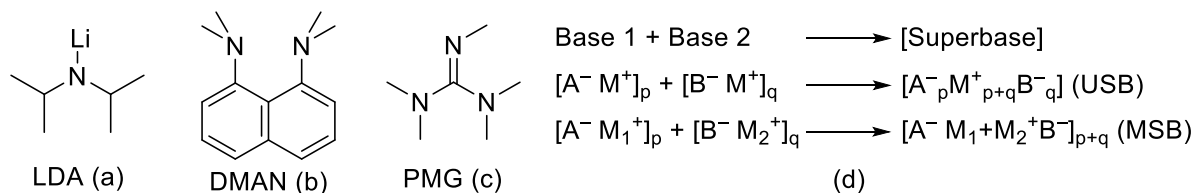
Schema 1.5: Definitionen für Gasphasenbasizität (GB) und Protonenaffinität (PA).

Als Supersäuren sind Säuren definiert, die stärker als 100%ige Schwefelsäure ($pK_S = -3.0$)^[13] sind.^[32,35] Für Superbasen hingegen sind in der Literatur verschiedene Definitionen vorhanden (Schema 1.6). Die IUPAC definiert Lithiumdi-*iso*-propylamid (LDA) mit einem pK_{BH^+} -Wert in THF von 36^[13] als Grenze zur Superbasizität.^[32] Mit dieser restriktiven Definition sollen hauptsächlich anorganische und metallorganische Basen adressiert werden, zu denen die Metallhydride, -alkoxide und -amide, sowie Metallorganyle gehören. Für Organosuperbasen existieren großzügigere Grenzen, wie der Protonenschwamm 1,8-Bis(dimethylamino)-naphthalin (DMAN) mit einer PA von $245 \text{ kcal} \cdot \text{mol}^{-1}$ und einem pK_{BH^+} -Wert von 18.3 in Acetonitril.^[4] Auch Pentamethylguanidin (PMG) wird als Fixpunkt für Superbasizität vorgeschlagen, da es mit einem pK_{BH^+} -Wert in Acetonitril von 25.0^[36] und einer GB von

⁶ Zwischen ähnlichen Lösungsmitteln kann oft eine lineare Korrelation angenommen werden. So sind z. B. ungeladene Basen in THF zu niedrigeren pK_{BH^+} -Werten verschoben mit $pK_{BH^+}(\text{THF}) = 0.86 \cdot pK_{BH^+}(\text{MeCN}) - 3.4$.^[30]

⁷ Für den Zusammenhang von GB und PA gilt: $\text{GB} = \text{PA} + T \cdot \Delta S$ mit T = Temperatur und S = Entropie.

1000 kJ·mol⁻¹ (239 kcal·mol⁻¹)^[37] herausstechende Werte besitzt.^[38] Für CAUBÈRE schließlich definiert sich eine Superbase nicht über ihre Basizität, sondern dadurch, dass sie als Kombination zweier oder mehrerer Basen inhärent neue Eigenschaften besitzt.^[39] So können, als Beispiel für seine *unimetal superbases* (USB), Natriumalkoholate die Aktivität von in organischen Lösungsmitteln unlöslichem Natriumamid durch Bildung löslicher Mischaggregate drastisch erhöhen. Auch *multimetal superbases* (MSB), wie die LOCHMANN-SCHLOSSER-Base, fallen unter diese Definition.^[40]



Schema 1.6: Grenzmoleküle und Definitionen für Superbasizität nach IUPAC (a),^[32] ISHIKAWA (b),^[4] SUNDERMEYER (c)^[38] und CAUBÈRE (d).^[39]

Dabei stellt sich die Frage, wieso eine Unterscheidung in der Definition für metallhaltige und organische Superbasen notwendig ist, bzw. warum letztere überhaupt als Superbasen in Betracht gezogen werden sollten, obwohl sie in ihrer Basizität um mehrere Größenordnungen schwächer sind. Anorganische und metallorganische Basen sind zwar hochreaktiv, erstere erlauben aufgrund ihrer oft begrenzten Löslichkeit jedoch häufig nur heterogene Reaktionsführungen, während metallorganische Basen auch als Nukleophil reagieren und die Selektivität der Reaktion und damit die Ausbeute deutlich herabsenken können. Auch die Anwesenheit potentiell LEWIS-saurer Metallkationen kann zur Bildung unerwünschter Nebenprodukte führen. Demgegenüber steht der häufige Einsatz vergleichsweise schwacher Aminbasen als Hilfsbasen in der Synthese. Tertiäre Amine können aufgrund sterischer Abschirmung des basischen Stickstoffatoms durch organische Substituenten eine sehr geringe Nukleophilie und gute Löslichkeit in organischen Lösungsmitteln aufweisen. Die entstehenden Ammoniumsalze lassen sich häufig einfach abtrennen und die Variation der Substituenten lässt eine gezielte Einstellung des pK_{BH^+} -Wertes zu, wodurch hochselektive Reaktionen ermöglicht werden. Die in Abbildung 1.1 gezeigten Vertreter sind schwächere Basen als PMG, demnach per hier verwendeter Definition keine Superbasen und sind dennoch als wichtige Reagenzien aus vielen Synthesen nicht mehr wegzudenken.^[2] Ihr breites Anwendungsspektrum ist nur durch ihre deutlich unterlegene Basizität gegenüber den beiden anderen Klassen von Basen limitiert. Sogenannte nicht-ionische, neutrale oder ungeladene (Organo-)Superbasen haben somit zum Ziel, unter Beibehaltung der guten Löslichkeit in organischen Lösungsmitteln und geringer Nukleophilie, in Basizitätsregionen vorzustoßen, die bisher anorganischen oder metallorganischen Basen vorenthalten war.

1 Einleitung

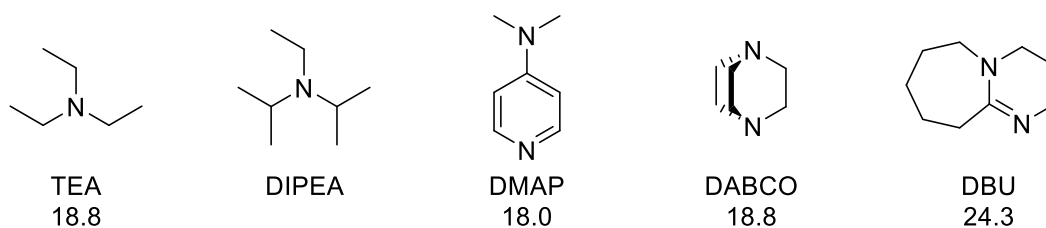


Abbildung 1.1: Strukturen der Basen Triethylamin (TEA), Di-*iso*-propylethylamin (DIPEA oder HÜNIG-Base), Dimethylaminopyridin (DMAP), 1,4-Diazabicyclo[2.2.2]octan (DABCO) und 1,8-Diazabicyclo[5.4.0]undec-7-en (DBU). Angegeben sind literaturbekannte pK_{BH^+} -Werte in Acetonitril.^[4]

1.2 Stickstoffsuperbasen

Die überwiegende Mehrheit ungeladener Superbasen weist ein Stickstoffatom als Basizitätszentrum auf.^[4] Dieses ist meist in Form eines Imins als *push-pull*-System an ein Molekülgerüst angebunden,^[41] da sich die Delokalisierung der bei Protonierung entstehenden positiven Ladung durch Konjugation, Aromatizität oder negativer Hyperkonjugation als fruchtvollster Ansatz herausgestellt hat.^[36] Erstere beiden Fälle sind in Guanidinen^[37,42] (Abbildung 1.2 (a)), Imidazolin-2-ylidenaminen (b),^[43] Cyclopropenimininen^[44–48] (c) und deren Kombinationen realisiert (d).^[16,29,49] Negative Hyperkonjugation machen sich die zu den zurzeit stärksten Superbasen gehörenden peralkylierten Polyaminophosphazene von SCHWESINGER *et al.* zu eigen, bei denen die positive Ladung über ein Phosphor- und Stickstoff-Heteroatomgrundgerüst delokalisiert wird.^[19] Das in Abbildung 1.3 gezeigte *N-tert*-Butyltris(dimethylamino)-phosphazene (dma)₁-*t*Bu besitzt einen pK_{BH^+} -Wert von 26.9 in Acetonitril, der sich durch basischere Pyrrolidinsubstituenten (pyrr) um 1.5 Größenordnungen steigern lässt.^[50] Einen noch größeren Effekt bewirkt das in der Literatur auch *battery cell* getaufte Konzept der Homologisierung, welches die Erweiterung des Heteroatomrückgrates um weitere Phosphazeneinheiten zu Superbasen höherer Ordnung bezeichnet.^[19,51] So liegt der pK_{BH^+} -Wert der stärksten kommerziell erhältlichen Superbase (dma)₄-*t*Bu bereits bei 42.7 (MeCN).^[19] Der basischste Vertreter der SCHWESINGER-Basen ist (pyrr)₅-*t*Bu mit einem pK_{BH^+} -Wert von 46.9 (MeCN),^[19] während sich die Grenzen der Homologisierung bei (dma)₇-*t*Bu (ohne Abbildung) zeigen, dessen protonierte Form bereits extrem säurelabil ist und dessen freie Basenform bislang nicht isoliert werden konnte.^[19,52]

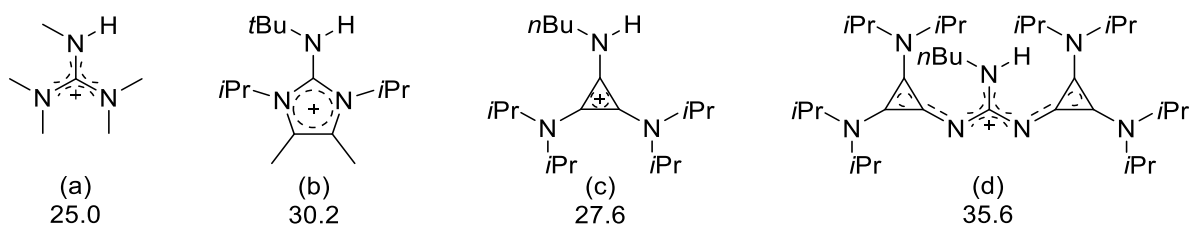


Abbildung 1.2: Veranschaulichung der Ladungsdelokalisierung und pK_{BH^+} -Werte (MeCN) von Guanidinen (a),^[36] Imidazolin-2-ylidenaminen (b)^[43] und Cyclopropenimininen (c)^[16] sowie einer beispielhaften Superbase höherer Ordnung (d).^[16]

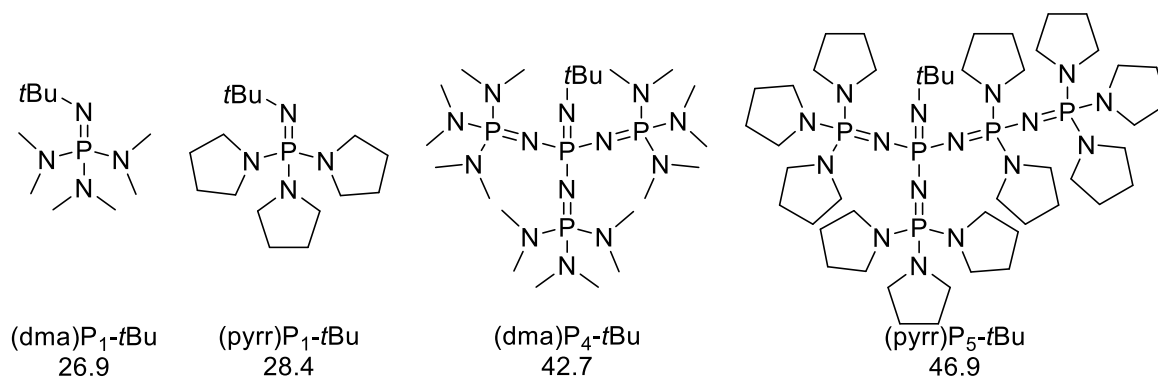


Abbildung 1.3: Strukturen und pK_{BH^+} -Werte (MeCN) ausgewählter SCHWESINGER-Basen.^[19,50]

Die überlegene Basizität von Phosphazenen gegenüber Guanidinen und Cyclopropenimininen wird in Abbildung 1.4 verdeutlicht. Aufgetragen ist der pK_{BH^+} -Wert von Superbasen höherer Ordnung als Funktion der pK_{BH^+} -Werte ihrer Substituenten.^[16] Die Steigung der Regressionsgeraden quantifiziert den Einfluss der Substituenten auf die Basizität und ist ein Maß dafür, wie gut das Kernmotiv die elektronendonierenden Eigenschaften der Substituenten über Wechselwirkungen mit der basischen Iminfunktion verbindet. Auf die Substituentenanzahl normiert ist dieser Wert bei Phosphazenen und Guanidinen als Kernmotiv mit 0.55 bzw. 0.57 fast dreimal so groß wie bei Cyclopropenimininen (0.21), was auf die hohe Stabilität des aromatischen Cyclopropeniumkations zurückzuführen ist. Der Vorteil von Phosphazenen gegenüber Guanidinen liegt in der Möglichkeit drei statt nur zwei Substituenten zu tragen, wodurch absolute Steigungswerte von 1.65 gegenüber 1.13 erzielt werden und Phosphazene sowohl als Kernmotiv wie auch als Substituent in Superbasen höherer Ordnung die größte Basizitätssteigerung erzielen. Aus diesem Grund sind die SCHWESINGER-Basen nach wie vor unerreichte Spitzenreiter in der großen Auswahl an Stickstoffsuperbasen.

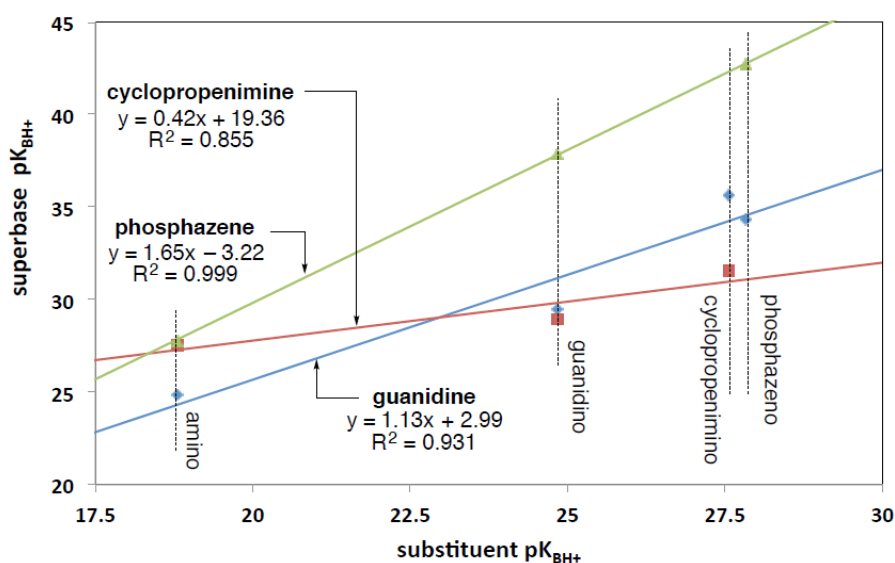
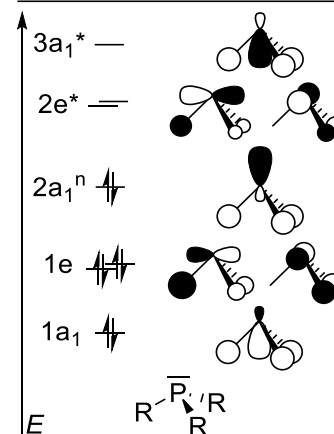
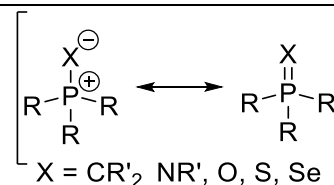


Abbildung 1.4: Aufgetragen sind pK_{BH^+} -Werte von Superbasen höherer Ordnung mit Phosphazen- (grün), Guanidin- (blau) und Cyclopropenimin-Kernmotiv (rot) in Abhängigkeit der pK_{BH^+} -Werte ihrer Amino-, Guanidino-, Cyclopropenimino- und Phosphazenylnsubstituenten. Ref.^[16] entnommen.

Exkurs: Negative Hyperkonjugation

Wie bei allen hyperkoordinierten Hauptgruppenverbindungen weist auch das Phosphor(V)atom in Phosphazenen eine Bindungsordnung von vier auf und besitzt lediglich acht Elektronen in bindenden Orbitalen. Zusätzliche fünfte oder sechste Bindungen werden entweder über Mehrzentrenbindungen wie z. B. in Phosphorpentachlorid oder im Hexafluoridphosphat-anion realisiert oder im Falle einer formalen Doppelbindung wie in Phosphazenen, Phosphoranen, Phosphorsäuren und anderen Phosphorchalkogeniden über negative Hyperkonjugation.^[53]

Ausgehend vom Orbitalschema eines Phosphans PR_3 (Schema 1.7, unten), bildet das freie Elektronenpaar $2a_1^n$ eine kovalente σ -Bindung mit dem Substituenten X aus, was der linken, ladungsseparierten LEWIS-Schreibweise in Schema 1.7 (oben) entspricht. Die rechte und gängige LEWIS-Schreibweise beschreibt

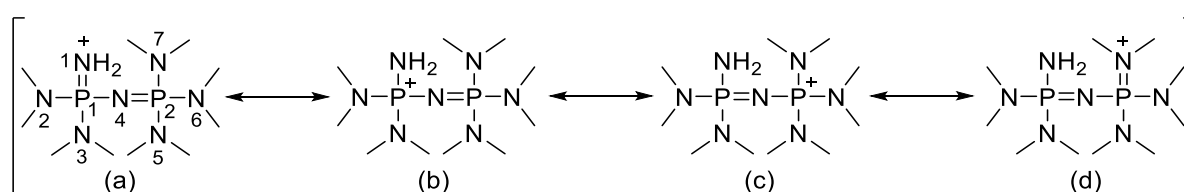


Schema 1.7: Mögliche LEWIS-Schreibweisen hyperkoordinierter Phosphorverbindungen R_3PX (oben) sowie das qualitative Orbitalschema eines Phosphans PR_3 (unten).

zusätzliche dative π -Wechselwirkungen, welche durch konstruktive Interferenz nicht-bindender p-Orbitale des Substituenten X mit dem antibindenden $2e^*$ -Orbital des PR_3 -Fragments ausgebildet werden.^[54] Diese Art der Bindung zwischen Hauptgruppenelementen ist analog zur σ -Donor- π -Akzeptor-Wechselwirkung in Übergangsmetallkomplexen.^[55] Der Doppelbindungscharakter sinkt mit steigender σ - und π -Donorfähigkeit der Substituenten R,^[56] wie auch mit steigender Polarisierbarkeit des Substituenten X (Polarisierbarkeit von Chalkogenen: $\text{O} < \text{S} < \text{Se}$; Doppelbindungsanteil: $\text{O} > \text{S} > \text{Se}$)^[57] und wird in (Imino-) Phosphoranen auch von mesomeren und induktiven Effekten der Substituenten R' beeinflusst.

Beim Vergleich der im Kristall vorliegenden Molekülstrukturen von $(\text{dma})\text{P}_2\text{-H}$ ^[58] und dessen Hydrochlorid^[59] wird die Delokalisierung der positiven Ladung durch negative Hyperkonjugation über das Heteroatomgrundgerüst deutlich (Schema 1.8): Die N–P-Bindung des basischen Iminstickstoffatoms (N1) verlängert sich durch Protonierung von einer Doppelbindung mit 1.565(2) Å zu einer Einfachbindung mit 1.614(1) Å, Grenzstruktur (a) hat demzufolge kaum Einfluss auf die Bindungssituation. Stattdessen verkürzt sich die formale Einfachbindung der P–N–P-Einheit (N4-P1) von 1.604(2) Å auf 1.574(1) Å und gleicht sich der formalen Doppelbindung an (N4-P2: 1.555(2) bzw. 1.559(1) Å). Zusammen mit einem aufgeweiteten P–N–P-Winkel (von 132.4(1)° zu 140.30(9)°), weist dies auf einen großen Anteil der Grenzstrukturen (b) und (c) an der Bindungssituation hin. Auch die P–N-Bindungen

der Dimethylaminosubstituenten verkürzen sich von durchschnittlich 1.66 Å auf 1.64 Å und die Winkelsummen um die Aminstickstoffatome nähern sich dem Wert von 360° für ideale Planarität an, was die Beteiligung der NR₂-Substituenten an der Delokalisierung mittels negativer Hyperkonjugation belegt (d). Dass einer von drei Substituenten der einzelnen Phosphoratome einen leicht größeren N–P-Abstand aufweist und stärker von idealer Planarität abweicht (N3 und N5), lässt sich über das Phänomen des sogenannten *special nitrogen* erklären. Dieser Effekt besagt, dass aufgrund von Orbitalsymmetrien lediglich zwei der drei Aminosubstituenten negative Hyperkonjugation ausbilden können, weshalb heteroleptische Bis(dialkylamino)alkylphosphane ((R₂N)₂(R′)P) teilweise stärkere Donorliganden sein können, als Tris(dialkylamino)phosphane ((R₂N)₃P).^[60]

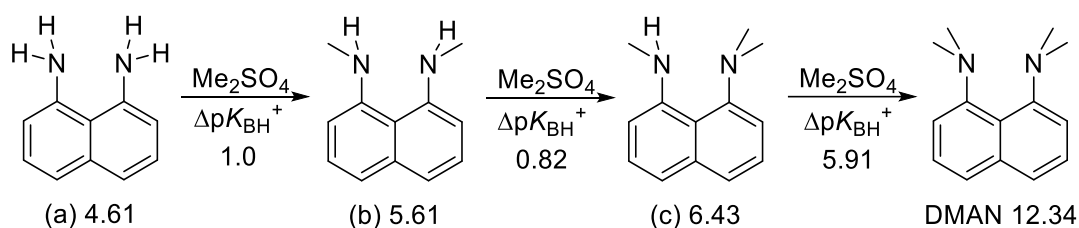


Schema 1.8: Ausgewählte mögliche mesomere Grenzstrukturen von (dma)₂P₂-H·H⁺. Vergleich ausgewählter Bindungslängen/Å und -winkel/° sowie Winkelsummen/° von (dma)₂P₂-H/(dma)₂P₂-H·HCl: N1-P1 1.565(2)/1.614(1), N2-P1 1.673(2)/1.631(1), N3-P1 1.689(2)/1.652(1), N4-P1 1.604(2)/1.574(1), N4-P2 1.555(2)/1.559(1), N5-P2 1.654(2)/1.645(1), N6-P2 1.650(2)/1.640(1), N7-P2 1.642(2)/1.640(1), P1-N4-P2 132.4(1)/140.30(9), N2 352/359, N3 351/351, N5 348/354, N6 355/359, N7 359/358.^[58,59]

Durch die geringe Ladungsdichte und Nukleophilie sowie eine gute Löslichkeit können nicht-ionische Superbasen hochreaktive nackte Anionen in Lösung erzeugen. Chirale Superbasen ermöglichen sogar den gezielten Aufbau von Stereozentren.^[61] So kommen Guanidine, Cyclopropenimine und Phosphazene zur katalytischen Erzeugung von Enolaten in der (asymmetrischen) MICHAEL-Addition,^[16,45,47,62] der HENRY-Reaktion^[63] oder der Aldol-Addition zum Einsatz.^[64] Auch Amine und Alkohole können durch katalytischen Einsatz von Superbasen für die Addition an Alkine,^[65] die Substitution der Methoxygruppe an Anisolen^[66] oder für die MANNICH-Reaktion^[46,67] aktiviert werden. SCHWESINGER-Basen ermöglichen durch die anti-MARKOVNIKOV-selektive Addition von Alkoholen an Vinylaryle einen direkten Zugang zu synthetisch wertvollen β-Phenethylethern (Ph(CH₂)(CH₂)OR).^[68] Auch der Zerfall von Trifluormethylcarbanionen in Difluorcarben und Fluoridionen wird durch (dma)₄-tBu verhindert und so die Übertragung von CF₃-Gruppen ermöglicht.^[69] Die Aktivierung der Nukleophile ist dabei nicht auf eine Deprotonierung beschränkt, auch silylgeschützte Verbindungen können katalytisch desilyliert und zur Reaktion gebracht werden.^[70] In der Polymerchemie kommen Superbasen sowohl in der radikalischen^[71] als auch in der anionischen Polymerisation zum Einsatz.^[72] Sie ermöglichen z. B. die metallfreie Polymerisation von Acrylaten,^[73] Lactonen,^[74] Lactamen,^[75] Siloxanen^[76] und Epoxiden.^[77]

Protonenschwämme und Protonenpinzetten

Neben der bisher beschriebenen Delokalisierung der positiven Ladung konnten auch mit Strukturen, die die protonierte Form der Base mithilfe einer oder mehrerer intramolekularer Wasserstoffbrückenbindungen (IHBs) stabilisieren, bemerkenswerte Ergebnisse erzielt werden. Ein weites und ausgearbeitetes Feld derartiger Verbindungen ist das der Protonenschwämme. 1986 entdeckten ALDER *et al.*, dass bei sukzessiver Methylierung von 1,8-Diaminonaphthalin (Schema 1.9 (a)) der pK_{BH^+} -Wert von *N,N,N'*-Trimethyl-1,8-diaminonaphthalin (c) zu 1,8-Bis(dimethylamino)naphthalin DMAN sprunghaft um sechs Größenordnungen anstieg.^[78] Diese unerwartet hohe Basizität des DMAN liegt an einer energetisch günstigen protonierten Spezies, die durch eine asymmetrische IHB mit schnellem intramolekularem Protonenaustausch zwischen den beiden Stickstoffbasizitätszentren stabilisiert wird,^[79] und einer destabilisierten freien Basenform, in der es durch Repulsion der freien Elektronenpaare der Stickstoffatome zu einer Verdrillung und damit partiellen Aufhebung der Aromatizität des Naphthalinrückgrates kommt.^[78] Der dadurch hervorgerufenen hohen thermodynamischen Basizität steht durch die stabilisierende IHB und die sterische Abschirmung des aciden Protons durch die Alkylsubstituenten ein kinetisch gehemmter intermolekularer Protonenaustausch gegenüber, was ALDER zu der bezeichnenden Namensgebung des Protonenschwammes inspirierte.



Schema 1.9: Basizitätsveränderung bei sukzessiver Methylierung von (a) zu DMAN (pK_{BH^+} -Werte in H_2O).^[78]

Auf Basis dieses Strukturmotives wurde eine große Auswahl chelatisierender Basen entwickelt. Den größten Einfluss auf die Basizität haben dabei die Substituenten an den Stickstoffatomen selbst, so konnten in der eigenen Arbeitsgruppe 1,8-Bisguanidinonaphthalin^[80,81] und 1,8-Bisphosphazenylnaphthalinprotonenschwämme^[82] dargestellt werden (Abbildung 1.5). Letztere markieren mit dem von KÖGEL synthetisierten P_2 -TPPN, welcher das Prinzip des Protonenschwammes mit dem Homologisierungskonzept verbindet, mit einem pK_{BH^+} -Wert von 40.2 (MeCN) den Rekordhalter für chelatisierende Basen.^[83] Cyclopropenimine wurden 2014 von DUDDING *et al.* in Protonenschwämmen eingesetzt.^[84,85] Durch Verwendung von (*R,R*)-1,2-Diaminocyclohexan^[86] oder 1(*S*)-(-)-2,2'-Diamino-1.1'-binaphthalin^[87] in Kombination mit (Di-)Phosphazenen konnte KÖGEL aus der eigenen Arbeitsgruppe chirale Protonenpinzetten erhalten.

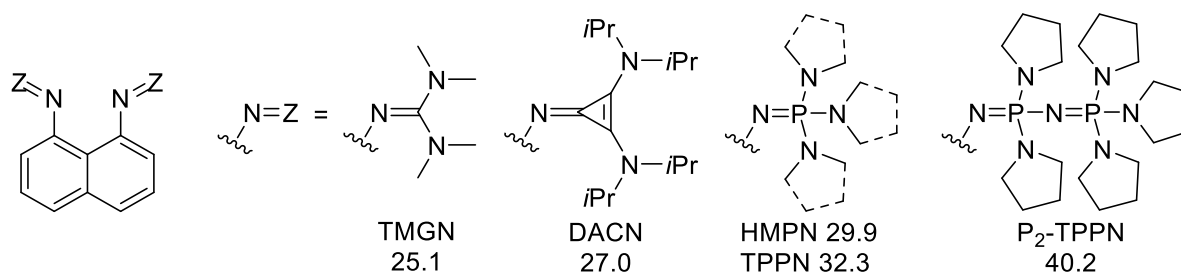


Abbildung 1.5: Strukturen und pK_{BH^+} -Werte (MeCN) der Protonenschwämme TMGN,^[80] DACN (berechneter Wert),^[84] HMPN,^[82] TPPN^[83] und P_2 -TPPN.^[83]

Auch Substitutionen am Naphthalinrückgrat haben Einfluss auf die Basizität. So können die beiden Basizitätszentren durch den *buttressing effect*, die Substitution in 2,7-Position durch sterisch anspruchsvolle Gruppen, in größere räumliche Nähe gezwungen werden, was die Repulsion der freien Elektronenpaare an den Stickstoffatomen und damit die Basizität erhöht.^[88] Der gleiche Effekt wird auch durch andere Grundgerüste, wie in STAABS 4,5-Bis(dimethylamino)fluoren^[89] und 4,5-Bis(dimethylamino)phenanthren,^[90] erzielt. Werden die Stickstoffatome hingegen in das aromatische Grundgerüst implementiert, steigt die kinetische Aktivität aufgrund fehlender sterischer Abschirmung der Basizitätszentren. Derartige chelatisierende Basen, zu denen SCHWESINGERS Vinamidin (Abbildung 1.6 (a)),^[91] STAABS Chino[7,8-*h*]chinolin^[92] oder POZHARSKIIs asymmetrische Benzo[*h*]quinoline (b) gehören, sollten daher besser als Pseudoprotonenschwämme bezeichnet werden, bei denen auch ein schneller intermolekularer Protonenaustausch möglich ist.^[93] In pyridinverbrückten Bisguanidinen (c) wird das acide Proton sogar über zwei zusätzliche IHBs chelatisiert.^[94]

Ein ähnliches Prinzip zur Erhöhung der Basizität ist der Korona-Effekt, bei dem eine IHB von einem Wasserstoffbrückenakzeptor am Ende einer Alkylkette unter Ringschluss zum aciden Proton ausgebildet wird,^[95] diese trägt bis zu $10 \text{ kcal} \cdot \text{mol}^{-1}$ zur PA bei.^[48] Der kooperative Einfluss multipler Korona-Effekte war bereits Gegenstand verschiedener theoretischer Studien,^[96] der bislang einzige synthetisch realisierte Vertreter ist *N,N',N''*-Tris(dimethylaminopropyl)guanidin (TDMPG).^[97] Die im Kristall vorliegende Molekülstruktur des Hexafluoridosphats bestätigte die Existenz dreier IHBs, die jedoch keine sechsgliedrigen

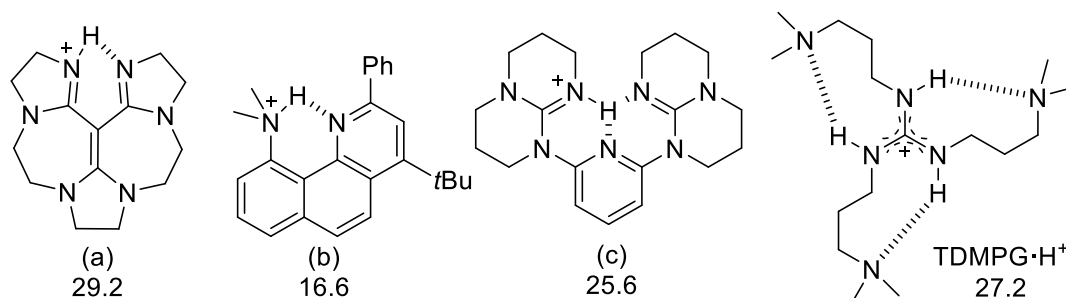
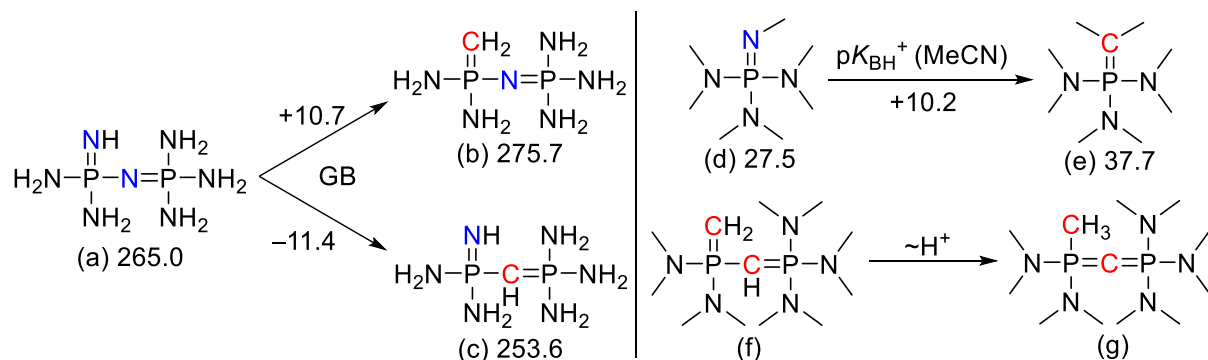


Abbildung 1.6: pK_{BH^+} -Werte (MeCN) vom Vinamidin- (a),^[91] Benzo[*h*]quinolin- (b)^[93] und Pyridinylen-bisguanidin-Pseudoprotonenschwämmen (c)^[94] sowie von TDMPG.^[98]

Ringe zwischen N–H-Donor und alkylverbrücktem Akzeptor ausbilden, sondern die in Abbildung 1.6 dargestellten Achtringe zu benachbarten Substituenten.^[97] Der Basizitätsgewinn in derartigen Modellsystemen liegt nicht nur in der durch Protonierung zusätzlich gebildeten IHB, sondern aufgrund der größeren Polarisierung der N–H-Bindungen darüber hinaus in einer Stärkung aller IHBs, wodurch TDMPG um 2.23 Größenordnungen basischer ist als das vom induktiven Effekt der Alkylgruppen vergleichbare *N,N',N''*-Tripropylguanidin.^[98]

1.3 Kohlenstoffsuperbasen

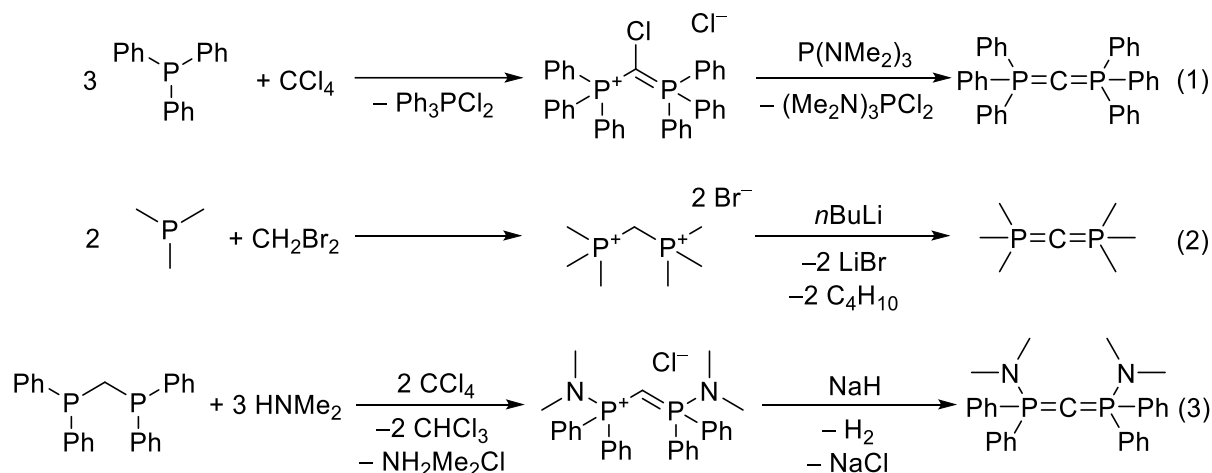
Neben der großen Auswahl an Stickstoffsuperbasen, haben auch Phosphorylide als Kohlenstoffsuperbasen Einzug in die Basizitätsskala gefunden.^[14,99] Diese machen sich die, im Vergleich zur Iminofunktion, intrinsisch höhere Basizität der Alkylidengruppe zunutze.^[100] Schema 1.10 zeigt, dass sich bei Substitution der basischen =NR-Funktion in (a) bzw. (d) durch eine =CR₂-Funktion in (b) bzw. (e) die GB um 10.7 kcal·mol⁻¹^[100] und der p*K*_{BH}⁺-Wert in Acetonitril um 10.2 Größenordnungen in den jeweiligen Beispielen erhöht.^[14] Als verbrückendes Strukturmotiv in Superbasen höherer Ordnung scheint die zur Iminobrücke (–N=) isolobale Methanylidengruppe (–CH=) dagegen einen gegenteiligen Effekt zu haben und reduziert die GB um 11.4 kcal·mol⁻¹ ((a) und (c)).^[100] Als Basizitätszentrum ist das Kohlenstoffatom aufgrund seiner geringeren Neigung zur negativen Hyperkonjugation, privilegiert um hohe Basizitäten zu erzielen. Als Motiv in stark elektronendonierenden Substituenten sollten Phosphazene dagegen den Phosphoryliden vorgezogen werden, da bei letzteren die positive Ladung weniger effizient delokalisiert werden kann. Bei ylidverbrückten Yliden (f) kommt es, sofern die hohe Elektronendichte an der Alkylidengruppe (=CR₂) nicht durch Konjugation (z. B. bei R = Ph) oder negative Hyperkonjugation (R = SiMe₃) reduziert wird, zur Tautomerisierung zum methylsubstituierten Carbodiphosphoran (g).^[101,102] Dies ist bei ylidverbrückten Iminophosphoranen (c) nicht der Fall, da die PA des Iminstickstoffatoms deutlich geringer ist als die erste PA des zentralen Kohlenstoffatoms.^[103]



Schema 1.10: GBs/kcal·mol⁻¹ von =NH und =CH₂ Basen (a-c)^[100] und experimentelle p*K*_{BH}⁺-Werte (MeCN) von Phosphazenen (d) und Yliden (e)^[14] sowie die experimentell beobachtete Tautomerisierung von (f) zu (g).^[101]

Auch bei Protonenschwämmen wurde der Sprung von Stickstoff- zu Kohlenstoffbasen schon untersucht. Das zum 1,8-Bis(hexamethyltriaminophosphazenylnaphthalin (HMPN, Abbildung 1.5, S.11) analoge, bisylidische 1,8-Bis(methanylid(en)hexamethyltriamino)phosphoranyl)naphthalin (MHPN), weist einen um 3.4 Größenordnungen höheren pK_{BH}^+ -Wert (33.3 in MeCN) auf.^[104] Dieser im Vergleich mit Monophosphazenen und -yliden (Schema 1.10, (d) und (e)) geringere Zuwachs und absolute pK_{BH}^+ -Wert ist auf das aromatische Naphthalinrückgrat zurückzuführen, das sich mit den Ylidfunktionen in Konjugation befindet und deren Elektronendichte reduziert. Anders als bei N,N' -Protonenschwämmen, wird die konjugierte Säure nicht über eine IHB stabilisiert, sondern über einen raschen Protonenaustausch zwischen beiden Ylidfunktionen ohne statische C–H \cdots C-Wechselwirkung. Der Basizitätsgewinn im Vergleich zum analogen Monoylid liegt dadurch bei $13.9 \text{ kcal}\cdot\text{mol}^{-1}$.^[104] Obwohl ihnen bereits auch superbasische Eigenschaften zugesprochen wurden, haben N -heterocyclische Carbene (NHCs),^[105] cyclische Alkylaminocarbone (CAACs),^[106] Carbodicarbene (CDCs)^[107] und Carbodiphosphorane (CDPs)^[108] bislang eher durch ihren Einsatz als starke LEWIS-Basen gegenüber Übergangs- und Hauptgruppenelementen, denn als BRØNSTED-Basen Bekanntheit erlangt. Für NHCs sind nur wenige experimentelle pK_{BH}^+ -Werte bekannt, welche um 22 ± 2 in THF und DMSO liegen,^[109] während die Basizität von CAACs, CDCs und CDPs lediglich theoretisch in Form berechneter PAs untersucht wurde.^[103,110] 2015 postulierten LEITO *et al.* Bisphosphazenylicarbene als privilegiertestes Strukturmotiv für die stärksten ungeladenen Superbasen mit GBs jenseits der $350 \text{ kcal}\cdot\text{mol}^{-1}$.^[111] FRENKING *et al.* konnten jedoch bereits 2008 durch den Vergleich der PAs von Carbenen und Carbodiphosphoranen zeigen, dass letztere sogar noch basischer sein sollten.^[103] Das erste CDP war das 1961 von RAMIREZ *et al.* synthetisierte Hexaphenylcarbodiphosphoran ((Ph)₆-CDP),^[112] dem bald weitere Verbindungen wie das Hexamethylcarbodiphosphoran ((Me)₆-CDP),^[113] das Hexakis(dimethylamino)carbodiphosphoran ((dma)₆-CDP)^[114] und gemischtsubstituierte Vertreter folgten.^[115–117] Die Synthese von CDPs erfolgt hauptsächlich über die APPEL- oder die SCHMIDBAUR-Route (Schema 1.11, (1) und (2)), bei denen Tetrachlorkohlenstoff^[118] bzw. Dibrommethan^[115,119] als C₁-Synthon mit Phosphanen zur Reaktion gebracht und anschließend dehalogeniert bzw. deprotoniert wird. Eine zusätzliche Möglichkeit für aminsubstituierte CDPs besteht in der Oxidation methylenverbrückter Bisphosphane mit Tetrachlorkohlenstoff in Gegenwart von Aminen als Nukleophil und Hilfsbase (Schema 1.11, (3)).^[114,116] Einen Sonderfall stellen PERINGERS multidentate, dppm-funktionalisierte CDP-Liganden dar (dppm = Bis(diphenylphosphino)methan), welche mithilfe von Nickel-, Palladium- oder Platinionen als Templatbildner synthetisiert werden.^[120]

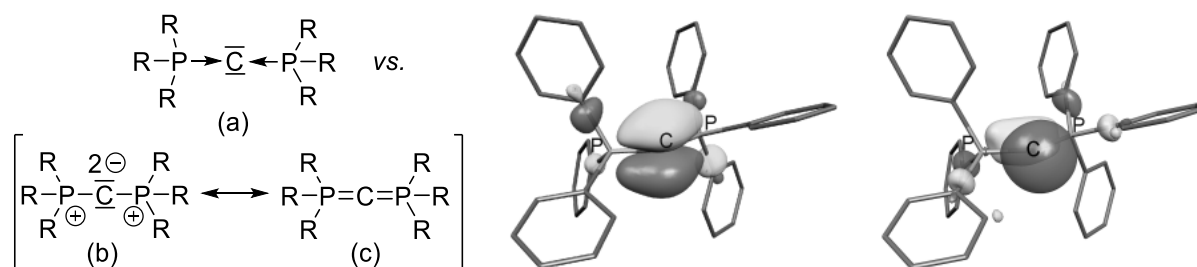
1 Einleitung



Schema 1.11: Mögliche Syntheserouten zur Darstellung von CDPs.

Sowohl die Bindungssituation als auch die Grundzustandsgeometrie wird in der Literatur kontrovers diskutiert. Die meisten im Kristall vorliegenden Molekülstrukturen zeigen eine gewinkelte P–C–P-Einheit,^[121] jedoch variiert der Winkel z. B. beim polymorphen (Ph)₆-CDP zwischen 130.1 und 143.8°^[122] und ist stark von den Kristallisationsbedingungen wie dem Lösungsmittel abhängig. 2017 wurde schließlich auch eine lineare Anordnung gefunden,^[123] wie sie bis *dato* einzig für (dma)₆-CDP bekannt war.^[114] In der Gasphase wurde für (Ph)₆-CDP eine mit 135.0°^[124] oder 136.9°^[125] gewinkelte Struktur im Grundzustand berechnet, wobei nur geringe Energieunterschiede zwischen linearer und gewinkelter Struktur gefunden wurden.^[123] Zur Darstellung der Bindungsverhältnisse in CDPs werden in der Literatur unterschiedliche LEWIS-Formeln verwendet. FRENKING *et al.* zeigten in theoretischen Untersuchungen, dass sowohl das *highest occupied molecular orbital* (HOMO) als auch das HOMO–1 größtenteils als freie Elektronenpaare mit π - bzw. σ -Symmetrie am zentralen Kohlenstoffatom lokalisiert sind (Schema 1.11, rechts) und kaum negativ hyperkonjugative Wechselwirkung zu den Phosphoratomen ausbilden.^[124] Sie interpretierten die P–C–P-Funktion als zweibindiges Kohlenstoff(0)atom, das durch zwei Phosphanliganden mittels dativer Hinbindung stabilisiert wird und propagieren daher die 1973 erstmalig von KASKA *et al.* vorgeschlagene Darstellung mit Pfeilen (Schema 1.12 (a)).^[126] Eine gleichwertige Beschreibung der Bindungssituation als kovalente Bindung wird über die bisylidische LEWIS-Formel (b) mit Formalladungen ausgedrückt.^[127] Unabhängig davon, ob dem zentralen Kohlenstoffatom die formale Oxidationsstufe 0 oder –IV zugeschrieben wird, macht dessen hohe Elektronendichte CDPs zu extrem starken BRØNSTED- und LEWIS-Basen, die nicht nur zwei-, sondern vier-Elektronen-Donorliganden sein können und in der Lage sind zwei Protonen aufzunehmen.⁸

⁸ Erste und zweite PA in kcal·mol⁻¹: (Ph)₆-CDP (280.0/185.6), (dma)₆-CDP (279.9/174.9), Hexapyrrolidino-carbodiphosphoran (pyrr)₆-CDP (287.6/188.9).^[103]



Schema 1.12: Mögliche LEWIS-Schreibweisen zur Veranschaulichung der Bindungssituation in CDPs (links).⁹ Die Abbildung von HOMO und HOMO-1 des (Ph)₆-CDPs ist Ref.^[124] entnommen (rechts).

1.4 Phosphorsuperbasen

Obwohl in den stärksten nicht-ionischen Superbasen essentieller Bestandteil, sind im oberen Teil der Basizitätsskala kaum Superbasen vertreten, bei denen Phosphoratome die Rolle des Basizitätszentrums einnehmen.^[14] Analog zu Carbenen liegt das bisherige Haupteinsatzgebiet von Phosphanen als Liganden in der Übergangsmetallchemie und -katalyse. Dabei beeinflussen elektronische und sterische Eigenschaften der Phosphane das Reaktionsvermögen und die Stabilität der resultierenden Komplexe, weshalb verschiedene Parameter entwickelt wurden, um Phosphanliganden beschreiben und katalogisieren zu können.^[128] Statt die Basizität mittels pK_{BH^+} -Werten anzugeben, wird die Donor-Akzeptor-Fähigkeit meist über TOLMANS elektronischen Parameter (TEP) quantifiziert, welcher die CO-Streckschwingung von Metallcarbonylen¹⁰ als Sonde verwendet.^[131] Je niedriger der TEP, desto stärkere Donor- und schwächere Akzeptorfähigkeit weist der untersuchte Ligand auf. Für eine hohe Donorfähigkeit kann auch eine geringe $^1J_{PSe}$ -Kopplungskonstante korrespondierender Phosphanselenide als Parameter herangezogen werden.^[132] Diese hängt maßgeblich vom s-Charakter der P-Se-Bindung ab, welcher nach der BENTSchen Regel mit geringerer Gruppenelektro negativität des PR_3 -Fragments sinkt.^[133] Der sterische Anspruch von Liganden wird über den TOLMAN Kegelwinkel θ beschrieben.^[131] Dieser ist definiert als Öffnungswinkel eines Kegels, dessen Spitze 2.28 \AA^{11} vom Phosphoratom entfernt ist und dessen Mantelfläche die VAN-DER-WAALS-Radien der äußersten Atome tangiert.¹² Auch das *buried volume* ($\%V_{Bur}$), welches den prozentualen Platzbedarf des Liganden innerhalb der ersten Koordinationssphäre quantifiziert, gibt Aufschluss über die sterische Abschirmung des Metallzentrums durch den Liganden.^[134,135]

⁹ Die in dieser Arbeit bevorzugte Heterokumulennotation (c) ist der Übersichtlichkeit geschuldet und bildet, analog zur formalen Doppelbindung in (Imino-)Phosphoranen (siehe Exkurs: Negative Hyperkonjugation, S. 8), weder die tatsächliche Bindungssituation innerhalb der P-C-P-Funktion, noch deren Geometrie ab.

¹⁰ Ursprünglich als Wellenzahl der A_1 -Carbonylstreckschwingung von Phosphannickeltri(carbonyl)komplexen definiert, werden mittlerweile auch Carbonylkomplexe des Rhodiums und Iridiums verwendet.^[129,130]

¹¹ Dieser willkürlich gewählte Wert entspricht der gemittelten Bindungslänge zwischen Übergangsmetallen und Phosphanliganden.^[131]

¹² Für asymmetrische Phosphane wird der Kegelwinkel aus den Halbkegelwinkel $\theta_i/2$ der einzelnen Substituenten gemäß $\theta = 2/3 \sum \theta_i/2$ berechnet.^[131]

1 Einleitung

Seltene Vertreter für Phosphorsuperbasen sind VERKADES Proazaphosphatrane, welche einen Bicyclus mit einem Stickstoff- und einem Phosphoratom als Brückenkopfatom darstellen. Bei Protonierung am Phosphoratom wird die resultierende positive Ladung sowohl durch negative Hyperkonjugation der NR-Donorgruppen als auch über eine unter Käfigkontraktion ausgebildete transannuläre dative N→P-Bindung stabilisiert (Abbildung 1.7).^[136] Durch diese stabilisierende Wechselwirkung wird eine PA von $261.0 \text{ kcal}\cdot\text{mol}^{-1}$ ^[137] und ein $\text{p}K_{\text{BH}^+}$ -Wert von 32.9 (MeCN) erzielt.^[17] SCHMUTZLER *et al.* versuchten in den 1990ern das mit einer PA von $278.8 \text{ kcal}\cdot\text{mol}^{-1}$ ^[137] potentiell sehr basische Tris(tetramethylguanidino)phosphan ($\text{P}(\text{tmg})_3$) zu synthetisieren, konnten jedoch lediglich die P-protonierte Form isolieren, da sämtliche Deprotonierungsversuche zur Zersetzung führten.^[138] Das Problem des Guanidinerfalls wurde 2017 von DIELMANN *et al.* gelöst indem strukturell verwandte Imidazolin-2-ylidenamino-Substituenten verwendet wurden. Der damit erreichte $\text{p}K_{\text{BH}^+}$ -Wert des Tris(imidazolin-2-ylidenamino)phosphans $\text{P}(\text{NI}i\text{Pr})_3$ liegt bei 31.0 (THF) und 40.3 (MeCN).^[139] Das zur SCHWESINGER-Base $(\text{dma})\text{P}_4\text{-}t\text{Bu}$ analoge Tris[tris(dimethylamino)phosphazeny]phosphan $((\text{dma})\text{P}_3\text{P})$ wurde bereits 1984 von KIRSANOV *et al.* aus Phosphortrichlorid und Tris(dimethylamino)phosphazenen synthetisiert.^[140] Für die Freisetzung des Phosphans aus der zunächst isolierten P-protonierten Form konnte kein anderer Weg als ein Anionenaustausch des Chlorids gegen Hydroxid mittels Silberoxid und anschließender Vakuumdehydratation der wässrigen Lösung gefunden werden. Obwohl die berechnete PA von $295.5 \text{ kcal}\cdot\text{mol}^{-1}$ ^[137] sogar die von $(\text{dma})\text{P}_4\text{-}t\text{Bu}$ ($280.0 \text{ kcal}\cdot\text{mol}^{-1}$)^[100] übersteigt, sind bislang keine experimentellen Untersuchungen zur Quantifizierung der Basizität dieser Verbindung literaturbekannt. Zu KIRSANOVs Phosphazenyphosphanen analoge, ylidverbrückte $\text{P}^{\text{III}}/\text{P}^{\text{V}}$ -Verbindungen wurden bereits 1970 von ISSLEIB synthetisiert.^[141] Diese scheinen jedoch aus den in Kapitel 1.3 (S. 12) erörterten Gründen nicht signifikant basischer zu sein als ihre Ausgangsverbindung, die Ylidbase $(\text{dma})_3\text{P}=\text{CH}_2$.

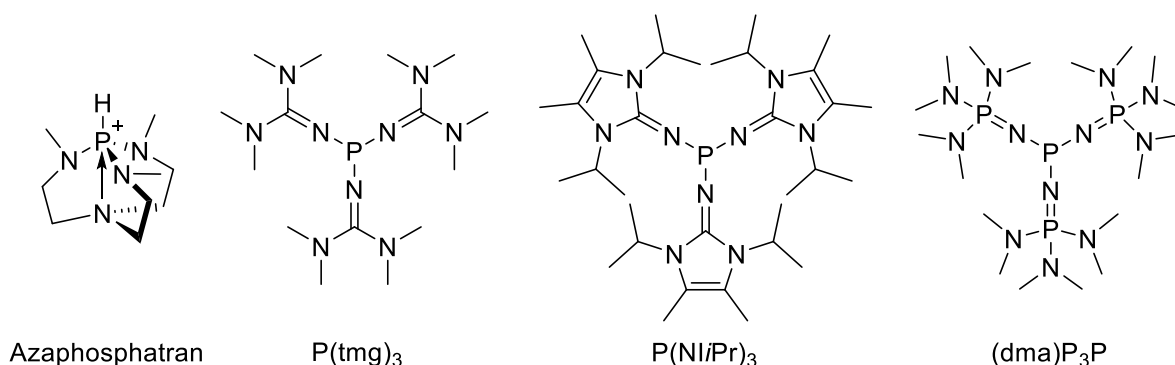


Abbildung 1.7: Kontraktion des tripodalen Käfigs durch Ausbildung einer transannulären, dativen Wechselwirkung im Azaphosphatran sowie Strukturen der (potentiellen) Phosphorsuperbasen $\text{P}(\text{tmg})_3$, $\text{P}(\text{NI}i\text{Pr})_3$ und $(\text{dma})\text{P}_3\text{P}$.

GESSNER *et al.* konnten 2018 zeigen, dass strukturell verwandte ylidfunktionalisierte Phosphane (YPhos), obwohl am Ylidkohlenstoffatom basischer als am Phosphor(III)atom, starke P-Donorliganden in der Übergangsmetallkatalyse darstellen. In Gold(I)komplexen haben sie Anwendung in der katalytischen Aktivierung von Alkinen, bei der der Goldkatalysator als π -Säure an die Dreifachbindung der Alkine koordiniert und diese für Nucleophile angreifbar macht. Dies wurde bereits erfolgreich in der Hydroaminierung und Hydratisierung sowie der Cyclisierung zu Lactonen und Cyclobutenen angewendet.^[142] Auch DIELMANNs IAPs wurden bereits in der goldkatalysierten Hydroaminierung von Acetylen getestet.^[143] Die in Abbildung 1.8 gezeigten Phosphane mit superbasischen Substituenten ermöglichen es durch ihren Donorcharakter, das Redoxpotential von Palladiumkatalysatoren soweit herabzusenken, dass sie in der Lage sind, oxidativ in die C–Cl-Bindung von (Hetero-)Aryl- und Vinylchloriden zu addieren und diese so für SUZUKI- und HARTWIG-BUCHWALD-Kupplungen einsetzbar zu machen.^[144–147]

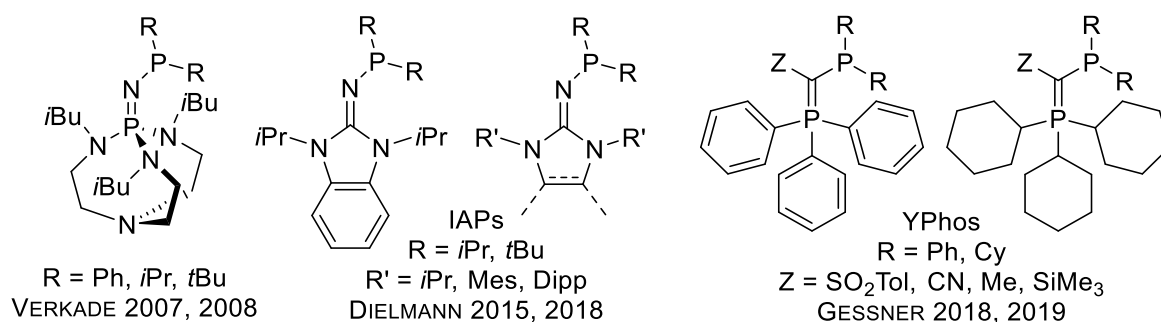


Abbildung 1.8: Strukturen elektronenreicher Phosphanliganden für die Übergangsmetallkatalyse.^[142–147]

Da bis 2017 VERKADES Proazaphosphatraner die stärksten bekannten Phosphor(III)superbasen waren, sind Anwendungen, bei denen Phosphane tatsächlich als Basen eingesetzt wurden, bislang auf diese Verbindungsklasse beschränkt. Beispiele sind die Trimerisierung von Isocyanaten,^[148] die Acylierung sterisch gehinderter Alkohole,^[149] die Dehalogenierung zu Olefinen,^[150] die HENRY-Reaktion^[151], die STRECKER-Reaktion,^[152] die MICHAEL-Addition,^[153] oder die Addition von Alkoholen und Aminen an Carbonylverbindungen.^[154] Auch als Organokatalysator zur (De-)Silylierung kamen Proazaphosphatraner zum Einsatz.^[155] KIRSANOVs (dma) P_3P wurde als Katalysator für die anionische Polymerisation von Epoxiden^[156] und korrespondierende Phosphazide als Organokatalysator für die Aktivierung silylgeschützter Nucleophile patentiert,^[157] Eingang in die Fachliteratur haben diese Anwendungen jedoch nicht gefunden. DIELMANN *et al.* nutzen ihre IAPs neben der Übergangsmetallkatalyse, auch zur Aktivierung kleiner Moleküle, wie Kohlenstoffdioxid,^[158] Schwefeldioxid^[159] oder gar Schwefelhexafluorid.^[160] Bei letzterem wird eine Fluoridabstraktion über einen $\text{S}_{\text{N}}2$ -Mechanismus postuliert, welcher niedrigere Barrieren

1 Einleitung

aufweist, als ein radikalischer Mechanismus. Der Terminus der Aktivierung ist dabei infrage zu stellen, da es sich stets um irreversible Reaktion handelt und die gebildeten Produkte bislang noch nicht zu einer weiteren Funktionalisierung genutzt werden können. Tabelle 1.1 stellt abschließend sterische und elektronische Parameter einiger vorgestellter Liganden zur Übersicht gegenüber.

Tabelle 1.1: Sterische und elektronische Parameter bekannter Liganden.

	TEP/cm ⁻¹	Kegelwinkel/°	%V _{bur} ^[a]	¹ J _{PSe} /Hz	pK _{BH} ⁺ (MeCN)
PPh ₃	2068.9 ^[131]	145 ^[131]	29.9 ^[161]	731 ^[128]	7.64 ^[162]
Proazaphosphatran ^[b]	2057.0 ^[163]	152 ^[163]	-	754 ^[164]	32.9 ^[17]
P(<i>t</i> Bu) ₃	2056.1 ^[131]	182 ^[131]	40.0 ^[129]	687 ^[128]	-
Y ₃ PCy ₂ ^[c]	2055.1 ^[142]	-	54.3 ^[142]	-	-
P(Ad) ₃ ^[d]	2052.1 ^[129]	179 ^[129]	40.5 ^[129]	670 ^[129]	-
NHC-IMes ^[e]	2050.7 ^[165]	-	31.6 ^[134]	-	-
(Ph) ₆ -CDP	2032 ^[166]	-	-	-	-
P(NiPr) ₃	2029.7 ^[139]	182 ^[139]	38.7 ^[139]	-	40.3 ^[139]

[a] aus den LAuCl-Komplexen bestimmt; [b] P[N(CH₃)CH₂CH₂]₃N; [c] Ph₃P=C(SO₂Tol)-P(Cy)₂; [d] Ad = Adamantyl; [e] 1,3-Dimesitylimidazol-2-ylidene.

Anders als Stickstoff- und Kohlenstoffprotonenschwämme, können 1,8-Bis(phosphan)-naphthalinderivate, wie sie bereits mit Methyl-, Phenyl-, Cyclohexyl-,^[167] Dimethylamino-^[168] und Methoxysubstituenten^[169] synthetisiert wurden, weder von einer IHB, noch von einem raschen Protonenaustausch profitieren. Zum einen können Phosphane zwar ähnlich gute Wasserstoffbrückenakzeptoren wie Amine sein, aufgrund der nur schwach polarisierten P-H-Bindung aber nur schlechte Wasserstoffbrückendonoren, weshalb der Energiegewinn durch eine IHB nur marginal ist (Abbildung 1.9). Zum anderen liegt der optimale P-P-Abstand für eine IHB durch den größeren VAN-DER-WAALS-Radius der Phosphoratome im Vergleich zu Elementen der zweiten Periode¹³ um 4.0 Å, weshalb es in der Molekülstruktur der konjugierten Säure des 1,8-Bis(phosphanyl)naphthalins sogar zu einer stärkeren Verzerrung im Molekül kommt als in der freien Basenform und sich das freie Elektronenpaar der PH₂-Gruppe zwischen zwei Protonen der PH₃⁺-Gruppe orientiert (Abbildung 1.10 (a)).^[171] Ein schneller intramolekularer Protonenaustausch konnte durch grundliniengetrennte Signale für die PH₂- und die PH₃⁺-Gruppe in ¹H- und ³¹P-NMR-Spektren ausgeschlossen werden.^[171] Anders als das Proton, werden Hauptgruppenelemente und Übergangsmetalle durchaus chelatisiert. So konnten neben klassischen Palladium(II)- und Platin(II)bisphosphankomplexen^[167] auch ein Bis(phospha)boroniumkation^[172] (b) oder ein Triphospheniumkation^[173] (c) erhalten werden.

¹³ VAN-DER-WAALS-Radien von Kohlenstoff: 1.70 Å; Stickstoff: 1.55 Å; Phosphor: 1.80 Å.^[170]

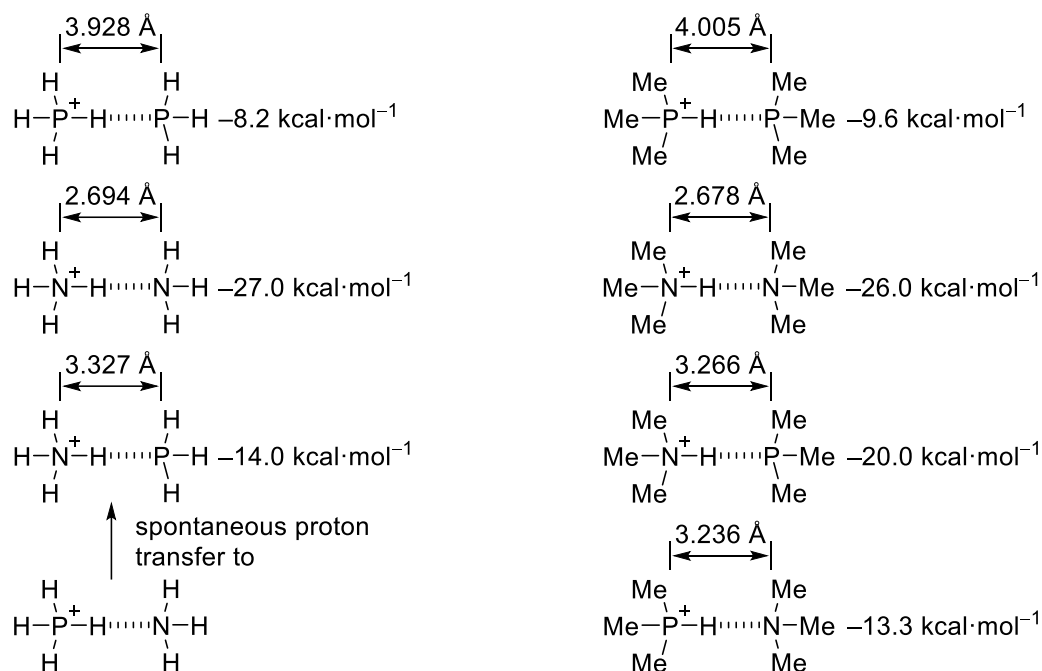


Abbildung 1.9: Vergleich von Energien und Abständen intermolekularer Wasserstoffbrückenbindungen zwischen Aminen und Phosphanen. Persönliche Kommunikation von BORISLAV KOVAČEVIĆ.^[174]

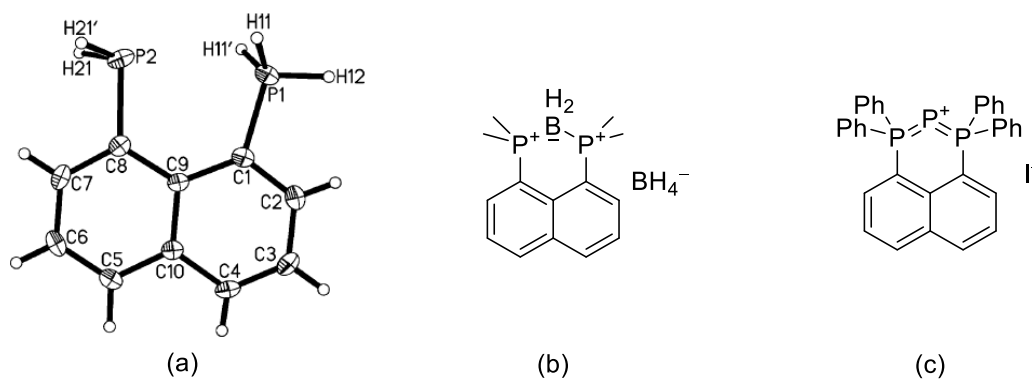
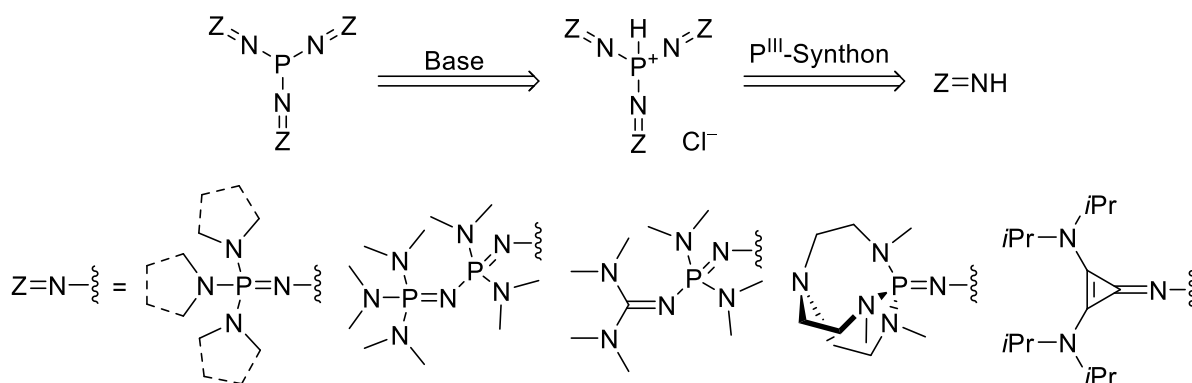


Abbildung 1.10: Im Kristall vorliegende Kationenstruktur der konjugierten Säure des 1,8-Bis(phosphanyl)naphthalins (a) (Ref.^[171] entnommen) sowie die LEWIS-Strukturen des Bis(phospha)boronium-tetrahydridoborats^[172] (b) und Triphospheniumiodids^[173] (c).

2 Aufgabenstellung

„Mein Ziel ist schneller, höher, weiter – denn ich bin lieber tot als Zweiter“;¹⁴ getreu diesem Motto war es das übergeordnete Ziel dieser Arbeit, mit ungeladenen Phosphor-, Kohlenstoff- und Stickstoffsuperbasen die obersten Sprossen der Basizitätsleiter zu erklimmen. Dazu sollten neue superbasische Phosphane, Carbodiphosphorane und Phosphazene entwickelt und hinsichtlich ihrer BRØNSTED- und LEWIS-Basizität untersucht werden.

Grundlage bildeten KIRSANOVs Tris[tris(dimethylamino)phosphazeny]phosphan^[140] (dma)P₃P und vorangehende Ergebnisse der eigenen Masterarbeit, in welcher die Superbase Tris[tris(pyrrolidino)phosphazeny]phosphan (pyrr)P₃P erstmalig dargestellt und eine verbesserte Synthese derartiger Phosphor(III)verbindungen entwickelt wurde.^[175] Darauf aufbauend sollten Phosphane mit verschiedenen, in Schema 2.1 gezeigten, superbasischen Substituenten synthetisiert und charakterisiert werden, um die Struktur-Eigenschafts-Beziehung der bislang weniger untersuchten Klasse der Phosphorsuperbasen besser zu verstehen. Neben der Quantifizierung des Elektronendonorcharakters dieser Verbindungen über die experimentelle bzw. theoretische Bestimmung von pK_{BH}⁺-Werten, Protonenaffinitäten, Gasphasenbasizitäten, TOLMANS elektronischem Parameter und ¹J_{PSe}-Kopplungskonstanten, sollten Reaktivitätsstudien gegenüber Alkylierungsmitteln und Metallkomplexen durchgeführt werden, um potentielle Anwendungsgebiete zu identifizieren.

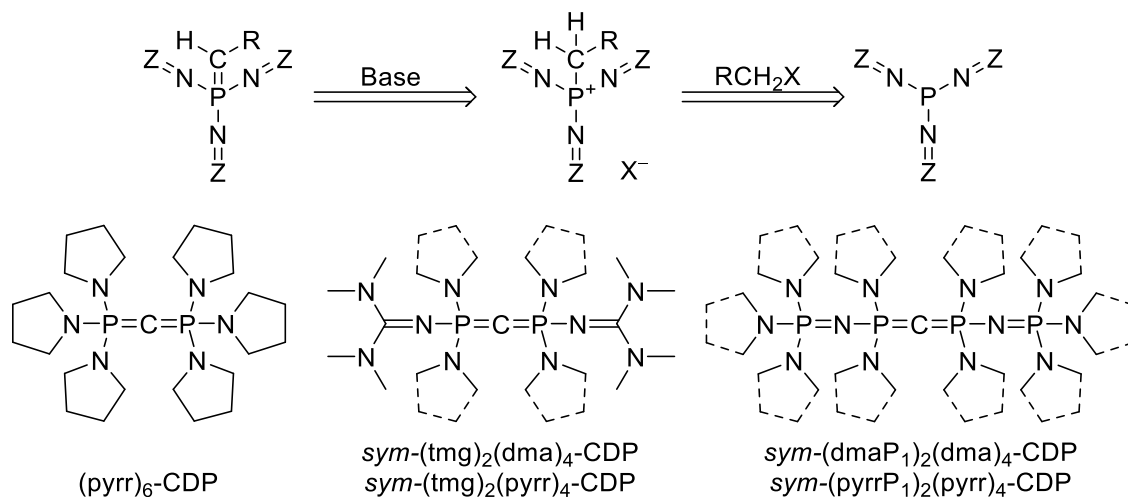


Schema 2.1: Retrosynthetischer Ansatz zur Darstellung potentiell superbasischer Phosphane.

Die durch Alkylierung der untersuchten superbasischen Phosphane erhaltenen Alkylphosphoniumsalze sollen dabei selbst als Präkursoren für superbasische Phosphorylide höherer Ordnung fungieren (Schema 2.2, oben). Um diese bislang noch nicht synthetisierten Kohlenstoffsuperbasen zugänglich zu machen sollte ein allgemeingültiges Deprotonierungsprotokoll entwickelt werden. Neben derartigen Monoyliden lag der Fokus auf potentiell noch basischeren Bisyliden. Da Carbodiphosphorane (CDPs) bislang nur theoretisch als Superbasen

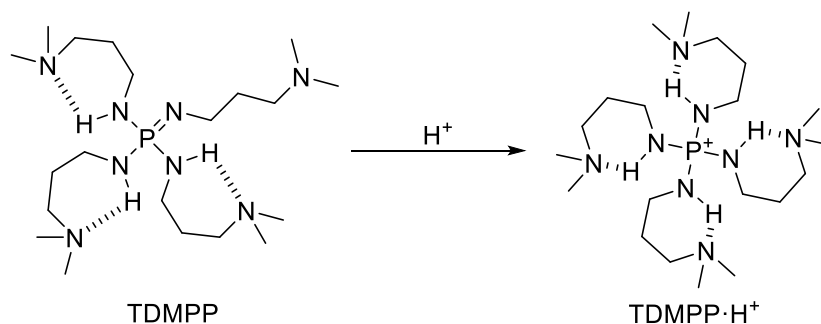
¹⁴ Aus *Testosteron* von RÜDIGER HOFFMANN.

untersucht wurden, sollten neue Vertreter dieser Verbindungsklasse synthetisiert und in der Basizitätsskala etabliert werden. Sowohl für das in theoretischen Untersuchungen bislang basischste (pyrr)₆-CDP als auch für Carbodiphosphoransuperbasen zweiter Ordnung, welche formal Phosphane mit einem superbasischen Substituenten inkorporieren (Schema 2.2, unten), sollte eine geeignete Synthesevorschrift entwickelt werden, weitere Erkenntnisse zu sterischen und elektronischen Eigenschaften gewonnen und erstmalig pK_{BH^+} -Werte von CDPs ermittelt werden.



Schema 2.2: Retrosynthetischer Ansatz zur Darstellung superbasischer Monoylide höherer Ordnung (oben) sowie die Zielmolekülstrukturen superbasischer CDPs erster und zweiter Ordnung (unten).

In Form des *N,N',N'',N'''*-Tetrakis(3-dimethylaminopropyl)triaminophosphazens (TDMPP) sollte abschließend auch ein neuartiger Vertreter der breit aufgestellten Klasse von Stickstoffsuperbasen entwickelt werden. Dieses kombiniert erstmalig die hohe intrinsische Basizität von Phosphazenen mit dem basizitätsverstärkenden Effekt multipler intramolekularer Wasserstoffbrückenbindungen (IHBs) (Schema 2.3). Eine geeignete Syntheseroute sollte entwickelt und die Existenz und Stärke des Korona-Effektes sowohl in Lösung als auch im Festkörper untersucht werden.



Schema 2.3: Die Protonierung von TDMPP soll zur Ausbildung einer vierten IHB unter Verkürzung und Stärkung aller im Molekül vorhandenen IHBs führen.

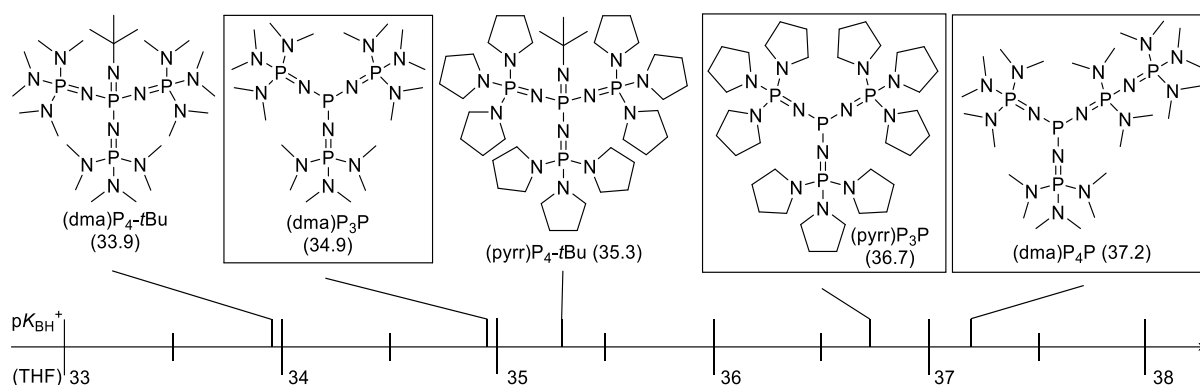
3 Kumulativer Teil

3.1 Phosphazenyolphosphate PAP: Die elektronenreichsten ungeladenen BRØNSTED- und LEWIS-Phosphor-Basen

Angew. Chem. Int. Ed. **2019**, *58*, 10335; *Angew. Chem.* **2019**, *131*, 10443.

Phosphazenyolphosphate PAP: The most electron rich uncharged phosphorus Brønsted and Lewis bases

Sebastian Ullrich, Borislav Kovačević, Xiulan Xie, Jörg Sundermeyer



Phosphorbasen können stärkere Protonenakzeptoren sein als Stickstoffbasen, dies ist die Kernaussage dieser Publikation. Ausgehend von KIRSANOVs ersten einfachen Vertretern von Phosphazenyolphosphaten und den Ergebnissen der eigenen Masterarbeit, wurden einfache Synthesevorschriften für die P-protonierten Phosphoniumsalze der Superbasen $(dma)P_3P$ und $(pyrr)P_3P$ entwickelt und gute bis quantitative Ausbeuten erzielt. Weiterhin wurde SCHWESINGERS Konzept der Homologisierung angewandt und die Verbindungen $(dma)P_4P \cdot HBF_4$ und $(dma)P_6P \cdot HBF_4$ erstmalig dargestellt und charakterisiert. Von allen vier Salzen wurden die im Kristall vorliegenden Molekülstrukturen erhalten, wodurch ein Einblick in die effiziente Delokalisierung der positiven Ladung mittels negativer Hyperkonjugation gewonnen wurde. Durch Deprotonierung mit Kaliumhexamethyldisilazan konnten die freien Phosphazenyolphosphate (PAP) erstmalig als farblose Feststoffe erhalten und ihre Reinheit mittels Elementaranalyse bestätigt werden. Einzig die Isolierung von $(dma)P_6P$ war nicht möglich. Diese außerordentlich starke Base konnte lediglich mit Kaliumpyrrolidid *in situ* freigesetzt werden und mittels ^{31}P -NMR-Spektroskopie und Folgereaktionen nachgewiesen werden. Die BRØNSTED-Basizität wurde sowohl über experimentelle pK_{BH^+} -Werte (THF), bestimmt durch NMR-Titration gegen SCHWESINGERS $(dma)P_4-tBu$ und $(pyrr)P_4-tBu$, als auch

durch kalkulierte pK_{BH^+} -Werte, Protonenaffinitäten und Gasphasenbasizitäten quantifiziert. Dabei stellten sich die Phosphane sowohl in der Gasphase, wie auch in Lösung als stärkere Basen denn ihre korrespondierenden Phosphazene heraus. Für (dma) P_6P wurde ein sehr hoher pK_{BH^+} -Wert von 41.9 (THF) berechnet. Der hohen thermodynamischen Basizität von PAPs steht ein kinetisch gehemmter Protonenaustausch gegenüber, dessen Barriere ebenfalls experimentell und theoretisch bestimmt wurde. Die LEWIS-Basizität wurde durch Reaktion mit Tetracarbonylnickel oder Oxidation mit grauem Selen als TEP und $^1J_{\text{PSe}}$ -Kopplungskonstante quantifiziert. Diese folgen dem Trend der BRØNSTED-Basizität und sind die niedrigsten für Phosphane bekannten Werte. Zusammen mit berechneten Kegelwinkeln von über 200° kombinieren PAPs sowohl elektronische als auch sterische Eigenschaften, wie sie in der Übergangsmetallkatalyse von großem Wert sind. Als Beispiel hierzu wurden lineare, heteroleptische 14-Valenzelektronen- Pt^0 -Komplexe synthetisiert. Die selektive Darstellung sowohl ausgehend von Pt^{II} - als auch von Pt^0 -Präkursoren verdeutlicht neben der hohen Basizität auch ein starkes Reduktionspotential. Auch im Platinkomplex wurden die Donoreigenschaften mittels ^{31}P - und ^{195}Pt -NMR-Spektroskopie sowie der Röntgenstrukturanalyse untersucht. Es konnten sehr hohe $^1J_{\text{PPt}}$ -Kopplungskonstanten und niedrige chemische ^{195}Pt -Verschiebungen detektiert werden, welche den reinen und starken σ -Donorcharakter der PAPs untermauern. Mit den präsentierten Phosphanen konnten nicht nur neue Phosphor(III)superbasen der von Stickstoff und Kohlenstoff dominierten Basizitätsskala hinzugefügt werden, diese konnten sogar die lange Zeit dominanten SCHWESINGER-Basen an der Spitze ablösen.

Erklärung der Eigenleistung

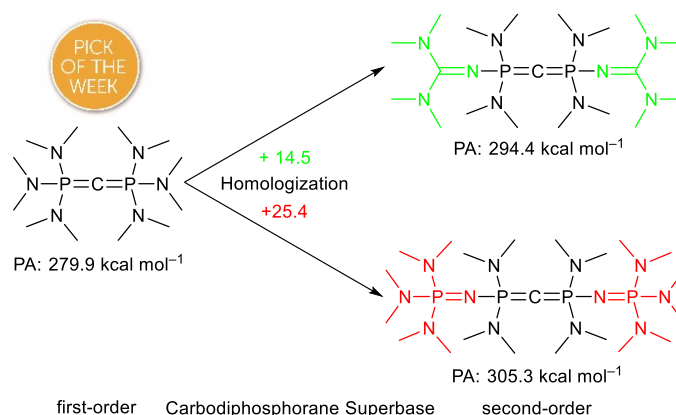
Sämtliche präparativen Arbeiten und die Auswertung der in den Serviceabteilungen des Fachbereichs aufgenommenen NMR-Spektren, Massenspektren, elementaranalytischen Daten und Einkristall-Röntgendiffraktogramme wurden von mir persönlich durchgeführt. ^{31}P -NMR-Spektren zur pK_{BH^+} -Bestimmung wurden von XIULAN XIE mit optimierten Relaxationszeiten und einem extra für die untersuchte Verbindungsklasse geschriebenen Parametersatz aufgenommen. Auch die Messungen und Auswertungen zum Protonenselbstaustausch erfolgten durch XIE. DFT-Kalkulationen wurden von BORISLAV KOVAČEVIĆ durchgeführt und ausgewertet. Das Manuskript und die *supporting information* wurden, mit Ausnahme der *theoretical section*, welche von KOVAČEVIĆ geschrieben wurde, von mir verfasst. Auch die Übersetzung des englischen Manuskriptes ins Deutsche erfolgte in Eigenregie. Mit meinem Betreuer JÖRG SUNDERMEYER wurden die wissenschaftliche Fragestellung und die Ergebnisse intensiv diskutiert.

3.2 Design nicht-ionischer Kohlenstoffsuperbasen: Carbodiphosphorane der zweiten Generation

Chem. Sci. **2019**, *10*, 9483.

Design of Non-Ionic Carbon Superbases: Second Generation Carbodiphosphoranes

Sebastian Ullrich, Borislav Kovačević, Björn Koch, Klaus Harms, Jörg Sundermeyer



Mit Carbodiphosphoranen (CDPs) eine neue Klasse von Kohlenstoffsuperbasen zu etablieren war das Ziel dieser Publikation. Ein synthetischer Zugang zum CDP erster Ordnung (pyrr)₆-CDP sowie den CDPs zweiter Ordnung *sym*-(tmg)₂(dma)₄-CDP und *sym*-(dmaP₁)₂(dma)₄-CDP wurde entwickelt. Bei letzterem konnte anstelle der Deprotonierung ein Zersetzungsmechanismus aufgeklärt werden, der eine potentielle Obergrenze der Stabilität phosphazenyhlaltiger Superbasen darstellt. Die NMR-spektroskopischen und XRD-strukturellen Charakteristika sowohl der freien Basen als auch der konjugierten Säuren wurden untersucht und erstmalig theoretische wie auch experimentelle pK_{BH}^+ -Werte für CDPs ermittelt. Diese bestätigen die herausragende Eignung von CDPs als nicht-ionische Superbasen und übertreffen bei deutlich geringerem Molekulargewicht sogar die Basizität der stärksten kommerziell erhältlichen ungeladenen Superbase (dma)P₄-*t*Bu.

Erklärung der Eigenleistung

Das Manuskript und die *supporting information* wurden, mit Ausnahme der *theoretical section*, die von BORISLAV KOVAČEVIĆ geschrieben wurde, von mir persönlich verfasst. Die Synthese und Charakterisierung der bisprotonierten und der freien CDPs erfolgte durch BJÖRN KOCH im Rahmen seiner unter meiner fachlichen und praktischen Anleitung angefertigten

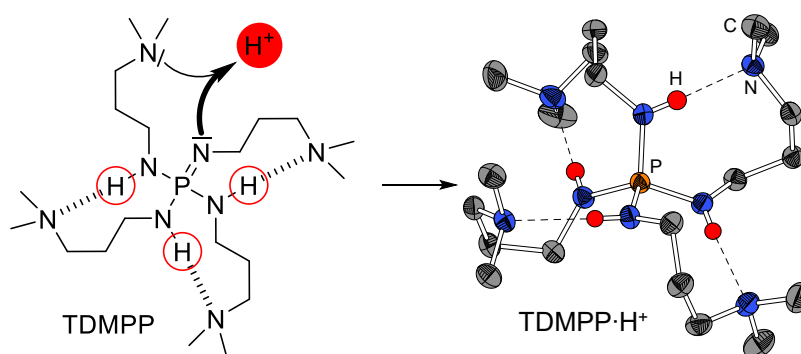
Bachelorarbeit.^[176] Die Synthese und Charakterisierung der monoprotonierten CDPs sowie die Aufklärung des Zersetzungsmechanismus von *sym*-(dmaP₁)₂(dma)₄-CDP wurden von mir durchgeführt. Auch die Auswertung der NMR-Titrationen zur p*K*_{BH}⁺-Bestimmung erfolgte in Eigenregie. Sämtliche XRD-Strukturen wurden, mit Ausnahme der Struktur von *sym*-(dmaP₁)₂(dma)₄-CDP·2HBF₄, welche durch KLAUS HARMS bearbeitet wurde, von mir gelöst und verfeinert. DFT-Kalkulationen wurden von KOVAČEVIĆ durchgeführt und ausgewertet. Mit meinem Betreuer JÖRG SUNDERMEYER wurden die wissenschaftliche Fragestellung und die Ergebnisse intensiv diskutiert.

3.3 Basizitätsverstärkung durch multiple intramolekulare Wasserstoffbrückenbindungen in der Organosuperbase *N,N',N'',N'''*-Tetrakis(3-dimethylaminopropyl)triaminophosphazen

Org. Lett. **2019**, DOI: 10.1021/acs.orglett.9b03521.

Basicity Enhancement by Multiple Intramolecular Hydrogen Bonding in Organic Superbase *N,N',N'',N'''*-Tetrakis(3-(dimethylamino)propyl)-triaminophosphazene

Sebastian Ullrich, Danijela Barić, Borislav Kovačević, Xiulan Xie, Jörg Sundermeyer



Mit der Synthese von *N,N',N'',N'''*-Tetrakis(3-dimethylaminopropyl)triaminophosphazen (TDMPP) wurde erstmalig eine ungeladene Stickstoffsuperbase präsentiert, deren intrinsisch hohe Basizität des Phosphazenmotivs durch den multiplen Korona-Effekt, den Ringschluss von Alkylketten durch intramolekulare Wasserstoffbrückenbindungen (IHBs), verstärkt wird. Die Einkristall-Röntgenstrukturanalyse der konjugierten Säure, temperaturabhängige NMR-Studien sowie theoretische Untersuchungen bestätigen die Existenz mehrfacher intra-

3 Kumulativer Teil

molekularer Wasserstoffbrückenbindungen und geben einen detaillierten Einblick zu deren Einfluss auf die Basizität im Festkörper, in Lösung und in der Gasphase. Der pK_{BH^+} -Wert wurde sowohl in THF (22.4) als auch in Acetonitril (30.4) experimentell ermittelt und stimmt gut mit den berechneten Werten überein (21.6 in THF bzw. 30.6 in MeCN). TDMPP ist damit die stärkste Stickstoffsuperbase erster Ordnung.

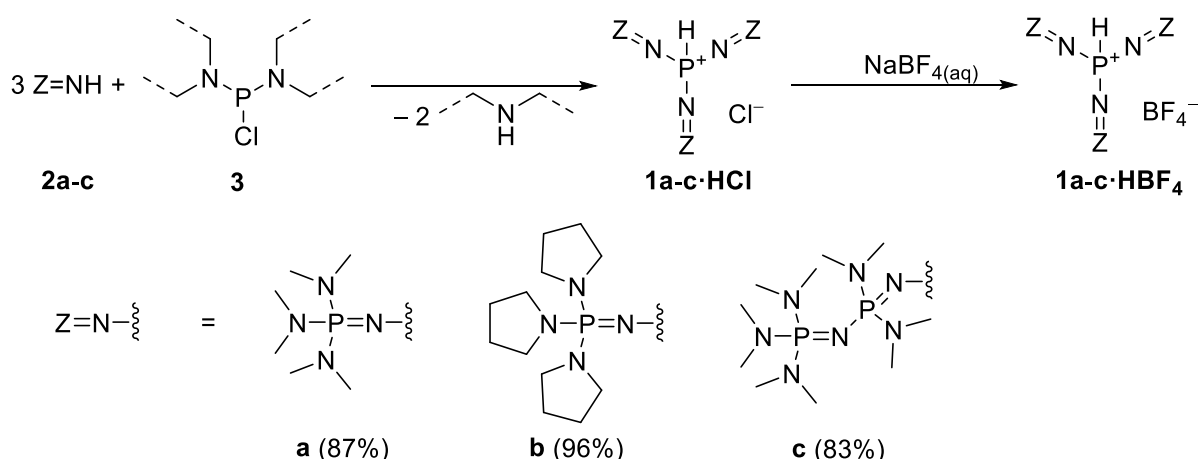
Erklärung der Eigenleistung

Sämtliche präparativen Arbeiten und die Auswertung der in den Serviceabteilungen des Fachbereichs aufgenommenen NMR-Spektren, Massenspektren, elementaranalytischen Daten und Einkristall-Röntgendiffraktogramme wurden von mir persönlich durchgeführt. ^{31}P -NMR-Spektren zur pK_{BH^+} -Bestimmung wurden von XIULAN XIE mit optimierten Relaxationszeiten und einem extra für die untersuchte Verbindungsklasse geschriebenen Parametersatz aufgenommen. DFT-Kalkulationen wurden von DANIJELA BARIĆ und BORISLAV KOVAČEVIĆ durchgeführt und ausgewertet. Das Manuskript und die *supporting information* wurden, mit Ausnahme der *theoretical section*, welche von BARIĆ und KOVAČEVIĆ geschrieben wurde, von mir verfasst. Mit meinem Betreuer JÖRG SUNDERMEYER wurden die wissenschaftliche Fragestellung und die Ergebnisse intensiv diskutiert.

4 Zusammenfassung

4.1 Beiträge zur Chemie superbasischer Phosphate

Über die Amineliminierung (Schema 4.1) konnte eine elegante Synthese P-protonierter Phosphoniumsalze (**1·HX**) mit superbasischen Substituenten entwickelt werden. Diese senkt die notwendigen Äquivalente des eingesetzten Nucleophils (**2**) im Vergleich zur Standardsynthese mit Phosphortrichlorid herab, weist lediglich flüchtige Amine als Nebenprodukt auf, vermeidet die aufwendige Trennung von Ammonium- und Phosphoniumsalzen und erzielt eine nahezu quantitative Ausbeute und hohe Reinheit. Da sich die erhaltenen Hydrochloride zwar als luft- und wasserstabil jedoch hygroskopisch herausstellten, wurden diese zu Lagerungszwecken durch Fällung aus wässriger Lösung in die Tetrafluoridoborate überführt. Über diese Reaktionsführung konnten die drei Superbasenvorläufer (dma)₃P·HBF₄ (**1a·HBF₄**), (pyrr)₃P·HBF₄ (**1b·HBF₄**) und (dma)₆P·HBF₄ (**1c·HBF₄**) als farblose Feststoffe erhalten werden.

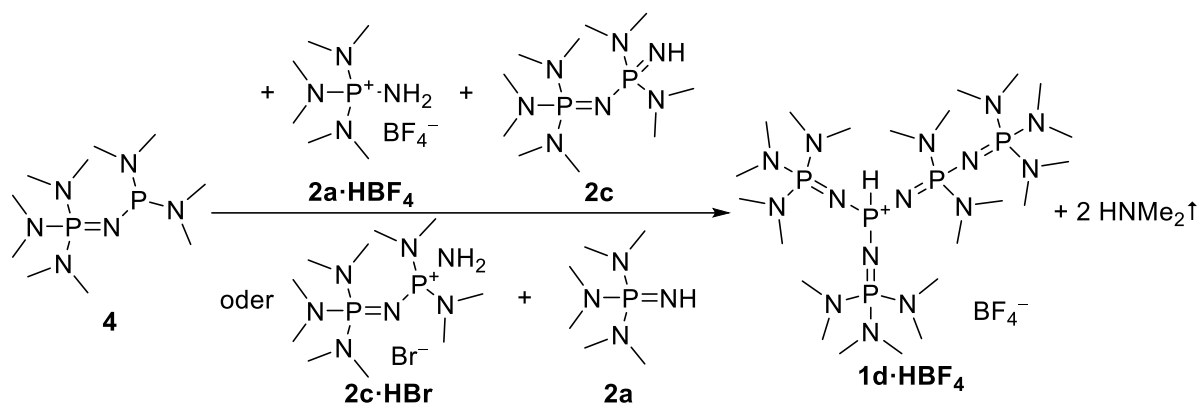


Schema 4.1: Synthese der Phosphoniumsalze **1·HCl** bzw. **1·HBF₄** über die Amineliminierung. Die angegebene Ausbeute ist auf die Produkte **1a·c·HBF₄** bezogen.

Für die Synthese des Diphosphazens **2c** wurde im Rahmen dieser Arbeit eine alternative Syntheseroute entwickelt. Anstelle einer Sauerstoff-Chlor-Substitution im Phosphanoxid (dma)₃P=N–P(dma)₂=O mit Phosphorylchlorid und anschließender Ammonolyse wie von SCHWESINGER *et al.* beschrieben,^[19] erfolgte die Darstellung erstmalig in einer Eintopfsynthese über die Bromierung und Ammonolyse des Monophosphazenyolphosphans **4**. Diese Syntheseroute verringert nicht nur die Anzahl der notwendigen Reaktionsschritte, sondern beinhaltet auch **4** als Zwischenprodukt. Dieses stellte sich als adäquates Edukt für die Darstellung des asymmetrischen (dma)₄P·HBF₄ (**1d·HBF₄**) heraus, welches zwei Monophosphazen- und einen Diphosphazensubstituenten inkorporiert (Schema 4.2). Der gemischtvalente P^{III}/P^V-Präkursor **4** reagiert nur mit den protonierten Formen **2a·HBF₄** oder **2c·HBr** und nicht mit deren freien

4 Zusammenfassung

Phosphazenen (**2a** oder **2c**). Die freien Basenformen reagieren hingegen selektiv mit dem intermediär gebildeten P-protonierten Phosphoniumsalz und bilden so **1d·HBF₄** unabhängig davon, welches Phosphazen in seiner freien oder protonierten Form vorliegt.



Schema 4.2: Darstellung von **1d·HBF₄**: Zuerst **4** und **2a·HBF₄** oder **2c·HBr**, dann **2c** bzw. **2a**, 94% Ausbeute. Bei Verwendung von **2c·HBr** folgt noch ein Anionenaustausch mit NaBF₄ aus wässriger Lösung.

Abbildung 4.1 zeigt die über Einkristall-Röntgendiffraktometrie (XRD) erhaltenen Strukturen der Phosphoniumkationen mit dem aciden Proton stets am zentralen Phosphoratom lokalisiert. Innerhalb der P–N=P–Einheiten sind die formalen Einfachbindungen mit durchschnittlichen 1.60 Å deutlich verkürzt und an die formalen Doppelbindungen (1.57 Å) angeglichen, die Winkel sind auf 129.0 bis 157.7° aufgeweitet. Dimethylaminosubstituenten zeigen durchschnittliche P–N-Abstände von 1.65 Å für terminale und 1.67 Å in verbrückenden Phosphazenygruppen. Pyrrolidinsubstituenten weisen Bindungslängen von 1.64 Å auf. Diese kurzen P–N-Bindungen zeigen die effiziente Delokalisierung der positiven Ladung durch negativ hyperkonjugative Wechselwirkungen über das gesamte Heteroatomgrundgerüst.

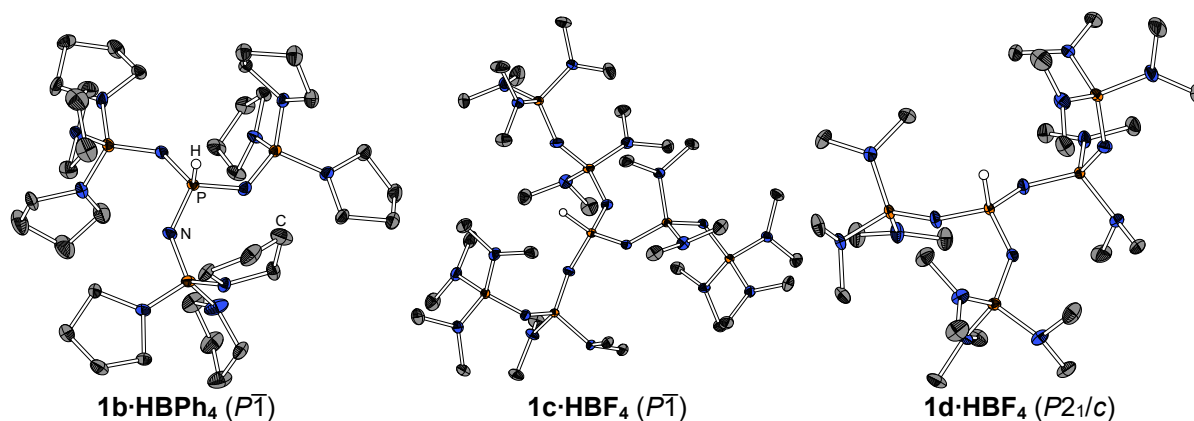


Abbildung 4.1: Im Kristall vorliegende Molekülstrukturen von (pyrr)₃P·HBPh₄ (**1b·HBPh₄**), (dma)₆P·HBF₄ (**1c·HBF₄**) und (dma)₄P·HBF₄ (**1d·HBF₄**). Für die XRD-Struktur von (dma)₃P·HBPh₄ (**1a·HBPh₄**, P_{21/n}) sei auf den kristallographischen Anhang verwiesen.¹⁵

¹⁵ Zur besseren Übersicht sind in dieser Arbeit mittels XRD erhaltene Molekülstrukturen ohne Anionen, kohlenstoffgebundene Wasserstoffatome (ausgenommen des zentralen Kohlenstoffatoms in protonierten CDPs), Fehlordinungen und nicht-kordinierende Lösungsmittelmoleküle dargestellt. Schwingungsellipsoide sind mit 50% Aufenthaltswahrscheinlichkeit abgebildet.

Die Freisetzung der Phosphazenyolphosphane (PAPs) (dma)P₃P (**1a**), (pyrr)P₃P (**1b**) und (dma)P₄P (**1d**) erfolgte durch Deprotonierung mit Kaliumhexamethyldisilazan (KHMDs) in sehr guten Ausbeuten von 87% (**1a**), 88% (**1b**) und 79% (**1d**). Lediglich die vermutlich stärkste ungeladene Superbase (dma)P₆P (**1c**) konnte bislang nicht isoliert werden, sondern wurde mit Kaliumpyrrolidid (Kpyrr) *in situ* generiert und mittels ³¹P-NMR-Spektroskopie sowie durch Folgereaktionen mit Tetracarbonylnickel oder grauem Selen nachgewiesen. Reduktive Bedingungen wie elementares Kalium in flüssigem Ammoniak oder Ethylendiamin führten aufgrund fehlender P–H-Bindungspolarisation zu keiner Reaktion, während Organolithiumbasen wie *n*- oder *tert*-Butyllithium zur teilweisen Zersetzung führten.

Um die Stärke von PAPs als BRØNSTED- und LEWIS-Basen quantifizieren zu können, wurden Protonenaffinitäten (PA), Gasphasenbasizitäten (GB), theoretische und experimentelle p*K*_{BH}⁺-Werte sowie TOLMANS elektronischer Parameter (TEP) aus den jeweiligen Nickeltricarbonylkomplexen und ¹J_{PSe}-Kopplungskonstanten korrespondierender Phosphanselenide ermittelt (Tabelle 4.1). Die p*K*_{BH}⁺-Werte in THF wurden über ³¹P-NMR-Titration gegen die SCHWESINGER-Basen (dma)P₄-*t*Bu (p*K*_{BH}⁺ in THF = 33.9)^[14] und (pyrr)P₄-*t*Bu (35.3)^[14] auf 34.9 (**1a**), 36.7 (**1b**) und 37.2 (**1d**) bestimmt. Diese sind nicht nur die für Phosphane höchsten bekannten p*K*_{BH}⁺-Werte, sie übersteigen sogar diejenigen ihrer korrespondierenden Phosphazenenbasen und sind damit neue Spitzenreiter der etablierten p*K*_{BH}⁺-Skala in THF. Aufgrund der geringen P–H-Bindungs-polarisation steht der hohen thermodynamischen Basizität ein kinetisch gehemmter Protonenaustausch gegenüber. Die über Austausch-NMR-Spektroskopie ermittelte Barriere liegt für **1a** bei 15.5 kcal·mol⁻¹ und für **1b** bei 16.5 kcal·mol⁻¹, was einer Austauschrate von 13 bzw. 3 Hz entspricht. Derart hohe Barrieren sind eher mit Protonenschwämmen vergleichbar als mit kinetisch aktiven Phosphazenen.^[15,19]

Tabelle 4.1: Berechnete Protonenaffinität (PA), Gasphasenbasizität (GB), Kegelwinkel (θ) und p*K*_{BH}⁺-Werte (in THF) sowie experimentelle p*K*_{BH}⁺-Werte (in THF), TOLMANS elektronischer Parameter (TEP) und ¹J_{PSe}-Kopplungskonstanten der untersuchten P^{III}-Superbasen.

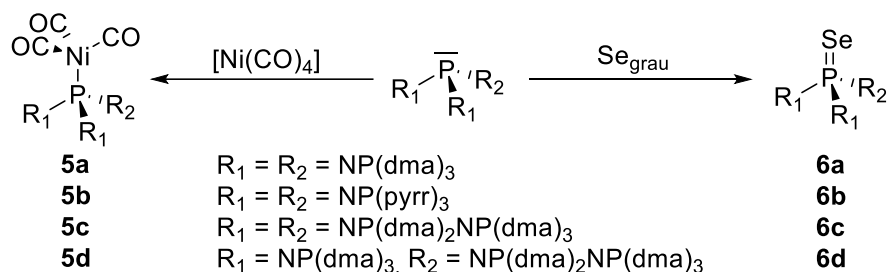
	PA /kcal·mol ⁻¹	GB /kcal·mol ⁻¹	p <i>K</i> _{BH} ⁺ (ber.)	p <i>K</i> _{BH} ⁺ (exp.)	TEP/cm ⁻¹	θ /°	¹ J _{PSe} /Hz
(dma)P ₃ P (1a)	297.4	291.3	34.9	34.9	2022.4	203.2	654
(pyrr)P ₃ P (1b)	307.5	300.2	37.8	36.7	2018.6	198.9	628
(dma)P ₄ P (1d)	304.3	295.4	37.0	37.2	2017.3	216.5	631
(dma)P ₆ P (1c)	315.4	306.8	41.9	-	2014.5	240.8	608

TEPs und ¹J_{PSe}-Kopplungskonstanten bestätigen den Trend in der Basizität und stellen die bisher niedrigsten publizierten Werte für Phosphane dar. PAPs sind damit nachweislich die stärksten Phosphor-BRØNSTED- und LEWIS-Basen. Zusammen mit Kegelwinkeln (θ) nahe oder sogar oberhalb von 200° kombinieren sie sterische und elektronische Eigenschaften, die beim

4 Zusammenfassung

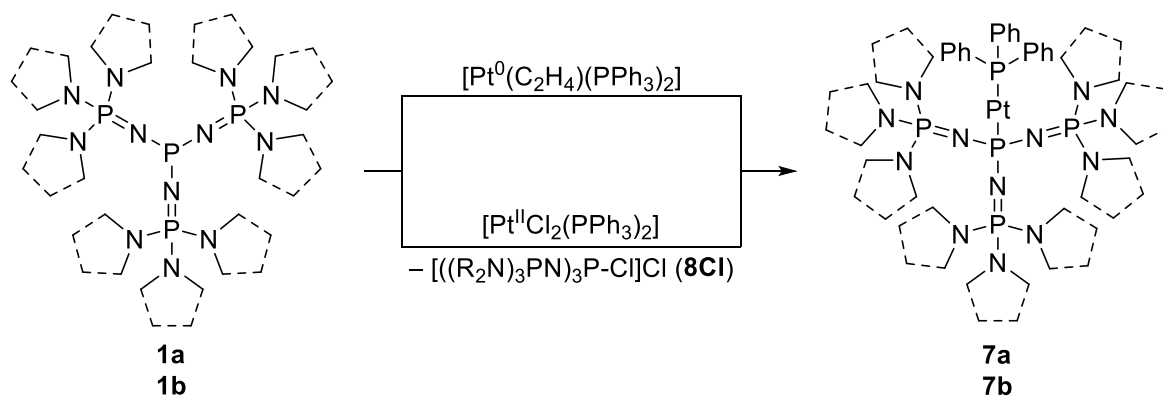
Design von Übergangsmetallkatalysatoren von großem Wert sind und übertreffen mit ihren Parametern andere superbasische Phosphane, die ihren Nutzen als Liganden in der Homogenkatalyse bereits demonstriert haben.^[142–147]

Die Darstellung der korrespondierenden Nickeltricarbonylkomplexe **5** und Phosphanselenide **6** erfolgte nach Schema 4.3 über die Reaktion mit Tetracarbonylnickel oder die Oxidation durch graues Selen. Mit Ausnahme von **5c** und **6c**, bei deren Synthese das Phosphan (dma)P₆P (**1c**) *in situ* mit Kaliumpyrrolidid freigesetzt wurde und es deshalb zu Nebenreaktionen kam, wurden alle dargestellten Nickelkomplexe und Phosphanselenide rein isoliert. Abbildung 4.2 zeigt beispielhafte XRD-Strukturen dieser Substanzen. Diese belegen in nicht-ionischen Verbindungen mit durchschnittlichen 1.65 Å zu 1.54 Å eine deutlichere Unterscheidung formaler Einfach- und Doppelbindungen innerhalb der P–N=P-Einheit.



Schema 4.3: Darstellung der Nickelcarbonylkomplexe **5** und Phosphanselenide **6**.

Die Eignung von PAPs als stark elektronendonierende Liganden wurde neben tetraedrischen Nickel(0)komplexen auch in Form linearer 14-Valenzelektronen-Platin(0)komplexe (**7**) dargelegt. Dabei ermöglicht das mit der hohen Basizität einhergehende hohe Reduktionspotential des Phosphor(III)atoms die Synthese sowohl aus Komplexpräkursoren der Oxidationsstufe 0 als auch der Oxidationsstufe +II (Schema 4.4). Sehr große ¹J_{Pt}-Kopplungskonstanten von 6153 (**7a**) bzw. 6223 Hz (**7b**) und niedrige chemische ¹⁹⁵Pt-NMR-Verschiebungen von –6238 bzw. –6219 ppm untermauern den extrem starken σ-Donor- und äußerst schwachen π-Akzeptorcharakter der Phosphazenyldiphosphanliganden.



Schema 4.4: Darstellung heteroleptischer Platin(0)komplexe (**7**). Mit [Pt⁰(C₂H₄)(PPh₃)₂] und **1** im Verhältnis 1:1, mit [Pt^{II}Cl₂(PPh₃)₂] und **1** im Verhältnis 1:2 unter Bildung von **8Cl** als Nebenprodukt.

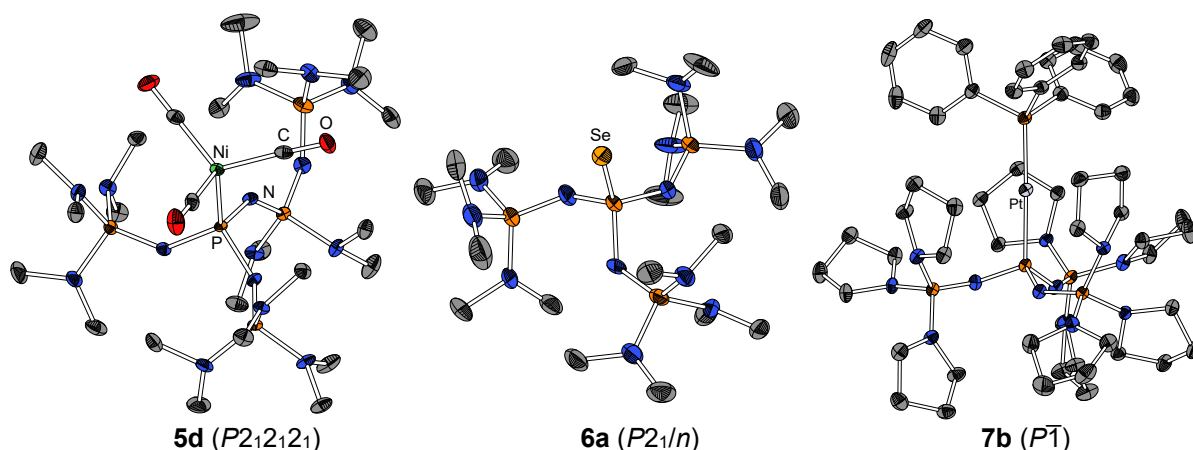
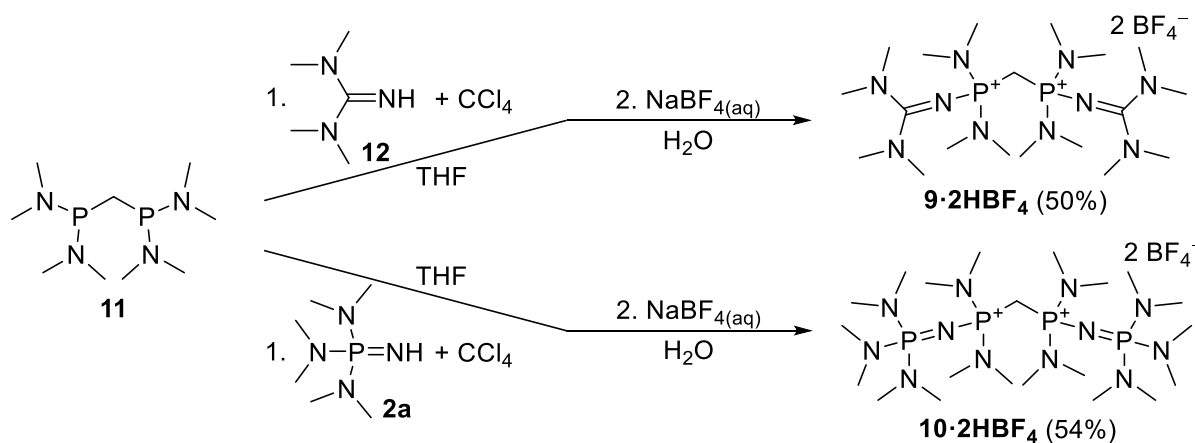


Abbildung 4.2: Im Kristall vorliegende Molekülstrukturen von $[(\text{dma})_4\text{P}_4\text{-Ni}(\text{CO})_3]$ (**5d**), $(\text{dma})_3\text{P}=\text{Se}$ (**6a**) und $[(\text{pyrr})_3\text{P}_3\text{-PtPPh}_3]$ (**7b**). Die XRD-Strukturen von $[(\text{dma})_3\text{P}_3\text{-Ni}(\text{CO})_3]$ (**5a**, $P\bar{1}$), $[(\text{pyrr})_3\text{P}_3\text{-Ni}(\text{CO})_3]$ (**5b**, $P\bar{1}$), $(\text{pyrr})_3\text{P}=\text{Se}$, (**6b**, $P2_1/c$) und $[(\text{dma})_3\text{P}_3\text{-PtPPh}_3]$ (**7a**, $Pa\bar{3}$) sind im kristallographischen Anhang zu finden.

4.2 Design ungeladener Kohlenstoffsuperbasen

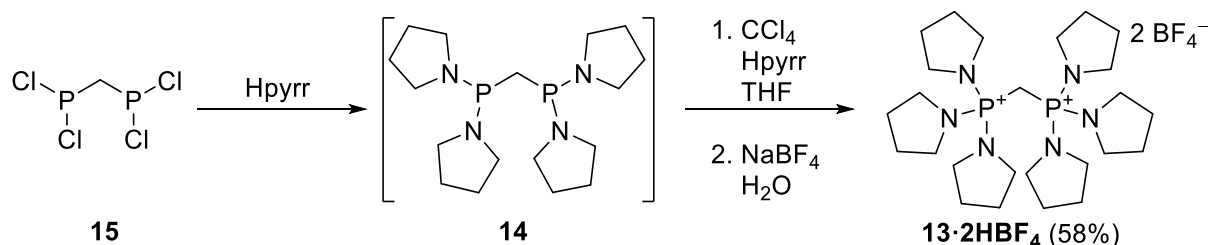
Die Synthese der protonierten CDPs zweiter Ordnung *sym*-(tmg)(dma)₂-CDP·2HBF₄ (**9·2HBF₄**) und *sym*-(dmaP₁)(dma)₂-CDP·2HBF₄ (**10·2HBF₄**) gelang wie in Schema 4.5 gezeigt über eine Erweiterung der Synthesestrategie von (dma)₆-CDP nach APPEL *et al.*^[114] Dabei wurde Bis[bis(dimethylamino)phosphino]methan (**11**) in Gegenwart von drei Äquivalenten Tetramethylguanidin (**12**) bzw. Tris(dimethylamino)phosphazen (**2a**) anstelle von Dimethylamin als Nukleophil und Hilfsbase mit Tetrachlorkohlenstoff oxidiert. Diese Reaktionsführung bietet den Vorteil der vorgeformten P–C–P-Einheit in **11**, welches in zwei Stufen in großem Maßstab zugänglich ist^[177] und macht die aufwändige Synthese der Phosphane (tmg)(dma)₂P bzw. **4** obsolet. Auch andere kommerziell erhältliche oder einfach zugängliche Nukleophile wie Cyclopropenimine, Imidazolin-2-ylidenamine *et al.*, könnten anstelle von **12** bzw. **2a** zu weiteren CDPs zweiter Ordnung funktionalisiert werden und so ein weites Feld neuer Kohlenstoffsuperbasen eröffnen.



Schema 4.5: Synthese der bisprotonierten CDPs **9·2HBF₄** und **10·2HBF₄**.

4 Zusammenfassung

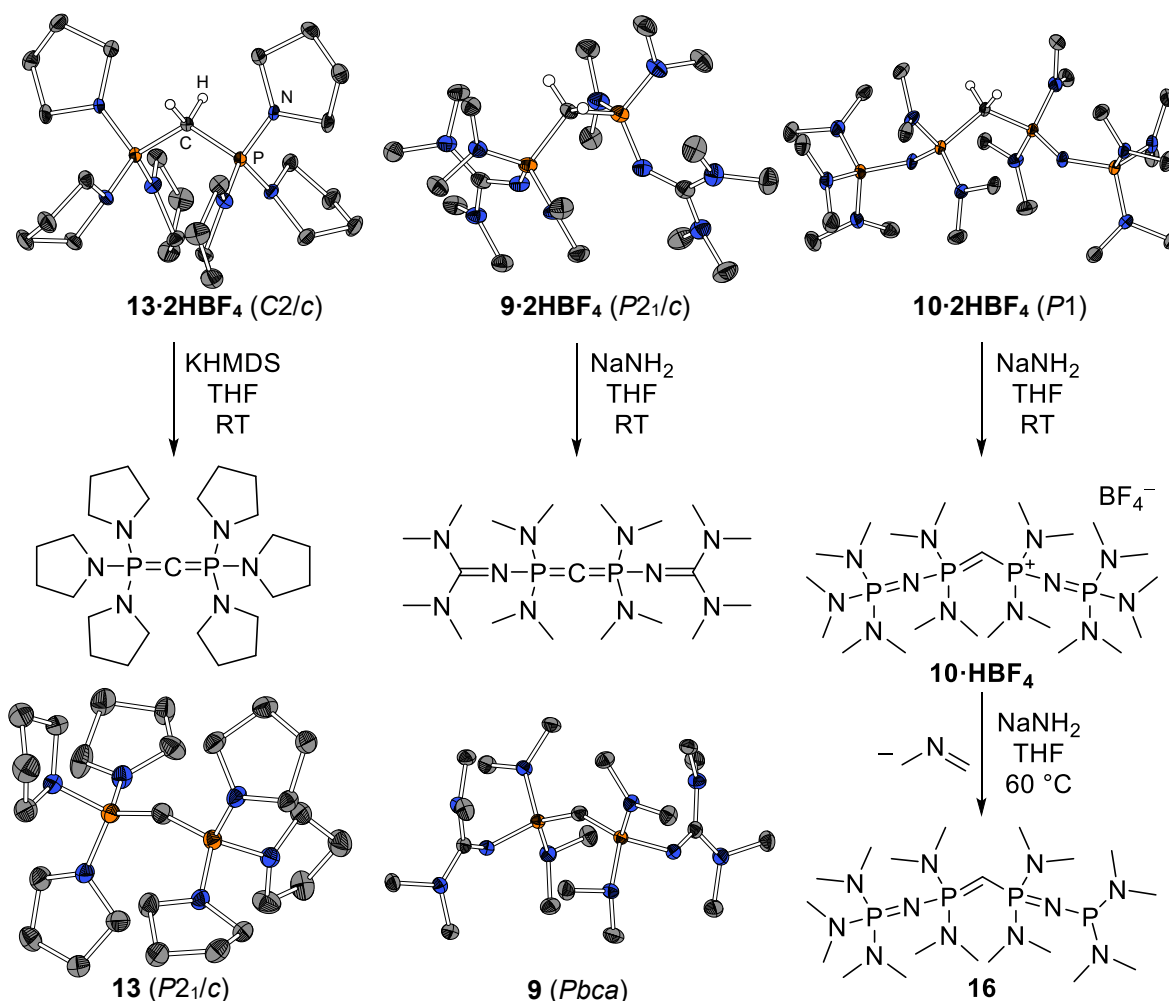
(pyrr)-CDP·2HBF₄ (**13**·2HBF₄) wurde analog nach Schema 4.6 synthetisiert. Da das Zwischenprodukt **14**, anders als **11**, nicht unzersetzt destillierbar ist und daher nicht in ausreichender Reinheit isoliert werden konnte, wurde die Reaktion ausgehend von Bis(dichlorophosphino)methan (**15**) mit einem Überschuss Pyrrolidin als Eintopfreaktion durchgeführt.



Schema 4.6: *In situ* Synthese von **14** und dessen anschließende Oxidation mit CCl₄ in Gegenwart überschüssigen Pyrrolidins (Hpyrr). Die Isolierung als Tetrafluoridoboratsalz erfolgt durch Ausfällen aus wässriger Lösung.

Bei allen drei Reaktionen wurde mittels ³¹P-NMR-Spektroskopie das monoprotonierte Hydrochlorid der CDPs als Produkt identifiziert, deren zweiter pK_{BH}⁺-Wert in THF liegt demzufolge unter dem der jeweiligen Hilfsbase Pyrrolidin (13.5),^[27] Tetramethylguanidin **12** (15.5)^[28] oder Tris(dimethylamino)phosphazen **2a** (19.7).^[28] Ein Anionenaustausch mit Natriumtetrafluoridoborat aus wässriger Lösung führte zur zweiten Protonierung am zentralen Kohlenstoffatom und einer stark alkalischen Lösung, weshalb selbst die monoprotonierten CDPs in wässrigem Medium starke kationische Basen darstellen.

Während für die Deprotonierung zum freien CDP **13** die Basizität von KHMDS ausreichend war, musste im Fall von **9** auf Natriumamid zurückgegriffen werden. Beide CDPs konnten aus *n*-Hexan als farbloser, kristalliner Feststoff in 70% (**13**) bzw. 60% (**9**) Ausbeute isoliert werden und liegen, anders als (dma)₆-CDP, im Einkristall mit 155.9(2)° (**13**) bzw. 147.30(9)° (**9**) gewinkelt vor (Schema 4.7). Beim Versuch **10**·2HBF₄ mit Natriumamid zu deprotonieren wurde bei Raumtemperatur lediglich das monoprotonierte **10**·HBF₄ erhalten. Bei erhöhter Temperatur wurde gemäß Schema 4.7 nicht das thermodynamisch acideste Proton am zentralen Kohlenstoffatom abstrahiert, sondern eine der peripheren, leicht zugänglichen Dimethylamino-Gruppen deprotoniert, welche anschließend als *N*-Methylmethanimin eliminierte und die terminale Phosphazanylgruppe zum Phosphan reduzierte. Diese Reaktion ist aufgrund der hohen Barriere des P–N-Bindungs-bruches langsam, läuft aber selektiv unter Bildung von **16** ab. Mit anderen Basen wie Benzylkalium, Kaliumhydrid oder *n*-Butyllithium kam es entweder ebenfalls zur Reduktion zu Phosphan **16** oder zu Zersetzungsreaktionen. Die monoprotonierten Spezies von **9** und **13** wurden zu Vergleichszwecken, entweder durch Kommutierung zwischen bisprotoniertem und freiem CDP oder durch Reaktion mit einem Äquivalent Bis(trifluormethansulfonyl)imid (HTFSI) in NMR-Experimenten dargestellt.



Schema 4.7: Deprotonierung der bisprotonierten Tetrafluoridoboratsalze zu den CDPs **13** bzw. **9** (mit ihren XRD-Strukturen) sowie zum monoprotinierten CDP **10·HBF₄** bei Raumtemperatur und zum Abbauprodukt **16** bei erhöhter Temperatur.

Der pK_{BH^+} -Wert von **13** konnte durch NMR-Titration gegen (tmg)P₁-*t*Bu und (dma)P₄-*t*Bu auf einen Wert zwischen 30.1 und 32.9 eingegrenzt werden. Für **9** konnte gegen (pyrr)P₄-*t*Bu ein pK_{BH^+} -Wert von 35.8 in THF ermittelt werden (Tabelle 4.2). Dieser ist für CDPs nicht nur der erste berichtete pK_{BH^+} -Wert, er zeigt auch, dass **9** sogar um 0.5 Größenordnungen basischer ist als die auf der THF-Basizitätsskala stärkste Stickstoffsuperbase (pyrr)P₄-*t*Bu. Das bisylidische CDP **9** ist zudem um 2.3 Größenordnungen basischer als die bislang stärkste Kohlenstoffsuperbase, das Monoylid H₂C=P(2,4,6-(MeO)₃-C₆H₂)₂Ph (pK_{BH^+} in THF: 33.5).^[14] Vor dem Hintergrund des deutlich geringeren Molekulargewichts stellen CDPs damit außergewöhnlich starke nicht-ionische Superbasen dar, um ein vielfaches basischer als Carbene wie NHCs oder CAACs.^[109,110] Ihr Donorcharakter gegenüber anderen LEWIS-Säuren als dem Proton wird zukünftig im Vergleich zu diesen klassischen C-Donorliganden zu untersuchen sein.

4 Zusammenfassung

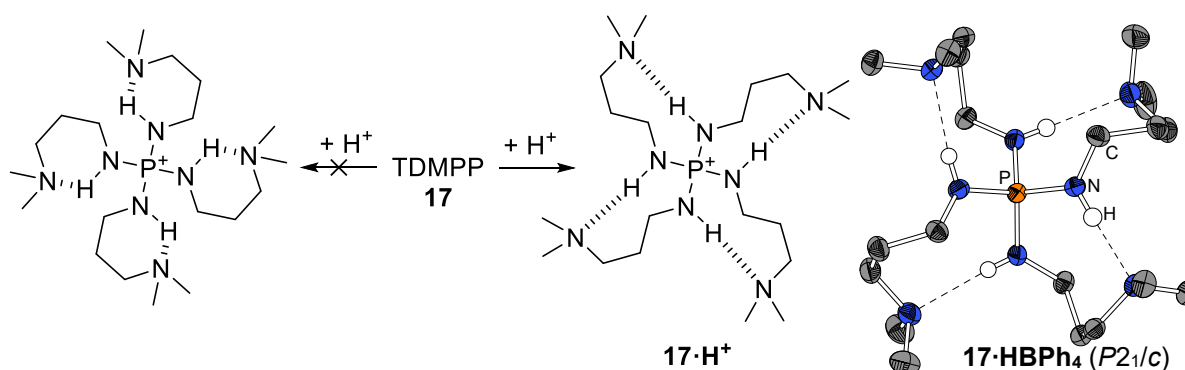
Tabelle 4.2: Berechnete erste und zweite Protonenaffinität (PA), Gasphasenbasizität (GB) und pK_{BH^+} -Werte (in THF) der präsentierten CDPs.

		PA/kcal·mol ⁻¹	GB/kcal·mol ⁻¹	pK_{BH^+} (THF) ^[a]
(pyrr) ₆ -CDP (13)	1.	291.1	282.2	32.8 (30.1-32.9)
	2.	191.6	184.0	
<i>sym</i> -(tmg)(dma) ₂ -CDP (9)	1.	294.4	287.2	34.9 (35.8)
	2.	202.0	194.1	
<i>sym</i> -(dmaP ₁)(dma) ₂ -CDP (10)	1.	305.3	299.7	39.1
	2.	212.1	202.2	
16	am C-Atom	275.9	268.7	24.4
	am P-Atom	276.2	268.8	21.1

[a] experimentell bestimmte Werte in Klammern.

4.3 Eine Phosphazenenbase mit Korona-Effekt

N,N',N'',N'''-Tetrakis(3-dimethylaminopropyl)triaminophosphazen (TDMPP, **17**) kombiniert erstmalig das Konzept der Basizitätsverstärkung durch den multiplen Korona-Effekt, den Ringschluss von *N*-Alkylaminosubstituenten durch intramolekulare H-Brücken (IHBs), mit der intrinsisch hohen Basizität von Phosphazenen und stellt somit einen neuen Vertreter für Stickstoffsuperbasen dar. **17** konnte aus den gängigen Chemikalien Phosphorpentachlorid und 3-Dimethylaminopropylamin in seiner protonierten Form als Tetraphenylborat in 68% Ausbeute synthetisiert werden. Die im Kristall vorliegende Molekülstruktur bestätigt das Vorliegen der vier IHBs im Festkörper. Analog zum Guanidin TDMPG·HPF₆ bilden die Dimethylaminopropylketten keine sechsgliedrigen Ringe, sondern Achtringe mit benachbarten N–H-Funktionen aus (Schema 4.8). Die Existenz der IHBs in Lösung wurde durch temperaturabhängige NMR-Spektroskopie in unterschiedlichen Lösungsmitteln bestätigt.



Schema 4.8: Mögliche Konformationen der konjugierten Säure von TDMPP (**17**). Die rechte Anordnung der IHBs wurde über die Einkristall-Röntgenstrukturanalyse und DFT-Kalkulationen als thermodynamisch bevorzugt ermittelt.

Für die Gasphase wurde eine individuelle Bindungsenergie der intramolekularen Wasserstoffbrücken im *S*₄-symmetrischen Kation **17·H⁺** von 5.8 kcal·mol⁻¹ berechnet. Diese liegt oberhalb der individuellen Bindungsenergie der drei IHBs in der asymmetrischen Neutral-

form **17** (3.5, 3.9 und 4.2 kcal·mol⁻¹) und trägt somit zur Basizitätssteigerung in der Superbase TDMPP bei. Der pK_{BH^+} -Wert von **17** konnte durch NMR-Titration gegen HMPN auf einen Wert von 22.4 in THF bzw. 30.4 in Acetonitril bestimmt werden. Der vierfache Korona-Effekt erhöht die Basizität damit um 1.7 (THF) bzw. 2.9 (MeCN) Größenordnungen im Vergleich mit (dma)P₁-Me und um 0.7 (THF) und 1.5 (MeCN) Größenordnungen im Vergleich zu (pyrr)P₁-Et, der bislang stärksten Phosphazenenbase erster Ordnung. Der Vorteil des tetrasubstituierten Phosphoratoms im Vergleich zum trisubstituierten Kohlenstoffatom in TDMPG manifestiert sich in einem um 2.8 Größenordnungen höheren pK_{BH^+} -Wert in Acetonitril.

4.4 Fazit

Mittels neuem Design und synthetischer Realisierung ungeladener Phosphor-, Kohlenstoff- und Stickstoffsüberbasen konnten weitere Sprossen in das obere Ende der Basizitätsleiter eingefügt werden. Die vorgestellten Phosphazenyldiphosphane (PAPs) stellten dabei nicht nur den Basizitätsrekord für Phosphorbasen auf, sie übertreffen sogar die lange Zeit dominierende Klasse von Phosphazenenbasen und sind Spitzenreiter der bislang untersuchten THF-Basizitätsskala. Die hohe Elektronendichte am Phosphoratom führt dabei nicht nur zu einer hohen BRØNSTED-Basizität, sondern resultiert auch in einer hohen LEWIS-Basizität und Reduktionskraft. Diese offenbarten sich in beispielhaften Reaktionen mit Übergangsmetallkomplexpräkursoren, dem Hauptgruppenelement Selen und dem simpelsten Elektrophil von allen, dem Proton.

Für die bislang als Superbasen vernachlässigte Klasse der Carbodiphosphorane (CDPs) wurde erstmals ein experimentell bestimmter pK_{BH^+} -Wert präsentiert. Dieser bestätigt das bisylidische Kohlenstoffatom als herausragendes Basizitätszentrum, welches mit deutlich geringeren Molekulargewichten in ähnliche Basizitätsregionen vorstößt, wie SCHWESINGERS P₄-Phosphazene. Die entwickelte Syntheseroute zu superbasischen CDPs zweiter Ordnung ermöglicht eine einfache Modulation der Substituenten und eröffnet damit ein weites Feld, fein abgestimmter Kohlenstoffsüberbasen am oberen Ende der Basizitätsskala.

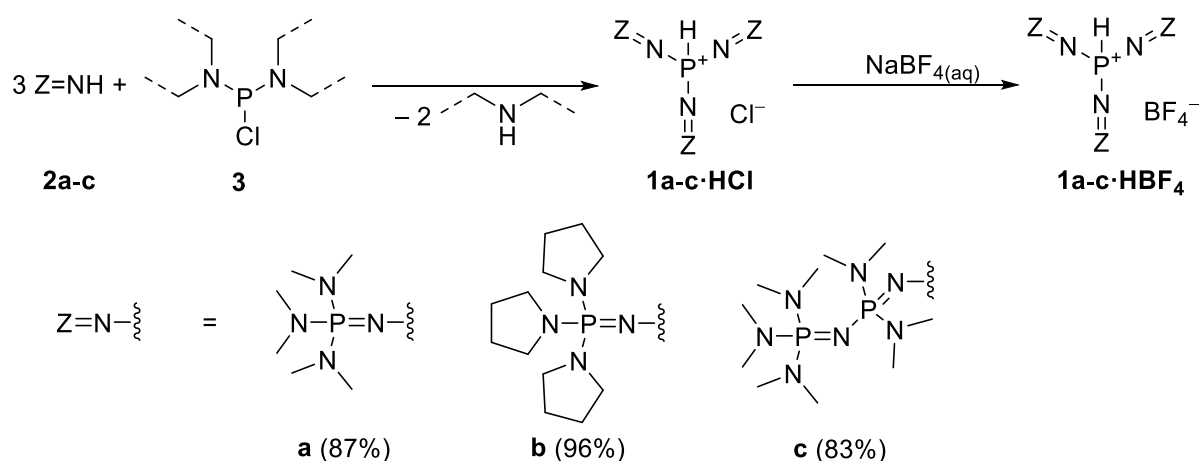
Erstmalig wurde ein Phosphazene vorgestellt, dessen Basizität durch multiple intramolekulare Wasserstoffbrückenbindungen (IHBs) drastisch gesteigert wird. Experimentelle und theoretische Untersuchungen beleuchteten dabei den Einfluss des Korona-Effektes auf die Basizität im Festkörper, in Lösung und in der Gasphase und offenbarten die stärkste Phosphazenenbase erster Ordnung.

Somit konnten neue Vertreter ungeladener Superbasen präsentiert werden, deren verschiedene Reaktivität gegenüber dem Proton und anderen LEWIS-Säuren der Unterschiedlichkeit des Phosphor-, Kohlenstoff- oder Stickstoffatoms als Basizitätszentrum Rechnung trägt.

5 Summary

5.1 Contributions to the Chemistry of Superbasic Phosphanes

The developed amine elimination (Scheme 5.1) enables an elegant synthesis of P-protonated phosphonium salts with superbasic substituents (**1·HX**). In comparison to the standard synthesis with phosphorus trichloride, the built-in auxiliary base in the electrophile **3** reduces the necessary amount of the nucleophile **2**, generates only volatile byproducts, and avoids difficult separation of a mixture of ammonium and phosphonium salts to provide the target compounds in nearly quantitative yields and high purity. Since the isolated hydrochlorides turned out to be air and moisture stable but hygroscopic, a precipitation step with sodium tetrafluoroborate from aqueous solution lead to infinitely storable P-H phosphonium salts **1·HBF₄**. The three superbase precursors (dma)₃P·HBF₄ (**1a·HBF₄**), (pyrr)₃P·HBF₄ (**1b·HBF₄**), and (dma)₆P·HBF₄ (**1c·HBF₄**) were prepared *via* this synthesis route.



Scheme 5.1: Preparation of phosphonium salts **1·HCl** and **1·HBF₄**, respectively, *via* amine elimination. Yield are given for the products **1a-c·HBF₄**.

Within this work an alternative approach for the synthesis of diphosphazene **2c** was developed. Instead of the substitution of oxygen by chlorine in the phosphane oxide (dma)₃P=N–P(dma)₂=O with phosphoryl chloride and subsequent ammonolysis as described by SCHWESINGER *et al.*,^[19] **2c** was prepared from monophosphazeny phosphane **4** by consecutive bromination and ammonolysis in a one-pot synthesis. This route decreases the number of synthetic steps and provides **4**, which is an intermediate required for the preparation of the asymmetric (dma)₄P·HBF₄ (**1i·HBF₄**) incorporating two monophosphazeny and one diphosphazeny substituents (Scheme 5.2). The mixed-valent P^{III}/P^V precursor **4** turned out to be an adequate starting material as it does not react with the phosphazenes (**2a** or **2c**), but exclusively with their protonated form (**2a·HBF₄** or **2c·HBr**) to the intermediate phosphonium

5 Summary

The liberation of phosphazanyl phosphanes (PAPs) (dma)P₃P (**1a**), (pyrr)P₃P (**1b**), and (dma)P₄P (**1d**) was conducted with potassium hexamethyldisilazide (KHMDs) in high yields of 87% (**1a**), 88% (**1b**), and 79% (**1d**), respectively. The probably strongest non-ionic superbases (dma)P₆P (**1c**) could not be isolated in its pure form yet, instead it was generated *in situ* with potassium pyrrolidide (Kpyrr) and could be trapped and further functionalized as phosphane selenide or nickel carbonyl complex. Under reductive conditions such as elemental potassium in liquid ammonia or ethylenediamine no reaction was observed due to low P–H bond polarization, whilst treatment with organolithium bases led to partial disintegration of the cation.

In order to quantify BRØNSTED and LEWIS basicities, proton affinities (PA), gas-phase basicities (GB), theoretical and experimental pK_{BH}^+ values, as well as the TOLMAN electronic parameters (TEP) of the respective nickel tricarbonyl complexes and $^1J_{\text{PSe}}$ coupling constants of corresponding phosphane selenides were determined (Table 5.1). Experimental pK_{BH}^+ values in THF were determined by ^{31}P NMR titration experiments against SCHWESINGER's (dma)P₄-*t*Bu (pK_{BH}^+ in THF = 33.9)^[14] or (pyrr)P₄-*t*Bu (35.3)^[14] as reference bases to values of 34.9 (**1a**), 36.7 (**1b**), and 37.2 (**1d**). These values are not only the highest obtained for any phosphorus superbases so far, but the basicity of phosphanes **1a** and **1b** even exceed the basicity of their phosphazene counter-parts. Thereby PAPs mark the new top-end of the established THF-based basicity scale. In contrast to the highly thermodynamic basicity, the kinetics of intermolecular proton exchange are slow due to small P–H bond polarization. The barriers were determined as 15.5 kcal·mol⁻¹ for **1a** and 16.5 kcal·mol⁻¹ for **1b**, complying with exchange rates of 13 or 3 Hz, respectively. Hence PAPs are kinetically low-active BRØNSTED bases, similar to proton sponges rather than to kinetically more active phosphazene bases.^[15,19]

Table 5.1: Calculated proton affinities (PA), gas-phase basicities (GB), cone angles (θ) and pK_{BH}^+ values (in THF) as well as experimental pK_{BH}^+ values (in THF), TOLMAN's electronic parameter (TEP), and $^1J_{\text{PSe}}$ coupling constants of the P^{III}-superbases.

	PA /kcal·mol ⁻¹	GB /kcal·mol ⁻¹	pK_{BH}^+ (calcd.)	pK_{BH}^+ (exp.)	TEP/cm ⁻¹	$\theta/^\circ$	$^1J_{\text{PSe}}/\text{Hz}$
(dma)P ₃ P (1a)	297.4	291.3	34.9	34.9	2022.4	203.2	654
(pyrr)P ₃ P (1b)	307.5	300.2	37.8	36.7	2018.6	198.9	628
(dma)P ₄ P (1d)	304.3	295.4	37.0	37.2	2017.3	216.5	631
(dma)P ₆ P (1c)	315.4	306.8	41.9	-	2014.5	240.8	608

TEPs and $^1J_{\text{PSe}}$ couplings are the so far lowest reported values for phosphanes and in accordance with the trend in phosphane basicity, validating PAPs as the strongest phosphorus BRØNSTED and LEWIS bases. Furthermore PAPs exhibit cone angles (θ) near or even greater than 200°.

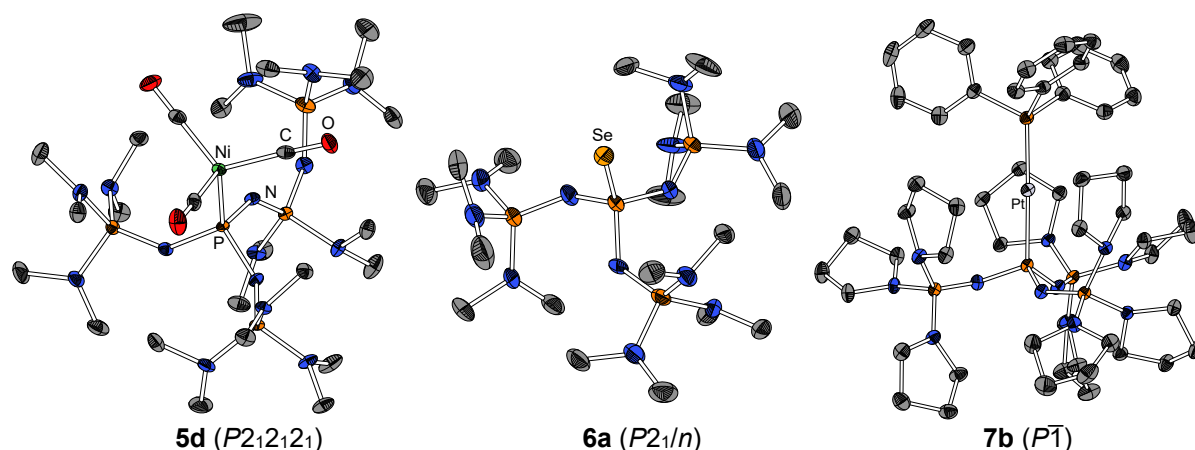
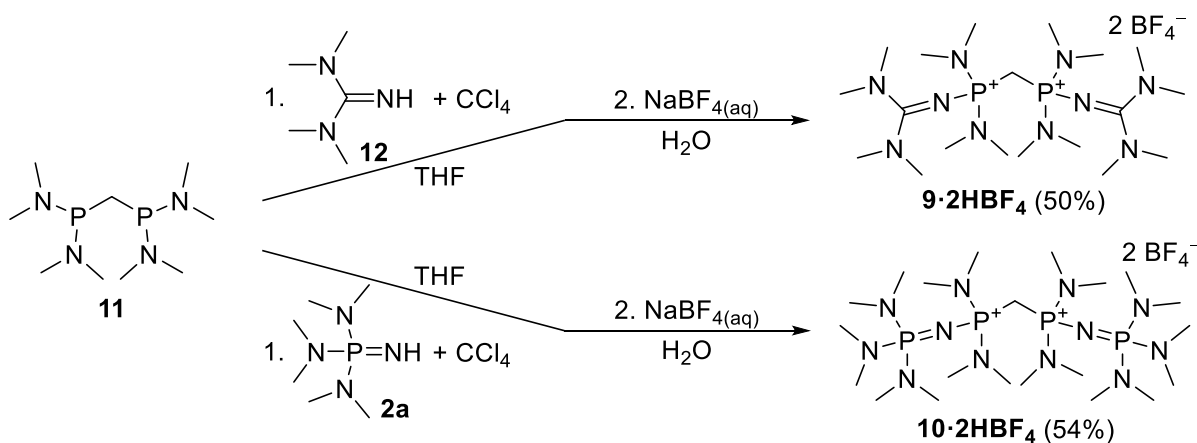


Figure 5.2: XRD structures of $[(\text{dma})\text{P}_4\text{P}-\text{Ni}(\text{CO})_3]$ (**5d**), $(\text{dma})\text{P}_3\text{P}=\text{Se}$ (**6a**), and $[(\text{pyrr})\text{P}_3\text{P}-\text{PtPPh}_3]$ (**7b**). Molecular structures of $[(\text{dma})\text{P}_3\text{P}-\text{Ni}(\text{CO})_3]$ (**5a**, $P\bar{1}$), $[(\text{pyrr})\text{P}_3\text{P}-\text{Ni}(\text{CO})_3]$ (**5b**, $P\bar{1}$), $(\text{pyrr})\text{P}_3\text{P}=\text{Se}$, (**6b**, $P2_1/c$), and $[(\text{dma})\text{P}_3\text{P}-\text{PtPPh}_3]$ (**7a**, $Pa\bar{3}$) are given in the crystallographic section.

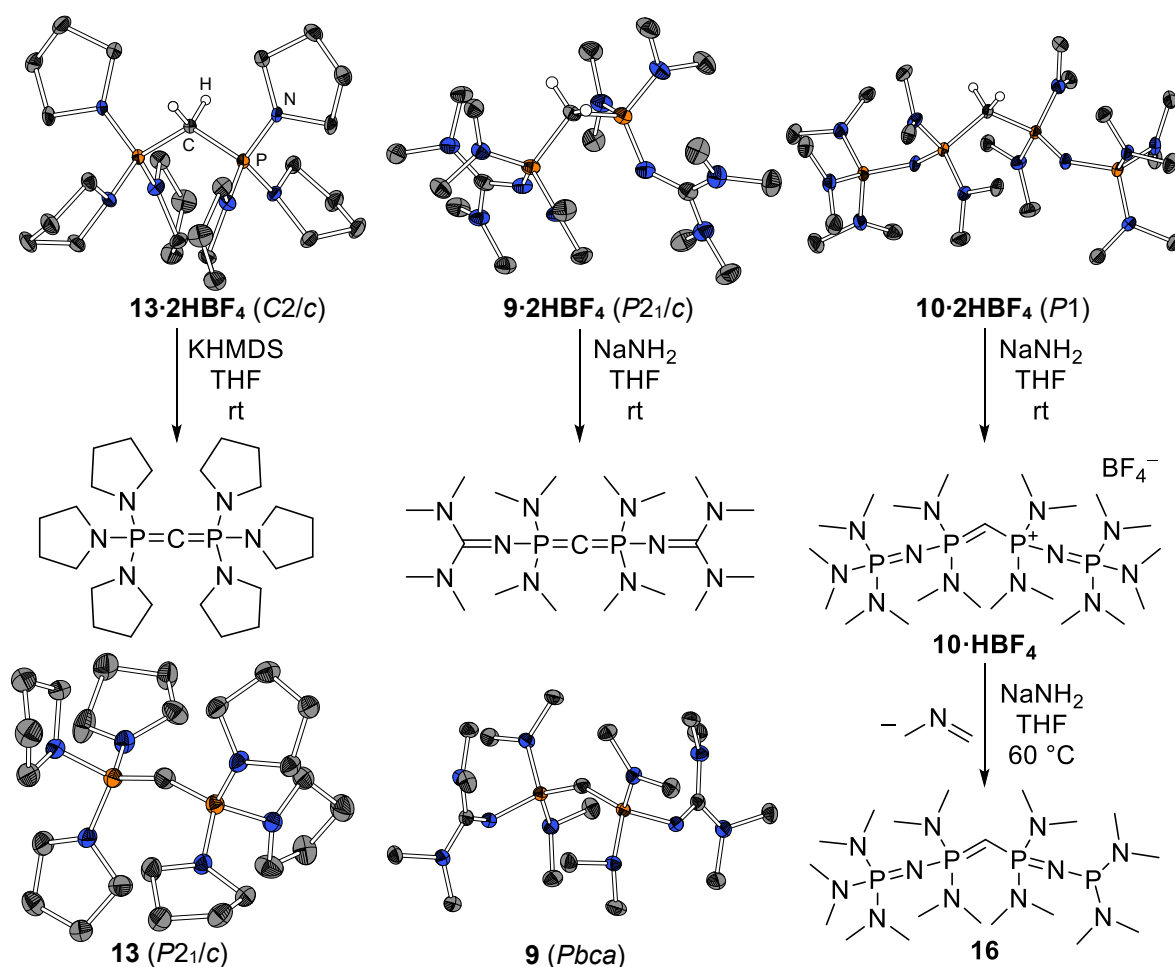
5.2 Design of Uncharged Carbon Superbases

For the synthesis of new superbasic carbodiphosphoranes an alternative synthesis strategy originally described for $(\text{dma})_6\text{-CDP}$ by APPEL *et al.*^[114] was further developed. The precursors for the second-order CDPs *sym*- $(\text{tmg})_2(\text{dma})_4\text{-CDP}$ (**9**) and *sym*- $(\text{dmaP}_1)_2(\text{dma})_4\text{-CDP}$ (**10**) were obtained as shown in Scheme 5.5. Bis[bis(dimethylamino)phosphino]methane (**11**) was oxidized with carbon tetrachloride in presence of tetramethylguanidine (**12**) or tris(dimethylamino)phosphazene (**2a**) instead of dimethylamine as nucleophile and auxiliary base. This reaction offers the advantage of preformed C–P bonds, wherefore the laborious preparation of the phosphanes $(\text{tmg})(\text{dma})_2\text{P}$ or **4** become obsolete. Instead **11** is readily obtainable in two steps on a large scale.^[177] In further developments the superbasic building blocks oxidatively introduced as nucleophiles can be varied for different commercially available or easily preparable building blocks, such as cyclopropenimines, imidazolin-2-ylidenamine, *et al.*, opening up a vast field of potentially new carbon superbases.



Scheme 5.5: Preparation of bisprotonated CDPs **9·2HBF₄** and **10·2HBF₄**.

5 Summary



Scheme 5.7: Deprotonation of bisprotonated tetrafluoridoborate salts to CDP **13** and **9** (with their respective XRD-structures) as well as to monoprotonated **10·HBF₄** at room temperature and the decomposition pathway to **16** at elevated temperatures.

The pK_{BH}^+ value of **13** could be estimated by NMR titration against (tmg)P₁-*t*Bu and (dma)P₄-*t*Bu to lie in-between 30.1 and 32.9. For **9** a value of 35.8 was determined against (pyrr)P₄-*t*Bu (Table 5.2). This is not only the first reported pK_{BH}^+ value for CDPs, it proves **9** to be by 0.5 orders of magnitude more basic than the strongest commercially available non-ionic nitrogen superbase on the THF basicity scale.

Table 5.2: Calculated first and second proton affinity (PA) and gas-phase basicity (GB) together with calculated pK_{BH}^+ values in THF.

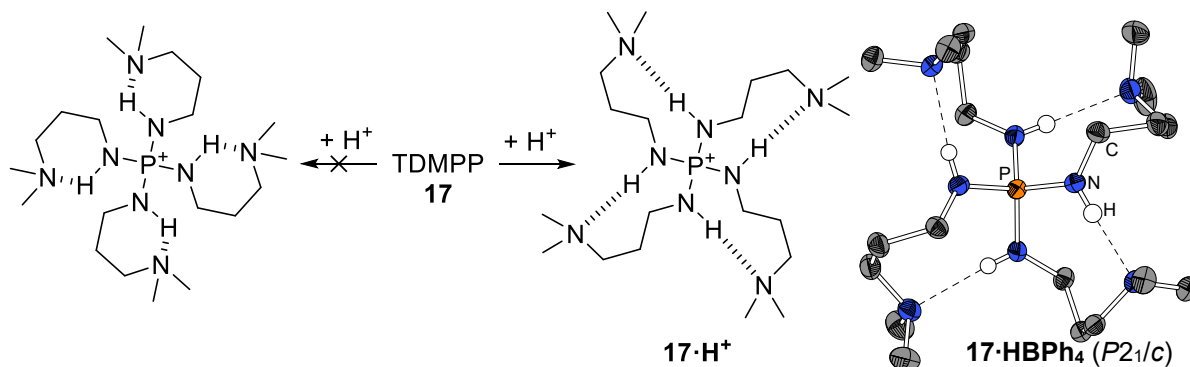
		PA/kcal·mol ⁻¹	GB/kcal·mol ⁻¹	$pK_{\text{BH}}^+(\text{THF})^{[a]}$
(pyrr) ₆ -CDP (13)	1 st	291.1	282.2	32.8 (30.1-32.9)
	2 nd	191.6	184.0	
<i>sym</i> -(tmg)(dma) ₂ -CDP (9)	1 st	294.4	287.2	34.9 (35.8)
	2 nd	202.0	194.1	
<i>sym</i> -(dmaP ₁)(dma) ₂ -CDP (10)	1 st	305.3	299.7	39.1
	2 nd	212.1	202.2	
16	at carbon	275.9	268.7	24.4
	at phosphorus	276.2	268.8	21.1

[a] experimental values in parentheses.

Furthermore bisylidic CDP **9** is 2.3 orders of magnitude more basic than the strongest non-ionic carbon superbase so far, the monoamid H₂C=P(2,4,6-(MeO)₃-C₆H₂)₂Ph (pK_{BH}⁺ in THF: 33.5).^[14] Thereby, in the light of a significantly lower molecular weight, CDPs turned out to be outstanding uncharged superbases, by far superior to carbenes like NHCs or CAACs.^[109,110] In future their donor character towards LEWIS acids other than the proton will be compared to such classical C-donor ligands.

5.3 A Phosphazene Base with Corona Effect

In *N,N',N'',N'''*-Tetrakis(3-dimethylaminopropyl)triaminophosphazene (TDMPP, **17**) the concept of basicity enhancement by the multiple corona effect, the formation of a crown-shaped ring by an *N*-alkylamino substituent *via* intramolecular hydrogen bonding (IHB), was incorporated in a phosphazene base for the first time to give a new type of nitrogen superbase. **17** was obtained from the common chemicals phosphorus pentachloride and 3-dimethylaminopropylamine in its protonated form as tetraphenylborate in 68% yield. The XRD structure confirmed the existence of four IHBs in solid state, forming eight-membered rings similar to those in guanidine analogue TDMPG·HPF₆ (Scheme 5.8). For validation of the IHBs existence in solution temperature dependent NMR studies in different solvents were conducted.



Scheme 5.8: Possible conformations of the conjugate acid of TDMPP (**17**). The one on the right-hand side was confirmed as energetically favoured *via* single crystal X-ray diffraction and DFT calculations.

The individual strength of the four IHBs in *S*₄-symmetric cation **17·H**⁺ was calculated to 5.8 kcal·mol⁻¹ in the gas-phase, which is higher than the individual strength of the three IHBs in asymmetric neutral form **17** (3.5, 3.9 and 4.2 kcal·mol⁻¹) and contributes therefore to the overall basicity enhancement in superbase TDMPP. The pK_{BH}⁺ value of **17** was determined by NMR titration against HMPN giving a value of 22.4 in THF and 30.4 in acetonitrile. The four-fold corona effect attributes 1.7 (THF) and 2.9 (MeCN) units, respectively, in comparison to (dma)P₁-Me as well as 0.7 (THF) and 1.5 (MeCN) units in comparison to the most basic first-order phosphazene superbase (pyrr)P₁-Et. The advantage of the tetrasubstituted phosphorus

5 Summary

atom to the trisubstituted carbon atom in TDMPG is manifested in a 2.8 orders of magnitude higher pK_{BH^+} value in acetonitrile.

5.4 Conclusion

With the design and synthesis of new uncharged phosphorus, carbon, and nitrogen superbases additional staves at the upper end of the basicity ladder were established. The presented phosphazenyl phosphanes (PAPs) are not only the record holder of phosphorus bases, but even surpass the long-time dominant phosphazene superbases, being the new top-end markers of the self-consistent THF-based basicity scale. High electron density at the phosphorus(III) atom results in high BRØNSTED basicity as well as in high LEWIS basicity and reduction potential. These attributes were validated in paradigmatic reactions with transition metal precursors, the main group element selenium and the simplest electrophile of all, the proton.

For the first time an experimental pK_{BH^+} value for carbodiphosphoranes (CDPs) was presented. It confirmed the bisylidic carbon atom as an exceptional basicity centre, reaching a similar basicity region as SCHWESINGER's P₄-phosphazenes, however with significantly lower molecular weight. The synthesis route to second-order CDPs opens-up a vast field of fine-tuned top-tier carbon superbases through simple modulation of the P-substituents.

A new nitrogen superbase was presented with augmented basicity through multiple intermolecular hydrogen bonding. Experimental and theoretical investigations shed light on the influence of the four-fold corona effect in solid state, in solution and in the gas-phase and revealed the strongest first-order phosphazene superbase.

Thus, several new representatives of non-ionic superbases were presented, which take into account the differences of phosphorus, carbon and nitrogen atom as basicity centres in their divergent reactivity towards the proton and other LEWIS acids.

6 Volltexte der Manuskripte

S. Ullrich, B. Kovačević, X. Xie, J. Sundermeyer, “Phosphazanyl Phosphines: The Most Electron-Rich Uncharged Phosphorus Brønsted and Lewis Bases”, *Angew. Chem. Int. Ed.* **2019**, *58*, 10335; *Angew. Chem.* **2019**, *131*, 10443. Copyright © 2019 Wiley-VCH Verlag GmbH & Co. KGaA, Weinheim. Lizenznummern: 4636461086423 & 4636470782468. Zu finden unter DOI: [10.1002/anie.201903342](https://doi.org/10.1002/anie.201903342) & DOI: [10.1002/ange.201903342](https://doi.org/10.1002/ange.201903342).

Angefügt sind die in Originalform veröffentlichten Manuskripte in englischer und deutscher Sprache sowie die in den *supporting information* aufgeführten Synthesevorschriften, NMR-Experimente und Details zu den Rechnungen. Auf die Reproduktion von Spektren, XRD-Strukturen und Tabellen berechneter Atomkoordinaten in der Gasphase wurde verzichtet.

S. Ullrich, B. Kovačević, B. Koch, K. Harms, J. Sundermeyer, “Design of Non-Ionic Carbon Superbases: Second Generation Carbodiphosphoranes”, *Chem. Sci.* **2019**, *10*, 9483. Published by The Royal Society of Chemistry. Zu finden unter DOI: [10.1039/C9SC03565F](https://doi.org/10.1039/C9SC03565F).

Angefügt ist das in Originalform veröffentlichte Manuskript sowie die in den *supporting information* aufgeführten NMR-Experimente und Details zu den Rechnungen. Auf die Reproduktion von Spektren, XRD-Strukturen und Tabellen berechneter Atomkoordinaten in der Gasphase wurde verzichtet.

S. Ullrich, D. Barić, X. Xie, B. Kovačević, J. Sundermeyer, “Basicity Enhancement by Multiple Intramolecular Hydrogen Bonding in Organic Superbase *N,N',N'',N'''*-Tetrakis(3-(dimethylamino)propyl)triaminophosphazene”, *Org. Lett.* **2019**, *article ASAP*. Reprinted with permission. Copyright © 2019 American Chemical Society. Zu finden unter DOI: [10.1021/acs.orglett.9b03521](https://doi.org/10.1021/acs.orglett.9b03521).

Angefügt ist online veröffentlichte Manuskript sowie die in den *supporting information* aufgeführten Synthesevorschriften, NMR-Experimente und Details zu den Rechnungen. Auf die Reproduktion von Spektren, XRD-Strukturen und Tabellen berechneter Atomkoordinaten in der Gasphase wurde verzichtet.



Phosphazeryl Phosphines: The Most Electron-Rich Uncharged Phosphorus Brønsted and Lewis Bases

Sebastian Ullrich, Borislav Kovačević, Xiulan Xie, and Jörg Sundermeyer*

Dedicated to Professor Helmut Werner on the occasion of his 85th birthday

Abstract: It was discovered that phosphazeryl phosphines (PAPs) can be stronger P-superbases than the corresponding Schwesinger type phosphazene N-superbases. A simple synthetic access to this class of PR_3 derivatives including their homologization is described. XRD structures, proton affinities (PA), and gas-phase basicities (GB) as well as calculated and experimental pK_{BH^+} values in THF are presented. In contrast to their N-basic counterparts, PAPs are also privileged ligands in transition metal chemistry. In fact, they are currently the strongest uncharged P-donors known, exceeding classical and more recently discovered ligands such as $PtBu_3$ and imidazolin-2-ylidenaminophosphines (IAPs) with respect to their low Tolman electronic parameters (TEPs) and large cone angles.

Over the past two decades uncharged organic superbases have become a veritable tool in organic synthesis.^[1] Marking the high-end record of the solvent-dependent pK_{BH^+} scale, Schwesinger's famous phosphazene N-superbases^[2] became commercially available and the subject of many investigations and applications in organic synthesis and catalysis.^[3] The homologization concept was utilized to achieve a similar trend for other uncharged nitrogen superbases such as guanidines,^[4] cyclopropenimines,^[5] and combinations thereof^[6,7] as well as their bidentate proton sponge derivatives.^[8] A similar molecular superbase design has been investigated by theory^[9] and experiment for uncharged carbon bases such as related phosphorus ylides^[10] and their bisylide pincers.^[11] Compared to the dominating class of N-bases, phosphorus(III) compounds have not been systematically considered as extremely strong proton acceptors.^[6,10] The main field of interest and application of these compounds lies in creating very strong donors in transition metal chemistry and catalysis. Verkade's proazaphosphatranes are early representatives of rare superbasic phosphines.^[12] Schmutzler et al. attempted to synthesize a potentially very

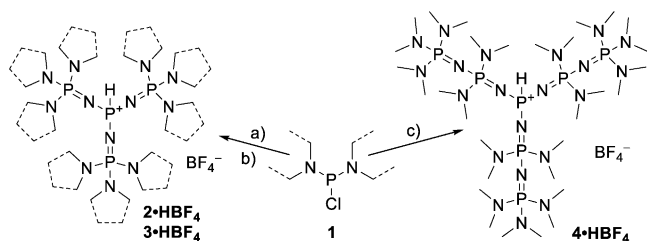
basic tris(tetramethylguanidino)phosphine. They were able to isolate the P-protonated form, but deprotonation leads to disintegration of this PR_3 derivative.^[13] In 2017 Dielmann et al. solved the problem of guanidine degradation by using related aromatically stabilized imidazolin-2-ylidenamino substituents to access the very interesting class of electron-rich imidazolin-2-ylidenaminophosphine (IAP) ligands with their high basicity as well as outstanding Tolman electronic parameters (TEPs) and large cone angles.^[14]

Here we report that Schwesinger's phosphazenes, the currently strongest known non-ionic superbases, surprisingly become even more basic, when formally the nitrene $tBuN$ unit at the P^V imine is reductively eliminated. Furthermore, the emerging class of phosphazeryl phosphines (PAPs) are, in contrast to phosphazenes, privileged to form a wide range of transition metal coordination compounds as well. PAPs thus complement other phosphine ligands incorporating superbasic structural motifs, which have already been utilized as catalysts in palladium^[15] and gold catalysis,^[16] and as activators of small molecules per se.^[14,17] We demonstrate that PAPs are indeed the most electron-rich uncharged PR_3 donors known so far, exceeding even IAPs with respect to their higher pK_{BH^+} and lower TEP values. A convenient synthesis for PAPs and an abbreviation related to Schwesinger's phosphazenes is introduced: " $(R_2N)P^V_xP^{III}$ " denotes a P^{III} base incorporating x phosphazeryl units. R_2N represents secondary amino substituents at the P^V phosphazene skeleton, typically dimethylamino (dma) and pyrrolidyl (pyrr) groups; however, other secondary amines are also suitable. The title compounds are readily prepared by the reaction of electrophiles $(Me_2N)_2PCl$ (**1a**) or $(Et_2N)_2PCl$ (**1b**), which have a built-in auxiliary base, and phosphazenes $(R_2N)_3P=NH$ (**5**) (Scheme 1). In contrast to the classical Kirsanov reaction applying PCl_3 and an excess of the nucleophile as auxiliary base, our PAP target compounds are formed in good yields and not as an inseparable mixture of ammonium and phosphonium salts.^[18] As PAP hydrochlorides turned out to be hygroscopic, a precipitation step with $NaBF_4$ from aqueous solution leads to crystalline, air-stable, and indefinitely storable P-H functional phosphonium salts $[PAP-H]BF_4$. In an early attempt to prepare the pure base $((Me_2N)_3P=N)_3P$ from its hydrochloride, Kirsanov et al. exchanged chloride for hydroxide (via moist Ag_2O).^[18] Vacuum dehydration of the aqueous solution of $[((R_2N)_3P=N)_3P-H]OH$ led to a viscous liquid, in part probably a hydrate of the base. The basicity of this species was never established experimentally but theoretically.^[19] We discovered that deprotonation of our class of salts $[PAP-H]BF_4$ by potassium hexamethyldisilazide

[*] S. Ullrich, Dr. X. Xie, Prof. Dr. J. Sundermeyer
Fachbereich Chemie, Philipps-Universität Marburg
Hans-Meerwein-Straße, 35032 Marburg (Germany)
E-mail: jsu@staff.uni-marburg.de

Dr. B. Kovačević
The Group for Computational Life Sciences
Rudjer Bošković Institute
Bijenička c. 54, 10000 Zagreb (Croatia)

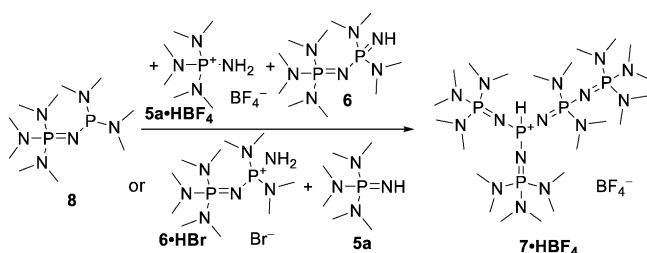
Supporting information and the ORCID identification number(s) for the author(s) of this article can be found under:
<https://doi.org/10.1002/anie.201903342>



Scheme 1. Preparation of P_3P and P_6P phosphonium salts: a) $(\text{dma})_3\text{P}=\text{NH}$ (**5a**) and **1a** or **1b** in THF, 3 h 60°C, 87%; b) $(\text{pyrr})_3\text{P}=\text{NH}$ (**5b**) and **1a** or **1b** in toluene, 3 h 90°C, 96%; c) $(\text{dma})_3\text{P}=\text{N}-\text{P}(\text{dma})_2=\text{NH}$ (**6**) and **1a** in THF, 72 h reflux, 83%. Workup by precipitation from aqueous NaBF_4 described in the Supporting Information

(KHMDS, or comparable metal amides) in toluene or THF leads to colorless solids as pure P^{III} bases.

Based on this strategy the protonated forms of the symmetric $(\text{dma})P_3P$ (**2·HBF₄**) and $(\text{pyrr})P_3P$ (**3·HBF₄**) were isolated in excellent yields. Furthermore it was possible to employ Schwesinger's homologization concept on corresponding phosphines and to synthesize the higher homologue $(\text{dma})P_6P\cdot\text{HBF}_4$ (**4·HBF₄**). For $(\text{dma})P_4P\cdot\text{HBF}_4$ (**7·HBF₄**), which has one bisphosphazanyl and two monophosphazanyl substituents, the standard procedure had to be varied as shown in Scheme 2. The mixed-valent $P^{\text{III}}/P^{\text{V}}$ precursor $(\text{dma})P_1P^{[\text{I}8]}$ (**8**) turned out to be an adequate starting



Scheme 2. Preparation of **7·HBF₄**: **8** and **5a·HBF₄** or **6·HBr** in THF, 1 h 60°C, then **6** or **5a**, respectively, 1 h 60°C, 94%. Workup described in the Supporting Information.

material as it does not react with the phosphazenes (**6** or **5a**), but only with their protonated form (**5a·HBF₄** or **6·HBr**) to the intermediate phosphonium salt. This in turn reacts selectively only with the added phosphazene to **7·HBF₄**, regardless of which building block is used in its free or protonated form.

In the ^{31}P NMR spectra the P^{III} atom in all protonated PAPs exhibits a quartet around $\delta = -30$ ppm, which splits without ^1H -BB decoupling to a doublet of quartets with a $^1J_{\text{PH}}$ coupling constant of ≈ 550 Hz. The phosphorus-bonded proton gives rise to a doublet of quartets between $\delta = 7.89$ and 7.58 ppm in the ^1H NMR spectra. Figure 1 shows the molecular structures of the phosphonium cations with the acidic protons always located at the central phosphorus atom. The formal $\text{P}-\text{N}$ single bonds are significantly shortened to an average bond length of 1.60 Å and approximate to the formal $\text{P}=\text{N}$ double bonds (1.57 Å) and reveal a strong influence of

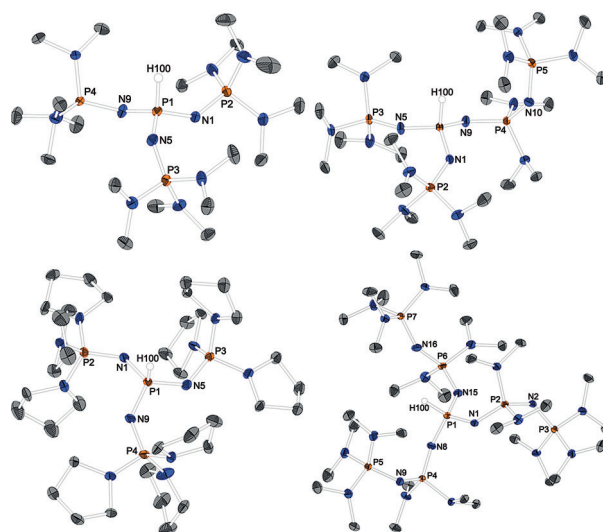


Figure 1. Molecular structures of **2·HBF₄**, **7·HBF₄**, **3·HBF₄**, and **4·HBF₄**. Carbon-bonded hydrogen atoms and anions omitted for clarity, ellipsoids at 50% probability, in the case of disorder only the major component is displayed. Selected bond lengths [Å] and angles [°]: **2·HBF₄**: $P2_1/n$ $P1-N1$ 1.594(1), $P1-N5$ 1.590(1), $P1-N9$ 1.607(1), $N1-P2$ 1.556(1), $N5-P3$ 1.556(1), $N9-P4$ 1.563(1), $P1-N1-P2$ 136.90(9), $P1-N5-P3$ 137.37(9), $P1-N9-P4$ 131.57(9). **7·HBF₄**: $P2_1/c$ $P1-N1$ 1.600(1), $P1-N5$ 1.590(1), $P1-N9$ 1.588(1), $N1-P2$ 1.566(1), $N5-P3$ 1.541(1), $N10-P5$ 1.567(1), $N9-P4$ 1.580(1), $P4-N10$ 1.588(1), $P4-N11$ 1.671(1), $P4-N12$ 1.657(1), $P1-N1-P2$ 137.46(8), $P1-N5-P3$ 157.67(9), $P1-N9-P4$ 133.27(8), $P4-N10-P5$ 132.26(8), $N9-P4-N10$ 120.09(7), $N11-P4-N12$ 111.28(7). **3·HBF₄**: $P-1$ $P1-N1$ 1.598(1), $P1-N5$ 1.602(1), $P1-N9$ 1.596(1), $N1-P2$ 1.568(1), $N5-P3$ 1.579(1), $N9-P4$ 1.562(1), $P1-N1-P2$ 133.00(9), $P1-N5-P3$ 129.02(9), $P1-N9-P4$ 134.0(1). **4·HBF₄**: $P-1$ $P1-N1$ 1.608(2), $P1-N15$ 1.593(2), $P2-N2$ 1.596(2), $P4-N9$ 1.598(2), $P6-N16$ 1.592(2), $N1-P2$ 1.574(2), $N8-P4$ 1.573(2), $N15-P6$ 1.564(2), $N2-P3$ 1.568(2), $N9-P5$ 1.563(2), $N16-P7$ 1.549(2), $P1-N1-P2$ 129.1(1), $P1-N8-P4$ 136.9(1), $P1-N15-P6$ 134.5(1), $P2-N2-P3$ 133.4(1), $P4-N9-P5$ 133.5(1), $P6-N16-P7$ 145.4(1).^[11]

negative hyperconjugation. The $\text{N}-\text{P}=\text{N}$ angles are expanded to between 129.0 and 157.7°. The dimethylamino groups have $\text{P}-\text{N}$ distances of 1.646 Å for terminal phosphazanyl groups, and 1.670 Å in bridging phosphazanyl groups. The pyrrolidine substituents are bonded with an average distance of 1.640 Å. Upon deprotonation the P^{III} atoms are magnetically deshielded with ^{31}P NMR shifts of around $\delta = 80$ ppm, whilst the P^{V} signals are slightly shifted to lower frequencies and the $^2J_{\text{PP}}$ coupling constants become smaller. So far, we have not isolated the free-base form of $(\text{dma})P_6P$ (**4**); however, we could generate it in situ in a suspension of a large excess freshly ground NaNH_2 in THF or potassium pyrrolidide (Kpyrr) in toluene. Deprotonation under the action of organolithium bases resulted in side reactions, whereas potassium in liquid ammonia or ethylenediamine showed no reactivity due to lack of proton acidity. The existence of this probably strongest known uncharged metal-free base **4** could, however, be proven by a combination of ^{31}P NMR spectroscopy and consecutive reactions as well as by calculations. Similar to Schwesinger's $(\text{dma})P_7-t\text{Bu}$ phosphazene counterpart^[2] isolation of an analytically pure sample of the base form $(\text{dma})P_6P$ remains a challenge for future work.

The electron-donor capability of PAPs was quantified by pK_{BH^+} values (Table 1), Tolman electronic parameters (TEPs),^[20] and $^1J_{\text{PSe}}$ coupling constants^[21] (Table 2). Evaluation of NMR titration experiments of the phosphonium salts

Table 1: Calculated proton affinity (PA) and gas-phase basicity (GB) together with calculated and experimental pK_{BH^+} values in THF.

	PA [kcal mol ⁻¹]	GB [kcal mol ⁻¹]	pK_{BH^+} [THF] calcd	pK_{BH^+} [THF] expt
(dma)P ₃ P	297.4	291.3	34.9	34.9 ^[b,c]
(pyrr)P ₃ P	307.5	300.2	37.8	36.7 ^[c]
(dma)P ₄ P	304.3	295.4	37.0	37.2 ^[c]
(dma)P ₆ P	315.4	306.8	41.9	–
P(Ni <i>i</i> Pr) ₃	294.9 ^[a]	288.0 ^[14]	33.8 ^[14]	31.0 ^[14]
Verkade base	259.2	288.0 ^[a]	31.4 ^[a]	
		251.0 ^[a]	–	24.1 ^[10]
(dma)P ₄ - <i>t</i> Bu	296.1	289.6	34.5	33.9 ^[10]
(pyrr)P ₄ - <i>t</i> Bu	303.2	295.6	36.3	35.3 ^[10]

[a] This work. [b] ³¹P NMR titration vs. (dma)P₄-*t*Bu. [c] ³¹P NMR titration vs. (pyrr)P₄-*t*Bu.

Table 2: TEP values and cone angles of nickel carbonyl complexes together with $^1J_{\text{PSe}}$ coupling constants of selenides.

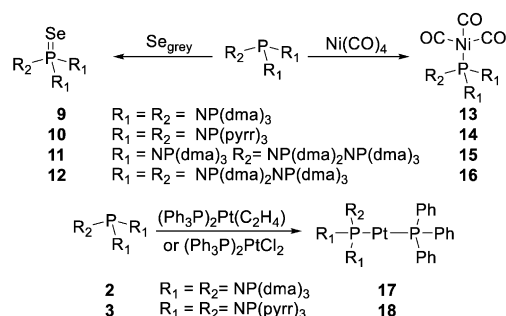
	TEP [cm ⁻¹] ^[a]	Cone angle [°] ^[b]	$^1J_{\text{PSe}}$ [Hz] ^[c]
(dma)P ₃ P	2022.4	203.2	654
(pyrr)P ₃ P	2018.6	198.9	628
(dma)P ₄ P	2017.3	216.5	631
(dma)P ₆ P	2014.5 ^[d]	240.8	608 ^[d]
P(Ni <i>i</i> Pr) ₃	2029.7 ^[14]	182 ^[14]	–
Verkade base	2057.0 ^[26]	173.5	
		152 ^[26]	754 ^[23]
P <i>t</i> Bu ₃	2056.7 ^[20]	147.2	
		168.0	687 ^[24]

[a] Determined via ATR-IR spectroscopy of neat substance. [b] Cone angles calculated in this work represent exact cone angles obtained by procedure described in Ref. [27] (for details see the Supporting Information). [c] $^1J_{\text{PSe}}$ coupling constants determined in this work via ³¹P and ⁷⁷Se NMR spectroscopy in C₆D₆ at room temperature. [d] Reaction of 4-HBF₄, Kpyrr, and Ni(CO)₄ or Se_{grey}, respectively; no pure compound isolated.

against Schwesinger's (dma)P₄-*t*Bu^[2] (pK_{BH^+} in THF: 33.9)^[10] or (pyrr)P₄-*t*Bu^[2] (35.3)^[10] as reference bases revealed the highest pK_{BH^+} values known so far for any phosphines. More importantly, the basicity of phosphines **2** and **3** exceeds the basicity of their corresponding reference phosphazenes by 0.9 and 1.4 units, respectively. Calculated pK_{BH^+} values are in excellent agreement with those obtained experimentally. Therefore, although superbase **4** was not isolated, we could determine its basicity with high accuracy. It appears that the pK_{BH^+} (THF) of **4** surpasses that of (dma)P₄-*t*Bu by 7.1 units. Inspection of data in Table S6 in the Supporting Information reveals that phosphines **2** and **3** possess higher pK_{BH^+} (THF) values than corresponding phosphazenes, whereas **7** and **4** are slightly less basic than the related phosphazenes. The origin of the higher pK_{BH^+} values of the former is their higher intrinsic (gas-phase) basicity, whereas solvation effects work into the

opposite direction: protonated phosphazenes are better solvated in THF than protonated phosphines. The slightly higher basicity of (dma)P₅-*t*Bu and (dma)P₇-*t*Bu phosphazenes in the gas phase and in THF could be attributed to the presence of weak intramolecular hydrogen bonds (IHB) in the conjugate acids (Figure S79) that do not exist in (dma)P₄-*t*Bu and (pyrr)P₄-*t*Bu, nor in any of studied phosphines. However, the influence of the IHB weakens in solvents of higher dielectric constants such as acetonitrile; therefore, in this solvent all studied phosphines are stronger bases than related phosphazenes. Small proton self-exchange rates are indicated by high coalescence temperatures of 1:1 mixtures of PAP bases and their acid forms in NMR solvents (p. S59 in the Supporting Information). These low rates are probably due to the small polarization of the P–H bond compared to N–H. Barriers for the intermolecular proton exchange are 15.5 kcal mol⁻¹ for **2** and 16.5 kcal mol⁻¹ for **3**, which complies with an exchange rate of 13 Hz and 3 Hz, respectively (all at 293 K) and are therefore more in the region of proton sponges rather than of their kinetic highly active phosphazene counterparts.^[2,22] Experimental barriers of proton self-exchange are in good agreement with those computationally obtained which are 14.6 and 18.5 kcal mol⁻¹ (at 298 K) for **2** and **3**, respectively.

Corresponding phosphine selenides **9–12** were obtained by oxidation of PAPs with gray selenium, [(PAP)Ni(CO)₃] complexes **13–16** by reaction with tetracarbonyl nickel (Scheme 3, top). A greater distinction between formal P–N



Scheme 3. Preparation of phosphine selenides **9–12** and nickel carbonyl complexes **13–16** (top) as well as the preparation of Pt⁰ complexes **17** and **18** (bottom): With [(Ph₃P)₂Pt(C₂H₄)] and PAP in a 1:1 ratio; with [(Ph₃P)₂PtCl₂] and PAP in a 1:2 ratio. Detailed conditions given in the Supporting Information.

single and double bonds, compared to that in protonated PAPs, was found in the XRD molecular structures of representative PAP complexes of nickel (**15**) and platinum (**17**) (Figure 2) as well as the selenide **10** (displayed in the Supporting Information) with average formal P=N and P–N bonds of 1.543 Å and 1.624 Å, respectively. The $^1J_{\text{PSe}}$ couplings are in accordance with the trend in PAP basicity: We observe drastically lower coupling constants compared to those of prominently basic phosphorus selenides.^[23,24] Most interestingly, the TEPs of PAPs are considerably lower than those of the recently published IAPs.^[14] Therefore we believe to have discovered the strongest uncharged electron-donating PR₃ ligands currently known. Together with cone angles close

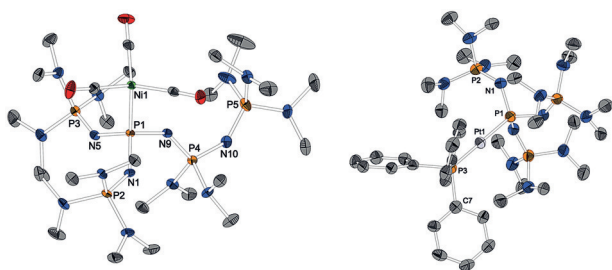


Figure 2. Molecular structures of **15** and **17**. Hydrogen atoms omitted for clarity, ellipsoids at 50% probability, in the case of disorder only the major component is displayed. Selected bond lengths [Å] and angles [°]: **15**: P2₁–P2₂, P1–Ni1 2.2640(7), P1–N1 1.657(2), P1–N5 1.666(2), P1–N9 1.648(2), N1–P2 1.536(2), N5–P3 1.540(2), N10–P5 1.548(2), N9–P4 1.554(2), P4–N10 1.608(2), P4–N11 1.684(2), P4–N12 1.666(2), P1–N1–P2 139.9(2), P1–N5–P3 138.4(2), P1–N9–P4 140.1(1), P4–N10–P5 138.8(2), N9–P4–N10 114.9(1), N11–P4–N12 103.1(1). **17**: P_a–P1–Pd1 2.312(2), P3–Pd1 2.213(2), P1–N1 1.653(3), N1–P2 1.544(3), P1–N1–P2 132.6(2), N1–P1–P3–C7 167.4(2).^[31]

to or even above 200°, PAPs combine steric and electronic properties that are highly valuable for the design of extremely electron-rich transition-metal bases.

The heteroleptic bisphosphine Pt⁰ complexes **17** and **18** were achieved either with Pt⁰ or Pt^{II} precursors (Scheme 3 bottom). In the latter case, the reducing power of PAPs leads to reductive elimination of [PAP–Cl]Cl and substitution of PPh₃ at [(Ph₃P)₂PtCl₂] to form linear 14-valence-electron bisphosphine complexes. XRD data of **17** reveal that the Pt–P bond to the sterically less demanding PPh₃ ligand (2.213 Å) is shorter than that to PAP (2.312 Å), indicating the importance of PPh₃ π-backbonding in contrast to the extreme PAP σ-donation in such heteroleptic model complexes. The assumption of an almost pure and strong PAP–Pt σ-bond is in agreement with results from ³¹P and ¹⁹⁵Pt NMR spectroscopy.^[28,29] The ¹J_{Pt}Pt–PPh₃ coupling constant of 3236 Hz is only about half as large as that of Pt–PAP (6153 Hz). So far this seems to be one of the largest ¹J_{Pt}Pt reported for Pt–PR₃ complexes.^[29] The ¹⁹⁵Pt NMR shift of **17** (δ = –6238 ppm) is in the range of homoleptic [Pt(PrBu₃)₂] (δ_{Pt} = –6471 ppm, ¹J_{Pt}Pt = 4420 Hz, Pt–P 2.249 Å).^[29,30] This indicates that the much stronger electron-donating PAP compensates for the better π-backbonding PPh₃ ligand in the overall shielding.

In summary, we have presented a convenient and high-yielding synthesis, a homologization strategy, and the structural characterization of a class of phosphazeny phosphines (PAPs). To our surprise such uncharged P^{III} superbases often are more basic than their corresponding Schwesinger N-bases. Their kinetic and thermodynamic basicity seems to depend on differences in P–H and N–H bond polarity and solvation effects. Furthermore, it was discovered that PAPs display very large cone angles. They are stronger donor ligands towards transition metals than any other known PR₃ ligand class; consequently they display the lowest Tolman electronic parameters (TEPs) of all PR₃ ligands. Our conclusions are based on experimental and calculated pK_{BH⁺} (THF) values, on calculated proton affinities and gas-phase basicities, on experimental NMR and IR data, and finally on XRD structures of PAP adducts with representative transition

metals, with the non-metal selenium and the simplest electrophile of all, the proton.

Acknowledgements

We thank DAAD (PPP Croatia, Proj. ID 57218955) for travel support. B.K. thanks the University of Zagreb Computing Centre (SRCE) for granting computational time.

Keywords: basicity · phosphane ligands · phosphanes · phosphazenes · superbases

How to cite: *Angew. Chem. Int. Ed.* **2019**, *58*, 10335–10339
Angew. Chem. **2019**, *131*, 10443–10447

- [1] T. Ishikawa, *Superbases for organic synthesis. Guanidines, amidines and phosphazenes and related organocatalysts*, Wiley, Chichester, **2009**.
- [2] a) R. Schwesinger, H. Schlemper, C. Hasenfratz, J. Willaredt, T. Dambacher, T. Breuer, C. Ottaway, M. Fletschinger, J. Boele, H. Fritz, et al., *Liebigs Ann./Recl.* **1996**, 1055; b) R. Schwesinger, C. Hasenfratz, H. Schlemper, L. Walz, E.-M. Peters, K. Peters, H. G. von Schnering, *Angew. Chem. Int. Ed. Engl.* **1993**, *32*, 1361; *Angew. Chem.* **1993**, *105*, 1420; c) R. Schwesinger, H. Schlemper, *Angew. Chem. Int. Ed. Engl.* **1987**, *26*, 1167; *Angew. Chem.* **1987**, *99*, 1212.
- [3] a) D. Zhang, S. K. Boopathi, N. Hadjichristidis, Y. Gnanou, X. Feng, *J. Am. Chem. Soc.* **2016**, *138*, 11117; b) H. Krawczyk, M. Dziegielewski, D. Deredas, A. Albrecht, Ł. Albrecht, *Chem. Eur. J.* **2015**, *21*, 10268; c) S. Boileau, N. Illy, *Prog. Polym. Sci.* **2011**, *36*, 1132; d) U. Köhn, M. Schulz, A. Schramm, W. Günther, H. Görls, S. Schenk, E. Anders, *Eur. J. Org. Chem.* **2006**, 4128; e) D. Uraguchi, S. Sakaki, T. Ooi, *J. Am. Chem. Soc.* **2007**, *129*, 12392; f) M. Ueno, C. Hori, K. Suzawa, M. Ebisawa, Y. Kondo, *Eur. J. Org. Chem.* **2005**, 1965.
- [4] a) K. Vazdar, R. Kunetskiy, J. Saame, K. Kaupmees, I. Leito, U. Jahn, *Angew. Chem. Int. Ed.* **2014**, *53*, 1435; *Angew. Chem.* **2014**, *126*, 1459; b) D. Barić, I. Dragičević, B. Kovačević, *J. Org. Chem.* **2013**, *78*, 4075; c) R. J. Schwamm, R. Vianello, A. Marsavelski, M. A. Garcia, R. M. Claramunt, I. Alkorta, J. Saame, I. Leito, C. M. Fitchett, A. J. Edwards, et al., *J. Org. Chem.* **2016**, *81*, 7612.
- [5] a) J. S. Bandar, A. Barthelme, A. Y. Mazori, T. H. Lambert, *Chem. Sci.* **2015**, *6*, 1537; b) J. S. Bandar, T. H. Lambert, *J. Am. Chem. Soc.* **2012**, *134*, 5552; c) Z. B. Maksić, B. Kovačević, *J. Phys. Chem. A* **1999**, *103*, 6678.
- [6] I. Kaljurand, J. Saame, T. Rodima, I. Koppel, I. A. Koppel, J. F. Kögel, J. Sundermeyer, U. Köhn, M. P. Coles, I. Leito, *J. Phys. Chem. A* **2016**, *120*, 2591–2604.
- [7] a) E. D. Nacsá, T. H. Lambert, *J. Am. Chem. Soc.* **2015**, *137*, 10246; b) A. A. Kolomeitsev, I. A. Koppel, T. Rodima, J. Barten, E. Lork, G.-V. Rösenthaller, I. Kaljurand, A. Kütt, I. Koppel, V. Mäemets, et al., *J. Am. Chem. Soc.* **2005**, *127*, 17656.
- [8] a) J. F. Kögel, B. Oelkers, B. Kovačević, J. Sundermeyer, *J. Am. Chem. Soc.* **2013**, *135*, 17768; b) J. F. Kögel, N.-J. Kneusels, J. Sundermeyer, *Chem. Commun.* **2014**, *50*, 4319; c) J. F. Kögel, B. Kovačević, S. Ullrich, X. Xie, J. Sundermeyer, *Chem. Eur. J.* **2017**, *23*, 2591; d) A. F. Pozharskii, V. A. Ozeryanskii, V. Y. Mikshiev, A. S. Antonov, A. V. Chernyshev, A. V. Metelitsa, G. S. Borodkin, N. S. Fedik, O. V. Dyablo, *J. Org. Chem.* **2016**, *81*, 5574; e) R. Schwesinger, M. Mißfeldt, K. Peters, H. G. von Schnering, *Angew. Chem. Int. Ed. Engl.* **1987**, *26*, 1165; *Angew. Chem.* **1987**, *99*, 1210; f) R. W. Alder, P. S. Bowman, W. R. S. Steele, D. R. Winterman, *Chem. Commun.* **1968**, 723.

- [9] a) I. A. Koppel, R. Schwesinger, T. Breuer, P. Burk, K. Herodes, I. Koppel, I. Leito, M. Mishima, *J. Phys. Chem. A* **2001**, *105*, 9575; b) I. Leito, I. A. Koppel, I. Koppel, K. Kaupmees, S. Tshepelevitsh, J. Saame, *Angew. Chem. Int. Ed.* **2015**, *54*, 9262; *Angew. Chem.* **2015**, *127*, 9394.
- [10] J. Saame, T. Rodima, S. Tshepelevitsh, A. Kütt, I. Kaljurand, T. Haljasorg, I. A. Koppel, I. Leito, *J. Org. Chem.* **2016**, *81*, 7349.
- [11] J. F. Kögel, D. Margetić, X. Xie, L. H. Finger, J. Sundermeyer, *Angew. Chem. Int. Ed.* **2017**, *56*, 3090; *Angew. Chem.* **2017**, *129*, 3136.
- [12] a) P. B. Kisanga, J. G. Verkade, R. Schwesinger, *J. Org. Chem.* **2000**, *65*, 5431; b) C. Lensink, S. K. Xi, L. M. Daniels, J. G. Verkade, *J. Am. Chem. Soc.* **1989**, *111*, 3478.
- [13] a) M. Freytag, V. Plack, P. G. Jones, R. Schmutzler, *Z. Naturforsch. B* **2004**, *59*, 499; b) J. Münchenberg, H. Thönnessen, P. G. Jones, R. Schmutzler, *Phosphorus Sulfur Silicon Relat. Elem.* **1997**, *123*, 57.
- [14] P. Mehlmann, C. Mück-Lichtenfeld, T. T. Y. Tan, F. Dielmann, *Chem. Eur. J.* **2017**, *23*, 5929.
- [15] a) C. V. Reddy, J. V. Kingston, J. G. Verkade, *J. Org. Chem.* **2008**, *73*, 3047; b) M. A. Wünsche, P. Mehlmann, T. Witteler, F. Buß, P. Rathmann, F. Dielmann, *Angew. Chem. Int. Ed.* **2015**, *54*, 11857; *Angew. Chem.* **2015**, *127*, 12024; c) T. Scherpf, C. Schwarz, L. T. Scharf, J.-A. Zur, A. Helbig, V. H. Gessner, *Angew. Chem. Int. Ed.* **2018**, *57*, 12859; *Angew. Chem.* **2018**, *130*, 13041.
- [16] a) T. Witteler, H. Darmandeh, P. Mehlmann, F. Dielmann, *Organometallics* **2018**, *37*, 3064; b) P. Weber, T. Scherpf, I. Rodstein, D. Lichte, L. T. Scharf, L. J. Gooßen, V. H. Gessner, *Angew. Chem. Int. Ed.* **2019**, *58*, 3203; *Angew. Chem.* **2019**, *131*, 3235.
- [17] a) F. Buß, P. Mehlmann, C. Mück-Lichtenfeld, K. Bergander, F. Dielmann, *J. Am. Chem. Soc.* **2016**, *138*, 1840; b) F. Buß, C. Mück-Lichtenfeld, P. Mehlmann, F. Dielmann, *Angew. Chem. Int. Ed.* **2018**, *57*, 4951; *Angew. Chem.* **2018**, *130*, 5045; c) F. Buß, P. Rotering, C. Mück-Lichtenfeld, F. Dielmann, *Dalton Trans.* **2018**, *47*, 10420.
- [18] A. P. Marchenko, G. N. Koidan, A. M. Pinchuk, A. V. Kirsanov, *J. Gen. Chem. USSR* **1984**, *54*, 1581.
- [19] B. Kovačević, Z. B. Maksić, *Chem. Commun.* **2006**, 1524.
- [20] C. A. Tolman, *Chem. Rev.* **1977**, *77*, 313.
- [21] W. McFarlane, D. S. Rycroft, *J. Chem. Soc. Dalton Trans.* **1973**, 2162.
- [22] J. F. Kögel, N. C. Abacılar, F. Weber, B. Oelkers, K. Harms, B. Kovačević, J. Sundermeyer, *Chem. Eur. J.* **2014**, *20*, 5994.
- [23] M. A. H. Laramay, J. G. Verkade, *J. Am. Chem. Soc.* **1990**, *112*, 9421.
- [24] Z. L. Niemeyer, A. Milo, D. P. Hickey, M. S. Sigman, *Nat. Chem.* **2016**, *8*, 610.
- [25] I. Kaljurand, I. A. Koppel, A. Kütt, E.-I. Rööm, T. Rodima, I. Koppel, M. Mishima, I. Leito, *J. Phys. Chem. A* **2007**, *111*, 1245.
- [26] Z. Thammavongsy, I. M. Kha, J. W. Ziller, J. Y. Yang, *Dalton Trans.* **2016**, *45*, 9853.
- [27] J. A. Bilbrey, A. H. Kazez, J. Locklin, W. D. Allen, *J. Comput. Chem.* **2013**, *34*, 1189.
- [28] O. Kühn, *Phosphorus-31 NMR Spectroscopy. A Concise Introduction for the Synthetic Organic and Organometallic Chemist*, Springer-Verlag, Berlin Heidelberg, **2009**.
- [29] R. Benn, H. Michael Büch, R.-D. Reinhardt, *Magn. Reson. Chem.* **1985**, *23*, 559.
- [30] K. J. Moynihan, C. Chieh, R. G. Goel, *Acta Crystallogr. Sect. B* **1979**, *35*, 3060.
- [31] CCDC 1898093 (**2-HBPh₄**), 1898095 (**3-HBPh₄**), 1898099 (**7-HBF₄**), 1898100 (**4-HBF₄**), 1898101 (**15**), 1898102 (**10**) and 1898103 (**17**) contain the supplementary crystallographic data for this paper. These data can be obtained free of charge from The Cambridge Crystallographic Data Centre.

Manuscript received: March 18, 2019
Revised manuscript received: April 29, 2019
Accepted manuscript online: April 30, 2019
Version of record online: June 24, 2019



Phosphazenyolphosphine: Die elektronenreichsten ungeladenen Brønsted- und Lewis-Phosphor-Basen

Sebastian Ullrich, Borislav Kovačević, Xiulan Xie und Jörg Sundermeyer*

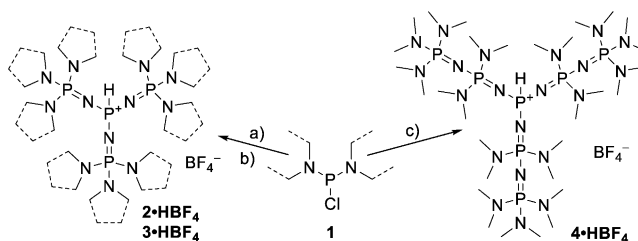
Professor Helmut Werner zum 85. Geburtstag gewidmet

Abstract: Wir entdeckten, dass Phosphazenyolphosphine (PAPs) stärkere P-Superbasen darstellen als ihre korrespondierenden Schwesinger-Phosphazen-N-Superbasen. Ein einfacher synthetischer Zugang zu diesen PR_3 -Derivaten sowie ihre Homologisierung, XRD-Strukturen, Protonenaffinitäten (PA) und Gasphasenbasizitäten (GB), berechnete wie auch experimentelle pK_{BH^+} -Werte werden beschrieben. Im Gegensatz zu ihren N-basischen Verwandten entpuppen PAPs sich darüber hinaus als privilegierte Liganden in der Übergangsmetallchemie. Tatsächlich stellen sie die stärksten bislang bekannten P-Donorliganden dar und überragen sowohl etablierte als auch kürzlich eingeführte Liganden, wie $PtBu_3$ oder Imidazolin-2-ylidenaminophosphine (IAPs), hinsichtlich niedrigerer elektronischer Tolman-Parameter (TEP) und größerer Kegelwinkel.

Ungeladene Superbasen entpuppten sich in den letzten Jahrzehnten als wertvolles Werkzeug in der organischen Synthese.^[1] Rekordhalter an der Spitze der pK_{BH^+} -Skala sind Schwesingers berühmte, gut untersuchte und kommerziell erhältliche Phosphazenenbasen.^[2] Ihr Anwendungsgebiet in der Synthese und Katalyse wächst zunehmend.^[3] Um ähnliche Basizitäten mit anderen nicht-ionischen Superbasen zu erzielen, wurde das Homologisierungskonzept auch auf Guanidine,^[4] Cyclopropenimine^[5] und deren Kombinationen,^[6,7] wie auch auf Protonenschwämme^[8] angewendet. Ein vergleichbares Moleküldesign wurde auch für Kohlenstoffbasen in Theorie und Praxis untersucht.^[9] Dazu gehören Phosphorylide^[10] und bisylidische Protonenpinzetten.^[11] Phosphor(III)-Verbindungen wurden hingegen kaum als starke Protonenakzeptoren in Betracht gezogen.^[6,10] Ihr Hauptaufgabengebiet beschränkte sich bislang auf die Komplexchemie und Übergangsmetallkatalyse. Verkades Proazaphosphatrane sind seltene Vertreter besonders basischer Phosphine.^[12] Schmutzler et al. versuchten das potenziell superbasische Tris(tetramethylguanidino)phosphin zu isolieren, scheiterten

jedoch aufgrund von Zersetzungsreaktionen an der Deprotonierung der P-protonierten konjugierten Säure.^[13] 2017 wurde das Problem der Guanidinzersetzung von Dielmann et al. gelöst, indem ein Imidazol-2-ylidenamin als Guanidin-/Imidazol-artiger Substituent gewählt und so die Klasse elektronenreicher Phosphane (IAPs) mit hoher Basizität und niedrigen elektronischen Tolman-Parametern (TEPs) zugänglich gemacht wurde.^[14]

Wir berichten hier, dass Schwesingers Phosphazene, die bis heute stärksten nicht-ionischen Superbasen, überraschenderweise noch basischer werden, wenn formal die *t*BuN-Nitreneinheit des P^V -Imins reaktiv eliminiert wird. Die daraus resultierende Klasse der Phosphazenyolphosphine (PAPs) ist, anders als Phosphazene, zusätzlich privilegiert, eine große Anzahl an Übergangsmetallkomplexen zu bilden. Somit ergänzen sie Phosphinliganden mit superbasischen Strukturmotiven, wie sie bereits in der Palladium-^[15] oder Goldkatalyse^[16] eingesetzt wurden. Darüber hinaus sind sie selbst auch dazu in der Lage, kleine Moleküle zu aktivieren.^[14,17] In der Tat stellen die über eine einfache Syntheseroute darstellbaren PAPs die stärksten ungeladenen PR_3 -Donoren dar und übertreffen sogar IAPs bezüglich ihrer höheren pK_{BH^+} - und niedrigeren TEP-Werte. In Anlehnung an Schwesingers Phosphazene führen wir folgende Nomenklatur ein: „ $(R_2N)_xP^V_xP^{III}$ “ bezeichnet eine P^{III} -Base, bestehend aus x Phosphazenyleinheiten. R_2N beschreibt dabei die Substituenten des P^V -Phosphazengerüsts, hauptsächlich Dimethylamino- (dma) und Pyrrolidinogruppen (pyrr), wobei auch andere sekundäre Amine verwendet werden können. Die Titelverbindungen sind einfach zugänglich über die Reaktion von Phosphazenen $(R_2N)_3P=NH$ (**5**) mit den Elektrophilen $(Me_2N)_2PCl$ (**1a**) oder $(Et_2N)_2PCl$ (**1b**), deren Aminosubstituenten als Hilfsbase fungieren (Schema 1). Im Gegensatz zur



Schema 1. Darstellung der P_3P und P_6P -Phosphoniumsalze: a) $(dma)_3P=NH$ (**5a**) und **1a** oder **1b** in THF, 3 h 60 °C, 87%; b) $(pyrr)_3P=NH$ (**5b**) und **1a** oder **1b** in Toluol, 3 h 90 °C, 96%; c) $(dma)_3P=N-P(dma)_2=NH$ (**6**) und **1a** in THF, 72 h unter Rückfluss, 83 %. Details zur Fällung als BF_4^- -Salz aus wässriger Lösung sind in den Hintergrundinformationen gegeben.

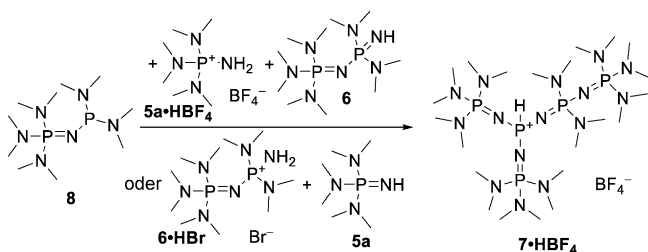
[*] S. Ullrich, Dr. X. Xie, Prof. Dr. J. Sundermeyer
Fachbereich Chemie, Philipps-Universität Marburg
Hans-Meerwein-Straße, 35032 Marburg (Deutschland)
E-Mail: jsu@staff.uni-marburg.de

Dr. B. Kovačević
The Group for Computational Life Sciences
Rudjer Bošković Institute
Bijenička 54, HR-10000 Zagreb (Kroatien)

Hintergrundinformationen und die Identifikationsnummer (ORCID) eines Autors sind unter:
<https://doi.org/10.1002/ange.201903342> zu finden.

klassischen Kirsanov-Reaktion von PCl_3 , mit einem Überschuss an Phosphazenen als Nukleophil und Hilfsbase, werden PAPs in hohen Ausbeuten und nicht in einem aufwendig zu trennenden Gemisch aus Ammonium- und Phosphoniumsalzen erhalten.^[18] Die stabilen, jedoch hygroskopischen Hydrochloride wurden über einen Anionenaustausch aus wässriger Lösung mit NaBF_4 in unbegrenzt lagerbare $[\text{PAP-H}]\text{BF}_4$ -Salze überführt, deren Deprotonierung mit Kaliumhexamethyldisilazid (KHMDs) oder vergleichbaren Metallamiden) in THF oder Toluol selektiv zu den reinen P^{III} -Basen in Form farbloser Feststoffe führte. In früheren Versuchen zur Isolierung der freien Base $((\text{Me}_2\text{N})_3\text{P}=\text{N})_3\text{P}$ aus ihrem Hydrochlorid tauschten Kirsanov et al. das Chloridion gegen Hydroxid über wässriges Ag_2O aus. Die anschließende Dehydratation der wässrigen Lösung von $[(\text{R}_2\text{N})_3\text{P}=\text{N}]_3\text{P-H}]\text{OH}$ führte zu einem viskosen Öl, das vermutlich teilweise aus einem Hydrat der Base bestand.^[18] Deren Basizität wurde bislang nie experimentell bestimmt, wohl aber theoretisch analysiert.^[19]

Mithilfe unserer Strategie konnten die protonierten Formen der symmetrischen Phosphine **(dma)P₃P** (**2-HBF₄**) und **(pyrr)P₃P** (**3-HBF₄**), wie auch die des höheren Homologen **(dma)P₆P-HBF₄** (**4-HBF₄**) in exzellenten Ausbeuten isoliert werden. Für das gemischtsubstituierte **(dma)P₄P-HBF₄** (**7-HBF₄**) musste die Standardprozedur wie in Schema 2 ge-



Schema 2. Darstellung von **7-HBF₄**: **8** und **5a-HBF₄** oder **6-HBr** in THF, 1 h 60 °C, dann **6** bzw. **5a**, 1 h 60 °C, 94 %.

zeigt variiert werden. Dabei stellte sich der gemischtvalente $\text{P}^{\text{III}}/\text{P}^{\text{V}}$ -Vorläufer **(dma)P₁P**^[18](**8**) als adäquates Edukt heraus, da dieses nur mit den protonierten Formen von **5a** oder **6** reagiert und nicht mit den freien Phosphazenen. Diese reagieren hingegen selektiv mit dem intermediär gebildeten P-protonierten Phosphoniumsalz und bilden so **7-HBF₄** als einziges Produkt, unabhängig davon, welches Phosphazen in seiner freien oder protonierten Form vorliegt.

In den ^{31}P -NMR-Spektren zeigen die P^{III} -Atome aller protonierten PAPs bei etwa $\delta = -30$ ppm Quartetts, die ohne ^1H -BB-Entkopplung zusätzlich zu Dubletts mit einer $^1J_{\text{PH}}$ -Kopplungskonstante um 550 Hz aufspalten. In den ^1H -NMR-Spektren zeigt das phosphorgebundene Proton ein Signal in Form eines Dubletts von Quartetts zwischen $\delta = 7.89$ und 7.58 ppm. In Abbildung 1 sind die Molekülstrukturen der Phosphoniumkationen dargestellt, die acid Protonen sind dabei stets am zentralen Phosphoratom lokalisiert. Innerhalb der P-N=P-Einheiten sind die formalen Einfachbindungen mit durchschnittlichen 1.60 Å deutlich verkürzt und an die formalen Doppelbindungen (1.57 Å) angeglichen, die Winkel sind auf 129.0 bis 157.7° aufgeweitet. Beide zeigen damit

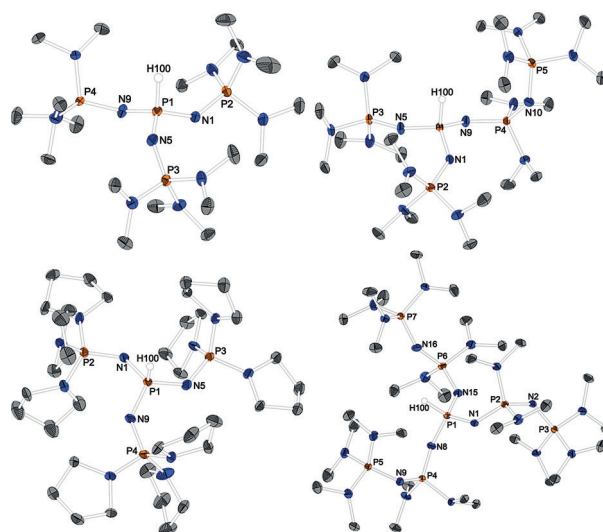


Abbildung 1. Molekülstrukturen von **2-HBF₄**, **7-HBF₄**, **3-HBF₄** und **4-HBF₄**. An Kohlenstoffatome gebundene Protonen, Minoritätskomponenten von Fehlordnungen, sowie die Anionen sind der Übersichtlichkeit halber nicht dargestellt. Ellipsoide bei 50%. Ausgewählte Bindungslängen [Å] und -winkel [°]: **2-HBF₄**: P_2/n P1-N1 1.594(1), P1-N5 1.590(1), P1-N9 1.607(1), N1-P2 1.556(1), N5-P3 1.556(1), N9-P4 1.563(1), P1-N1-P2 136.90(9), P1-N5-P3 137.37(9), P1-N9-P4 131.57(9). **7-HBF₄**: P_2/c P1-N1 1.600(1), P1-N5 1.590(1), P1-N9 1.588(1), N1-P2 1.566(1), N5-P3 1.541(1), N10-P5 1.567(1), N9-P4 1.580(1), P4-N10 1.588(1), P4-N11 1.671(1), P4-N12 1.657(1), P1-N1-P2 137.46(8), P1-N5-P3 157.67(9), P1-N9-P4 133.27(8), P4-N10-P5 132.26(8), N9-P4-N10 120.09(7), N11-P4-N12 111.28(7). **3-HBF₄**: P-1 P1-N1 1.598(1), P1-N5 1.602(1), P1-N9 1.596(1), N1-P2 1.568(1), N5-P3 1.579(1), N9-P4 1.562(1), P1-N1-P2 133.00(9), P1-N5-P3 129.02(9), P1-N9-P4 134.0(1). **4-HBF₄**: P-1 P1-N1 1.608(2), P1-N8 1.590(2), P1-N15 1.593(2), P2-N2 1.596(2), P4-N9 1.598(2), P6-N16 1.592(2), N1-P2 1.574(2), N8-P4 1.573(2), N15-P6 1.564(2), N2-P3 1.568(2), N9-P5 1.563(2), N16-P7 1.549(2), P1-N1-P2 129.1(1), P1-N8-P4 136.9(1), P1-N15-P6 134.5(1), P2-N2-P3 133.4(1), P4-N9-P5 133.5(1), P6-N16-P7 145.4(1).^[31]

starken Einfluss negativer Hyperkonjugation. Dimethylaminosubstituenten zeigen durchschnittliche P-N-Abstände von 1.646 Å für terminale und 1.670 Å in verbrückenden Phosphazenygruppen. Pyrrolidinsubstituenten weisen Bindungslängen von 1.640 Å auf. Durch die Deprotonierung wird das P^{III} -Atom magnetisch entschirmt und zeigt ^{31}P -NMR-Verschiebungen um $\delta = 80$ ppm, während die P^{V} -Signale zu leicht niedrigeren Frequenzen verschoben werden und sich die $^2J_{\text{PP}}$ -Kopplungskonstanten verringern. Leider war es uns bislang nicht möglich, die freie Basenform von **(dma)P₆P** (**4**) zu isolieren; wir konnten sie lediglich in situ in einer Suspension aus NaNH_2 in THF oder Kaliumpyrrolidid (Kpyrr) in Toluol generieren. Der Einsatz von Organolithiumbasen führte zu Nebenreaktionen, während Kalium in flüssigem Ammoniak oder Ethylendiamin aufgrund fehlender P-H-Acidität keine Reaktion zeigte. Die Existenz dieser vermutlich stärksten aller ungeladenen, metallfreien Basen konnte jedoch sowohl über ^{31}P -NMR-Spektroskopie wie auch durch Folgereaktionen belegt werden. Analog zu Schwesingers korrespondierendem **(dma)P₇-tBu**-Phosphazen^[2] bleibt die Isolierung von **(dma)P₆P** in Reinsubstanz eine Herausforderung für die Zukunft.

Tabelle 1: Vergleich berechneter Protonenaffinitäten (PA) und Gasphasenbasizitäten (GB) sowie berechneter und experimenteller pK_{BH^+} -Werte.

	PA [kcal mol ⁻¹]	GB [kcal mol ⁻¹]	pK_{BH^+} (THF) berechnet	pK_{BH^+} (THF) experimentell
(dma)P ₃ P	297.4	291.3	34.9	34.9 ^[b,c]
(pyrr)P ₃ P	307.5	300.2	37.8	36.7 ^[c]
(dma)P ₄ P	304.3	295.4	37.0	37.2 ^[c]
(dma)P ₆ P	315.4	306.8	41.9	–
P(NiPr) ₃	294.9 ^[a]	288.0 ^[14]	33.8 ^[14]	31.0 ^[14]
		288.0 ^[a]	31.4 ^[a]	
Verkades Base	259.2	259.0 ^[25]	–	24.1 ^[10]
		251.0 ^[a]		
(dma)P ₄ -tBu	296.1	289.6	34.5	33.9 ^[10]
(pyrr)P ₄ -tBu	303.2	295.6	36.3	35.3 ^[10]

[a] Diese Arbeit; [b] ³¹P-NMR-Titration gegen (dma)P₄-tBu; [c] ³¹P-NMR-Titration gegen (pyrr)P₄-tBu.

Tabelle 2: Vergleich von TEP-Werten, Kegelwinkeln und ¹J_{PSe}-Kopplungskonstanten.

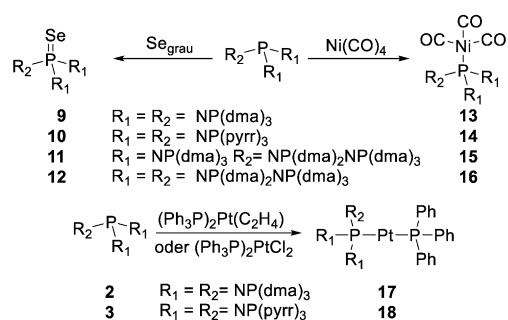
	TEP [cm ⁻¹] ^[a]	Kegelwinkel [°] ^[b]	¹ J _{PSe} [Hz] ^[c]
(dma)P ₃ P	2022.4	203.2	654
(pyrr)P ₃ P	2018.6	198.9	628
(dma)P ₄ P	2017.3	216.5	631
(dma)P ₆ P	2014.5 ^[d]	240.8	608 ^[d]
P(NiPr) ₃	2029.7 ^[14]	182 ^[14] /173.5 ^[b]	–
Verkades Base	2057.0 ^[26]	152 ^[26] /147.2 ^[b]	754 ^[23]
PtBu ₃	2056.1 ^[20]	182 ^[20] /168.0 ^[b]	687 ^[24]

[a] Bestimmt via ATR-IR-Spektroskopie der Reinsubstanzen; [b] Kegelwinkel in dieser Arbeit entsprechen nach Lit. [27] erhaltenen, exakten Kegelwinkeln (Details in den Hintergrundinformationen); [c] ¹J_{PSe}-Kopplungen in dieser Arbeit wurden durch ³¹P- und ⁷⁷Se-NMR-Spektroskopie in C₆D₆ bei Raumtemperatur bestimmt; [d] Reaktion von **4**-HBF₄, Kpyrr und Ni(CO)₄ bzw. Se_{grau}, es konnte kein homogenes Produkt isoliert werden.

Die Stärke von PAPs als Elektronendonoren wurde mittels pK_{BH^+} -Werten (Tabelle 1), den TEPs^[20] und der ¹J_{PSe}-Kopplung korrespondierender Phosphinselenide^[21] (Tabelle 2) quantifiziert. NMR-Titrationen gegen Schwesingers (dma)P₄-tBu^[2] (pK_{BH^+} in THF: 33.9)^[10] oder (pyrr)P₄-tBu^[2] (35.3)^[10] als Referenzbasen offenbarten die höchsten pK_{BH^+} -Werte für Phosphine. Die Basizität von **2** und **3** übersteigt sogar diejenige ihrer korrespondierenden Phosphazene um 0.9 bzw. 1.4 Größenordnungen. Berechnete pK_{BH^+} -Werte stimmen gut mit den experimentellen überein, weshalb wir auch die Basizität der nicht isolierten Superbase **4** präzise vorhersagen können. Es scheint, dass der pK_{BH^+} -Wert (THF) von **4** um 7.1 Größenordnungen über dem von (dma)P₄-tBu liegt. Die Auswertung von Tabelle S6 in den Hintergrundinformationen zeigt, dass die Phosphine **2** und **3** höhere pK_{BH^+} -Werte (THF) als ihre korrespondierenden Phosphazene besitzen, während **7** und **4** im direkten Vergleich marginal weniger basisch sind. Die Ursache für die höheren pK_{BH^+} -Werte der Phosphine liegt in der höheren intrinsischen Gasphasenbasizität, während sich Solvatationseffekte gegenteilig auswirken – protonierte Phosphazene sind in THF besser solvatisiert als protonierte Phosphine. Die im direkten Vergleich leicht höhere Basizität von (dma)P₅-tBu und (dma)P₇-tBu in der Gasphase und in THF kann auf eine intramolekulare

Wasserstoffbrückenbindung (IHB) in der konjugierten Säure zurückgeführt werden (Abbildung S79), die weder in (dma)P₄-tBu oder (pyrr)P₄-tBu, noch in einem der untersuchten Phosphine existiert. Da IHBs in polarerer Lösungsmitteln wie z. B. Acetonitril geschwächt werden, sind in diesem Lösungsmittel alle untersuchten Phosphine basischer als ihre Phosphazene Gegenstücke. Der hohen thermodynamischen Basizität von PAPs steht ein kinetisch gehemmter Protonenaustausch gegenüber (Seite S59 in den Hintergrundinformationen), der vermutlich auf die geringe Polarisierung der P-H-Bindung im Gegensatz zur N-H-Bindung zurückgeführt werden kann. Die Barrieren für den intermolekularen Protonenaustausch liegen bei 15.5 kcal mol⁻¹ für **2** und 16.5 kcal mol⁻¹ für **3**, was einer Austauschrate (bei 293 K) von 13 bzw. 3 Hz entspricht. Sie befinden sich damit eher in der Region von Protonenschwämmen als von kinetisch aktiven Phosphazenen.^[2,22] Die experimentellen Werte stimmen gut mit den berechneten überein, die bei 14.6 kcal mol⁻¹ für **2** bzw. 18.5 kcal mol⁻¹ für **3** liegen (bei 298 K).

Die korrespondierenden Phosphinselenide **9–12** wurden durch Oxidation mit grauem Selen, [(PAP)Ni(CO)₃]-Komplexe **13–16** durch Reaktion mit Tetracarbonylnickel erhalten (Schema 3, oben). In den XRD-Molekülstrukturen reprä-

**Schema 3.** Darstellung der Phosphinselenide **9–12** und Nickelcarbonylkomplexe **13–16** (oben), sowie die Darstellung der Pt⁰-Komplexe **17** und **18** (unten): Aus [(Ph₃P)₂Pt(C₂H₄)] und PAP im Verhältnis 1:1, aus [(Ph₃P)₂PtCl₂] und PAP im Verhältnis 1:2.

sentativer PAP-Komplexe des Nickels (**15**) und Platins (**17**) (Abbildung 2) liegt eine deutlichere Unterscheidung formaler P-N-Einfach- und -Doppelbindungen vor, ebenso im Phosphinselenid **10** (abgebildet in den Hintergrundinformationen) mit durchschnittlichen formalen P=N- und P-N-Bindungslängen von 1.543 Å bzw. 1.624 Å. Die ¹J_{PSe}-Kopplungen bestätigen den Trend in der Basizität und zeigen drastisch kleinere Kopplungskonstanten im Vergleich zu literaturbekannten Phosphinseleniden.^[23,24] Die bestimmten TEPs von PAPs sind sogar deutlich niedriger als die der kürzlich publizierten IAPs,^[14] weshalb wir vermutlich die bislang stärksten elektronendonierenden PR₃-Liganden entdeckt haben. In Verbindung mit Kegelwinkeln nahe oder sogar jenseits der 200° kombinieren PAPs sterische und elektronische Eigenschaften, die beim Design extrem elektronenreicher Übergangsmetallkomplexe von hohem Wert sind.

Die heteroleptischen Bisphosphin-Pt⁰-Komplexe **17** und **18** konnten sowohl aus Pt⁰- als auch Pt^{II}-Präkursoren erhalten

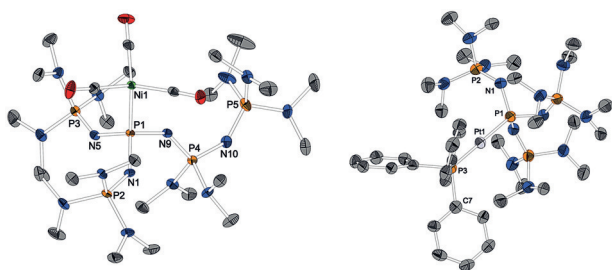


Abbildung 2. Molekülstrukturen von **15** und **17**. Protonen und Minoritätskomponenten von Fehlordnungen sind der Übersichtlichkeit halber nicht dargestellt. Ellipsoide bei 50%. Ausgewählte Bindungslängen [Å] und -winkel [°]: **15**: P2₁,2₁ P1-Ni1 2.2640(7), P1-N1 1.657(2), P1-N5 1.666(2), P1-N9 1.648(2), N1-P2 1.536(2), N5-P3 1.540(2), N10-P5 1.548(2), N9-P4 1.554(2), P4-N10 1.608(2), P4-N11 1.684(2), P4-N12 1.666(2), P1-N1-P2 139.9(2), P1-N5-P3 138.4(2), P1-N9-P4 140.1(1), P4-N10-P5 138.8(2), N9-P4-N10 114.9(1), N11-P4-N12 103.1(1). **17**: Pa-3 P1-Pd1 2.312(2), P3-Pd1 2.213(2), P1-N1 1.653(3), N1-P2 1.544(3), P1-N1-P2 132.6(2), N1-P1-P3-C7 167.4(2).^[31]

werden (Schema 3, unten). Bei letzterem führt das Reduktionspotential der PAPs zu einer Substitution von PPh₃ sowie einer reduktiven Eliminierung von [PAP-Cl]Cl und so zur Bildung linearer 14-Valenzelektronen-Komplexe. Die Molekülstruktur von **17** zeigt eine kürzere Pt-P-Bindung zum sterisch weniger anspruchsvollen PPh₃-Liganden (2.213 Å) als zum PAP (2.312 Å), was auf π -Rückbindungsanteile des PPh₃ zurückzuführen ist, im Kontrast zur extrem starken PAP σ -Hinbindung in diesen heteroleptischen Modellkomplexen. Die Annahme einer reinen und starken PAP-Pt- σ -Bindung wird durch die Ergebnisse aus ³¹P- und ¹⁹⁵Pt-NMR-Spektroskopie gestützt.^[28,29] Die ¹J_{PtP}-Kopplungskonstante zwischen Metallzentrum und PPh₃-Ligand ist mit 3236 Hz nur halb so groß wie die Pt-PAP-Kopplung (6153 Hz), die zu den größten literaturbekannten ¹J_{PtP}-Kopplungskonstanten gehört.^[29] Die ¹⁹⁵Pt-NMR-Verschiebung von **17** ($\delta = -6238$ ppm) liegt im Bereich des homoleptischen Komplexes [Pt(PtBu₃)₂] ($\delta_{Pt} = -6471$ ppm, ¹J_{PtP} = 4420 Hz, Pt-P 2.249 Å)^[29,30] und belegt die Kompensation der elektronenziehenden π -Rückbindung des PPh₃-Liganden durch die σ -Hinbindung des stark elektronendonierenden PAP-Liganden.

Zusammenfassend präsentierten wir eine einfache und zuverlässige Synthese, die Homologisierung sowie die spektroskopische und strukturelle Charakterisierung von Phosphazenyldiphosphanen (PAPs). Zu unserer Überraschung überträgt die Basizität derartiger ungeladener P^{III}-Superbasen oft die ihrer korrespondierenden Schwesinger-N-Basen. Kinetische und thermodynamische Basizität scheinen dabei maßgeblich von Unterschieden in der P-H- bzw. N-H-Bindungspolarisation sowie Solvationseffekten abhängig zu sein. Als die stärksten elektronendonierenden PR₃-Liganden in Kombination mit ihren großen Kegelwinkeln von bis über 200°, scheinen PAPs auch für die Verwendung in Übergangsmetall-Komplexen prädestiniert zu sein. Unsere Schlussfolgerungen beruhen auf experimentellen und berechneten pK_{BH+}-Werten in THF, auf berechneten Protonenaffinitäten und Gasphasenbasizitäten sowie auf NMR-, IR- und XRD-Daten von PAP-Addukten mit repräsentativen Übergangsmetallen, dem Hauptgruppenelement Selen und

schließlich dem einfachsten Elektrophil von allen, dem Proton.

Danksagung

Wir danken dem DAAD (PPP Croatia, Proj. ID 57218955) für Reisekostenbeihilfe. B.K. dankt dem Computerzentrum der Univ. Zagreb (SRCE) für die Bereitstellung von Rechenzeit.

Interessenkonflikt

Die Autoren erklären, dass keine Interessenkonflikte vorliegen.

Stichwörter: Basizität · Phosphane · Phosphanliganden · Phosphazene · Superbasen

Zitierweise: *Angew. Chem. Int. Ed.* **2019**, *58*, 10335–10339
Angew. Chem. **2019**, *131*, 10443–10447

- [1] T. Ishikawa, *Superbases for organic synthesis. Guanidines, amidines and phosphazenes and related organocatalysts*, Wiley, Chichester, **2009**.
- [2] a) R. Schwesinger, H. Schlemper, C. Hasenfratz, J. Willaredt, T. Dambacher, T. Breuer, C. Ottaway, M. Fletschinger, J. Boele, H. Fritz, et al., *Liebigs Ann./Recl.* **1996**, 1055; b) R. Schwesinger, C. Hasenfratz, H. Schlemper, L. Walz, E.-M. Peters, K. Peters, H. G. von Schnering, *Angew. Chem. Int. Ed. Engl.* **1993**, *32*, 1361; *Angew. Chem.* **1993**, *105*, 1420; c) R. Schwesinger, H. Schlemper, *Angew. Chem. Int. Ed. Engl.* **1987**, *26*, 1167; *Angew. Chem.* **1987**, *99*, 1212.
- [3] a) D. Zhang, S. K. Boopathi, N. Hadjichristidis, Y. Gnanou, X. Feng, *J. Am. Chem. Soc.* **2016**, *138*, 11117; b) H. Krawczyk, M. Dzięgielewski, D. Deredas, A. Albrecht, Ł. Albrecht, *Chem. Eur. J.* **2015**, *21*, 10268; c) S. Boileau, N. Illy, *Prog. Polym. Sci.* **2011**, *36*, 1132; d) U. Köhn, M. Schulz, A. Schramm, W. Günther, H. Görls, S. Schenk, E. Anders, *Eur. J. Org. Chem.* **2006**, 4128; e) D. Uraguchi, S. Sakaki, T. Ooi, *J. Am. Chem. Soc.* **2007**, *129*, 12392; f) M. Ueno, C. Hori, K. Suzawa, M. Ebisawa, Y. Kondo, *Eur. J. Org. Chem.* **2005**, 1965.
- [4] a) K. Vazdar, R. Kunetskiy, J. Saame, K. Kaupmees, I. Leito, U. Jahn, *Angew. Chem. Int. Ed.* **2014**, *53*, 1435; *Angew. Chem.* **2014**, *126*, 1459; b) D. Barić, I. Dragičević, B. Kovačević, *J. Org. Chem.* **2013**, *78*, 4075; c) R. J. Schwamm, R. Vianello, A. Marsavelski, M. A. Garcia, R. M. Claramunt, I. Alkorta, J. Saame, I. Leito, C. M. Fitchett, A. J. Edwards, et al., *J. Org. Chem.* **2016**, *81*, 7612.
- [5] a) J. S. Bandar, A. Barthelme, A. Y. Mazori, T. H. Lambert, *Chem. Sci.* **2015**, *6*, 1537; b) J. S. Bandar, T. H. Lambert, *J. Am. Chem. Soc.* **2012**, *134*, 5552; c) Z. B. Maksić, B. Kovačević, *J. Phys. Chem. A* **1999**, *103*, 6678.
- [6] I. Kaljurand, J. Saame, T. Rodima, I. Koppel, I. A. Koppel, J. F. Kögel, J. Sundermeyer, U. Köhn, M. P. Coles, I. Leito, *J. Phys. Chem. A* **2016**, *120*, 2591–2604.
- [7] a) E. D. Nacsa, T. H. Lambert, *J. Am. Chem. Soc.* **2015**, *137*, 10246; b) A. A. Kolomeitsev, I. A. Koppel, T. Rodima, J. Barten, E. Lork, G.-V. Rösenthaller, I. Kaljurand, A. Kütt, I. Koppel, V. Mäemets, et al., *J. Am. Chem. Soc.* **2005**, *127*, 17656.
- [8] a) J. F. Kögel, B. Oelkers, B. Kovačević, J. Sundermeyer, *J. Am. Chem. Soc.* **2013**, *135*, 17768; b) J. F. Kögel, N.-J. Kneusels, J. Sundermeyer, *Chem. Commun.* **2014**, *50*, 4319; c) J. F. Kögel, B. Kovačević, S. Ullrich, X. Xie, J. Sundermeyer, *Chem. Eur. J.*

- 2017, 23, 2591; d) A. F. Pozharskii, V. A. Ozeryanskii, V. Y. Mikshiev, A. S. Antonov, A. V. Chernyshev, A. V. Metelitsa, G. S. Borodkin, N. S. Fedik, O. V. Dyablo, *J. Org. Chem.* **2016**, 81, 5574; e) R. Schwesinger, M. Mißfeldt, K. Peters, H. G. von Schnering, *Angew. Chem. Int. Ed. Engl.* **1987**, 26, 1165; *Angew. Chem.* **1987**, 99, 1210; f) R. W. Alder, P. S. Bowman, W. R. S. Steele, D. R. Winterman, *Chem. Commun.* **1968**, 723.
- [9] a) I. A. Koppel, R. Schwesinger, T. Breuer, P. Burk, K. Herodes, I. Koppel, I. Leito, M. Mishima, *J. Phys. Chem. A* **2001**, 105, 9575; b) I. Leito, I. A. Koppel, I. Koppel, K. Kaupmees, S. Tshepelevitsh, J. Saame, *Angew. Chem. Int. Ed.* **2015**, 54, 9262; *Angew. Chem.* **2015**, 127, 9394.
- [10] J. Saame, T. Rodima, S. Tshepelevitsh, A. Kütt, I. Kaljurand, T. Haljasorg, I. A. Koppel, I. Leito, *J. Org. Chem.* **2016**, 81, 7349.
- [11] J. F. Kögel, D. Margetić, X. Xie, L. H. Finger, J. Sundermeyer, *Angew. Chem. Int. Ed.* **2017**, 56, 3090; *Angew. Chem.* **2017**, 129, 3136.
- [12] a) P. B. Kisanga, J. G. Verkade, R. Schwesinger, *J. Org. Chem.* **2000**, 65, 5431; b) C. Lensink, S. K. Xi, L. M. Daniels, J. G. Verkade, *J. Am. Chem. Soc.* **1989**, 111, 3478.
- [13] a) M. Freytag, V. Plack, P. G. Jones, R. Schmutzler, *Z. Naturforsch. B* **2004**, 59, 499; b) J. Münchenberg, H. Thönnessen, P. G. Jones, R. Schmutzler, *Phosphorus Sulfur Silicon Relat. Elem.* **1997**, 123, 57.
- [14] P. Mehlmann, C. Mück-Lichtenfeld, T. T. Y. Tan, F. Dielmann, *Chem. Eur. J.* **2017**, 23, 5929.
- [15] a) C. V. Reddy, J. V. Kingston, J. G. Verkade, *J. Org. Chem.* **2008**, 73, 3047; b) M. A. Wünsche, P. Mehlmann, T. Witteler, F. Buß, P. Rathmann, F. Dielmann, *Angew. Chem. Int. Ed.* **2015**, 54, 11857; *Angew. Chem.* **2015**, 127, 12024; c) T. Scherpf, C. Schwarz, L. T. Scharf, J.-A. Zur, A. Helbig, V. H. Gessner, *Angew. Chem. Int. Ed.* **2018**, 57, 12859; *Angew. Chem.* **2018**, 130, 13041.
- [16] a) T. Witteler, H. Darmandeh, P. Mehlmann, F. Dielmann, *Organometallics* **2018**, 37, 3064; b) P. Weber, T. Scherpf, I. Rodstein, D. Lichte, L. T. Scharf, L. J. Gooßen, V. H. Gessner, *Angew. Chem. Int. Ed.* **2019**, 58, 3203; *Angew. Chem.* **2019**, 131, 3235.
- [17] a) F. Buß, P. Mehlmann, C. Mück-Lichtenfeld, K. Bergander, F. Dielmann, *J. Am. Chem. Soc.* **2016**, 138, 1840; b) F. Buß, C. Mück-Lichtenfeld, P. Mehlmann, F. Dielmann, *Angew. Chem. Int. Ed.* **2018**, 57, 4951; *Angew. Chem.* **2018**, 130, 5045; c) F. Buß, P. Rotering, C. Mück-Lichtenfeld, F. Dielmann, *Dalton Trans.* **2018**, 47, 10420.
- [18] A. P. Marchenko, G. N. Koidan, A. M. Pinchuk, A. V. Kirsanov, *J. Gen. Chem. USSR* **1984**, 54, 1581.
- [19] B. Kovačević, Z. B. Maksić, *Chem. Commun.* **2006**, 1524.
- [20] C. A. Tolman, *Chem. Rev.* **1977**, 77, 313.
- [21] W. McFarlane, D. S. Rycroft, *J. Chem. Soc. Dalton Trans.* **1973**, 2162.
- [22] J. F. Kögel, N. C. Abacılar, F. Weber, B. Oelkers, K. Harms, B. Kovačević, J. Sundermeyer, *Chem. Eur. J.* **2014**, 20, 5994.
- [23] M. A. H. Laramay, J. G. Verkade, *J. Am. Chem. Soc.* **1990**, 112, 9421.
- [24] Z. L. Niemeyer, A. Milo, D. P. Hickey, M. S. Sigman, *Nat. Chem.* **2016**, 8, 610.
- [25] I. Kaljurand, I. A. Koppel, A. Kütt, E.-I. Rööm, T. Rodima, I. Koppel, M. Mishima, I. Leito, *J. Phys. Chem. A* **2007**, 111, 1245.
- [26] Z. Thammavongsy, I. M. Kha, J. W. Ziller, J. Y. Yang, *Dalton Trans.* **2016**, 45, 9853.
- [27] J. A. Bilbrey, A. H. Kazez, J. Locklin, W. D. Allen, *J. Comput. Chem.* **2013**, 34, 1189.
- [28] O. Köhl, *Phosphorus-31 NMR Spectroscopy. A Concise Introduction for the Synthetic Organic and Organometallic Chemist*, Springer-Verlag, Berlin Heidelberg, **2009**.
- [29] R. Benn, H. Michael Büch, R.-D. Reinhardt, *Magn. Reson. Chem.* **1985**, 23, 559.
- [30] K. J. Moynihan, C. Chieh, R. G. Goel, *Acta Crystallogr. Sect. B* **1979**, 35, 3060.
- [31] CCDC 1898093 (**2-HBPh₄**), 1898095 (**3-HBPh₄**), 1898099 (**7-HBF₄**), 1898100 (**4-HBF₄**), 1898101 (**15**), 1898102 (**10**) und 1898103 (**17**) enthalten die ausführlichen kristallographischen Daten zu dieser Veröffentlichung. Die Daten sind kostenlos beim Cambridge Crystallographic Data Centre erhältlich.

Manuskript erhalten: 18. März 2019

Veränderte Fassung erhalten: 29. April 2019

Akzeptierte Fassung online: 30. April 2019

Endgültige Fassung online: 24. Juni 2019

Supporting Information

Phosphazanyl Phosphines: The Most Electron-Rich Uncharged Phosphorus Brønsted and Lewis Bases

*Sebastian Ullrich, Borislav Kovačević, Xiulan Xie, and Jörg Sundermeyer**

anie_201903342_sm_miscellaneous_information.pdf

Supporting Information

Table of Content

Synthetic Details	S1
NMR Studies (exp. pK_{BH^+} and proton self-exchange)	S50
Crystallographic Details (CCDC Codes)	S60
Computational Details	S64
References	S136

Synthetic Details

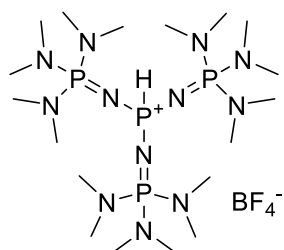
General Remarks

All reactions with air or moisture sensitive substances were carried out under inert atmosphere using standard Schlenk techniques. Air or moisture sensitive substances were stored in a nitrogen-flushed glovebox. Solvents were purified according to common literature procedures and stored under an inert atmosphere over molsieve (3 Å or 4 Å).^[1] Pyrrolidine was distilled from CaH_2 . Potassium bis(trimethylsilyl)amide,^[2] benzyl potassium,^[3] (η^2 -ethylene)bis(triphenylphosphane)platinum(0),^[4] bis(dimethylamino)phosphorus chloride^[5] (**1a**), tris(dimethylamino)phosphazene^[6] (**5a**), tris(pyrrolidino)phosphazene^[6] (**5b**) and (pyrr) P_4 -*t*Bu^[6] were prepared according to literature-known procedures. (dma) P_4 -*t*Bu was purchased as 1M solution in *n*-hexan and dried in high vacuum. All other reagents were used as provided.

^1H , ^{13}C , ^{31}P and ^{77}Se NMR spectra were recorded on a Bruker Avance III HD 250, Avance II 300, Avance III HD 300 or Avance III HD 500 spectrometer. Chemical shift δ is denoted relatively to SiMe_4 (^1H , ^{13}C), 85% H_3PO_4 (^{31}P), SeMe_2 (^{77}Se) or K_2PtCl_6 (^{195}Pt). ^1H and ^{13}C NMR spectra were referenced to the solvent signals,^[7] ^{195}Pt NMR spectra externally to K_2PtCl_4 (0.5M in D_2O , $\delta = -1617.5$ ppm). Multiplicity is abbreviated as follows: s (singlet), d (doublet), t (triplet), q (quartet), m (multiplet), br. (broad signal). High resolution mass spectrometry were performed on a Thermo Fisher Scientific LTQ-FT Ultra or a Jeol AccuTOF GCv., elemental analysis on an Elementar Vario Micro Cube. IR spectra were recorded in a glovebox on a Bruker Alpha ATR-FT-IR.

Tris[tris(dimethylamino)phosphazeny]phosponium tetrafluoridoborate (dma) $P_3P \cdot HBF_4 (2 \cdot HBF_4)$

The preparation of the hydrochloride $2 \cdot HCl$ from phosphorus trichloride was described by Kirsanov et al.^[8]

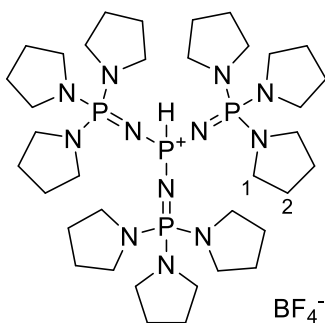


1a (326 mg, 2.11 mmol, 1.00 eq), dissolved in THF (10 mL), was added to a solution of **5a** (1.15 g, 6.45 mmol, 3.06 eq) in THF (30 mL). After stirring for 1 h at room temperature the mixture was heated for 3 h at 60 °C. All volatile components were removed in vacuo and the residue washed with diethyl ether (3x 40 mL). After drying in high

vacuum the hygroscopic $2 \cdot HCl$ was converted to its tetrafluoridoborate salt as described in the general procedure to afford $2 \cdot HBF_4$ (1.196 g, 1.84 mmol, 87%) as colorless solid.

$[C_{18}H_{55}BF_4N_{12}P_4]$ (650.42 $g \cdot mol^{-1}$) 1H -NMR (500.2 MHz, C_6D_6): δ (ppm) = 7.65 (dq, $^1J_{PH} = 554$ Hz, $^3J_{PH} = 5$ Hz, 1H, PH), 2.49 (d, $^3J_{PH} = 10$ Hz, 54H, $N(CH_3)_2$). $^{13}C\{^1H\}$ -NMR (125.8 MHz, C_6D_6): δ (ppm) = 37.1 (d, $^2J_{PC} = 4$ Hz). $^{31}P\{^1H\}$ -NMR (202.5 MHz, C_6D_6): δ (ppm) = 21.5 (d, $^2J_{PP} = 30$ Hz, $P(dma)_3$), -28.9 (q, $^2J_{PP} = 31$ Hz, PH). ^{31}P -NMR (202.5 MHz, C_6D_6): δ (ppm) = 21.5 (br. m, $P(dma)_3$), -28.9 (dq, $^1J_{PH} = 554$ Hz, $^2J_{PP} = 31$ Hz, PH). ESI(+)-MS (MeOH): m/z (%) = 563.7 (100) $[M-BF_4]^+$. ESI(+)-HRMS: m/z $[M-BF_4]^+$ calcd. 563.3618, found 563.3628. Elemental analysis: calcd. C 33.24%, H 8.52%, N 25.84%; found C 32.90%, H 8.52%, N 25.49%. IR (neat): $\tilde{\nu}$ (cm^{-1}) = 2883 (m, CH_3), 2848 (m, CH_3), 2803 (m, CH_3), 2300 (w, PH), 1457 (m), 1289 (m), 1230 (s), 1179 (s), 1094 (m), 1050 (s), 969 (vs), 854 (m), 832 (m), 766 (m), 740 (s), 642 (m), 612 (m), 500 (s). XRD: For single crystal X-ray structure determination BPh_4^- was used instead of BF_4^- . Suitable single crystals were obtained by slowly cooling a concentrated solution in methanol/water.

Tris[tris(pyrrolidino)phosphazeny]phosponium tetrafluoridoborate (pyrr) $P_3P \cdot HBF_4$ ($3 \cdot HBF_4$)

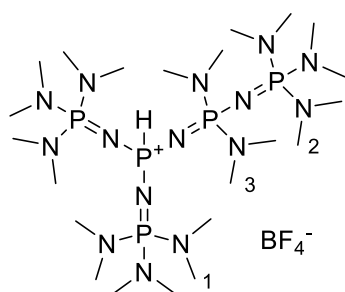


5b (4.494 g, 17.53 mmol, 3.06 eq) was dissolved in toluene (10 mL), added to a solution of **1a** (0.884 g, 5.72 mmol, 1.00 eq) in toluene (10 mL) and stirred for 3 h at 90 °C. All volatile components were removed in vacuo and the resulting colorless solid was washed with diethyl ether (3x 20 mL) to extract the excess of phosphazene. After drying in high vacuum the hygroscopic $3 \cdot HCl$ was converted to its tetrafluoridoborate salt as

described in the general procedure to afford **3**·HBF₄ (4.839 g, 5.47 mmol, 96%) as colorless solid.

[C₃₆H₇₃BF₄N₁₂P₄] (884.76 g·mol⁻¹) ¹H-NMR (300.2 MHz, C₆D₆): δ (ppm) = 7.89 (dq, ¹J_{PH} = 556 Hz, ³J_{PH} = 4 Hz, 1H, PH), 3.21-3.17 (m, 36H, HI), 1.77-1.73 (m, 36H, H2). ¹³C{¹H}-NMR (75.5 MHz, C₆D₆): δ (ppm) = 47.2 (d, ²J_{PC} = 5 Hz, C1), 26.9 (d, ³J_{PC} = 8 Hz, C2). ³¹P{¹H}-NMR (101.3 MHz, C₆D₆): δ (ppm) = 7.9 (d, ²J_{PP} = 24 Hz, P(pyrr)₃), -29.3 (q, ²J_{PP} = 23 Hz, PH). ³¹P-NMR (101.3 MHz, C₆D₆): δ (ppm) = 7.9 (br. d, ²J_{PP} = 24 Hz, P(pyrr)₃), -29.3 (dq, ¹J_{PH} = 555 Hz, ²J_{PP} = 23 Hz, PH). ESI(+)-MS (MeOH): m/z (%) = 798.0 (100) [M-BF₄]⁺. ESI(+)-HRMS: m/z [M-BF₄]⁺ calcd. 797.5026, found 797.5030. Elemental analysis: calcd. C 48.87%, H 8.32%, N 19.00%; found C 48.68%, H 8.36%, N 18.95%. IR (neat): $\tilde{\nu}$ (cm⁻¹) = 2949 (m, CH₂), 2853 (m, CH₂), 2292 (w, PH), 1448 (w), 1345 (w), 1313 (w), 1223 (m), 1202 (s), 1125 (s), 1079 (s), 1046 (s), 994 (s), 912 (m), 866 (m), 813 (m), 765 (m), 701 (w), 587(s), 560 (s), 501 (s). XRD: For single crystal X-ray structure determination BPh₄⁻ was used instead of BF₄⁻. Suitable single crystals were obtained by dissolving in toluene and layering with diethyl ether.

[Pentakis(dimethylamino)diphosphazeny]bis[tris(dimethylamino)phosphazeny]-phosponium tetrafluoridoborate (dma)P₄P·HBF₄ (7·HBF₄)



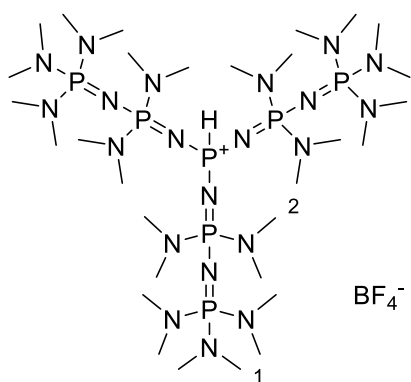
8 (1.519 g, 5.12 mmol, 1.17 eq) was added to a suspension of **5a**·HBF₄ (1.165 g, 4.38 mmol, 1.00 eq) in THF (60 mL) and stirred for 1 h at 60 °C. After cooling to room temperature **6** (1.364 g, 4.38 mmol, 1.00 eq) was added and the mixture was stirred for one additional hour at 60 °C. All volatile components were removed in vacuo and the resulting oil was diluted with *n*-

hexane (40 mL) to precipitate the product, which was washed after decantation of the supernatant solvent with more *n*-hexane (2x 40 mL). Drying in high vacuum afforded **7**·HBF₄ (3.230 g, 4.122 mmol, 94%) as colorless solid.

[C₂₂H₆₇BF₄N₁₅P₅] (783.56 g·mol⁻¹) ¹H-NMR (500.1 MHz, C₆D₆): δ (ppm) = 7.60 (ddt, ¹J_{PH} = 549 Hz, ³J_{PH} = 6 Hz, ³J_{PH} = 2 Hz, 1H, PH), 2.57 (d, ³J_{PH} = 11 Hz, 12H, H3), 2.54 (d, ³J_{PH} = 10 Hz, 18H, H2), 2.53 (d, ³J_{PH} = 10 Hz, 36H, HI). ¹³C{¹H}-NMR (125.8 MHz, C₆D₆): δ (ppm) = 37.6 (d, ²J_{PC} = 4 Hz, C3), 37.2 (d, ²J_{PC} = 5 Hz, C1), 31.1 (d, ²J_{PC} = 5 Hz, C2). ³¹P{¹H}-NMR (101.3 MHz, C₆D₆): δ (ppm) = 19.9 (d, ²J_{PP} = 27 Hz, P1), 16.6 (d, ²J_{PP} = 54 Hz, P2), 2.2 (dd, ²J_{PP} = 54 Hz, ²J_{PP} = 27 Hz, P3), -28.8 (dt, 2x ²J_{PP} = 27 Hz, PH). ³¹P-NMR (101.3 MHz, C₆D₆): δ (ppm) = 19.9 (br. m, P1), 16.6 (br. m, P2), 2.2 (br. m, P3), -28.8 (ddt, ¹J_{PH} = 549 Hz, 2x ²J_{PP}

= 27 Hz, *PH*). ESI(+)-MS (MeOH): m/z (%) = 696.6 (100) $[M-BF_4]^+$. ESI(+)-HRMS: m/z $[M-BF_4]^+$ calcd. 696.4386, found 696.4402. Elemental analysis: calcd. C 33.72%, H 8.62%, N 26.81%; found C 33.64%, H 8.26%, N 26.81%. IR (neat): $\tilde{\nu}$ (cm^{-1}) = 2996 (w, CH_3), 2885 (br. m, CH_3), 2848 (m, CH_3), 2807 (w, CH_3), 2316 (w, *PH*), 1455 (w), 1361 (w), 1269 (s), 1232 (s), 1181 (s), 1093 (m), 1049 (s), 1035 (sh. s), 966 (vs), 860 (m), 808 (w), 794 (w), 736 (s), 642 (m), 591 (w), 499 (s), 480 (m), 447 (m). XRD: For single crystal X-ray structure determination suitable single crystals were obtained by dissolving in toluene and layering with *n*-hexane.

Tris[*pentakis*(dimethylamino)diphosphazeny]phosphonium tetrafluoridoborate
(*dma*)P₆P·HBF₄ (4·HBF₄)



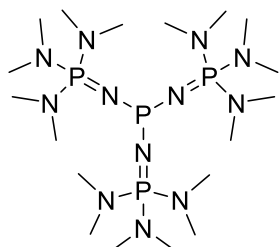
1a (329 mg, 2.13 mmol, 1.00 eq), dissolved in 5 mL THF, was added to a solution of **6** (2.00 g, 6.43 mmol, 3.01 eq) in THF (20 mL). After stirring for 1 h at room temperature a reflux condenser with a bubbler was mounted and the clear reaction mixture was heated for 72 h under reflux conditions. All volatile components were removed in vacuo, *n*-hexane (40 mL) was added to the residue to precipitate the product as colorless solid and separate it from the supernatant solvent

by decantation. After washing with *n*-hexane (2x 20 mL) and drying in high vacuum the hygroscopic **4·HCl** was converted to its tetrafluoridoborate salt as described in the general procedure to afford **4·HBF₄** (1.858 g, 1.77 mmol, 83%) as colorless solid.

$[C_{30}H_{91}BF_4N_{21}P_7]$ (1049.83 $g \cdot mol^{-1}$) 1H -NMR (300.2 MHz, C_6D_6): δ (ppm) = 7.58 (dq, $^1J_{PH} = 540$ Hz, $^3J_{PH} = 5$ Hz, 1H, *PH*), 2.67 (d, $^3J_{PH} = 11$ Hz, 36H, *H2*), 2.57 (d, $^3J_{PH} = 10$ Hz, 54H, *H1*). $^{13}C\{^1H\}$ -NMR (75.5 MHz, C_6D_6): δ (ppm) = 38.0 (d, $^2J_{PC} = 4$ Hz, *C2*), 37.1 (d, $^2J_{PC} = 5$ Hz, *C1*). $^{31}P\{^1H\}$ -NMR (101.3 MHz, C_6D_6): δ (ppm) = 15.3 (d, $^2J_{PP} = 54$ Hz, *P1*), 0.1 (dd, $^2J_{PP} = 54$ Hz, $^2J_{PP} = 23$ Hz, *P2*), -30.6 (q, $^2J_{PP} = 24$ Hz, *PH*). ^{31}P -NMR (101.3 MHz, C_6D_6): δ (ppm) = 15.3 (br. m, *P1*), 0.1 (br. m, *P2*), -30.6 (dq, $^1J_{PH} = 540$ Hz, $^2J_{PP} = 24$ Hz, *PH*). ESI(+)-MS (MeOH): m/z (%) = 962. 8 (100) $[M-BF_4]^+$. ESI(+)-HRMS: m/z $[M-BF_4]^+$ calcd. 962.5924, found 962.5926. Elemental analysis: calcd. C 34.32%, H 8.74%, N 28.02%; found C 34.22%, H 8.65%, N 28.03%. IR (neat): $\tilde{\nu}$ (cm^{-1}) = 2874 (br. m, CH_3), 2796 (m, CH_3), 2308 (w, *PH*), 1456 (m), 1271 (s), 1230 (s), 1178 (s), 1093 (m), 1049 (s), 963 (vs), 857 (s), 786 (m), 736 (m), 641 (s), 586 (m), 507 (s), 479 (s). XRD: For single crystal X-ray structure determination suitable crystals were obtained by slowly evaporating a concentrated solution in diethyl ether.

Tris[tris(dimethylamino)phosphazeny]phosphine (dma)P₃P (2)

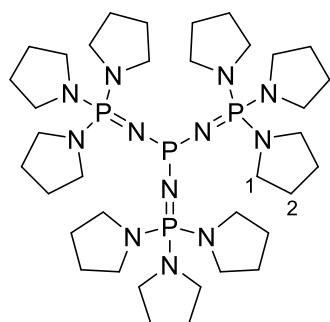
In an early attempt to prepare the free base from its hydrochloride, Kirsanov et al. exchanged chloride for hydroxide (via moist Ag₂O). Vacuum dehydration of [(dma)P₃P-H]OH_{aq} led to a viscous liquid.^[8]



A solution of potassium bis(trimethylsilyl)amide (403 mg, 2.02 mmol, 1.00 eq) in toluene (20 mL) was added slowly to a solution of **2**·HBF₄ (1.314 g, 2.02 mmol, 1.00 eq) and stirred for 30 min at room temperature. Precipitated potassium tetrafluoridoborate was centrifuged off and all volatiles of the clear solution were removed in vacuo. The resulting oil was dissolved in *n*-pentane (30 mL) and filtered over celite. Evaporation of the solvent and drying in high vacuum yielded **2** (985 mg, 1.75 mmol, 87%) as colorless solid.

[C₁₈H₅₄N₁₂P₄] (562.61 g·mol⁻¹) ¹H-NMR (500.2 MHz, C₆D₆): δ (ppm) = 2.74 (d, ³J_{PH} = 10 Hz, 54H). ¹³C{¹H}-NMR (125.8 MHz, C₆D₆): δ (ppm) = 38.2 (dd, ²J_{PC} = 3 Hz, ⁴J_{PC} = 3 Hz). ³¹P{¹H}-NMR (202.5 MHz, C₆D₆): δ (ppm) = 83.4 (q, ²J_{PP} = 19 Hz, P^{III}), 14.4 (d, ²J_{PP} = 21 Hz, P(dma)₃). LIFDI(+)-MS (toluene): m/z (%) = 562.4 (20) [M]⁺, 563.4 (100) [M+H]⁺. LIFDI(+)-HRMS: m/z [M]⁺ calcd. 562.35448, found 562.35234. Elemental analysis: calcd. C 38.43%, H 9.67%, N 29.88%; found C 38.33%, H 9.83%, N 30.15%. IR (neat): $\tilde{\nu}$ (cm⁻¹) = 2991 (w, CH₃), 2865 (m, CH₃), 2831 (m, CH₃), 2788 (m, CH₃), 1453 (m), 1282 (m), 1166 (vs), 1064 (m), 990 (sh. s), 959, (vs), 765 (m), 720 (vs), 609 (m), 572 (s), 518, (w), 481 (m), 442 (m), 414 (w).

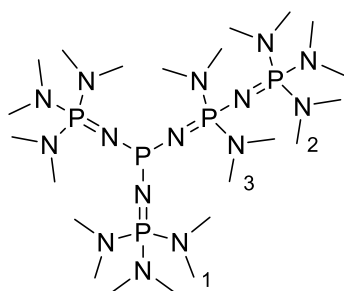
Tris[tris(pyrrolidino)phosphazeny]phosphine (pyrr)P₃P (3)



A solution of potassium bis(trimethylsilyl)amide (341 mg, 1.71 mmol, 1.00 eq) in toluene (20 mL) was added slowly to a solution of **3**·HBF₄ (1.510 g, 1.71 mmol, 1.00 eq) in toluene (30 mL) and stirred for 90 min at room temperature. Precipitated potassium tetrafluoridoborate was centrifuged off and all volatile components of the clear solution were removed in vacuo. The residue was dissolved in *n*-pentane (20 mL), filtered over celite and the filter cake extracted with *n*-pentane (20 mL). The solvent was evaporated and the resulting oil dried in high vacuum until crystallization set in. **3** (1.202 g, 1.51 mmol, 88%) was isolated as colourless solid.

[C₃₆H₇₂N₁₂P₄] (796.95 g·mol⁻¹) ¹H-NMR (500.1 MHz, C₆D₆): δ (ppm) = 3.45-3.41 (m, 36H, *H1*), 1.78-1.73 (m, 36H, *H2*). ¹³C{¹H}-NMR (125.8 MHz, C₆D₆): δ (ppm) = 47.4 (dd, ²J_{PC} = 4 Hz, ⁴J_{PC} = 4 Hz *C1*), 26.9 (d, ³J_{PC} = 8 Hz, *C2*). ³¹P{¹H}-NMR (202.5 MHz, C₆D₆): δ (ppm) = 81.1 (q, ²J_{PP} = 10 Hz, *P^{III}*), 1.35 (d, ²J_{PP} = 12 Hz, *P(pyrr)₃*). ³¹P-NMR (202.5 MHz, C₆D₆): δ (ppm) = 81.1 (q, ²J_{PP} = 10 Hz, *P^{III}*), 1.35 (br. s, *P(pyrr)₃*). LIFDI(+)-MS (THF): m/z (%) = 796.5 (34) [M]⁺, 797.5 (100) [M+H]⁺. LIFDI(+)-HRMS: m/z [M]⁺ calcd. 796.49533, found 796.49287. Elemental analysis: calcd. C 54.26%, H 9.11%, N 21.09%; found C 53.55%, H 9.14%, N 20.92%. IR (neat): $\tilde{\nu}$ (cm⁻¹) = 2953 (m, CH₂), 2843 (m, CH₂), 1456 (w), 1342 (w), 1290 (w), 1179 (s), 1129 (vs), 1059 (vs), 995 (s), 911 (m), 872 (m), 809 (w), 756 (s), 690 (m), 562 (s), 477 (s), 424 (m).

[Pentakis(dimethylamino)diphosphazeny]bis[tris(dimethylamino)phosphazeny]-phosphine (dma)P₄P (7)



A solution of potassium bis(trimethylsilyl)amide (275 mg, 1.38 mmol, 1.01 eq) in 20 mL toluene was added slowly to a solution of **7**·HBF₄ (1.070 g, 1.37 mmol, 1.00 eq) in 30 mL toluene. The yellow suspension was stirred at 90 C for 3 h and centrifuged after cooling to room temperature. All volatiles of the clear solution were removed in vacuo, the residue dissolved in

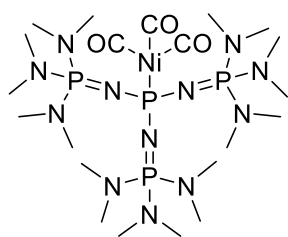
25 mL *n*-hexane and filtered over celite. The filtrate was evaporated and dried in high vacuum to obtain **7** (752 mg, 1.08 mmol, 79%) as pale yellow oil.

[C₂₂H₆₆N₁₅P₅] (695.74 g·mol⁻¹) ¹H-NMR (500.2 MHz, C₆D₆): δ (ppm) = 2.99 (d, ³J_{PH} = 11 Hz, 12H, *H3*), 2.79 (d, ³J_{PH} = 10 Hz, 36H, *H1*), 2.66 (d, ³J_{PH} = 10 Hz, 18H, *H2*). ¹³C{¹H}-NMR (125.8 MHz, C₆D₆): δ (ppm) = 39.0 (dd, *J*_{PC} = 5 Hz, *J*_{PC} = 4 Hz, *C3*), 38.4 (dd, 2x *J*_{PC} = 4 Hz, *C1*), 37.7 (dd, *J*_{PC} = 4 Hz, *J*_{PC} = 3 Hz, *C2*). ³¹P{¹H}-NMR (202.5 MHz, C₆D₆): δ (ppm) = 84.7 (dt, ²J_{PP} = 48 Hz, ²J_{PP} = 18 Hz, *P^{III}*), 19.4 (d, ²J_{PP} = 43 Hz, *P2*), 11.2 (d, ²J_{PP} = 18 Hz, *P1*), 1.0 (dd, 2x ²J_{PP} = 46 Hz, *P3*). ³¹P-NMR (202.5 MHz, C₆D₆): δ (ppm) = 84.7 (dt, ²J_{PP} = 48 Hz, ²J_{PP} = 18 Hz, *P^{III}*), 19.7-19.1 (m, *P2*), 11.2 (br. s, *P1*), 1.0 (br. s, *P3*). LIFDI(+)-MS (THF): m/z (%) = 695.4 (100) [M]⁺. LIFDI(+)-HRMS: m/z [M]⁺ calcd. 695.43137, found 695.43108. IR (neat): $\tilde{\nu}$ (cm⁻¹) = 2991 (w, CH₃), 2867 (sh. m, CH₃), 2834 (s, CH₃), 2788 (s, CH₃), 1455 (m), 1281 (s), 1165 (vs), 1065 (m), 959 (vs), 810 (w), 719 (vs), 635 (m), 622 (m), 568 (s), 485 (s).

General procedure for the preparation of nickeltricarbonyl complexes 9-11

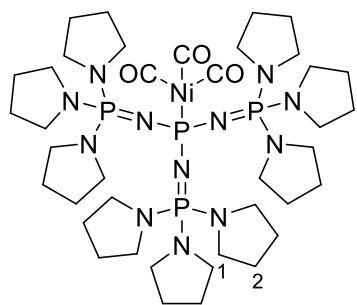
The nickeltricarbonyl complexes of **2**, **3** and **4** were prepared as follows: A solution of the respective phosphine in toluene (5 mL) was added to a solution of tetracarbonylnickel in toluene (5 mL) at 0 °C. The mixture was warmed to room temperature, all volatiles were removed in vacuo, the residue dissolved in *n*-pentane (20 mL) and cleared via syringe filtration. Evaporation of the solvent and drying in high vacuum gave the respective nickeltricarbonyl complexes as colourless to pale yellow solids.

[Tricarbonyl{tris[tris(dimethylamino)phosphazeny]phosphine}nickel(0)] (**9**)



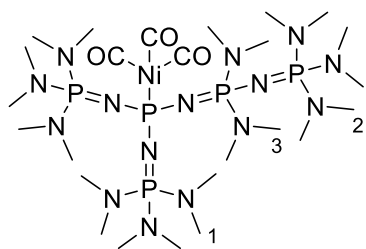
2 (103 mg, 183 μmol , 1 eq) and tetracarbonylnickel (0.03 mL, 0.2 mmol, 1 eq) gave **9** (72 mg, 0.10 mmol, 56%) as pale yellow solid. $[\text{C}_{21}\text{H}_{54}\text{N}_{12}\text{NiO}_3\text{P}_4]$ (705.33 $\text{g}\cdot\text{mol}^{-1}$) $^1\text{H-NMR}$ (500.2 MHz, C_6D_6): δ (ppm) = 2.64 (d, $^3J_{\text{PH}} = 10$ Hz, 54H). $^{13}\text{C}\{^1\text{H}\}\text{-NMR}$ (125.8 MHz, C_6D_6): δ (ppm) = 203.4 (d, $^2J_{\text{PC}} = 9$ Hz, CO), 37.8 (d, $^2J_{\text{PC}} = 4$ Hz, $\text{N}(\text{CH}_3)_2$). $^{31}\text{P}\{^1\text{H}\}\text{-NMR}$ (202.5 MHz, C_6D_6): δ (ppm) = 53.2 (q, $^2J_{\text{PP}} = 18$ Hz, PNi), 3.1 (d, $^2J_{\text{PP}} = 18$ Hz, $\text{P}(\text{dma})_3$). LIFDI(+)-MS (toluene): m/z (%) = 704.3 (100) $[\text{M}]^+$. LIFDI(+)-HRMS: m/z $[\text{M}]^+$ calcd. 704.27458, found 704.27597. Elemental analysis: calcd. C 35.76%, H 7.72%, N 23.83%; found C 36.96%, H 7.72%, N 24.06%. IR (neat): $\tilde{\nu}$ (cm^{-1}) = 2997 (w, CH_3), 2871 (sh. m, CH_3), 2836 (m, CH_3), 2793 (m, CH_3), 2022 (m, CO), 1929 (vs, CO), 1480 (w), 1454 (m), 1409 (w), 1244 (s), 1190 (s), 1065 (m), 967 (vs), 775 (m), 722 (s), 572 (s), 486 (s), 471 (s), 444 (m).

[Tricarbonyl{tris[tris(pyrrolidino)phosphazeny]phosphine}nickel(0)] (**10**)



3 (144 mg, 181 μmol , 1.0 eq) and tetracarbonylnickel (0.10 mL, 0.44 mmol, 2.4 eq) gave **10** as colourless solid. $[\text{C}_{39}\text{H}_{72}\text{N}_{12}\text{NiO}_3\text{P}_4]$ (939.67 $\text{g}\cdot\text{mol}^{-1}$) $^1\text{H-NMR}$ (300.2 MHz, C_6D_6): δ (ppm) = 3.37-3.31 (m, 36H, *HI*), 1.75-1.71 (m, 36H, *H2*). $^{13}\text{C}\{^1\text{H}\}\text{-NMR}$ (75.5 MHz, C_6D_6): δ (ppm) = 203.9 (d, $^2J_{\text{PC}} = 9$ Hz, CO), 47.0 (d, $^2J_{\text{PC}} = 5$ Hz, *CI*), 26.8 (d, $^3J_{\text{PC}} = 9$ Hz, *C2*). $^{31}\text{P}\{^1\text{H}\}\text{-NMR}$ (101.3 MHz, C_6D_6): δ (ppm) = 51.0 (q, $^2J_{\text{PP}} = 21$ Hz, PNi), -11.6 (d, $^2J_{\text{PP}} = 21$ Hz, $\text{P}(\text{pyrr})_3$). LIFDI(+)-MS (toluene): m/z (%) = 797.5 (50) $[\text{M}+\text{H}-\text{Ni}(\text{CO})_3]^+$, 938.4 (100) $[\text{M}]^+$. LIFDI(+)-HRMS: m/z $[\text{M}]^+$ calcd. 938.41543, found 938.41557. IR (neat): $\tilde{\nu}$ (cm^{-1}) = 2959 (m, CH_2), 2861 (m, CH_2), 2019 (m, CO), 1928 (vs, CO), 1902 (sh. w), 1458 (w), 1305 (m), 1290 (m), 1227 (vs), 1196 (s), 1130 (s), 1074 (vs), 1007 (vs), 913 (w), 870 (w), 765 (w), 740 (w), 707 (w), 676 (w), 577 (s), 558 (s), 517 (w), 472 (s).

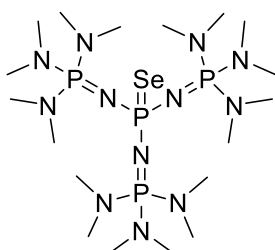
[Tricarbonyl{[pentakis(dimethylamino)diphosphazeny]bis[tris(dimethylamino)-phosphazeny]phosphine}nickel(0)] (11)



7 (138 mg, 198 μmol , 1 eq) and tetracarbonylnickel (0.03 ml, 0.2 mmol, 1 eq) gave **11** (148 mg, 177 μmol , 89%) as colourless crystalline solid.

[$\text{C}_{25}\text{H}_{66}\text{N}_{15}\text{NiO}_3\text{P}_5$] (838.47 $\text{g}\cdot\text{mol}^{-1}$) ^1H -NMR (300.2 MHz, C_6D_6): δ (ppm) = 2.88 (d, $^3J_{\text{PH}} = 11$ Hz, 12H, *H3*), 2.71 (d, $^3J_{\text{PH}} = 10$ Hz, 36H, *H1*), 2.51 (d, $^3J_{\text{PH}} = 10$ Hz, 18H, *H2*). $^{13}\text{C}\{^1\text{H}\}$ -NMR (75.5 MHz, C_6D_6): δ (ppm) = 204.0 (d, $^2J_{\text{PC}} = 9$ Hz, CO), 38.8 (d, $^2J_{\text{PC}} = 4$ Hz, C3), 37.9 (d, $^2J_{\text{PC}} = 4$ Hz, C1), 37.5 (d, $^2J_{\text{PC}} = 4$ Hz, C2). $^{31}\text{P}\{^1\text{H}\}$ -NMR (101.3 MHz, C_6D_6): δ (ppm) = 48.6 (d, $^2J_{\text{PP}} = 69$ Hz, PNi), 12.3 (d, $^2J_{\text{PP}} = 52$ Hz, P2), 1.24 (s, P1), -10.3 (dd, $^2J_{\text{PP}} = 68$ Hz, $^2J_{\text{PP}} = 52$ Hz, P3). LIFDI(+)-MS (benzene): m/z (%) = 696.4 (100) [$\text{M}+\text{H}-\text{Ni}(\text{CO})_3$], 837.4 (29) [M] $^+$. LIFDI(+)-HRMS: m/z [M] $^+$ calcd. 837.35146, found 837.35139. Elemental analysis: calcd. C 35.81%, H 7.93%, N 25.06%; found C 35.34%, H 7.98%, N 24.73%. IR (neat): $\tilde{\nu}$ (cm^{-1}) = 3003 (w, CH_3), 2872 (m, CH_3), 2833 (m) CH_3), 2793 (m, CH_3), 2017 (m, CO), 1927 (vs, CO), 1898 (sh. w), 1482 (m), 1454 (m), 1285 (s), 1180 (vs), 1062 (m), 962 (vs), 820 (w), 770 (s), 723 (s), 705 (s), 624 (m), 582 (m), 564 (m), 525 (m), 493 (s), 467 (s), 438 (sh. m). XRD: The isolated product was suitable for single crystal X-ray structure determination.

Tris[tris(dimethylamino)phosphazeny]phosphine selenide (13)



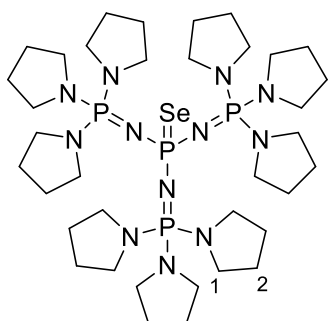
A solution of potassium bis(trimethylsilyl)amide (40 mg, 0.20 mmol, 1.0 eq) in toluene (5 mL) was added to a solution of **2**· HBF_4 (126 mg, 194 μmol , 1.0 eq) in toluene (5 mL). After stirring for 1 h at room temperature, gray selenium (16 mg, 0.20 mmol, 1.0 eq) was added and stirred for 1 h at 90 $^\circ\text{C}$. After cooling to room temperature the mixture

was centrifuged, the supernatant clear solution separated and all volatiles were removed in vacuo. The residue was dissolved in *n*-pentane (10 mL) and cleared via syringe filtration. Removal of the solvent and drying in high vacuum gave **13** as pale yellow solid.

[$\text{C}_{18}\text{H}_{54}\text{N}_{12}\text{P}_4\text{Se}$] (642.27 $\text{g}\cdot\text{mol}^{-1}$) ^1H -NMR (300.2 MHz, C_6D_6): δ (ppm) = 2.79 (d, $^3J_{\text{PH}} = 10$ Hz, 54H). $^{13}\text{C}\{^1\text{H}\}$ -NMR (125.8 MHz, C_6D_6): δ (ppm) = 38.1 (d, $^2J_{\text{PC}} = 4$ Hz). $^{31}\text{P}\{^1\text{H}\}$ -NMR (121.5 MHz, C_6D_6): δ (ppm) = 13.0 (d, $^2J_{\text{PP}} = 35$ Hz, $\text{P}(\text{dma})_3$), -6.7 (q, $^2J_{\text{PP}} = 35$ Hz, $^1J_{\text{PSe}} = 645$ Hz (satellites), PSe). $^{77}\text{Se}\{^1\text{H}\}$ -NMR (95.4 MHz, C_6D_6): δ (ppm) = 137.9 (d, $^1J_{\text{PSe}} = 645$ Hz). LIFDI(+)-MS (toluene): m/z (%) = 642.3 (100) [M] $^+$. LIFDI(+)-HRMS: m/z [M] $^+$

calcd. 642.27108, found 642.26810. Elemental analysis: calcd. C 33.70%, H 8.48%, N 26.20%; found C 34.09%, H 8.46%, N 25.66%.

Tris[tris(pyrrolidino)phosphazeny]phosphine selenide (**14**)

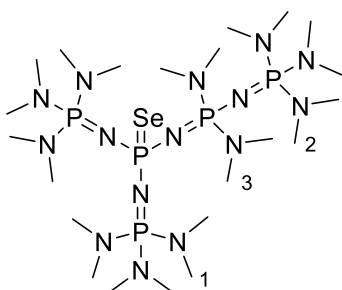


A solution of potassium bis(trimethylsilyl)amide (34 mg, 0.17 mmol, 1.3 eq) in toluene (10 mL) was added to a solution of **3**·HBF₄ (114 mg, 129 μmol, 1.0 eq) in toluene (10 mL) and stirred for 1 h at room temperature. Gray selenium (18 mg, 0.23 mmol, 1.8 eq) was added and the mixture stirred at room temperature overnight. The brown mixture was centrifuged and all volatiles of the clear yellow solution were removed in vacuo. The residue was

dissolved in *n*-pentane (20 mL) and cleared via syringe filtration. The solvent was evaporated slowly and colourless crystalline **14** dried in high vacuum.

[C₃₆H₇₂N₁₂P₄Se] (875.91 g·mol⁻¹) ¹H-NMR (500.2 MHz, C₆D₆): δ (ppm) = 3.52-3.48 (m, 36H, *HI*), 1.83-1.80 (m 36H, *H2*). ¹³C{¹H}-NMR (125.8 MHz, C₆D₆): δ (ppm) = 47.3 (d, ²J_{PC} = 4 Hz, *C2*), 26.9 (d, ³J_{PC} = 9 Hz, *C2*). ³¹P{¹H}-NMR (202.5 MHz, C₆D₆): δ (ppm) = 0.6 (d, ²J_{PP} = 22 Hz, *P*(pyrr)₃), -5.5 (q, ²J_{PP} = 22 Hz, ¹J_{PSe} = 628 Hz (satellites), *PSe*). ⁷⁷Se{¹H}-NMR (95.4 MHz, C₆D₆): δ (ppm) = 190.9 (d, ¹J_{PSe} = 628 Hz). LIFDI(+)-MS (toluene): *m/z* (%) = 876.4 (100) [M]⁺. LIFDI(+)-HRMS: *m/z* [M]⁺ calcd. 876.41216, found 876.41236. Elemental analysis: calcd. C 49.37%, H 8.29%, N 19.19%; found C 49.30%, H 8.38%, N 18.47%. XRD: The isolated product was suitable for single crystal X-ray structure determination.

[Pentakis(dimethylamino)diphosphazeny]bis[tris(dimethylamino)phosphazeny]-phosphine selenide (**15**)



Toluene (20 mL) was added to a mixture of **7**·HBF₄ (170 mg, 217 μmol, 1.0 eq) and potassium bis(trimethylsilyl)amide (44 mg, 0.22 mmol, 1.0 eq) and the mixture was stirred for 1 h at room temperature and 1 h at 90 °C. Gray selenium (19 mg, 0.24 mmol, 1.1 eq) was added and stirred for one additional hour at 90 °C. The solid was centrifuged off and all volatiles of the solution were

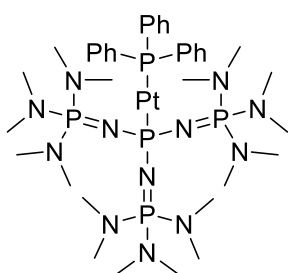
removed in vacuo. The residue was dissolved in *n*-pentane (10 mL), cleared via syringe filtration and dried in high vacuum. **15** was obtained as pale yellow solid.

[C₂₂H₆₆N₁₅P₅Se] (775.35 g·mol⁻¹) ¹H-NMR (300.2 MHz, C₆D₆): δ (ppm) = 2.98 (d, ³J_{PH} = 11 Hz, 12H, *H3*), 2.83 (d, ³J_{PH} = 10 Hz, 36H, *HI*), 2.65 (d, ³J_{PH} = 10 Hz, 18H, *H2*).

$^{13}\text{C}\{^1\text{H}\}$ -NMR (75.5 MHz, C_6D_6): δ (ppm) = 38.9 (d, $^2J_{\text{PC}} = 4$ Hz, C3), 38.2 (d, $^2J_{\text{PC}} = 4$ Hz, C1), 37.6 (d, $^2J_{\text{PC}} = 4$ Hz, C2). $^{31}\text{P}\{^1\text{H}\}$ -NMR (121.5 MHz, C_6D_6): δ (ppm) = 19.0 (d, $^2J_{\text{PP}} = 44$ Hz, P2), 11.2 (d, $^2J_{\text{PP}} = 42$ Hz, P1), -6.9 (dd, $^2J_{\text{PP}} = 44$ Hz, $^2J_{\text{PP}} = 12$ Hz, P3), -13.1 (dt, $^2J_{\text{PP}} = 42$ Hz, $^2J_{\text{PP}} = 12$ Hz, $^1J_{\text{PSe}} = 631$ Hz (satellites), PSe). $^{77}\text{Se}\{^1\text{H}\}$ -NMR (57.3 MHz, C_6D_6): δ (ppm) = 127.6 (d, $^1J_{\text{PSe}} = 631$ Hz). LIFDI(+)-MS (benzene): m/z (%) = 775.3 (100) $[\text{M}]^+$. LIFDI(+)-HRMS: m/z $[\text{M}]^+$ calcd. 775.34801, found 775.34666.

[[Tris[tris(dimethylamino)phosphazanyl]phosphine}(triphenylphosphine)platinum(0)]

(17)

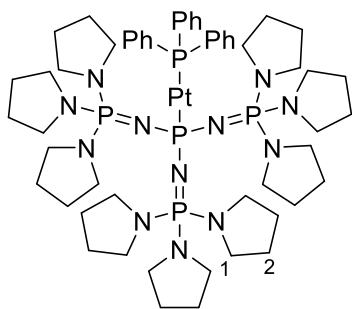


Toluene (10 mL) was added to a mixture of **2**· HBF_4 (173 mg, 265 μmol , 1.0 eq) and potassium bis(trimethylsilyl)amide (58 mg, 0.29 mmol, 1.1 eq) and stirred for 90 min at room temperature. Precipitated potassium tetrafluoridoborate was separated by centrifugation and the supernatant added to a solution of $(\eta^2$ -ethylene)bis(triphenylphosphane)platinum(0) (204 mg, 273 μmol ,

1.0 eq) in toluene (5 mL) and stirred over weekend at room temperature. All volatiles were removed in vacuo, the residue dissolved in *n*-pentane (10 mL) and filtered. The filtrate was stored at -25 $^\circ\text{C}$, the resulting crystals separated by decantation, washed with cold *n*-pentane (4 mL) and dried in high vacuum to isolate **17** as yellow crystals containing one equivalent *n*-pentane as cocrystallize.

$[\text{C}_{36}\text{H}_{69}\text{N}_{12}\text{P}_5\text{Pt}]$ (1019.98 $\text{g}\cdot\text{mol}^{-1}$) ^1H -NMR (300.3 MHz, $\text{THF-}d_8$): δ (ppm) = 7.72-7.66 (m, 6H, *m-H*), 7.21-7.18 (m, 9H, *o,p-H*), 2.76 (d, $^3J_{\text{PH}} = 10$ Hz, 54H, CH_3). $^{13}\text{C}\{^1\text{H}\}$ -NMR (125.8 MHz, C_6D_6): δ (ppm) = 140.2 (d, $^1J_{\text{PC}} = 37$ Hz, *i-C*), 134.9 (d, $^3J_{\text{PC}} = 13$ Hz, *m-C*), 128.3 (overlapped with the solvent signal, *p-C*), 127.6 (d, $^2J_{\text{PC}} = 9$ Hz, *o-C*), 38.3 (d, $^2J_{\text{PC}} = 3$ Hz, CH_3). $^{31}\text{P}\{^1\text{H}\}$ -NMR (121.5 MHz, $\text{THF-}d_8$): δ (ppm) = 87.8 (dq, $^2J_{\text{PP}} = 549$ Hz, $^2J_{\text{PP}} = 26$ Hz, $^1J_{\text{PPt}} = 6147$ Hz (satellites), N_3PPt), 47.1 (d, $^2J_{\text{PP}} = 549$ Hz, $^1J_{\text{PPt}} = 3229$ Hz (satellites), Ph_3PPt), 12.3 (d, $^2J_{\text{PP}} = 26$ Hz, $\text{P}(\text{dma})_3$). $^{195}\text{Pt}\{^1\text{H}\}$ -NMR (64.54 MHz, $\text{THF-}d_8$): δ (ppm) = -6238 (dd, $^1J_{\text{PPt}} = 6153$ Hz, $^1J_{\text{PPt}} = 3236$ Hz). LIFDI(+)-MS (*n*-hexane): m/z (%) = 1019.4 (100) $[\text{M}]^+$. LIFDI(+)-HRMS: m/z $[\text{M}]^+$ calcd. 1019.41039, found 1019.41330. XRD: The isolated crystalline product was suitable for single crystal X-ray structure determination.

[[Tris[tris(pyrrolidino)phosphazeny]phosphine}(triphenylphosphine)platinum(0)] (**18**)



Toluene (15 mL) was added to a mixture of **3**·HBF₄ (242 mg, 274 μmol, 1.0 eq) and potassium bis(trimethylsilyl)amide (60 mg, 0.30 mmol, 1.1 eq) and stirred for 90 min at room temperature. Precipitated potassium tetrafluoroborate was separated by centrifugation and the supernatant added to a solution of (η²-ethylene)bis(triphenylphosphane)platinum(0)

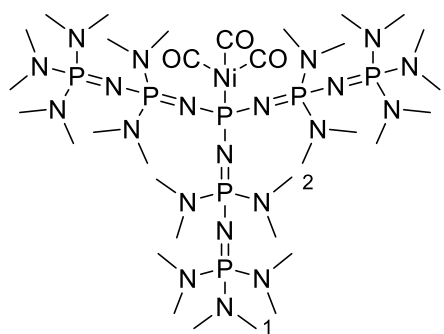
(204 mg, 273 μmol, 1.0 eq) in toluene (5 mL) and stirred for 3 h at 90 °C. All volatiles were removed in vacuo, the residue dissolved in *n*-hexane (20 mL) and filtered. The filtrate was stored at -35 °C, the resulting crystals separated by decantation, washed with cold *n*-pentane (2 mL) and dried in high vacuum to isolate **18** as yellow crystals.

[C₅₄H₈₇N₁₂P₅Pt] (1254.33 g·mol⁻¹) ¹H-NMR (300.3 MHz, THF-*d*₈): δ (ppm) = * 64 (m, 6H, *m*-H), 7.19-7.17 (m, 9H, *o,p*-H), 3.41-3.35 (m, 36H, *HI*), 1.72-1.64 (m, 36H, *H2*). ¹³C{¹H}-NMR (75.7 MHz, C₆D₆): δ (ppm) = 140.8 (dd, ¹J_{PC} = 35 Hz, ³J_{PC} = 2 Hz, *i*-C), 135.0 (dd, ³J_{PC} = 14 Hz, ⁵J_{PC} = 2 Hz, *m*-C), 128.3 (d, ⁴J_{PC} = 1 Hz, *p*-C), 127.5 (d, ²J_{PC} = 9 Hz, *o*-C), 47.7 (d, ²J_{PC} = 4 Hz, *CI*), 27.0 (d, ³J_{PC} = 9 Hz, *C2*). ³¹P{¹H}-NMR (121.5 MHz, THF-*d*₈): δ (ppm) = 87.9 (dq, ²J_{PP} = 553 Hz, ²J_{PP} = 12 Hz, ¹J_{PPt} = 6222 Hz (satellites), N₃PPt), 45.9 (dd, ²J_{PP} = 553 Hz, ⁴J_{PP} = 2 Hz, ¹J_{PPt} = 3185 Hz (satellites), Ph₃PPt), -0.6 (dd, ²J_{PP} = 12 Hz, ⁴J_{PP} = 1 Hz, P(*dma*)₃). ¹⁹⁵Pt{¹H}-NMR (64.54 MHz, THF-*d*₈): δ (ppm) = -6219 (dd, ¹J_{PPt} = 6225 Hz, ¹J_{PPt} = 3183 Hz). LIFDI(+)-MS (*n*-hexane): *m/z* (%) = 1253.6 (100) [M]⁺. LIFDI(+)-HRMS: *m/z* [M]⁺ calcd. 1253.55124, found 1253.55229. Elemental analysis: calcd. C 51.71%, H 6.99%, N 13.40%; found C 51.84%, H 6.96%, N 13.78%.

Deprotonation attempts of (dma)₃P₆P·HBF₄ (**4**·HBF₄)

Several bases were tested for deprotonation of **4**·HBF₄, such as lithium di-*iso*-propylamid, potassium bis(trimethylsilyl)amide, potassium hydrid, benzyl potassium, elemental potassium and *n*- or *t*- butyllithium, which showed either no reaction or decomposition. Only excess of sodium amide in THF lead to a mixture of free **4** and **4**·HBF₄ Finally potassium pyrrolidid in toluene fully deprotonated the starting material for consecutive reactions but isolation of the free base was not possible.

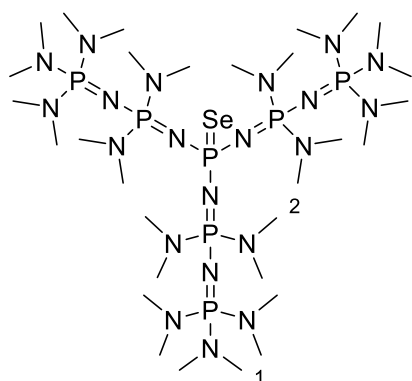
[Tricarbonyl{tris[pentakis(dimethylamino)diphosphazeny]phosphine}nickel(0)] (12)



4·HBF₄ (49 mg, 47 μmol, 1 eq) was dissolved in toluene (5 mL) and cooled to 0 °C. A solution of potassium pyrrolidid (5 mg, 0.05 mmol, 1 eq) in toluene (7 mL) was added slowly, the mixture allowed to warm to room temperature and added afterwards to a solution of tetracarbonylnickel (0.01 mL, 0.08 mmol, 1 eq) in toluene (8 mL). All volatiles were removed in vacuo the residue

dissolved in *n*-pentane (10 mL) and cleared via syringe filtration. The solvent was evaporated and the residue used for analytics. [C₃₃H₉₀N₂₁NiO₃P₇] (1104.74 g·mol⁻¹) ³¹P{¹H}-NMR (101.3 MHz, C₆D₆): δ (ppm) = 46.4 (q, ²J_{PP} = 23 Hz, PNi), 7.4 (d, ²J_{PP} = 56 Hz, P1), -13.9 (dd, ²J_{PP} = 56 Hz, ²J_{PP} = 23 Hz, P2). IR (neat): $\tilde{\nu}$ (cm⁻¹) = 2015 (w, CO), 1926 (s, CO). Since no pure product could be isolated, the IR spectrum was calculated to ensure the correct bands were assigned.

Tris[pentakis(dimethylamino)diphosphazeny]phosphine selenide (16)



4·HBF₄ (49 mg, 47 μmol, 1 eq) was dissolved in toluene (5 mL) and cooled to 0 °C. A solution of potassium pyrrolidid (5 mg, 0.05 mmol, 1 eq) in toluene (7 mL) was added slowly, the mixture allowed to warm to room temperature and added afterwards to a suspension of gray selenium (4 mg, 0.05 mmol, 1 eq) in toluene (8 mL). The mixture was stirred at room temperature over night, all volatiles were removed in vacuo the residue dissolved in *n*-

pentane (10 mL) and cleared via syringe filtration. The solvent was evaporated and the residue dissolved in C₆D₆.

[C₃₀H₉₀N₂₁P₇Se] (1040.97g·mol⁻¹) ³¹P{¹H}-NMR (202.5 MHz, C₆D₆): δ (ppm) = 12.1 (d, ²J_{PP} = 54 Hz, P1), -9.7 (dd, ²J_{PP} = 54 Hz, ²J_{PP} = 21 Hz, P2), -17.6 (q, ²J_{PP} = 21 Hz, ¹J_{PSe} = 608 Hz (satellites), PSe). ⁷⁷Se-NMR (95.4 MHz, C₆D₆): δ (ppm) = 120.4 (d, ¹J_{PSe} = 609 Hz). LIFDI(+)-MS (C₆D₆): m/z (%) = 978.6 (100) [M+O-Se], 1039.5 (27) [M]⁺. LIFDI(+)-HRMS: m/z [M]⁺ calcd. 1039.50244, found 1039.50367.

NMR Studies

NMR Titration Experiments

The pK_{BH^+} values of three phosphine super bases (dma)P₃P (**2**), (pyrr)P₃P (**3**), (dma)P₄P (**7**) were determined via NMR titration. The general procedure for NMR titration experiments for the determination of pK_{BH^+} values was described elsewhere.^[9] Adding to the initial amount of a super base in its protonated form a similar amount of a Schwesinger base in THF, an equilibrium in competition of protons in solution was quickly reached. In order to have quantitative ³¹P NMR spectra relaxation times of all ³¹P signals were first determined using the standard inversion recovery procedure. Quantitative ³¹P NMR spectra were thus recorded by inverse gated decoupling method with a relaxation delay of 30 s. Therefore, signal intensities of the central phosphorus (P^{III}) in its free and protonated form, as well as the terminal phosphorus (P^V) of the Schwesinger base in its free and protonated form, revealed the molar ratio of the different species at equilibrium. On the bases of these signal intensities equilibrium constants were thus calculated and the unknown pK_{BH^+} values determined.

A mixture of (dma)P₃P·HBF₄ and (dma)P₄-*t*Bu (pK_{BH^+} (THF) = 33.9)^[10] in THF did show a neat signal at 82 ppm which was due to P^{III} in its free form, whereas in a similar experiment of (pyrr)P₃P·HBF₄ or (dma)P₄P·HBF₄ mixed with (dma)P₄-*t*Bu, no signal corresponding to the free base could be observed. This meant that a basicity of both higher than that of (dma)P₄-*t*Bu could be expected and a stronger base was necessary for the purpose. Thus, experiments were then carried out with (pyrr)P₄-*t*Bu (pK_{BH^+} (THF) = 35.3)^[10] in THF.

Results. Results of thermal dynamic basicity determination are shown in Tables S1-S3. Thus, the pK_{BH^+} of THF scale of super bases **2**, **3** and **7** were determined to be 34.9 ± 0.2 , 36.7 ± 0.1 and 37.2 ± 0.1 . The ³¹P NMR spectra of the titration experiments are given in Figures S65-S76.

Table S1: ³¹P NMR titration experiments for pK_{BH^+} determination of (dma)P₃P (**2**).

Experiment 1	2 ·HBF ₄	(dma)P ₄ - <i>t</i> Bu	2	(dma)P ₄ - <i>t</i> Bu·HBF ₄
Initial weight / mg	6.478	6.337	0.00	0.00
Initial amount / μmol	9.96	10.00	0.00	0.00
Final amount / μmol	7.66	7.70	2.30	2.30
pK_{BH^+} (2) = pK_{BH^+} ((pyrr)P ₄ - <i>t</i> Bu) – log $K = 33.9 - \log [2.30^2 \div (7.65 \times 7.70)] = 35.0$				
Experiment 2	2 ·HBF ₄	(dma)P ₄ - <i>t</i> Bu	2	(dma)P ₄ - <i>t</i> Bu·HBF ₄
Initial weight / mg	5.976	5.941	0.00	0.00
Initial amount / μmol	9.19	9.38	0.00	0.00
Final amount / μmol	7.24	7.43	1.95	1.95
pK_{BH^+} (2) = pK_{BH^+} ((pyrr)P ₄ - <i>t</i> Bu) – log $K = 33.9 - \log [1.95^2 \div (7.24 \times 7.43)] = 35.1$				

Experiment 3	2 ·HBF ₄	(pyrr)P ₄ - <i>t</i> Bu	2	(pyrr)P ₄ - <i>t</i> Bu·HBF ₄
Initial weight / mg	7.276	9.007	0.00	0.00
Initial amount / μmol	11.19	10.38	0.00	0.00
Final amount / μmol	4.60	3.16	6.59	7.22
$pK_{BH^+}(\mathbf{2}) = pK_{BH^+}((pyrr)P_4-tBu) - \log K = 35.3 - \log [(6.59 \times 7.22) \div (4.60 \times 3.79)] = 34.9$				
Experiment 4	2 ·HBF ₄	(pyrr)P ₄ - <i>t</i> Bu	2	(pyrr)P ₄ - <i>t</i> Bu·HBF ₄
Initial weight / mg	6.958	9.195	0.00	0.00
Initial amount / μmol	10.70	10.59	0.00	0.00
Final amount / μmol	4.02	3.47	6.68	7.12
$pK_{BH^+}(\mathbf{2}) = pK_{BH^+}((pyrr)P_4-tBu) - \log K = 35.3 - \log [(6.68 \times 7.12) \div (4.02 \times 3.47)] = 34.8$				

Table S2: ³¹P NMR titration experiments for pK_{BH⁺} determination of (pyrr)P₃P (**3**).

Experiment 1	3 ·HBF ₄	(pyrr)P ₄ - <i>t</i> Bu	3	(pyrr)P ₄ - <i>t</i> Bu·HBF ₄
Initial weight / mg	5.284	5.533	0.00	0.00
Initial amount / μmol	5.97	6.37	0.00	0.00
Final amount / μmol	5.33	4.80	0.64	1.57
$pK_{BH^+}(\mathbf{2}) = pK_{BH^+}((pyrr)P_4-tBu) - \log K = 35.3 - \log [(0.64 \times 1.57) \div (5.33 \times 4.80)] = 36.7$				
Experiment 2	3 ·HBF ₄	(pyrr)P ₄ - <i>t</i> Bu	3	(pyrr)P ₄ - <i>t</i> Bu·HBF ₄
Initial weight / mg	5.763	6.130	0.00	0.00
Initial amount / μmol	6.51	7.06	0.00	0.00
Final amount / μmol	5.63	5.63	0.88	1.43
$pK_{BH^+}(\mathbf{3}) = pK_{BH^+}((pyrr)P_4-tBu) - \log K = 35.3 - \log [(0.88 \times 1.43) \div (5.63 \times 5.63)] = 36.7$				
Experiment 3	3 ·HBF ₄	(pyrr)P ₄ - <i>t</i> Bu	3	(pyrr)P ₄ - <i>t</i> Bu·HBF ₄
Initial weight / mg	5.791	6.049	0.00	0.00
Initial amount / μmol	6.55	6.97	0.00	0.00
Final amount / μmol	5.62	5.53	0.93	1.44
$pK_{BH^+}(\mathbf{3}) = pK_{BH^+}((pyrr)P_4-tBu) - \log K = 35.3 - \log [(0.93 \times 1.44) \div (5.62 \times 5.53)] = 36.7$				

Table S3: ^{31}P NMR titration experiments for $\text{p}K_{\text{BH}^+}$ determination of (dma) P_4P (**7**).

Experiment 1	7 · HBF_4	(pyrr) P_4 - <i>t</i> Bu	7	(pyrr) P_4 - <i>t</i> Bu· HBF_4
Initial weight / mg	6.517	7.309	0.00	0.00
Initial amount / μmol	8.32	8.42	0.00	0.00
Final amount / μmol	7.92	6.74	0.39	1.68
$\text{p}K_{\text{BH}^+}(\mathbf{7}) = \text{p}K_{\text{BH}^+}(\text{(pyrr)}\text{P}_4\text{-}t\text{Bu}) - \log K = 35.3 - \log [(0.39 \times 1.68) \div (7.92 \times 6.74)] = 37.2$				
Experiment 2	7 · HBF_4	(pyrr) P_4 - <i>t</i> Bu	7	(pyrr) P_4 - <i>t</i> Bu· HBF_4
Initial weight / mg	8.951	12.705	0.00	0.00
Initial amount / μmol	11.42	14.65	0.00	0.00
Final amount / μmol	10.67	12.35	0.75	2.30
$\text{p}K_{\text{BH}^+}(\mathbf{7}) = \text{p}K_{\text{BH}^+}(\text{(pyrr)}\text{P}_4\text{-}t\text{Bu}) - \log K = 35.3 - \log [(0.75 \times 2.30) \div (10.67 \times 12.35)] = 37.2$				
Experiment 3	7 · HBF_4	(pyrr) P_4 - <i>t</i> Bu	7	(pyrr) P_4 - <i>t</i> Bu· HBF_4
Initial weight / mg	9.730	14.320	0.00	0.00
Initial amount / μmol	12.42	16.50	0.00	0.00
Final amount / μmol	11.54	13.91	0.88	2.59
$\text{p}K_{\text{BH}^+}(\mathbf{7}) = \text{p}K_{\text{BH}^+}(\text{(pyrr)}\text{P}_4\text{-}t\text{Bu}) - \log K = 35.3 - \log [(0.88 \times 2.59) \div (11.54 \times 15.62)] = 37.2$				

Self-Exchange Results

Both ^1H and ^{31}P spectra of the free base and the corresponding protonated species of **2** and **3** in THF were recorded for sample control. Spectrometer was Bruker AV III 500 installed with a cryo Prodigy probe head. The ^{31}P – ^{31}P exchange spectra were recorded with the pulse sequence EXSYX for observing slow exchange between two sites of heteronuclear with ^1H decoupling in acquisition time.^[11] Relaxation time of the ^{31}P resonances was measured. The spectral width for the 2D EXSYX was 140 ppm, with a relaxation delay of 9 s. Mixing times were 10, 20, and 30 ms for sample A; 15, 30, 50 ms for sample B, throughout temperatures at 293, 303, 313, and 323 K.

Sample A: **2**· HBF_4 (15.512 mg, 23.849 μmol , 1.00 eq) and **2** (13.842 mg, 24.603 μmol , 1.03 eq) in 0.5 mL THF-*d*₈.

Sample B: **3**· HBF_4 (15.666 mg, 17.706 μmol , 1.00 eq) and **3** (14.090 mg, 17.680 μmol , 1.00 eq) in 0.5 mL THF-*d*₈.

Detailed procedure for the study of the kinetic basicity of a super base through observing its proton self-exchange by two-dimensional NMR exchange spectroscopy has been published previously.^[9] The EXSYX results on **2** and **3** self-exchange in THF are summarized in Table S4 and S5.

Table S4: Self-exchange kinetics of **2** with $2\cdot\text{H}^+$ (mole ratio 1:1) in THF- d_8 .

Temperature/K	Exchange Rate k/s^{-1}	Free Energy $\Delta G^\ddagger/\text{kJ}\cdot\text{mol}^{-1}$
293	13	65.0
303	26	66.0
313	43	66.9
323	60	67.9

Table S5: Self-exchange kinetics of **3** with $3\cdot\text{H}^+$ (mole ratio 1:1) in THF- d_8 .

Temperature/K	Exchange Rate k/s^{-1}	Free Energy $\Delta G^\ddagger/\text{kJ}\cdot\text{mol}^{-1}$
293	3	69.1
303	8	69.5
313	16	70.0
323	31	70.4

Eyring plots on the basis of four temperatures were obtained and shown in Figure S77 and S78.

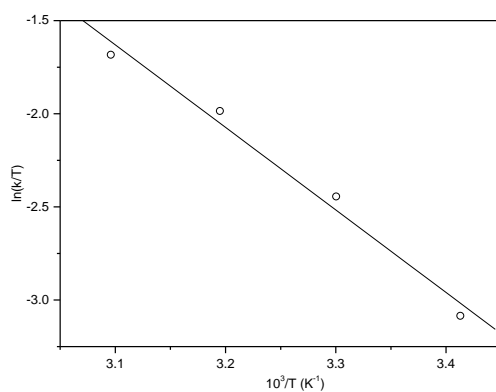


Figure S77: Eyring plot of proton self-exchange of **2** with $2\cdot\text{H}^+$ (0.5 : 0.5) in THF- d_8 .

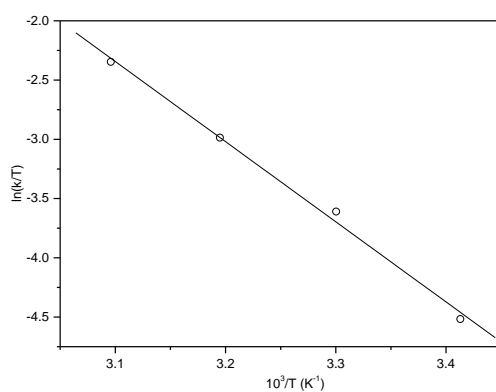


Figure S78: Eyring plot of proton self-exchange of **3** with $3\cdot\text{H}^+$ (0.5 : 0.5) in THF- d_8 .

Computational Details

Calculations in the gas phase are performed at the B3LYP-D3/6-311+G(2df,p)//B3LYP-D3/6-31+G(d) level of theory. All structures were optimized without any geometry constraints and confirmed to be an energy minimum on potential energy surface by computing their vibrational frequencies analytically. Free energies of solvation for acetonitrile and THF solvent were obtained with the SMD model utilizing M062X functional and 6-31+G(d) basis set. Calculations has been performed with Gaussian09 program package.^[19]

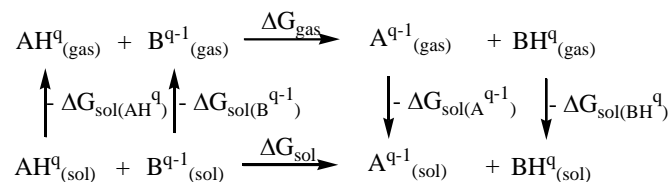
Gas phase basicities (GB) have been calculated as the Gibbs free energy ΔG of the (gas phase) reaction: $B + H^+ \rightarrow BH^+$

So, the gas basicity is calculated as: $GB = G(BH^+) - [G(B) + G(H^+)]$.

G of the neutral and protonated species contains the electronic energy E_{el} obtained at B3LYP-D3/6-311+G(2df,p)//B3LYP-D3/6-31+G(d)) level of theory and the thermal correction to free energy, G_{therm} , which sums the zero point vibrational energy (ZPVE), enthalpic and entropic contribution at 298 K.

Proton affinities (PA) in the gas phase are calculated as the enthalpy of the aforementioned reaction. $PA = H(BH^+) - [H(B) + H(H^+)]$.

pK_a values have been estimated as a relative values utilizing following thermodynamic cycle:^[20]



Total charge of the acids and the conjugate bases are represented by q and q^{-1} , respectively. The main advantage of this approximation in pK_a calculations is the expected error cancellation of solvation free energies of the charged molecules in both sides of the chemical equation. Reference base was selected on the basis of similar geometry, electronic structure and accurately measured pK_a value. Tricyclohexylphosphine (PCy₃) with pK_a value of 9.7^[21] and trimethylphosphine (PCH₃)₃ with pK_a value of 15.5^[22] served as a reference bases for calculaton of pK_a values in THF and MeCN solvents, respectively. According to the above thermodynamic cycle, the basicity of a base **B** can be calculated relative to the known basicity of base **A** by following equation:

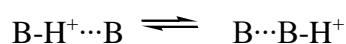
$$pK(BH^+) = pK(AH^+) + \{G_{gas}(B) - G_{gas}(A) - G_{gas}(BH^+) + G_{gas}(AH^+) + \Delta G_{sol}(B) - \Delta G_{sol}(A) - \Delta G_{sol}(BH^+) + \Delta G_{sol}(AH^+)\}/2.303RT$$

where symbols have their usual meaning.

Table S6: Calculated gas phase proton affinity (PA) and gas phase basicity (GB) together with calculated pK_{BH^+} values in THF and MeCN of P_xP phosphines and corresponding phosphazenes.

	PA / kcal·mol ⁻¹	GB / kcal·mol ⁻¹	pK_{BH^+} (THF)	pK_{BH^+} (MeCN)
(dma)P ₃ P	297.4	291.3	34.9	41.7
(dma)P ₄ -tBu	296.1	289.6	34.5	41.5
(pyrr)P ₃ P	307.5	300.2	37.8	43.8
(pyrr)P ₄ -tBu	303.2	295.6	36.3	42.8
(dma)P ₄ P	304.3	295.4	37.0	43.8
(dma)P ₅ -tBu	304.5	297.7	37.7	43.7
(dma)P ₆ P	315.4	306.8	41.9	46.8
(dma)P ₇ -tBu	315.0	307.6	42.0	46.6
(pyrr)P ₆ P	320.0	315.3	45.0	48.6
(pyrr)P ₇ -tBu	318.9	311.8		

Proton exchange barriers are calculated as a free energy of activation at 298K for proton transfer reaction between protonated and neutral phosphine:



Free energies are obtained at B3LYP-D3/6-311+G(2df,p)//B3LYP-D3/6-31+G(d) level of theory.

Cone angles are calculated according to a mathematically rigorous method developed by Bilbrey *et al.*^[23] This method is based on solving for the most acute right circular cone that contains the entire ligand. A Mathematica^[24] package FindConeAngle developed by the authors^[25] was used to compute the /° cone angles and visualize the solutions. The inputs for cone angle calculations were B3LYP-D3/6-31+G(d)/LANL2DZ optimized geometries of mono(phosphine)nickel (0)complexes.

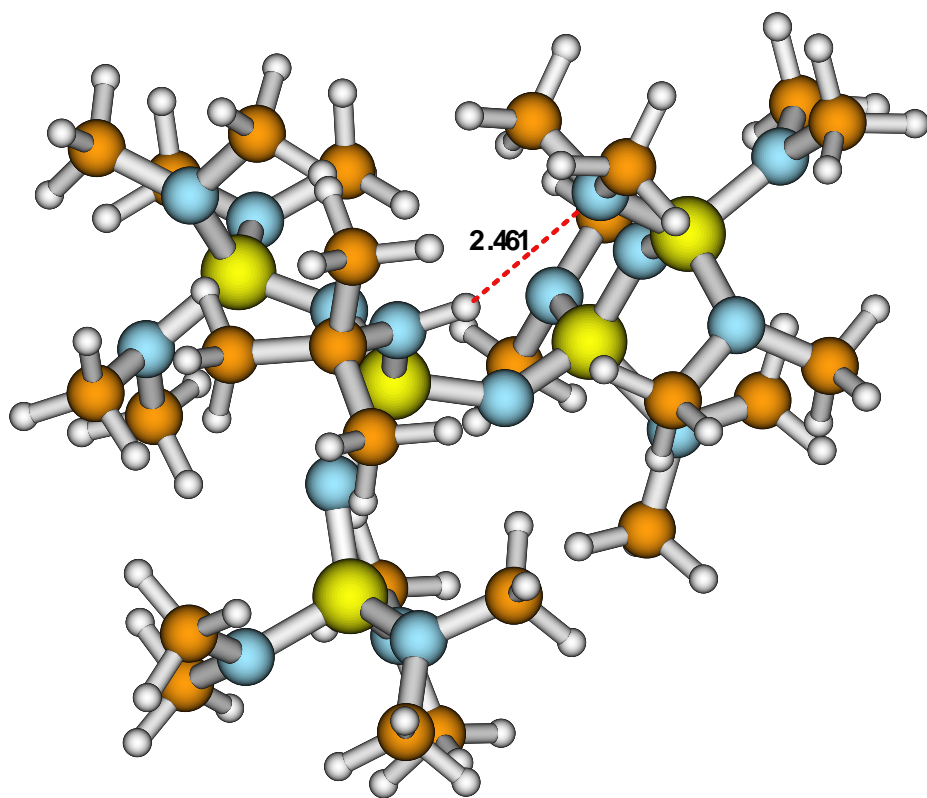


Figure S79: Conjugate acid of (dma)P₅-tBu (top view).

References

- [1] W. L. F. Armarego, D. D. Perrin, *Purification of laboratory chemicals*, Butterworth Heinemann, Oxford, Boston, **1996**.
- [2] J. Åhman, P. Somfai, *Synthetic Commun.* **1995**, *25*, 2301.
- [3] P. J. Bailey, R. A. Coxall, C. M. Dick, S. Fabre, L. C. Henderson, C. Herber, S. T. Liddle, D. Loroño-González, A. Parkin, S. Parsons, *Chem. Eur. J.* **2003**, *9*, 4820.
- [4] U. Nagel, *Chem. Ber.* **1982**, *115*, 1998.
- [5] U. Berens, U. Englert, S. Geysler, J. Runsink, A. Salzer, *Eur. J. Org. Chem.* **2006**, *2006*, 2100.
- [6] R. Schwesinger, H. Schlemper, C. Hasenfratz, J. Willaredt, T. Dambacher, T. Breuer, C. Ottaway, M. Fletschinger, J. Boele, H. Fritz et al., *Liebigs Ann./Recl.* **1996**, *1996*, 1055.
- [7] G. R. Fulmer, Miller, Alexander J. M., N. H. Sherden, H. E. Gottlieb, A. Nudelman, B. M. Stoltz, J. E. Bercaw, K. I. Goldberg, *Organometallics* **2010**, *29*, 2176.
- [8] A. P. Marchenko, G. N. Koidan, A. M. Pinchuk, A. V. Kirsanov, *J. Gen. Chem. USSR* **1984**, *54*, 1581.
- [9] J. F. Kögel, X. Xie, E. Baal, D. Gesevičius, B. Oelkers, B. Kovačević, J. Sundermeyer, *Chem. Eur. J.* **2014**, *20*, 7670.
- [10] J. Saame, T. Rodima, S. Tshepelevitsh, A. Kütt, I. Kaljurand, T. Haljasorg, I. A. Koppel, I. Leito, *J. Org. Chem.* **2016**, *81*, 7349.
- [11] X. Xie, F. Bönisch, *Magn. Reson. Chem.* **2015**, *53*, 801.
- [12] a) *Apex3*, Bruker AXS Inc., Madison, Wisconsin, USA, **2016**; b) *SAINT*, Bruker AXS Inc., Madison, Wisconsin, USA, **2015**; c) *SADABS. Bruker AXS area detector scaling and absorption correction*, Bruker AXS Inc., Madison, Wisconsin, USA, **2016**.
- [13] a) *X-Area Pilatus3_SV*, STOE & Cie GmbH, Darmstadt, Germany, **2016**; b) *X-Area Recipe*, STOE & Cie GmbH, Darmstadt, Germany, **2015**; c) *X-Area Integrate*, STOE & Cie GmbH, Darmstadt, Germany, **2016**; d) *X-Area LANA*, STOE & Cie GmbH, Darmstadt, Germany, **2016**.
- [14] G. M. Sheldrick, *Acta Cryst.* **2015**, *A71*, 3.
- [15] G. M. Sheldrick, *Acta Cryst.* **2015**, *C71*, 3.
- [16] L. J. Farrugia, *J Appl Crystallogr* **2012**, *45*, 849.
- [17] C. B. Hübschle, G. M. Sheldrick, B. Dittrich, *J. Appl. Crystallogr.* **2011**, *44*, 1281.
- [18] K. Brandenburg, H. Putz, *Diamond - Crystal and Molecular Structure Visualization v4*, Crystal Impact GbR, Bonn, Germany, **2014**.

- [19] Gaussian 09, Revision D.01, M. J. Frisch, G. W. Trucks, H. B. Schlegel, G. E. Scuseria, M. A. Robb, J. R. Cheeseman, G. Scalmani, V. Barone, G. A. Petersson, H. Nakatsuji, X. Li, M. Caricato, A. Marenich, J. Bloino, B. G. Janesko, R. Gomperts, B. Mennucci, H. P. Hratchian, J. V. Ortiz, A. F. Izmaylov, J. L. Sonnenberg, D. Williams-Young, F. Ding, F. Lipparini, F. Egidi, J. Goings, B. Peng, A. Petrone, T. Henderson, D. Ranasinghe, V. G. Zakrzewski, J. Gao, N. Rega, G. Zheng, W. Liang, M. Hada, M. Ehara, K. Toyota, R. Fukuda, J. Hasegawa, M. Ishida, T. Nakajima, Y. Honda, O. Kitao, H. Nakai, T. Vreven, K. Throssell, J. A. Montgomery, Jr., J. E. Peralta, F. Ogliaro, M. Bearpark, J. J. Heyd, E. Brothers, K. N. Kudin, V. N. Staroverov, T. Keith, R. Kobayashi, J. Normand, K. Raghavachari, A. Rendell, J. C. Burant, S. S. Iyengar, J. Tomasi, M. Cossi, J. M. Millam, M. Klene, C. Adamo, R. Cammi, J. W. Ochterski, R. L. Martin, K. Morokuma, O. Farkas, J. B. Foresman, and D. J. Fox, Gaussian, Inc., Wallingford CT, 2016.
- [20] A. M. Toth, M. D. Liptak, D. L. Phillips, G. C. Shields, *J. Chem. Phys.* **2001**, *114*, 4595.
- [21] K. Abdur-Rashid, T. P. Fong, B. Greaves, D. G. Gusev, J. G. Hinman, S. E. Landau, A. J. Lough, R. H. Morris, *J. Am. Chem. Soc.* **2000**, *122*, 9155.
- [22] K. Haav, J. Saame, A. Kütt, I. Leito, *Eur. J. Org. Chem.* **2012**, *2012*, 2167.
- [23] J. A. Bilbrey, A. H. Kazez, J. Locklin, W. D. Allen, *J. Comput. Chem.* **2013**, *34*, 1189.
- [24] *Mathematica 8.0*, Wolfram Research, Inc., Champaign, IL, **2010**.
- [25] can be found under <http://www.psicode.org/>.

EDGE ARTICLE

Cite this: *Chem. Sci.*, 2019, 10, 9483

All publication charges for this article have been paid for by the Royal Society of Chemistry

Received 18th July 2019

Accepted 15th August 2019

DOI: 10.1039/c9sc03565f

rsc.li/chemical-science

Design of non-ionic carbon superbases: second generation carbodiphosphoranes†

Sebastian Ullrich,^a Borislav Kovačević,^b Björn Koch,^a Klaus Harms^{ID}^a and Jörg Sundermeyer^{ID}^{*a}

A new generation of carbodiphosphoranes (CDPs), incorporating pyrrolidine, tetramethylguanidine, or tris(dimethylamino)phosphazene as substituents is introduced as the most powerful class of non-ionic carbon superbases on the basicity scale to date. The synthetic approach as well as NMR spectroscopic and structural characteristics in the free and protonated form are described. Investigation of basicity in solution and in the gas phase by experimental and theoretical means provides the to our knowledge first reported pK_{BH}^+ values for CDPs in the literature and suggest them as upper tier superbases.

Introduction

Much theoretical and synthetic effort has been devoted to lift non-ionic organic bases to the basicity level of common inorganic or metalorganic bases.^{1,2} With his famous phosphazenes Schwesinger established a widely used and commercially available class of (organo-)superbases.^{3,4} His homologization concept, the stepwise expansion of the molecular scaffold in order to better delocalize the positive charge formed upon protonation, was also applied to synthesize higher-order N-superbases of guanidines,^{5,6} imidazolidine amines⁷ and cyclopropeneimines.^{8,9} However, such basicity enhancement is accompanied by an unwanted growth of the bases' molecular weight. Therefore, other strategies for augmenting the intrinsic proton affinity have been investigated: in proton sponges, a second nitrogen basicity centre in close proximity to the first one increases the pK_{BH}^+ value up to 16 orders of magnitude by intramolecular hydrogen bonding compared to corresponding non chelating bases.¹⁰ Additional thermodynamic driving force comes from relief of strain of the aromatic backbone.¹¹ Many derivatives of such proton sponges were designed by combining aforementioned superbasic functionalities with the 1,8-diaminonaphthalene structural motif¹² or as proton pincers with different backbones.¹³

Atoms other than nitrogen as basicity centre were also applied, such as phosphorus.^{14,15} Recently, we demonstrated, that N-phosphazanyl substituted phosphines (PAPs) possess higher pK_{BH}^+ values as P^{III} bases than their corresponding

phosphazene P^VN_tBu counterparts as N bases.¹⁶ So far the limit of homologization is reached at the P₇ level both in phosphazanyl phosphazenes and phosphazanyl phosphines as both P₇ benchmark bases have only been isolated in their protonated form.^{16,17}

Non-ionic carbon is another contender to extend the basicity ladder to unmatched regions.¹⁸ In this respect phosphorus (mono-)ylides^{19,20} as well as bisylidic proton sponges²¹ were investigated on theoretical and experimental level. Although identified as potential superbases, the application of N-heterocyclic carbenes (NHCs),²² cyclic alkyl amino carbenes (CAACs),²³ carbodicarbenes (CDCs),²⁴ and carbodiphosphoranes (CDPs)²⁵ has been exploited predominantly as strong Lewis bases towards transition and main group elements other than the proton.²⁶

The prototypic hexaphenyl carbodiphosphorane ((Ph)₆-CDP) was first synthesized 1961 by Ramirez *et al.*²⁷ Further compounds like the hexamethyl carbodiphosphorane ((Me)₆-CDP),²⁸ hexakis(dimethylamino) carbodiphosphorane ((dma)₆-CDP),²⁹ and mixed representatives followed.^{30–32}

Herein we promote carbodiphosphoranes with their electron-rich R₃P–C–PR₃ functionality as exceptionally strong carbon Brønsted bases. As bisylides with a π-symmetric HOMO and σ-symmetric HOMO–1, both mainly located as lone pairs at the carbon, only slightly stabilized by back-bonding *via* negative hyperconjugation,³³ they provide outstanding pK_{BH}^+ values in particular for the first of two protonation steps. We present a synthesis for hexa(pyrrolidino) carbodiphosphorane ((pyrr)₆-CDP) with its calculated first and second proton affinity (PA) of 287.6 and 188.9 kcal mol⁻¹,³⁴ which exceeds the PAs of (Ph)₆-CDP (280.0 and 185.6 kcal mol⁻¹)³⁴ and (dma)₆-CDP (279.9 and 174.9 kcal mol⁻¹).³⁴ Furthermore we apply the homologization concept to CDPs by introducing PR₂R' units bearing one intrinsically superbasic substituent R' to access CDP

^aFachbereich Chemie, Philipps-University Marburg, Hans-Meerwein-Straße, 35032 Marburg, Germany. E-mail: jsu@staff.uni-marburg.de

^bThe Group for Computational Life Sciences, Rudjer Bošković Institute, Bijenička c. 54, HR-10000 Zagreb, Croatia

† Electronic supplementary information (ESI) available. CCDC 1903830, 1903833, 1903838, 1903840, 1903841 and 1903843. For ESI and crystallographic data in CIF or other electronic format see DOI: 10.1039/c9sc03565f

superbases of second-order.⁸ We thereby focused on *N*-tetramethylguanidynyl (tmg) and *N*-tris(dimethylamino)phosphazanyl (dmaP₁) substituents targeting new carbodiphosphoranes *sym*-(tmg)₂(dma)₄-CDP and *sym*-(dmaP₁)₂(dma)₄-CDP.

Results and discussion

Synthesis

We experienced, that the established synthesis routes to CDPs are inappropriate for phosphines more electron-rich than P(NMe₂)₃: reactions between such phosphines P(NR₂)₂R' and CCl₄ did not follow the pattern outlined in ref. 32 and 35 but exclusively led to chlorination of the phosphine, whilst reactions with methylene bromide did not selectively follow the path outlined in ref. 30 and 36, but led to a 1 : 1-mixture of the methylated phosphonium bromide [R'(NR₂)₂P-Me]Br and the brominated species [R'(NR₂)₂P-Br]Br. Therefore we further developed an alternative strategy laid out by Appel *et al.* for the synthesis of (dma)₆-CDP.²⁹ The doubly protonated precursors of the second-order carbodiphosphorane superbases, *sym*-(tmg)₂(dma)₄-CDP (**1**) and *sym*-(dmaP₁)₂(dma)₄-CDP (**2**), were obtained in an oxidative imination sequence as shown in Scheme 1. Bis[bis(dimethylamino)phosphino]methane (**3**) was oxidized by CCl₄ in presence of tetramethylguanidine (Htmg) or tris(dimethylamino)phosphazene ((dma)₃P₁-H) instead of dimethylamine as nucleophile and auxiliary base. This reaction offers the advantage of preformed C–P bonds avoiding the preparation of respective P^{III} nucleophiles.^{15,20,37} **3** is readily synthesized in two steps on a large scale³⁸ and the selected superbasic building blocks oxidatively introduced as nucleophiles are either commercially available or easily accessible in few steps.⁴

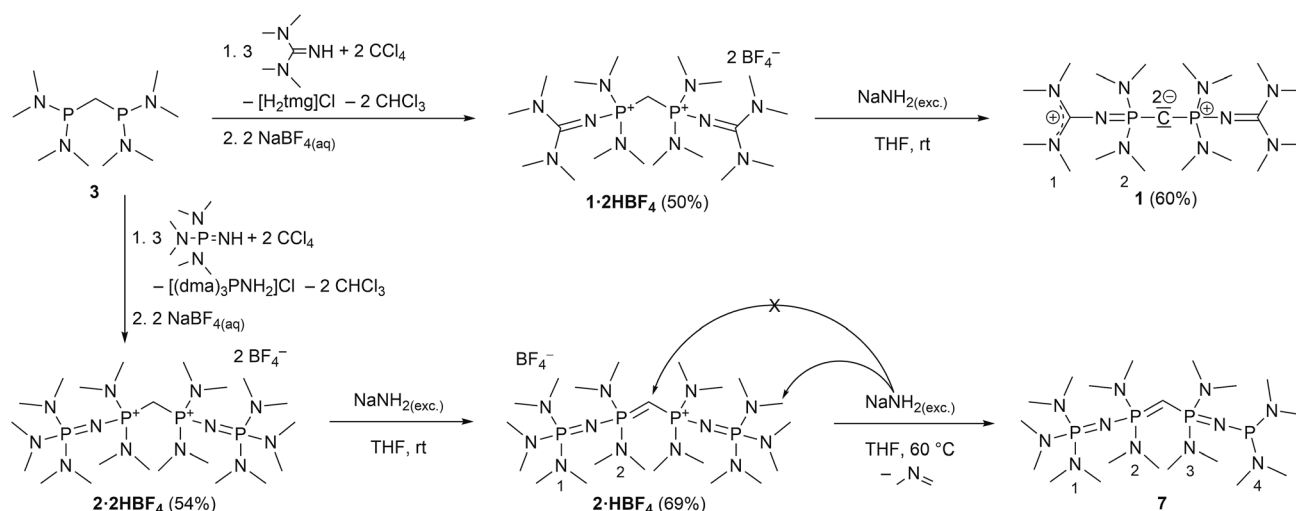
The synthesis of **4**·2HBF₄, the precursor for (pyrr)₆-CDP **4**, was accomplished in a one-pot synthesis (Scheme 2), since the intermediate bis[di(pyrrolidino)phosphino]methane (**5**) turned

out to decompose upon vacuum distillation. Starting from bis(dichlorophosphino)methane³⁸ (**6**), **5** was prepared *in situ* with an excess of pyrrolidine (Fig. S1 in the ESI†) and directly oxidized with CCl₄.

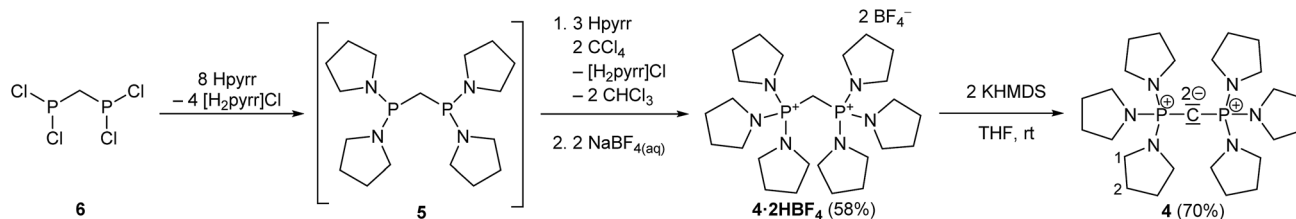
In all three reactions the respective monoprotonated hydrochloride adducts were identified as products *via* ³¹P NMR spectroscopy. Therefore the second p*K*_{BH}⁺ values in THF of these new CDPs are obviously lower than that of the auxiliary base pyrrolidine (13.5),³⁹ tetramethylguanidine (15.5),⁴⁰ or tris(dimethylamino)phosphazene **2a** (19.7),⁴⁰ respectively. For purification, the crude products were precipitated with NaBF₄ from aqueous solution. These conditions lead to second protonation at the central carbon atom and a strongly alkaline solution. Therefore, even the monoprotonated CDPs can be considered as strong cationic bases in aqueous medium. Similar behaviour was found for (Ph)₆-CDP in water, although the latter is slowly hydrolysed under ambient conditions,²⁷ which is not the case for peraminated CDPs **1**, **2** and **4** reported here.

The bis(tetrafluoridoborate) salts of **1**, **2** and **4** were obtained in 50–60% yield as water and air stable, colourless solids, indefinitely storable. They are well soluble in polar organic solvents like methanol, acetonitrile or DMSO but insoluble in less polar solvents such as ethers and hydrocarbons.

For the liberation of the free CDPs different suitable bases were identified: for **4** potassium bis(trimethylsilyl)amide (KHMSD) is of sufficient basicity, whilst for **1** the more basic sodium amide (NaNH₂) is necessary for full deprotonation. Both new bases **1** and **4** could be isolated in 70% and 60% yield, respectively, from *n*-hexane as pure colourless crystalline solids, indefinitely storable at room temperature under inert conditions. Contrastingly we were not able to isolate **2** as free CDP base form. Sodium amide in liquid ammonia or suspended in THF at room temperature selectively abstracts the first proton under formation of **2**·HBF₄ as colourless solid in 69% yield. At elevated temperature the central carbon atom is not further



Scheme 1 Preparation of CDP precursors **1**·2HBF₄ and **2**·2HBF₄ together with subsequent deprotonation to **1** (one exemplary mesomeric structure displayed) and **7**, respectively. Numbering schemes refer to assigned NMR signals in the experimental section.



Scheme 2 *In situ* preparation of 5 with subsequent oxidation by CCl₄ in presence of excess of pyrrolidine (Hpyrr) to 4·2HBF₄. Deprotonation with KHMDS lead to the free CDP 4 (displayed in exemplarily bisylidic notation). The numbering scheme refers to assigned NMR signals in the experimental section.

deprotonated, even though it is the thermodynamically most acidic site (see Theoretical Calculations). Instead NaNH₂ deprotonates selectively one of the dimethylamino groups at the terminal phosphazene moiety which results in the irreversible elimination of *N*-methylmethanimine and reduction of the phosphazene to a phosphine (Scheme 1). A related deprotonation and reduction of tetrakis(dimethylamino)phosphonium bromide under the action of NaNH₂ was described by Pinchuk *et al.*⁴¹ In case of 2 this reaction is slow but highly selective and 7 could be obtained as sole product as pale yellow highly viscous oil. The proposed configuration was confirmed *via* ¹H, ¹³C, and ³¹P NMR spectroscopy and by HR mass spectrometry. 7 can be considered as a hybrid between mixed valence phosphazanyl phosphines^{15,16} and ylidic P^{III}/P^V compounds of the type (Me₂N)₃P=C(H)-PR₂ (ref. 42) or other ylide-functionalized phosphines.⁴³ Further attempts to deprotonate 2·2HBF₄ with other bases or reducing agents resulted either in only single deprotonation (benzyl potassium in THF), in an unselective disintegration (*n*BuLi) or in the same deprotonation of the P-NMe₂ group (potassium in liquid ammonia, ethylene diamine, THF, or DME or an excess of benzyl potassium in THF). The reaction of potassium hydride in THF gave a mixture of 7 as minor component and presumably free CDP 2 as major product by means of ³¹P NMR spectroscopy (Fig. S29 in the ESI[†]). Clearly the acidity of P^V-attached NMe₂ groups limits the accessibility of 2. Under the action of excess of strong inorganic bases at elevated temperatures the stability limit of these phosphazene moieties seems to have been reached.

For analytical reasons the monoprotonated forms of 1 and 4 were prepared on NMR scale either *via* commutation between the free CDP and its bisprotonated form or by protonating the free CDPs with one equivalent triflimidic acid (HTFSI).

Structural features

For X-ray structure determination suitable single crystals were obtained from *n*-hexane for both presented CDPs 4 and 1. They crystallize solvent-free in space group *P2₁/c* or *Pbca*, respectively, with one complete molecule per asymmetric unit (Fig. 1). Contrary to the parent compound (dma)₆-CDP, one of the hitherto two reported linear CDPs,^{29,44} a bent structure with P-C-P angles of 155.9(2)° and 147.30(9)°, respectively is found. Since the potential for bending at the central P-C-P carbon atom in polymorphic (Ph)₆-CDP is very flat⁴⁴ and reveals high dependence of the crystallization method,⁴⁵ the obtained

crystals of (dma)₆-CDP from the melt are maybe the reason for its linearity.²⁹ The P-C_{central} distances are with 1.606 Å (4) and 1.618 Å (1) in the for CDPs reported range: (dma)₆-CDP: 1.584(1) Å,²⁹ (Me)₆-CDP: 1.594(3) Å,⁴⁶ (Ph)₆-CDP: 1.601–1.635 Å.^{44,47} On average, pyrrolidine N-P distances in 4 are 1.68 Å while those of dma and tmg groups in 1 are 1.70 Å and 1.66 Å respectively.

Single crystals obtained from reaction control samples during the synthesis of 4·2HBF₄ turned out to be a cocrystallizate of 4·2HCl and pyrrolidinium chloride (Fig. 2). Cations and anions form a C-H...Cl...H-N hydrogen bond network with C...Cl distances of 3.600(2) Å and N...Cl distances of 3.018(2) Å and

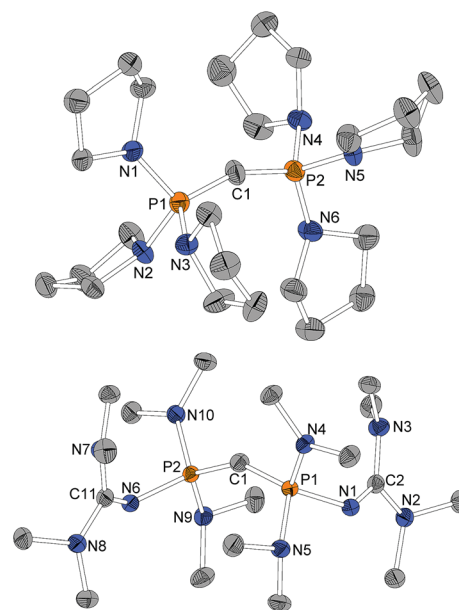


Fig. 1 Molecular structure of 4 (top) and 1 (bottom). Hydrogen atoms omitted for clarity, ellipsoids at 50% probability. Selected bond length/Å and angles/°: 4 P1-C1 1.605(2), P1-N1 1.672(2), P1-N2 1.678(2), P1-N3 1.694(2), P2-C1 1.606(2), P2-N4 1.699(2), P2-N5 1.669(2), P2-N6 1.671(2), P1-C1-P2 155.9(2), C1-P1-N1 110.2(1), C1-P1-N2 115.1(1), C1-P1-N3 121.8(1), C1-P2-N4 118.4(1), C1-P2-N5 111.3(1), C1-P2-N6 117.1(1), N1-P1-C1-P2 168.0(4), N4-P2-C1-P1 130.6(4). 1 P1-C1 1.619(1), P1-N4 1.680(1), P1-N5 1.714(1), P1-N1 1.665(1), N1-C2 1.298(2), N2-C2 1.377(2), N3-C2 1.382(2), P2-C1 1.617(1), P2-N9 1.719(1), P2-N10 1.680(1), P2-N6 1.664(1), N6-C11 1.299(2), N7-C11 1.376(2), N8-C11 1.379(2), P2-C1-P1 147.30(9), C1-P1-N4 109.52(6), C1-P1-N5 121.56(6), C1-P1-N1 119.85(6), C2-N1-P1 128.1(1), C1-P2-N9 120.76(6), C1-P2-N10 110.08(6), C1-P2-N6 119.47(6), C11-N6-P2 127.3(1), N4-P1-C1-P2 162.2(2), N10-P2-C1-P1 155.8(2).

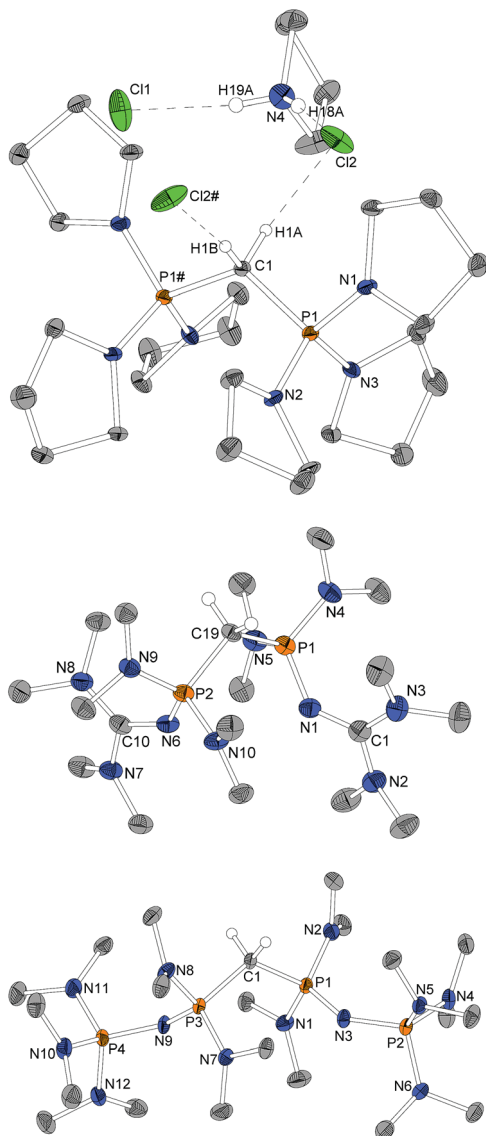


Fig. 2 Molecular structure of $4 \cdot 2\text{HCl}$ with pyrrolidinium chloride as cocrystallite as well as of $1 \cdot 2\text{HBF}_4$ and $2 \cdot 2\text{HBF}_4$ (only one of the two independent molecules depicted, structure factors given for both). Peripheral hydrogen atoms and BF_4^- anions omitted for clarity, ellipsoids at 50% probability. # marked atoms generated via a 2-fold axis through C1. Selected bond length/Å and angles/ $^\circ$: $4 \cdot 2\text{HCl}$ P1–C1 1.799(1), P1–N1 1.612(2), P1–N2 1.630(2), P1–N3 1.616(2), P1–C1–P1# 119.5(1), N1–P1–C1 103.26(9), N2–P1–C1 109.07(7), N3–P1–C1 115.21(8), N1–P1–C1–P1# 177.03(7), C1–H1A...Cl2 3.600(2), 173.8; C1–H1B...Cl2# 3.600(2), 173.8; N4–H18A...Cl2 3.048(2), 174(3); N4–H19A...C1 3.018(2), 172(3). $1 \cdot 2\text{HBF}_4$ P1–C19 1.820(2), P1–N4 1.644(2), P1–N5 1.639(2), P1–N1 1.580(2), N1–C1 1.330(3), N2–C1 1.351(3), N3–C1 1.346(3), P2–C19 1.822(2), P2–N9 1.640(2), P2–N10 1.643(2), P2–N6 1.586(2), N6–C10 1.335(3), N7–C10 1.332(3), N8–C10 1.349(3), P1–C19–P2 113.4(1), N4–P1–C19 104.3(1), N5–P1–C19 109.7(1), N1–P1–C19 110.8(1), C1–N1–P1 136.1(2), N9–P2–C19 105.4(1), N10–P2–C19 108.8(1), N6–P2–C19 111.8(1), C10–N6–P2 132.6(2), N4–P1–C19–P2 169.1(1), N9–P2–C19–P1 165.2(1). $2 \cdot 2\text{HBF}_4$ P1–C1/P5–C22 1.820(4)/1.822(4), P1–N1/P5–N19 1.626(4)/1.630(4), P1–N2/P5–N20 1.642(4)/1.650(4), P1–N3/P5–N21 1.573(4)/1.571(4), P2–N3/P6–N21 1.582(4)/1.589(4), P2–N4/P6–N22 1.648(4)/1.639(4), P2–N5/P6–N23 1.639(4)/1.639(4), P2–N6/P6–N24 1.650(4)/1.655(4), P3–C1/P7–C22 1.819(5)/1.817(5), P3–N7/P7–N13 1.636(4)/1.645(4), P3–N8/P7–N14 1.647(4)/1.635(4), P3–N9/P7–N15 1.575(4)/1.567(4), P4–N9/P8–N15 1.577(4)/

3.048(2) Å, the slightly longer distance involving the bridging chlorine atom. Similar weak hydrogen bonds were described for $(\text{Ph})_6\text{-CDP} \cdot 2\text{H}^+$ with $[\text{InCl}_4]^-$ (3.60 Å and 4.03 Å),⁴⁸ $[\text{BeCl}_4]^{2-}$ (3.55 Å and 3.58 Å),⁴⁹ I^- (3.80 Å and 3.81 Å)⁵⁰ and Cl^- (3.38 Å)⁴⁹ anions. The difference between the latter and $4 \cdot 2\text{HCl}$ probably arise from a less polarized C–H bond due to the stronger electron pair donor **4**. Single crystals of the isolated $4 \cdot 2\text{HBF}_4$ were additionally obtained from chloroform and exhibits no significant differences in the structural properties (displayed in the ESI[†]). Fig. 2 shows the molecular structures of $1 \cdot 2\text{HBF}_4$ and $2 \cdot 2\text{HBF}_4$ as well. All three bisprotonated CDPs exhibit a strong influence of charge delocalization as the reason for their extraordinary basicity: upon protonation the P–C bonds elongate from 1.606 Å (**4**) and 1.618 Å (**1**) to 1.799 Å in $4 \cdot 2\text{HCl}$ and 1.821 Å in $1 \cdot 2\text{HBF}_4$ and $2 \cdot 2\text{HBF}_4$, whilst the P–N bonds become shorter to average 1.62 Å for pyrrolidine and 1.64 Å for dimethylamine substituents. This complies with distances found in protonated phosphazenes⁵¹ and phosphorus ylids⁵² and proves the electron donating effect of the amino substituents. The P–N bonds to the tmg groups in $1 \cdot 2\text{HBF}_4$ exhibits with 1.58 Å (1.66 Å in **1**) clearly double-bond character. The P–N=C angles are expanded from 127° and 128° to 132° and 136°. A diminishing difference of formal N–C single and double bonds in the tmg group indicates the conjugation within the CN_3 moiety. The formal P–N single and double bonds of the phosphazene substituents in $2 \cdot 2\text{HBF}_4$ equalize at 1.57–1.59 Å with P–N–P angles between 134° and 142°. Similar influence of negative hyperconjugation for charge delocalization was found in superbasic PAPS¹⁶ and protonated diphosphazenes.⁵³ The P–C–P angles in the bisprotonated forms (**4**: 120°, **1**: 113°, **2**: 121°) are more acute than in the free CDPs (**4**: 156°, **1**: 147°). The difference to ideal tetrahedral geometry presumably arise from the bulkiness of the PR_3 moieties.

NMR spectroscopic features

All six presented compounds were characterized by ^1H , ^{13}C , and ^{31}P NMR spectroscopy. Selected chemical shifts and couplings are collected in Table 1. Proton shifts of bis- and monoprotated CDPs lie around 3 ppm for CH_2 and below 1 ppm for CH groups, both decreasing with increasing basicity of the parent CDP indicating less polarized C–H bonds. This shielding trend is not observed in the ^{13}C NMR shifts of the carbon nuclei: the most basic CDP **1** exhibits a triplet at 9.5 ppm compared to –1.6 ppm (**4**) and –6.8 ppm ($(\text{dma})_6\text{-CDP}$).²⁹ Surprisingly the ^{13}C chemical shift for **1** is even higher than for its monoprotated form ($1 \cdot \text{HTFSI}$: 9.3 ppm) contrasting the typical trend

1.579(4), P4–N10/P8–N16 1.644(4)/1.652(4), P4–N11/P8–N17 1.636(4)/1.648(4), P4–N12/P8–N18 1.655(4)/1.637(4), P3–C1–P1/P5–C22–P7 120.9(2)/121.7(2), N1–P1–C1/N19–P5–C22 110.8(2)/109.8(2), N2–P1–C1/N20–P5–C22 103.8(2)/104.0(2), N3–P1–C1/N21–P5–C22 107.9(2)/108.4(2), P1–N3–P2/P5–N21–P6 138.2(3)/135.7(3), N7–P3–C1/N14–P7–C22 111.2(2)/112.4(2), N8–P3–C1/N13–P7–C22 105.0(2)/103.2(2), N9–P3–C1/N15–P7–C22 107.9(2)/107.4(2), P3–N9–P4/P7–N15–P8 133.6(3)/141.6(3), N2–P1–C1–P3/N20–P5–C22–P7 164.8(3)/166.8(3), N8–P3–C1–P1/N13–P7–C22–P5 165.6(3)/164.4(3).

Table 1 NMR shifts δ /ppm and couplings J /Hz of the presented compounds

	δ_{H} ($^2J_{\text{PH}}/^4J_{\text{PH}}$)	δ_{C} ($^1J_{\text{PC}}/^3J_{\text{PC}}$)	δ_{P}
4·2HBF ₄ ^a	3.43 (19)	26.4 (110)	32.7
4·HTFSI ^b	0.93 (7)	10.3 (192)	40.1
4 ^c	—	−1.6 (280)	11.5
1·2HBF ₄ ^a	3.16 (17)	25.2 (112)	20.8
1·HTFSI ^b	0.55 (4)	9.3 (185)	37.1
1 ^c	—	9.5 (209)	18.2
2·2HBF ₄ ^a	2.87 (19)	25.6 (122/7)	23.2–22.7, 20.6–20.3
2·HBF ₄ ^a	0.25 (6/3)	12.6 (194/4)	34.3–33.6, 16.5–15.8
2 ^d	—	—	7.7–7.0, 6.2–5.6
7 ^c	0.42 (3/2)	13.0 (187/186/2)	109.9, 39.9, 37.0, 15.1

^a In CD₃CN. ^b In THF-*d*₃. ^c In C₆D₆. ^d In C₆D₆, assigned from the isolated mixture of the reaction between 2·2HBF₄ and KH in THF (Fig. S29 in the ESI).

observed for other CDPs.^{31,54} The $^1J_{\text{PC}}$ couplings drastically increase with step by step deprotonation indicating larger s-character of the ylidic P–C bonds. In the ^{31}P NMR spectra signals for the monoprotonated forms lie between the bisprotonated at higher and the free CDPs at lower values and correlate with the group electronegativity of the phosphines ((dma)₆-CDP: 27.72 ppm; (dma)₆-CDP·HCl: 54.16 ppm).²⁹ This is not exactly the case for the bisprotonated and free CDPs. The ^{31}P NMR signals of all three forms of **2** are multiplets corresponding to an AA'XX' spin system with $^2J_{\text{PP}}$ and $^4J_{\text{PP}}$ coupling (Fig. S22, S25, and S29 in the ESI[†]). **7** exhibits four individual signals in shape of two doublets of doublets for bridging phosphorus atoms and two doublets for terminal phosphorus atoms with the P^{III} atom being characteristically deshielded.^{15,16} ^1H and ^{13}C NMR signals are slightly shifted to higher frequencies in comparison with 2·HBF₄, indicating that the mixed valent P^{III}/P^V phosphanylphosphazene substituent is a poorer donor than corresponding P₂ bisphosphazene.

NMR titration experiments were conducted for **4** against (tmg)P₁-*t*Bu ($\text{p}K_{\text{BH}}^+$ in THF: 29.1)⁶ and (dma)P₄-*t*Bu ($\text{p}K_{\text{BH}}^+$ in THF: 33.9).²⁰ The $\text{p}K_{\text{BH}}^+$ value for **4** therefore has to be in between 30.1 and 32.9, since only free (tmg)P₁-*t*Bu and protonated **4** or protonated (dma)P₄-*t*Bu and free **4** were detected, respectively. Basicity of **1** was determined *via* titration against (pyrr)P₄-*t*Bu ($\text{p}K_{\text{BH}}^+$ in THF: 35.3)²⁰ as reference. Protonated and base forms of both species were quantified by ^{31}P NMR integration and a $\text{p}K_{\text{BH}}^+$ value of 35.8 in THF was determined for **1**. To our knowledge this is the first report of an experimental $\text{p}K_{\text{BH}}^+$ value for a carbodiphosphorane. It approves **1** to be an exceptional strong non-ionic carbon base, 0.5 orders of magnitude more basic than the strongest uncharged Schwesinger-type nitrogen superbases measured in THF²⁰ and 2.3 orders of magnitude more basic than the so far strongest uncharged carbon superbases H₂C=P(2,4,6-(MeO)₃-C₆H₂)₂Ph ($\text{p}K_{\text{BH}}^+$ in THF: 33.5).²⁰ Singlet carbenes such as NHCs and CAACs are weak carbon bases in comparison, according to $\text{p}K_{\text{BH}}^+$ values around 23 in THF and DMSO⁵⁵ or calculated PAs.^{34,56} The exceptional C-basicity of the title compounds is

only surpassed by our PAP phosphorus superbases (pyrr)P₃P (36.7) and (dma)P₄P (37.2).¹⁶

Quantumchemical calculations

First and second proton affinity (PA) and gas-phase basicity (GB) of carbodiphosphoranes **1**, **2**, **4** and phosphine **7** are calculated utilizing M06-2X/6-11+G(2df,p)//M06-2X/6-31+G(d) theoretical model. $\text{p}K_{\text{BH}}^+$ values in THF are obtained using the same functional and basis set whereas solvent is treated as dielectric continuum utilizing the SMD solvation model. $\text{p}K_{\text{BH}}^+$ values are calculated as relative values using an isodesmic reaction approach⁵⁷ where Schwesingers (dma)P₄-*t*Bu phosphazene with $\text{p}K_{\text{BH}}^+$ of 33.9 (ref. 20) has served as a reference base. Calculated values for protonation at central carbon atom, and in case of **7** protonation at the P^{III} atom as well, are presented in Table 2. It appears that the first proton affinity as well as $\text{p}K_{\text{BH}}^+$ values of **1** and **2** are higher than in Schwesingers (dma)P₄-*t*Bu phosphazene which has PA of 293.3 kcal mol^{−1} calculated at the same level of theory. Interestingly first GB of **1** is slightly lower than the GB of (dma)P₄-*t*Bu (GB = 288.2 kcal mol^{−1}) implying that the higher $\text{p}K_{\text{BH}}^+$ value of **1** relative to (dma)P₄-*t*Bu is a result of a more pronounced solvation effect in the carbodiphosphorane. This is unexpected considering that the N–H bond in a protonated phosphazene has a higher polarity than the C–H bond in protonated CDP as a result of lower electronegativity of carbon relative to nitrogen. The calculated $\text{p}K_{\text{BH}}^+$ (THF) 39.1 of **2** would be far higher than the $\text{p}K_{\text{BH}}^+$ (THF) 33.9 of (dma)P₄-*t*Bu, the strongest commercially available superbases. As described isolation of neutral base **2** is not achieved experimentally as other C–H bonds in the precursor 2·H⁺ seemed to have a higher kinetic and thermodynamic acidity. In order to understand the deprotonation path of 2·H⁺ under the action of NaNH₂, the reaction profile is calculated and presented in Fig. S36 in the ESI.[†] It appears, that the deprotonation of peripheral NMe₂ group in combination with the irreversible elimination of *N*-methylmethanimine is thermodynamically feasible (exergonic), however, kinetically hindered by a high barrier ($\Delta G^\ddagger = 32.8$ kcal mol^{−1}). This explains, that deprotonation induced degradation is competitive to deprotonation of central carbon atom at elevated temperatures, though the central carbon atom in 2·H⁺ is the thermodynamically most acidic site. It appears that decomposition product – phosphine **7** – has a gas-phase

Table 2 Calculated first and second proton affinity (PA) and gas phase basicity (GB) together with $\text{p}K_{\text{BH}}^+$ values in THF

	PA/kcal mol ^{−1}	GB/kcal mol ^{−1}	$\text{p}K_{\text{BH}}^+$ in THF ^a	
4	1 st	291.1	282.2	32.8 (30.1–32.9)
	2 nd	191.6	184.0	—
1	1 st	294.4	287.2	34.9 (35.8 ± 1)
	2 nd	202.0	194.1	—
2	1 st	305.3	299.7	39.1
	2 nd	212.1	202.2	—
7	At carbon	275.9	268.7	24.4
	At phosphorus	276.2	268.8	21.1

^a Experimental values in parentheses.

basicity ($30.9 \text{ kcal mol}^{-1}$) much lower than CDP 2. Interestingly, GB value for protonation at central carbon and P^{III} phosphorus of 7 is almost the same, whereas $\text{p}K_{\text{BH}}^+$ in THF for protonation at P^{III} is by 3.3 orders of magnitude lower than $\text{p}K_{\text{BH}}^+$ for protonation at carbon, which again indicates a more pronounced solvation effect in C-protonated CDP.

Conclusions

In this work we presented the most basic uncharged carbon bases known so far. A convenient synthesis for first- and novel second-order carbodiphosphorane superbases was presented. The CDPs (pyrr)₆-CDP 4 and *sym*-(tmg)₂(dma)₄-CDP 1 were synthesized as free base as well as in their mono- and bisprotonated forms. In our attempt to synthesize the even more outstanding base *sym*-(dmaP₁)₂(dma)₄-CDP 2 an unexpected, but highly selective deprotonation at peripheral PNCH₃ bonds induced an irreversible elimination path towards phosphine 7. This reaction is indicating a potential basicity limit for phosphazene containing superbases. Structural as well as spectroscopic features were investigated and the basicity was quantified by theoretical and experimental means. Remarkable $\text{p}K_{\text{BH}}^+$ values for 4 and 1 confirm them as benchmark breakers for non-ionic carbon bases on the THF basicity scale. Compared to the top Schwesinger bases, this basicity is even more outstanding, if their molecular weight below 500 g mol^{-1} is considered. We expect, that such simply synthesized carbodiphosphoranes with water stable protonated forms will enter the field of organic superbase catalysis.¹

Experimental section

General

All Reactions with air or moisture sensitive substances were carried out under inert atmosphere using standard Schlenk techniques. Air or moisture sensitive substances were stored in a nitrogen-flushed glovebox. Solvents were purified according to common literature procedures and stored under an inert atmosphere over molsieve (3 Å or 4 Å).⁵⁸ Pyrrolidine and tetramethylguanidine were distilled from CaH₂, triflimidic acid was purified by sublimation under argon. Bis(dichlorophosphino) methane³⁸ (6), bis[bis(dimethylamino)phosphino]methane³⁸ (3), tris(dimethylamino)phosphazene⁴ and (pyrr)₄-tBu⁴ were prepared according to literature-known procedures. (dma)₄-tBu was purchased as 1 M solution in *n*-hexane and dried in high vacuum. All other reagents were used as provided.

¹H, ¹³C, and ³¹P NMR spectra were recorded on a Bruker Avance III HD 250, Avance II 300, Avance III HD 300 or Avance III HD 500 spectrometer. Chemical shift δ is denoted relatively to SiMe₄ (¹H, ¹³C) or 85% H₃PO₄ (³¹P). ¹H and ¹³C NMR spectra were referenced to the solvent signals.⁵⁹ Multiplicity is abbreviated as follows: s (singlet), d (doublet), t (triplet), q (quartet), m (multiplet), br. (broad signal). High resolution mass spectrometry were performed on a Thermo Fisher Scientific LTQ-FT Ultra (ESI(+)) or a Jeol AccuTOF GCv (LIFDI(+) = liquid injection field desorption ionization), elemental analysis on an Elementar Vario Micro Cube. IR spectra were recorded in a glovebox on

a Bruker Alpha ATR-FT-IR. CCDC 1903830 (4·2HCl + HpyrrCl), 1903833 (1·2HBF₄), 1903838 (2·2HBF₄), 1903840 (1), 1903841 (4·2HBF₄), and 1903843 (4) contain the supplementary crystallographic data for this paper.†

General procedure for the precipitation of BF₄-salts

The crude product was dissolved in a minimum amount of water and a concentrated aqueous sodium tetrafluoroborate solution (2.0 eq.) was added. The resulting precipitate was filtered off, rinsed three times with small portions of cold water, washed with THF and dried in high vacuum.

(pyrr)₆-CDP·2HBF₄ (4·2HBF₄)

6 (3.60 g, 16.5 mmol, 1.00 eq.) was dissolved in THF (60 mL), cooled to $-78 \text{ }^\circ\text{C}$ and pyrrolidine (17.7 mL, 216 mmol, 13.1 eq.) was added dropwise. Afterwards the cooling bath was removed and the mixture stirred for additional 6 h. Carbon tetrachloride (3.12 mL, 32.3 mmol, 1.96 eq.) was added at $-78 \text{ }^\circ\text{C}$ and the mixture allowed to warm to room temperature overnight. The suspension was filtered under air and the filter cake extracted with THF ($3 \times 60 \text{ mL}$). The solvent was removed under reduced pressure and the residue dried in high vacuum. The crude product was converted to its tetrafluoroborate salt as described in the general procedure and recrystallized from methanol/ethanol. 4·2HBF₄ (6.38 g, 9.52 mmol, 58%) was obtained as colourless solid.

[C₂₅H₅₀B₂F₈N₆P₂] ($670.27 \text{ g mol}^{-1}$) ¹H NMR (500.2 MHz, CD₃CN): δ (ppm) = 3.43 (t, ²J_{PH} = 19 Hz, 2H, CH₂), 3.25–3.22 (m, 24H, H1), 1.97–1.95 (m, 24H, H2, (overlapped with the solvent signal)). ¹³C{¹H} NMR (125.8 MHz, CD₃CN): δ (ppm) = 48.7 (s, C1), 26.9–26.8 (m, C2), 26.4 (t, ¹J_{PC} = 110 Hz, CH₂). ³¹P{¹H} NMR (121.5 MHz, CD₃CN): δ (ppm) = 32.7. ESI(+) MS (MeOH): *m/z* (%) = 495.6 (100) [M – H – 2BF₄]⁺, 583.2 (5) [M – BF₄]⁺. ESI(+) HRMS: *m/z* [M – H – 2BF₄]⁺ calcd 495.3488, found 495.3505; [M – BF₄]⁺ calcd 583.3600, found 583.3611. Elemental analysis: calcd C 44.80%, H 7.52%, N 12.54%; found C 44.49%, H 7.50%, N 12.46%. IR (neat): $\tilde{\nu}$ (cm⁻¹) = 2970 (w), 2879 (w), 1458 (w), 1251 (w), 1210 (m), 1134 (m), 1047 (vs.), 1021 (vs.), 918 (m), 870 (m), 824 (m), 779 (m), 699 (m), 581 (w), 549 (w), 517 (m) 484 (s). XRD: for single crystal X-ray structure determination suitable single crystals were obtained by slow evaporation of a concentrated solution in chloroform.

sym-(tmg)₂(dma)₄-CDP·2HBF₄ (1·2HBF₄)

3 (831 mg, 3.29 mmol, 1.00 eq.) and tetramethylguanidine (1.14 g, 9.88 mmol, 3.00 eq.) were dissolved in THF (60 mL). Carbon tetrachloride (640 μL , 6.62 mmol, 2.01 eq.) was added at $-78 \text{ }^\circ\text{C}$ and the mixture allowed to warm to room temperature overnight. The suspension was filtered under air and the filter cake extracted with THF ($3 \times 20 \text{ mL}$). The solvent was removed under reduced pressure and the residue dried in high vacuum. The crude product was converted to its tetrafluoroborate salt as described in the general procedure and recrystallized from ethanol. 1·2HBF₄ (1.08 g, 1.66 mmol, 50%) was isolated as colourless solid.

[C₁₀H₅₀B₂F₈N₁₀P₂] (654.24 g mol⁻¹) ¹H NMR (500.2 MHz, CD₃CN): δ (ppm) = 3.16 (t, ²J_{PH} = 17 Hz, 2H, CH₂), 2.91 (s, 24H, H1), 25.3 (d, ³J_{PH} = 10 Hz, 24H, H2). ¹³C{¹H} NMR (125.8 MHz, CD₃CN): δ (ppm) = 161.6 (dd, 2 × ²J_{PC} = 2 Hz, CN₃), 40.9 (s, C1), 37.1 (dd, 2 × ²J_{PC} = 2 Hz, C2), 25.2 (t, ¹J_{PC} = 112 Hz, CH₂). ³¹P{¹H} NMR (202.5 MHz, CD₃CN): δ (ppm) = 20.8 (s, ¹J_{PC} = 113 Hz (satellites)). ESI(+) MS (MeOH): *m/z* (%) = 479.5 (100) [M - H - 2BF₄]⁺. ESI(+) HRMS: *m/z* [M - H - 2BF₄]⁺ calcd. 479.3622, found 479.3625. Elemental analysis: calcd C 34.88%, H 7.70%, N 21.41%; found C 34.98%, H 7.84%, N 21.39%. IR (neat): $\tilde{\nu}$ (cm⁻¹) = 2911 (br. w.), 1539 (s), 1486 (m), 1429 (m), 1401 (m), 1356 (m), 1289 (m), 1235 (w), 1186 (m), 1161 (m), 1046 (vs.), 1034 (vs.), 979 (vs.), 933 (vs.), 784 (s), 771 (s), 739 (m), 716 (m), 690 (w), 672 (w), 618 (w), 572 (m), 519 (m), 459 (m), 437 (m). XRD: for single crystal X-ray structure determination suitable single crystals were obtained from ethanol at -25 °C.

sym-(dmaP₁)₂(dma)₄-CDP · 2HBF₄ (2 · 2HBF₄)

3 (1.55 g, 6.14 mmol, 1.00 eq.) and tris(dimethylamino)phosphazene (3.28 g, 18.4 mmol, 3.00 eq.) were dissolved in THF (60 mL). Carbon tetrachloride (1.19 mL, 12.3 mmol, 2.00 eq.) was added at -78 °C and the mixture allowed to warm to room temperature overnight. The suspension was filtered under air and the filter cake extracted with THF (3 × 20 mL). The solvent was removed under reduced pressure and the residue dried in high vacuum. The crude product was converted to its tetrafluoroborate salt as described in the general procedure and recrystallized from ethanol/*n*-hexane. **2 · 2HBF₄** (2.58 g, 3.31 mmol, 54%) was isolated as colourless solid.

[C₂₁H₆₂B₂F₈N₁₂P₄] (780.31 g mol⁻¹) ¹H NMR (500.2 MHz, CD₃CN): δ (ppm) = 2.87 (t, ²J_{PH} = 19 Hz, 2H, CH₂), 2.68 (d, ³J_{PH} = 11 Hz, 24H, H2), 2.65 (d, ³J_{PH} = 10 Hz, 36H, H1). ¹³C{¹H} NMR (125.8 MHz, CD₃CN): δ (ppm) = 37.3 (m, C1, C2), 25.6 (tt, ¹J_{PC} = 122 Hz, ³J_{PC} = 7 Hz, CH₂). ³¹P{¹H} NMR (202.5 MHz, CD₃CN): δ (ppm) = 23.2–22.7 (m, P1), 20.6–20.3 (m, P2). ESI(+) MS (MeOH): *m/z* (%) = 303.5 (25) [M - 2BF₄]²⁺, 605.6 (60) [M - H - 2BF₄]⁺, 693.5 (100) [M - BF₄]⁺. ESI(+) HRMS: *m/z* [M - 2BF₄]²⁺ calcd 303.2080, found 303.2088; [M - H - 2BF₄]⁺ calcd 605.4087, found 605.4104; [M - BF₄]⁺ calcd 693.4195, found 693.4215. Elemental analysis: calcd C 32.32%, H 8.01%, N 21.54%; found C 31.94%, H 7.70%, N 21.18%. IR (neat): $\tilde{\nu}$ (cm⁻¹) = 2886 (w), 1539 (s), 1486 (m), 1429 (m), 1401 (m), 1356 (m), 1298 (m), 1234 (m), 1186 (w), 1161 (m), 1047 (vs.), 1035 (vs.), 979 (vs.), 933 (s), 784 (s), 771 (s), 739 (m), 715 (m), 690 (m), 672 (m), 572 (m), 519 (m), 459 (m), 439 (m). XRD: for single crystal X-ray structure determination suitable single crystals were obtained from ethanol/*n*-hexane at -25 °C.

(pyrr)₆-CDP (4)

A solution of potassium bis(trimethylsilyl)amide (558 mg, 2.80 mmol, 2.09 eq.) in THF (15 mL) was added to a suspension of **4 · 2HBF₄** (938 mg, 1.34 mmol, 1.00 eq.) in THF (40 mL) and stirred for 16 h at room temperature. All volatiles were removed *in vacuo*, the residue dissolved in *n*-hexane (20 mL) and filtered over Celite. The filter cake was extracted with *n*-hexane (2 × 15 mL) and the filtrate evaporated to dryness. **4** (481 mg,

973 μmol, 70%) was isolated as colourless solid. [C₂₅H₄₈N₆P₂] (494.65 g mol⁻¹) ¹H NMR (500.2 MHz, C₆D₆): δ (ppm) = 3.33–3.23 (m, 24H, H1), 1.75–1.64 (m, 24H, H2). ¹³C{¹H} NMR (125.8 MHz, C₆D₆): δ (ppm) = 47.4 (s, C1), 28.9 (s, C2), -1.6 (t, ¹J_{PC} = 280 Hz, PCP). ³¹P{¹H}-NMR (202.5 MHz, C₆D₆): δ (ppm) = 11.5. LIFDI(+) MS (*n*-hexane): *m/z* (%) = 495.4 (100) [M + H]⁺. LIFDI(+) HRMS: *m/z* [M + H]⁺ calcd 495.34939, found 495.35037. Elemental analysis: calcd C 60.70%, H 9.78%, N 16.99%; found C 60.39%, H 9.62%, N 17.42%. IR (neat): $\tilde{\nu}$ (cm⁻¹) = 2952 (m), 2836 (m), 1492 (w), 1435 (s), 1338 (m), 1319 (m), 1289 (w), 1191 (m), 1134 (m), 1046 (vs.), 1000 (vs.), 980 (vs.), 909 (s), 870 (m), 742 (m), 546 (vs.), 497 (vs.). XRD: for single crystal X-ray structure determination suitable single crystals were obtained from *n*-hexane at -25 °C.

sym-(tmg)₂(dma)₄-CDP (1)

A mixture of **1 · 2HBF₄** (190 mg, 290 μmol, 1.00 eq.) and sodium amide (113 mg, 2.90 mmol, 10.0 eq.) was stirred in THF (15 mL) for 16 h at room temperature. The suspension was filtered over Celite and the filter cake extracted with THF (3 × 5 mL). All volatiles were removed *in vacuo*, *n*-hexane (10 mL) added to the residue, filtered again over Celite and extracted with *n*-hexane (3 × 4 mL). Evaporation of the solvent and drying in high vacuum yielded **1** (86 mg, 0.17 mmol, 60%) as colourless solid. [C₁₉H₄₈N₁₀P₂] (478.61 g mol⁻¹) ¹H NMR (500.2 MHz, C₆D₆): δ (ppm) = 2.88 (dd, 2 × ^{3,5}J_{PH} = 5 Hz, 24H, H2), 2.73 (s, 24H, H1). ¹³C{¹H} NMR (125.8 MHz, C₆D₆): δ (ppm) = 156.0 (s, CN₃), 40.1 (s, C1), 38.3 (s, C2), 9.5 (t, ¹J_{PC} = 209 Hz, PCP). ³¹P{¹H} NMR (121.5 MHz, C₆D₆): δ (ppm) = 18.2. LIFDI(+) MS (*n*-hexane): *m/z* (%) = 479.4 (100) [M + H]⁺. LIFDI(+) HRMS: *m/z* [M + H]⁺ calcd 479.36169, found 479.36229. Elemental analysis: calcd C 47.68%, H 10.11%, N 29.27%; found C 47.54%, H 9.96%, N 29.47%. IR (neat): $\tilde{\nu}$ (cm⁻¹) = 3006 (w), 2847 (m), 2810 (m), 2778 (m), 1566 (vs.), 1496 (s), 1472 (m), 1453 (m), 1440 (m), 1421 (m), 1358 (vs.), 1281 (m), 1251 (m), 1235 (m), 1211 (m), 1173 (m), 1128 (s), 1052 (m), 971 (s), 949 (vs.), 917 (m), 860 (vs.), 796 (m), 748 (m), 685 (s), 652 (s), 629 (vs.), 568 (m), 527 (s), 452 (s). XRD: for single crystal X-ray structure determination suitable single crystals were obtained from *n*-hexane at -25 °C.

Attempted synthesis of *sym*-(dmaP₁)₂(dma)₄-CDP (2)

A mixture of **2 · 2HBF₄** (136 mg, 174 μmol, 1.0 eq.) and freshly ground sodium amide (75 mg, 1.9 mmol, 11 eq.) was suspended in THF (15 mL) and stirred for 72 h at 60 °C. The solid was removed by filtration over Celite and the filtrate evaporated to dryness. The residue was dissolved in *n*-pentane (20 mL), cleared *via* syringe filtration, the solvent removed and the residue dried in high vacuum to give **7** as pale yellow high viscous oil.

[C₁₉H₅₅N₁₀P₄] (561.62 g mol⁻¹) ¹H NMR (300.3 MHz, C₆D₆): δ (ppm) = 2.99 (d, ³J_{PH} = 9 Hz, 12H, H4), 2.88 (d, ³J_{PH} = 10 Hz, 12H, H3), 2.83 (d, ³J_{PH} = 11 Hz, 12H, H2), 2.32 (d, ³J_{PH} = 10 Hz, 18H, H1), 0.42 (dddd, 2 × ²J_{PH} = 3 Hz, 2 × ⁴J_{PH} = 2 Hz, 1H, CH). ¹³C{¹H} NMR (75.5 MHz, C₆D₆): δ (ppm) = 38.5 (dd, ²J_{PC} = 4 Hz, ⁴J_{PC} = 3 Hz, C3), 38.4 (d, ²J_{PC} = 16 Hz, C4), 38.1 (dd, ²J_{PC} = 4 Hz, ⁴J_{PC} = 1 Hz, C2) 37.1 (d, ²J_{PC} = 4 Hz, C1), 13.0 (ddd, ¹J_{PC} =

187 Hz, $^1J_{PC} = 186$ Hz, $^3J_{PC} = 2$ Hz, CH). $^{31}\text{P}\{^1\text{H}\}$ NMR (121.5 MHz, C_6D_6): δ (ppm) = 109.9 (d, $^2J_{PP} = 100$ Hz, P4), 39.9 (dd, $^2J_{PP} = 50$ Hz, $^2J_{PP} = 41$ Hz, P2), 37.0 (dd, $^2J_{PP} = 100$ Hz, $^2J_{PP} = 41$ Hz, P3), 15.1 (d, $^2J_{PP} = 50$ Hz, P1). LIFDI(+) MS (*n*-hexane): m/z (%) = 561.4 (100) $[\text{M}]^+$. LIFDI(+) HRMS: m/z $[\text{M}]^+$ calcd 561.35924, found 561.35562.

(pyrr)₆-CDP·HTFSI (4·HTFSI)

4 (8.954 mg, 18.10 μmol , 1.04 eq.) and triflimidic acid (4.911 mg, 17.46 μmol , 1.00 eq.) were mixed in THF-*d*₈ (0.5 mL) and used for analytics.

$[\text{C}_{27}\text{H}_{49}\text{F}_6\text{N}_7\text{O}_4\text{P}_2\text{S}_2]$ (775.79 g mol⁻¹) ^1H NMR (500.2 MHz, THF-*d*₈): δ (ppm) = 3.20–3.17 (m, 24H, H1), 1.88–1.85 (m, 24H, H2), 0.93 (t, $^2J_{PH} = 7$ Hz, 1H, CH). $^{13}\text{C}\{^1\text{H}\}$ NMR (125.8 MHz, THF-*d*₈): δ (ppm) = 121.1 (q, $^1J_{FC} = 323$ Hz, CF₃), 47.8 (s, C1), 26.9 (dd, $2 \times J_{PC} = 4$ Hz, C2), 10.3 (t, $^1J_{PC} = 192$ Hz, CH). $^{31}\text{P}\{^1\text{H}\}$ NMR (121.5 MHz, THF-*d*₈): δ (ppm) = 40.1. LIFDI(+) MS (THF): m/z (%) = 495.4 (100) $[\text{M} - \text{TFSI}]^+$. LIFDI(+) HRMS: m/z $[\text{M} - \text{TFSI}]^+$ calcd 495.34939, found 495.35146.

sym-(tmg)₂(dma)₄-CDP·HTFSI (1·HTFSI)

1 (9.273 mg, 19.38 μmol , 1.00 eq.) and triflimidic acid (5.517 mg, 19.62 μmol , 1.01 eq.) were mixed in THF-*d*₈ (0.5 mL) and used for analytics.

$[\text{C}_{21}\text{H}_{49}\text{F}_6\text{N}_{11}\text{O}_4\text{P}_2\text{S}_2]$ (759.75 g mol⁻¹) ^1H NMR (300.3 MHz, THF-*d*₈): δ (ppm) = 2.90 (s, 24H, H1), 2.67–2.64 (m, 24H, H2), 0.55 (t, $^2J_{PH} = 4$ Hz, 1H, CH). $^{13}\text{C}\{^1\text{H}\}$ NMR (75.5 MHz, THF-*d*₈): δ (ppm) = 161.1 (s, CN₃), 121.1 (q, $^1J_{FC} = 322$ Hz, CF₃), 40.3 (s, C1), 37.7 (dd, $2 \times ^2J_{PC} = 2$ Hz, C2), 9.3 (t, $^1J_{PC} = 185$ Hz, CH). $^{31}\text{P}\{^1\text{H}\}$ NMR (121.5 MHz, C_6D_6): δ (ppm) = 37.1. LIFDI(+) MS (THF): m/z (%) = 479.4 (100) $[\text{M} - \text{TFSI}]^+$. LIFDI(+) HRMS: m/z $[\text{M} - \text{TFSI}]^+$ calcd 479.36169, found 479.36232.

sym-(dmaP)₂(dma)₄-CDP·HBF₄ (2·HBF₄)

A mixture of 2·2HBF₄ (600 mg, 769 μmol , 1.00 eq.) and finely ground sodium amide (321 mg, 8.23 mmol, 10.7 eq.) was suspended in THF (20 mL), cooled to -78 °C and ammonia (ca. 40 mL) was condensed in. The mixture was allowed to warm to room temperature overnight, the solid removed by centrifugation and the supernatant evaporated to dryness. The residue was dissolved in dichloromethane (40 mL) and filtered over Celite. All volatiles were removed *in vacuo*, the residue washed with diethyl ether (2×40 mL) and dried in high vacuum. 2·HBF₄ (365 mg, 527 μmol , 69%) was isolated as colorless solid. $[\text{C}_{21}\text{H}_{61}\text{BF}_4\text{N}_{10}\text{P}_4]$ (692.50 g mol⁻¹) ^1H NMR (500.2 MHz, CD₃CN): δ (ppm) = 2.64 (d, $^3J_{PH} = 10$ Hz, 36H, H1), 2.60–2.57 (m, 24H, H2), 0.25 (tt, $^2J_{PH} = 6$ Hz, $^4J_{PH} = 3$ Hz, 1H, CH). $^{13}\text{C}\{^1\text{H}\}$ NMR (125.8 MHz, CD₃CN): δ (ppm) = 37.9 (d, $^2J_{PC} = 2$ Hz, C2), 37.4 (d, $^2J_{PC} = 5$ Hz, C1), 12.6 (tt, $^1J_{PC} = 194$ Hz, $^3J_{PC} = 4$ Hz, CH). $^{31}\text{P}\{^1\text{H}\}$ NMR (121.5 MHz, CD₃CN): δ (ppm) = 34.3–33.6 (m, P2), 16.5–15.8 (m, P1). LIFDI(+) MS (THF): m/z (%) = 605.4 (100) $[\text{M} - \text{BF}_4]^+$. LIFDI(+) HRMS: m/z $[\text{M} - \text{BF}_4]^+$ calcd 605.40926, found 605.41147. Elemental analysis: calcd C 36.42%, H 8.88%, N 24.27%; found C 36.25%, H 8.59%, N 24.21%. IR (neat): $\tilde{\nu}$ (cm⁻¹) = 3000 (w), 2883 (m), 2846 (m), 2804 (m), 1458 (m), 1288 (s), 1243 (m), 1183 (m), 1167 (m), 1092 (m), 1048 (s), 976 (vs.), 955

(vs.), 845 (m), 823 (m), 770 (m), 740 (s), 715 (s), 660 (s), 598 (m), 551 (w), 527 (m), 498 (s), 454 (m), 420 (w).

Conflicts of interest

The authors have no conflicts to declare.

Acknowledgements

This work was supported by Philipps-Universität Marburg.

Notes and references

- 1 T. Ishikawa, *Superbases for organic synthesis. Guanidines, amidines and phosphazenes and related organocatalysts*, Wiley, Chichester, West Sussex, U.K, 2009.
- 2 E. D. Raczyńska, J.-F. Gal and P.-C. Maria, *Chem. Rev.*, 2016, **116**, 13454.
- 3 R. Schwesinger and H. Schlemper, *Angew. Chem., Int. Ed. Engl.*, 1987, **26**, 1167; *Angew. Chem.*, 1987, **99**, 1212.
- 4 R. Schwesinger, H. Schlemper, C. Hasenfratz, J. Willaredt, T. Dambacher, T. Breuer, C. Ottaway, M. Fletschinger, J. Boele, H. Fritz, D. Putzas, H. W. Rotter, F. G. Bordwell, A. V. Satish, G.-Z. Ji, E.-M. Peters, K. Peters, H. G. von Schnering and L. Walz, *Liebigs Ann./Recl.*, 1996, **1996**, 1055.
- 5 B. Kovačević and Z. B. Maksić, *Org. Lett.*, 2001, **3**, 1523.
- 6 A. A. Kolomeitsev, I. A. Koppel, T. Rodima, J. Barten, E. Lork, G.-V. Rösenthaller, I. Kaljurand, A. Kütt, I. Koppel, V. Mäemets and I. Leito, *J. Am. Chem. Soc.*, 2005, **127**, 17656.
- 7 (a) R. A. Kunetskiy, S. M. Polyakova, J. Vavřík, I. Císařová, J. Saame, E. R. Nerut, I. Koppel, I. A. Koppel, A. Kütt, I. Leito and I. M. Lyapkalo, *Chem.-Eur. J.*, 2012, **18**, 3621; (b) K. Vazdar, R. Kunetskiy, J. Saame, K. Kaupmees, I. Leito and U. Jahn, *Angew. Chem., Int. Ed.*, 2014, **53**, 1435; *Angew. Chem.*, 2014, **126**, 1459.
- 8 E. D. Nacsá and T. H. Lambert, *J. Am. Chem. Soc.*, 2015, **137**, 10246.
- 9 B. Kovačević, Z. B. Maksić and R. Vianello, *J. Chem. Soc., Perkin Trans. 2*, 2001, 886.
- 10 J. F. Kögel, B. Oelkers, B. Kovačević and J. Sundermeyer, *J. Am. Chem. Soc.*, 2013, **135**, 17768.
- 11 R. W. Alder, P. S. Bowman, W. R. S. Steele and D. R. Winterman, *Chem. Commun.*, 1968, 723.
- 12 (a) V. Raab, J. Kipke, R. M. Gschwind and J. Sundermeyer, *Chem.-Eur. J.*, 2002, **8**, 1682; (b) V. Raab, E. Gauchenova, A. Merkoulov, K. Harms, J. Sundermeyer, B. Kovačević and Z. B. Maksić, *J. Am. Chem. Soc.*, 2005, **127**, 15738; (c) L. Belding and T. Dudding, *Chem.-Eur. J.*, 2014, **20**, 1032; (d) L. Belding, P. Stoyanov and T. Dudding, *J. Org. Chem.*, 2016, **81**, 6.
- 13 (a) H. A. Staab, T. Saupe and C. Krieger, *Angew. Chem., Int. Ed. Engl.*, 1983, **22**, 731; *Angew. Chem.*, 1983, **95**, 748; (b) T. Saupe, C. Krieger and H. A. Staab, *Angew. Chem., Int. Ed. Engl.*, 1986, **25**, 451; *Angew. Chem.*, 1986, **98**, 460; (c) M. A. Zirnstein and H. A. Staab, *Angew. Chem., Int. Ed. Engl.*, 1987, **26**, 460; *Angew. Chem.*, 1987, **99**, 460; (d) R. Schwesinger, M. Mißfeldt, K. Peters and H. G. von

- Schnering, *Angew. Chem., Int. Ed. Engl.*, 1987, **26**, 1165; *Angew. Chem.*, 1987, **99**, 1210; (e) A. F. Pozharskii, O. V. Ryabtsova, V. A. Ozeryanskii, A. V. Degtyarev, O. N. Kazheva, G. G. Alexandrov and O. A. Dyachenko, *J. Org. Chem.*, 2003, **68**, 10109; (f) A. V. Degtyarev, O. V. Ryabtsova, A. F. Pozharskii, V. A. Ozeryanskii, Z. A. Starikova, L. Sobczyk and A. Filarowski, *Tetrahedron*, 2008, **64**, 6209; (g) J. F. Kögel, N.-J. Kneusels and J. Sundermeyer, *Chem. Commun.*, 2014, **50**, 4319; (h) A. F. Pozharskii, V. A. Ozeryanskii, V. Y. Mikshiev, A. S. Antonov, A. V. Chernyshev, A. V. Metelitsa, G. S. Borodkin, N. S. Fedik and O. V. Dyablo, *J. Org. Chem.*, 2016, **81**, 5574; (i) R. J. Schwamm, R. Vianello, A. Marsavelski, M. A. Garcia, R. M. Claramunt, I. Alkorta, J. Saame, I. Leito, C. M. Fitchett, A. J. Edwards and M. P. Coles, *J. Org. Chem.*, 2016, **81**, 7612; (j) J. F. Kögel, B. Kovačević, S. Ullrich, X. Xie and J. Sundermeyer, *Chem.-Eur. J.*, 2017, **23**, 2591.
- 14 (a) C. Lensink, S. K. Xi, L. M. Daniels and J. G. Verkade, *J. Am. Chem. Soc.*, 1989, **111**, 3478; (b) J. Münchenberg, H. Thönnessen, P. G. Jones and R. Schmutzler, *Phosphorus, Sulfur Silicon Relat. Elem.*, 1997, **123**, 57; (c) P. Mehlmann, C. Mück-Lichtenfeld, T. T. Y. Tan and F. Dielmann, *Chem.-Eur. J.*, 2017, **23**, 5929.
- 15 A. P. Marchenko, G. N. Koidan, A. M. Pinchuk and A. V. Kirsanov, *J. Gen. Chem. USSR*, 1984, **54**, 1581.
- 16 S. Ullrich, B. Kovačević, X. Xie and J. Sundermeyer, *Angew. Chem., Int. Ed.*, 2019, **58**, 10335; *Angew. Chem.*, 2019, **131**, 10443.
- 17 R. Schwesinger, C. Hasenfratz, H. Schlemper, L. Walz, E.-M. Peters, K. Peters and H. G. von Schnering, *Angew. Chem., Int. Ed. Engl.*, 1993, **32**, 1361; *Angew. Chem.*, 1993, **105**, 1420.
- 18 I. Leito, I. A. Koppel, I. Koppel, K. Kaupmees, S. Tshepelevitsh and J. Saame, *Angew. Chem., Int. Ed.*, 2015, **54**, 9262; *Angew. Chem.*, 2015, **127**, 9394.
- 19 (a) S. Goumri-Magnet, O. Guerret, H. Gornitzka, J. B. Cazaux, D. Bigg, F. Palacios and G. Bertrand, *J. Org. Chem.*, 1999, **64**, 3741; (b) I. A. Koppel, R. Schwesinger, T. Breuer, P. Burk, K. Herodes, I. Koppel, I. Leito and M. Mishima, *J. Phys. Chem. A*, 2001, **105**, 9575.
- 20 J. Saame, T. Rodima, S. Tshepelevitsh, A. Kütt, I. Kaljurand, T. Haljasorg, I. A. Koppel and I. Leito, *J. Org. Chem.*, 2016, **81**, 7349.
- 21 J. F. Kögel, D. Margetić, X. Xie, L. H. Finger and J. Sundermeyer, *Angew. Chem., Int. Ed.*, 2017, **56**, 3090; *Angew. Chem.*, 2017, **129**, 3136.
- 22 (a) A. J. Arduengo, R. L. Harlow and M. Kline, *J. Am. Chem. Soc.*, 1991, **113**, 361; (b) W. A. Herrmann, *Angew. Chem., Int. Ed.*, 2002, **41**, 1290; *Angew. Chem.*, 2002, **114**, 1342; (c) M. N. Hopkinson, C. Richter, M. Schedler and F. Glorius, *Nature*, 2014, **510**, 485; (d) V. Nesterov, D. Reiter, P. Bag, P. Frisch, R. Holzner, A. Porzelt and S. Inoue, *Chem. Rev.*, 2018, **118**, 9678; (e) A. Doddi, M. Peters and M. Tamm, *Chem. Rev.*, 2019, **119**, 6994.
- 23 (a) V. Lavallo, Y. Canac, C. Präsang, B. Donnadieu and G. Bertrand, *Angew. Chem., Int. Ed.*, 2005, **44**, 5705; *Angew. Chem.*, 2005, **117**, 5851; (b) M. Soleilhavoup and G. Bertrand, *Acc. Chem. Res.*, 2015, **48**, 256; (c) Z. R. Turner, *Chem.-Eur. J.*, 2016, **22**, 11461; (d) M. Melaimi, R. Jazzar, M. Soleilhavoup and G. Bertrand, *Angew. Chem., Int. Ed.*, 2017, **56**, 10046; *Angew. Chem.*, 2017, **129**, 10180; (e) C. M. Weinstein, G. P. Junor, D. R. Tolentino, R. Jazzar, M. Melaimi and G. Bertrand, *J. Am. Chem. Soc.*, 2018, **140**, 9255.
- 24 (a) C. A. Dyker, V. Lavallo, B. Donnadieu and G. Bertrand, *Angew. Chem., Int. Ed.*, 2008, **47**, 3206; *Angew. Chem.*, 2008, **120**, 3250; (b) A. Fürstner, M. Alcarazo, R. Goddard and C. W. Lehmann, *Angew. Chem., Int. Ed.*, 2008, **47**, 3210; *Angew. Chem.*, 2008, **120**, 3254; (c) O. Kauffhold and F. E. Hahn, *Angew. Chem., Int. Ed.*, 2008, **47**, 4057; *Angew. Chem.*, 2008, **120**, 4122; (d) C. Pranckevicius, L. Liu, G. Bertrand and D. W. Stephan, *Angew. Chem., Int. Ed.*, 2016, **55**, 5536; *Angew. Chem.*, 2016, **128**, 5626; (e) W.-C. Chen, W.-C. Shih, T. Jurca, L. Zhao, D. M. Andrada, C.-J. Peng, C.-C. Chang, S.-K. Liu, Y.-P. Wang, Y.-S. Wen, G. P. A. Yap, C.-P. Hsu, G. Frenking and T.-G. Ong, *J. Am. Chem. Soc.*, 2017, **139**, 12830; (f) S.-C. Chan, P. Gupta, X. Engelmann, Z. Z. Ang, R. Ganguly, E. Bill, K. Ray, S. Ye and J. England, *Angew. Chem., Int. Ed.*, 2018, **57**, 15717; *Angew. Chem.*, 2018, **130**, 15943.
- 25 (a) W. C. Kaska, D. K. Mitchell and R. F. Reichelderfer, *J. Organomet. Chem.*, 1973, **47**, 391; (b) W. Petz and G. Frenking, in *Transition Metal Complexes of Neutral eta1-Carbon Ligands*, ed. R. Chauvin and Y. Canac, Springer Berlin Heidelberg, Berlin, Heidelberg, 2010, vol. 30, pp. 49–92; (c) W. Petz, *Coord. Chem. Rev.*, 2015, **291**, 1; (d) J. E. Münzer, N.-J. H. Kneusels, B. Weinert, B. Neumüller and I. Kuzu, *Dalton Trans.*, 2019, **48**, 11076.
- 26 (a) R. Tonner and G. Frenking, *Chem.-Eur. J.*, 2008, **14**, 3260; (b) R. Tonner and G. Frenking, *Chem.-Eur. J.*, 2008, **14**, 3273; (c) M. Alcarazo, C. W. Lehmann, A. Anoop, W. Thiel and A. Fürstner, *Nat. Chem.*, 2009, **1**, 295.
- 27 F. Ramirez, N. B. Desai, B. Hansen and N. McKelvie, *J. Am. Chem. Soc.*, 1961, **83**, 3539.
- 28 O. Gasser and H. Schmidbaur, *J. Am. Chem. Soc.*, 1975, **97**, 6281.
- 29 R. Appel, U. Baumeister and F. Knoch, *Chem. Ber.*, 1983, **116**, 2275.
- 30 H. Schmidbaur, O. Gasser and M. S. Hussain, *Chem. Ber.*, 1977, **110**, 3501.
- 31 R. Appel and K. Waid, *Z. Naturforsch. B Chem. Sci.*, 1981, **36**, 131.
- 32 A. P. Marchenko, G. N. Koidan, V. A. Oleinik, I. S. Zal'tsman and A. M. Pinchuk, *J. Gen. Chem. USSR*, 1988, **58**, 1485.
- 33 R. Tonner, F. Öxler, B. Neumüller, W. Petz and G. Frenking, *Angew. Chem., Int. Ed.*, 2006, **45**, 8038; *Angew. Chem.*, 2006, **118**, 8206.
- 34 R. Tonner, G. Heydenrych and G. Frenking, *ChemPhysChem*, 2008, **9**, 1474.
- 35 (a) R. Appel, F. Knoll, W. Mische, W. Morbach, H.-D. Wihler and H. Veltmann, *Chem. Ber.*, 1976, **109**, 58; (b) R. Appel, F. Knoll, H. Schöler and H.-D. Wihler, *Angew. Chem., Int. Ed. Engl.*, 1976, **15**, 702; *Angew. Chem.*, 1976, **88**, 769; (c)

- R. Appel and H. Veltmann, *Tetrahedron Lett.*, 1977, **18**, 399;
- (d) A. P. Marchenko, G. N. Koidan, V. A. Oleinik, A. A. Kudryavtsev and A. M. Pinchuk, *J. Gen. Chem. USSR*, 1987, **57**, 1916; (e) V. A. Oleinik, A. P. Marchenko, G. N. Koidan and A. M. Pinchuk, *J. Gen. Chem. USSR*, 1988, **58**, 625; (f) G. N. Koidan, A. P. Marchenko, V. A. Oleinik and A. M. Pinchuk, *J. Gen. Chem. USSR*, 1988, **58**, 1304.
- 36 F. Ramirez and N. McKelvie, *J. Am. Chem. Soc.*, 1957, **79**, 5829.
- 37 (a) J. Münchenberg, O. Böge, A. K. Fischer, P. G. Jones and R. Schmutzler, *Phosphorus, Sulfur Silicon Relat. Elem.*, 1994, **86**, 103; (b) J. F. Kögel, N. C. Abacılar, F. Weber, B. Oelkers, K. Harms, B. Kovačević and J. Sundermeyer, *Chem.–Eur. J.*, 2014, **20**, 5994.
- 38 Z. S. Novikova, A. A. Prishchenko and I. F. Lutsenko, *J. Gen. Chem. USSR*, 1977, **47**, 707.
- 39 T. Rodima, I. Kaljurand, A. Pihl, V. Mäemets, I. Leito and I. A. Koppel, *J. Org. Chem.*, 2002, **67**, 1873.
- 40 I. Kaljurand, T. Rodima, A. Pihl, V. Mäemets, I. Leito, I. A. Koppel and M. Mishima, *J. Org. Chem.*, 2003, **68**, 9988.
- 41 A. P. Marchenko, G. N. Koidan and A. M. Pinchuk, *J. Gen. Chem. USSR*, 1984, **54**, 2405.
- 42 K. Issleib and M. Lischewski, *J. Prakt. Chem.*, 1970, **312**, 135.
- 43 (a) T. Scherpf, C. Schwarz, L. T. Scharf, J.-A. Zur, A. Helbig and V. H. Gessner, *Angew. Chem., Int. Ed.*, 2018, **57**, 12859; *Angew. Chem.*, 2018, **130**, 13041; (b) P. Weber, T. Scherpf, I. Rodstein, D. Lichte, L. T. Scharf, L. J. Gooßen and V. H. Gessner, *Angew. Chem., Int. Ed.*, 2019, **58**, 3203; *Angew. Chem.*, 2019, **131**, 3235.
- 44 P. J. Quinlivan and G. Parkin, *Inorg. Chem.*, 2017, **56**, 5493.
- 45 H. Schmidbaur, G. Hasslberger, U. Deschler, U. Schubert, C. Kappenstein and A. Frank, *Angew. Chem., Int. Ed. Engl.*, 1979, **18**, 408; *Angew. Chem.*, 1979, **91**, 437.
- 46 E. A. V. Ebsworth, T. E. Fraser, D. W. H. Rankin, O. Gasser and H. Schmidbaur, *Chem. Ber.*, 1977, **110**, 3508.
- 47 (a) A. T. Vincent and P. J. Wheatley, *J. Chem. Soc., Dalton Trans.*, 1972, 617; (b) G. E. Hardy, J. I. Zink, W. C. Kaska and J. C. Baldwin, *J. Am. Chem. Soc.*, 1978, **100**, 8001.
- 48 W. Petz, M. Fahlbusch, E. Gromm and B. Neumüller, *Z. Anorg. Allg. Chem.*, 2008, **634**, 682.
- 49 W. Petz, K. Dehnicke and B. Neumüller, *Z. Anorg. Allg. Chem.*, 2011, **637**, 1761.
- 50 R. Ganguly and V. Jevtovic, *Acta Crystallogr., Sect. E: Crystallogr. Commun.*, 2017, **73**, 1259.
- 51 (a) S. Ullrich, CCDC 1903847: Experimental Crystal Structure Determination; (b) S. Ullrich, CCDC 1903849: Experimental Crystal Structure Determination.
- 52 H. Vogt, D. Wulff-Molder, F. Ritschl, M. Mücke, U. Skrabei and M. Meisel, *Z. Anorg. Allg. Chem.*, 1999, **625**, 1025.
- 53 S. Ullrich, CCDC 1903848: Experimental Crystal Structure Determination.
- 54 M. Gruber, W. Bauer, H. Maid, K. Schöll and R. R. Tykwinski, *Inorg. Chim. Acta*, 2017, **468**, 152.
- 55 (a) R. W. Alder, P. R. Allen and S. J. Williams, *Chem. Commun.*, 1995, 1267; (b) Y.-J. Kim and A. Streitwieser, *J. Am. Chem. Soc.*, 2002, **124**, 5757; (c) N. Wang, J. Xu and J. K. Lee, *Org. Biomol. Chem.*, 2018, **16**, 8230.
- 56 (a) R. W. Alder, M. E. Blake and J. M. Oliva, *J. Phys. Chem. A*, 1999, **103**, 11200; (b) R. Tonner and G. Frenking, *Angew. Chem., Int. Ed.*, 2007, **46**, 8695; *Angew. Chem.*, 2007, **119**, 8850; (c) A. A. Tukov, A. T. Normand and M. S. Nechaev, *Dalton Trans.*, 2009, 7015.
- 57 S. Sastre, R. Casasnovas, F. Muñoz and J. Frau, *Phys. Chem. Chem. Phys.*, 2016, **18**, 11202.
- 58 W. L. F. Armarego and D. D. Perrin, *Purification of laboratory chemicals*, Butterworth Heinemann, Oxford, Boston, 4th edn, 1996.
- 59 G. R. Fulmer, A. J. M. Miller, N. H. Sherden, H. E. Gottlieb, A. Nudelman, B. M. Stoltz, J. E. Bercaw and K. I. Goldberg, *Organometallics*, 2010, **29**, 2176.

Design of Non-Ionic Carbon Superbases: Second Generation of Carbodiphosphoranes

Sebastian Ullrich,^a Borislav Kovačević,^b Björn Koch,^a Klaus Harms^a and Jörg Sundermeyer^{*a}

^aFachbereich Chemie, Philipps-Universität Marburg, Hans-Meerwein-Straße, 35032 Marburg, Germany.

^bThe Group for Computational Life Sciences, Rudjer Bošković Institute, Bijenička c. 54, HR-10000 Zagreb, Croatia.

*E-mail: jsu@staff.uni-marburg.de

Supporting Information

Table of Content

NMR Titration Experiments	S1
NMR Spectra	S3
Crystallographic Section	S20
Computational Section	S24
References	S48

NMR titration experiments

The experimental pK_{BH}^+ values in THF of **1** and **4** were determined via NMR titration. The general procedure for NMR titration experiments for the determination of pK_{BH}^+ values was described elsewhere.¹ The carbodiphosphorane (CDP) in its free form was mixed with a similar amount of a reference superbase in its protonated form ($((tmg)P_1-tBu \cdot HBF_4$, pK_a in THF: 29.1)² or with similar amounts of a reference base ($((dma)P_4-tBu$, pK_{BH}^+ in THF: 33.9; $(pyrr)P_4-tBu$, pK_{BH}^+ in THF: 35.3)² and triflimidic acid (HTFSI) in THF- d_8 . An equilibrium in competition of protons in solution was quickly reached. Quantitative $^{31}P\{^1H\}$ NMR spectra were recorded by inverse gated decoupling method with a relaxation delay of 25 s. Since proton exchange between the free CDP and its conjugate acid is slow on NMR timescale, neat signals were observed and used to determine the molar ratio of the different species at equilibrium. On the bases of these signal intensities equilibrium constants were thus calculated and the unknown pK_{BH}^+ values determined.

Sample A: **4** (5.281 mg, 10.68 μmol , 1.00eq), (dma) P_4 -*t*Bu (7.101 mg, 11.20 μmol , 1.05 eq) and HTFSI (3.415 mg, 12.15 μmol , 1.14 eq) were mixed in THF- d_8 (0.6 mL).

Sample B: **4** (5.986 mg, 12.10 μmol , 1.00eq) and (tmg) P_1 -*t*Bu·HBF₄ (6.659 mg, 12.05 μmol , 1.00 eq) were mixed in THF- d_8 (0.6 mL).

The $^{31}\text{P}\{^1\text{H}\}$ NMR spectra of the titration experiment in THF- d_8 are given in Figures S30-S32. In case of (tmg) P_1 -*t*Bu as reference base, **4** deprotonated the used (tmg) P_1 -*t*Bu·HBF₄ quantitatively, indicating a $\text{p}K_{\text{BH}^+}$ value at least one order of magnitude higher than 29.1. In case of (dma) P_4 -*t*Bu only the reference base was protonated by HTFSI with **4** remaining quantitatively in its free base form, indicating a $\text{p}K_{\text{BH}^+}$ value one order of magnitude lower than 33.9. The $\text{p}K_{\text{BH}^+}$ value of **4** can therefore be assigned between 30.1 and 32.9.

Sample C: **1** (3.423 mg, 7.152 μmol , 1.01 eq), (dma) P_4 -*t*Bu (4.640 mg, 7.320 μmol , 1.03 eq) and HTFSI (1.997 mg, 7.103 μmol , 1.00 eq) were mixed in THF- d_8 (0.6 mL).

Sample D: **1** (7.772 mg, 16.24 μmol , 1.02 eq), (pyrr) P_4 -*t*Bu (14.166 mg, 16.32 μmol , 1.03 eq) and HTFSI (4.470 mg, 15.90 μmol , 1.00 eq) were mixed in THF- d_8 (0.6 mL).

The $^{31}\text{P}\{^1\text{H}\}$ NMR spectra of the titration experiment in THF- d_8 are given in Figures S33-S35. In case of (dma) P_4 -*t*Bu as reference base, only **1** was protonated by HTFSI with (dma) P_4 -*t*Bu remaining quantitatively in its free base form, indicating a $\text{p}K_{\text{BH}^+}$ value of **1** at least one order of magnitude higher than 33.9. In case of (pyrr) P_4 -*t*Bu as reference base, signals for **1**, **1**·HTFSI, (pyrr) P_4 -*t*Bu and (pyrr) P_4 -*t*Bu·HTFSI were detected in the $^{31}\text{P}\{^1\text{H}\}$ NMR spectrum. Results of thermal dynamic basicity determination are shown in Table S1. Thus, the $\text{p}K_{\text{BH}^+}$ of **1** was determined to be 35.8 ± 1 in THF.

Table S1: $^{31}\text{P}\{^1\text{H}\}$ NMR titration experiments between **1** and (pyrr) P_4 -*t*Bu with HTFSI in THF- d_8 .

	1	(pyrr) P_4 - <i>t</i> Bu	1 ·H ⁺	(pyrr) P_4 - <i>t</i> Bu·H ⁺
Initial weight/mg	7.772	14.166	0.00	0.00
Initial amount/ μmol	16.24	16.32	0.00	0.00
Final amount/ μmol	5.65	10.64	10.59	5.68
$\text{p}K_{\text{BH}^+}(\mathbf{1}) = \text{p}K_{\text{BH}^+}((\text{pyrr})\text{P}_4\text{-}t\text{Bu}) - \log K = 35.3 - \log [(5.65 \cdot 5.68) \div (10.64 \cdot 10.59)] = 35.8$				

Computational Section

PA and GB calculation

Calculations in the gas phase are performed at the M06-2X/6-311+G(2df,p)//M06-2X/6-31+G(d) level of theory. All structures were optimized without any geometry constraints and confirmed to be an energy minimum on potential energy surface by computing their vibrational frequencies analytically.

Gas phase basicities (GB) have been calculated as the Gibbs free energy ΔG of the (gas phase) reaction: $B + H^+ \rightarrow BH^+$

Therefore, the gas basicity is calculated as: $GB = G(BH^+) - [G(B) + G(H^+)]$.

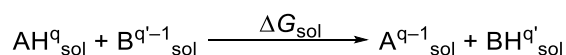
G of the neutral and protonated species contains the electronic energy E_{el} obtained at M06-2X/6-311+G(2df,p)//M06-2X/6-31+G(d) level of theory and the thermal correction to free energy, G_{therm} , which sums the zero point vibrational energy (ZPVE), enthalpic and entropic contribution at 298 K.

Proton affinities (PA) in the gas phase are calculated as the enthalpy of the aforementioned reaction. $PA = H(BH^+) - [H(B) + H(H^+)]$

All structures were optimized and characterized as energy minima by the absence of imaginary frequencies. All calculations were performed with the Gaussian09 software.¹¹

pK_a calculation

To calculate the pK_{BH^+} in THF we have used the isodesmic reaction approach (Scheme S1).



Scheme S1: Isodesmic reaction where proton exchange between an acidic species and a reference acid molecule.

The charge of the acids and the conjugate bases are represented by q/q' and $q-1/q'-1$, respectively.

The pK_a values calculated by the following equation:

$$pK_a(AH^q) = \frac{\Delta G_{sol}}{RT \cdot \ln 10} + pK_a(BH^{q'})$$

$pK_a(BH^{q'})$ is experimentally known and the free energies of deprotonation in solution (ΔG_{sol}) are obtained by following equation:

$$\Delta G_{sol} = G_{sol}(A^{q-1}) + G_{sol}(BH^{q'}) - G_{sol}(AH^q) - G_{sol}(B^{q'-1})$$

The ΔG_{sol} values in this study were calculated using SMD/M06-2X/6-311+G(2df,p)//SMD/M06-2X/6-31+G(d) computational model in THF solvent.

Deprotonation/decomposition reaction

Reaction profile for deprotonation/decomposition reaction of **2**·H⁺ in THF under the action of NH₂⁻ is presented on Figure S36. Reaction profile is calculated utilizing SMD/M06-2X/6-311+G(2df,p)//SMD/M06-2X/6-31+G(d) computational model. Transition states are characterized by the presence of one imaginary frequency. The Intrinsic Reaction Coordinate (IRC) calculation has also been performed to confirm the smooth connection of the TS to the reactant and the product. Transition states TS1 and TS1' correspond to proton transfer between **2**·H⁺ and NH₂⁻. TS1 is the activation barrier for proton transfer between central C atom of **2**·H⁺ whereas TS1' is the activation barrier for proton transfer between peripheral NCH₃ group and NH₂⁻ base. TS2 correspond to the activation barrier for P-N bond breaking with elimination of CH₂=N-CH₃ and formation of **7**.

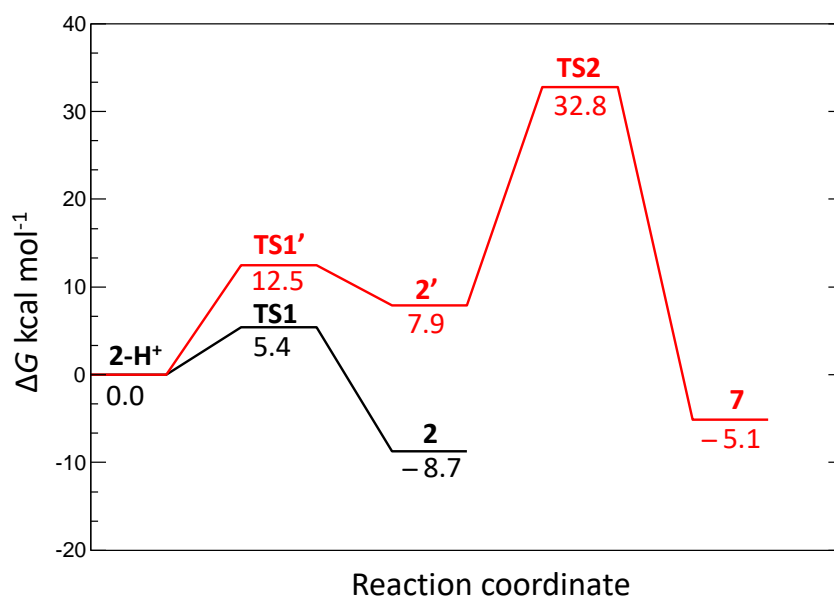


Figure S36. Relative energy profile for deprotonation/decomposition pathway of **2**·H⁺ in THF under the action of NH₂⁻ calculated at SMD/M06-2X/6-311+G(2df,p)//SMD/M06-2X/6-31G(d) level of theory. Energy profile for deprotonation of central C atom is denoted by black line, whereas deprotonation of peripheral NCH₃ (TS1') together with elimination of N-methylmethanimine (TS2) and formation of **7** is denoted by red.

References

- 1 J. F. Kögel, X. Xie, E. Baal, D. Gesevičius, B. Oelkers, B. Kovačević and J. Sundermeyer, *Chem. Eur. J.*, 2014, **20**, 7670.
- 2 J. Saame, T. Rodima, S. Tshepelevitsh, A. Kütt, I. Kaljurand, T. Haljasorg, I. A. Koppel and I. Leito, *J. Org. Chem.*, 2016, **81**, 7349.
- 3 a) Apex3, Bruker AXS Inc., Madison, Wisconsin, USA, 2016; b) SAINT, Bruker AXS Inc., Madison, Wisconsin, USA, 2015; c) SADABS. Bruker AXS area detector scaling and absorption correction, Bruker AXS Inc., Madison, Wisconsin, USA, 2016;
- 4 a) X-Area Pilatus3_SV, STOE & Cie GmbH, Darmstadt, Germany, 2016; b) X-Area Recipe, STOE & Cie GmbH, Darmstadt, Germany, 2015; c) X-Area Integrate, STOE & Cie GmbH, Darmstadt, Germany, 2016; d) X-Area LANA, STOE & Cie GmbH, Darmstadt, Germany, 2016;
- 5 G. M. Sheldrick, *Acta Cryst.*, 2015, **A71**, 3.
- 6 G. M. Sheldrick, *Acta Cryst.*, 2015, **C71**, 3.
- 7 L. J. Farrugia, *J. Appl. Crystallogr.*, 2012, **45**, 849.
- 8 C. B. Hübschle, G. M. Sheldrick and B. Dittrich, *J. Appl. Crystallogr.*, 2011, **44**, 1281.
- 9 K. Brandenburg and H. Putz, *Diamond - Crystal and Molecular Structure Visualization v4*, Crystal Impact GbR, Bonn, Germany, 2014.
- 10 Jmol colors, <http://jmol.sourceforge.net/jscolors/>, (accessed 1 May 2019).
- 11 Gaussian 09, Revision D.01, M. J. Frisch, G. W. Trucks, H. B. Schlegel, G. E. Scuseria, M. A. Robb, J. R. Cheeseman, G. Scalmani, V. Barone, G. A. Petersson, H. Nakatsuji, X. Li, M. Caricato, A. Marenich, J. Bloino, B. G. Janesko, R. Gomperts, B. Mennucci, H. P. Hratchian, J. V. Ortiz, A. F. Izmaylov, J. L. Sonnenberg, D. Williams-Young, F. Ding, F. Lipparini, F. Egidi, J. Goings, B. Peng, A. Petrone, T. Henderson, D. Ranasinghe, V. G. Zakrzewski, J. Gao, N. Rega, G. Zheng, W. Liang, M. Hada, M. Ehara, K. Toyota, R. Fukuda, J. Hasegawa, M. Ishida, T. Nakajima, Y. Honda, O. Kitao, H. Nakai, T. Vreven, K. Throssell, J. A. Montgomery, Jr., J. E. Peralta, F. Ogliaro, M. Bearpark, J. J. Heyd, E. Brothers, K. N. Kudin, V. N. Staroverov, T. Keith, R. Kobayashi, J. Normand, K. Raghavachari, A. Rendell, J. C. Burant, S. S. Iyengar, J. Tomasi, M. Cossi, J. M. Millam, M. Klene, C. Adamo, R. Cammi, J. W. Ochterski, R. L. Martin, K. Morokuma, O. Farkas, J. B. Foresman, and D. J. Fox, Gaussian, Inc., Wallingford CT, 2016.

Basicity Enhancement by Multiple Intramolecular Hydrogen Bonding in Organic Superbase N,N',N'',N''' -Tetrakis(3-(dimethylamino)propyl)triaminophosphazene

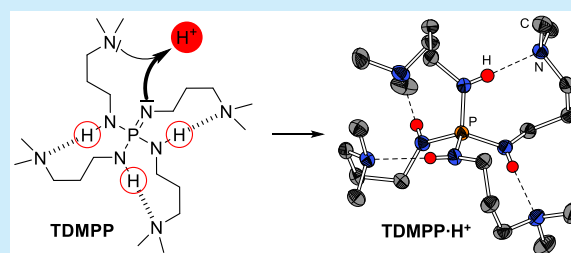
Sebastian Ullrich,[†] Danijela Barić,[‡] Xiulan Xie,[†] Borislav Kovačević,[‡] and Jörg Sundermeyer^{*,†}

[†]Fachbereich Chemie, Philipps-Universität Marburg, Hans-Meerwein-Straße, 35032 Marburg, Germany

[‡]The Group for Computational Life Sciences, Ruđer Bošković Institute, Bijenička c. 54, HR-10000 Zagreb, Croatia

Supporting Information

ABSTRACT: With the synthesis of N,N',N'',N''' -tetrakis(3-(dimethylamino)propyl)triaminophosphazene (TDMPP, **1**), we present the first phosphazene superbase with enhanced basicity through the effect of multiple intramolecular hydrogen bonding (IHB). Due to intramolecular solvation of four NH protons, the proton affinity is even higher than that of second-order phosphazene (dma) P_2 -*t*Bu. X-ray structural proof, NMR titration experiments, and computational investigations provide a more detailed quantitative description of the IHB influence on the superbasicity of **1** in solid-state, solution, and the gas-phase.



In the run for the upper staves of the basicity ladder, much effort has been devoted to the design of nonionic organic superbases.¹ The most common principle to reach superbasicity is to delocalize the positive charge either by π -resonance, aromatization, negative hyperconjugation, or proton hopping. Such concepts are realized in guanidines,^{2,3} cyclopropenimines,^{4,5} phosphazenes,⁶ and bis-P-ylides.⁷ Further amplification of basicity is accomplished by combining these structural motifs in superbases of higher-order.⁸ The top of the range nonionic nitrogen, phosphorus, and carbon superbases following this homologization concept are the long-time application-approved Schwesinger polyaminophosphazenes⁹ or even more basic phosphazanyl phosphines (PAP)¹⁰ and corresponding carbodiphosphoranes.

Additional structural features to unleash enhanced basicity other than by enlarging the molecules' scaffold are the formation of a *transannular* P→N dative bond in Verkade's proazaphosphatranes¹² or the strain relief upon protonation and formation of one intramolecular hydrogen bond (IHB), a concept exploited in the vast field of proton sponges.^{13,14} The amplification of basicity by *N*-alkylamino substituents prone to form a crown-shaped ring upon protonation via a IHB is termed as the *corona* effect (Figure 1 (I)).^{4,15} Such IHB contributes approximately 10 kcal·mol⁻¹ to the proton affinity

(PA).⁴ The cooperative effect of multiple intramolecular hydrogen bonding was elaborated for bases with different aryl- or alkylamine scaffolds¹⁶ or for a series of bases with a central guanidine moiety and different intramolecular ligand functionalities (Figure 1) L = NMe₂ (IIa),^{17,18} 2-pyridyl (IIb),¹⁹ phosphazanyl (IIc),²⁰ or cyclopropeniminyl (IId).²¹ Here the ligand L is an electron pair donor functionality toward a proton, similar as it is in coordination chemistry toward a metal Lewis acid.

Basicity measurements of N,N',N'' -tris(3-(dimethylamino)propyl)guanidine¹⁸ (TDMPG, IIa) determined a pK_a of 27.15 in acetonitrile, 2.23 pK_a units higher than corresponding N,N',N'' -tripropylguanidine possessing no IHB.²² Another series of *corona*-type bases incorporating cyclopropenimine as central moiety and as proton pincers L has been investigated computationally. Such designer base (IIId) with intrinsically better H-bond acceptors than simple dimethylamino functionalities (IIIa)²³ has a PA of 306.0 kcal·mol⁻¹ in theory.²¹ In the following fundamental investigation we extend this concept to the first-order phosphazene superbase N,N',N'',N''' -tetrakis(3-(dimethylamino)propyl)triaminophosphazene (TDMPP, **1**). We analyze by theory and experiment the increase of PA and pK_a by a multiple IHB *corona* effect. The influence of multiple hydrogen bond networks on basicity is believed to be of fundamental interest in understanding collaborative IHB effects in proteins and nucleic acids.

Tetrakis(3-(dimethylamino)propylamino)phosphonium tetraphenylborate **1**·HBPh₄ was prepared from commercially available starting materials phosphorus pentachloride and 3-

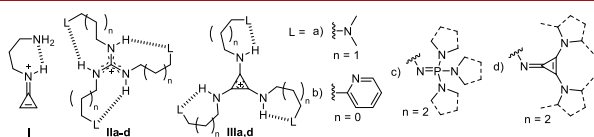
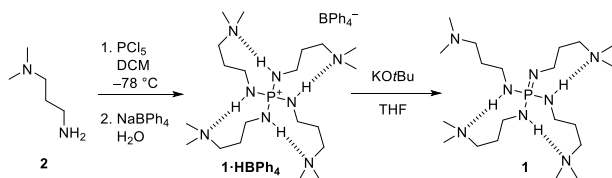


Figure 1. A selection of superbasic structural motifs incorporating the *corona* effect.

Received: October 4, 2019

(dimethylamino)propylamine **2**. The latter is acting as nucleophile and auxiliary base (Scheme 1). To our surprise

Scheme 1. Preparation of **1**^a



^aExperimental details are given in the Supporting Information.

the resulting hydrochloride **1·HCl** was obtained as highly viscous oil, even soluble in ether. Obviously, chloride is strongly solvated by the multi-NH functional cation. For purification, it is an option to exchange the chloride ion by much weaker hydrogen bond acceptor anion BPh_4^- . **1·HBPh₄** precipitated from an aqueous solution in 68% yield. Liberation of the free base was conducted with potassium *tert*-butoxide in THF to give **1** in 98% yield.

1·HBPh₄ crystallizes from ethyl acetate in space group $P2_1/c$ (Figure 2). The cation forms four equivalent IHB, building

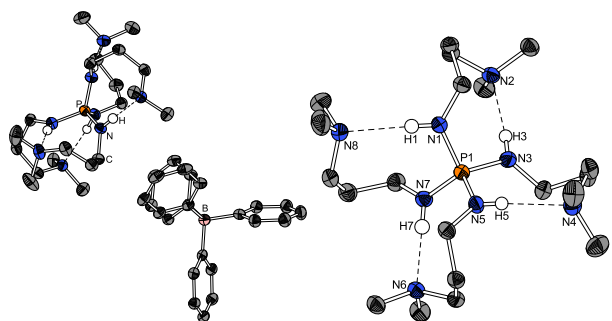


Figure 2. Molecular structure of **1·HBPh₄** (left) and substructure of the phosphonium cation (right). Carbon bonded hydrogen atoms omitted for clarity, ellipsoids at 50% probability. Selected bond length (Å) and angles (°): P1–N1 1.627(1), P1–N3 1.629(1), P1–N5 1.614(1), P1–N7 1.613(1), N1–P1–N3 103.15(6), N1–P1–N5 121.41(7), N1–P1–N7 103.81(7), N3–P1–N5 103.71(7), N3–P1–N7 121.46(7), N5–P1–N7 104.69(7), N1–H1···N8 3.049(2), 173.7(2); N3–H3···N2 2.979(2), 171(2); N5–H5···N4 2.988(2), 176(2); N7–H7···N6 2.842(2), 178(2).

eight-membered rings with a neighboring 3-(dimethylamino)propylamine substituent as shown in Scheme 1. A related arrangement of three IHB was found in the X-ray structure of guanidine **TDMPG·HPF₆** (Figure 1, IIa).¹⁸ Clearly, six-membered rings with N–H···N bond to one and the same 3-(dimethylamino)propyl substituent are thermodynamically not favored. This arrangement leads to a distortion of the tetrahedral configuration at the phosphorus atom and a flattening of the ion sphere with two expanded N–P–N angles. The P–N distances range from 1.613(1) to 1.627(1) Å and are similar to those in (dma)₃P₁–H·H⁺.²⁴ The average N–H···N distance within the H-bonds is 2.96 Å and lies in between the N–H···O bonds found in (dma)₃P₁Me·CH₃COOH (3.102(4) and 2.876(4) Å).²⁵ It is slightly longer than in **TDMPG·HPF₆** (2.886(4) Å).¹⁸ Within these asymmetric H-bonds, the protons, which were located in the

Fourier map and isotropically refined, are more strongly bound to the more basic P-amino and not C-amino groups.

The B3LYP+D3/6-31G(d) optimized gas phase structure of **1·H⁺** exhibits S_4 symmetry and is in good agreement with the experimental XRD structure: the calculated N–H···N distance is 2.90 Å and P–N distances are 1.64 Å. The alternative conformer where all IHB are established through formation of six-membered rings within one and the same dimethylaminoalkyl functionality (Figure S12 in the Supporting Information) is less stable by 13.5 kcal·mol⁻¹. The most stable conformer of neutral base **1** possesses three intramolecular hydrogen bonds with the shape similar to the conjugate acid. However, N–H···N distances in neutral base are between 3.00 and 3.05 Å implying that H-bonds in the base are weaker than in the protonated base.

The proton affinity (PA) of **1**, calculated by B3LYP+D3/6-311+G(2df,p)//B3LYP+D3/6-31G(d) model, is 286.7 kcal·mol⁻¹, whereas gas-phase basicity (GB) is 276.6 kcal·mol⁻¹. It appears that **1** has a higher by 26.5 kcal·mol⁻¹ PA than Schwesinger's phosphazene (dma)₃P₁-tBu, which is unsupported by *corona* effects, and even a higher by 12.7 kcal·mol⁻¹ PA than our bisphosphazene proton sponge 1,8-bis-(hexamethyltriaminophosphazenylnaphthalene (**HMPN**).¹⁴ Remarkably, the PA of **1** is only lower by 2.1 kcal·mol⁻¹ than that of Schwesinger's triphosphazene (dma)₃P₃-tBu.²⁶ These findings imply a strong impact of multiple IHB to the PA of **1**.

High frequency chemical shifts for the NH protons at 300 K of 6.23 (CDCl₃), 6.16 (THF), and 6.24 ppm (MeCN), respectively, with a linear chemical shift/temperature dependence and a $\Delta\delta/\Delta T$ of -11 ppb·K⁻¹ prove the existence of hydrogen bonds in the protonated form in solution (Figure S7 in the Supporting Information).²⁷ Upon deprotonation the signal in THF is shifted to 3.32 ppm with $\Delta\delta/\Delta T$ of -17 ppb·K⁻¹. Thus, IHB are existing in the protonated form as well as in the neutral base, although they are weaker in the base form **1**. A dynamic fluctuation of N–H···N bonds is suggested, since only a single signal set is observed in the ¹H NMR spectrum even at 210 K. Solvents with a high H-bond affinity are capable of breaking up the IHB in **1·HBPh₄** and form H-bonds per se. Thus, in DMSO the chemical shift of **1·HBPh₄** is 5.55 ppm at 300 K with a temperature dependency of -5 ppb·K⁻¹. The ³¹P{¹H} NMR signal of **1·HBPh₄** is a singlet with a chemical shift of 27.5 in THF-*d*₈ and 26.6 in MeCN-*d*₃. Upon deprotonation the phosphorus atom gets magnetically more shielded to 16.2 ppm in THF-*d*₈ and 18.1 ppm in MeCN-*d*₃. Proton exchange in a mixture of protonated and free base form in MeCN-*d*₃ is rapid, since the ³¹P{¹H} NMR spectrum at 203 MHz shows an averaged signal even at a temperature as low as 233 K. Both the NMR and X-ray data confirm that IHB are weaker in the tetrahedral phosphonium cation **TDMPP·H⁺** (**1·H⁺**) than in the trigonal planar guanidinium cation **TDMPG·H⁺**. In other words, the CN–H protons in **TDMPG·H⁺** are more acidic with more polarized N–H bonds than PN–H protons in **1·H⁺**.

The pK_a value of **1** was determined via NMR titration against reference base **HMPN**^{14,28} in MeCN and THF (Table 1, experimental details are given in the Supporting Information pp. S8–S11). It appears that the quadruple *corona* effect increases basicity by 1.7 orders of magnitude (in THF) and 2.9 (in MeCN) compared to *noncorona* standard base (dma)₃P₁-Me and at least 0.7 (THF) and 1.5 (MeCN) orders of magnitude compared to the most basic standard P₁-

Table 1. Experimental and Calculated pK_a Values of **1 in Comparison with the Reference base HMPN**

molecule	THF- d_6		MeCN- d_3	
	pK_a (exp)	pK_a (calc)	pK_a (exp)	pK_a (calc)
1	22.4	21.6	30.4	30.6
HMPN	21.9 ¹⁰		29.9 ²⁰	

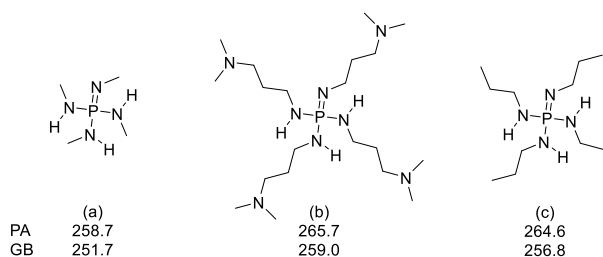
phosphazene (pyrr)P₁-Et.²⁹ TDMPP (**1**) has a pK_a in MeCN 2.8 orders of magnitude higher than known *corona-archetypical* standard TDMPG.²²

Basicity of **1** in THF and MeCN solution is calculated as a relative value utilizing thermodynamic cycle where HMPN again served as a reference base (details given in the Supporting Information). Calculated pK_a values are in excellent agreement with experimental data (Table 1). It appears that solution-phase basicity is not as pronounced as the basicity in the gas-phase. Notably, in contrast to the gas-phase, monophosphazene **1** is less basic than bisphosphazene (dma)₂P₂-*t*Bu both, in THF and MeCN. This is due to the internal solvation effect in **1** caused by the alkylamino side chains,² which is more pronounced in the gas phase than in THF and MeCN. As mentioned above, the gas phase structure of **1** possesses three intramolecular hydrogen bonds. Upon protonation the fourth IHB is formed, while the already existing three IHB become stronger than they were in the neutral base. This induces additional stabilization of the conjugate acid. As mentioned before, solvents with even more pronounced H-bond donating or accepting ability than that of THF and MeCN, such as DMSO, will hinder formation of IHBs in **1**, causing further decrease of its basicity.

From comparison of the PA of **1** and other superbases such as (dma)P₁-*t*Bu, it is obvious that the presence of dimethylaminopropyl side chains substantially increases the PA of **1**. Detailed analysis of IHB-triggered superbases introduced earlier reveals that the occurrence of IHB is not the only factor impacting basicity.^{20,21} Namely, the *N*-alkylene chain itself acts as an electron donor, thus increasing the basicity of central core of either guanidine or cyclopropenimine type.^{20,21} Finally, the inductive effect of H-bond accepting ligand L has a significant impact on the basicity in some cases.²⁰ In our previous work, we introduced the term ΔPA_{total} , which represents the increase in PA of the studied superbase due to a presence of IHB forming side chains equipped with donor L.^{20,21} It is calculated as a difference in PA of the studied IHB superbase and the appropriate reference molecule—the one that possesses the same central molecular core as the investigated IHB superbase but without side chains. For superbase **1**, the corresponding reference molecule is *N,N',N'',N'''*-tetramethyltriaminophosphazene, (TMAP, Figure 3 (a)) with a calculated PA of 258.7 kcal·mol⁻¹. We proposed that ΔPA_{total} may be presented as a sum of three terms: the strength of intramolecular H-bonds (ΔPA_{IHB}), the inductive effect of alkyl chain (ΔPA_{alkyl}), and the inductive effect of the substituent L placed at the end of the side chain (ΔPA_L):

$$\begin{aligned} \Delta PA_{\text{total}} &= PA(\text{superbase}) - PA(\text{reference molecule}) \\ &= \Delta PA_{\text{IHB}} + \Delta PA_{\text{alkyl}} + \Delta PA_L \end{aligned} \quad (1)$$

The increase of proton affinity due to the presence of intramolecular H-bonds, ΔPA_{IHB} , is calculated as difference between the PA of the examined superbase in its IHB-folded conformations (Scheme 1) and PA of its unfolded conformers

**Figure 3.** PA and GB (in kcal·mol⁻¹) of reference molecule *N,N',N'',N'''*-tetramethyltriaminophosphazene, TMAP (a), superbase **1** in unfolded (zigzag) conformation (b), and *N,N',N'',N'''*-tetrapropyltriaminophosphazene (c).

(Figure 3(b)). The difference in stability between unfolded and folded conformers of neutral and protonated molecule, respectively, is larger for protonated form, as expected. The second term, the influence of propyl substituent, ΔPA_{alkyl} is obtained as a difference in PAs between *N,N',N'',N'''*-tetrapropyltriaminophosphazene (Figure 3(c)) and the reference molecule TMAP. The last term, ΔPA_L , which describes the contribution to the PA due to inductive effect of the H-bond accepting substituent L at the end of alkyl chain, is calculated as a difference in PAs between the unfolded conformer of **1** (b) and *N,N',N'',N'''*-tetrapropyltriaminophosphazene (c). Results are presented in Table 2. As expected, the

Table 2. Calculated PA and GB of **1 and Contributions to Its Total Increase Relative to the PA and GB of the Reference Molecule TMAP^a**

	1	Δ_{total}	Δ_{IHB}	Δ_{alkyl}	Δ_L
PA	286.7	28.0	21.0	5.9	1.1
GB	276.6	24.9	17.6	5.1	2.2

^aAll values are given in kcal·mol⁻¹.

largest total contribution to the PA enhancement in **1** originates from the presence of four intramolecular H-bonds. Given that the protonated superbase **1** possesses *S*₄ symmetry, the strength of each hydrogen bond is 5.25 kcal·mol⁻¹, according to this analysis. The magnitude of the second contribution, the effect of propyl chain, is in accordance with previously calculated values for IHB stabilized superbases,^{20,21} while the inductive effect of the dimethylamino substituent has a negligible influence to proton affinity enhancement. This is similar to TDMPG where this effect contributes less than 1 kcal·mol⁻¹.²⁰ The same analysis was performed for the increase in GB (Table 2). Expectedly, the contribution of IHBs to the increase of GB is smaller than to the increase of PA value; the difference is 3.4 kcal·mol⁻¹. The effect of alkyl chains is less pronounced too (5.1 vs 5.9 kcal·mol⁻¹ for GB and PA, respectively). This is partially compensated by the influence of L, which enhances GB for 2.2 kcal·mol⁻¹, whereas for PA this increase is only 1.1 kcal·mol⁻¹.

To verify whether the above analysis gives realistic estimation of the H-bond strength, we employed another approach for its evaluation, based on the QTAIM analysis.³⁰ The IHB strength can be determined from the electron density (ρ) calculated at the bond critical point³¹ (BCP) of intramolecular hydrogen bond using the correlation of Afonin et al.:³²

$$E_{\text{HB}}(\rho^{\text{BCP}}) = 191.4\rho^{\text{BCP}} - 1.78 \quad (\text{in kcal}\cdot\text{mol}^{-1}) \quad (2)$$

According to these calculations, the strength of each IHB in the protonated superbases ($1\cdot\text{H}^+$) is $5.8\text{ kcal}\cdot\text{mol}^{-1}$, which is close to the value presented in Table 2; the strength of all four IHB is $21.0\text{ kcal}\cdot\text{mol}^{-1}$, meaning that on average each IHB contributes by $5.25\text{ kcal}\cdot\text{mol}^{-1}$. Using the AIM approach, we were also able to calculate the strength of three H-bonds that are present in a neutral form of superbases 1. Since the neutral molecule 1 is of lower symmetry, these three H-bonds are not equally strong as in S_4 symmetric $1\cdot\text{H}^+$. The calculated strength of three IHB is 3.5, 3.9, and $4.2\text{ kcal}\cdot\text{mol}^{-1}$, respectively. As already discussed, due to a lower positive charge on hydrogen atoms of N–H group in neutral base than in the conjugate acid, they are weaker than the IHB in protonated form.

It would be interesting to examine whether the increase in PA is linearly dependent on the number of IHB; i.e., does the strength of IHB decrease if their number increases? In order to answer this question, we calculated the individual IHB strength in $1\cdot\text{H}^+$ for cases where it accommodates only one to up to four IHB (Table S3 in the Supporting Information). It turns out that a saturation effect occurs: the strength of already present IHB decreases with formation of new ones. It ranges from $7.1\text{ kcal}\cdot\text{mol}^{-1}$ in a structure with one IHB to $5.8\text{ kcal}\cdot\text{mol}^{-1}$ in $1\cdot\text{H}^+$ with all four IHB.

In summary we presented the synthesis of TDMPP (1), the first phosphazene superbases with a drastic basicity enhancement by the effect of cooperative multiple intramolecular hydrogen bonds. The nature of the IHB was investigated in gas-phase, in solution, and in solid-state by experimental and computational methods. It appears that first-order phosphazene 1 possesses high pK_a values in THF and MeCN of 22.4 and 30.4, respectively, superior to those of the bisphosphazene proton sponge HMPN. The PA of $286.7\text{ kcal}\cdot\text{mol}^{-1}$ turned out to be even in a range between Schwesinger's higher-order phosphazenes $(\text{dma})_2\text{P}_2\text{-tBu}$ and $(\text{dma})_3\text{P}_3\text{-tBu}$, which are not supported by any multiple IHB corona effect. The combination of such high basicity with the straightforward synthesis, the low molecular weight, and water stability of the protonated form are encouraging for the use of 1 as versatile superbases in synthesis and organocatalysis.

■ ASSOCIATED CONTENT

Supporting Information

The Supporting Information is available free of charge on the ACS Publications website at DOI: [10.1021/acs.orglett.9b03521](https://doi.org/10.1021/acs.orglett.9b03521).

Experimental and computational details (PDF)

Accession Codes

CCDC 1912279 contains the supplementary crystallographic data for this paper. These data can be obtained free of charge via www.ccdc.cam.ac.uk/data_request/cif, or by emailing data_request@ccdc.cam.ac.uk, or by contacting The Cambridge Crystallographic Data Centre, 12 Union Road, Cambridge CB2 1EZ, UK; fax: +44 1223 336033.

■ AUTHOR INFORMATION

Corresponding Author

*E-mail: jsu@staff.uni-marburg.de.

ORCID

Danijela Barić: 0000-0002-5614-5167

Borislav Kovačević: 0000-0002-8000-4508

Jörg Sundermeyer: 0000-0001-8244-8201

Notes

The authors declare no competing financial interest.

■ ACKNOWLEDGMENTS

We thank DAAD (PPP Croatia, Proj. ID 57218955) for travel support. B.K. and D.B. thank the Univ. of Zagreb Computing Centre (SRCE) for granting computational time.

■ REFERENCES

- (1) (a) Ishikawa, T. *Superbases for Organic Synthesis: Guanidines, Amidines and Phosphazenes and Related Organocatalysts*; Wiley: Chichester, U.K., 2009. (b) Maksić, Z. B.; Kovačević, B.; Vianello, R. *Chem. Rev.* **2012**, *112*, 5240–5270. (c) Raczynska, E. D.; Gal, J.-F.; Maria, P.-C. *Chem. Rev.* **2016**, *116*, 13454–13511.
- (2) Raczynska, E. D.; Maria, P.-C.; Gal, J.-F.; Decouzon, M. *J. Phys. Org. Chem.* **1994**, *7*, 725–733.
- (3) (a) Kovačević, B.; Maksić, Z. B. *Org. Lett.* **2001**, *3*, 1523–1526. (b) Raczynska, E. D.; Cyrański, M. K.; Gutowski, M.; Rak, J.; Gal, J.-F.; Maria, P.-C.; Darowska, M.; Duczmal, K. *J. Phys. Org. Chem.* **2003**, *16*, 91–106. (c) Vazdar, K.; Kunetskiy, R.; Saame, J.; Kaupmees, K.; Leito, I.; Jahn, U. *Angew. Chem., Int. Ed.* **2014**, *53*, 1435–1438; *Angew. Chem.* **2014**, *126*, 1459–1462. (d) Schwamm, R. J.; Vianello, R.; Marsavelski, A.; Garcia, M. A.; Claramunt, R. M.; Alkorta, I.; Saame, J.; Leito, I.; Fitchett, C. M.; Edwards, A. J.; Coles, M. P. *J. Org. Chem.* **2016**, *81*, 7612–7625.
- (4) Maksić, Z. B.; Kovačević, B. *J. Phys. Chem. A* **1999**, *103*, 6678–6684.
- (5) (a) Bruns, H.; Patil, M.; Carreras, J.; Vázquez, A.; Thiel, W.; Goddard, R.; Alcarazo, M. *Angew. Chem., Int. Ed.* **2010**, *49*, 3680–3683; *Angew. Chem.* **2010**, *122*, 3762–3766. (b) Bandar, J. S.; Lambert, T. H. *J. Am. Chem. Soc.* **2012**, *134*, 5552–5555. (c) Bandar, J. S.; Lambert, T. H. *J. Am. Chem. Soc.* **2013**, *135*, 11799–11802. (d) Bandar, J.; Lambert, T. *Synthesis* **2013**, *45*, 2485–2498. (e) Bandar, J. S.; Barthelme, A.; Mazori, A. Y.; Lambert, T. H. *Chem. Sci.* **2015**, *6*, 1537–1547.
- (6) (a) Schwesinger, R.; Schlemper, H. *Angew. Chem., Int. Ed. Engl.* **1987**, *26*, 1167–1169; *Angew. Chem.* **1987**, *99*, 1212–1214. (b) Köhn, U.; Schulz, M.; Schramm, A.; Günther, W.; Görls, H.; Schenk, S.; Anders, E. *Eur. J. Org. Chem.* **2006**, *2006*, 4128–4134. (c) Uruguchi, D.; Sakaki, S.; Ooi, T. *J. Am. Chem. Soc.* **2007**, *129*, 12392–12393. (d) Núñez, M. G.; Farley, A. J. M.; Dixon, D. J. *J. Am. Chem. Soc.* **2013**, *135*, 16348–16351. (e) Krawczyk, H.; Dziegielewski, M.; Deredas, D.; Albrecht, A.; Albrecht, L. *Chem. - Eur. J.* **2015**, *21*, 10268–10277.
- (7) Kögel, J. F.; Margetić, D.; Xie, X.; Finger, L. H.; Sundermeyer, J. *Angew. Chem., Int. Ed.* **2017**, *56*, 3090–3093; *Angew. Chem.* **2017**, *129*, 3136–3139.
- (8) (a) Nacsa, E. D.; Lambert, T. H. *J. Am. Chem. Soc.* **2015**, *137*, 10246–10253. (b) Koppel, I. A.; Schwesinger, R.; Breuer, T.; Burk, P.; Herodes, K.; Koppel, I.; Leito, I.; Mishima, M. *J. Phys. Chem. A* **2001**, *105*, 9575–9586. (c) Kolomeitsev, A. A.; Koppel, I. A.; Rodima, T.; Barten, J.; Lork, E.; Röschenhaler, G.-V.; Kaljurand, I.; Kütt, A.; Koppel, I.; Mäemets, V.; Leito, I. *J. Am. Chem. Soc.* **2005**, *127*, 17656–17666. (d) Leito, I.; Koppel, I. A.; Koppel, I.; Kaupmees, K.; Tshepelevitsh, S.; Saame, J. *Angew. Chem., Int. Ed.* **2015**, *54*, 9262–9265; *Angew. Chem.* **2015**, *127*, 9394–9397.
- (9) (a) Schwesinger, R.; Hasenfratz, C.; Schlemper, H.; Walz, L.; Peters, E.-M.; Peters, K.; von Schnering, H. G. *Angew. Chem., Int. Ed. Engl.* **1993**, *32*, 1361–1363; *Angew. Chem.* **1993**, *105*, 1420–1422. (b) Schwesinger, R.; Schlemper, H.; Hasenfratz, C.; Willaredt, J.; Dambacher, T.; Breuer, T.; Ottaway, C.; Fletschinger, M.; Boele, J.; Fritz, H.; Putzas, D.; Rotter, H. W.; Bordwell, F. G.; Satish, A. V.; Ji, G.-Z.; Peters, E.-M.; Peters, K.; von Schnering, H. G.; Walz, L. *Liebigs Ann./Recl.* **1996**, *1996*, 1055–1081.

- (10) Ullrich, S.; Kovačević, B.; Xie, X.; Sundermeyer, J. *Angew. Chem., Int. Ed.* **2019**, *58*, 10335–10339; *Angew. Chem.* **2019**, *131*, 10443–10447.
- (11) Ullrich, S.; Kovačević, B.; Koch, B.; Harms, K.; Sundermeyer, J. *Chem. Sci.* **2019**, *10*, 9483–9492.
- (12) (a) Lensink, C.; Xi, S. K.; Daniels, L. M.; Verkade, J. G. *J. Am. Chem. Soc.* **1989**, *111*, 3478–3479. (b) Kisanga, P. B.; Verkade, J. G.; Schwesinger, R. *J. Org. Chem.* **2000**, *65*, 5431–5432.
- (13) (a) Alder, R. W.; Bowman, P. S.; Steele, W. R. S.; Winterman, D. R. *Chem. Commun.* **1968**, 723–724. (b) Raab, V.; Kipke, J.; Gschwind, R. M.; Sundermeyer, J. *Chem. - Eur. J.* **2002**, *8*, 1682–1693. (c) Kögel, J. F.; Oelkers, B.; Kovačević, B.; Sundermeyer, J. *J. Am. Chem. Soc.* **2013**, *135*, 17768–17774. (d) Kögel, J. F.; Kneusels, N.-J.; Sundermeyer, J. *Chem. Commun.* **2014**, *50*, 4319–4321. (e) Belding, L.; Dudding, T. *Chem. - Eur. J.* **2014**, *20*, 1032–1037. (f) Kögel, J. F.; Kovačević, B.; Ullrich, S.; Xie, X.; Sundermeyer, J. *Chem. - Eur. J.* **2017**, *23*, 2591–2598.
- (14) Raab, V.; Gauchenova, E.; Merkoulov, A.; Harms, K.; Sundermeyer, J.; Kovačević, B.; Maksić, Z. B. *J. Am. Chem. Soc.* **2005**, *127*, 15738–15743.
- (15) Maksić, Z. B.; Glasovac, Z.; Despotovi, I. *J. Phys. Org. Chem.* **2002**, *15*, 499–508.
- (16) (a) Tian, Z.; Fattahi, A.; Lis, L.; Kass, S. R. *Croat. Chem. Acta* **2009**, *82*, 41–45. (b) Bachrach, S. M.; Wilbanks, C. C. *J. Org. Chem.* **2010**, *75*, 2651–2660. (c) Bachrach, S. M. *Org. Lett.* **2012**, *14*, 5598–5601. (d) Lo, R.; Singh, A.; Kesharwani, M. K.; Ganguly, B. *Chem. Commun.* **2012**, *48*, 5865–5867. (e) Bachrach, S. M. *J. Org. Chem.* **2013**, *78*, 10909–10916. (f) Bachrach, S. M. *J. Org. Chem.* **2019**, *84*, 3467–3476.
- (17) Kovačević, B.; Glasovac, Z.; Maksić, Z. B. *J. Phys. Org. Chem.* **2002**, *15*, 765–774.
- (18) Glasovac, Z.; Kovačević, B.; Meštrović, E.; Eckert-Maksić, M. *Tetrahedron Lett.* **2005**, *46*, 8733–8736.
- (19) Glasovac, Z.; Pavošević, F.; Štrukil, V.; Eckert-Maksić, M.; Schlangen, M.; Kretschmer, R. *Int. J. Mass Spectrom.* **2013**, *354–355*, 113–122.
- (20) Barić, D.; Dragičević, I.; Kovačević, B. *J. Org. Chem.* **2013**, *78*, 4075–4082.
- (21) Barić, D.; Dragičević, I.; Kovačević, B. *Tetrahedron* **2014**, *70*, 8571–8576.
- (22) Eckert-Maksić, M.; Glasovac, Z.; Trošelj, P.; Kütt, A.; Rodima, T.; Koppel, I.; Koppel, I. A. *Eur. J. Org. Chem.* **2008**, *2008*, 5176–5184.
- (23) Gattin, Z.; Kovačević, B.; Maksić, Z. B. *Eur. J. Org. Chem.* **2005**, *2005*, 3206–3213.
- (24) (a) Ullrich, S. CCDC 1903847: Experimental Crystal Structure Determination; Cambridge Crystallographic Data Centre. (b) Ullrich, S. CCDC 1903849: Experimental Crystal Structure Determination; Cambridge Crystallographic Data Centre.
- (25) Hartmann, F.; Mootz, D.; Schwesinger, R. *Z. Naturforsch., B: J. Chem. Sci.* **1996**, *51*, 1369–1374.
- (26) Kovačević, B.; Barić, D.; Maksić, Z. B. *New J. Chem.* **2004**, *28*, 284–288.
- (27) (a) Kessler, H. *Angew. Chem., Int. Ed. Engl.* **1982**, *21*, 512–523; *Angew. Chem.* **1982**, *94*, 509–520. (b) Gellman, S. H.; Adams, B. R.; Dado, G. P. *J. Am. Chem. Soc.* **1990**, *112*, 460–461. (c) Gellman, S. H.; Dado, G. P.; Liang, G. B.; Adams, B. R. *J. Am. Chem. Soc.* **1991**, *113*, 1164–1173. (d) Andrade-Lopez, N.; Ariza-Castolo, A.; Contreras, R.; Vazquez-Olmos, A.; Barba Behrens, N.; Tlahuext, H. *Heteroat. Chem.* **1997**, *8*, 397–410. (e) Chen, J.; Willis, P.; Parkin, S.; Cammers, A. *Eur. J. Org. Chem.* **2005**, *2005*, 171–178. (f) Xu, W.; Arieno, M.; Löw, H.; Huang, K.; Xie, X.; Cruchter, T.; Ma, Q.; Xi, J.; Huang, B.; Wiest, O.; Gong, L.; Meggers, E. *J. Am. Chem. Soc.* **2016**, *138*, 8774–8780.
- (28) Kaljurand, I.; Saame, J.; Rodima, T.; Koppel, I.; Koppel, I. A.; Kögel, J. F.; Sundermeyer, J.; Köhn, U.; Coles, M. P.; Leito, I. *J. Phys. Chem. A* **2016**, *120*, 2591–2604.
- (29) (a) Kaljurand, I.; Rodima, T.; Pihl, A.; Mäemets, V.; Leito, I.; Koppel, I. A.; Mishima, M. *J. Org. Chem.* **2003**, *68*, 9988–9993.
- (b) Kaljurand, I.; Kütt, A.; Sooväli, L.; Rodima, T.; Mäemets, V.; Leito, I.; Koppel, I. A. *J. Org. Chem.* **2005**, *70*, 1019–1028.
- (30) Bader, R. F. W. *Atoms in Molecules: A Quantum Theory*; Clarendon Press: Oxford, 1994.
- (31) Espinosa, E.; Molins, E.; Lecomte, C. *Chem. Phys. Lett.* **1998**, *285*, 170–173.
- (32) Afonin, A. V.; Vashchenko, A. V.; Sigalov, M. V. *Org. Biomol. Chem.* **2016**, *14*, 11199–11211.

Basicity Enhancement by Multiple Intramolecular Hydrogen Bonding in Organic Superbase *N,N',N'',N'''*-Tetrakis(3-dimethylaminopropyl)triaminophosphazene

Sebastian Ullrich,[†] Danijela Barić,[‡] Xiulan Xie,[†] Borislav Kovačević,[‡] and Jörg Sundermeyer^{†*}

[†]Fachbereich Chemie, Philipps-Universität Marburg, Hans-Meerwein-Straße, 35032 Marburg, Germany

[‡]The Group for Computational Life Sciences, Ruđer Bošković Institute, Bijenička c. 54, HR-10000 Zagreb, Croatia

*E-mail: jsu@staff.uni-marburg.de

Supporting Information

Table of Contents

<i>Synthetic Details</i>	S1
<i>NMR Studies</i>	S8
<i>Figure S7, Temperature dependencies of chemical shift</i>	S8
<i>Computational Details</i>	S12
<i>Figure S12, Alternative conformer of $\mathbf{1}\cdot\mathbf{H}^+$</i>	S13
<i>Table S3, Individual IHB strength in different conformations of $\mathbf{1}\cdot\mathbf{H}^+$</i>	S13
<i>Coordinates of optimized geometries of $\mathbf{1}$ and $\mathbf{1}\cdot\mathbf{H}^+$</i>	S14
<i>References</i>	S16

Synthetic Details

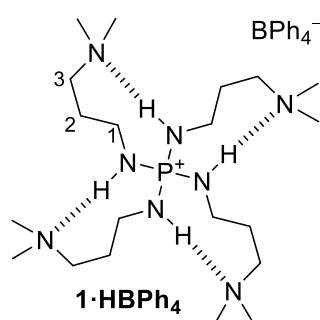
General Remarks

¹H, ¹³C, ³¹P NMR spectra and were recorded on a Bruker Avance III HD 250, Avance II 300, Avance III HD 300 or Avance III HD 500 spectrometer. Chemical shift δ is denoted relatively to SiMe₄ (¹H, ¹³C) or 85% H₃PO₄ (³¹P). ¹H and ¹³C NMR spectra were referenced to the solvent residual signals.¹ Multiplicity is abbreviated as follows: s (singlet), d (doublet), t (triplet), m (multiplet), br. (broad signal). High resolution mass spectrometry were performed on a Thermo Fisher Scientific LTQ-FT Ultra or a Jeol AccuTOF GCv., elemental analysis on an Elementar Vario Micro Cube. IR spectra were recorded in a glovebox on a Bruker Alpha ATR-FT-IR.

XRD data were collected with a Stoe STADIVARI diffractometer equipped with $\text{CuK}\alpha$ radiation, a graded multilayer mirror monochromator ($\lambda = 1.54178 \text{ \AA}$) and a DECTRIS PILATUS 300K detector using an oil-coated shock-cooled crystal at 100(2) K. Data collection, reduction, cell refinement and semi-empirical absorption correction (multi-scan) were performed within Stoe X-Area.² Structures were solved with dual-space methods using ShelXT³ and refined against F^2 with ShelXL,⁴ all within the user interface of WinGX⁵ and ShelXL.⁶ Carbon bonded hydrogen atoms were calculated in their idealized positions and refined with fixed isotropic thermal parameters. Hydrogen atoms connected to heteroatoms were located on the Fourier map and refined isotropically. All molecular structures were illustrated with Diamond 4⁷ using thermal ellipsoids at the 50% probability level.

All reactions with air or moisture sensitive substances were carried out under inert atmosphere using standard Schlenk techniques. Air or moisture sensitive substances were stored in a nitrogen-flushed glovebox. Solvents were purified according to common literature procedures and stored under an inert atmosphere over molsieve (3 \AA or 4 \AA).⁸ All other reagents were used as provided.

Tetrakis(3-dimethylaminopropylamino)phosphonium tetraphenylborat (**1·HBPh₄**)

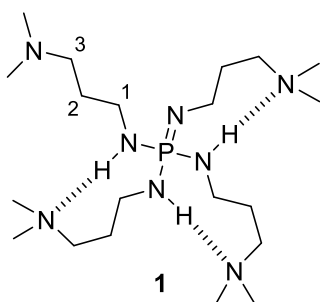


Phosphorus pentachloride (5.00 g, 24.0 mmol, 1.00 eq) was dissolved in dichloromethane (100 mL), cooled to $-78 \text{ }^\circ\text{C}$ and a solution of 3-dimethylamino-1-propylamine (24.2 mL, 192 mmol, 8.01 eq) in dichloromethane (25 mL) was added dropwise. The reaction mixture was allowed to warm to room temperature overnight, filtered under air and the filtercake extracted with dichloromethane (3x 25 mL). The filtrate was washed first with a solution of sodium tetraphenylborate (8.21 g, 24.0 mmol, 1.00 eq) in (50 mL) water and then with pure water (50 mL). The combined aqueous phase was extracted with dichloromethane (2x 50 mL) and the combined organic phase dried over sodium sulfate. All volatiles were removed in vacuo, the residue dissolved in ethyl acetate (300 mL), filtered and the filter cake extracted with ethyl acetate (2x 100 mL). The solvent was evaporated and the off-white solid **1·HBPh₄** (12.2 g, 16.2 mmol, 68%) dried in high vacuum.

$[\text{C}_{44}\text{H}_{72}\text{BN}_8\text{P}]$ ($754.90 \text{ g}\cdot\text{mol}^{-1}$) ^1H NMR (500.2 MHz, CDCl_3): δ (ppm) = 7.42 (br. s, 8H, *o-H*), 7.06 (t, $^3J_{\text{HH}} = 7 \text{ Hz}$, 8H, *m-H*), 6.91 (t, $^3J_{\text{HH}} = 7 \text{ Hz}$, 4H, *p-H*), 6.23 (dt, $^2J_{\text{PH}} = 13 \text{ Hz}$, $^3J_{\text{HH}} = 6 \text{ Hz}$, 4H, *NH*), 2.83 (dtt, $^3J_{\text{PH}} = 17 \text{ Hz}$, $2 \times ^3J_{\text{HH}} = 6 \text{ Hz}$, 8H, *HI*), 2.34 (t, $^3J_{\text{HH}} = 6 \text{ Hz}$, 8H, *H3*), 2.16 (s, 24H, *CH₃*), 1.53 (tt, $2 \times ^3J_{\text{HH}} = 6 \text{ Hz}$, *H2*). $^{13}\text{C}\{^1\text{H}\}$ -NMR (125.8 MHz, CDCl_3): δ (ppm) = 164.4 (q, $^1J_{\text{BC}} = 49 \text{ Hz}$, *i-C*), 136.4 (s, *o-C*), 125.6 (q, $^3J_{\text{BC}} = 2 \text{ Hz}$, *m-C*), 121.8 (s, *p-*

C), 54.3 (s, C3), 44.4 (s, CH₃), 37.6 (s, CI), 27.7 (d, ³J_{PC} = 5 Hz, C2). ³¹P{¹H}-NMR (202.5 MHz, CDCl₃): δ (ppm) = 25.4. ³¹P{¹H}-NMR (121.5 MHz, MeCN-*d*₃): δ (ppm) = 26.6. ³¹P{¹H}-NMR (202.5 MHz, THF-*d*₈): δ (ppm) = 27.5. ³¹P{¹H}-NMR (202.5 MHz, DMSO-*d*₆): δ (ppm) = 29.8. ESI(+)-MS (MeOH): m/z (%) = 218.4 (90) [M-BPh₄+H]²⁺, 435.5 (100) [M-BPh₄]⁺. ESI(+)-HRMS: m/z [M-BPh₄]⁺ calcd. 435.4047, found 435.4059, [M-BPh₄+H]²⁺ calcd. 218.2060, found 218.2065. ESI(-)-MS (MeOH): m/z (%) = 319.2 (100) [BPh₄]⁻. ESI(-)-HRMS: m/z [BPh₄]⁻ calcd. 319.1668, found 319.1670. Elemental analysis: calcd. C 70.01%, H 9.61%, N 14.84%; found C 69.59%, H 9.31%, N 14.61%. IR (neat): $\tilde{\nu}$ (cm⁻¹) = 3336 (m, NH), 3054 (m), 3000 (w), 3983 (w), 2943 (m), 2856 (m), 2817 (m), 2800 (m), 2781 (m), 2717 (m), 1580 (w), 1501 (m), 1464 (s), 1425 (m), 1408 (m), 1384 (m), 1355 (w), 1298 (w), 1267 (m), 1226 (m), 1173 (m), 1158 (s), 1130 (s), 1099 (m), 1074 (m), 1033 (s), 1007 (m), 991 (m), 909 (m), 856 (m), 828 (m), 746 (m), 729 (s), 702 (vs), 623 (w), 611 (s), 581(m), 543 (w), 512 (w), 484 (m), 465 (m). XRD: For single crystal X-ray structure determination suitable single crystals were obtained by slowly cooling a concentrated solution in ethyl acetate.

N,N',N'',N'''-tetrakis(3-dimethylaminopropyl)triaminophosphazene (**1**)



A solution of potassium *tert*-butoxide (180 mg, 902 μmol, 1.06 eq) in THF (200 mL) was added to a solution of **1**·HBPh₄ (640 mg, 848 μmol, 1.00 eq) in THF (20 mL) and stirred for 30 min at room temperature. Precipitated potassium tetraphenylborate was separated by centrifugation and the clear solution evaporated to dryness. The residue was dissolved in *n*-pentane (20 mL), filtered over celite and the filter cake extracted with *n*-pentane (20 mL). Removal of the solvent and drying in high vacuum yielded **1** (360 mg, 828 μmol, 98%) as yellow waxy solid.

[C₂₀H₅₁N₈P] (434.66 g·mol⁻¹) ¹H NMR (500.1 MHz, THF-*d*₈): δ (ppm) = 3.32 (s, 3H, NH), 2.90 (dt, ³J_{PH} = 11 Hz, ³J_{HH} = 7 Hz, 8H, HI), 2.29 (t, ³J_{HH} = 7 Hz, 8H, H3), 2.14 (s, 24H, CH₃), 1.56 (tt, 2x ³J_{HH} = 7 Hz, H2). ¹³C{¹H} NMR (125.8 MHz, THF-*d*₈): δ (ppm) = 58.4 (s, C3), 45.7 (s, CH₃), 40.6 (s, CI), 31.9 (d, ³J_{PC} = 9 Hz, C2). ³¹P{¹H} NMR (121.5 MHz, THF-*d*₈): δ (ppm) = 16.2. ³¹P{¹H} NMR (121.5 MHz, CD₃CN): δ (ppm) = 18.1. ³¹P{¹H} NMR (121.5 MHz, C₆D₆): δ (ppm) = 16.3. ³¹P{¹H} NMR (121.5 MHz, DMSO-*d*₆): δ (ppm) = 19.0. LIFDI(+) MS (*n*-hexane): m/z (%) = 435.4 (100) [M+H]⁺. LIFDI(+) HRMS: m/z [M+H]⁺ calcd. 435.40525, found 435.40591. IR (neat): $\tilde{\nu}$ (cm⁻¹) = 3130 (br. w, NH), 2937 (s), 2854 (m), 2811 (s), 2759 (vs), 1586 (w), 1458 (s), 1375 (m), 1299 (w), 1262 (m), 1227 (m), 1201 (s), 1173 (s), 1152 (s), 1092 (vs), 1063 (s), 1041 (s), 1011 (s), 970 (s), 936 (m), 826 (m), 748 (m), 560 (m), 484 (m), 412 (w).

NMR Studies

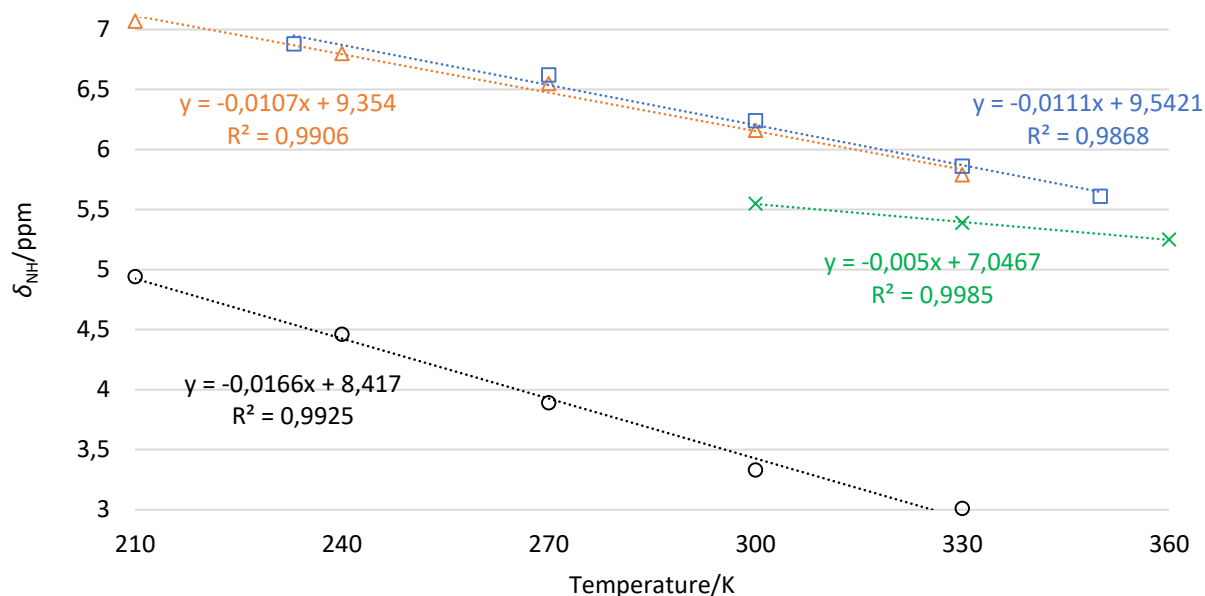


Figure S1: Temperature dependency of the NH protons chemical shift δ_{NH} of **1**·HBPh₄ in THF- d_8 (orange triangles), MeCN- d_3 (blue squares), and DMSO- d_6 (green crosses), as well as of the free base **1** in THF- d_8 (black circles).

The pK_a values of **1** in MeCN- d_3 and THF- d_8 were determined via NMR titration. The general procedure for NMR titration experiments for the determination of pK_a values was described elsewhere.⁹ Adding to the initial amount of a super base in its protonated form a similar amount of a reference super base **HMPN**¹⁰ with known basicity in the respective solvents, an equilibrium in competition of protons in solution was quickly reached. In order to have quantitative ³¹P NMR spectra relaxation times of all ³¹P signals were first determined using the standard inversion recovery procedure. Quantitative ³¹P NMR spectra were thus recorded by inverse gated decoupling method with a relaxation delay of 30 s. A mixture of **1**·HBPh₄ and **HMPN** ($pK_a = 29.9$ (MeCN)/21.9 (THF))^{10,11} in both solvents show neat signals of **HMPN** in its free and protonated forms, respectively, whereas a single average signal was observed for **1** due to fast exchange between **1** and **1**·H⁺ in all the solvents studied. Therefore, signal intensities of the reference base **HMPN** in its free and protonated forms were used to determine the molar ratio of the different species at equilibrium. On the bases of these signal intensities equilibrium constants were thus calculated and the unknown pK_a values determined. Results of thermal dynamic basicity determination are shown in Tables S1-S2. Thus, the pK_a of **1** was determined to be 30.4 and 22.4 in MeCN and THF, respectively. The ³¹P{¹H} NMR spectra of the titration experiment are given in Figures S8-S11.

Table S1: ^{31}P NMR titration experiments between **1**·HBPh₄ and HMPN in MeCN-*d*₃.

Experiment 1	1 ·HBPh ₄	HMPN	1	HMPN·HBPh ₄
Initial weight (mg)	9.073	5.777	0.00	0.00
Initial amount (μmol)	12.02	12.02	0.00	0.00
Final amount (μmol)	7.71	7.71	4.31	4.31
$\text{p}K_{\text{a}}(\mathbf{1}) = \text{p}K_{\text{a}}(\text{HMPN}) - \log K = 29.9 - \log [4.31^2 \div 7.71^2] = 30.4$				
Experiment 2	1 ·HBPh ₄	HMPN	1	HMPN·HBPh ₄
Initial weight (mg)	10.169	6.447	0.00	0.00
Initial amount (μmol)	13.47	13.42	0.00	0.00
Final amount (μmol)	8.69	8.63	4.79	4.79
$\text{p}K_{\text{a}}(\mathbf{1}) = \text{p}K_{\text{a}}(\text{HMPN}) - \log K = 29.9 - \log [4.79^2 \div (8.69 \times 8.63)] = 30.4$				

Table S2: ^{31}P NMR titration experiments between **1**·HBPh₄ and HMPN in THF-*d*₈.

Experiment 1	1 ·HBPh ₄	HMPN	1	HMPN·HBPh ₄
Initial weight (mg)	8.693	5.522	0.00	0.00
Initial amount (μmol)	11.52	11.49	0.00	0.00
Final amount (μmol)	7.36	7.33	4.16	4.16
$\text{p}K_{\text{a}}(\mathbf{1}) = \text{p}K_{\text{a}}(\text{HMPN}) - \log K = 21.9 - \log [4.16^2 \div (7.36 \times 7.33)] = 22.4$				
Experiment 2	1 ·HBPh ₄	HMPN	1	HMPN·HBPh ₄
Initial weight (mg)	8.043	5.152	0.00	0.00
Initial amount (μmol)	10.65	10.72	0.00	0.00
Final amount (μmol)	6.75	6.82	3.91	3.91
$\text{p}K_{\text{a}}(\mathbf{1}) = \text{p}K_{\text{a}}(\text{HMPN}) - \log K = 21.9 - \log [3.91^2 \div (6.75 \times 6.82)] = 22.4$				

Computational Details

Gas phase calculations are carried out at B3LYP+D3/6-311+G(2df,p)// B3LYP+D3/6-31G(d) level of theory, where term D3 indicates the explicit inclusion of Grimme's D3 atom-pair-wise dispersion correction.¹² The energy minima on potential energy surface was confirmed by vibrational analysis for all examined structures. Proton affinity (PA) is obtained according to the equation:

$$PA = H^{298}(\text{B}) + (5/2)RT - H^{298}(\text{BH}^+) \quad (1)$$

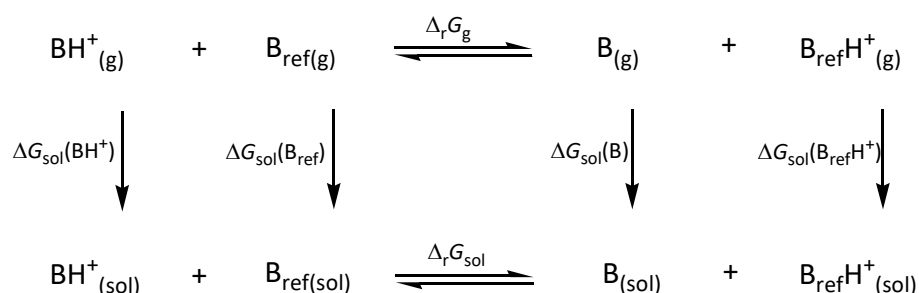
where $H^{298}(\text{B})$ and $H^{298}(\text{BH}^+)$ represent the enthalpies at 298 K of the neutral (B) and protonated base (BH^+), calculated at B3LYP+D3/6-311+G(2df,p)//B3LYP+D3/6-31G(d) level of theory, while $(5/2)RT$ corresponds to the enthalpy of proton. Gas basicity (GB) is calculated using Gibbs energies of neutral and protonated base:

$$GB = G^{298}(\text{B}) + G^{298}(\text{H}^+) - G^{298}(\text{BH}^+) \quad (2)$$

The Gibbs energy of the proton in the gas phase, $G^{298}(\text{H}^+)$, has a value of $-6.29 \text{ kcal}\cdot\text{mol}^{-1}$,¹³ and Gibbs energy of B and BH^+ , respectively, is obtained as a sum of the total energy and thermal correction to Gibbs energy calculated at the level of theory mentioned above.

$\text{p}K_{\text{a}}$ value in acetonitrile (MeCN) and in tetrahydrofuran (THF) were calculated using Truhlar's SMD model of solvation¹⁴ for both solvents, MeCN and THF. We utilized thermodynamic cycle presented in Scheme S1, with **HMPN** as a reference base B_{ref} with experimental $\text{p}K_{\text{a}}$ values of 29.9 in MeCN¹⁰ and 21.9 in THF.¹¹

Scheme S1: Thermodynamic cycle used for calculation of $\text{p}K_{\text{a}}$ values by SMD approach.



$\text{p}K_{\text{a}}$ values of investigated superbase was given as:

$$\text{p}K_{\text{a}}(\text{B}) = \Delta_r G_{\text{sol}}/RT \ln 10 + \text{p}K_{\text{a}}(\text{B}_{\text{ref}}) \quad (5)$$

The overall Gibbs energy reaction change in solution, $\Delta_r G_{\text{sol}}$, is calculated as follows:

$$\Delta_r G_{\text{sol}} = (G_{\text{g}}(\text{B}) + \Delta G_{\text{sol}}(\text{B}) + G_{\text{g}}(\text{B}_{\text{ref}}\text{H}^+) + \Delta G_{\text{sol}}(\text{B}_{\text{ref}}\text{H}^+)) - (G_{\text{g}}(\text{BH}^+) + \Delta G_{\text{sol}}(\text{BH}^+) + G_{\text{g}}(\text{B}_{\text{ref}}) + \Delta G_{\text{sol}}(\text{B}_{\text{ref}})) \quad (6)$$

where Gibbs energies in the gas phase (G_{g}) represent a sum of total energy calculated at B3LYP+D3/6-311+G(2df,p)//B3LYP+D3/6-31G(d) level of theory and thermal correction for Gibbs energy. Values of ΔG_{sol} are given as differences in energy of the structure in solution and in the gas phase and calculated using (SMD)/M06-2X/6-311+G(d,p)//B3LYP+D3/6-31G(d) model. All structure optimizations, vibrational frequency calculations and single point energies were carried out using the Gaussian 09¹⁵ package whereas the topology of the electron density was analysed using program package AIMAll.¹⁶

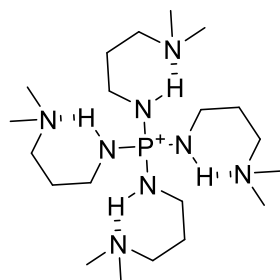


Figure S12: Conformer of $1 \cdot \text{H}^+$ with four IHB established by interaction of dimethylaminoalkyl side chain with N–H group bearing the same substituent. Calculated PA=273.2 kcal·mol⁻¹.

Table S3: Individual IHB strength (in kcal·mol⁻¹) in different conformations of $1 \cdot \text{H}^+$, calculated by QTAIM approach.

7.1	6.6	6.3	5.8
	6.5	6.0	5.8
		5.9	5.8
			5.8

References

- (1) Fulmer, G. R.; Miller, Alexander J. M.; Sherden, N. H.; Gottlieb, H. E.; Nudelman, A.; Stoltz, B. M.; Bercaw, J. E.; Goldberg, K. I. *Organometallics* **2010**, 29, 2176–2179.
- (2) a) *X-Area Pilatus3_SV*; STOE & Cie GmbH, Darmstadt, Germany, 2016; b) *X-Area Recipe*; STOE & Cie GmbH, Darmstadt, Germany, 2015; c) *X-Area Integrate*; STOE & Cie GmbH, Darmstadt, Germany, 2016; d) *X-Area LANA*; STOE & Cie GmbH, Darmstadt, Germany, 2016;
- (3) Sheldrick, G. M. *Acta Cryst.* **2015**, A71, 3–8.
- (4) Sheldrick, G. M. *Acta Cryst.* **2015**, C71, 3–8.
- (5) Farrugia, L. J. *J. Appl. Crystallogr.* **2012**, 45, 849–854.
- (6) Hübschle, C. B.; Sheldrick, G. M.; Dittrich, B. *J. Appl. Crystallogr.* **2011**, 44, 1281–1284.
- (7) Brandenburg, K.; Putz, H. *Diamond - Crystal and Molecular Structure Visualization v4*; Crystal Impact GbR, Bonn, Germany, 2014.
- (8) W. L. F. Armarego; D. D. Perrin. *Purification of laboratory chemicals*, 4th ed; Butterworth Heinemann, Oxford, Boston, 1996.
- (9) Kögel, J. F.; Xie, X.; Baal, E.; Gesevičius, D.; Oelkers, B.; Kovačević, B.; Sundermeyer, J. *Chem. Eur. J.* **2014**, 20, 7670–7685.
- (10) Raab, V.; Gauchenova, E.; Merkoulov, A.; Harms, K.; Sundermeyer, J.; Kovačević, B.; Maksić, Z. B. *J. Am. Chem. Soc.* **2005**, 127, 15738–15743.
- (11) Kaljurand, I.; Saame, J.; Rodima, T.; Koppel, I.; Koppel, I. A.; Kögel, J. F.; Sundermeyer, J.; Köhn, U.; Coles, M. P.; Leito, I. *J. Phys. Chem. A* **2016**.
- (12) Grimme, S.; Ehrlich, S.; Goerigk, L. *J. Comput. Chem.* **2011**, 32, 1456–1465.
- (13) Fifen, J. J.; Dhaouadi, Z.; Nsangou, M. *J. Phys. Chem. A* **2014**, 118, 11090–11097.
- (14) Marenich, A. V.; Cramer, C. J.; Truhlar, D. G. *J. Phys. Chem. B* **2009**, 113, 6378–6396.
- (15) Gaussian 09, Revision D.01, Frisch, M. J.; Trucks, G. W.; Schlegel, H. B.; Scuseria, G. E.; Robb, M. A.; Cheeseman, J. R.; Scalmani, G.; Barone, V.; Petersson, G. A.; Nakatsuji, H.; Li, X.; Caricato, M.; Marenich, A.; Bloino, J.; Janesko, B. G.; Gomperts, R.; Mennucci, B.; Hratchian, H. P.; Ortiz, J. V.; Izmaylov, A. F.; Sonnenberg, J. L.; Williams-Young, D.; Ding, F.; Lipparini, F.; Egidi, F.; Goings, J.; Peng, B.; Petrone, A.; Henderson, T.; Ranasinghe, D.; Zakrzewski, V. G.; Gao, J.; Rega, N.; Zheng, G.; Liang, W.; Hada, M.; Ehara, M.; Toyota, K.; Fukuda, R.; Hasegawa, J.; Ishida, M.; Nakajima, T.; Honda, Y.; Kitao, O.; Nakai, H.; Vreven, T.; Throssell, K.; Montgomery Jr., J. A.; Peralta, J. E.; Ogliaro, F.; Bearpark, M.; Heyd, J. J.; Brothers, E.; Kudin, K. N.; Staroverov, V. N.; Keith, T.; Kobayashi, R.; Normand, J.; Raghavachari, K.; Rendell, A.; Burant, J. C.; Iyengar, S.

S.; Tomasi, J.; Cossi, M.; Millam, J. M.; Klene, M.; Adamo, C.; Cammi, R.; Ochterski, J. W.; Martin, R. L.; Morokuma, K.; Farkas, O.; Foresman, J. B.; Fox, D. J. Gaussian, Inc., Wallingford CT, 2016.

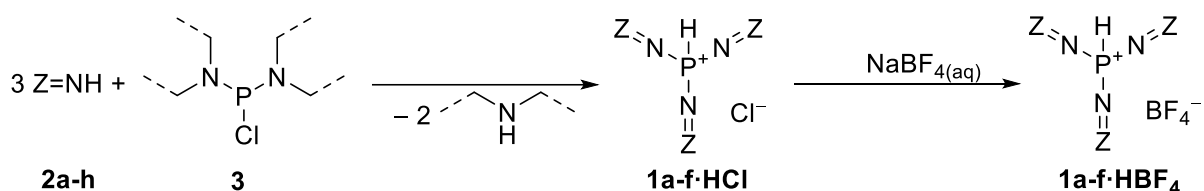
(16) Keith, T. A. *AIMAll*; TK Gristmill Software, Overland Park KS, USA, 2019.

7 Appendix

In diesem Kapitel werden Synthesen und Experimente diskutiert, die im Rahmen dieser Arbeit entwickelt und durchgeführt wurden, aber in keinem der drei Manuskripte enthalten sind. Dazu gehören grundlegende Untersuchungen, auf die die in den Manuskripten veröffentlichten Ergebnisse aufbauen, wie auch weiterführende Studien, deren Veröffentlichung noch aussteht. Um eine Publikation in Fachzeitschriften zu vereinfachen, ist der experimentelle Teil in englischer Sprache verfasst.

7.1 Diskussion

Neben dimethylamin- und pyrrolidinsubstituierten Phosphazenyldiphosphanen konnten über die Amineliminierung (Schema 7.1) drei weitere P-protonierte Phosphoniumsalze (**1·HX**) mit superbasischen Substituenten dargestellt werden, indem auch die aus Tabelle 7.1 aufgeführten Nukleophile **2e-g** eingesetzt wurden.

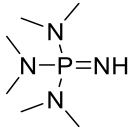
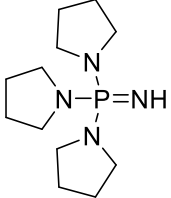
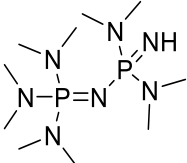
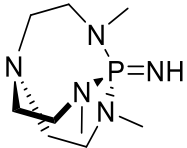
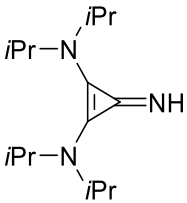
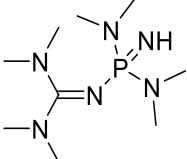
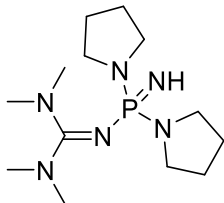
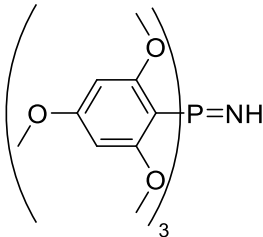


Schema 7.1: Synthese der Phosphoniumsalze **1·HCl** bzw. **1·HBF₄** über die Amineliminierung. Die Kennzeichnung der Substituenten Z=N– sowie die erzielte Ausbeute ist Tabelle 7.1 zu entnehmen.

Für die Synthese des Iminoproazaphosphatrans **2e** wurde erstmalig eine Eintopfreaktion aus STAUDINGER-Reaktion mit Trimethylsilylazid und anschließender Methanolyse durchgeführt, anstelle der zweistufigen Oxidation des Proazaphosphatrans mit Brom oder Iod und anschließender Ammonolyse.^[144,145,178] Die guanidinsubstituierten Phosphazene **2g** und **2h** sowie Tris(2,4,6-trimethoxyphenyl)iminophosphoran **2i** wurden mittels Bromierung bzw. Iodierung und anschließender Ammonolyse und Deprotonierung aus den literaturbekannten Phosphanen^[14,179] erstmalig synthetisiert.

Während sich die nach Schema 7.1 dargestellten Phosphoniumsalze **1a-f·HBF₄** selektiv bildeten, kam es bei der Synthese von **1g·HBF₄** und **1h·HBF₄** zu Nebenreaktionen. Diese sind auf die Reaktivität intermediär gebildeter freier Phosphane gegenüber dem Guanidin-substituenten zurückzuführen, weshalb die dimethylaminosubstituierte Verbindung **1g·HBF₄** nur in 16% Ausbeute rein isoliert und das pyrrolidinsubstituierte Analogon **1h·HBF₄** lediglich in Spuren nachgewiesen werden konnte. Auch im Falle des 2,4,6-trimethoxyphenyl-funktionalisierten Präkursors **2i** wurde sowohl bei Verwendung von Bis(dimethylamino)-phosphorchlorid (**3**) als auch von Phosphortrichlorid als Elektrophil keine selektive Reaktion beobachtet.

Tabelle 7.1: Übersicht der im Rahmen dieser Arbeit synthetisierten Nucleophile **2a-i** für die Darstellung superbasischer Phosphate.

Eintrag	Nucleophil	Anzahl der Stufen ^[a] (davon literaturbekannt)	P ^{III} -Basenvorläufer ^[b]
a		2 (2), ^[19] auch kommerziell erhältlich	(dma) ₃ P·HBF ₄ (87%)
b		2 (2), ^[19] auch kommerziell erhältlich	(pyrr) ₂ P·HBF ₄ (96%)
c		6 (5), ^[19] alternative Syntheseroute entwickelt	(dma) ₆ P·HBF ₄ (83%)
d	Kombination aus a und c für die Synthese nach Schema 4.2, S. 28		(dma) ₄ P·HBF ₄ (94%)
e		4 (3), ^[180] alternative Syntheseroute entwickelt	(Me ₃ tren) ₃ P·HBF ₄ ^[c] (64%)
f		2 (2) ^[116]	(cpi) ₃ P·HCl ^[d] (84%)
g		3 (2), ^[14] erstmalig synthetisiert	(tmg)(dma) ₂ P·HBF ₄ (16%)
h		3 (2), ^[14] erstmalig synthetisiert	(tmg)(pyrr) ₂ P·HBF ₄ (nur in Spuren nachweisbar)
i		4 (1), ^[179] erstmalig synthetisiert	(tmp) ₃ P·HBF ₄ ^[e] (nicht erhalten)

[a] Anzahl der im Rahmen dieser Arbeit durchgeführten Reaktionsschritte; [b] Bezeichnung und Ausbeute der nach Schema 7.1 synthetisierten P-protonierten Phosphorsuperbasen **1·HX**; [c] Me₃tren = Tris(2-N-methylaminoethyl)amin; [d] cpi = 2,3-bis(di-*iso*-propylamino)cyclopropenimin; [e] tmp = 2,4,6-Trimethoxyphenyl.

Abbildung 7.1 zeigt die über Einkristall-Röntgendiffraktometrie (XRD) erhaltenen Strukturen der Phosphoniumkationen von $(\text{Me}_3\text{tren})\text{P}_3\text{P}\cdot\text{HBPh}_4$ (**1e** $\cdot\text{HBPh}_4$) und $(\text{tmg})(\text{dma})_2\text{P}_3\text{P}\cdot\text{HBF}_4$ (**1g** $\cdot\text{HBF}_4$). Die P–N-Abstände in beiden Phosphoniumionen sind mit 1.60 Å und 1.57 Å für formale Einfach- bzw. Doppelbindungen zu denen in **1a-d** $\cdot\text{H}^+$ identisch, Guanidinsubstituenten in **1g** $\cdot\text{HBF}_4$ weisen P–N-Bindungslängen von 1.62 Å auf. Der Abstand der Brückenkopf-atome in **1e** $\cdot\text{HBPh}_4$ ist mit durchschnittlich 3.22 Å nur wenig geringer als die Summe ihrer VAN-DEER-WAALS-Radien (3.35 Å)^[170] und zeigt somit einen vernachlässigbaren stabilisierenden Einfluss einer transannularen dativen N→P-Bindung.

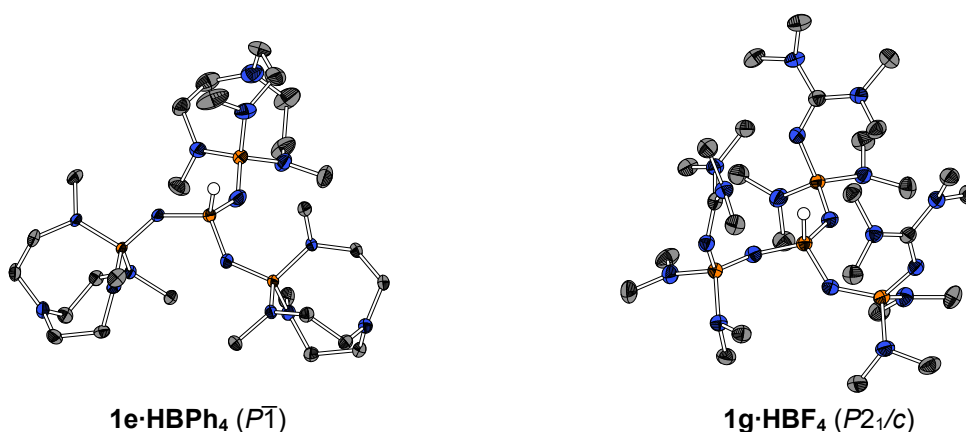


Abbildung 7.1: Im Kristall vorliegende Molekülstrukturen von $(\text{Me}_3\text{tren})\text{P}_3\text{P}\cdot\text{HBPh}_4$ (**1e** $\cdot\text{HBPh}_4$) und $(\text{tmg})(\text{dma})_2\text{P}_3\text{P}\cdot\text{HBF}_4$ (**1g** $\cdot\text{HBF}_4$).

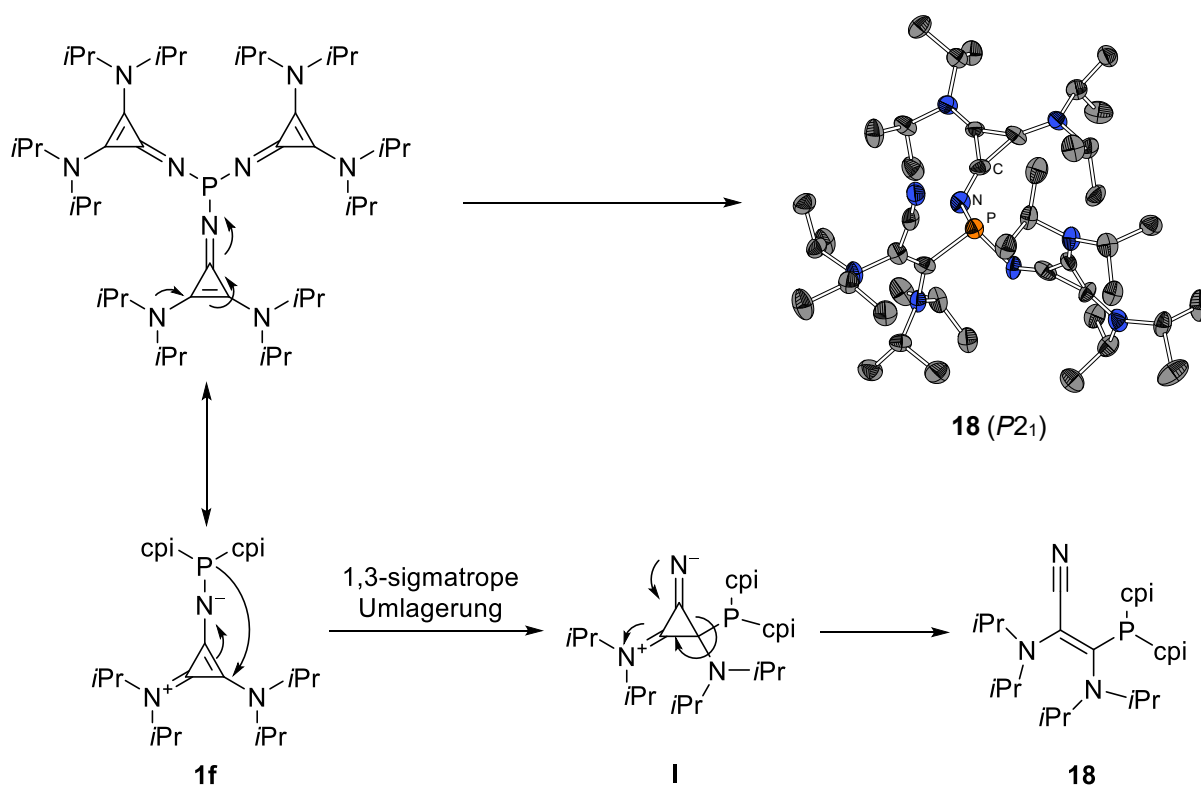
Während die Superbase $(\text{Me}_3\text{tren})\text{P}_3\text{P}$ (**1e**) mit Natriumamid in 87% Ausbeute freigesetzt werden konnte, war es nicht möglich die freie Basenform von $(\text{tmg})(\text{dma})_2\text{P}_3\text{P}$ (**1g**) zu isolieren. Analog zu seinem niedrigeren Homologen $\text{P}(\text{tmg})_3$ kam es unter Baseneinwirkung zu Zersetzungsreaktionen. Da tetramethylguanidinhaltige Phosphazenenbasen wie $(\text{tmg})_3\text{P}-t\text{Bu}$ stabil sind,^[29] ist die Instabilität auf das Phosphor(III)atom zurückzuführen, welches vermutlich in der Lage ist, das Guanidinkohlenstoffatom nukleophil anzugreifen. Aufgrund derartiger Nebenreaktionen war bereits die Synthese der protonierten Form **1g** $\cdot\text{HBF}_4$ nur in 16% Ausbeute möglich. Die Stabilisierung in einem aromatischen System, wie in Imidazolin-2-ylidenaminen (analog zu DIELMANNs IAPs),^[139] könnte hier Abhilfe schaffen. Weiterhin konnte gezeigt werden, dass die freie Basenform von $(\text{cpi})_3\text{P}$ (**1f**) durch die hohe Elektronendichte am Phosphoratom intrinsisch instabil ist und selektiv über eine 1,3-sigmatrope Umlagerung unter Ringöffnung eines elektronendonierenden Cyclopropeniminsubstituenten zu einem elektronenziehenden Acrylonitril in das weniger basische Phosphan **18** relaxiert (Schema 7.2).

Tabelle 7.2 vergleicht die NMR- und IR-spektroskopischen Daten der dargestellten Phosphane und ihrer konjugierten Säuren untereinander. Obwohl die Werte der unterschiedlichen Superbasen alle in einem ähnlichen Bereich liegen, scheint ein allgemeiner Trend, der Rückschlüsse auf die Basizität zulässt, aus diesen spektroskopischen Daten nicht ersichtlich zu sein.

Tabelle 7.2: NMR- und IR-spektroskopische Charakteristika der dargestellten Phosphane und ihrer konjugierten Säure, soweit nicht anders angegeben in C₆D₆ als Lösungsmittel.

	δ_P /ppm ($^2J_{PP}/\text{Hz}$) ^[a]	δ_P /ppm ($^2J_{PP}/\text{Hz}$) ^[b]	δ_H /ppm ($^1J_{PH}/\text{Hz}$) ^[c]	ν_{PH}/cm^{-1} ^[d]
(dma)P ₃ P (1a)	83.4 (20)	-28.9 (30)	7.65 (554)	2300
(pyrr)P ₃ P (1b)	81.1 (10)	-29.3 (24)	7.89 (556)	2292
(dma)P ₄ P (1d)	84.7 (48/18)	-28.8 (27)	7.60 (549)	2316
(dma)P ₆ P (1c)	87.6 (89) ^[e]	-30.6 (24)	7.58 (540)	2308
(Me ₃ tren)P ₃ P (1e)	90.2 (76) ^[h]	-34.0 (34) ^[i]	7.51 (554) ^[i]	2321
(cpi) ₃ P (1f)	113.6 ^[f]	10.6 ^[g]	7.76 (508) ^[g]	2337
(tmg)(dma) ₂ P ₃ P (1g)	-	-28.6(26)	7.61 (528)	2301

[a] P^{III}-Atom des freien Phosphans; [b] P^{III}-Atom der konjugierten Säure; [c] phosphorgebundenes Proton der konjugierten Säure; [d] Bande der PH-Valenzschwingung im ATR-IR-Spektrum der konjugierten Säure in Reinsubstanz; [e] in Toluol; [f] Umlagerungsprodukt **18**; [g] in CDCl₃; [h] in THF-*d*₈; [i] in CD₃CN.

Schema 7.2: 1,3-Sigmatrope Umlagerung von **1f** zu **18** inklusive dessen im Kristall vorliegender Molekülstruktur.

Zum Vergleich sind in Tabelle 7.3 die elektronischen und sterischen Eigenschaften aller diskutierten PAPs aufgelistet. Durch die fehlende Stabilisierung einer transannularen dativen N→P-Bindung in **1e**, liegt dieses von seiner Basizität lediglich aufgrund des induktiven Effektes des Me₃tren-Substituenten zwischen der von **1a** und **1b**. Während die Homologisierung von (dma)P₃P (**1a**) zu (dma)P₆P (**1c**) den berechneten pK_{BH}⁺-Wertes um 7.0 Größenordnungen steigert, ist dies bei Verwendung von Guanidinsubstituenten in **1g** immer noch um 5.3 Größenordnungen der Fall, weshalb die Synthese eines vergleichbaren imidazolin-2-ylidenamin-funktionalisierten PAPs mit höherer Stabilität ein lohnendes Ziel darstellt.

7 Appendix

Tabelle 7.3: Berechnete Protonenaffinität (PA), Gasphasenbasizität (GB), Kegelwinkel (θ) und pK_{BH^+} -Werte (in THF) sowie experimentelle pK_{BH^+} -Werte (in THF), TOLMANS elektronischer Parameter (TEP), $^1J_{\text{PSe}}$ -Kopplungskonstanten und das *buried volume* ($\%V_{\text{bur}}$) der untersuchten P^{III} -Superbasen.

	PA /kcal·mol ⁻¹	GB /kcal·mol ⁻¹	pK_{BH^+} (ber.)	pK_{BH^+} (exp.)	TEP /cm ⁻¹	$\theta/^\circ$	$^1J_{\text{PSe}}$ /Hz	$\%V_{\text{bur}}^{\text{[a]}}$
(dma)P ₃ P (1a)	297.4	291.3	34.9	34.9	2022.4	203.2	654	37.8 48.7 ^[b]
(pyrr)P ₃ P (1b)	307.5	300.2	37.8	36.7	2018.6	198.9	628	40.9
(dma)P ₄ P (1d)	304.3	295.4	37.0	37.2	2017.3	216.5	631	42.6
(dma)P ₆ P (1c)	315.4	306.8	41.9	-	2014.5	240.8	608	-
(Me ₃ tren)P ₃ P (1e)	304.9 ^[c]	296.7 ^[c]	36.6 ^[c]	-	2015.2	-	636	38.4
(cpi) ₃ P (1f)	300.4 ^[c]	291.5 ^[c]	29.0 ^[c]	-	-	-	669 ^[d]	-
(tmg)(dma) ₂ P ₃ P (1g)	309.6 ^[c]	302.8 ^[c]	40.2 ^[c]	-	-	-	-	-

[a] aus den Strukturen der LNi(CO)₃-Komplexe **5** mit SambVca 2.0^[135] ermittelt ($r = 3.50 \text{ \AA}$, $d = 2.28 \text{ \AA}$, Bondi radien skaliert mit 1.17); [b] aus der Struktur des LAuCl-Komplexes **19a** (Abbildung 7.2) ermittelt; [c] persönliche Kommunikation von BORISLAV KOVAČEVIĆ;^[174] [d] Phosphanselenid des Umlagerungsprodukts **18**.

Das *buried Volume* wurde sowohl aus korrespondierenden tetraedrischen Nickeltricarbonyl-komplexen (**5**) auf Werte um 40% als auch im Fall von (dma)P₃P (**1a**) aus dem linearen Chloridogold(I)komplex **19a** (Abbildung 7.2) auf wesentlich größere 48.7% ermittelt. Es überragt andere Phosphanliganden wie Tri-*tert*-butylphosphan (40.0%),^[129] Triadamantylphosphan (40.5%)^[129] oder Tris(imidazolin-2-ylidenamino)phosphan (38.7%)^[139] deutlich.

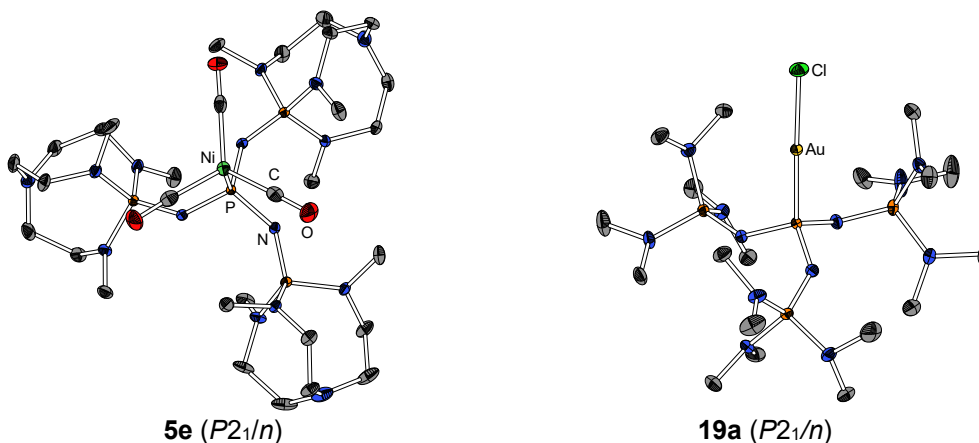
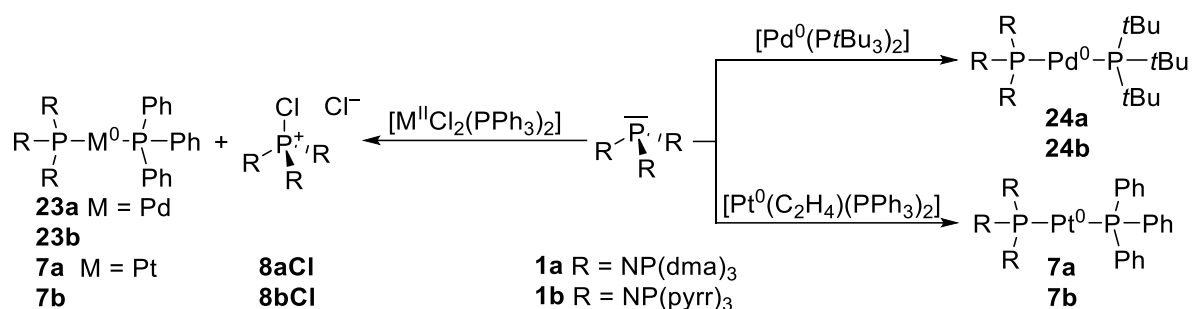


Abbildung 7.2: Im Kristall vorliegende Molekülstrukturen von [(Me₃tren)P₃P–Ni(CO)₃] (**5e**) und [(dma)P₃P–AuCl] (**19a**).

Neben tetraedrischen Nickel(0)- (**5**) und linearen Gold(I)komplexen (**19**), konnten auch die in Abbildung 7.3 dargestellten quadratisch-planaren Rhodium(I)- (**20**), Palladium(II)- (**21**) und Platin(II)komplexe (**22**) synthetisiert werden. Letztere zwei Chloridokomplexe stellten sich dabei nur im Festkörper als langzeitstabil heraus, in Lösung dagegen kam es stets zur reduktiven Eliminierung der elementaren Metalle unter Bildung des Chlorophosphoniumsalzes **8**. Das niedrige Redoxpotential der superbasischen Phosphanliganden ermöglicht im Gegenzug die Synthese linearer heteroleptischer Palladium(0)- (**23** und **24**) und Platin(0)komplexe (**7**) sowohl

aus Präkursoren der Oxidationsstufe 0 als auch der Oxidationsstufe +II (Schema 7.3). Eine zweifache Substitution zu homoleptischen Palladium(0)- und Platin(0)komplexen ist aus thermodynamischen Gründen nicht möglich. Zwar ist auch eine zweite Metall-PAP-Bindung stärker als die Metall-PPh₃-Bindung, die freiwerdende Enthalpie wird allerdings durch einen negativen Entropieterm überkompensiert, da die Freiheitsgrade beider PAPs bei Koordination an ein Metallzentrum stark reduziert werden und die Reaktion insgesamt endergonisch wird.¹⁷



Schema 7.3: Synthese linearer Pd⁰- (**23** und **24**) und Pt⁰-Komplexe (**7**). Mit [M^{II}Cl₂(PPh₃)₂] und **1** im Verhältnis 1:2 unter Bildung von **8Cl** als Nebenprodukt; mit [Pd⁰(PtBu₃)₂] bzw. [Pt⁰(C₂H₄)(PPh₃)₂] und **1** im Verhältnis 1:1.

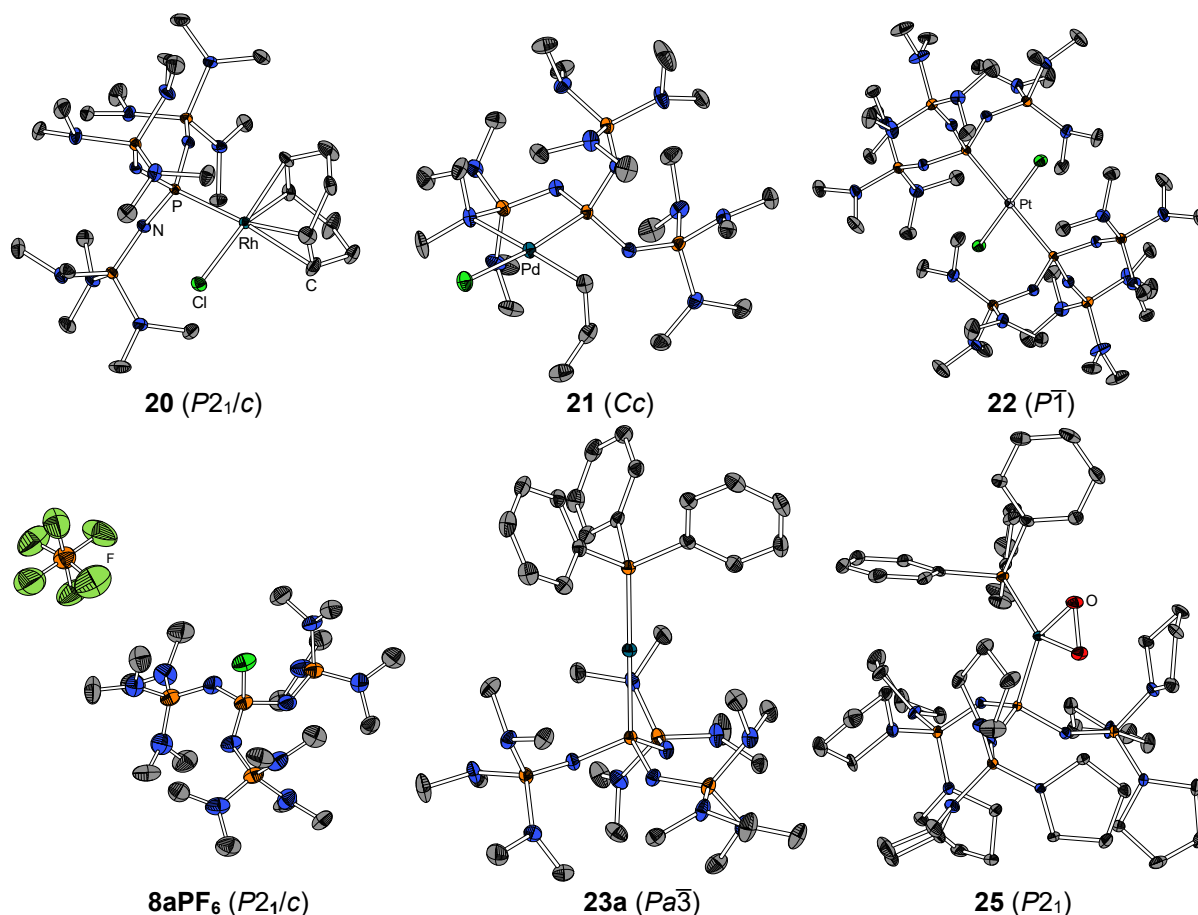
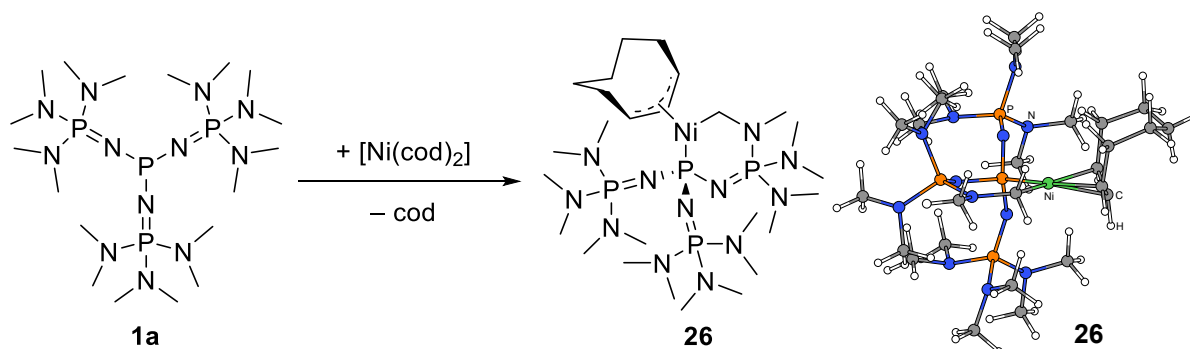


Abbildung 7.3: Im Kristall vorliegende Molekülstrukturen von [(dma)₃P₃P–Rh(cod)Cl] (**20**, cod = 1,5-Cyclo-octadien), [(dma)₃P₃P–Pd(allyl)Cl] (**21**), [{(dma)₃P₃P}₂PtCl₂] (**22**), [(dma)₃P₃P–Cl]PF₆ (**8aPF₆**, nach Anionenaustausch mit AgPF₆ erhalten), [(dma)₃P₃P–PdPPh₃] (**23a**) und [(pyrr)₃P₃P–Pd(O₂)PPh₃] (**25**).

¹⁷ Thermodynamik der Reaktion von [(dma)₃P₃P–Pt–PPh₃] (**7a**) und (dma)₃P₃P (**1a**) bei 298 K: ΔH = –4.6 kcal·mol^{–1}, ΔG = 5.8 kcal·mol^{–1}. Persönliche Kommunikation von BORISLAV KOVAČEVIĆ.^[174]

Die linearen Palladium(0)- (**23** und **24**) und Platin(0)komplexe (**7**), sind unter inerten Bedingungen sowohl in Lösung als auch im Festkörper stabil, werden jedoch leicht durch (Luft-)Sauerstoff oxidiert. So kristallisierte aus einer Lösung von **23b** in *n*-Hexan der Peroxidkomplex **25** aus. Analog zu den Palladium(II)- und Platin(II)komplexen **21** und **22** ist auch dieser nur im Festkörper langzeitstabil und zerfällt in Lösung in die korrespondierenden Phosphanoxide und elementares Palladium.

Komplex **21** ist das bislang einzige Beispiel, bei dem PAPs nicht nur über das Phosphor(III)-atom koordinieren, sondern auch chelatisierend über ein Dimethylaminostickstoffatom einen fünfgliedrigen Ring ausbilden. Obwohl die Stickstoffatome durch den Einbezug ihres freien Elektronenpaares in negative Hyperkonjugation nur schwach LEWIS-basisch sind, wird dabei sogar der Allylligand aus dem üblichen η^3 - in einen η^1 -Koordinationsmodus gedrängt. Ein einzelnes Signal für die Phosphazenylylsubstituenten im ^{31}P -NMR-Spektrum weist dabei auf eine Fluktuation innerhalb des Liganden hin. Um diesen unüblichen Koordinationsmodus in anderen Komplexen zu reproduzieren, wurden Reaktionen mit Bis(cyclooctadien)nickel(0) und -platin(0) durchgeführt, um den PAP-Liganden durch Verdrängen eines zweizähligen Cyclooctadiens in den chelatisierenden Koordinationsmodus zu zwingen. Während mit letzterem keine selektive Reaktion beobachtet wurde, konnte im Fall der Reaktion mit Bis(cyclooctadien)nickel(0) Komplex **26** als einziges Produkt rein isoliert werden (Schema 7.4).



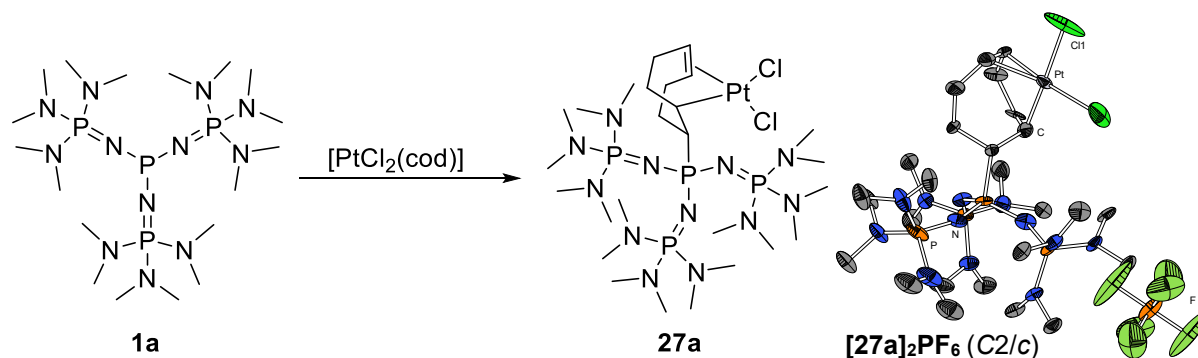
Schema 7.4: Reaktion von (dma) P_3P (**1a**) mit $[\text{Ni}(\text{cod})_2]$ zu **26** inklusive dessen berechneter Struktur.¹⁸

Dieser diamagnetische, quadratisch-planare Nickel(II)komplex entsteht vermutlich durch eine oxidative Addition des Nickel(0)atoms in eine der C–H-Bindungen einer Dimethylamino-Gruppe. Induziert wird die oxidative Addition durch das Redoxpotential des Metallzentrums, welches durch das stark elektronendonierende Phosphazenylylphosphan **1a**, das zuvor ein Cyclooctadien als Liganden substituiert hat, deutlich herabgesenkt wird. Mehrere anschließende Hydrometallierungs- und β -Hydrideliminierungsschritte am verbliebenen

¹⁸ Persönliche Kommunikation von BORISLAV KOVAČEVIĆ.^[174]

Cycloocta-1,5-dienliganden resultieren letztendlich im Nickel(II)komplex **26** mit einem allylisch gebundenen η^3 -Cyclooct-2-en-1-yliganden und einem über das Phosphor(III)atom wie auch eine CH₂-N-Gruppe sechsgliedrig chelatisierenden PAP-Liganden. In Ermangelung einer XRD-Struktur wurden die Ergebnisse aus NMR-Spektroskopie, Massenspektrometrie und der Elementaranalyse zusätzlich durch DFT-Kalkulationen gestützt, diese identifizierten die in Schema 7.4 rechts gezeigte optimierte Struktur als energetisches Minimum.¹⁸

Bei der Reaktion zwischen PAPs und Dichlorido(cyclooctadien)platin(II) kam es nicht unter Bildung eines kationischen Komplexes zur Substitution eines Chloridoliganden, sondern durch die hohe Nukleophilie des Phosphans addierte dieses an eine der Doppelbindungen und bildete so einen zwitterionischen 8-Phosphonium-cyclooct-4-en-1-yliganden im Platin(II)komplex **27a** (Schema 7.5).



Schema 7.5: Addition von **1a** an $[\text{PtCl}_2(\text{cod})]$ zu **27a**. Rechts ist die die asymmetrische Einheit der XRD-Struktur des Dimers $[\text{27a}]_2\text{PF}_6$ (erhalten durch Ausfällen eines halben Äquivalentes AgCl) abgebildet, welche über eine zweizählige Achse durch C11 vervollständigt wird.

Als Alternative zu den in Lösung instabilen Palladium(II)komplexen wurde versucht Cobalt(II)komplexe darzustellen, wie sie bereits mit stark elektronendonierenden NHC-Liganden für die palladiumfreie SUZUKI-Kupplung von Arylchloriden verwendet wurden.^[181] Der erhaltene tiefblaue Feststoff stellte sich jedoch *via* ^{31}P -NMR-Spektroskopie und Einkristall-Röntgenstrukturanalyse als $[(\text{dma})\text{P}_3\text{P}-\text{H}]_2[\text{Co}_2\text{Cl}_6]$ (**1a**: $\text{H}_2\text{Co}_2\text{Cl}_6$) heraus.¹⁹ Reaktionen mit Dichlorido(*para*-cymol)ruthenium(II)-Dimer $[\text{Ru}^{\text{II}}\text{Cl}_2(\text{cym})]_2$ sowie dem GRUBBS-II-Katalysator^[182] Dichlorido(3-phenyl-1H-inden-1-ylidene)bis(tricyclohexylphosphan)ruthenium(II) $[(\text{ind})\text{Ru}^{\text{II}}\text{Cl}_2(\text{PCy}_3)_2]$ führten zu keiner selektiven Reaktion. Gegenüber der harten LEWIS-Säure Titantrichlorid reagieren PAPs als reine Reduktionsmittel zum Chlorophosphoniumchlorid und violetten Titan(III)spezies. Mit Tris(pentafluorophenyl)boran konnte als Hauptprodukt das Phosphan-Boran-Addukt $[(\text{pyrr})\text{P}_3\text{P}-\text{B}(\text{C}_6\text{F}_5)_3]$ (**28**) erhalten werden.

¹⁹ Bindungslängen und -winkel im Kation sind identisch mit der im Kristall vorliegenden Struktur von **1a**·**HBPh**₄, weshalb auf eine Abbildung verzichtet und auf den kristallografischen Teil verwiesen wird.

7 Appendix

Tabelle 7.4 listet die durchgeführten Komplexierungsreaktionen mit PAPs auf, Tabelle 7.5 vergleicht die chemischen Verschiebungen der isolierten Komplexe in der ^{31}P -NMR-Spektroskopie.

Tabelle 7.4: Durchgeführte Reaktionen von PAPs mit LEWIS-Säuren.

Reaktand	Produkt	Anmerkungen
CoCl_2	$[(\text{dma})\text{P}_3\text{P-H}]_2[\text{Cl}_6\text{Co}_2]$ (11a) $\cdot\text{H}_2\text{Co}_2\text{Cl}_6$)	CoCl_2 vermutlich mit HCl kontaminiert
$[\text{Ni}^0(\text{CO})_4]$	$[(\text{R}_2\text{N})\text{P}_x\text{P-Ni}^0(\text{CO})_3]^{[\text{a}]}$ (5)	
Se	$(\text{R}_2\text{N})\text{P}_x\text{P=Se}^{[\text{a}]}$ (6)	
$[\text{Pt}^{\text{II}}\text{Cl}_2(\text{PPh}_3)_2]$	$[(\text{dma})\text{P}_3\text{P-Pt}^0\text{PPh}_3]$ (7a)	$[(\text{dma})\text{P}_3\text{P-Cl}]\text{Cl}$ (8aCl) als Nebenprodukt
$[\text{Pt}^0(\text{C}_2\text{H}_4)(\text{PPh}_3)_2]$	$[(\text{R}_2\text{N})\text{P}_3\text{P-Pt}^0\text{PPh}_3]^{[\text{b}]}$ (7)	
TiCl_4	$[(\text{dma})\text{P}_3\text{P-Cl}]\text{Cl}$ (8aCl)	Reduktion zu Ti^{III} -Spezies
$[\text{Au}^{\text{I}}\text{Cl}(\text{PPh}_3)]$	$[(\text{R}_2\text{N})\text{P}_3\text{P-Au}^{\text{I}}\text{Cl}]^{[\text{b}]}$ (19)	
$[\text{Au}^{\text{I}}\text{Cl}(\text{tht})]$	$[(\text{R}_2\text{N})\text{P}_3\text{P-Au}^{\text{I}}\text{Cl}]^{[\text{b}]}$ (19)	
$[\text{Rh}^{\text{I}}\text{Cl}(\text{cod})_2]$	$[(\text{dma})\text{P}_3\text{P-Rh}^{\text{I}}\text{Cl}(\text{cod})]$ (20)	
$[\text{Pd}^{\text{II}}(\text{allyl})\text{Cl}]_2$	$[(\text{dma})\text{P}_3\text{P-Pd}^{\text{II}}(\text{allyl})\text{Cl}]$ (21)	in Lösung instabil
PtCl_2	$[(\text{dma})\text{P}_3\text{P-Pt}^{\text{II}}\text{Cl}_2-\text{P}_3\text{P}(\text{dma})]$ (22)	in Lösung instabil, nicht isoliert
$[\text{Pd}^{\text{II}}\text{Cl}_2(\text{PPh}_3)_2]$	$[(\text{R}_2\text{N})\text{P}_3\text{P-Pd}^0\text{PPh}_3]^{[\text{b}]}$ (23)	$[(\text{R}_2\text{N})\text{P}_3\text{P-Cl}]\text{Cl}$ (8Cl) als Nebenprodukt
$[\text{Pd}^0(\text{PtBu}_3)_2]$	$[(\text{R}_2\text{N})\text{P}_3\text{P-Pd}^0\text{PtBu}_3]^{[\text{b}]}$ (24)	
$[\text{Ni}^0(\text{cod})_2]$	$[\kappa^2-\{[(\text{CH}_2\text{NMe})(\text{dma})_2\text{PN}][(\text{dma})_3\text{PN}]_2\text{P}\}-\text{Ni}^{\text{II}}(\eta^3-\text{C}_8\text{H}_{13})]$ (26)	
$[\text{Pt}^{\text{II}}\text{Cl}_2(\text{cod})]$	$[\{(\text{R}_2\text{N})\text{P}_3\text{P-C}_8\text{H}_{12}\}\text{Pt}^{\text{II}}\text{Cl}_2]^{[\text{b}]}$ (27)	
$\text{B}(\text{C}_6\text{F}_5)_3$	$[(\text{pyrr})\text{P}_3\text{P-B}(\text{C}_6\text{F}_5)_3]$ (28)	nicht rein isoliert
$[\text{Pd}^0(\text{PPh}_3)_4]$	-	Gleichgewicht mit schnellem Austausch in Lösung beobachtet, nur Edukt reisoliert
$[\text{Pt}^0(\text{cod})_2]$	-	keine selektive Reaktion
$[\text{Ru}^{\text{II}}\text{Cl}_2(\text{cym})_2]$	-	keine selektive Reaktion
$[(\text{ind})\text{Ru}^{\text{II}}\text{Cl}_2(\text{PCy}_3)_2]$	-	keine selektive Reaktion

[a] $(\text{R}_2\text{N})\text{P}_x\text{P} = (\text{dma})\text{P}_3\text{P}/(\text{pyrr})\text{P}_3\text{P}/(\text{Me}_3\text{tren})\text{P}_3\text{P}/(\text{dma})\text{P}_4\text{P}/(\text{dma})\text{P}_6\text{P}$; [b] $(\text{R}_2\text{N})\text{P}_3\text{P} = (\text{dma})\text{P}_3\text{P}/(\text{pyrr})\text{P}_3\text{P}$.

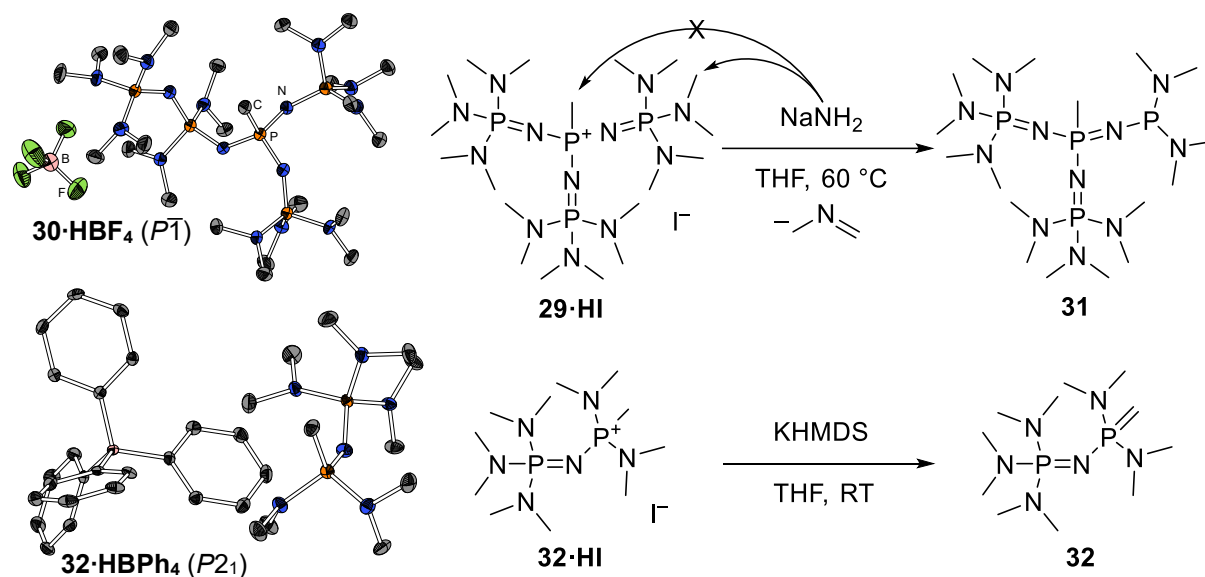
Tabelle 7.5: Chemische Verschiebung δ_{P} und Kopplungskonstanten J des zentralen Phosphoratoms in Verbindungen der Form $(\text{dma})\text{P}_3\text{P-X}$; sofern nicht anders angegeben in C_6D_6 als Lösungsmittel.

X	-	$\text{Cl}^{[\text{a}]}$	$\text{Ni}^0(\text{CO})_3$	$\text{Ni}^{\text{II}}(\text{C}_8\text{H}_{13})$	Pd^0PPh_3	$\text{Pd}^0\text{P}(\text{tBu})_3$	$\text{Pd}^{\text{II}}(\text{allyl})\text{Cl}$
$\delta_{\text{P}}/\text{ppm}$	83.4	-22.7	53.2	56.2	61.7	64.0	25.7
$^2J_{\text{PP}}/\text{Hz}$	20	29	18	66/50/10	23 (400) ^[b]	6 (383) ^[c]	3
X	H	CH_3	Se	$\text{Rh}^{\text{I}}\text{Cl}(\text{cod})$	$\text{Pt}^0\text{PPh}_3^{[\text{d}]}$	$\text{Pt}^{\text{II}}\text{Cl}_2[\text{P}_3\text{P}(\text{dma})]$	$\text{Au}^{\text{I}}\text{Cl}$
$\delta_{\text{P}}/\text{ppm}$	-28.9	-12.5	-6.7	26.1	87.8	16.0	22.3
$^2J_{\text{PP}}/\text{Hz}$	31	36	35	- ^[e]	26 (549) ^[b]	- ^[e]	60
$^1J_{\text{PX}}/\text{Hz}$	554	127	645	179	6150	2947	-

[a] in CDCl_3 ; [b] $^2J_{\text{PP}}$ -Kopplung zu PPh_3 ; [c] $^2J_{\text{PP}}$ -Kopplung zu $\text{P}(\text{tBu})_3$; [d] in $\text{THF-}d_8$; [e] nicht aufgelöst.

Neben der hohen BRØNSTED-Basizität, führt die gezeigte hohe Affinität von PAPs gegenüber anderen LEWIS-Säuren als dem Proton auch zu einer hohen Nukleophilie: Bei der Konkurrenzreaktion zwischen Ethylierung *via* nukleophiler Substitution und Iodwasserstoff-Eliminierung an Iodethan wurde bei den untersuchten Basen (dma)P₃P (**1a**), (pyrr)P₃P (**1b**) und (Me₃tren)P₃P (**1e**) fast ausschließlich ethyliertes Substitutionsprodukt nachgewiesen.²⁰ Diese hohe Nukleophilie kann bei einer potentiellen Anwendung als Superbase zu unerwünschten Nebenprodukten führen, im Gegenzug können die generierten Alkylphosphoniumsalze selbst Präkursoren zu äußerst starken Kohlenstoffsuperbasen darstellen.

Beim Versuch derartige Phosphormonoylide höherer Ordnung aus den protonierten Vorläufern [(dma)P₃P–Me]I (**29·HI**) und [(dma)P₄P–Me]I (**30·HI**), welche zunächst durch Reaktion von PAPs mit Iodmethan synthetisiert wurden, darzustellen wurde jedoch ein analoger Reaktionsmechanismus wie für das Carbodiphosphoran *sym*-(dmaP₁)(dma)₂-CDP (**10**) beobachtet (Schema 7.6). Während es bei Raumtemperatur zu keiner Reaktion kam, bildete sich bei erhöhter Temperatur nicht das ungeladene Phosphorylid **29**, sondern langsam, aber selektiv, Phosphan **31**. Lediglich das P₂-Ylid **32** konnte erhalten werden, da dieses mit KHMDS in Lösung deprotoniert werden konnte.

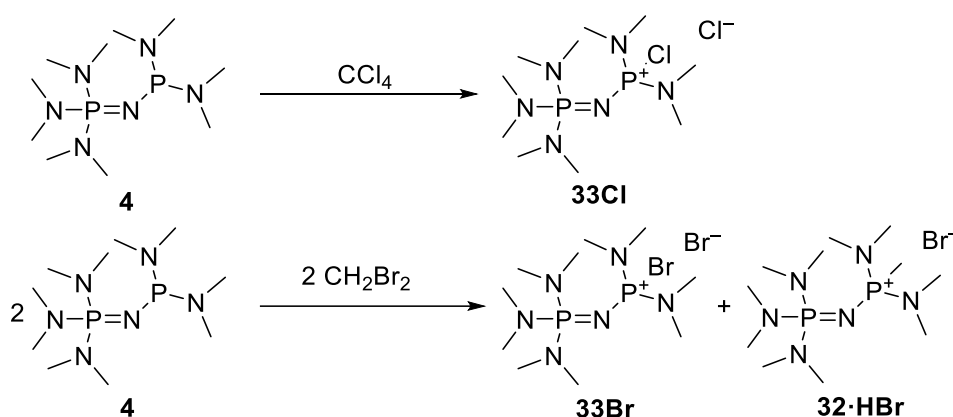


Schema 7.6: Reaktion von **33·HI** mit Natriumamid zu **35** unter Abspaltung von *N*-Methylmethanimin und Deprotonierung von **36·HI** mit KHMDS zum Phosphorylid **36** sowie die im Kristall vorliegenden Strukturen von **34·HBF₄** und **36·HPh₄** (beide durch Anionenaustausch mit NaBF₄ bzw. NaBPh₄ aus wässriger Lösung erhalten).

Anders als die Darstellung von Carbodiphosphoranen über die Oxidation methylenverbrückter Bisphosphane mit Tetrachlorkohlenstoff in Gegenwart von Iminen als Nukleophil und Hilfsbase (Schema 4.5, S. 31) stellten sich die etablierten Synthesewege von CDPs als nicht

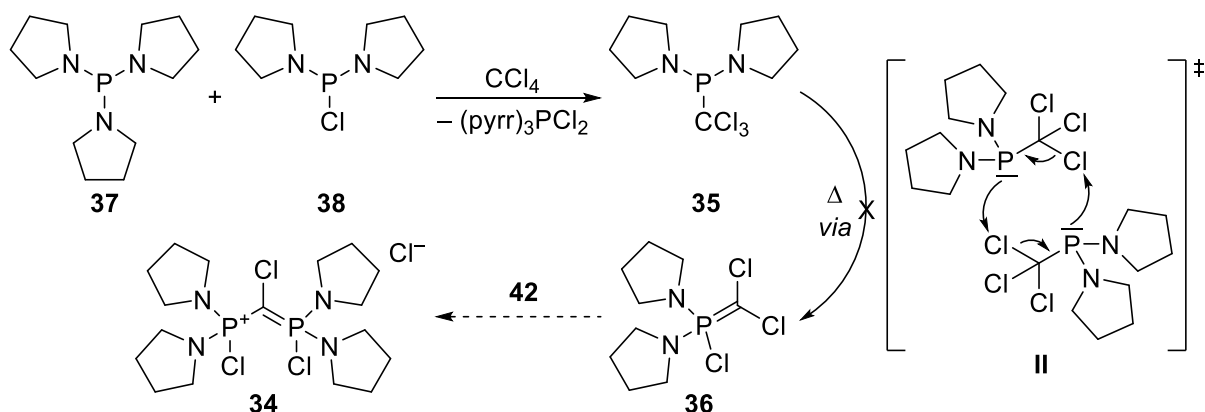
²⁰ Anteil an alkylierter Spezies [PAP–Et]I bei der Reaktion zwischen PAPs und Ethyliodid in THF, nachgewiesen *via* ³¹P-NMR-Spektroskopie: (dma)P₃P (83%), (pyrr)P₃P (88%), (Me₃tren)P₃P (83%).

zielführend heraus (Schema 7.7). Bei basischeren und damit reduzierenderen Phosphanen als Hexamethylphosphortriamin kommt es bei der APPEL-Route durch Tetrachlorkohlenstoff lediglich zur Chlorierung des Monophosphazenylyphosphans **4** zu **33Cl** (Schema 7.7, oben), während über die SCHMIDBAUR-Route mit Dibrommethan ein 1:1-Gemisch aus bromierter (**33Br**) und methylierter Spezies (**32·HBr**) erhalten und mittels ^{31}P -NMR-Spektroskopie und Massenspektrometrie nachgewiesen wurde (Schema 7.7, unten). Vermutlich wird das intermediäre Bromomethylphosphoniumbromid $[(\text{dma})_3\text{PN}](\text{dma})_2\text{P-CH}_2\text{Br}]^+\text{Br}^-$ durch einen nukleophilen Angriff eines weiteren Moleküls **4** in das σ^* -Orbital der Brom-Kohlenstoff-Bindung zum Ylid **32** reduziert und **4** dabei zu **33Br** oxidiert. Das entstandene Ylid **32** ist so basisch, dass es in der Lage ist verbliebenes Dibrommethan zu deprotonieren.



Schema 7.7: Beobachtete Reaktionen von **4** mit Tetrachlorkohlenstoff bzw. Dibrommethan.

Auch die Synthese des potentiellen CDP-Präkursors **34**, dessen analoge dimethylaminosubstituierte Verbindung bereits von PINCHUK *et al.* dargestellt wurde,^[117,183] scheiterte an der durch die Pyrrolidinsubstitution erhöhte Reaktivität. So konnte zwar das trichlormethylfunktionalisierte Phosphan **36** *in situ* generiert werden, zeigte jedoch eine noch höhere Instabilität als die analoge Dimethylaminospezies und konnte weder unzersetzt isoliert, noch selektiv in das Ylid **36** umgelagert und weiter umgesetzt werden (Schema 7.8).



Schema 7.8: Versuchte Synthese des Präkursors **38**, in Analogie zu den dimethylaminosubstituierten Verbindungen von PINCHUK *et al.*^[117,183]

7.2 Zusammenfassung

Zusätzlich zu dimethylamin- und pyrrolidinsubstituierten Phosphazenyolphosphanen (PAPs) konnten Azaphosphatrane, Cyclopropenimine und Guanidine als superbasische Struktur motive in Phosphanbasen implementiert werden. Aufgrund der hohen Elektronendichte am Phosphor(III)atom zeigten sich dabei in einigen Fällen jedoch unerwartete Reaktions- und Zersetzungspfade. Mit mehreren beispielhaften Übergangsmetallkomplexpräkursoren konnte eine Reihe verschiedener extrem elektronenreicher PAP-Metallkomplexe dargestellt werden, darunter Ni^{0/II}-, Rh^I-, Pd^{0/II}-, Pt^{0/II}- und Au^I-Verbindungen. Gegenüber Alkylierungsmitteln offenbarten PAPs eine hohe Nukleophilie. Für die resultierenden Alkylphosphoniumsalze wurde versucht, eine Deprotonierungsvorschrift zu entwickeln, um das bisher experimentell erreichte Basizitätslimit mit neuen Phosphorylidbasen höherer Ordnung noch weiter zu verschieben. Dabei limitierte jedoch die Stabilität der Phosphazenylobstituenten in derart extremen Basizitätsregionen analog zu den präsentierten Carbodiphosphoranen die Freisetzung der Basenform bislang auf unbekannte P₂-Ylide.

7.3 Experimenteller Teil

General

All Reactions with air or moisture sensitive substances were carried out under argon atmosphere using standard SCHLENK techniques or in a nitrogen-flushed glovebox. Solvents were purified according to common literature procedures and stored under argon atmosphere over molsieve (3 Å or 4 Å).^[184] Potassium bis(trimethylsilyl)amide (KHMDs),^[185] bis(dimethylamino)-phosphorus chloride (**3a**),^[186] bis(diethylamino)phosphorus chloride (**3b**),^[180] 2,3-bis(di-*iso*-propylamino)cyclopropeneimine (**2f**),^[16] 2,8,9-trimethyl-2,5,8,9-tetraaza-1-phospha-bicyclo-[3.3.3]undecane,^[180] bis(dimethylamino)tetramethylguanidinophosphane,^[14] tris(2,4,6-trimethoxyphenyl)phosphane,^[179] [tris(dimethylamino)phosphazanyl]bis(dimethylamino)-phosphane (**4**),^[140] *trans*-dichloridobis(triphenylphosphane)palladium(II),^[187] dichlorido(1,5-cyclooctadiene)platinum(II),^[187] and chlorido(triphenylphosphane)gold(I)^[187] were prepared according to literature-known procedures. All other reagents were used as provided.

¹H, ¹¹B, ¹³C, ¹⁹F ³¹P, ⁷⁷Se, and ¹⁹⁵Pt NMR spectra were recorded on a Bruker Avance III HD 250, Avance II 300, Avance III HD 300 or Avance III HD 500 spectrometer. Chemical shift δ is denoted relatively to SiMe₄ (¹H, ¹³C), BF₃·OEt₂ (¹¹B), CFCl₃ (¹⁹F), 85% H₃PO₄ (³¹P), SeMe₂ (⁷⁷Se), or K₂PtCl₆ (¹⁹⁵Pt). ¹H and ¹³C NMR spectra were referenced to the solvent residual signals,^[188] ¹⁹⁵Pt NMR spectra externally to K₂PtCl₄ (0.5M in D₂O, δ = -1617.5 ppm). Multiplicity is abbreviated as follows: s (singlet), d (doublet), t (triplet), q (quartet), quint.

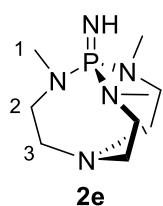
(quintet), sext. (sextet), sept. (septet), m (multiplet), br. (broad signal). High resolution mass spectrometry were performed on a Thermo Fisher Scientific LTQ-FT Ultra or a Jeol AccuTOF GCv., elemental analysis on an Elementar Vario Micro Cube. IR spectra were recorded in a glovebox on a Bruker Alpha ATR-FT-IR.

General procedure for the preparation of PAP containing solutions

A mixture of the respective phosphonium tetrafluoridoborate (**1**·HBF₄) and a 10% excess of potassium bis(trimethylsilyl)amide was stirred for 90 min in toluene or THF, centrifuged and the supernatant clear solution used for subsequent reactions.

1-Imino-2,8,9-trimethyl-2,5,8,9-tetraaza-1-phospha-bicyclo[3.3.3]undecane (2e)

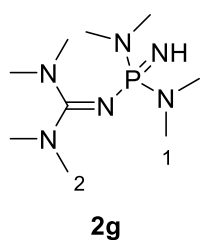
The compound was originally obtained by VERKADE *et al.* via the iodination of proazaphosphatrane 2,8,9-trimethyl-2,5,8,9-tetraaza-1-phospha-bicyclo[3.3.3]undecane and consecutive ammonolysis and deprotonation.^[144,145] Here a one-pot synthesis via the STAUDINGER reaction with subsequent methanolysis is presented:



Trimethylsilylazide (0.60 mL, 4.6 mmol, 1.3 eq) was added to a solution of 2,8,9-trimethyl-2,5,8,9-tetraaza-1-phospha-bicyclo[3.3.3]undecane (767 mg, 3.55 mmol, 1.0 eq) in toluene (60 mL) and the mixture stirred under reflux conditions overnight. All volatiles were removed *in vacuo* and the residue stirred in methanol (30 mL) at 60 °C overnight. Removal of the solvent and sublimation at 100 °C and $5 \cdot 10^{-2}$ mbar gave 1-imino-2,8,9-trimethyl-2,5,8,9-tetraaza-1-phospha-bicyclo[3.3.3]undecane (**2e**) (712 g, 3.08 mmol, 87%) as colourless solid.

[C₉H₂₂N₅P] (231.28 g·mol⁻¹) ¹H NMR (300.2 MHz, C₆D₆): δ (ppm) = 2.66 (d, ³J_{PH} = 8 Hz, 9H, HI), 2.57-2.49 (m, 6H, H₂), 2.38 (t, ³J_{HH} = 5 Hz, 6H, H₃). ¹³C{¹H} NMR (75.5 MHz, C₆D₆): δ (ppm) = 51.9 (d, ²J_{PC} = 3 Hz, C₂), 50.1 (s, C₃), 35.9 (d, ²J_{PC} = 6 Hz, C₁). ³¹P{¹H} NMR (121.5 MHz, C₆D₆): δ (ppm) = 34.4.

Bis(dimethylamino)tetramethylguanidinophosphazene (2g)

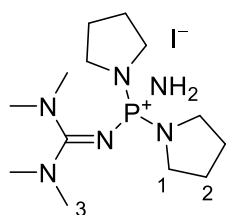


Bromine (1.75 mL, 34.1 mmol, 1.01 eq) was added dropwise at -40 °C to a solution of bis(dimethylamino)tetramethylguanidinophosphane (7.90 g, 33.9 mmol, 1.00 eq) in toluene (150 mL). The mixture was allowed to warm to room temperature overnight. After the precipitate had settled, the clear supernatant was decanted, and the solid dried *in vacuo*. It was dissolved in dichloromethane (200 mL), cooled to 0 °C, and saturated with ammonia. Ammonium bromide

was filtered off and extracted with more dichloromethane. All volatiles were removed *in vacuo*, the residue dissolved in an aqueous solution of sodium tetrafluoridoborate (4.48 g, 40.8 mmol, 1.20 eq), extracted with dichloromethane (3x 20 mL), dried over sodium sulfate, and evaporated to dryness. The resulting **2g**·HBF₄ was dissolved in THF (100 mL) and a solution of potassium *tert*-butoxide (3.91 g, 34.8 mmol, 1.03 eq) in THF (50 mL) was added. The mixture was stirred for two hours at room temperature, filtered, and the filtercake extracted with THF (2x 20 mL). All volatiles were removed *in vacuo* and the residue was distilled at 80 °C and 5.0·10⁻³ mbar to isolate bis(dimethylamino)tetramethylguanidinophosphazene (**2g**) (6.58 g, 26.5 mmol, 78%) as colourless liquid.

[C₉H₂₅N₆P] (248.31 g·mol⁻¹) ¹H NMR (300.2 MHz, C₆D₆): δ (ppm) = 2.77 (d, ³J_{PH} = 10 Hz, 12H, *HI*), 2.56 (s, 12H, *H2*), 0.63 (br. s, 1H, *NH*). ¹³C{¹H} NMR (75.5 MHz, C₆D₆): δ (ppm) = 39.8 (s, *C2*), 38.1 (d, ²J_{PC} = 2 Hz, *CI*), the CN₃ signal was not observed. ³¹P{¹H} NMR (101.3 MHz, C₆D₆): δ (ppm) = 28.9. LIFDI(+) MS (toluene): m/z (%) = 249.2 (100) [M+H]⁺. LIFDI(+) HRMS: m/z [M+H]⁺ calcd. 249.19511, found 249.19809.

Aminotetramethylguanidinobispyrrolidinophosphonium iodide (**2h**·HI)



2h·HI

A mixture of tris(pyrrolidino)phosphane, tetramethylguanidino-bis(pyrrolidino)phosphane and bis(tetramethylguanidino)pyrrolidino-phosphane (14.9 g, 20 : 71 : 9), prepared according to Ref. [14], was dissolved in toluene (60 mL) and cooled to 0 °C. Iodine (13.7 g, 108 mmol) was added and the mixture stirred at room temperature overnight. The solvent was evaporated, the brown solid dissolved in dichloromethane (120 mL), and saturated with ammonia. The suspension was filtered, the filtrate washed with water, and the solvent removed under reduced pressure. The residue was digested with ethyl acetate to precipitate a brown solid, which was recrystallized first from water, then from ethyl acetate to isolate aminotetramethylguanidino(bispyrrolidino)phosphonium iodide (**2h**·HI) (2.21 g, 5.16 mmol) as brown solid.

[C₁₃H₃₀IN₆P] (428.30 g·mol⁻¹) ¹H NMR (300.2 MHz, CDCl₃): δ (ppm) = 4.03 (br. s, 2H, *NH*₂), 3.29-3.18 (m, 8H, *HI*), 3.01 (s, 12H, *H3*), 1.91-1.87 (m, 8H, *H2*). ¹³C{¹H} NMR (75.5 MHz, CDCl₃): δ (ppm) = 47.2 (d, ²J_{PC} = 5 Hz, *CI*), 40.5 (s, *C3*), 26.5 (d, ³J_{PC} = 8 Hz, *C2*), The CN₃ signal was not observed. ³¹P{¹H} NMR (101.3 MHz, CDCl₃): δ (ppm) = 9.4. ESI(+) MS (MeOH): m/z (%) = 301.4 (100) [M-I]⁺. ESI(+) HRMS: m/z [M-I]⁺ calcd. 301.2264, found 301.2269. XRD: For single crystal X-ray structure determination suitable single crystals were obtained by recrystallization from water.

Iodotris(2,4,6-trimethoxyphenyl)phosphonium iodide

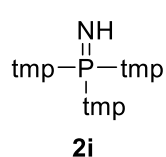
$$\begin{array}{c} \text{I}^- \\ | \\ \text{tmp}-\text{P}^+-\text{tmp} \\ | \\ \text{tmp} \end{array}$$
 Tris(2,4,6-trimethoxyphenyl)phosphane (9.90 g, 18.6 mmol, 1.00 eq) was suspended in toluene (250 mL) and iodine (4.72 g, 18.6 mmol, 1.00 eq) was added. The suspension was stirred at room temperature for three days, the yellow solid filtered off, and washed with toluene (2x 20 mL). Drying *in vacuo* afforded iodotris(2,4,6-trimethoxyphenyl)phosphonium iodide (13.8 g, 17.5 mmol, 94%) as yellow powder.

$[\text{C}_{27}\text{H}_{33}\text{I}_2\text{O}_9\text{P}]$ (786.33 $\text{g}\cdot\text{mol}^{-1}$) ^1H NMR (300.2 MHz, CDCl_3): δ (ppm) = 6.11 (d, $^4J_{\text{PH}} = 5$ Hz, 6H, *m-H*), 3.91 (s, 9H, *p-OCH}_3*), 3.64 (s, 18H, *o-OCH}_3*). $^{13}\text{C}\{^1\text{H}\}$ NMR (75.5 MHz, CDCl_3): δ (ppm) = 166.4 (d, $^2J_{\text{PC}} = 2$ Hz, *o-C*), 163.8 (d, $^4J_{\text{PC}} = 1$ Hz, *p-C*), 91.8 (d, $^3J_{\text{PC}} = 8$ Hz, *m-C*), 56.3 (s, *o-OCH}_3*), 56.2 (s, *p-OCH}_3*), the *i-C* signal was not observed. $^{31}\text{P}\{^1\text{H}\}$ NMR (101.3 MHz, CDCl_3): δ (ppm) = -65.7. LIFDI(+) MS (CH_2Cl_2): m/z (%) = 548.1 (100) $[\text{C}_{27}\text{H}_{33}\text{O}_9\text{P}=\text{O}]^+$, 659.0 (60) $[\text{M}-\text{I}]^+$. LIFDI(+) HRMS: m/z $[\text{M}-\text{I}]^+$ calcd. 659.09069, found 659.09230. Elemental analysis: calcd. C 41.24%, H 4.23%, found C 41.55%, H 4.27%.

Aminotris(2,4,6-trimethoxyphenyl)phosphonium iodide (2i·HI)

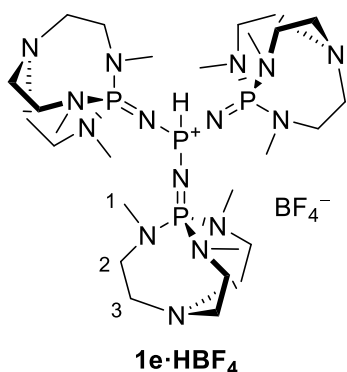
$$\begin{array}{c} \text{NH}_2 \quad \text{I}^- \\ | \\ \text{tmp}-\text{P}^+-\text{tmp} \\ | \\ \text{tmp} \end{array}$$
2i·HI
 Ammonia was passed into a suspension of iodotris(trimethoxyphenyl)phosphonium iodide (13.4 g, 17.1 mmol, 1.00 eq) in dichloromethane (200 mL) until it turned colourless. Precipitated ammonium iodide was filtered off and extracted with dichloromethane (50 mL). The filtrate was washed with water (3x 100 mL) and dried over magnesium sulfate. The solvent was removed under reduced pressure and the crude product recrystallized from THF to yield aminotris(trimethoxyphenyl)phosphonium iodide (**2i·HI**) (11.1 g, 16.4 mmol, 96%) as off-white solid.

$[\text{C}_{27}\text{H}_{35}\text{INO}_9\text{P}]$ (675.45 $\text{g}\cdot\text{mol}^{-1}$) ^1H NMR (300.2 MHz, C_6D_6): δ (ppm) = 6.07 (d, $^4J_{\text{PH}} = 5$ Hz, 6H, *m-H*), 3.86 (br. d, $^2J_{\text{PH}} = 2$ Hz, 2H, NH_2), 3.84 (s, 9H, *p-OCH}_3*), 3.60 (s, 18H, *o-OCH}_3*). $^{13}\text{C}\{^1\text{H}\}$ NMR (75.5 MHz, C_6D_6): δ (ppm) = 165.6 (d, $^4J_{\text{PC}} = 1$ Hz, *p-C*), 163.4 (d, $^2J_{\text{PC}} = 2$ Hz, *o-C*), 96.2 (d, $^1J_{\text{PC}} = 126$ Hz, *i-C*), 91.2 (d, $^3J_{\text{PC}} = 8$ Hz, *m-C*), 56.5 (s, *o-OCH}_3*), 56.1 (s, *p-OCH}_3*). $^{31}\text{P}\{^1\text{H}\}$ NMR (101.3 MHz, C_6D_6): δ (ppm) = 20.5. ESI(+) MS (MeOH): m/z (%) = 548.5 (100) $[\text{M}-\text{I}]^+$. ESI(+) HRMS: m/z $[\text{M}-\text{I}]^+$ calcd. 548.2044, found 548.2036. XRD: For single crystal X-ray structure determination suitable single crystals were obtained from methanol/water at 0 °C.

Tris(2,4,6-trimethoxyphenyl)iminophosphorane (2i)

Aminotris(2,4,6-trimethoxyphenyl)phosphonium iodide (**2i·HI**) (5.53 g, 8.18 mmol, 1.00 eq) was suspended in THF (60 mL) and a solution of potassium *tert*-butoxide (926 mg, 8.25 mmol, 1.01 eq) in THF (40 mL) was added. The mixture was stirred at room temperature overnight, filtered over celite, and the filtercake extracted with THF (60 mL). The filtrate was evaporated to dryness, the residue washed with *n*-hexane (3x 20 mL), and dried in high vacuum. Tris(2,4,6-trimethoxyphenyl)iminophosphorane (**2i**) (1.025 g, 1.87 mmol, 23%) was isolated as off-white solid.

[C₂₇H₃₄NO₉P] (547.54 g·mol⁻¹) ¹H NMR (300.2 MHz, CD₃CN): δ (ppm) = 6.08 (d, ⁴J_{PH} = 4 Hz, 6H, *m-H*), 3.79 (s, 9H, *p-OCH*₃), 3.52 (s, 18H, *o-OCH*₃), 3.46 (br. s, 1H, *NH*). ¹³C{¹H} NMR (75.5 MHz, CD₃CN): δ (ppm) = 163.8 (s, *o-C*), 163.5 (d, ⁴J_{PC} = 5 Hz, *p-C*), 91.5 (d, ³J_{PC} = 6 Hz, *m-C*), 56.1 (s, *o-OCH*₃), 56.0 (s, *p-OCH*₃), the *i-C* signal was not observed. ³¹P{¹H} NMR (101.3 MHz, CD₃CN): δ (ppm) = 1.3. LIFDI(+) MS (THF): *m/z* (%) = 547.2 (100) [M]⁺. LIFDI(+) HRMS: *m/z* [M]⁺ calcd. 547.19712, found 547.19594.

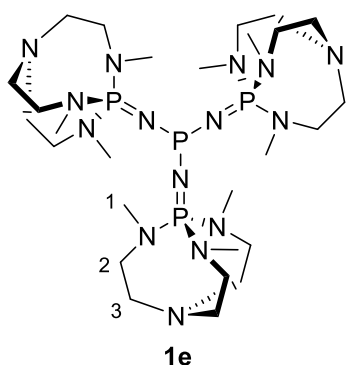
Tris[1-imino-2,8,9-trimethyl-2,5,8,9-tetraaza-1-phospha-bicyclo[3.3.3]undecane]-phosphonium tetrafluoridoborate (Mestren)P₃P·HBF₄ (1e·HBF₄)

Bis(diethylamino)phosphorus chloride (**3b**) (876 mg, 4.16 mmol, 1.00 eq) was added to a solution of 1-imino-2,8,9-trimethyl-2,5,8,9-tetraaza-1-phospha-bicyclo[3.3.3]undecane (**2e**) (2.88 g, 12.5 mmol, 3.01 eq) in THF (150 mL), stirred at 60 °C for 5 h and at room temperature overnight. The precipitate was filtered off and dried in high vacuum. The crude **1e·HCl** was converted to its BF₄-salt by dissolving in a minimum amount of water and adding sodium tetrafluoridoborate (503 mg, 4.58 mmol, 1.10 eq), dissolved in a minimum amount of water. The precipitate was filtered off and rinsed with three portions of cold water. Washing with THF (2x 20 mL) and diethyl ether (2x 20 mL) and drying in high vacuum afforded tris[1-imino-2,8,9-trimethyl-2,5,8,9-tetraaza-1-phospha-bicyclo[3.3.3]undecane]phosphonium tetrafluoridoborate (**1e·HBF₄**) (2.14 g, 2.64 mmol, 64%) as colourless solid.

[C₂₇H₆₄BF₄N₁₅P₄] (809.61 g·mol⁻¹) ¹H NMR (300.3 MHz, CD₃CN): δ (ppm) = 7.51 (dq, ¹J_{PH} = 554 Hz, ³J_{PH} = 6 Hz, 1H, *PH*), 2.89-2.81 (m, 18H, *H2*), 2.76 (t, ³J_{HH} = 5 Hz, 18H, *H3*), 2.74 (d, ³J_{PH} = 9 Hz, 27H, *H1*). ¹³C{¹H} NMR (75.5 MHz, CD₃CN): δ (ppm) = 52.2 (d, ²J_{PC} = 4 Hz, *C2*), 50.2 (s, *C3*), 35.4 (d, ²J_{PC} = 6 Hz, *C1*). ³¹P{¹H} NMR (121.5 MHz, CD₃CN): δ (ppm) = 14.7 (d, ²J_{PP} = 34 Hz, *P*(Me₃tren)), -34.0 (q, ²J_{PP} = 34 Hz, *PH*). ³¹P NMR (121.5 MHz, CD₃CN):

δ (ppm) = 14.7 (br. s, $P(\text{Me}_3\text{tren})$), -34.0 (dq, $^1J_{\text{PH}} = 554$ Hz, $^2J_{\text{PP}} = 34$ Hz, PH). ESI(+) MS (MeOH): m/z (%) = 722.72 (100) $[\text{M}-\text{BF}_4]^+$. ESI(+) HRMS: m/z $[\text{M}-\text{BF}_4]^+$ calcd. 722.4414, found 722.4431. Elemental analysis: calcd. C 40.06%, H 7.97%, N 25.95%; found C 39.81%, H 7.91%, N 25.74%. IR (neat): $\tilde{\nu}$ (cm^{-1}) = 2920 (m, CH_3 , CH_2), 2872 (m, CH_3 , CH_2), 2817 (m, CH_3 , CH_2), 2321 (w, PH), 1670 (w), 1452 (m), 1425 (w), 1382 (m), 1355 (m), 1333 (m), 1277 (s), 1223 (s), 1131 (s), 1116 (s), 1091 (m), 1048 (s), 1033 (s), 1013 (vs), 995 (vs), 901 (s), 879 (vs), 870 (vs), 790 (m), 723 (s), 600 (s), 544 (s), 509 (s), 486 (s), 449 (m), 410 (m). XRD: For single crystal X-ray structure determination NaBPh_4 was used instead of NaBF_4 . Suitable single crystals were obtained from methanol/water at -25 °C.

Tris[1-imino-2,8,9-trimethyl-2,5,8,9-tetraaza-1-phospha-bicyclo[3.3.3]undecane]-phosphane (Me_3tren) P_3P (1e**)**

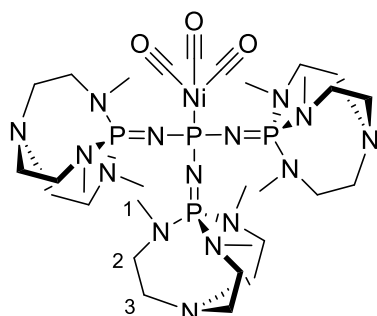


Tris[1-imino-2,8,9-trimethyl-2,5,8,9-tetraaza-1-phospha-bicyclo[3.3.3]undecane]phosphonium tetrafluoridoborate (**1e**· HBF_4) (1.20 g, 1.48 mmol, 1.00 eq) and sodium amide (430 mg, 11.0 mmol, 7.43 eq) were stirred in THF (50 mL) at room temperature overnight. All volatiles were removed *in vacuo*, the residue diluted with toluene (50 mL) and filtered over celite. The solvent was evaporated, the residue washed with *n*-pentane (3x

10 mL), and dried in high vacuum. Tris[1-imino-2,8,9-trimethyl-2,5,8,9-tetraaza-1-phospha-bicyclo[3.3.3]undecane]phosphane (**1e**) (930 mg, 1.29 mmol, 87%) was obtained as off-white solid.

$[\text{C}_{27}\text{H}_{63}\text{N}_{15}\text{P}_4]$ (721.80 $\text{g}\cdot\text{mol}^{-1}$) ^1H NMR (300.3 MHz, $\text{THF}-d_8$): δ (ppm) = 2.83 (br. d, $^3J_{\text{PH}} = 8$ Hz, 18H, H_2), 2.79 (d, $^3J_{\text{PH}} = 8$ Hz, 27H, H_1), 2.74 (t, $^3J_{\text{HH}} = 5$ Hz, 18H, H_3). $^{13}\text{C}\{^1\text{H}\}$ NMR (75.5 MHz, $\text{THF}-d_8$): δ (ppm) = 52.5 (s, C_2), 54.3 (s, C_3), 35.8 (d, $^2J_{\text{PC}} = 10$ Hz, C_1). $^{31}\text{P}\{^1\text{H}\}$ NMR (121.5 MHz, $\text{THF}-d_8$): δ (ppm) = 90.2 (q, $^2J_{\text{PP}} = 76$ Hz, P^{III}), 14.8 (d, $^2J_{\text{PP}} = 76$ Hz, $P(\text{Me}_3\text{tren})$). ^{31}P NMR (121.5 MHz, $\text{THF}-d_8$): δ (ppm) = 90.2 (q, $^2J_{\text{PP}} = 76$ Hz, P^{III}), 14.8 (br. d, $^2J_{\text{PP}} = 76$ Hz, $P(\text{Me}_3\text{tren})$). LIFDI(+) MS (toluene): m/z (%) = 722.4 (100) $[\text{M}+\text{H}]^+$. LIFDI(+) HRMS: m/z $[\text{M}+\text{H}]^+$ calcd. 722.44196, found 722.44504. IR (neat): $\tilde{\nu}$ (cm^{-1}) = 2922 (w, CH_3 , CH_2), 2870 (w, CH_3 , CH_2), 2811 (w, CH_3 , CH_2), 1455 (w), 1379 (w), 1355 (w), 1333 (m), 1225 (m), 1117 (vs), 1047 (s), 1011 (vs), 918 (w), 894 (m), 865 (s), 745 (s), 715 (m), 629 (w), 592 (m), 540 (w), 510 (m), 481 (w), 443 (w), 411 (w).

Tricarbonyl{tris[1-imino-2,8,9-trimethyl-2,5,8,9-tetraaza-1-phospha-bicyclo[3.3.3]undecane]phosphane}nickel(0) (5e)



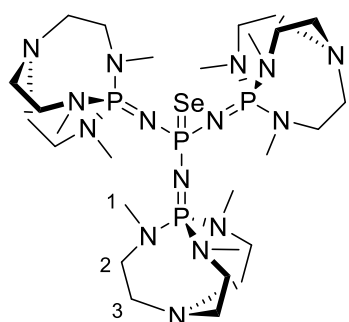
5e

Tetracarbonylnickel (0.2 mL, 2 mmol, 4 eq) was added at 0 °C to a solution of (Me₃tren)P₃P (**1e**) (399 mg, 553 μmol, 1 eq) in toluene (20 mL) and stirred for 1 h at room temperature. The mixture was centrifuged, the supernatant evaporated to dryness, and the residue stirred in diethyl ether (20 mL) overnight. The solution was cleared *via* syringe filtration, the solvent removed *in vacuo* and the residue dried in high vacuum.

Tricarbonyl{tris[1-imino-2,8,9-trimethyl-2,5,8,9-tetraaza-1-phospha-bicyclo[3.3.3]undecane]phosphane}nickel(0) (**5e**) was isolated as colourless solid.

[C₃₀H₆₃N₁₅NiO₃P₄] (864.52 g·mol⁻¹) ¹H NMR (500.2 MHz, C₆D₆): δ (ppm) = 2.93 (d, ³J_{PH} = 8 Hz, 27H, *H1*), 2.69 (br. s, 18H, *H2*), 2.51 (t, ³J_{HH} = 5 Hz, 18H, *H3*). ¹³C{¹H} NMR (125.8 MHz, C₆D₆): δ (ppm) = 204.1 (d, ²J_{PC} = 10 Hz, CO), 52.0 (d, ²J_{PC} = 4 Hz, C2), 50.3 (s, C3), 35.9 (d, ²J_{PC} = 7 Hz, C1). ³¹P{¹H} NMR (202.5 MHz, C₆D₆): δ (ppm) = 48.6 (q, ²J_{PP} = 25 Hz, PNi), -3.2 (d, ²J_{PP} = 25 Hz, P(Me₃tren)). Elemental analysis: calcd. C 41.68%, H 7.35%, N 24.30%; found C 42.33%, H 7.38%, N 24.67%. IR (neat): $\tilde{\nu}$ (cm⁻¹) = 2010 (m), 2868 (m), 2809 (m), 2015 (m, CO), 1931 (vs, CO), 1918 (vs, CO), 1469 (w), 1448 (m), 1423 (w), 1377 (m), 1353 (m), 1331 (m), 1254 (s), 1224 (vs), 1116 (s), 1048 (m), 1012 (vs), 894 (m), 878 (m), 863 (s), 793 (w), 751 (m), 713 (s), 581 (m), 539 (m), 508 (m), 476 (s), 436 (m), 411 (w).

Tris[1-imino-2,8,9-trimethyl-2,5,8,9-tetraaza-1-phospha-bicyclo[3.3.3]undecane]phosphorus selenide (6e)



6e

Grey selenium (44 mg, 0.56 mmol, 1.0 eq) was added to a stirred solution of (Me₃tren)P₃P (**1e**) (401 mg, 556 μmol, 1.0 eq) in toluene (20 mL) and the mixture was stirred for 6 h at 90 °C and at room temperature overnight. The solid was separated by centrifugation and all volatiles of the clear supernatant removed *in vacuo*. The residue was extracted with diethyl ether (2x 20 mL), evaporated to dryness, and dried in high vacuum.

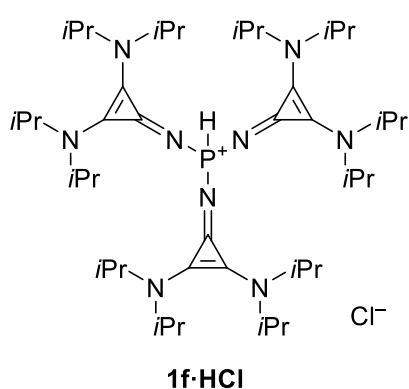
Tris[1-imino-2,8,9-trimethyl-2,5,8,9-tetraaza-1-phospha-bicyclo[3.3.3]undecane]phosphorus selenide (**6e**) was obtained as pale yellow solid.

[C₂₇H₆₃N₁₅P₄Se] (800.76 g·mol⁻¹) ¹H NMR (500.2 MHz, C₆D₆): δ (ppm) = 3.09 (d, ³J_{PH} = 8 Hz, 27H, *H1*), 2.68 (br. s, 18H, *H2*), 2.46 (t, ³J_{HH} = 5 Hz, 18H, *H3*). ¹³C{¹H} NMR (125.8 MHz,

7 Appendix

C₆D₆): δ (ppm) = 52.2 (d, $^2J_{PC}$ = 4 Hz, C2), 50.1 (s, C3), 36.4 (d, $^2J_{PC}$ = 6 Hz, C1). $^{31}\text{P}\{^1\text{H}\}$ NMR (202.5 MHz, C₆D₆): δ (ppm) = 1.7 (d, $^2J_{PP}$ = 40 Hz, P(Me₃tren)), -14.2 (q, $^2J_{PP}$ = 41 Hz, $^1J_{PSe}$ = 636 Hz (satellites), PSe). ^{77}Se NMR (95.4 MHz, C₆D₆): δ (ppm) = 89.4 (d, $^1J_{PSe}$ = 636 Hz). LIFDI(+) MS (toluene): m/z (%) = 801.4 (100) [M]⁺. LIFDI(+) HRMS: m/z [M]⁺ calcd. 801.35065, found 801.35128. IR (neat): $\tilde{\nu}$ (cm⁻¹) = 2918 (w, CH₃, CH₂), 2868 (w, CH₃, CH₂), 2809 (m, CH₃, CH₂), 1449 (w), 1378 (m), 1353 (w), 1332 (m), 1311 (w), 1252 (m), 1222 (vs), 1131 (s), 1117 (s), 1048 (s), 1012 (vs), 895 (m), 882 (m), 865 (s), 780 (m), 717 (s), 657 (w), 583 (m), 541 (m), 509 (s), 484 (m), 446 (w), 411 (w).

Tris[(2,3-bis(di-*iso*-propylamino)cycloprop-2-en-1-ylidene)amino]phosphonium chloride (cpi)₃P·HCl (**1f**·HCl)

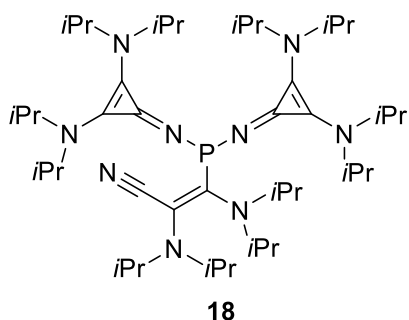


Bis(dimethylamino)phosphorus chloride (**3a**) (65 mg, 0.42 mmol, 3.1 eq) was added to a solution of 2,3-bis(di-*iso*-propylamino)cyclopropeneimine (**2f**) (327 mg, 1.3 mmol, 3.1 eq) in chlorobenzene (20 mL). After stirring for 1 h at room temperature all volatiles were removed *in vacuo*, the residue dissolved in THF (20 mL), filtered over celite, and the filtercake extracted with THF (5 mL). The solvent was removed under reduced pressure and the crude product

stirred in toluene (20 mL) overnight. The solid was separated by centrifugation and dried in high vacuum. Tris[(2,3-bis(di-*iso*-propylamino)cycloprop-2-en-1-ylidene)amino]-phosphonium chloride (**1f**·HCl) (289 mg, 353 μmol , 84%) was isolated as colourless solid.

[C₄₅H₈₅ClN₉P] (818.66 g·mol⁻¹) ^1H NMR (300.2 MHz, CDCl₃): δ (ppm) = 7.76 (d, $^1J_{PH}$ = 508 Hz, 1H, PH), 3.85 (sept., $^3J_{HH}$ = 7 Hz, 12H, CH(CH₃)₂), 1.25 (d, $^3J_{HH}$ = 7 Hz, 72H, CH(CH₃)₂). ^{13}C NMR (75.5 MHz, CDCl₃): δ (ppm) = 122.7 (d, $^2J_{PC}$ = 2 Hz, PNC), 119.0 (d, $^3J_{PC}$ = 24 Hz, CN(*i*Pr)₂), 49.6 (s, CH(CH₃)₂), 22.3 (s, CH(CH₃)₂). $^{31}\text{P}\{^1\text{H}\}$ NMR (101.3 MHz, CDCl₃): δ (ppm) = 10.6. ^{31}P NMR (101.3 MHz, CDCl₃): δ (ppm) = 10.6 (d, $^1J_{PH}$ = 508 Hz). ESI(+) MS (toluene): m/z (%) = 782.8 (100) [M-Cl]⁺. ESI(+)-HMRS: m/z [M-Cl]⁺ calcd. 782.6660, found 782.6653. Elemental analysis: calcd. C 66.02%, H 10.47%, N 15.40%; found C 65.57%, H 10.41%, N 15.37%. IR (neat): $\tilde{\nu}$ (cm⁻¹) = 2967 (m, CH₃, CH), 2932 (w, CH₃, CH), 2872 (w, CH₃, CH), 2337 (w, PH), 1899 (w), 1539 (w), 1471 (s), 1444 (s), 1368 (m), 1325 (m), 1219 (m), 1195 (m), 1160 (m), 1124 (m), 1027 (m), 1004 (m), 950 (s), 883 (m), 790 (m), 741 (m), 708 (m), 667 (w), 618 (w), 599 (w), 557 (m), 530 (m), 502 (m), 456 (w).

Deprotonation of tris[(2,3-bis(di-*iso*-propylamino)cycloprop-2-en-1-ylidene)amino]-phosphonium chloride (1f**·HCl) (1f·HCl)**

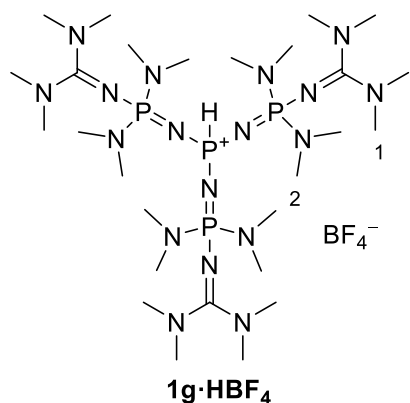


A solution of potassium bis(trimethylsilyl)amide (35 mg, 0.18 mmol, 1.0 eq) in toluene (10 mL) was added to a solution of tris[(2,3-bis(di-*iso*-propylamino)cycloprop-2-en-1-ylidene)amino]phosphonium chloride (**1f**·HCl) (144 mg, 176 μ mol, 1.0 eq) in toluene (20 mL) and stirred for 1 h at room temperature. All volatiles of the resulting yellow mixture were removed *in vacuo*, the residue dissolved in

n-pentane (20 mL), and filtered over celite. The solvent was evaporated and the residue dried in high vacuum to give **18** as intense yellow solid.

[C₄₅H₈₄N₉P] (782.20 g·mol⁻¹) ¹H NMR (300.2 MHz, C₆D₆): δ (ppm) = 6.21 (sept., ³J_{HH} = 7 Hz, 2H, CH(CH₃)₂), 3.81 (sept., ³J_{HH} = 7 Hz, 8H, CH(CH₃)₂), 3.54 (sept., ³J_{HH} = 7 Hz, 2H, CH(CH₃)₂), 1.59 (d, ³J_{HH} = 7 Hz, 12H, CH(CH₃)₂), 1.37 (d, ³J_{HH} = 7 Hz, 12H, CH(CH₃)₂), 1.24 (d, ³J_{HH} = 7 Hz, 24H, CH(CH₃)₂), 1.20 (d, ³J_{HH} = 7 Hz, 24H, CH(CH₃)₂). ¹³C{¹H} NMR (75.5 MHz, C₆D₆): δ (ppm) = 141.5 (s, PCCCN), 129.3 (d, ³J_{PC} = 34 Hz, PCCCN), 122.7 (s, PNC(CN(*i*Pr)₂)₂), 116.6 (d, ³J_{PC} = 16 Hz, PNC(CN(*i*Pr)₂)₂), 98.9 (d, ¹J_{PC} = 81 Hz, PCCCN), 50.5 (s, CH(CH₃)₂), 50.2 (s, CH(CH₃)₂), 49.4 (s, CH(CH₃)₂), 49.3 (s, CH(CH₃)₂), 24.6 (s, CH(CH₃)₂), 22.6 (s, CH(CH₃)₂), 22.5 (s, CH(CH₃)₂), 21.6 (s, CH(CH₃)₂). ³¹P{¹H} NMR (101.3 MHz, C₆D₆): δ (ppm) = 113.6. LIFDI(+) MS (toluene): m/z (%) = 642.3 (100) [M]⁺. LIFDI(+) HRMS: m/z [M]⁺ calcd. 642.27108, found 642.26810. Elemental analysis: calcd. C 69.10%, H 10.82%, N 16.12%; found C 68.16%, H 10.54%, N 15.82%. IR (neat): $\tilde{\nu}$ (cm⁻¹) = 2966 (m, CH₃, CH), 2930 (w, CH₃, CH), 2870 (w, CH₃, CH), 2137 (w, CN), 1873 (w), 1621 (w), 1521 (m), 1484 (s), 1459 (s), 1426 (s), 1363 (m), 1307 (s), 1271 (m), 1219 (m), 1199 (m), 1162 (m), 1121 (m), 1102 (m), 1065 (m), 1019 (w), 965 (w), 862 (w), 791 (m), 770 (w), 707 (m), 668 (m), 656 (m), 610 (w), 592 (w), 557 (w), 493 (w), 436 (w), 420 (w). XRD: For single crystal X-ray structure determination suitable single crystals were obtained by slow evaporation of a solution in *n*-pentane.

Tris[bis(dimethylamino)tetramethylguanidinophosphazeny]phosphonium tetrafluoridoborate (tmg)(dma)₂P₃P·HBF₄ (1g**·HBF₄)**

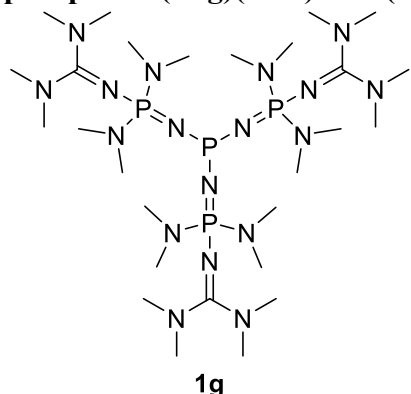


Bis(dimethylamino)tetramethylguanidinophosphazene (**2g**) (5.87 g, 23.6 mmol, 3.00 eq), dissolved in THF (20 mL) was added to a solution of bis(dimethylamino)phosphorus chloride (**3a**) (1.22 g, 7.87 mmol, 1.00 eq) in THF (50 mL), and stirred at room temperature overnight. All volatiles were removed *in vacuo* and the residue was washed with diethyl ether (2x 40 mL). After drying in high vacuum the crude product was converted to its tetrafluoridoborate salt by

dissolving in a minimum amount of water and adding sodium tetrafluoridoborate (950 mg, 8.65 mmol, 1.10 eq), dissolved in a minimum amount of water. The precipitate was filtered off, rinsed with cold water and dried in high vacuum. Tris[bis(dimethylamino)tetramethylguanidinophosphazeny]phosphonium tetrafluoridoborate (**1g**·HBF₄) (1.09 g, 1.27 mmol, 16%) was isolated as colourless solid.

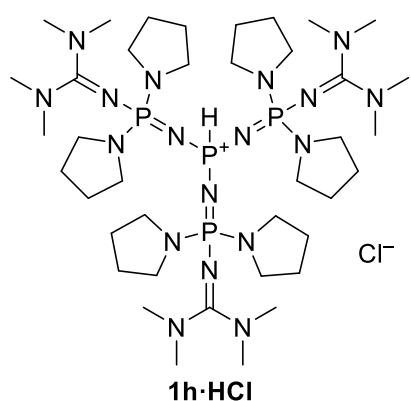
[C₂₇H₇₃BF₄N₁₈P₄] (860.71 g·mol⁻¹) ¹H NMR (500.1 MHz, C₆D₆): δ (ppm) = 7.61 (dq, ¹J_{PH} = 528 Hz, ³J_{PH} = 3 Hz, 1H, PH), 2.78 (s, 36H, HI), 2.62 (d, ³J_{PH} = 10 Hz, 36H, H2). ¹³C{¹H} NMR (125.8 MHz, C₆D₆): δ (ppm) = 160.8 (d, ²J_{PC} = 4 Hz, CN₃), 40.2 (s, CI), 37.4 (d, ²J_{PC} = 4 Hz, C2). ³¹P{¹H} NMR (202.5 MHz, C₆D₆): δ (ppm) = 5.1 (d, ²J_{PP} = 26 Hz, P2), -28.6 (q, ²J_{PP} = 26 Hz, PH). ³¹P NMR (202.5 MHz, C₆D₆): δ (ppm) = 5.33-4.91 (m, P2), -28.6 (dq, ¹J_{PH} = 528 Hz, ²J_{PP} = 26 Hz, PH). ESI(+) MS (MeCN): m/z (%) = 773.8 (100) [M-BF₄]⁺. ESI(+) HRMS: m/z [M-BF₄]⁺ calcd. 773.5211, found 773.5218. Elemental analysis: calcd. C 37.68%, H 8.55%, N 29.29%; found C 37.50%, H 8.38%, N 29.10%. IR (neat): $\tilde{\nu}$ (cm⁻¹) = 2868 (m, CH₃), 1829 (m, CH₃), 2791 (m, CH₃), 2301 (w, PH), 1563 (s), 1519 (s), 1478 (m), 1427 (m), 1410 (m), 1387 (s), 1345 (w), 1280 (m), 1233 (s), 1187 (vs), 1143 (s), 1091 (s), 1048 (vs), 1018 (s), 969 (vs), 920 (s), 900 (vs), 816 (m), 748 (m), 712 (s), 679 (s), 623 (m), 576 (m), 532 (m), 491 (s). XRD: For single crystal X-ray structure determination suitable single crystals were obtained from methanol/water at -25 °C.

Attempted synthesis of tris[bis(dimethylamino)tetramethylguanidinophosphazeny]-phosphane (tmg)(dma)₂P₃P (**1g**)



Tris[bis(dimethylamino)tetramethylguanidinophosphazeny]phosphonium tetrafluoroborate (**1g**·HBF₄) (280 mg, 0.33 mmol, 1.0 eq) and potassium bis(trimethylsilyl)amide (69 mg, 0.35 mmol, 1.1 eq) were stirred in toluene (15 mL) for 90 min at room temperature. Reaction control *via* ³¹P NMR spectroscopy revealed complete disintegration of the starting material.

Attempted synthesis of tris[tetramethylguanidinobis(pyrrolidino)phosphazeny]-phosphonium chloride (tmg)(pyrr)₂P₃P·HBF₄ (**1h**·HCl)

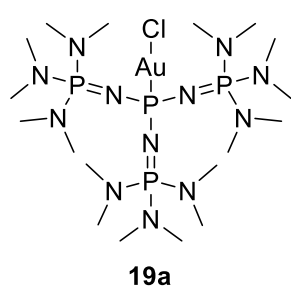


Aminotetramethylguanidinobis(pyrrolidino)phosphonium iodide (**2h**·HI) (1.18 g, 2.74 mmol, 3.11 eq) and potassium bis(trimethylsilyl)amide (552 mg, 2.77 mmol, 3.15 eq) were stirred in THF (20 mL) at room temperature overnight. The precipitate was separated by centrifugation, bis(dimethylamino)phosphorus chloride (135 mg, 880 μmol, 1.00 eq) was added to the supernatant and the reaction mixture stirred for 3 h at room temperature. Traces of tris[tetramethylguanidino-

bis(pyrrolidino)phosphazeny]phosphonium chloride (**1h**·HCl) were identified by ³¹P NMR spectroscopy, but were inseparable from byproducts.

³¹P{¹H} NMR (101.3 MHz, THF): δ (ppm) = -2.13 (d, ²J_{PP} = 23 Hz, P(tmg)(pyrr)₂), -27.9 (q, ²J_{PP} = 24 Hz, PH).

Chlorido{tris[tris(dimethylamino)phosphazeny]phosphane}gold(I) (**19a**)

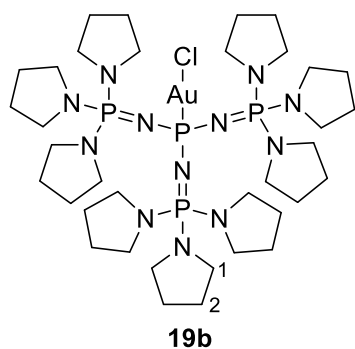


A (dma)₃P₃P (**1a**) containing solution in toluene (20 mL, 0.52 mmol, 1.0 eq), prepared according to the general procedure, was added to a suspension of (chlorido)(triphenylphosphane)gold(I) (256 mg, 517 μmol, 1.0 eq) in toluene (10 mL). All volatiles were removed *in vacuo*, the residue dissolved in boiling *n*-hexane (20 mL), and filtered hot. Chlorido{tris[tris(dimethylamino)phosphazeny]phosphane}-

gold(I) (**19a**) (340 mg, 428 μmol, 83%) was crystallized at -25 °C as colourless solid and washed once with cold *n*-pentane (5 mL).

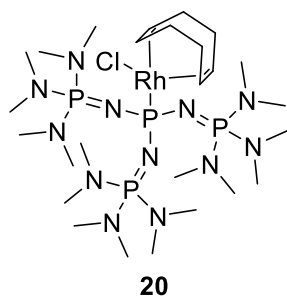
[C₁₈H₅₄AuClN₁₂P₄] (795.03 g·mol⁻¹) ¹H NMR (300.3 MHz, C₆D₆): δ (ppm) = 2.65 (d, ³J_{PH} = 10 Hz, 54H). ¹³C{¹H} NMR (75.5 MHz, C₆D₆): δ (ppm) = 37.9 (d, ²J_{PC} = 4 Hz). ³¹P{¹H} NMR (121.5 MHz, C₆D₆): δ (ppm) = 22.3 (q, ²J_{PP} = 40 Hz, PAu), 15.3 (d, ²J_{PP} = 40 Hz, P(dma)₃). LIFDI(+) MS (toluene): m/z (%) = 597.3 (100) [M–Au]⁺, 794.3 (70) [M]⁺. LIFDI(+) HRMS: m/z [M]⁺ calcd. 794.28989, found 794.28457. Elemental analysis: calcd. C 27.19%, H 6.85%, N 21.14%; found C 27.35%, H 6.80%, N 21.51%. XRD: The isolated crystalline product was suitable for single crystal X-ray structure determination.

Chlorido{tris[tris(pyrrolidino)phosphazeny]phosphane}gold(I) (19b)



A (pyrr)₃P (**1b**) containing solution in toluene (15 mL, 0.29 mmol, 1.0 eq), prepared according to the general procedure, was added to a suspension of (chlorido)(triphenylphosphane)-gold(I) (150 mg, 0.30 mmol, 1.0 eq) in toluene (5 mL). All volatiles were removed *in vacuo*, the residue dissolved in boiling *n*-hexane (20 mL), and filtered hot. The filtrate was reduced to the half and chlorido{tris[tris(pyrrolidino)phosphazeny]phosphane}gold(I) (**19b**) (244 mg, 237 μmol, 81%) crystallized at –25 °C as colourless solid. [C₃₆H₇₂AuClN₁₂P₄] (1029.37 g·mol⁻¹) ¹H NMR (300.3 MHz, C₆D₆): δ (ppm) = 3.38-3.33 (m, 36H, *H1*), 1.80-1.76 (m, 36H, *H2*). ¹³C{¹H} NMR (75.5 MHz, C₆D₆): δ (ppm) = 47.3 (d, ²J_{PC} = 4 Hz, *Cl*), 26.8 (d, ²J_{PC} = 9 Hz, *C2*). ³¹P{¹H} NMR (121.5 MHz, C₆D₆): δ (ppm) = 20.7 (q, ²J_{PP} = 23 Hz, PAu), 1.4 (d, ²J_{PP} = 23 Hz, P(pyrr)₃). LIFDI(+) MS (toluene): m/z (%) = 1028.4 (100) [M]⁺. LIFDI(+) HRMS: m/z [M]⁺ calcd. 1028.43074, found 1028.41066.

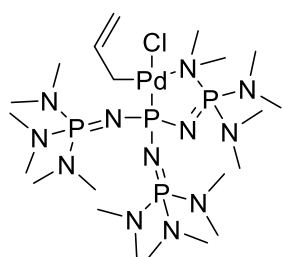
Chlorido(1,5-cyclooctadiene){tris[tris(dimethylamino)phosphazeny]phosphane}rhodium(I) (20)



A (dma)₃P (**1a**) containing solution in toluene (5.0 mL, 0.16 mmol, 2.0 eq), prepared according to the general procedure, was added to a solution of [(chlorido)(cyclooctadiene)rhodium(I)] dimer (39 mg, 79 μmol, 1.0 eq) in toluene (5 mL). All volatiles were removed *in vacuo*, the residue dissolved in *n*-pentane (15 mL), and cleared *via* syringe filtration. Drying in high vacuum gave (chlorido)(1,5-cyclooctadiene){tris[tris(dimethylamino)phosphazeny]phosphane}rhodium(I) (**20**) as intense yellow solid.

[C₂₆H₆₆ClN₁₂RhP₄] (809.15 g·mol⁻¹) ¹H NMR (500.1 MHz, C₆D₆): δ (ppm) = 5.56 (d, ³J_{HH} = 3 Hz, 2H, CH), 3.91 (dd, ³J_{PH} = 3 Hz, ³J_{HH} = 3 Hz, 2H, CH) 2.74 (d, ³J_{PH} = 10 Hz, 54H, N(CH₃)₂), 2.58-2.53 (m, 2H, CH₂), 2.42-2.35 (m, 2H, CH₂), 2.14-2.03 (m, 4H, CH₂). ¹³C {¹H} NMR (125.8 MHz, C₆D₆): δ (ppm) = 99.5 (dd, ¹J_{RhC} = 20 Hz, ²J_{PC} = 6 Hz, CH), 66.8 (d, ¹J_{RhC} = 16 Hz, CH), 38.1 (d, ²J_{PC} = 5 Hz, N(CH₃)₂), 34.0 (d, ³J_{PC} = 3 Hz, CH₂), 29.4 (d, ³J_{PC} = 3 Hz, CH₂). ³¹P {¹H} NMR (202.5 MHz, C₆D₆): δ (ppm) = 26.1 (d, ¹J_{PRh} = 179 Hz, PRh), 3.7 (s, P(dma)₃). LIFDI(+) MS (toluene): m/z (%) = 563.3 (20) [M-RhCl(cod)+H]⁺, 597.3 (40) [M-Rh(cod)]⁺, 773.3 (100) [M-Cl]⁺, 808.3 (20) [M]⁺. LIFDI(+) HRMS: m/z [M]⁺ calcd. 808.32274, found 808.32282. Elemental analysis: calcd. C 38.59%, H 8.22%, N 20.77%; found C 38.16%, H 8.06%, N 18.63%. IR (neat): $\tilde{\nu}$ (cm⁻¹) = 2961 (w), 2866 (m), 2838 (m), 2739 (m), 1456 (m), 1345 (m), 1256 (vs), 1194 (s), 1093 (s), 1067 (s), 1021 (s), 973 (vs), 861 (m), 797 (s), 724 (s), 572 (s), 511 (s), 486 (s), 442 (s). XRD: For single crystal X-ray structure determination suitable single crystals were obtained from *n*-pentane at -25 °C.

(η^1 -Allyl)(chlorido){ κ^2 -tris[tris(pyrrolidino)phosphazeny]phosphane}palladium(II) (21)

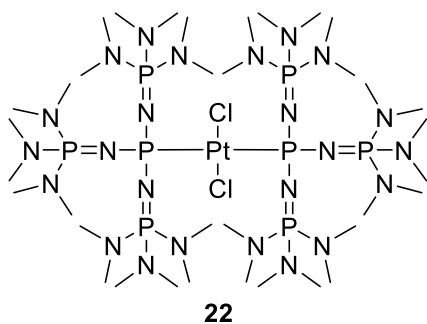


21

A (dma)₃P₃P (**1a**) containing solution in toluene (5.0 mL, 0.16 mmol, 1.9 eq), prepared according to the general procedure, was added to a solution of (allyl)(chlorido)palladium(II) dimer (30 mg, 82 μmol, 1.0 eq) in toluene (5 mL). All volatiles were removed *in vacuo*, the residue dissolved in *n*-pentane (15 mL), and cleared *via* syringe filtration. Drying in high vacuum gave (η^1 -allyl)chlorido{ κ^2 -tris-

[tris(pyrrolidino)phosphazeny]phosphane}palladium(II) (**21**) as yellow crystalline solid. The substance's instability in solution allowed no analytics other than ³¹P NMR spectroscopy and single crystal X-ray structure determination.

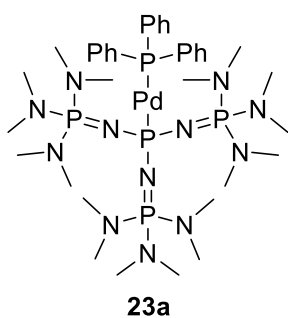
[C₂₁H₅₉ClN₁₂PdP₄] (745.55 g·mol⁻¹) ³¹P {¹H} NMR (202.5 MHz, C₆D₆): δ (ppm) = 25.7 (q, ²J_{PP} = 3 Hz, PPD), 12.6 (br. s, P(dma)₃). XRD: The obtained crystalline solid was suitable for single crystal X-ray structure determination.

Dichloridobis{tris[tris(dimethylamino)phosphazeny]phosphane}platinum(II) (22)

A (dma)₃P (1a) containing solution in toluene (5.0 mL, 0.16 mmol, 1.9 eq), prepared according to the general procedure, was added to a suspension of platinum(II) chloride (22 mg, 83 μmol, 1.0 eq) in toluene (5 mL). All volatiles were removed *in vacuo*, the residue dissolved in diethyl ether (20 mL), and cleared *via* syringe filtration. The solution was stored at -25 °C to obtain suitable single

crystals for single crystal X-ray structure determination. For ³¹P NMR spectroscopy the solvent was evaporated and the residue dissolved in C₆D₆. Due to the substance's instability in solution no further analytics were possible.

[C₃₆H₁₀₈Cl₂N₂₄P₈Pt] (1391.20 g·mol⁻¹) ³¹P{¹H} NMR (202.5 MHz, C₆D₆): δ (ppm) = 16.0 (s, ¹J_{PPt} = 2947 Hz (satellites), PPt), 0.59 (s, ³J_{PPt} = 33 Hz (satellites), P(dma)₃). XRD: For single crystal X-ray structure determination suitable single crystals were obtained by cooling a concentrated solution in diethyl ether.

{Tris[tris(dimethylamino)phosphazeny]phosphane}(triphenylphosphane)palladium(0) (23a)

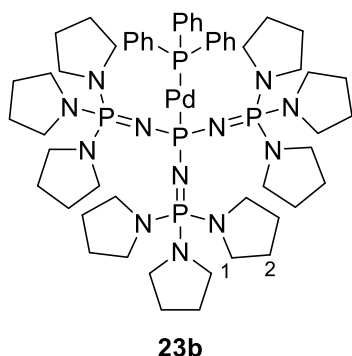
A (dma)₃P (1a) containing solution in toluene (14 mL, 0.13 mmol, 2.4 eq), prepared according to the general procedure, was added to a suspension of dichloridobis(triphenylphosphane)palladium(II) (59 mg, 84 μmol, 1.0 eq) in toluene (5 mL) and stirred overnight at room temperature. The orange suspension was centrifuged and the clear supernatant evaporated to dryness. The residue was dissolved in *n*-pentane (20 mL), filtered, and the filtercake extracted with

n-pentane (2x 20 mL). The filtrate was reduced to a minimum and stored at -25 °C to isolate {tris[tris(dimethylamino)phosphazeny]phosphane}(triphenylphosphane)palladium(0) (23a) as orange crystals containing one equivalent *n*-pentane as cocrystallize.

[C₃₆H₆₉N₁₂P₅Pd] (931.32 g·mol⁻¹) ¹H NMR (300.2 MHz, C₆D₆): δ (ppm) = 7.96-7.90 (m, 6H, *m*-H), 7.19-7.14 (m, 6H, *o*-H), 7.11-7.06 (m, 3H, *p*-H), 2.85 (d, ³J_{PH} = 10 Hz, 54H, N(CH₃)₂). ¹³C{¹H} NMR (75.5 MHz, C₆D₆): δ (ppm) = 140.9 (d, ¹J_{PC} = 23 Hz, *i*-C), 134.9 (d, ³J_{PC} = 17 Hz, *m*-C), 128.2 (*p*-C, overlapped with the solvent signal), 127.9 (d, ²J_{PC} = 9 Hz, *o*-C), 38.3 (dd, ²J_{PC} = 4 Hz, ⁴J_{PC} = 2 Hz, N(CH₃)₂). ³¹P{¹H} NMR (121.5 MHz, C₆D₆): δ (ppm) = 61.7 (dq, ²J_{PP} = 401 Hz, ²J_{PP} = 23 Hz, N₃PPd), 26.5 (d, ²J_{PP} = 400 Hz, Ph₃PPd), 11.2 (d, ²J_{PP} = 24 Hz,

$P(\text{dma})_3$). XRD: The isolated crystalline product was suitable for single crystal X-ray structure determination.

{Tris[tris(pyrrolidino)phosphazeny]phosphane}(triphenylphosphane)palladium(0)
(23b)

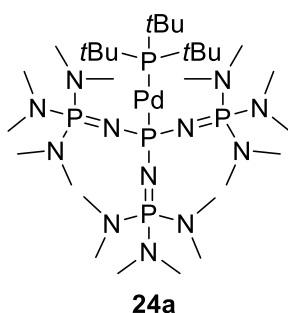


A (pyrr) P_3P (**1b**) containing solution in toluene (20 mL, 0.46 mmol, 2.1 eq), prepared according to the general procedure, was added to a suspension of dichloridobis(triphenylphosphane)palladium(II) (153 mg, 0.22 mmol, 1.0 eq) in toluene (5 mL) and stirred for 6 h at 60 °C. All volatiles were removed *in vacuo*, the residue dissolved in *n*-hexane (20 mL), filtered over celite, and the filtercake extracted with *n*-hexane (2x 20 mL). The

solvent was evaporated and the residue dried in high vacuum. {Tris[tris(pyrrolidino)phosphazeny]phosphane}(triphenylphosphane)palladium(0) (**23b**) was obtained as orange solid.

[$C_{54}H_{87}N_{12}P_5Pd$] (1165.66 $\text{g}\cdot\text{mol}^{-1}$) ^1H NMR (300.3 MHz, C_6D_6): δ (ppm) = 7.96-7.90 (m, 6H, *m-H*), 7.21-7.15 (m, 6H, *o-H*), 7.13-7.07 (m, 3H, *p-H*), 3.58-3.52 (m, 36H, *H1*), 1.77-1.73 (m, 36H, *H2*). $^{13}\text{C}\{^1\text{H}\}$ NMR (75.5 MHz, C_6D_6): δ (ppm) = 141.3 (d, $^1J_{PC} = 23$ Hz, *i-C*), 134.9 (d, $^3J_{PC} = 17$ Hz, *m-C*), 128.1 (*p-C*, overlapped with the solvent signal), 127.9 (d, $^2J_{PC} = 9$ Hz, *o-C*), 47.6 (dd, $^2J_{PC} = 4$ Hz, $^4J_{PC} = 2$ Hz, *CI*), 27.0 (d, $^3J_{PC} = 8$ Hz, *C2*). $^{31}\text{P}\{^1\text{H}\}$ NMR (121.5 MHz, C_6D_6): δ (ppm) = 61.0 (dq, $^2J_{PP} = 407$ Hz, $^2J_{PP} = 6$ Hz, N_3PPd), 26.6 (d, $^2J_{PP} = 407$ Hz, Ph_3PPd), -1.4 (d, $^2J_{PP} = 6$ Hz, $P(\text{dma})_3$). LIFDI(+) MS (*n*-hexane): m/z (%) = 278.1 (10) [$Ph_3P=O$] $^+$, 812.5 (100) [(pyrr) $P_3P=O$] $^+$, 1164.5 (10) [M] $^+$. LIFDI(+) HRMS: m/z [M] $^+$ calcd. 1164.48995, found 1164.49267.

{Tris[tris(dimethylamino)phosphazeny]phosphane}(tri-*tert*-butylphosphane)-palladium(0) (24a)

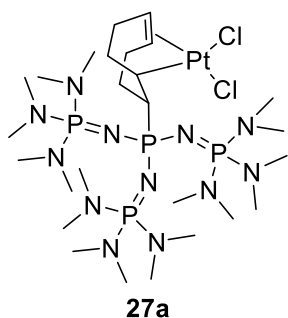


A (dma) P_3P (**1a**) containing solution in toluene (20 mL, 0.47 mmol, 1.0 eq), prepared according to the general procedure, was added to a solution of bis(tri-*tert*-butylphosphane)palladium(0) (256 mg, 0.50 mmol, 1.1 eq) in toluene (5 mL) and stirred over weekend at room temperature. All volatiles were removed *in vacuo*, the residue dissolved in *n*-pentane (15 mL), and filtered over celite. The solvent

was evaporated and the residue dried for 8 h at 50 °C and $7.4\cdot 10^{-7}$ mbar. {Tris[tris(dimethyl-

[C₂₆H₆₆N₁₂NiP₄] (729.49 g·mol⁻¹) ¹H NMR (500.1 MHz, C₆D₆): δ (ppm) = 5.16 (t, ³J_{HH} = 8 Hz, 1H, CHCHCH₂), 3.77 (ddd, ³J_{PH} = 15 Hz, ²J_{HH} = 11 Hz, ³J_{PH} = 2 Hz, 1H, HI), 3.62 (ddd, ³J_{PH} = 12 Hz, ²J_{HH} = 11 Hz, ³J_{PH} = 2 Hz, 1H, HI), 3.62 (ddt, 2x ³J_{HH} = 8 Hz, ³J_{PH} = 1 Hz, 1H, CHCHCH₂), 3.30 (ddt, 2x ³J_{HH} = 8 Hz, ³J_{PH} = 7 Hz, 1H, CHCHCH₂), 2.90 (d, ³J_{PH} = 9 Hz, 3H, H₂), 2.72 (d, ³J_{PH} = 10 Hz, 18H, H₄), 2.68 (d, ³J_{PH} = 10 Hz, 6H, H₃), 2.66 (d, ³J_{PH} = 10 Hz, 6H, H₃), 2.62 (d, ³J_{PH} = 10 Hz, 18H, H₄), 2.56-2.49 (m, 3H, CH₂), 2.47-2.40 (m, 2H, CH₂), 1.87 (quint. ³J_{HH} = 5 Hz, 2H, CH₂), 1.78 (quint. ³J_{HH} = 5 Hz, 2H, CH₂), 1.55 (dt, ²J_{HH} = 14 Hz, ³J_{HH} = 4 Hz, 1H, CHCHCH₂). ¹³C{¹H} NMR (125.8 MHz, C₆D₆): δ (ppm) = 107.8 (s, CHCHCH₂), 68.1 (d, ²J_{PC} = 35 Hz, CHCHCH₂) 66.1 (d, ²J_{PC} = 3 Hz, CHCHCH₂), 42.3 (dd, ²J_{PC} = 23 Hz, ²J_{PC} = 17 Hz, CI), 41.3 (dd, ²J_{PC} = 5 Hz, ⁴J_{PC} = 3 Hz, C2), 38.1 (d, ²J_{PC} = 4 Hz, C4), 37.8 (d, ²J_{PC} = 4 Hz, C4), 37.7 (d, ²J_{PC} = 3 Hz, C3), 37.3 (d, ²J_{PC} = 3 Hz, C3), 32.9 (s, CH₂), 32.3 (d, ²J_{PC} = 5 Hz, CH₂), 30.7 (d, ²J_{PC} = 2 Hz, CH₂), 30.5 (d, ²J_{PC} = 7 Hz, CH₂), 24.8 (s, CH₂). ³¹P{¹H} NMR (121.5 MHz, C₆D₆): δ (ppm) = 56.2 (ddd, ²J_{PP} = 66 Hz, ²J_{PP} = 50 Hz, ²J_{PP} = 10 Hz, PNi), 27.0 (d, ²J_{PP} = 50 Hz, P3), 7.0 (d, ²J_{PP} = 66 Hz, P4), 4.5 (d, ²J_{PP} = 10 Hz, P4). LIFDI(+) MS (*n*-hexan): m/z (%) = 728.4 (100) [M]⁺. LIFDI(+) HRMS: m/z [M]⁺ calcd. 728.38373, found 728.38675. Elemental analysis: calcd. C 42.81%, H 9.12%, N 23.04%; found C 43.07%, H 8.85%, N 22.61%.

Dichlorido[8-{{tris(dimethylamino)phosphazeny]phosphonio}cyclooct-4-en-1-yl]-platinum(II) (27a)



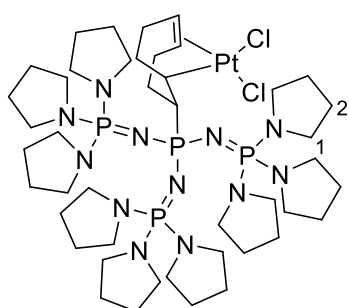
A (dma)₃P (1a) containing solution in toluene (20 mL, 0.59 mmol, 1.0 eq), prepared according to the general procedure, was added to a suspension of dichlorido(1,5-cyclooctadiene)platinum(II) (220 mg, 0.59 mmol, 1.0 eq) in toluene (5 mL) and stirred overnight at room temperature. The solid was separated by centrifugation and recrystallized from THF at -25 °C. After washing with toluene (10 mL) and *n*-pentane (20 mL) and drying in high vacuum

dichlorido[8-{{tris(dimethylamino)phosphazeny]phosphonio}cyclooct-4-en-1-yl]platinum(II) (27a) (370 mg, 395 μmol, 67%) was isolated as colourless solid.

[C₂₆H₆₆Cl₂N₁₂P₄Pt] (936.78 g·mol⁻¹) ¹H NMR (500.2 MHz, CDCl₃): δ (ppm) = 4.96 (br. s, ²J_{PH} = 81 Hz (satellites), 1H, CH), 4.65 (br. s, ²J_{PH} = 94 Hz (satellites), 1H, CH), 3.63 (br. d, ²J_{PH} = 13 Hz, ²J_{PH} = 118 Hz (satellites), 1H, CH), 2.60 (d, ³J_{PH} = 10 Hz, 54H, CH₃), 2.29-2.26 (m, 1H, CH₂), 2.17 (d, ³J_{PH} = 16 Hz, 1H, CH₂), 2.11-2.05 (m, 1H, CH₂), 1.96-1.85 (m, 5H, PCH, CH₂), 1.60-1.56 (m, 1H, CH₂). ¹³C{¹H} NMR (125.8 MHz, CDCl₃): δ (ppm) = 79.2 (br. s ¹J_{PC} =

260 Hz, CH), 74.3 (br. s $^1J_{PtC} = 251$ Hz, CH), 50.3 (dq, $^1J_{PC} = 123$ Hz, $^3J_{PC} = 3$ Hz, PCH), 37.3 (d, $^2J_{PC} = 5$ Hz, CH₃), 36.8 (s, CH₂), 29.5 (s, CH₂), 29.3 (d, $J_{PC} = 20$ Hz, CH₂), 24.7 (br. s, CH, CH₂). $^{31}P\{^1H\}$ NMR (121.5 MHz, CDCl₃): δ (ppm) = 10.4 (d, $^2J_{PP} = 26$ Hz, $P(dma)_3$), -11.3 (q, $^2J_{PP} = 26$ Hz, $^3J_{PPt} = 303$ Hz (satellites), PCH). $^{195}Pt\{^1H\}$ NMR (64.54 MHz, CDCl₃): δ (ppm) = -3400 (d, $^3J_{PPt} = 302$ Hz). ESI(+) MS (MeCN): m/z (%) = 900.9 (100) [M-Cl]⁺. ESI(+) HRMS: m/z [M-Cl]⁺ calcd. 901.3812, found 901.3811. XRD: For single crystal X-ray structure determination suitable single crystals were obtained by treating a solution in dichloromethane with silver hexafluoridophosphate and layering the decanted supernatant with diethyl ether.

Dichlorido[8-[[tris(pyrrolidino)phosphazeny]phosphonio]cyclooct-4-en-1-yl]-platinum(II) (27b)



27b

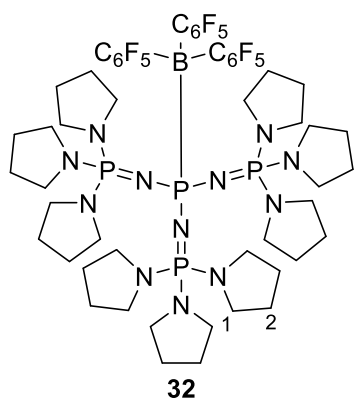
A (pyrr)P₃P (**1b**) containing solution in toluene (20 mL, 0.59 mmol, 1.0 eq), prepared according to the general procedure, was added to a suspension of dichlorido(1,5-cyclooctadiene)-platinum(II) (220 mg, 0.59 mmol, 1.00 eq) in toluene (5 mL) and stirred for 2 h at 90 °C. The solid was separated by centrifugation and recrystallized from THF at -25 °C. After washing with toluene (10 mL) and *n*-pentane (20 mL) and drying in high

vacuum dichlorido[8-[[tris(pyrrolidino)phosphazeny]phosphonio]cyclooct-4-en-1-yl]-platinum(II) (**27b**) (400 mg, 342 μ mol, 58%) was isolated as colourless solid.

[C₄₄H₈₄Cl₂N₁₂P₄Pt] (1171.12 g·mol⁻¹) 1H NMR (500.2 MHz, CDCl₃): δ (ppm) = 4.96 (br. s, $^2J_{PtH} = 84$ Hz (satellites), 1H, CH), 4.65 (br. s, $^2J_{PtH} = 94$ Hz (satellites), 1H, CH), 3.67 (br. d, $^2J_{PH} = 7$ Hz, $^2J_{PtH} = 118$ Hz (satellites), 1H, CH), 3.13-3.10 (m, 36H, HI), 2.30-2.22 (m, 1H, CH₂), 2.15 (d, $^3J_{PH} = 17$ Hz, 1H, CH₂), 2.07-1.98 (m, 3H, PCH, CH₂), 1.90-1.82 (m, 3H, CH₂), 1.78-1.74 (m, 36H, H₂), 1.60-1.52 (m, 1H, CH₂). $^{13}C\{^1H\}$ NMR (125.8 MHz, CDCl₃): δ (ppm) = 78.8 (br. s $^1J_{PtC} = 260$ Hz, CH), 74.7 (br. s $^1J_{PtC} = 255$ Hz, CH), 50.6 (dq, $^1J_{PC} = 125$ Hz, $^3J_{PC} = 3$ Hz, PCH), 46.5 (d, $^2J_{PC} = 5$ Hz, CI), 37.1 (s, CH₂), 29.6 (s, CH₂), 29.4 (s, CH₂), 26.5 (d, $^2J_{PC} = 9$ Hz, C₂), 25.5 (br. s, CH), 24.9 (s, CH₂). $^{31}P\{^1H\}$ NMR (121.5 MHz, CDCl₃): δ (ppm) = -5.8 (d, $^2J_{PP} = 24$ Hz, $P(pyrr)_3$), -12.7 (q, $^2J_{PP} = 23$ Hz, $^3J_{PPt} = 300$ Hz (satellites), PCH). $^{195}Pt\{^1H\}$ NMR (64.54 MHz, CDCl₃): δ (ppm) = -3406 (d, $^3J_{PPt} = 308$ Hz). ESI(+) MS (MeCN): m/z (%) = 1135.7 (100) [M-Cl]⁺. ESI(+) HRMS: m/z [M-Cl]⁺ calcd. 1135.5226, found 1135.5182.

Tris[tris(pyrrolidino)phosphazeny]phosphane tris(pentafluorophenyl)borane adduct

(28)



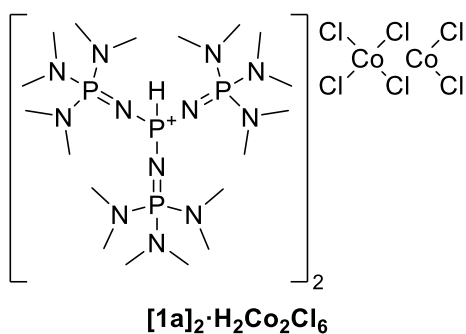
Tris(pentafluorophenyl)borane (28 mg, 54 μmol , 1.0) was dissolved in toluene (5 mL) and cooled to $-78\text{ }^\circ\text{C}$. (pyrr) P_3P (**2b**) (43 mg, 54 μmol , 1.0 eq), dissolved in toluene (5 mL), was added dropwise and the mixture allowed to warm to room temperature overnight. All volatiles were removed *in vacuo*, the residue dissolved in *n*-pentane (20 mL), and filtered over celite. The filtercake was extracted with *n*-pentane (3x 20 mL) and the solvent evaporated. A colourless solid, containing

tris[tris(pyrrolidino)phosphazeny]phosphane tris(pentafluorophenyl)borane adduct (**28**) as major component, was obtained.

$[\text{C}_{54}\text{H}_{72}\text{BF}_{15}\text{N}_{12}\text{P}_4]$ ($1308.94\text{ g}\cdot\text{mol}^{-1}$) ^1H NMR (300.3 MHz, C_6D_6): δ (ppm) = 2.90-2.84 (m, 36H, *HI*), 1.60-1.55 (m, 36H, *H2*). ^{11}B NMR (96.33 MHz, C_6D_6): δ (ppm) = -11.2 (d, $^1J_{\text{PB}} = 210$ Hz). $^{19}\text{F}\{^1\text{H}\}$ NMR (282.5 MHz, C_6D_6): δ (ppm) = -133.9 - -134.1 (m, *o-F*), -163.0 (t, $J_{\text{FF}} = 21$ Hz, *p-F*), -166.8 - -167.0 (m, *m-F*). $^{31}\text{P}\{^1\text{H}\}$ NMR (121.5 MHz, C_6D_6): δ (ppm) = -6.8 (q, $^1J_{\text{PB}} = 209$ Hz, *PB*), -21.9 (br. s, *P(pyrr)* $_3$).

Tris[tris(dimethylamino)phosphazeny]phosphonium hexachloridodicobaltate

$[(\text{dma})\text{P}_3\text{P}]_2\cdot\text{H}_2\text{Co}_2\text{Cl}_6$ ($[\mathbf{1a}]_2\cdot\text{H}_2\text{Co}_2\text{Cl}_6$)



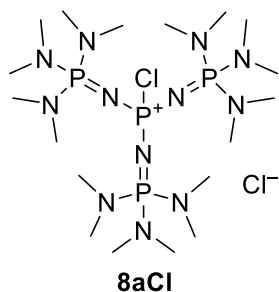
A (dma) P_3P (**1a**) containing solution in toluene (10 mL, 0.15 mmol, 1.0 eq), prepared according to the general procedure, was added to a stirred suspension of anhydrous cobalt(II) chloride (22 mg, 0.17 mmol, 1.1 eq) in toluene (5 mL). All volatiles of the deep blue solution were removed *in vacuo* and the residue washed with *n*-pentane (3x 15 mL). Drying in high vacuum gave

tris[tris(dimethylamino)phosphazeny]phosphonium hexachloridodicobaltate ($[\mathbf{1a}]_2\cdot\text{H}_2\text{Co}_2\text{Cl}_6$) as intense blue solid.

$[\text{C}_{36}\text{H}_{110}\text{Cl}_6\text{Co}_2\text{N}_{24}\text{P}_8]$ ($1457.80\text{ g}\cdot\text{mol}^{-1}$) $^{31}\text{P}\{^1\text{H}\}$ NMR (121.5 MHz, C_6D_6): δ (ppm) = 23.7 (br. d, $^2J_{\text{PP}} = 32$ Hz, *P(dma)* $_3$), -17.7 (br. s, *PH*). ^{31}P NMR (121.5 MHz, C_6D_6): δ (ppm) = 24.7 (br. s, *P(dma)* $_3$), -17.0 (br. d, $^1J_{\text{PH}} = 569$ Hz, *PH*). LIFDI(+) MS (benzene): m/z (%) = 563.4 (100) $[(\text{dma})\text{P}_3\text{P}-\text{H}]^+$. LIFDI(+) HRMS: m/z $[(\text{dma})\text{P}_3\text{P}-\text{H}]^+$ calcd. 563.36231, found 563.36342.

XRD: For single crystal X-ray structure determination suitable single crystals were obtained by dissolving in toluene and layering with *n*-pentane.

Chlorotris[tris(dimethylamino)phosphazeny]phosphonium chloride (**8aCl**)



The compound was not synthesized on purpose but occurred in different complexation reactions as side product and was isolated as colourless precipitate from the reaction mixtures.

[C₁₈H₅₄Cl₂N₁₂P₄] (633.51 g·mol⁻¹) ¹H NMR (300.2 MHz, CDCl₃): δ (ppm) = 2.69 (d, ³J_{PH} = 10 Hz, 54H). ¹³C{¹H} NMR (75.5 MHz, CDCl₃): δ (ppm) = 37.3 (d, ²J_{PC} = 4 Hz). ³¹P{¹H} NMR (121.5 MHz, CDCl₃): δ (ppm) = 19.1 (d, ²J_{PP} = 29 Hz, P(dma)₃), -22.7 (q, ²J_{PP} = 29 Hz, PCl). LIFDI(+) MS (THF): m/z (%) = 597.3 (100) [M-Cl]⁺. LIFDI(+) HRMS: m/z [M-Cl]⁺ calcd. 597.32334, found 597.35479. XRD: For single crystal X-ray structure determination the anion was exchanged for PF₆⁻ by treating a solution in THF with AgPF₆ and layering the decanted supernatant with *n*-pentane.

Reaction of [tris(dimethylamino)phosphazeny]phosphane (**1a**) with titanium tetrachloride

A (dma)₃P₃P (**1a**) containing solution in THF (5.0 mL, 0.17 mmol, 1 eq), prepared according to the general procedure, was added to a solution of titanium tetrachloride (0.05 mL, 0.5 mmol, 3 eq) in THF (2 mL). The mixture immediately turned deep purple, indicating the reduction to titanium(III) species. Chlorotris[tris(dimethylamino)phosphazeny]phosphonium chloride (**8aCl**) was detected *via* ³¹P NMR spectroscopy and HR massspectrometry.

Reactions of PAs with ruthenium precursors

A (dma)₃P₃P (**1a**) containing solution in toluene (5.0 mL, 0.11 mmol, 2.2 eq), prepared according to the general procedure, was added to a solution of dichlorido(*para*-cymene)ruthenium(II) dimer (31 mg, 51 μmol, 1.1 eq) in toluene (5 mL). No selective reaction was observed *via* ³¹P NMR spectroscopy.

(pyrr)₃P₃P (**1b**) (68 mg, 85 μmol, 2.2 eq), dissolved in toluene, was added to a solution of dichlorido(3-phenyl-1H-inden-1-ylidene)bis(tricyclohexylphosphane)ruthenium(II) (36 mg, 39 μmol, 1.0 eq) in toluene (5 mL). No selective reaction was observed *via* ³¹P NMR spectroscopy.

Reactivity studies of PAPs towards iodoethane

The respective PAP was dissolved in THF (5 mL) and iodoethane was added under stirring. All volatiles were removed *in vacuo*, the residue dissolved in CD₃CN and analyzed by NMR spectroscopy and mass spectrometry. The alkylation/protonation ratio was determined on the bases of the central phosphorus atoms' signal intensities. The spectroscopic data of the ethylated products are given below.

Tris[tris(dimethylamino)phosphazanyl]phosphane (**1a**) (21 mg, 37 μmol, 1.0 eq) and iodoethane (50 μL, 62 μmol, 1.7 eq) gave a [(dma)P₃P-Et]⁺/[(dma)P₃P-H]⁺-ratio of 83/17.

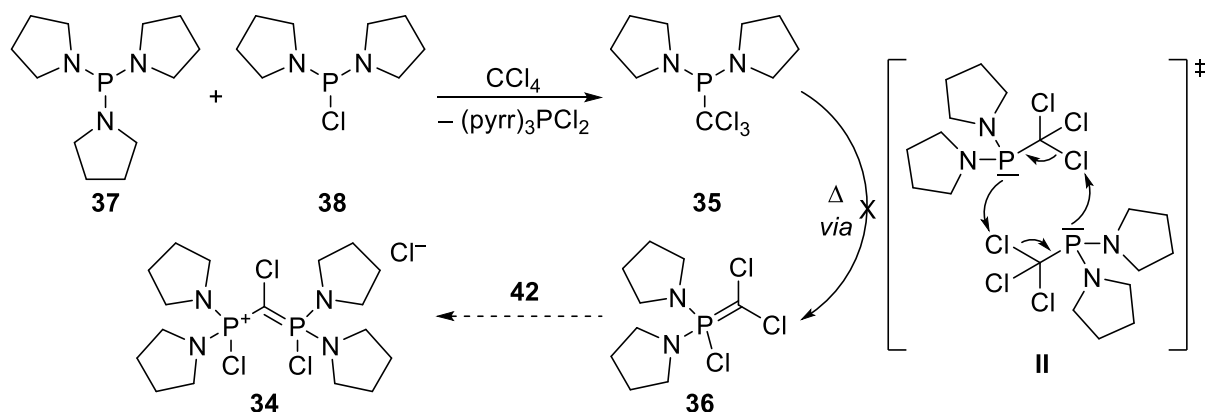
¹H NMR (250.1 MHz, CD₃CN): δ (ppm) = 2.63 (d, ³J_{PP} = 10 Hz, 54H, N(CH₃)₂), 1.66 (dq, ²J_{PH} = 15 Hz, ³J_{HH} = 8 Hz, 2H, PCH₂CH₃), 1.12 (dt, ³J_{PH} = 20 Hz, ³J_{HH} = 8 Hz, 3H, PCH₂CH₃). ³¹P{¹H} NMR (121.5 MHz, CD₃CN): δ (ppm) = 13.2 (d, ²J_{PP} = 36 Hz, P(dma)₃), -10.1 (q, ²J_{PP} = 35 Hz, PEt). ESI(+) MS (MeCN): m/z (%) = 563.6 (10) [(dma)P₃P-H]⁺, 591.6 (100) [(dma)P₃P-Et]⁺. ESI(+) HRMS: m/z [(dma)P₃P-Et]⁺ calcd. 591.3931, found 591.3926.

Tris[tris(pyrrolidino)phosphazanyl]phosphane (**1b**) (18 mg, 23 μmol, 1.0 eq) and iodoethane (50 μL, 62 μmol, 2.7 eq) gave a [(pyrr)P₃P-Et]⁺/[(pyrr)P₃P-H]⁺-ratio of 88/12.

¹H NMR (250.1 MHz, CD₃CN): δ (ppm) = 3.17-3.11 (m, 36H, N(CH₂CH₂)₂), 1.80-1.75 (m, 36H, N(CH₂CH₂)₂), 1.62 (dq, ²J_{PH} = 16 Hz, ³J_{HH} = 8 Hz, 2H, PCH₂CH₃), 1.11 (dt, ³J_{PH} = 20 Hz, ³J_{HH} = 8 Hz, 3H, PCH₂CH₃). ³¹P{¹H} NMR (121.5 MHz, CD₃CN): δ (ppm) = -0.7 (d, ²J_{PP} = 32 Hz, P(pyrr)₃), -10.3 (q, ²J_{PP} = 33 Hz, PEt). ESI(+) MS (MeCN): m/z (%) = 797.8 (10) [(pyrr)P₃P-H]⁺, 825.7 (100) [(pyrr)P₃P-Et]⁺. ESI(+) HRMS: m/z [(pyrr)P₃P-Et]⁺ calcd. 825.5339, found 825.5354.

Tris[1-imino-2,8,9-trimethyl-2,5,8,9-tetraaza-1-phospha-bicyclo[3.3.3]undecane]phosphane (**1e**) (22 mg, 30 μmol, 1.0 eq) and iodoethane (50 μL, 62 μmol, 2.1 eq) gave a [(Me₃tren)P₃P-Et]⁺/[(Me₃tren)P₃P-H]⁺-ratio of 83/17.

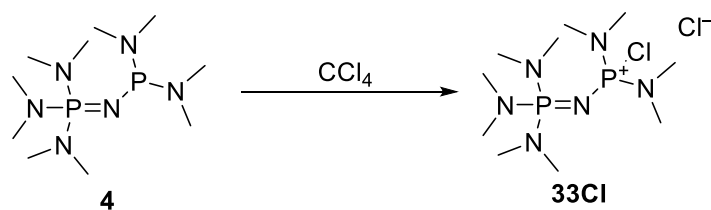
¹H NMR (250.1 MHz, CD₃CN): δ (ppm) = 2.90-2.83 (m, 18H, P(N(CH₃)CH₂CH₂)₃N), 2.75 (t, ³J_{HH} = 5 Hz, 18H, P(N(CH₃)CH₂CH₂)₃N), 2.72 (d, ³J_{PH} = 9 Hz, 27H, P(N(CH₃)CH₂CH₂)₃N), 1.60 (dq, ²J_{PH} = 16 Hz, ³J_{HH} = 8 Hz, 2H, PCH₂CH₃), 1.11 (dt, ³J_{PH} = 20 Hz, ³J_{HH} = 8 Hz, 3H, PCH₂CH₃). ³¹P{¹H} NMR (121.5 MHz, CD₃CN): δ (ppm) = 8.7 (d, ²J_{PP} = 37 Hz, P(Me₃tren)₃), -15.4 (q, ²J_{PP} = 37 Hz, PEt). ESI(+) MS (MeCN): m/z (%) = 722.7 (10) [(Me₃tren)P₃P-H]⁺, 750.7 (100) [(Me₃tren)P₃P-Et]⁺. ESI(+) HRMS: m/z [(Me₃tren)P₃P-Et]⁺ calcd. 750.4727, found 750.4735.

In situ synthesis of trichloromethylbis(pyrrolidino)phosphane (39)

Carbon tetrachloride (0.13 mL, 1.3 mmol, 1.0 eq) was dissolved in diethyl ether (20 mL) and cooled to $-78\text{ }^{\circ}\text{C}$. A mixture of trispyrrolidinophosphane (**37**) (316 mg, 1.31 mmol 1.0 eq) and bispyrrolidinophosphorus chloride (**38**) (271 mg, 1.31 mmol, 1.0 eq) in diethyl ether (10 mL) was added dropwise and stirred for 30 min at $-78\text{ }^{\circ}\text{C}$ and 30 min at room temperature. The precipitate was filtered off, extracted with diethyl ether (10 mL) and dried in high vacuum to give chlorotris(pyrrolidino)phosphonium chloride (410 mg, 1.31 mmol, 100%) as tan solid. The combined filtrate, containing **39**, was added to a solution of bispyrrolidinophosphorus chloride (**38**) (272 mg, 1.31 mmol, 1.0 eq) in 10 mL diethyl ether and stirred at room temperature overnight. Since no reaction was observed *via* ^{31}P NMR spectroscopy, chlorobenzene (20 mL) was added, the diethyl ether removed under reduced pressure and the solution stirred at $90\text{ }^{\circ}\text{C}$ overnight, which resulted in unselective reactions.

35 [$\text{C}_9\text{H}_{16}\text{Cl}_3\text{N}_2\text{P}$] ($289.57\text{ g}\cdot\text{mol}^{-1}$) $^{31}\text{P}\{^1\text{H}\}$ NMR (101.3 MHz, Et_2O): δ (ppm) = 100.2.

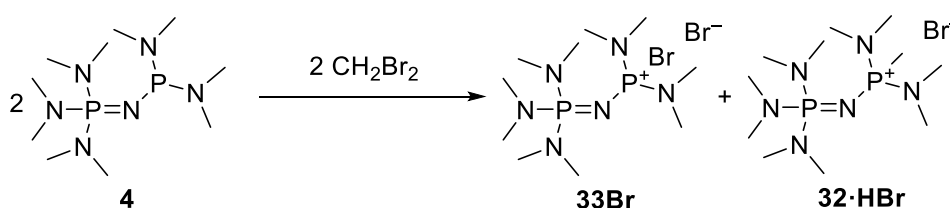
(pyrr)₃PCl₂ [$\text{C}_{12}\text{H}_{24}\text{Cl}_2\text{N}_3\text{P}$] ($312.22\text{ g}\cdot\text{mol}^{-1}$) ^1H NMR (300.1 MHz, CDCl_3): δ (ppm) = 3.52-3.46 (m, 12H, $\text{N}(\text{CH}_2\text{CH}_2)_2$), 2.10-2.06 (m, 12H, $\text{N}(\text{CH}_2\text{CH}_2)_2$). $^{31}\text{P}\{^1\text{H}\}$ NMR (101.3 MHz, CDCl_3): δ (ppm) = 36.1.

Attempted synthesis of *sym*-(dmaP₁)₂(dma)₄-CDP·2HBF₄ *via* the APPEL or SCHMIDBAUR route

[Tris(dimethylamino)phosphazeny]bis(dimethylamino)phosphane (**4**) (606 mg, 2.17 mmol 2.11 eq), dissolved in toluene (10 mL), was added dropwise at $0\text{ }^{\circ}\text{C}$ to a solution of carbon tetrachloride (100 μL , 1.03 mmol, 1.00 eq) in toluene (10 mL). The dark brown precipitate was

separated by decantation and dried *in vacuo* to give chloro[tris(dimethylamino)phosphazeny]bis(dimethylamino)phosphonium chloride (**33Cl**).

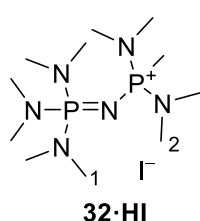
[C₁₀H₃₀Cl₂N₆P₂] (367.24 g·mol⁻¹) ¹H NMR (300.2 MHz, CDCl₃): δ (ppm) = 2.79 (d, ³J_{PH} = 14 Hz, 12H, *H2*), 2.69 (d, ³J_{PH} = 11 Hz, 18H, *H1*). ¹³C{¹H} NMR (75.5 MHz, CDCl₃): δ (ppm) = 37.3 (d, ²J_{PC} = 4 Hz, *C2*), 37.1 (d, ²J_{PC} = 5 Hz, *C1*). ³¹P{¹H} NMR (101.3 MHz, CDCl₃): δ (ppm) = 23.6 (d, ²J_{PP} = 57 Hz, *P1*), 16.9 (d, ²J_{PP} = 57 Hz, *P2*). LIFDI(+) MS (CDCl₃): m/z (%) = 331.2 (100) [M-Cl]⁺. LIFDI(+) HRMS: m/z [M-Cl]⁺ calcd. 331.16957, found 331.16859.



[Tris(dimethylamino)phosphazeny]bis(dimethylamino)phosphane (**4**) (425 mg, 1.43 mmol 1.00 eq), dissolved in toluene (10 mL), was added dropwise at -50 °C to a solution of dibromomethane (100 μL, 1.43 mmol, 1.00 eq) in toluene (10 mL). During warming to room temperature a brown oil separated, which was isolated by decantation, washed with diethyl ether (20 mL) and dried in high vacuum to give a 1:1 mixture of bromo[tris(dimethylamino)phosphazeny]bis(dimethylamino)phosphonium bromide (**33Br**) and methyl[tris(dimethylamino)phosphazeny]bis(dimethylamino)phosphonium bromide (**32·HBr**).

33Br [C₁₀H₃₀Br₂N₆P₂] (456.15 g·mol⁻¹) ¹H NMR (300.2 MHz, CDCl₃): δ (ppm) = 2.79 (d, ³J_{PH} = 15 Hz, 12H, *H2*), 2.72 (d, ³J_{PH} = 11 Hz, 18H, *H1*). ¹³C{¹H} NMR (75.5 MHz, CDCl₃): δ (ppm) = 37.9 (d, ²J_{PC} = 4 Hz, *C2*), 37.2 (d, ²J_{PC} = 4 Hz, *C1*). ³¹P{¹H} NMR (101.3 MHz, CDCl₃): δ (ppm) = 23.4 (d, ²J_{PP} = 56 Hz, *P1*), 6.9 (d, ²J_{PP} = 55 Hz, *P2*). LIFDI(+) MS (CDCl₃): m/z (%) = 311.2 (100) [32+H]⁺, 375.1 (10) [33Br]⁺ LIFDI(+) HRMS: m/z [33Br]⁺ calcd. 375.11851, found 375.06709. The analytical data for **32·HBr** are identical to those of **32·HI** given below.

Methyl[tris(dimethylamino)phosphazeny]bis(dimethylamino)phosphonium iodide (**32·HI**)

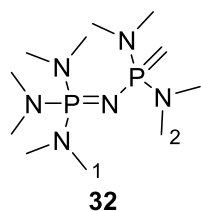


[Tris(dimethylamino)phosphazeny]bis(dimethylamino)phosphane (**4**) (382 mg, 1.29 mmol, 1.00 eq) was dissolved in THF (7 mL) and added dropwise to a solution of iodomethane (258 mg, 1.82 mmol, 1.41 eq) in THF (3 mL). The solvent was evaporated and the colourless residue washed with diethyl ether (2x 10 mL). Drying in high vacuum afforded

methyl[tris(dimethylamino)phosphazeny]bis(dimethylamino)phosphonium iodide (**32·HI**) (477 mg, 1.09 mmol, 85%) as colourless solid.

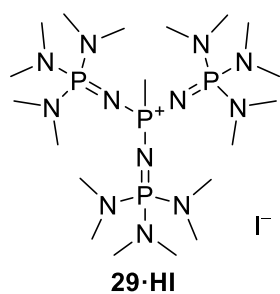
[C₁₁H₃₃IN₆P₂] (438.28 g·mol⁻¹) ¹H NMR (300.2 MHz, CDCl₃): δ (ppm) = 2.67 (d, ³J_{PH} = 10 Hz, 18H, *HI*), 2.66 (d, ³J_{PH} = 11 Hz, 12H, *H2*), 1.76 (d, ²J_{PH} = 14 Hz, 3H, *PCH*₃). ¹³C{¹H} NMR (75.5 MHz, CDCl₃): δ (ppm) = 37.3 (d, ²J_{PC} = 5 Hz, *CI*), 36.5 (d, ²J_{PC} = 5 Hz, *C2*), 13.0 (d, ¹J_{PC} = 111 Hz, *PCH*₃) ³¹P{¹H} NMR (101.3 MHz, CDCl₃): δ (ppm) = 29.3 (d, ²J_{PP} = 58 Hz, *P2*), 22.5 (d, ²J_{PP} = 58 Hz, *PI*). ESI(+) MS (MeOH): m/z (%) = 311.4 (100) [M-I]⁺. ESI(+) HRMS: m/z [M-I]⁺ calcd. 311.2236, found. 311.2234. Elemental analysis: calcd. C 30.15%, H 7.59%, N 19.18%; found C 29.63%, H 7.40%, N 18.92%. XRD: For single crystal X-ray structure determination the anion was exchanged for BPh₄⁻ by dissolving in water, adding an aqueous solution of sodium tetraphenylborate and filtration of the resulting precipitate. Suitable single crystals were obtained by dissolving in THF and layering with diethyl ether.

Methylidene[tris(dimethylamino)phosphazeny]bis(dimethylamino)phosphorane (**32**)



Methyl[tris(dimethylamino)phosphazeny]bis(dimethylamino)phosphonium iodide (406 mg, 926 μmol, 1.00 eq) and potassium bis(trimethylsilyl)amide (187 mg, 937 μmol, 1.01 eq) were stirred in THF (15 mL) for 15 min, the resulting suspension was centrifuged and the solid extracted with THF (8 mL). All volatiles of the clear solution were removed in vacuo, the residue dissolved in *n*-pentane (5 mL), and filtered over celite. The solvent was and evaporated and the resulting pale yellow oil dried in high vacuum to give methylidene[tris(dimethylamino)phosphazeny]bis(dimethylamino)phosphorane (**32**).

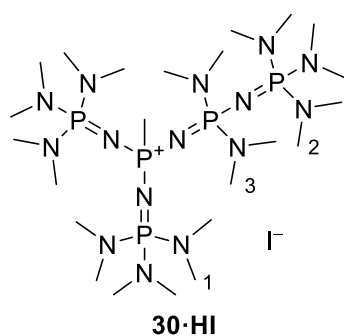
[C₁₁H₃₂N₆P₂] (310.37 g·mol⁻¹) ¹H NMR (300.2 MHz, C₆D₆): δ (ppm) = 2.81 (d, ³J_{PH} = 11 Hz, 12H, *H2*), 2.44 (d, ³J_{PH} = 10 Hz, 18H, *HI*), the methylidene signal was not observable. ¹³C{¹H} NMR (75.5 MHz, C₆D₆): δ (ppm) = 38.4 (d, ²J_{PC} = 3 Hz, *C2*), 37.3 (d, ²J_{PC} = 4 Hz, *CI*), -1.5 (d, ¹J_{PC} = 164 Hz, *PCH*₂). ³¹P{¹H} NMR (101.3 MHz, C₆D₆): δ (ppm) = 52.6 (d, ²J_{PP} = 52 Hz, *P2*), 20.1 (d, ²J_{PP} = 51 Hz, *PI*).

Methyltris[tris(dimethylamino)phosphazeny]phosphonium iodide (29·HI)

A mixture of (dma)₃P₃P·HBF₄ (**1a·HBF₄**) (505 mg, 776 μmol, 1.00 eq) and potassium bis(trimethylsilyl)amide (397 mg, 1.99 mmol, 2.56 eq) was stirred in THF (20 mL) at room temperature overnight. Precipitated potassium tetrafluoroborate was centrifuged off and iodomethane (250 μL, 4.02 mmol, 5.18 eq) was added to the clear solution. The precipitate was centrifuged off and extracted with THF (2x 20 mL). All

volatiles were removed *in vacuo*, the residue washed with diethyl ether (2x 10 mL) and dried in high vacuum to afford methyltris[tris(dimethylamino)phosphazeny]phosphonium iodide (**29·HI**) (375 mg, 532 μmol, 69%) as colourless solid.

[C₁₉H₅₇IN₁₂P₄] (704.55 g·mol⁻¹) ¹H NMR (500.2 MHz, CDCl₃): δ (ppm) = 2.64 (d, ³J_{PH} = 10 Hz, 54H, N(CH₃)₂), 1.48 (d, ²J_{PH} = 15 Hz, 3H, PCH₃). ¹³C {¹H} NMR (125.8 MHz, CDCl₃): δ (ppm) = 37.4 (d, ²J_{PC} = 4 Hz, N(CH₃)₂), 25.6 (dq, ¹J_{PC} = 127 Hz, ³J_{PC} = 2 Hz, PCH₃). ³¹P {¹H} NMR (202.5 MHz, CDCl₃): δ (ppm) = 15.8 (d, ²J_{PP} = 36 Hz, P(dma)₃), -12.5 (q, ²J_{PP} = 36 Hz, PCH₃). ³¹P NMR (202.5 MHz, CDCl₃): δ (ppm) = 15.8 (br. m, P(dma)₃), -12.5 (qq, ²J_{PP} = 36 Hz, ²J_{PH} = 15 Hz, PCH₃). ESI(+) MS (MeOH): m/z (%) = 577.6 (100) [M-I]⁺. ESI(+) HRMS: m/z [M-I]⁺ calcd. 577.3774, found 577.3771. Elemental analysis: calcd. C 32.39%, H 8.16%, N 23.86%; found C 31.52%, H 7.87%, N 23.05%. IR (neat): $\tilde{\nu}$ (cm⁻¹) = 2994 (w, CH₃), 2882 (w, CH₃), 2843 (w, CH₃), 2803 (w, CH₃), 1458 (w), 1416 (w), 1252 (s), 1177 (s), 1067 (m), 1000 (m), 974 (vs), 901 (s), 806 (m), 738 (s), 691 (m), 598 (m), 492 (s). XRD: For single crystal X-ray structure determination suitable single crystals were obtained by slow evaporation of a solution in MeCN.

Methyl[pentakis(dimethylamino)diphosphazeny]bis[tris(dimethylamino)-phosphazeny]phosphonium iodide (30·HI)

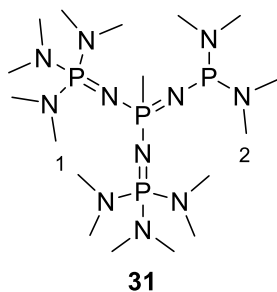
A solution of potassium bis(trimethylsilyl)amide (272 mg, 1.36 mmol, 1.02 eq) in toluene (10 mL) was added to a solution of (dma)₄P₄P·HBr (**1d·HBr**) (1.04 g, 1.34 mmol, 1.00 eq) in toluene (10 mL) and stirred for 90 min at 90 °C. The precipitate was removed by centrifugation and iodomethane (100 μL, 1.61 mmol, 1.20 eq) was added to the clear solution. The precipitate was centrifuged off and extracted with THF (2x 20 mL). All volatiles

were removed *in vacuo*, the residue washed with *n*-hexane and dried in high vacuum to afford

methyl[pentakis(dimethylamino)diphosphazeny]bis[tris(dimethylamino)phosphazeny]phosphonium iodide (**30·HI**) as colourless solid.

[C₂₃H₆₉IN₁₅P₅] (837.68 g·mol⁻¹) ¹H NMR (500.2 MHz, CDCl₃): δ (ppm) = 2.63 (d, ³J_{PH} = 10 Hz, 54H, *HI*,2), 2.57 (d, ³J_{PH} = 11 Hz, 12H, *H3*), 1.44 (d, ²J_{PH} = 15 Hz, 3H, *PCH*₃). ¹³C{¹H} NMR (125.8 MHz, CDCl₃): δ (ppm) = 37.6 (d, ²J_{PC} = 4 Hz, *C3*), 37.4 (d, ²J_{PC} = 4 Hz, *CI*), 37.3 (d, ²J_{PC} = 4 Hz, *C2*), 24.8 (d, ¹J_{PC} = 124 Hz, *PCH*₃). ³¹P{¹H} NMR (202.5 MHz, CDCl₃): δ (ppm) = 15.1 (d, ²J_{PP} = 31 Hz, *PI*), 14.1 (d, ²J_{PP} = 54 Hz, *P2*), -1.3 (dd, ²J_{PP} = 28 Hz, ²J_{PP} = 56 Hz, *P3*), -12.0 (dt, 2x ²J_{PP} = 30 Hz, *PCH*₃). ³¹P NMR (202.5 MHz, CDCl₃): δ (ppm) = 15.1 (br. m, *PI*), 14.1 (br. m, *P2*), -1.3 (br. m, *P3*), -12.0 (dtq, 2x ²J_{PP} = 30 Hz, ³J_{PH} = 15 Hz, *PCH*₃). ESI(+) MS (MeOH): m/z (%) = 710.7 (100) [M-I]⁺. ESI(+) HRMS: m/z [M-I]⁺ calcd. 710.4543, found 710.4560. XRD: For single crystal X-ray structure determination the anion was exchanged for BF₄⁻ by dissolving in water, adding an aqueous solution of sodium tetrafluoridoborate and filtration of the resulting precipitate. Suitable single crystals were obtained from methanol/water at -25 °C.

Attempted synthesis of methylidenetris[tris(dimethylamino)phosphazeny]phosphorane (**29**)



Methyltris[tris(dimethylamino)phosphazeny]phosphonium iodide (**29·HI**) (98 mg, 0.14 mmol, 1.0 eq) and sodium amide (23 mg, 0.59 mmol, 4.2 eq) was stirred in THF (2 mL) at 60 °C for two weeks. The suspension was diluted with *n*-pentane (20 mL), cleared *via* syringe filtration, and evaporated to dryness to give **31** as a pale yellow oil.

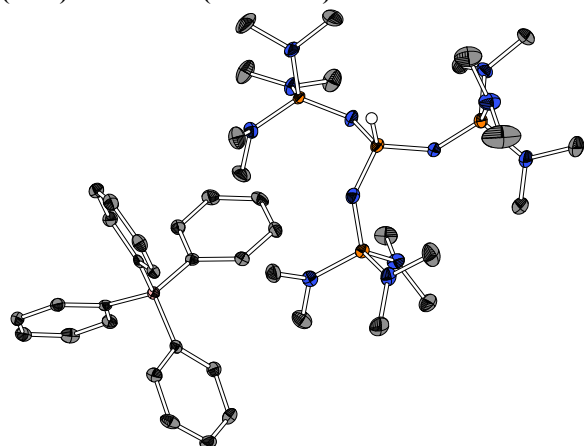
[C₁₇H₅₁N₁₁P₄] (533.57 g·mol⁻¹) ¹H NMR (500.2 MHz, C₆D₆): δ (ppm) = 3.04 (d, ³J_{PH} = 9 Hz, 12H, *HI*), 2.58 (d, ³J_{PH} = 10 Hz, 12H, *H2*), 1.82 (ddt, ²J_{PH} = 15 Hz, 2x ⁴J_{PH} = 1 Hz, 3H, *PCH*₃). ¹³C{¹H} NMR (125.8 MHz, C₆D₆): δ (ppm) = 28.5 (d, ²J_{PC} = 15 Hz, *C2*), 37.5 (dd, ²J_{PC} = 4 Hz, ⁴J_{PC} = 1 Hz, *CI*), 25.3 (ddt, ¹J_{PC} = 122 Hz, ³J_{PC} = 3 Hz, ³J_{PC} = 6 Hz, *PCH*₃). ³¹P{¹H} NMR (121.5 MHz, C₆D₆): δ (ppm) = 113.1 (d, ²J_{PP} = 129 Hz, *P2*), 13.5 (d, ²J_{PP} = 28 Hz, *PI*), -3.4 (dt, ²J_{PP} = 129 Hz, ²J_{PP} = 28 Hz, *PCH*₃). ³¹P NMR (121.5 MHz, C₆D₆): δ (ppm) = 113.1 (br. d, ²J_{PP} = 129 Hz, *P2*), 12.4-11.7 (m, *PI*), -3.4 (dtq, ²J_{PP} = 129 Hz, ²J_{PP} = 28 Hz, ²J_{PH} = 14 Hz, *PCH*₃). LIFDI(+) MS (*n*-hexane): m/z (%) = 533.2 (100) [M]⁺. LIFDI(+) HRMS: m/z [M]⁺ calcd. 533.32794, found 533.32951.

8 Kristallographischer Anhang

XRD Data were collected with a Bruker D8 Quest area detector diffractometer equipped with MoK α radiation, a graded multilayer mirror monochromator ($\lambda = 0.71073 \text{ \AA}$) and a Photon-100 CMOS detector or with a Stoe Stadivari diffractometer equipped with CuK α radiation, a graded multilayer mirror monochromator ($\lambda = 1.54178 \text{ \AA}$) and a Dectris Pilatus 300K detector both using an oil-coated shock-cooled crystal at 100(2) K. Data collection, reduction, cell refinement and semi-empirical absorption correction (multi-scan) were performed within Bruker Apex3^[189] or Stoe X-Area.^[190] Structures were solved with dual-space methods using ShelXT^[191] and refined against F² with ShelXL,^[192] all within the user interface of WinGX^[193] and ShelXLe.^[194] Carbon bonded hydrogen atoms were calculated in their idealized positions and refined with fixed isotropic thermal parameters. Hydrogen atoms connected to heteroatoms were located on the Fourier map and refined isotropically. All molecular structures were illustrated with Diamond 4^[195] using thermal ellipsoids at the 50% probability level. Peripheral protons as well as non-coordinating solvent molecules are omitted for clarity. In case of disorder only the major component is displayed. Atom colours are assigned as shown below with reference to Jmol.^[196]

H																
Li	Be											B	C	N	O	F
Na	Mg											Al	Si	P	S	Cl
K	Ca	Sc	Ti	V	Cr	Mn	Fe	Co	Ni	Cu	Zn	Ga	Ge	As	Se	Br
Rb	Sr	Y	Zr	Nb	Mo	Tc	Ru	Rh	Pd	Ag	Cd	In	Sn	Sb	Te	I
Cs	Ba		Hf	Ta	W	Re	Os	Ir	Pt	Au	Hg	Tl	Pb	Bi		

Tris[tris(dimethylamino)phosphazeny]phosphonium tetraphenylborate
(dma)₃P₃P·HBPh₄ (1a·HBPh₄)

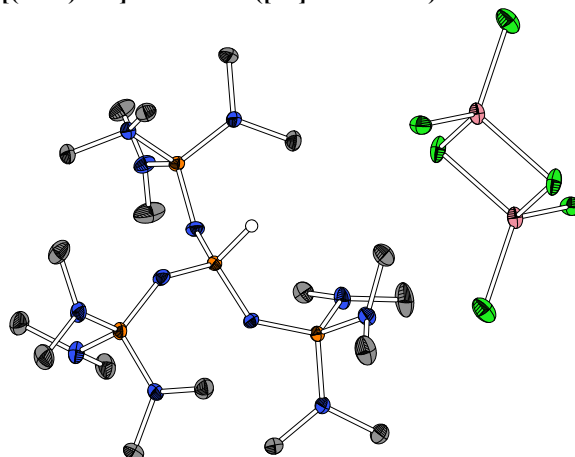


CCDC code	1892093
Crystal growth	Sebastian Ullrich
Solution and refinement	Sebastian Ullrich
Identification code	SUdmaP3P
Habitus, colour	block, clear colourless
Crystal size	0.488 x 0.311 x 0.134 mm ³
Crystal system	Monoclinic
Space group	<i>P</i> 2 ₁ / <i>n</i> <i>Z</i> = 4
Unit cell dimensions	
<i>a</i> = 13.2940(5) Å	<i>α</i> = 90°
<i>b</i> = 13.8234(6) Å	<i>β</i> = 103.5100(10)°
<i>c</i> = 27.4487(11) Å	<i>γ</i> = 90°
Volume	4904.6(3) Å ³
Cell determination	9632 peaks with <i>θ</i> 2.4 to 25.4°
Empirical formula	C ₄₂ H ₇₃ BN ₁₂ P ₄
Formula weight	882.83
Density (calculated)	1.196 g·cm ⁻³
Absorption coefficient	0.197 mm ⁻¹
F(000)	1904
Diffractometer type	Bruker D8 Quest
Wavelength	0.71073 Å
Temperature	100(2) K
Theta range for data collection	2.157 to 25.419°
Index ranges	
	-16 ≤ <i>h</i> ≤ 16, -16 ≤ <i>k</i> ≤ 16, -33 ≤ <i>l</i> ≤ 33
Reflections collected	104292
Independent reflections	9033 [<i>R</i> (int) = 0.0266]
Completeness to <i>θ</i> = 25.000°	99.9%
Observed reflections	8248 [<i>I</i> > 2σ(<i>I</i>)]
Reflections used for refinement	9033
Absorption correction	Semi-empirical from equivalents
Max. and min. transmission	0.7452 and 0.7217
Largest diff. peak and hole	1.031 and -0.511 e·Å ⁻³
Solution	dual/difmap
Refinement	Full-matrix least-squares on <i>F</i> ²
Treatment of hydrogen atoms	mixed/hetero
Data / restraints / parameters	9033 / 0 / 554
Goodness-of-fit on <i>F</i> ²	1.021
<i>R</i> index (all data)	<i>R</i> ₁ = 0.0392 <i>wR</i> ₂ = 0.0966
<i>R</i> index conventional [<i>I</i> > 2σ(<i>I</i>)]	<i>R</i> ₁ = 0.0354 <i>wR</i> ₂ = 0.0933

Refinement special details

One reflection was omitted from the least-squares refinement using OMIT. High residual density of 1.031 e·Å⁻³ is close to P1 and rooted in a slight, non-addressable disorder.

Tris[tris(dimethylamino)phosphazeny]phosphonium hexachloridodicobaltat
[(dma)₃P₃P]₂·H₂Co₂Cl₆ ([1a]₂·H₂Co₂Cl₆)

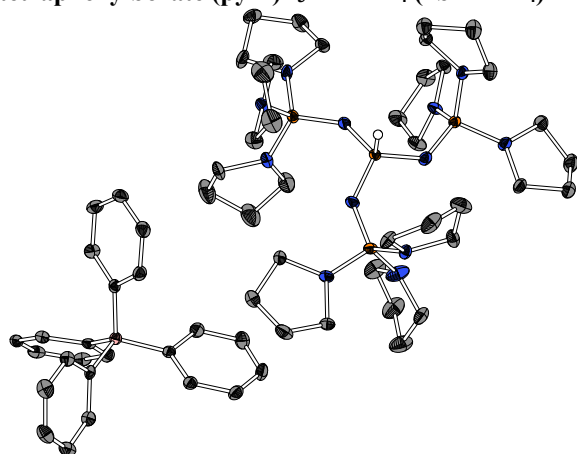


CCDC code	1903850
Crystal growth	Sebastian Ullrich
Solution and refinement	Sebastian Ullrich
Identification code	SU060Co
Habitus, colour	block, clear blue
Crystal size	0.514 x 0.254 x 0.220 mm ³
Crystal system	Triclinic
Space group	<i>P</i> $\bar{1}$ <i>Z</i> = 2
Unit cell dimensions	
<i>a</i> = 11.3907(5) Å	<i>α</i> = 98.7615(18)°
<i>b</i> = 11.6029(5) Å	<i>β</i> = 106.7020(17)°
<i>c</i> = 14.3399(6) Å	<i>γ</i> = 98.9224(16)°
Volume	1754.06(13) Å ³
Cell determination	9943 peaks with <i>θ</i> 2.6 to 27.1°
Empirical formula	C ₁₈ H ₅₅ Cl ₃ CoN ₁₂ P ₄
Formula weight	728.90
Density (calculated)	1.380 g·cm ⁻³
Absorption coefficient	0.930 mm ⁻¹
F(000)	770
Diffractometer type	Bruker D8 Quest
Wavelength	0.71073 Å
Temperature	100(2) K
Theta range for data collection	2.343 to 27.161°
Index ranges	
	-14 ≤ <i>h</i> ≤ 14, -14 ≤ <i>k</i> ≤ 14, -18 ≤ <i>l</i> ≤ 18
Reflections collected	19874
Independent reflections	7497 [<i>R</i> (int) = 0.0291]
Completeness to <i>θ</i> = 25.000°	97.9%
Observed reflections	5997 [<i>I</i> > 2σ(<i>I</i>)]
Reflections used for refinement	7497
Absorption correction	Semi-empirical from equivalents
Max. and min. transmission	0.7455 and 0.6731
Largest diff. peak and hole	0.671 and -0.354 e·Å ⁻³
Solution	dual/difmap
Refinement	Full-matrix least-squares on <i>F</i> ²
Treatment of hydrogen atoms	mixed/mixed
Data / restraints / parameters	7497 / 0 / 364
Goodness-of-fit on <i>F</i> ²	1.040
<i>R</i> index (all data)	<i>R</i> ₁ = 0.0552 <i>wR</i> ₂ = 0.0801
<i>R</i> index conventional [<i>I</i> > 2σ(<i>I</i>)]	<i>R</i> ₁ = 0.0346 <i>wR</i> ₂ = 0.0727

Refinement special details

The asymmetric unit contains a half anion fragment completed by inversion. The phosphorus bonded proton was refined with isotropic temperature factors at 1.5 times that of the carrier atom.

Tris[tris(pyrrolidino)phosphazeny]phosphonium tetraphenylborate (pyrr) $P_3P \cdot HBPh_4$ (1b \cdot HBPh $_4$)

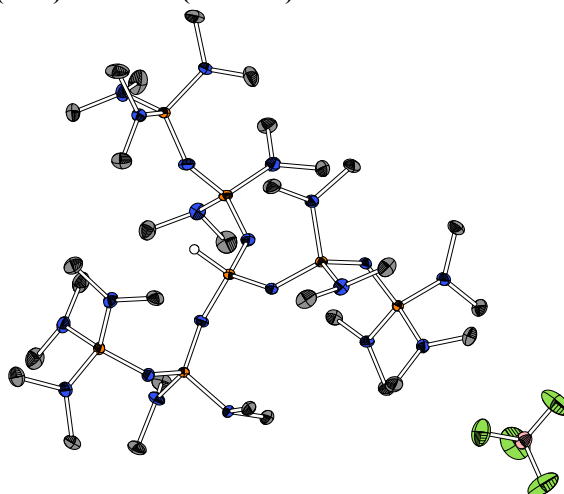


CCDC code	1898095
Crystal growth	Sebastian Ullrich
Solution and refinement	Sebastian Ullrich
Identification code	SU009BPh4
Habitus, colour	block, clear colourless
Crystal size	0.376 x 0.205 x 0.136 mm ³
Crystal system	Triclinic
Space group	<i>P</i> 1 <i>Z</i> = 2
Unit cell dimensions	
<i>a</i> = 13.4229(6) Å	<i>a</i> = 87.977(2)°
<i>b</i> = 13.9112(7) Å	<i>b</i> = 73.297(2)°
<i>c</i> = 16.8452(7) Å	<i>c</i> = 87.239(2)°
Volume	3008.5(2) Å ³
Cell determination	9852 peaks with θ 2.2 to 27.1°
Empirical formula	C ₆₀ H ₉₃ BN ₁₂ P ₄
Formula weight	1117.15
Density (calculated)	1.233 g·cm ⁻³
Absorption coefficient	0.175 mm ⁻¹
F(000)	1204
Diffractometer type	Bruker D8 Quest
Wavelength	0.71073 Å
Temperature	100(2) K
Theta range for data collection	2.116 to 27.177°
Index ranges	
-17 ≤ <i>h</i> ≤ 17, -17 ≤ <i>k</i> ≤ 17, -19 ≤ <i>l</i> ≤ 21	
Reflections collected	128088
Independent reflections	13373 [<i>R</i> (int) = 0.0952]
Completeness to theta = 25.000°	99.9%
Observed reflections	10277 [<i>I</i> > 2σ(<i>I</i>)]
Reflections used for refinement	13373
Absorption correction	Semi-empirical from equivalents
Max. and min. transmission	0.7455 and 0.7214
Largest diff. peak and hole	0.276 and -0.393 e·Å ⁻³
Solution	dual/difmap
Refinement	Full-matrix least-squares on F ²
Treatment of hydrogen atoms	mixed/mixed
Data / restraints / parameters	13373 / 150 / 785
Goodness-of-fit on F ²	1.017
<i>R</i> index (all data)	<i>R</i> ₁ = 0.0616 <i>wR</i> ₂ = 0.1005
<i>R</i> index conventional [<i>I</i> > 2σ(<i>I</i>)]	<i>R</i> ₁ = 0.0401 <i>wR</i> ₂ = 0.0926

Refinement special details

Four pyrrolidin rings were refined in 2-component disorder using SAME and RIGU restraints. The phosphorus bonded proton was refined with isotropic temperature factors at 1.5 times that of the carrier atom.

Tris[pentakis(dimethylamino)diphosphazeny]-phosphonium tetrafluoridoborate (dma) $P_6P \cdot HBF_4$ (1c \cdot HBF $_4$)

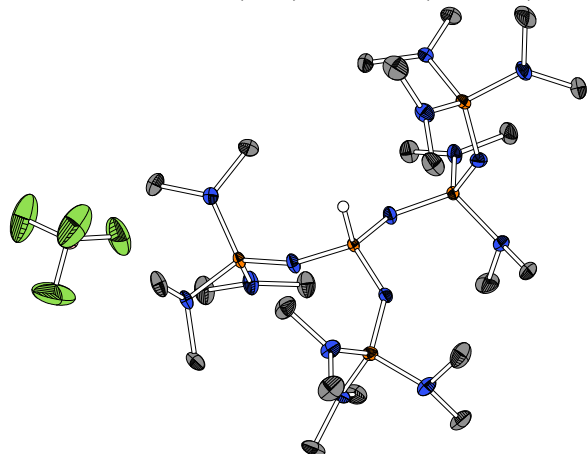


CCDC code	1898100
Crystal growth	Sebastian Ullrich
Solution and refinement	Sebastian Ullrich
Identification code	SU013hmds
Habitus, colour	needle, clear colourless
Crystal size	0.479 x 0.132 x 0.080 mm ³
Crystal system	Triclinic
Space group	<i>P</i> 1 <i>Z</i> = 2
Unit cell dimensions	
<i>a</i> = 9.9662(6) Å	<i>a</i> = 95.439(2)°
<i>b</i> = 14.2411(8) Å	<i>b</i> = 98.325(2)°
<i>c</i> = 19.4485(11) Å	<i>c</i> = 95.562(2)°
Volume	2701.7(3) Å ³
Cell determination	9618 peaks with θ 2.4 to 27.1°
Empirical formula	C ₃₀ H ₉₁ BF ₄ N ₂₁ P ₇
Formula weight	1049.83
Density (calculated)	1.291 g·cm ⁻³
Absorption coefficient	0.288 mm ⁻¹
F(000)	1128
Diffractometer type	Bruker D8 Quest
Wavelength	0.71073 Å
Temperature	100(2) K
Theta range for data collection	2.183 to 27.198°
Index ranges	
-12 ≤ <i>h</i> ≤ 12, -18 ≤ <i>k</i> ≤ 18, -25 ≤ <i>l</i> ≤ 24	
Reflections collected	89005
Independent reflections	11983 [<i>R</i> (int) = 0.0677]
Completeness to theta = 25.000°	99.9%
Observed reflections	9473 [<i>I</i> > 2σ(<i>I</i>)]
Reflections used for refinement	11983
Absorption correction	Semi-empirical from equivalents
Max. and min. transmission	0.7455 and 0.6811
Largest diff. peak and hole	0.443 and -0.376 e·Å ⁻³
Solution	dual/difmap
Refinement	Full-matrix least-squares on F ²
Treatment of hydrogen atoms	mixed/mixed
Data / restraints / parameters	11983 / 125 / 677
Goodness-of-fit on F ²	1.035
<i>R</i> index (all data)	<i>R</i> ₁ = 0.0609 <i>wR</i> ₂ = 0.0895
<i>R</i> index conventional [<i>I</i> > 2σ(<i>I</i>)]	<i>R</i> ₁ = 0.0405 <i>wR</i> ₂ = 0.0828

Refinement special details

One dimethylamino group was refined in 2-component disorder using RIGU and SAME restraints. The BF₄ anion was refined in 2-component disorder using RIGU, SAME and ISOR restraints. The phosphorus bonded proton was refined with isotropic temperature factors at 1.5 times that of the carrier atom.

[Pentakis(dimethylamino)diphosphazeny]bis-[tris(dimethylamino)phosphazeny]phosphonium tetrafluoridoborate (dma)P₄P·HBF₄ (1d·HBF₄)

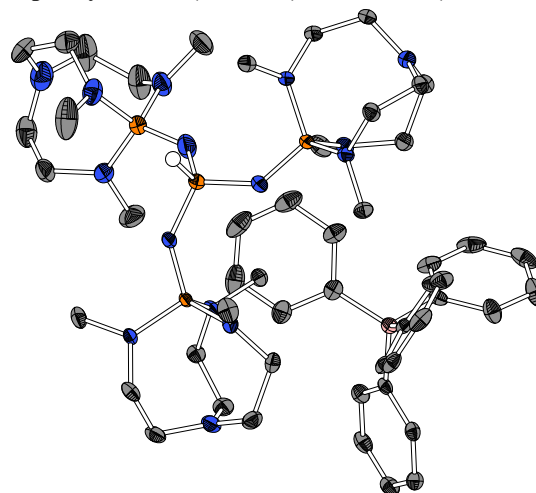


CCDC code	1898099
Crystal growth	Sebastian Ullrich
Solution and refinement	Sebastian Ullrich
Identification code	SU021BF4
Habitus, colour	plate, clear colourless
Crystal size	0.428 x 0.198 x 0.084 mm ³
Crystal system	Monoclinic
Space group	<i>P</i> 2 ₁ / <i>c</i> <i>Z</i> = 4
Unit cell dimensions	
<i>a</i> = 14.2537(6) Å	<i>α</i> = 90°
<i>b</i> = 8.3923(4) Å	<i>β</i> = 93.8430(10)°
<i>c</i> = 33.7165(15) Å	<i>γ</i> = 90°
Volume	4024.1(3) Å ³
Cell determination	9714 peaks with <i>θ</i> 2.5 to 27.1°
Empirical formula	C ₂₂ H ₆₇ BF ₄ N ₁₅ P ₅
Formula weight	783.56
Density (calculated)	1.293 g·cm ⁻³
Absorption coefficient	0.283 mm ⁻¹
F(000)	1680
Diffractometer type	Bruker D8 Quest
Wavelength	0.71073 Å
Temperature	100(2) K
Theta range for data collection	2.422 to 27.156°
Index ranges	
	-18 ≤ <i>h</i> ≤ 18, -10 ≤ <i>k</i> ≤ 10, -43 ≤ <i>l</i> ≤ 43
Reflections collected	101405
Independent reflections	8911 [<i>R</i> (int) = 0.0339]
Completeness to <i>θ</i> = 25.000°	99.9%
Observed reflections	7943 [<i>I</i> > 2σ(<i>I</i>)]
Reflections used for refinement	8911
Absorption correction	Semi-empirical from equivalents
Max. and min. transmission	0.7455 and 0.7076
Largest diff. peak and hole	0.412 and -0.382 e·Å ⁻³
Solution	dual/difmap
Refinement	Full-matrix least-squares on F ²
Treatment of hydrogen atoms	mixed/hetero
Data / restraints / parameters	8911 / 91 / 493
Goodness-of-fit on F ²	1.081
<i>R</i> index (all data)	<i>R</i> ₁ = 0.0380 <i>wR</i> ₂ = 0.0821
<i>R</i> index conventional [<i>I</i> > 2σ(<i>I</i>)]	<i>R</i> ₁ = 0.0322 <i>wR</i> ₂ = 0.0791

Refinement special details

The BF₄ anion was refined in 3-component disorder using ISOR and RIGU restraints as variable metric rigid group. One reflection was omitted from the least-squares refinement using OMIT.

Tris[1-imino-2,8,9-trimethyl-2,5,8,9-tetraaza-1-phospha-bicyclo[3.3.3]undecane]phosphonium tetraphenylborate (Me₃tren)P₃P·HBPh₄ (1e·HBPh₄)

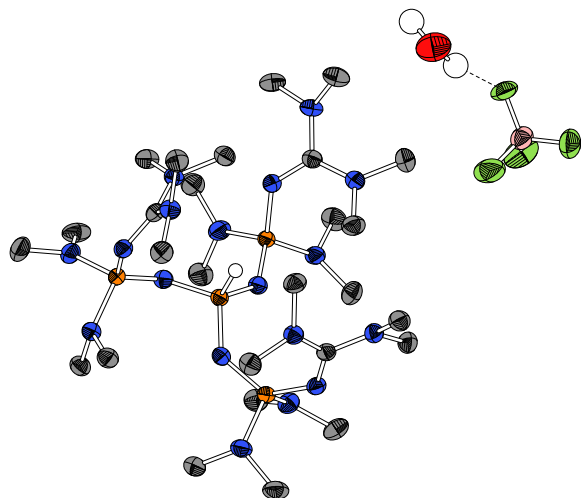


Crystal growth	Sebastian Ullrich
Solution and refinement	Sebastian Ullrich
Identification code	SU033
Habitus, colour	needle, clear colourless
Crystal size	0.476 x 0.157 x 0.056 mm ³
Crystal system	Triclinic
Space group	<i>P</i> <i>1</i> <i>Z</i> = 2
Unit cell dimensions	
<i>a</i> = 13.3016(6) Å	<i>α</i> = 106.9098(16)°
<i>b</i> = 14.4956(7) Å	<i>β</i> = 95.8703(16)°
<i>c</i> = 14.7347(7) Å	<i>γ</i> = 90.8842(15)°
Volume	2700.9(2) Å ³
Cell determination	9774 peaks with <i>θ</i> 2.4 to 27.2°
Empirical formula	C ₅₁ H ₈₄ BN ₁₅ P ₄
Formula weight	1042.02
Density (calculated)	1.281 g·cm ⁻³
Absorption coefficient	0.191 mm ⁻¹
F(000)	1120
Diffractometer type	Bruker D8 Quest
Wavelength	0.71073 Å
Temperature	100(2) K
Theta range for data collection	2.180 to 27.168°
Index ranges	
	-17 ≤ <i>h</i> ≤ 17, -18 ≤ <i>k</i> ≤ 18, -18 ≤ <i>l</i> ≤ 18
Reflections collected	55059
Independent reflections	11958 [<i>R</i> (int) = 0.0473]
Completeness to <i>θ</i> = 25.000°	99.9%
Observed reflections	9149 [<i>I</i> > 2σ(<i>I</i>)]
Reflections used for refinement	11958
Absorption correction	Semi-empirical from equivalents
Max. and min. transmission	0.7455 and 0.7088
Largest diff. peak and hole	1.417 and -0.831 e·Å ⁻³
Solution	dual/difmap
Refinement	Full-matrix least-squares on F ²
Treatment of hydrogen atoms	mixed/hetero
Data / restraints / parameters	11958 / 0 / 653
Goodness-of-fit on F ²	1.050
<i>R</i> index (all data)	<i>R</i> ₁ = 0.0859 <i>wR</i> ₂ = 0.1563
<i>R</i> index conventional [<i>I</i> > 2σ(<i>I</i>)]	<i>R</i> ₁ = 0.0613 <i>wR</i> ₂ = 0.1442

Refinement special details

High residual density of 1.417 e·Å⁻³ is close to P1 and rooted in a slight, non-addressable disorder.

**Tris[bis(dimethylamino)tetramethylguanidino]-
phosphazeny]phosphonium tetrafluoroborate
hydrate (tmg)(dma)₂P₃P·HBF₄·H₂O (1g·HBF₄·H₂O)**

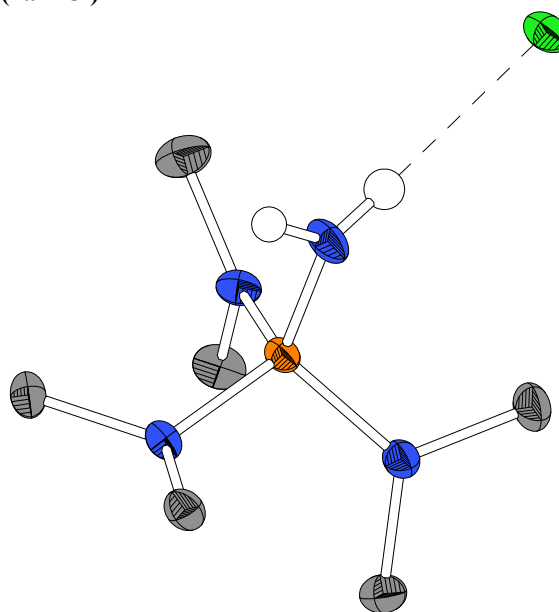


Crystal growth	Sebastian Ullrich
Solution and refinement	Sebastian Ullrich
Identification code	SU079
Habitus, colour	plate, colourless
Crystal size	0.252 x 0.153 x 0.041 mm ³
Crystal system	Monoclinic
Space group	<i>P</i> 2 ₁ / <i>c</i> <i>Z</i> = 4
Unit cell dimensions	
<i>a</i> = 20.3271(3) Å	<i>α</i> = 90°
<i>b</i> = 11.0531(2) Å	<i>β</i> = 90.8290(10)°
<i>c</i> = 20.2773(3) Å	<i>γ</i> = 90°
Volume	4555.38(13) Å ³
Cell determination	35017 peaks with <i>θ</i> 4.3 to 75.9°
Empirical formula	C ₂₇ H ₇₅ BF ₄ N ₁₈ OP ₄
Formula weight	878.74
Density (calculated)	1.281 g·cm ⁻³
Absorption coefficient	0.228 mm ⁻¹
F(000)	1888
Diffractometer type	Stoe Stadivari
Wavelength	0.71073 Å
Temperature	100(2) K
Theta range for data collection	2.004 to 26.546°
Index ranges	
-25 ≤ <i>h</i> ≤ 23, -11 ≤ <i>k</i> ≤ 13, -23 ≤ <i>l</i> ≤ 25	
Reflections collected	47099
Independent reflections	9371 [<i>R</i> (int) = 0.0454]
Completeness to theta = 26.546°	98.9%
Observed reflections	7097 [<i>I</i> > 2σ(<i>I</i>)]
Reflections used for refinement	9371
Extinction coefficient	<i>X</i> = 0.0024(4)
Absorption correction	Semi-empirical from equivalents
Max. and min. transmission	1.0000 and 0.5052
Largest diff. peak and hole	0.642 and -0.597 e·Å ⁻³
Solution	dual/difmap
Refinement	Full-matrix least-squares on F ²
Treatment of hydrogen atoms	mixed/mixed
Data / restraints / parameters	9371 / 82 / 568
Goodness-of-fit on F ²	1.001
<i>R</i> index (all data)	<i>R</i> ₁ = 0.0573 <i>wR</i> ₂ = 0.1288
<i>R</i> index conventional [<i>I</i> > 2σ(<i>I</i>)]	<i>R</i> ₁ = 0.0451 <i>wR</i> ₂ = 0.1246

Refinement special details

The BF₄ anion was refined in 2-component disorder using SADI and RIGU restraints. The O-H-bond length were restrained to 0.95(1) Å using DFIX with the protons isotropic temperature factors refined at 1.5 times that of the carrier atom.

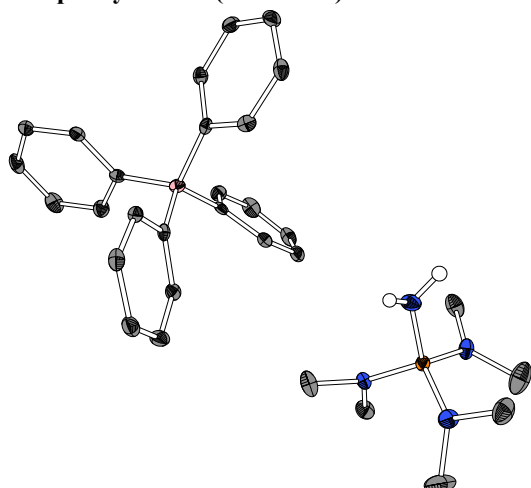
**Aminotris(dimethylamino)phosphonium chloride
(2a·HCl)**



CCDC code	1903847
Crystal growth	Björn Koch
Solution and refinement	Sebastian Ullrich
Identification code	BK12
Habitus, colour	block, colourless
Crystal size	0.176 x 0.162 x 0.139 mm ³
Crystal system	Monoclinic
Space group	<i>P</i> 2 ₁ / <i>n</i> <i>Z</i> = 4
Unit cell dimensions	
<i>a</i> = 9.3721(3) Å	<i>α</i> = 90°
<i>b</i> = 9.9456(3) Å	<i>β</i> = 100.494(3)°
<i>c</i> = 12.2423(4) Å	<i>γ</i> = 90°
Volume	1122.03(6) Å ³
Cell determination	14985 peaks with <i>θ</i> 5.5 to 76.5°
Empirical formula	C ₆ H ₂₀ ClN ₄ P
Formula weight	214.68
Density (calculated)	1.271 g·cm ⁻³
Absorption coefficient	4.051 mm ⁻¹
F(000)	464
Diffractometer type	Stoe Stadivari
Wavelength	1.54178 Å
Temperature	100(2) K
Theta range for data collection	5.488 to 75.676°
Index ranges	
-11 ≤ <i>h</i> ≤ 10, -12 ≤ <i>k</i> ≤ 8, -15 ≤ <i>l</i> ≤ 15	
Reflections collected	17221
Independent reflections	2330 [<i>R</i> (int) = 0.0559]
Completeness to theta = 70.000°	99.9%
Observed reflections	1928 [<i>I</i> > 2σ(<i>I</i>)]
Reflections used for refinement	2330
Absorption correction	Semi-empirical from equivalents
Max. and min. transmission	1.0000 and 0.3915
Largest diff. peak and hole	0.536 and -0.436 e·Å ⁻³
Solution	dual/difmap
Refinement	Full-matrix least-squares on F ²
Treatment of hydrogen atoms	mixed/mixed
Data / restraints / parameters	2330 / 2 / 123
Goodness-of-fit on F ²	1.029
<i>R</i> index (all data)	<i>R</i> ₁ = 0.0474 <i>wR</i> ₂ = 0.1151
<i>R</i> index conventional [<i>I</i> > 2σ(<i>I</i>)]	<i>R</i> ₁ = 0.0399 <i>wR</i> ₂ = 0.1127

Refinement special details

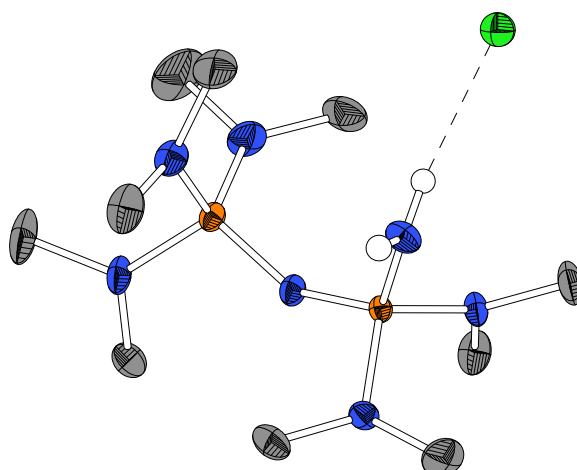
The N-H-bond length were restrained to 0.86(2) Å using DFIX. One reflection was omitted from the least-squares refinement using OMIT.

Aminotris(dimethylamino)phosphonium tetraphenylborate (2a-HBPh₄)

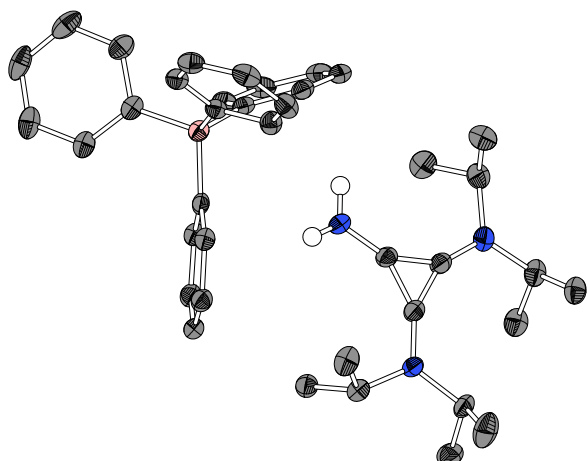
CCDC code	1903849
Crystal growth	Sebastian Ullrich
Solution and refinement	Sebastian Ullrich
Identification code	SU019BPh4
Habitus, colour	needle, clear colourless
Crystal size	0.629 x 0.131 x 0.102 mm ³
Crystal system	Orthorhombic
Space group	<i>Fdd2</i> <i>Z</i> = 16
Unit cell dimensions	
<i>a</i> = 31.9531(15) Å	<i>a</i> = 90°
<i>b</i> = 33.9460(14) Å	<i>b</i> = 90°
<i>c</i> = 10.2730(5) Å	<i>c</i> = 90°
Volume	11142.9(9) Å ³
Cell determination	9396 peaks with θ 2.5 to 27.1°
Empirical formula	C ₃₀ H ₄₀ BN ₄ P
Formula weight	498.44
Density (calculated)	1.189 g·cm ⁻³
Absorption coefficient	0.124 mm ⁻¹
F(000)	4288
Diffractometer type	Bruker D8 Quest
Wavelength	0.71073 Å
Temperature	100(2) K
Theta range for data collection	2.167 to 27.131°
Index ranges	
	-40 ≤ <i>h</i> ≤ 40, -43 ≤ <i>k</i> ≤ 36, -11 ≤ <i>l</i> ≤ 13
Reflections collected	21469
Independent reflections	5547 [<i>R</i> (int) = 0.0486]
Completeness to theta = 25.000°	100.0%
Observed reflections	4877 [<i>I</i> > 2σ(<i>I</i>)]
Reflections used for refinement	5547
Absorption correction	Semi-empirical from equivalents
Max. and min. transmission	0.7455 and 0.7000
Flack parameter (absolute struct.)	0.05(5)
Largest diff. peak and hole	0.241 and -0.337 e·Å ⁻³
Solution	dual/difmap
Refinement	Full-matrix least-squares on F ²
Treatment of hydrogen atoms	mixed/hetero
Data / restraints / parameters	5547 / 1 / 339
Goodness-of-fit on F ²	1.068
<i>R</i> index (all data)	<i>R</i> ₁ = 0.0556 <i>wR</i> ₂ = 0.0865
<i>R</i> index conventional [<i>I</i> > 2σ(<i>I</i>)]	<i>R</i> ₁ = 0.0426 <i>wR</i> ₂ = 0.0821

Refinement special details

No Flack check done due to low Friedel pair coverage (78%).

Amino[tris(dimethylamino)phosphazeny]bis(dimethylamino)phosphonium chloride (2c-HCl)

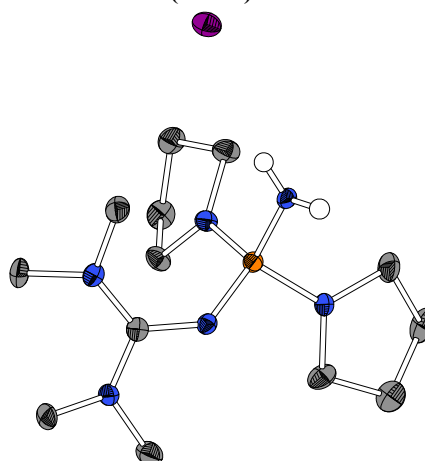
CCDC code	1903848
Crystal growth	Sebastian Ullrich
Solution and refinement	Sebastian Ullrich
Identification code	SU013Cl
Habitus, colour	block, clear colourless
Crystal size	0.410 x 0.323 x 0.146 mm ³
Crystal system	Monoclinic
Space group	<i>P2₁/n</i> <i>Z</i> = 4
Unit cell dimensions	
<i>a</i> = 10.8631(6) Å	<i>a</i> = 90°
<i>b</i> = 13.6470(7) Å	<i>b</i> = 105.069(2)°
<i>c</i> = 13.2356(7) Å	<i>c</i> = 90°
Volume	1894.69(18) Å ³
Cell determination	9849 peaks with θ 2.2 to 27.2°
Empirical formula	C ₁₀ H ₃₂ ClN ₇ P ₂
Formula weight	347.82
Density (calculated)	1.219 g·cm ⁻³
Absorption coefficient	0.374 mm ⁻¹
F(000)	752
Diffractometer type	Bruker D8 Quest
Wavelength	0.71073 Å
Temperature	100(2) K
Theta range for data collection	2.168 to 27.172°
Index ranges	
	-13 ≤ <i>h</i> ≤ 13, -17 ≤ <i>k</i> ≤ 17, -16 ≤ <i>l</i> ≤ 16
Reflections collected	54878
Independent reflections	4200 [<i>R</i> (int) = 0.0376]
Completeness to theta = 25.000°	100.0%
Observed reflections	3706 [<i>I</i> > 2σ(<i>I</i>)]
Reflections used for refinement	4200
Absorption correction	Semi-empirical from equivalents
Max. and min. transmission	0.7455 and 0.7074
Largest diff. peak and hole	0.281 and -0.337 e·Å ⁻³
Solution	dual/difmap
Refinement	Full-matrix least-squares on F ²
Treatment of hydrogen atoms	mixed/hetero
Data / restraints / parameters	4200 / 0 / 199
Goodness-of-fit on F ²	1.063
<i>R</i> index (all data)	<i>R</i> ₁ = 0.0367 <i>wR</i> ₂ = 0.0745
<i>R</i> index conventional [<i>I</i> > 2σ(<i>I</i>)]	<i>R</i> ₁ = 0.0297 <i>wR</i> ₂ = 0.0716

1-Amino(bis-2,3-(di-*iso*-propylamino)cyclopropenium tetraphenylborate (2e·HBPh₄)


Crystal growth	Andres Gonzales
Solution and refinement	Sebastian Ullrich
Identification code	AG0500
Habitus, colour	prism, colourless
Crystal size	0.259 x 0.196 x 0.100 mm ³
Crystal system	Triclinic
Space group	$P\bar{1}$ $Z = 2$
Unit cell dimensions	
$a = 11.3100(2)$ Å	$\alpha = 68.5820(10)^\circ$
$b = 12.6300(2)$ Å	$\beta = 74.8570(10)^\circ$
$c = 12.9852(2)$ Å	$\gamma = 77.2480(10)^\circ$
Volume	1650.53(5) Å ³
Cell determination	26559 peaks with θ 3.7 to 70.1°
Empirical formula	C ₃₉ H ₅₀ BN ₃
Formula weight	571.63
Density (calculated)	1.150 g·cm ⁻³
Absorption coefficient	0.497 mm ⁻¹
F(000)	620
Diffractometer type	Stoe Stadivari
Wavelength	1.54178 Å
Temperature	100(2) K
Theta range for data collection	3.731 to 69.824°
Index ranges	
	$-13 \leq h \leq 13, -15 \leq k \leq 8, -15 \leq l \leq 10$
Reflections collected	29644
Independent reflections	6106 [$R(\text{int}) = 0.0229$]
Completeness to theta = 69.824°	97.9%
Observed reflections	5199 [$I > 2\sigma(I)$]
Reflections used for refinement	6106
Absorption correction	Semi-empirical from equivalents
Max. and min. transmission	1.0000 and 0.5982
Largest diff. peak and hole	0.360 and -0.291 e·Å ⁻³
Solution	dual/difmap
Refinement	Full-matrix least-squares on F ²
Treatment of hydrogen atoms	mixed/mixed
Data / restraints / parameters	6106 / 15 / 402
Goodness-of-fit on F ²	1.077
R index (all data)	$R_1 = 0.0486$ $wR_2 = 0.1107$
R index conventional [$I > 2\sigma(I)$]	$R_1 = 0.0414$ $wR_2 = 0.1067$

Refinement special details

The nitrogen bonded protons were refined with isotropic temperature factors at 1.5 times that of the carrier atom. One di-*iso*-propylamino group was restrained with SIMU and RIGU.

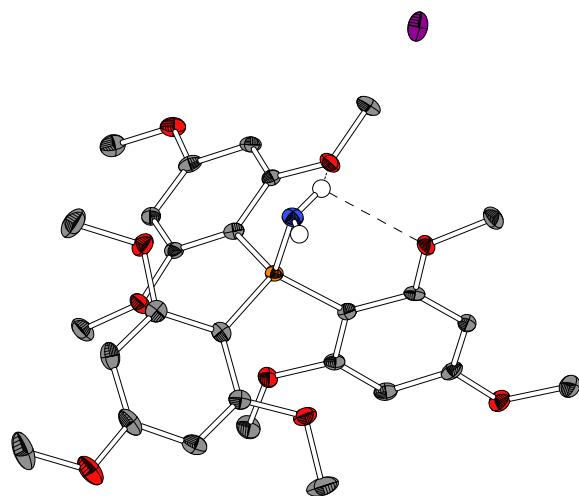
Aminobis(dimethylamino)(tetramethylguanidino)-phosphonium iodide (2h·HI)


Crystal growth	Sebastian Ullrich
Solution and refinement	Sebastian Ullrich
Identification code	SU066
Habitus, colour	prism, colourless
Crystal size	0.150 x 0.115 x 0.073 mm ³
Crystal system	Monoclinic
Space group	$C2/c$ $Z = 4$
Unit cell dimensions	
$a = 15.7993(6)$ Å	$\alpha = 90^\circ$
$b = 12.0039(4)$ Å	$\beta = 91.275(3)^\circ$
$c = 19.8350(9)$ Å	$\gamma = 90^\circ$
Volume	3760.8(3) Å ³
Cell determination	15409 peaks with θ 2.6 to 33.4°
Empirical formula	C ₂₆ H ₆₂ N ₁₂ OP ₂
Formula weight	874.61
Density (calculated)	1.545 g·cm ⁻³
Absorption coefficient	14.243 mm ⁻¹
F(000)	1784
Diffractometer type	Stoe Stadivari
Wavelength	1.54178 Å
Temperature	100(2) K
Theta range for data collection	5.602 to 89.590°
Index ranges	
	$-20 \leq h \leq 20, -15 \leq k \leq 15, -25 \leq l \leq 25$
Reflections collected	20221
Independent reflections	4289 [$R(\text{int}) = 0.0582$]
Completeness to theta = 70.000°	99.8%
Observed reflections	3378 [$I > 2\sigma(I)$]
Reflections used for refinement	4289
Absorption correction	Semi-empirical from equivalents
Max. and min. transmission	1.0000 and 0.2738
Largest diff. peak and hole	1.054 and -0.543 e·Å ⁻³
Solution	dual/difmap
Refinement	Full-matrix least-squares on F ²
Treatment of hydrogen atoms	mixed/hetero
Data / restraints / parameters	4289 / 0 / 230
Goodness-of-fit on F ²	0.997
R index (all data)	$R_1 = 0.0522$ $wR_2 = 0.0367$
R index conventional [$I > 2\sigma(I)$]	$R_1 = 0.0956$ $wR_2 = 0.0879$

Refinement special details

The asymmetric unit contains a half water molecule completed by a twofold axis. One pyrrolidine ring was refined in 2-component disorder.

Amino[tris(trimethoxyphenyl)phosphonium] iodide (2i-HI)

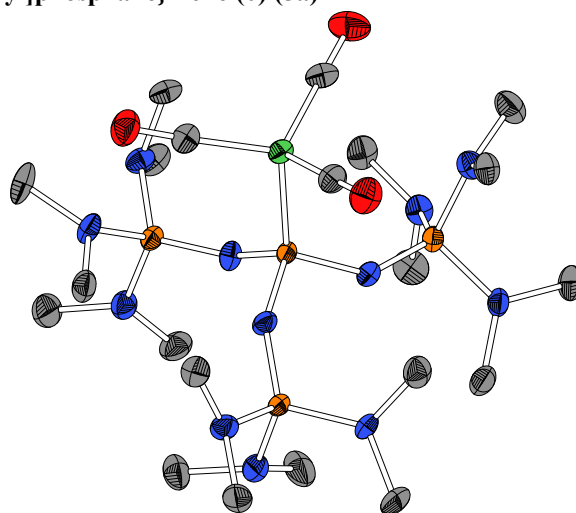


Crystal growth	Sebastian Ullrich
Solution and refinement	Sebastian Ullrich
Identification code	SU051
Habitus, colour	block, clear colourless
Crystal size	0.283 x 0.213 x 0.169 mm ³
Crystal system	Orthorhombic
Space group	<i>Pbca</i> $Z = 8$
Unit cell dimensions	
$a = 14.4603(6)$ Å	$\alpha = 90^\circ$
$b = 12.8073(5)$ Å	$\beta = 90^\circ$
$c = 34.0422(14)$ Å	$\gamma = 90^\circ$
Volume	6304.5(4) Å ³
Cell determination	9269 peaks with θ 2.2 to 25.4°
Empirical formula	C ₃₀ H ₃₈ INO ₉ P
Formula weight	714.48
Density (calculated)	1.505 g·cm ⁻³
Absorption coefficient	1.119 mm ⁻¹
F(000)	2920
Diffractometer type	Bruker D8 Quest
Wavelength	0.71073 Å
Temperature	100(2) K
Theta range for data collection	2.207 to 25.411°
Index ranges	
$-17 \leq h \leq 17, -15 \leq k \leq 15, -41 \leq l \leq 41$	
Reflections collected	63002
Independent reflections	5802 [$R(\text{int}) = 0.0253$]
Completeness to $\theta = 25.000^\circ$	99.9%
Observed reflections	5287 [$I > 2\sigma(I)$]
Reflections used for refinement	5802
Absorption correction	Semi-empirical from equivalents
Max. and min. transmission	0.7452 and 0.6967
Largest diff. peak and hole	1.008 and -0.546 e·Å ⁻³
Solution	dual/difmap
Refinement	Full-matrix least-squares on F ²
Treatment of hydrogen atoms	mixed/hetero
Data / restraints / parameters	5802 / 0 / 406
Goodness-of-fit on F ²	1.099
R index (all data)	$R_1 = 0.0359$ $wR_2 = 0.0811$
R index conventional [$I > 2\sigma(I)$]	$R_1 = 0.0317$ $wR_2 = 0.0789$

Refinement special details

The iodine anion was refined in 2-component disorder. The asymmetric unit contains a half benzene molecule completed by inversion.

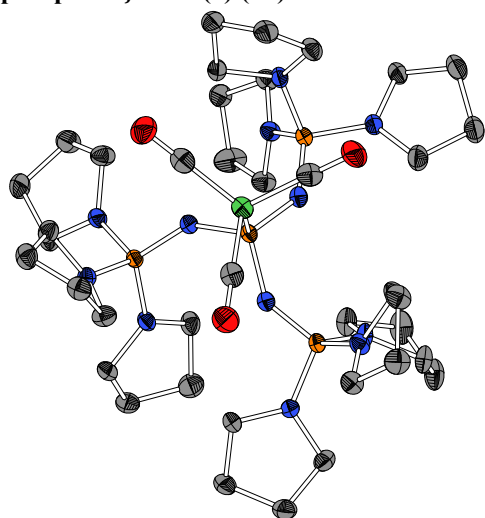
Tricarbonyl{tris[tris(dimethylamino)phosphazeny]phosphane}nickel(0) (5a)



Crystal growth	Sebastian Ullrich
Solution and refinement	Sebastian Ullrich
Identification code	SU060Ni
Habitus, colour	block, colourless
Crystal size	0.264 x 0.242 x 0.228 mm ³
Crystal system	Triclinic
Space group	<i>P</i> $\bar{1}$ $Z = 8$
Unit cell dimensions	
$a = 11.9751(4)$ Å	$\alpha = 92.172(2)^\circ$
$b = 24.4333(7)$ Å	$\beta = 95.020(2)^\circ$
$c = 24.4999(7)$ Å	$\gamma = 95.129(2)^\circ$
Volume	7104.8(4) Å ³
Cell determination	63876 peaks with θ 2.3 to 34.0°
Empirical formula	C ₂₁ H ₅₄ N ₁₂ NiO ₃ P ₄
Formula weight	705.35
Density (calculated)	1.319 g·cm ⁻³
Absorption coefficient	0.768 mm ⁻¹
F(000)	3008
Diffractometer type	Stoe Stadivari
Wavelength	0.71073 Å
Temperature	100(2) K
Theta range for data collection	2.282 to 34.767°
Index ranges	
$-19 \leq h \leq 19, -38 \leq k \leq 38, -37 \leq l \leq 38$	
Reflections collected	54269
Independent reflections	54269 [$R(\text{int}) = 0.0777$]
Completeness to $\theta = 25.000^\circ$	99.7%
Observed reflections	32408 [$I > 2\sigma(I)$]
Reflections used for refinement	54269
Absorption correction	Semi-empirical from equivalents
Max. and min. transmission	1.0000 and 0.3090
Largest diff. peak and hole	1.068 and -0.925 e·Å ⁻³
Solution	dual/difmap
Refinement	Full-matrix least-squares on F ²
Treatment of hydrogen atoms	geom/constr
Data / restraints / parameters	54269 / 0 / 1550
Goodness-of-fit on F ²	0.980
R index (all data)	$R_1 = 0.1296$ $wR_2 = 0.2150$
R index conventional [$I > 2\sigma(I)$]	$R_1 = 0.0696$ $wR_2 = 0.1760$

Refinement special details

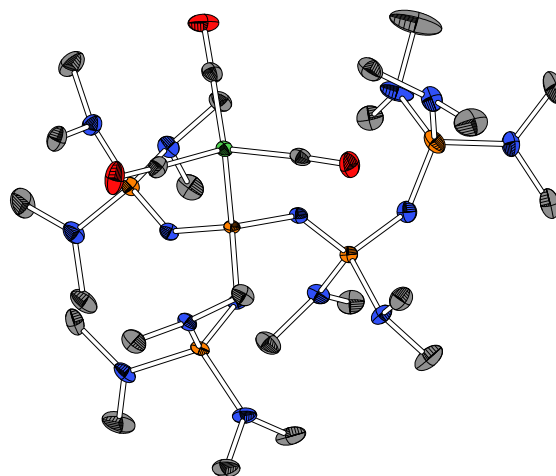
The asymmetric unit contains four independent molecules. Refined as 2-component twin. Four reflections were omitted from the least-squares refinement using OMIT.

Tricarbonyl{tris[tris(pyrrolidino)phosphazeny]-phosphane}nickel(0) (5b)

Crystal growth	Sebastian Ullrich
Solution and refinement	Klaus Harms
Identification code	SU062Ni
Habitus, colour	block, colourless
Crystal size	0.29 x 0.13 x 0.10 mm ³
Crystal system	Triclinic
Space group	$P\bar{1}$ Z = 2
Unit cell dimensions	
$a = 13.0970(2)$ Å	$a = 106.9620(10)^\circ$
$b = 18.2651(2)$ Å	$\beta = 99.0610(10)^\circ$
$c = 22.2152(3)$ Å	$\gamma = 90.0250(10)^\circ$
Volume	5013.61(12) Å ³
Cell determination	70238 peaks with θ 3.4 to 72.8°
Empirical formula	C ₈₈ H ₁₅₉ N ₂₄ Ni ₂ O ₆ P ₈
Formula weight	2014.56
Density (calculated)	1.334 g·cm ⁻³
Absorption coefficient	2.176 mm ⁻¹
F(000)	2158
Diffractometer type	Stoe Stadivari
Wavelength	1.54178 Å
Temperature	100(2) K
Theta range for data collection	3.421 to 72.502°
Index ranges	
$-16 \leq h \leq 10, -22 \leq k \leq 18, -25 \leq l \leq 27$	
Reflections collected	94831
Independent reflections	19241 [$R(\text{int}) = 0.0434$]
Completeness to theta = 67.679°	99.1%
Observed reflections	15064 [$I > 2\sigma(I)$]
Reflections used for refinement	19241
Absorption correction	Semi-empirical from equivalents
Max. and min. transmission	0.7353 and 0.2489
Largest diff. peak and hole	0.790 and -0.537 e·Å ⁻³
Solution	dual/difmap
Refinement	Full-matrix least-squares on F ²
Treatment of hydrogen atoms	geom/constr
Data / restraints / parameters	19241 / 109 / 1214
Goodness-of-fit on F ²	1.026
R index (all data)	$R_1 = 0.0496$ $wR_2 = 0.1088$
R index conventional [$I > 2\sigma(I)$]	$R_1 = 0.0384$ $wR_2 = 0.1048$

Refinement special details

The asymmetric unit contains two independent molecules, one toluene and a half *n*-hexane molecule, completed *via* inversion. Two pyrrolidine rings were refined in 2-component disorder. The *n*-hexane molecules was refined with SADI, RIGU and ISOR restraints. One reflection was omitted from the least-squares refinement using OMIT.

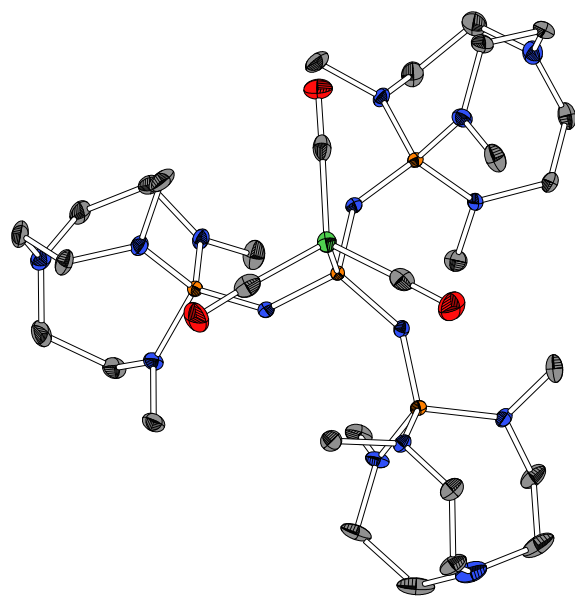
Tricarbonyl{[pentakis(dimethylamino)diphosphazeny]bis[tris(dimethylamino)phosphazeny]-phosphane}nickel(0) (5d)

CCDC code	1898101
Crystal growth	Sebastian Ullrich
Solution and refinement	Sebastian Ullrich
Identification code	SU061Ni
Habitus, colour	needle, clear colourless
Crystal size	0.670 x 0.103 x 0.083 mm ³
Crystal system	Orthorhombic
Space group	$P2_12_12_1$ Z = 4
Unit cell dimensions	
$a = 10.1549(4)$ Å	$\alpha = 90^\circ$
$b = 18.8634(8)$ Å	$\beta = 90^\circ$
$c = 22.3971(10)$ Å	$\gamma = 90^\circ$
Volume	4290.3(3) Å ³
Cell determination	9803 peaks with θ 2.3 to 27.1°
Empirical formula	C ₂₅ H ₆₆ N ₁₅ NiO ₃ P ₅
Formula weight	838.48
Density (calculated)	1.298 g·cm ⁻³
Absorption coefficient	0.684 mm ⁻¹
F(000)	1792
Diffractometer type	Bruker D8 Quest
Wavelength	0.71073 Å
Temperature	100(2) K
Theta range for data collection	2.115 to 27.142°
Index ranges	
$-11 \leq h \leq 13, -24 \leq k \leq 23, -28 \leq l \leq 28$	
Reflections collected	50450
Independent reflections	9490 [$R(\text{int}) = 0.0472$]
Completeness to theta = 25.000°	100.0%
Observed reflections	8685 [$I > 2\sigma(I)$]
Reflections used for refinement	9490
Absorption correction	Semi-empirical from equivalents
Max. and min. transmission	0.7455 and 0.6861
Flack parameter (absolute struct.)	$-0.009(4)$
Largest diff. peak and hole	0.307 and -0.287 e·Å ⁻³
Solution	dual/difmap
Refinement	Full-matrix least-squares on F ²
Treatment of hydrogen atoms	geom/constr
Data / restraints / parameters	9490 / 78 / 494
Goodness-of-fit on F ²	1.042
R index (all data)	$R_1 = 0.0340$ $wR_2 = 0.0582$
R index conventional [$I > 2\sigma(I)$]	$R_1 = 0.0277$ $wR_2 = 0.0582$

Refinement special details

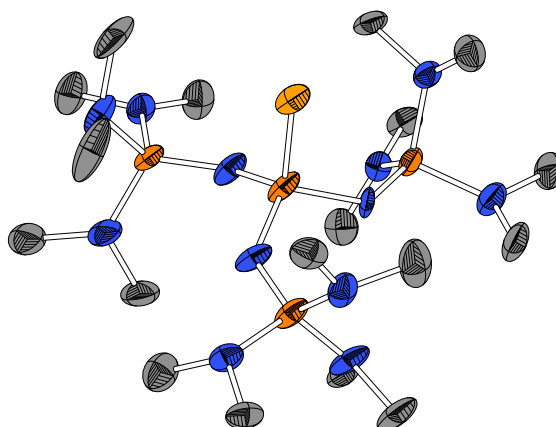
One dimethylamino group was refined in 2-component disorder using SIMU restraints.

Tricarbonyl{Tris[1-imino-2,8,9-trimethyl-2,5,8,9-tetraaza-1-phospha-bicyclo[3.3.3]undecane]-phosphane}nickel(0) (5e)

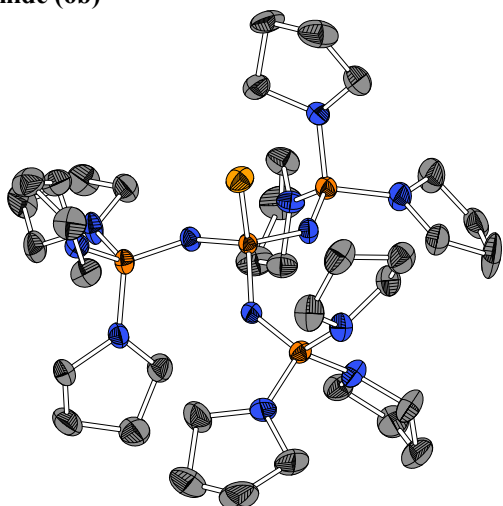


Crystal growth	Sebastian Ullrich
Solution and refinement	Sebastian Ullrich
Identification code	SU08300
Habitus, colour	prism, clear colourless
Crystal size	0.317 x 0.142 x 0.069 mm ³
Crystal system	Monoclinic
Space group	$P2_1/n$ $Z = 4$
Unit cell dimensions	
$a = 13.3073(6)$ Å	$\alpha = 90^\circ$
$b = 18.5171(8)$ Å	$\beta = 104.8380(10)^\circ$
$c = 17.6350(7)$ Å	$\gamma = 90^\circ$
Volume	4200.6(3) Å ³
Cell determination	9895 peaks with θ 2.4 to 25.3°
Empirical formula	C ₃₀ H ₆₃ N ₁₅ NiO ₃ P ₄
Formula weight	864.54
Density (calculated)	1.367 g·cm ⁻³
Absorption coefficient	0.665 mm ⁻¹
F(000)	1840
Diffractometer type	Bruker D8 Quest
Wavelength	0.71073 Å
Temperature	100(2) K
Theta range for data collection	2.200 to 25.423°
Index ranges	
	$-16 \leq h \leq 15, -22 \leq k \leq 22, -21 \leq l \leq 21$
Reflections collected	67944
Independent reflections	7730 [$R(\text{int}) = 0.0939$]
Completeness to theta = 25.000°	99.9%
Observed reflections	6000 [$I > 2\sigma(I)$]
Reflections used for refinement	7730
Absorption correction	Semi-empirical from equivalents
Largest diff. peak and hole	0.339 and -0.350 e·Å ⁻³
Solution	dual/difmap
Refinement	Full-matrix least-squares on F ²
Treatment of hydrogen atoms	geom/constr
Data / restraints / parameters	7730 / 0 / 487
Goodness-of-fit on F ²	1.024
R index (all data)	$R_1 = 0.0608$ $wR_2 = 0.0781$
R index conventional [$I > 2\sigma(I)$]	$R_1 = 0.0376$ $wR_2 = 0.0711$

Tris[tris(dimethylamino)phosphazeny]phosphane selenide (6a)



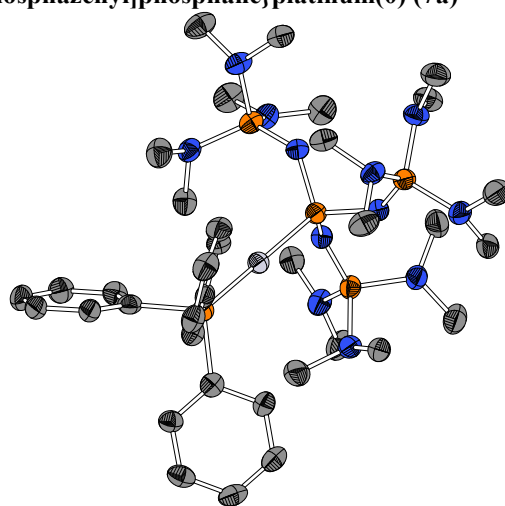
Crystal growth	Sebastian Ullrich
Solution and refinement	Sebastian Ullrich
Identification code	SU06000
Habitus, colour	needle, colourless
Crystal size	0.264 x 0.122 x 0.044 mm ³
Crystal system	Monoclinic
Space group	$P2_1/n$ $Z = 4$
Unit cell dimensions	
$a = 11.3081(4)$ Å	$\alpha = 90^\circ$
$b = 18.2574(5)$ Å	$\beta = 93.620(3)^\circ$
$c = 15.6852(6)$ Å	$\gamma = 90^\circ$
Volume	3231.85(19) Å ³
Cell determination	27112 peaks with θ 3.7 to 75.2°
Empirical formula	C ₁₈ H ₅₄ N ₁₂ P ₄ Se
Formula weight	641.57
Density (calculated)	1.319 g·cm ⁻³
Absorption coefficient	3.682 mm ⁻¹
F(000)	1360
Diffractometer type	Stoe Stadivari
Wavelength	1.54178 Å
Temperature	100(2) K
Theta range for data collection	3.719 to 75.262°
Index ranges	
	$-13 \leq h \leq 14, -22 \leq k \leq 15, -19 \leq l \leq 19$
Reflections collected	32182
Independent reflections	6573 [$R(\text{int}) = 0.0784$]
Completeness to theta = 70.000°	99.8%
Observed reflections	4487 [$I > 2\sigma(I)$]
Reflections used for refinement	6573
Absorption correction	Semi-empirical from equivalents
Max. and min. transmission	1.0000 and 0.1607
Largest diff. peak and hole	1.192 and -0.432 e·Å ⁻³
Solution	dual/difmap
Refinement	Full-matrix least-squares on F ²
Treatment of hydrogen atoms	geom/constr
Data / restraints / parameters	6573 / 79 / 471
Goodness-of-fit on F ²	0.930
R index (all data)	$R_1 = 0.0727$ $wR_2 = 0.1328$
R index conventional [$I > 2\sigma(I)$]	$R_1 = 0.0508$ $wR_2 = 0.1254$
Refinement special details	
	One phosphazeny group was refined in 2-component disorder using SIMU and RIGU restraints. One additional dimethylamino group was refined in 2-component disorder using SIMU.

Tris[tris(pyrrolidino)phosphazeny]phosphane selenide (6b)


CCDC code	1898102
Crystal growth	Sebastian Ullrich
Solution and refinement	Sebastian Ullrich
Identification code	SU062
Habitus, colour	needle, clear colourless
Crystal size	0.517 x 0.150 x 0.097 mm ³
Crystal system	Monoclinic
Space group	<i>P2₁/c</i> <i>Z</i> = 4
Unit cell dimensions	
<i>a</i> = 12.2499(6) Å	<i>a</i> = 90°
<i>b</i> = 20.7457(10) Å	<i>β</i> = 102.638(2)°
<i>c</i> = 17.6678(9) Å	<i>γ</i> = 90°
Volume	4381.2(4) Å ³
Cell determination	9920 peaks with <i>θ</i> 2.4 to 24.9°
Empirical formula	C ₃₆ H ₇₂ N ₁₂ P ₄ Se
Formula weight	875.89
Density (calculated)	1.328 g·cm ⁻³
Absorption coefficient	1.045 mm ⁻¹
F(000)	1864
Diffractometer type	Bruker D8 Quest
Wavelength	0.71073 Å
Temperature	230(2) K
Theta range for data collection	2.291 to 25.322°
Index ranges	
-14 ≤ <i>h</i> ≤ 14, -24 ≤ <i>k</i> ≤ 24, -21 ≤ <i>l</i> ≤ 21	
Reflections collected	121600
Independent reflections	7969 [<i>R</i> (int) = 0.0890]
Completeness to <i>θ</i> = 25.000°	99.9%
Observed reflections	5791 [<i>I</i> > 2σ(<i>I</i>)]
Reflections used for refinement	7969
Absorption correction	Semi-empirical from equivalents
Max. and min. transmission	0.7452 and 0.6750
Largest diff. peak and hole	0.300 and -0.300 e·Å ⁻³
Solution	dual/difmap
Refinement	Full-matrix least-squares on F ²
Treatment of hydrogen atoms	geom/constr
Data / restraints / parameters	7969 / 139 / 536
Goodness-of-fit on F ²	1.037
<i>R</i> index (all data)	<i>R</i> ₁ = 0.0687 <i>wR</i> ₂ = 0.0904
<i>R</i> index conventional [<i>I</i> > 2σ(<i>I</i>)]	<i>R</i> ₁ = 0.0401 <i>wR</i> ₂ = 0.0805

Refinement special details

Three pyrrolidine rings were refined in 2-component disorder using SADI, SIMU and RIGU restraints.

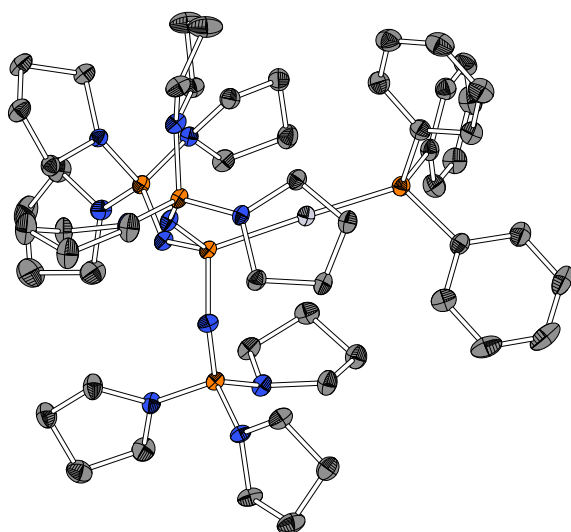
Triphenylphosphane{tris[tris(dimethylamino)-phosphazeny]phosphane}platinum(0) (7a)


CCDC code	1898103
Crystal growth	Sebastian Ullrich
Solution and refinement	Sebastian Ullrich
Identification code	SU060Pt2
Habitus, colour	block, yellow
Crystal size	0.191 x 0.171 x 0.156 mm ³
Crystal system	Cubic
Space group	<i>Pa</i> ³ <i>Z</i> = 8
Unit cell dimensions	
<i>a</i> = 21.6117(3) Å	<i>α</i> = 90°
<i>b</i> = 21.6117(3) Å	<i>β</i> = 90°
<i>c</i> = 21.6117(3) Å	<i>γ</i> = 90°
Volume	10094.1(4) Å ³
Cell determination	12622 peaks with <i>θ</i> 3.5 to 71.9°
Empirical formula	C ₃₆ H ₆₉ N ₁₂ P ₃ Pt
Formula weight	1019.97
Density (calculated)	1.342 g·cm ⁻³
Absorption coefficient	6.987 mm ⁻¹
F(000)	4176
Diffractometer type	Stoe Stadivari
Wavelength	1.54178 Å
Temperature	100(2) K
Theta range for data collection	3.542 to 71.766°
Index ranges	
-24 ≤ <i>h</i> ≤ 14, -21 ≤ <i>k</i> ≤ 26, -19 ≤ <i>l</i> ≤ 26	
Reflections collected	19660
Independent reflections	3288 [<i>R</i> (int) = 0.0499]
Completeness to <i>θ</i> = 70.000°	99.8%
Observed reflections	2495 [<i>I</i> > 2σ(<i>I</i>)]
Reflections used for refinement	3288
Absorption correction	Semi-empirical from equivalents
Max. and min. transmission	0.9999 and 0.3054
Largest diff. peak and hole	0.719 and -1.034 e·Å ⁻³
Solution	dual/difmap
Refinement	Full-matrix least-squares on F ²
Treatment of hydrogen atoms	geom/constr
Data / restraints / parameters	3288 / 0 / 169
Goodness-of-fit on F ²	1.019
<i>R</i> index (all data)	<i>R</i> ₁ = 0.0509 <i>wR</i> ₂ = 0.0371
<i>R</i> index conventional [<i>I</i> > 2σ(<i>I</i>)]	<i>R</i> ₁ = 0.0997 <i>wR</i> ₂ = 0.0962

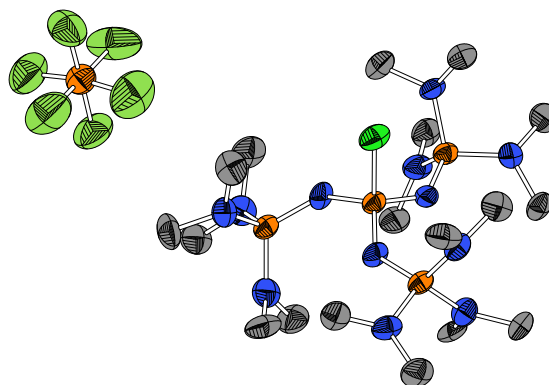
Refinement special details

The asymmetric unit contains a third of a molecule completed by a threefold axis alongside the P-Pt bonds. A half *n*-pentane molecule lies on an inversion center with a threefold axis and could therefore not be refined distinctly and was addressed by SQUEEZE routine.

Triphenylphosphane{tris[tris(pyrrolidino)phosphazeny]lphosphane}platinum(0) (7b)

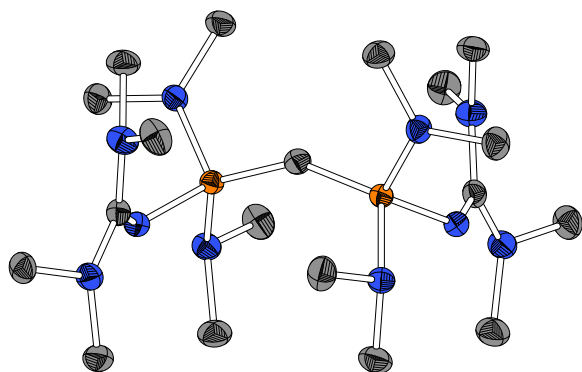


Crystal growth	Sebastian Ullrich
Solution and refinement	Sebastian Ullrich
Identification code	SU062Pt
Habitus, colour	block, yellow
Crystal size	0.270 x 0.224 x 0.201 mm ³
Crystal system	Triclinic
Space group	<i>P</i> $\bar{1}$ Z = 2
Unit cell dimensions	
<i>a</i> = 12.82796(24) Å	α = 102.2660(14)°
<i>b</i> = 13.32761(22) Å	β = 90.6850(15)°
<i>c</i> = 18.9168(3) Å	γ = 116.7670(13)°
Volume	2800.11(9) Å ³
Cell determination	109189 peaks with θ 2.3 to 34.2°
Empirical formula	C ₅₄ H ₈₇ N ₁₂ P ₅ Pt
Formula weight	1254.29
Density (calculated)	1.488 g·cm ⁻³
Absorption coefficient	2.697 mm ⁻¹
F(000)	1296
Diffractometer type	Stoe Stadivari
Wavelength	0.71073 Å
Temperature	100(2) K
Theta range for data collection	2.257 to 34.726°
Index ranges	
$-20 \leq h \leq 20$, $-21 \leq k \leq 15$, $-29 \leq l \leq 30$	
Reflections collected	169741
Independent reflections	23135 [<i>R</i> (int) = 0.0892]
Completeness to $\theta = 25.000^\circ$	99.9%
Observed reflections	17333 [<i>I</i> > 2 σ (<i>I</i>)]
Reflections used for refinement	23135
Absorption correction	Semi-empirical from equivalents
Max. and min. transmission	1.0000 and 0.3295
Largest diff. peak and hole	2.144 and -1.497 e·Å ⁻³
Solution	dual/ difmap
Refinement	Full-matrix least-squares on F ²
Treatment of hydrogen atoms	geom, constr
Data / restraints / parameters	23135 / 0 / 649
Goodness-of-fit on F ²	0.988
<i>R</i> index (all data)	<i>R</i> ₁ = 0.0673 <i>wR</i> ₂ = 0.0923
<i>R</i> index conventional [<i>I</i> > 2 σ (<i>I</i>)]	<i>R</i> ₁ = 0.0398 <i>wR</i> ₂ = 0.0847

Chlorotris[tris(dimethylamino)phosphazeny]lphosphonium hexafluoridophosphate (8aPF₆)

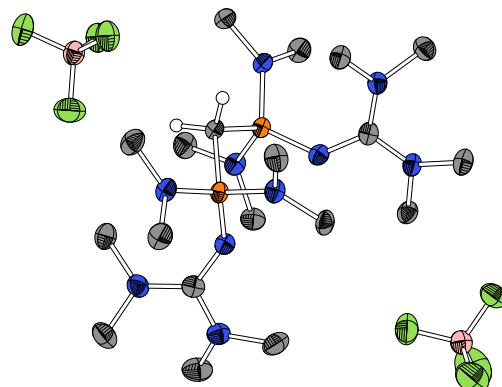
Crystal growth	Sebastian Ullrich
Solution and refinement	Sebastian Ullrich
Identification code	SUdmaP ₃ Cl
Habitus, colour	needle, colourless
Crystal size	0.680 x 0.356 x 0.044 mm ³
Crystal system	Monoclinic
Space group	<i>P</i> ₂ / <i>c</i> Z = 8
Unit cell dimensions	
<i>a</i> = 21.7586(8) Å	α = 90°
<i>b</i> = 8.6727(2) Å	β = 91.233(3)°
<i>c</i> = 37.4080(13) Å	γ = 90°
Volume	7057.5(4) Å ³
Cell determination	49948 peaks with θ 4.1 to 76.3°
Empirical formula	C ₁₈ H ₅₄ ClF ₆ N ₁₂ P ₅
Formula weight	743.03
Density (calculated)	1.399 g·cm ⁻³
Absorption coefficient	3.668 mm ⁻¹
F(000)	3136
Diffractometer type	Stoe Stadivari
Wavelength	1.54178 Å
Temperature	100(2) K
Theta range for data collection	3.083 to 76.194°
Index ranges	
$-27 \leq h \leq 26$, $-10 \leq k \leq 10$, $-46 \leq l \leq 46$	
Reflections collected	13219
Independent reflections	13219 [<i>R</i> (int) = 0.0796]
Completeness to $\theta = 70.000^\circ$	92.3%
Observed reflections	9709 [<i>I</i> > 2 σ (<i>I</i>)]
Reflections used for refinement	13219
Absorption correction	Semi-empirical from equivalents
Max. and min. transmission	1.0000 and 0.2782
Largest diff. peak and hole	1.399 and -1.008 e·Å ⁻³
Solution	dual/difmap
Refinement	Full-matrix least-squares on F ²
Treatment of hydrogen atoms	geom/constr
Data / restraints / parameters	13219 / 36 / 794
Goodness-of-fit on F ²	1.039
<i>R</i> index (all data)	<i>R</i> ₁ = 0.2106 <i>wR</i> ₂ = 0.1853
<i>R</i> index conventional [<i>I</i> > 2 σ (<i>I</i>)]	<i>R</i> ₁ = 0.4972 <i>wR</i> ₂ = 0.4852
Refinement special details	
Poor data due to thinness of the needle do not allow detailed structure analysis. The asymmetric unit contains two independent molecules. Refined as 2-component twin. Two dimethylamino groups were refined using RIGU and SIMU restraints.	

Tetrakis(dimethylamino)bis(tetramethylguanidino) carbodiphosphorane *sym*-(tmg)₂(dma)₄-CDP (9)



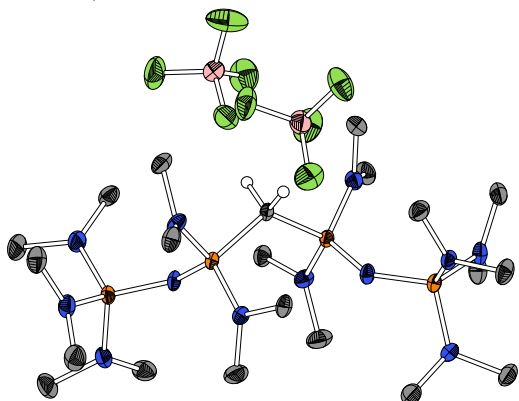
CCDC code	1903840
Crystal growth	Björn Koch
Solution and refinement	Sebastian Ullrich
Identification code	BK23
Habitus, colour	block, colourless
Crystal size	0.230 x 0.180 x 0.153 mm ³
Crystal system	Orthorhombic
Space group	<i>Pbca</i> <i>Z</i> = 8
Unit cell dimensions	
<i>a</i> = 17.0571(2) Å	<i>α</i> = 90°
<i>b</i> = 16.2524(3) Å	<i>β</i> = 90°
<i>c</i> = 19.3230(2) Å	<i>γ</i> = 90°
Volume	5356.70(13) Å ³
Cell determination	41617 peaks with <i>θ</i> 3.5 to 75.9°
Empirical formula	C ₁₉ H ₄₈ N ₁₀ P ₂
Formula weight	478.61
Density (calculated)	1.187 g·cm ⁻³
Absorption coefficient	1.677 mm ⁻¹
F(000)	2096
Diffractometer type	Stoe Stadivari
Wavelength	1.54178 Å
Temperature	100(2) K
Theta range for data collection	4.399 to 75.699°
Index ranges	
	-15 ≤ <i>h</i> ≤ 21, -20 ≤ <i>k</i> ≤ 20, -22 ≤ <i>l</i> ≤ 24
Reflections collected	53455
Independent reflections	5520 [<i>R</i> (int) = 0.0374]
Completeness to theta = 70.000°	99.9%
Observed reflections	4504 [<i>I</i> > 2σ(<i>I</i>)]
Reflections used for refinement	5520
Absorption correction	Semi-empirical from equivalents
Max. and min. transmission	1.0000 and 0.5130
Largest diff. peak and hole	0.319 and -0.342 e·Å ⁻³
Solution	dual/difmap
Refinement	Full-matrix least-squares on F ²
Treatment of hydrogen atoms	geom/constr
Data / restraints / parameters	5520 / 0 / 296
Goodness-of-fit on F ²	1.059
<i>R</i> index (all data)	<i>R</i> ₁ = 0.0425
	<i>wR</i> ₂ = 0.1024
<i>R</i> index conventional [<i>I</i> > 2σ(<i>I</i>)]	<i>R</i> ₁ = 0.0349
	<i>wR</i> ₂ = 0.0997

Methylenebis{tris(dimethylamino)phosphazeny]-bis(dimethylamino)phosphonium} tetrafluoroborate *sym*-(tmg)₂(dma)₄-CDP·2HBF₄ (9·2HBF₄)



CCDC code	1903833
Crystal growth	Björn Koch
Solution and refinement	Sebastian Ullrich
Identification code	BK14
Habitus, colour	needle, colourless
Crystal size	0.208 x 0.109 x 0.057 mm ³
Crystal system	Monoclinic
Space group	<i>P2₁/c</i> <i>Z</i> = 4
Unit cell dimensions	
<i>a</i> = 12.0045(4) Å	<i>α</i> = 90°
<i>b</i> = 25.5119(9) Å	<i>β</i> = 115.832(3)°
<i>c</i> = 11.6750(4) Å	<i>γ</i> = 90°
Volume	3218.3(2) Å ³
Cell determination	27616 peaks with <i>θ</i> 3.5 to 75.7°
Empirical formula	C ₁₉ H ₅₀ B ₂ F ₈ N ₁₀ P ₂
Formula weight	654.25
Density (calculated)	1.350 g·cm ⁻³
Absorption coefficient	1.901 mm ⁻¹
F(000)	1384
Diffractometer type	Stoe Stadivari
Wavelength	1.54178 Å
Temperature	100(2) K
Theta range for data collection	4.091 to 75.792°
Index ranges	
	-15 ≤ <i>h</i> ≤ 12, -25 ≤ <i>k</i> ≤ 32, -14 ≤ <i>l</i> ≤ 14
Reflections collected	33222
Independent reflections	6614 [<i>R</i> (int) = 0.0570]
Completeness to theta = 70.000°	100.0%
Observed reflections	4171 [<i>I</i> > 2σ(<i>I</i>)]
Reflections used for refinement	6614
Absorption correction	Semi-empirical from equivalents
Max. and min. transmission	0.9990 and 0.1961
Largest diff. peak and hole	0.532 and -0.419 e·Å ⁻³
Solution	dual/difmap
Refinement	Full-matrix least-squares on F ²
Treatment of hydrogen atoms	geom/constr
Data / restraints / parameters	6614 / 0 / 386
Goodness-of-fit on F ²	0.872
<i>R</i> index (all data)	<i>R</i> ₁ = 0.0734
	<i>wR</i> ₂ = 0.1259
<i>R</i> index conventional [<i>I</i> > 2σ(<i>I</i>)]	<i>R</i> ₁ = 0.0484
	<i>wR</i> ₂ = 0.1204

Methylenebis{tris(dimethylamino)phosphazenyll}-bis(dimethylamino)phosphonium} tetrafluoroborate *sym*-(dmaP₁)₂(dma)₄-CDP·2HBF₄ (10·2HBF₄)

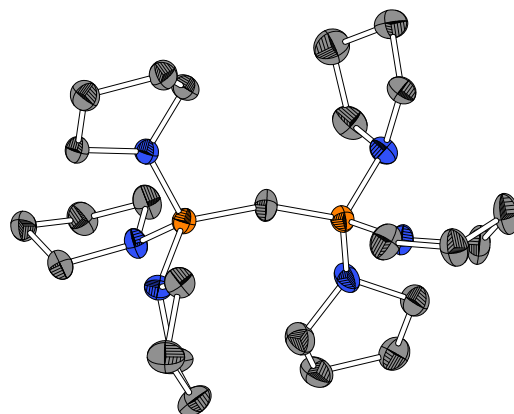


CCDC code	1903838	
Crystal growth	Björn Koch	
Solution and refinement	Klaus Harms	
Identification code	BK17	
Habitus, colour	needle, colourless	
Crystal size	0.56 x 0.07 x 0.07 mm ³	
Crystal system	Triclinic	
Space group	<i>P</i> 1	<i>Z</i> = 2
Unit cell dimensions		
<i>a</i> = 11.3316(5) Å	<i>a</i> = 94.444(4)°	
<i>b</i> = 11.7062(5) Å	<i>b</i> = 93.147(4)°	
<i>c</i> = 14.3391(7) Å	<i>c</i> = 92.843(3)°	
Volume	1890.73(15) Å ³	
Cell determination	59460 peaks with θ 3.1 to 76.0°	
Empirical formula	C ₂₁ H ₆₂ B ₂ F ₈ N ₁₂ P ₄	
Formula weight	780.32	
Density (calculated)	1.371 g·cm ⁻³	
Absorption coefficient	2.495 mm ⁻¹	
F(000)	828	
Diffractometer type	Stoe Stadivari	
Wavelength	1.54186 Å	
Temperature	100(2) K	
Theta range for data collection	3.097 to 74.933°	
Index ranges		
-14 ≤ <i>h</i> ≤ 14, -14 ≤ <i>k</i> ≤ 14, -10 ≤ <i>l</i> ≤ 17		
Reflections collected	33471	
Independent reflections	10558 [<i>R</i> (int) = 0.0454]	
Completeness to theta = 70.000°	98.6%	
Observed reflections	9844 [<i>I</i> > 2σ(<i>I</i>)]	
Reflections used for refinement	10558	
Absorption correction	Semi-empirical from equivalents	
Max. and min. transmission	0.6922 and 0.1438	
Flack parameter (absolute struct.)	0.48(2)	
Largest diff. peak and hole	0.556 and -0.457 e·Å ⁻³	
Solution	dual/difmap	
Refinement	Full-matrix least-squares on F ²	
Treatment of hydrogen atoms	geom/constr	
Data / restraints / parameters	10558 / 3 / 888	
Goodness-of-fit on F ²	1.027	
<i>R</i> index (all data)	<i>R</i> ₁ = 0.0485 <i>wR</i> ₂ = 0.1214	
<i>R</i> index conventional [<i>I</i> > 2σ(<i>I</i>)]	<i>R</i> ₁ = 0.0442 <i>wR</i> ₂ = 0.1180	

Refinement special details

The asymmetric unit contains two independent molecules. Refined as 2-component inversion twin.

Hexakis(pyrrolidino) carbodiphosphorane (pyrr)₆-CDP (13)

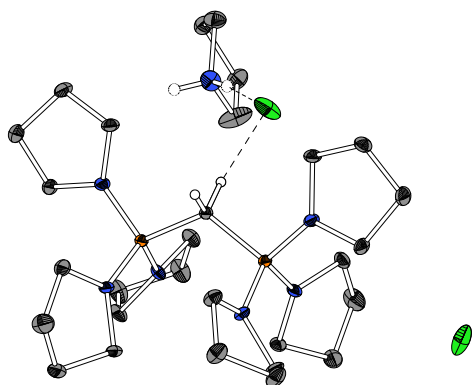


CCDC code	1903843	
Crystal growth	Björn Koch	
Solution and refinement	Sebastian Ullrich	
Identification code	BK1601	
Habitus, colour	block, colourless	
Crystal size	0.174 x 0.153 x 0.131 mm ³	
Crystal system	Monoclinic	
Space group	<i>P</i> 2 ₁ / <i>c</i>	<i>Z</i> = 4
Unit cell dimensions		
<i>a</i> = 10.8041(3) Å	<i>a</i> = 90°	
<i>b</i> = 14.3736(3) Å	<i>b</i> = 100.201(2)°	
<i>c</i> = 17.1480(5) Å	<i>c</i> = 90°	
Volume	2620.88(12) Å ³	
Cell determination	20435 peaks with θ 4.0 to 75.6°	
Empirical formula	C ₂₅ H ₄₈ N ₆ P ₂	
Formula weight	494.63	
Density (calculated)	1.254 g·cm ⁻³	
Absorption coefficient	1.691 mm ⁻¹	
F(000)	1080	
Diffractometer type	Stoe Stadivari	
Wavelength	1.54178 Å	
Temperature	100(2) K	
Theta range for data collection	4.040 to 75.169°	
Index ranges		
-6 ≤ <i>h</i> ≤ 13, -17 ≤ <i>k</i> ≤ 17, -21 ≤ <i>l</i> ≤ 21		
Reflections collected	32319	
Independent reflections	5312 [<i>R</i> (int) = 0.0556]	
Completeness to theta = 70.000°	99.3 %	
Observed reflections	3613 [<i>I</i> > 2σ(<i>I</i>)]	
Reflections used for refinement	5312	
Absorption correction	Semi-empirical from equivalents	
Max. and min. transmission	0.0332 and 0.0101	
Largest diff. peak and hole	0.633 and -0.288 e·Å ⁻³	
Solution	dual/difmap	
Refinement	Full-matrix least-squares on F ²	
Treatment of hydrogen atoms	geom/constr	
Data / restraints / parameters	5312 / 30 / 337	
Goodness-of-fit on F ²	0.902	
<i>R</i> index (all data)	<i>R</i> ₁ = 0.0658 <i>wR</i> ₂ = 0.1126	
<i>R</i> index conventional [<i>I</i> > 2σ(<i>I</i>)]	<i>R</i> ₁ = 0.0431 <i>wR</i> ₂ = 0.1070	

Refinement special details

Three pyrrolidine rings were refined in 2-component disorder using RIGU restraints.

Methylenebis[tris(pyrrolidino)phosphonium] chloride pyrrolidinium chloride (pyrr)₆-CDP·2HCl·2HpyrrCl (13·2HCl + Hpyrr)

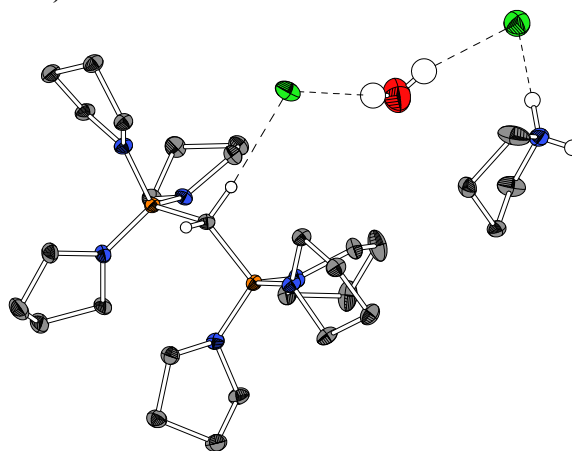


CCDC code	1903830
Crystal growth	Sebastian Ullrich
Solution and refinement	Sebastian Ullrich
Identification code	SU03900
Habitus, colour	block, clear colourless
Crystal size	0.330 x 0.220 x 0.140 mm ³
Crystal system	Orthorhombic
Space group	<i>P</i> 2 ₁ 2 ₁ 2 <i>Z</i> = 2
Unit cell dimensions	
<i>a</i> = 11.5410(4) Å	α = 90°
<i>b</i> = 21.5098(8) Å	β = 90°
<i>c</i> = 8.3299(3) Å	γ = 90°
Volume	2067.85(13) Å ³
Cell determination	9440 peaks with θ 2.6 to 27.1°
Empirical formula	C ₃₃ H ₇₀ Cl ₄ N ₈ P ₂
Formula weight	782.71
Density (calculated)	1.257 g·cm ⁻³
Absorption coefficient	0.398 mm ⁻¹
F(000)	844
Diffractometer type	Bruker D8 Quest
Wavelength	0.71073 Å
Temperature	100(2) K
Theta range for data collection	2.445 to 27.130°
Index ranges	
	-14 ≤ <i>h</i> ≤ 14, -27 ≤ <i>k</i> ≤ 25, -10 ≤ <i>l</i> ≤ 10
Reflections collected	27117
Independent reflections	4569 [<i>R</i> (int) = 0.0281]
Completeness to theta = 25.242°	99.6%
Observed reflections	4385 [<i>I</i> > 2σ(<i>I</i>)]
Reflections used for refinement	4569
Extinction coefficient	<i>X</i> = 0.0047(9)
Absorption correction	Semi-empirical from equivalents
Max. and min. transmission	0.746 and 0.672
Flack parameter (absolute struct.)	-0.21(6)
Largest diff. peak and hole	0.255 and -0.288 e·Å ⁻³
Solution	dual/difmap
Refinement	Full-matrix least-squares on F ²
Treatment of hydrogen atoms	mixed/hetero
Data / restraints / parameters	4569 / 0 / 223
Goodness-of-fit on F ²	1.082
<i>R</i> index (all data)	<i>R</i> ₁ = 0.0285 <i>wR</i> ₂ = 0.0656
<i>R</i> index conventional [<i>I</i> > 2σ(<i>I</i>)]	<i>R</i> ₁ = 0.0265 <i>wR</i> ₂ = 0.0646

Refinement special details

The asymmetric unit contains a half molecule completed by a twofold axis. Refined as 2-component inversion twin.

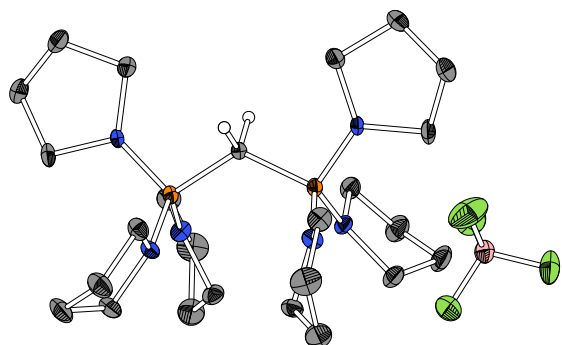
Methylenebis[tris(pyrrolidino)phosphonium] chloride pyrrolidinium chloride hydrate (pyrr)₆-CDP·2HCl·2HpyrrCl·H₂O (13·2HCl + Hpyrr + H₂O)



Crystal growth	Björn Koch
Solution and refinement	Sebastian Ullrich
Identification code	BK04
Habitus, colour	block, colourless
Crystal size	0.248 x 0.235 x 0.214 mm ³
Crystal system	Orthorhombic
Space group	<i>P</i> 2 ₁ 2 ₁ 2 <i>Z</i> = 2
Unit cell dimensions	
<i>a</i> = 11.0732(3) Å	α = 90°
<i>b</i> = 22.5457(6) Å	β = 90°
<i>c</i> = 8.2662(2) Å	γ = 90°
Volume	2063.68(9) Å ³
Cell determination	16928 peaks with θ 5.4 to 76.4°
Empirical formula	C ₃₃ H ₇₂ Cl ₄ N ₈ OP ₂
Formula weight	800.73
Density (calculated)	1.289 g·cm ⁻³
Absorption coefficient	3.627 mm ⁻¹
F(000)	864
Diffractometer type	Stoe Stadivari
Wavelength	1.54178 Å
Temperature	100(2) K
Theta range for data collection	5.351 to 75.754°
Index ranges	
	-13 ≤ <i>h</i> ≤ 13, -28 ≤ <i>k</i> ≤ 28, -10 ≤ <i>l</i> ≤ 4
Reflections collected	11420
Independent reflections	4125 [<i>R</i> (int) = 0.0264]
Completeness to theta = 70.000°	99.1 %
Observed reflections	4050 [<i>I</i> > 2σ(<i>I</i>)]
Reflections used for refinement	4125
Absorption correction	Semi-empirical from equivalents
Max. and min. transmission	1.0000 and 0.4398
Flack parameter (absolute struct.)	0.41(2)
Largest diff. peak and hole	0.693 and -0.305 e·Å ⁻³
Solution	dual/difmap
Refinement	Full-matrix least-squares on F ²
Treatment of hydrogen atoms	mixed/mixed
Data / restraints / parameters	4125 / 0 / 247
Goodness-of-fit on F ²	1.060
<i>R</i> index (all data)	<i>R</i> ₁ = 0.0374 <i>wR</i> ₂ = 0.0972
<i>R</i> index conventional [<i>I</i> > 2σ(<i>I</i>)]	<i>R</i> ₁ = 0.0368 <i>wR</i> ₂ = 0.0969

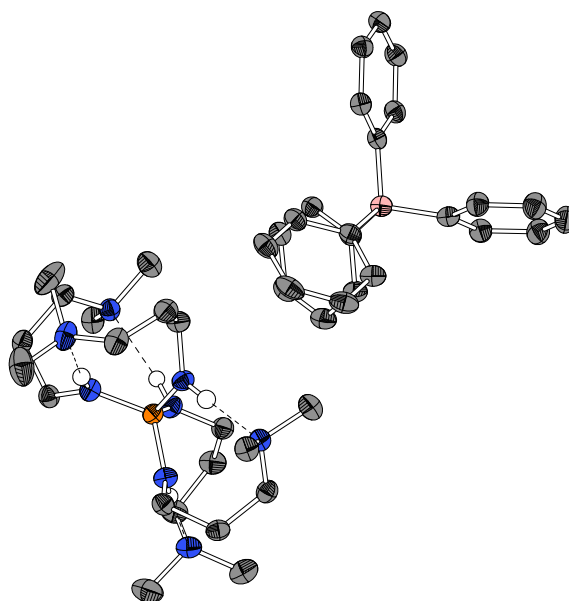
Refinement special details

The asymmetric unit contains a half molecule completed by a twofold axis. Refined as 2-component inversion twin. Protons attached to heteroatoms were refined with isotropic temperature factors at 1.5 times that of the carrier atom.

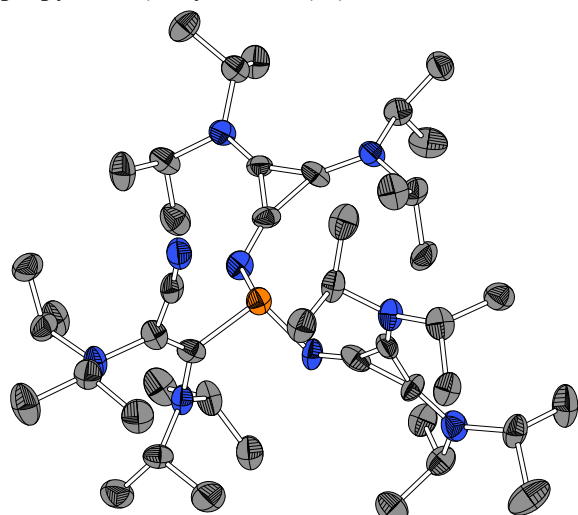
Methylenebis[tris(pyrrolidino)phosphonium] tetrafluoridoborate (pyrr)₆-CDP·2HBF₄ (13·2HBF₄)


CCDC code	1903841
Crystal growth	Björn Koch
Solution and refinement	Sebastian Ullrich
Identification code	BK0400
Habitus, colour	prism, colourless
Crystal size	0.369 x 0.258 x 0.093 mm ³
Crystal system	Monoclinic
Space group	<i>C2/c</i> $Z = 4$
Unit cell dimensions	
$a = 19.6853(6)$ Å	$\alpha = 90^\circ$
$b = 9.0107(2)$ Å	$\beta = 108.791(2)^\circ$
$c = 28.7299(10)$ Å	$\gamma = 90^\circ$
Volume	4824.4(3) Å ³
Cell determination	17841 peaks with θ 4.8 to 76.0°
Empirical formula	C ₂₉ H ₅₄ B ₂ Cl ₂ F ₈ N ₆ P ₂
Formula weight	1147.74
Density (calculated)	1.580 g·cm ⁻³
Absorption coefficient	7.494 mm ⁻¹
F(000)	2344
Diffractometer type	Stoe Stadivari
Wavelength	1.54178 Å
Temperature	100(2) K
Theta range for data collection	4.746 to 75.728°
Index ranges	
$-24 \leq h \leq 23, -10 \leq k \leq 4, -35 \leq l \leq 35$	
Reflections collected	21625
Independent reflections	4801 [$R(\text{int}) = 0.0593$]
Completeness to $\theta = 70.000^\circ$	98.3%
Observed reflections	3360 [$I > 2\sigma(I)$]
Reflections used for refinement	4801
Absorption correction	Semi-empirical from equivalents
Max. and min. transmission	1.0000 and 0.2029
Largest diff. peak and hole	0.757 and -0.610 e·Å ⁻³
Solution	dual/difmap
Refinement	Full-matrix least-squares on F ²
Treatment of hydrogen atoms	geom/constr
Data / restraints / parameters	4801 / 0 / 267
Goodness-of-fit on F ²	0.925
R index (all data)	$R_1 = 0.0672$ $wR_2 = 0.1241$
R index conventional [$I > 2\sigma(I)$]	$R_1 = 0.0469$ $wR_2 = 0.1182$

Refinement special details
The asymmetric unit contains a half molecule completed by a twofold axis and two chloroform molecules.

Tetrakis(3-dimethylaminopropylamino)phosphonium tetraphenylborat (17)


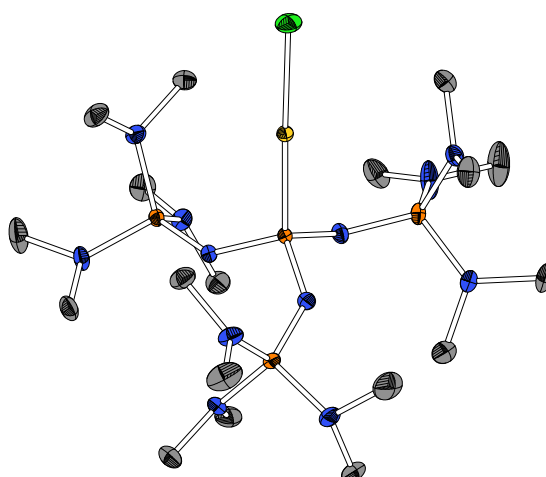
CCDC code	1912279
Crystal growth	Sebastian Ullrich
Solution and refinement	Sebastian Ullrich
Identification code	SU064
Habitus, colour	plate, colourless
Crystal size	0.250 x 0.169 x 0.058 mm ³
Crystal system	Monoclinic
Space group	<i>P2₁/c</i> $Z = 4$
Unit cell dimensions	
$a = 13.0091(2)$ Å	$\alpha = 90^\circ$
$b = 14.6924(2)$ Å	$\beta = 91.2000(10)^\circ$
$c = 23.8620(4)$ Å	$\gamma = 90^\circ$
Volume	4559.86(12) Å ³
Cell determination	33833 peaks with θ 3.4 to 76.0°
Empirical formula	C ₄₄ H ₇₂ BN ₈ P
Formula weight	754.87
Density (calculated)	1.100 g·cm ⁻³
Absorption coefficient	0.817 mm ⁻¹
F(000)	1648
Diffractometer type	Stoe Stadivari
Wavelength	1.54178 Å
Temperature	100(2) K
Theta range for data collection	3.398 to 76.015°
Index ranges	
$-15 \leq h \leq 16, -15 \leq k \leq 18, -30 \leq l \leq 22$	
Reflections collected	49498
Independent reflections	9436 [$R(\text{int}) = 0.0413$]
Completeness to $\theta = 70.000^\circ$	99.8%
Observed reflections	7110 [$I > 2\sigma(I)$]
Reflections used for refinement	9436
Absorption correction	Semi-empirical from equivalents
Max. and min. transmission	1.0000 and 0.4804
Largest diff. peak and hole	0.212 and -0.472 e·Å ⁻³
Solution	dual/difmap
Refinement	Full-matrix least-squares on F ²
Treatment of hydrogen atoms	mixed/hetero
Data / restraints / parameters	9436 / 0 / 511
Goodness-of-fit on F ²	1.012
R index (all data)	$R_1 = 0.0551$ $wR_2 = 0.1126$
R index conventional [$I > 2\sigma(I)$]	$R_1 = 0.0420$ $wR_2 = 0.1086$

(E)-3-(Bis((2,3-bis(di-*iso*-propylamino)cycloprop-2-en-1-ylidene)amino)phosphaneyl)-2,3-bis-(di-*iso*-propylamino)acrylonitrile (18)

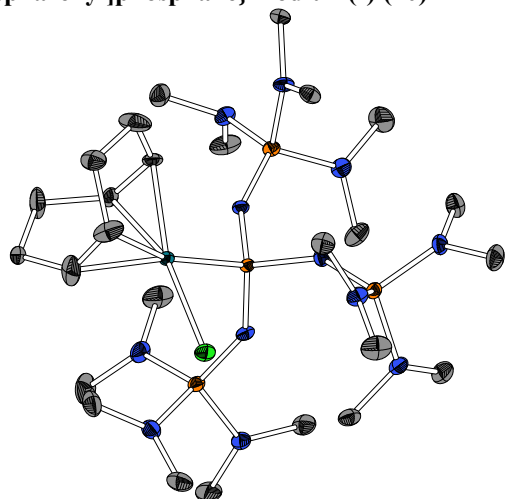
Crystal growth	Andres Gonzales
Solution and refinement	Klaus Harms
Identification code	AG017
Habitus, colour	needle, clear, yellow
Crystal size	0.30 x 0.04 x 0.03 mm ³
Crystal system	Monoclinic
Space group	<i>P</i> 2 ₁ <i>Z</i> = 4
Unit cell dimensions	
<i>a</i> = 11.5431(8) Å	<i>α</i> = 90°
<i>b</i> = 23.601(2) Å	<i>β</i> = 96.943(5)°
<i>c</i> = 18.2845(11) Å	<i>γ</i> = 90°
Volume	4944.7(6) Å ³
Cell determination	5471 peaks with <i>θ</i> 3.1 to 71.5°
Empirical formula	C ₄₅ H ₈₄ N ₉ P
Formula weight	782.18
Density (calculated)	1.051 g·cm ⁻³
Absorption coefficient	0.772 mm ⁻¹
<i>F</i> (000)	1728
Diffractometer type	Stoe Stadivari
Wavelength	1.54186 Å
Temperature	100(2) K
Theta range for data collection	2.434 to 69.994°
Index ranges	
-13 ≤ <i>h</i> ≤ 13, -28 ≤ <i>k</i> ≤ 27, -22 ≤ <i>l</i> ≤ 10	
Reflections collected	50157
Independent reflections	16853 [<i>R</i> (int) = 0.2617]
Completeness to theta = 67.686°	99.5%
Observed reflections	5329 [<i>I</i> > 2σ(<i>I</i>)]
Reflections used for refinement	16853
Absorption correction	Semi-empirical from equivalents
Max. and min. transmission	1.0000 and 0.0953
Flack parameter (absolute struct.)	0.06(4)
Largest diff. peak and hole	0.392 and -0.303 e·Å ⁻³
Solution	dual/difmap
Refinement	Full-matrix least-squares on <i>F</i> ²
Treatment of hydrogen atoms	geom/constr
Data / restraints / parameters	16853 / 1 / 1039
Goodness-of-fit on <i>F</i> ²	0.703
<i>R</i> index (all data)	<i>R</i> ₁ = 0.1974 <i>wR</i> ₂ = 0.1689
<i>R</i> index conventional [<i>I</i> > 2σ(<i>I</i>)]	<i>R</i> ₁ = 0.0709 <i>wR</i> ₂ = 0.1346

Refinement special details

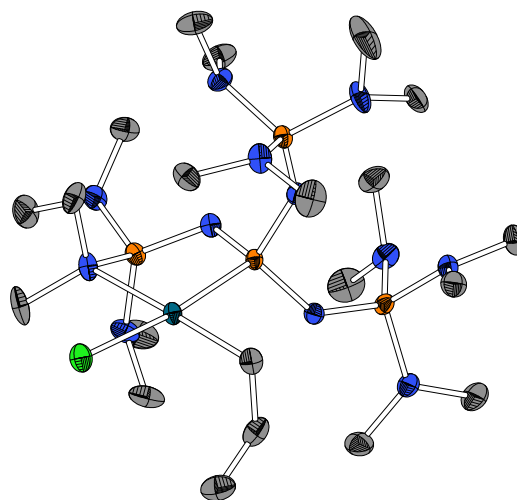
Poor data with *R*(int) greater than 0.25 do not allow detailed structure analysis.

Chlorido{tris[tris(dimethylamino)phosphazeny]-phosphane}gold(I) (19a)

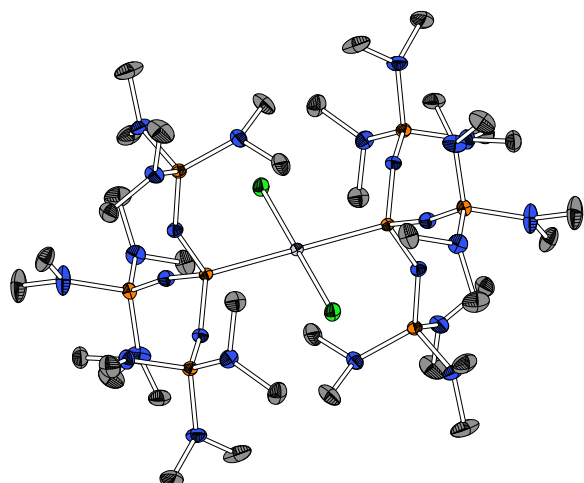
Crystal growth	Sebastian Ullrich
Solution and refinement	Sebastian Ullrich
Identification code	SU06013
Habitus, colour	needle, clear colourless
Crystal size	0.423 x 0.090 x 0.086 mm ³
Crystal system	Monoclinic
Space group	<i>P</i> 2 ₁ / <i>n</i> <i>Z</i> = 4
Unit cell dimensions	
<i>a</i> = 11.1116(5) Å	<i>α</i> = 90°
<i>b</i> = 18.1829(9) Å	<i>β</i> = 95.033(2)°
<i>c</i> = 16.3234(7) Å	<i>γ</i> = 90°
Volume	3285.3(3) Å ³
Cell determination	9008 peaks with <i>θ</i> 2.4 to 27.1°
Empirical formula	C ₁₈ H ₅₄ AuClN ₁₂ P ₄
Formula weight	795.03
Density (calculated)	1.607 g·cm ⁻³
Absorption coefficient	4.784 mm ⁻¹
<i>F</i> (000)	1608
Diffractometer type	Bruker D8 Quest
Wavelength	0.71073 Å
Temperature	105(2) K
Theta range for data collection	2.133 to 27.157°
Index ranges	
-14 ≤ <i>h</i> ≤ 14, -23 ≤ <i>k</i> ≤ 23, -20 ≤ <i>l</i> ≤ 20	
Reflections collected	104167
Independent reflections	7292 [<i>R</i> (int) = 0.0539]
Completeness to theta = 25.000°	100.0%
Observed reflections	6471 [<i>I</i> > 2σ(<i>I</i>)]
Reflections used for refinement	7292
Absorption correction	Semi-empirical from equivalents
Max. and min. transmission	0.7455 and 0.5709
Largest diff. peak and hole	0.423 and -0.517 e·Å ⁻³
Solution	direct/difmap
Refinement	Full-matrix least-squares on <i>F</i> ²
Treatment of hydrogen atoms	geom/constr
Data / restraints / parameters	7292 / 0 / 343
Goodness-of-fit on <i>F</i> ²	1.040
<i>R</i> index (all data)	<i>R</i> ₁ = 0.0249 <i>wR</i> ₂ = 0.0352
<i>R</i> index conventional [<i>I</i> > 2σ(<i>I</i>)]	<i>R</i> ₁ = 0.0182 <i>wR</i> ₂ = 0.0338

Chlorido(cyclooctadien){tris[tris(pyrrolidino)-phosphazeny]phosphane}rhodium(I) (20)

Crystal growth	Sebastian Ullrich
Solution and refinement	Sebastian Ullrich
Identification code	SU060Rh
Habitus, colour	block, clear yellow
Crystal size	0.540 x 0.438 x 0.423 mm ³
Crystal system	Monoclinic
Space group	<i>P</i> 2 ₁ / <i>c</i> <i>Z</i> = 4
Unit cell dimensions	
<i>a</i> = 10.8921(8) Å	<i>α</i> = 90°
<i>b</i> = 21.4392(15) Å	<i>β</i> = 105.752(2)°
<i>c</i> = 17.2190(12) Å	<i>γ</i> = 90°
Volume	3869.9(5) Å ³
Cell determination	9574 peaks with <i>θ</i> 2.2 to 27.2°
Empirical formula	C ₂₆ H ₆₆ ClN ₁₂ P ₄ Rh
Formula weight	809.14
Density (calculated)	1.389 g·cm ⁻³
Absorption coefficient	0.711 mm ⁻¹
F(000)	1712
Diffractometer type	Bruker D8 Quest
Wavelength	0.71073 Å
Temperature	100(2) K
Theta range for data collection	2.211 to 27.267°
Index ranges	
-14 ≤ <i>h</i> ≤ 13, -27 ≤ <i>k</i> ≤ 27, -21 ≤ <i>l</i> ≤ 22	
Reflections collected	86185
Independent reflections	8635 [<i>R</i> (int) = 0.0525]
Completeness to theta = 25.000°	99.9%
Observed reflections	7671 [<i>I</i> > 2σ(<i>I</i>)]
Reflections used for refinement	8635
Absorption correction	Semi-empirical from equivalents
Max. and min. transmission	0.7455 and 0.6803
Largest diff. peak and hole	0.524 and -0.667 e·Å ⁻³
Solution	dual/difmap
Refinement	Full-matrix least-squares on F ²
Treatment of hydrogen atoms	geom/constr
Data / restraints / parameters	8635 / 0 / 434
Goodness-of-fit on F ²	1.167
<i>R</i> index (all data)	<i>R</i> ₁ = 0.0417
	<i>wR</i> ₂ = 0.0717
<i>R</i> index conventional [<i>I</i> > 2σ(<i>I</i>)]	<i>R</i> ₁ = 0.0343
	<i>wR</i> ₂ = 0.0697
Refinement special details	
Two CH ₂ groups of the cyclooctadien were refined in 2-component disorder.	

(*η*¹-Allyl)chlorido{*κ*²-tris[tris(dimethylamino)-phosphazeny]phosphane}palladium(II) (21)

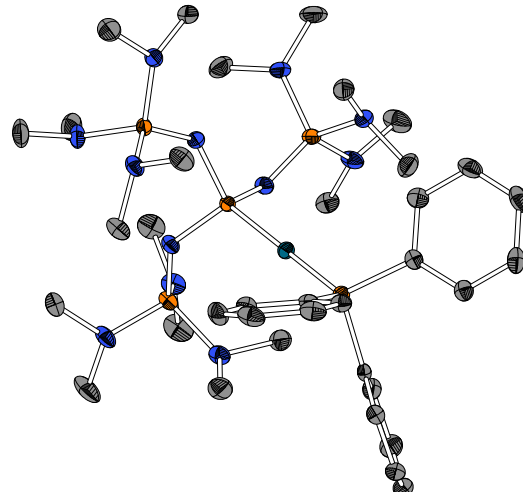
Crystal growth	Sebastian Ullrich
Solution and refinement	Sebastian Ullrich
Identification code	SU060Pd
Habitus, colour	plate, clear yellow
Crystal size	0.390 x 0.387 x 0.070 mm ³
Crystal system	Monoclinic
Space group	<i>Cc</i> <i>Z</i> = 4
Unit cell dimensions	
<i>a</i> = 11.7813(8) Å	<i>α</i> = 90°
<i>b</i> = 21.5773(14) Å	<i>β</i> = 98.293(2)°
<i>c</i> = 14.2651(10) Å	<i>γ</i> = 90°
Volume	3588.4(4) Å ³
Cell determination	9747 peaks with <i>θ</i> 3.3 to 27.1°
Empirical formula	C ₂₁ H ₅₉ ClN ₁₂ P ₄ Pd
Formula weight	745.53
Density (calculated)	1.380 g·cm ⁻³
Absorption coefficient	0.802 mm ⁻¹
F(000)	1568
Diffractometer type	Bruker D8 Quest
Wavelength	0.71073 Å
Temperature	100(2) K
Theta range for data collection	2.302 to 27.160°
Index ranges	
-15 ≤ <i>h</i> ≤ 15, -27 ≤ <i>k</i> ≤ 27, -18 ≤ <i>l</i> ≤ 18	
Reflections collected	42651
Independent reflections	7642 [<i>R</i> (int) = 0.0234]
Completeness to theta = 25.000°	99.9%
Observed reflections	7418 [<i>I</i> > 2σ(<i>I</i>)]
Reflections used for refinement	7642
Absorption correction	Semi-empirical from equivalents
Max. and min. transmission	0.7455 and 0.6836
Flack parameter (absolute struct.)	0.185(14)
Largest diff. peak and hole	0.176 and -0.528 e·Å ⁻³
Solution	dual/difmap
Refinement	Full-matrix least-squares on F ²
Treatment of hydrogen atoms	geom/constr
Data / restraints / parameters	7642 / 2 / 371
Goodness-of-fit on F ²	1.076
<i>R</i> index (all data)	<i>R</i> ₁ = 0.0182
	<i>wR</i> ₂ = 0.0168
<i>R</i> index conventional [<i>I</i> > 2σ(<i>I</i>)]	<i>R</i> ₁ = 0.0407
	<i>wR</i> ₂ = 0.0399
Refinement special details	
Refined as 2-component inversion twin.	

Dichloridobis{tris[tris(pyrrolidino)phosphazeny]-phosphane}platinum(II) (22)

Crystal growth	Sebastian Ullrich
Solution and refinement	Sebastian Ullrich
Identification code	SU060Pt
Habitus, colour	block, clear colourless
Crystal size	0.810 x 0.335 x 0.222 mm ³
Crystal system	Triclinic
Space group	$P\bar{1}$ $Z = 1$
Unit cell dimensions	
$a = 11.6541(8)$ Å	$\alpha = 112.565(2)^\circ$
$b = 12.3635(9)$ Å	$\beta = 93.079(2)^\circ$
$c = 14.3798(10)$ Å	$\gamma = 117.734(2)^\circ$
Volume	1623.7(2) Å ³
Cell determination	9594 peaks with θ 2.9 to 27.2°
Empirical formula	C ₃₆ H ₁₀₈ Cl ₂ N ₂₄ P ₈ Pt
Formula weight	1391.20
Density (calculated)	1.423 g·cm ⁻³
Absorption coefficient	2.487 mm ⁻¹
F(000)	724
Diffractometer type	Bruker D8 Quest
Wavelength	0.71073 Å
Temperature	100(2) K
Theta range for data collection	2.808 to 27.305°
Index ranges	
	$-14 \leq h \leq 14, -15 \leq k \leq 15, -18 \leq l \leq 18$
Reflections collected	56753
Independent reflections	7241 [$R(\text{int}) = 0.0332$]
Completeness to theta = 25.000°	99.8%
Observed reflections	7237 [$I > 2\sigma(I)$]
Reflections used for refinement	7242
Extinction coefficient	$X = 0.0071(4)$
Absorption correction	Semi-empirical from equivalents
Max. and min. transmission	0.7455 and 0.5101
Largest diff. peak and hole	1.299 and -1.360 e·Å ⁻³
Solution	dual/difmap
Refinement	Full-matrix least-squares on F ²
Treatment of hydrogen atoms	geom/constr
Data / restraints / parameters	7241 / 0 / 341
Goodness-of-fit on F ²	1.063
R index (all data)	$R_1 = 0.0174$ $wR_2 = 0.0460$
R index conventional [$I > 2\sigma(I)$]	$R_1 = 0.0174$ $wR_2 = 0.0459$

Refinement special details

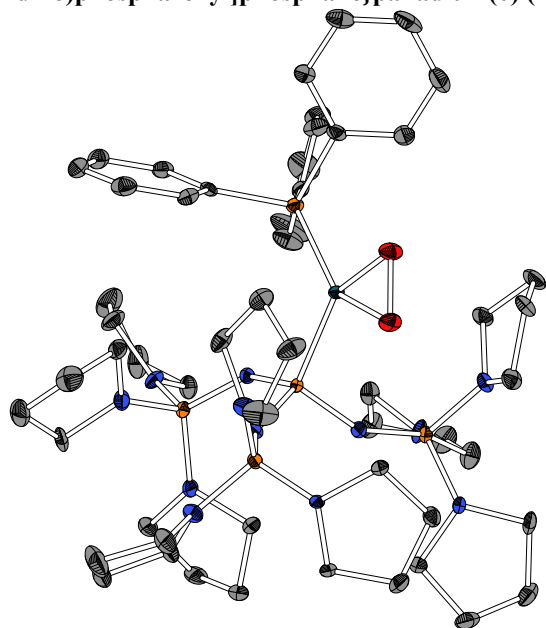
The asymmetric unit contains a half molecule completed by inversion. Four reflections were omitted from the least-squares refinement using OMIT.

Triphenylphosphane{tris[tris(dimethylamino)-phosphazeny]phosphane}palladium(0) (23a)

Crystal growth	Sebastian Ullrich
Solution and refinement	Sebastian Ullrich
Identification code	SU06033
Habitus, colour	block, clear orange
Crystal size	0.328 x 0.264 x 0.261 mm ³
Crystal system	Cubic
Space group	$P\bar{a}3$ $Z = 8$
Unit cell dimensions	
$a = 21.6458(7)$ Å	$\alpha = 90^\circ$
$b = 21.6458(7)$ Å	$\beta = 90^\circ$
$c = 21.6458(7)$ Å	$\gamma = 90^\circ$
Volume	10141.9(10) Å ³
Cell determination	9336 peaks with θ 2.3 to 27.1°
Empirical formula	C ₃₆ H ₆₉ N ₁₂ P ₅ Pd
Formula weight	931.28
Density (calculated)	1.220 g·cm ⁻³
Absorption coefficient	0.560 mm ⁻¹
F(000)	3920
Diffractometer type	Bruker D8 Quest
Wavelength	0.71073 Å
Temperature	100(2) K
Theta range for data collection	2.305 to 27.101°
Index ranges	
	$-26 \leq h \leq 27, -27 \leq k \leq 27, -23 \leq l \leq 27$
Reflections collected	54567
Independent reflections	3737 [$R(\text{int}) = 0.0687$]
Completeness to theta = 25.000°	99.9%
Observed reflections	3106 [$I > 2\sigma(I)$]
Reflections used for refinement	3737
Absorption correction	Semi-empirical from equivalents
Max. and min. transmission	0.7455 and 0.6595
Largest diff. peak and hole	0.403 and -0.371 e·Å ⁻³
Solution	dual/difmap
Refinement	Full-matrix least-squares on F ²
Treatment of hydrogen atoms	geom/constr
Data / restraints / parameters	3737 / 0 / 169
Goodness-of-fit on F ²	1.027
R index (all data)	$R_1 = 0.0418$ $wR_2 = 0.0717$
R index conventional [$I > 2\sigma(I)$]	$R_1 = 0.0299$ $wR_2 = 0.0673$

Refinement special details

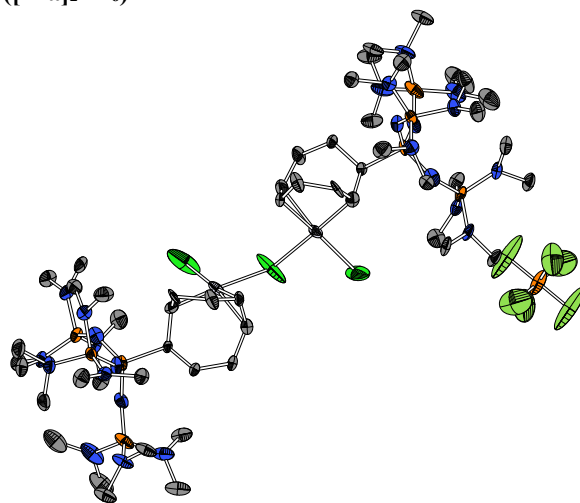
The asymmetric unit contains a third of a molecule completed by a threefold axis alongside the P–Pd bonds. A half *n*-pentane molecule lies on an inversion center with a threefold axis and could therefore not be refined distinctly and was addressed by SQUEEZE routine. One reflection was omitted from the least-squares refinement using OMIT.

(η^2 -Peroxyd)(triphenylphosphane){tris[tris(pyrrolidino)phosphazeny]lphosphane;palladium(0)} (25)

Crystal growth	Sebastian Ullrich
Solution and refinement	Sebastian Ullrich
Identification code	SU06214
Habitus, colour	block, clear yellow
Crystal size	0.388 x 0.217 x 0.146 mm ³
Crystal system	Monoclinic
Space group	$P2_1$ $Z = 4$
Unit cell dimensions	
$a = 11.8617(5)$ Å	$\alpha = 90^\circ$
$b = 24.3936(12)$ Å	$\beta = 93.591(2)^\circ$
$c = 19.8992(9)$ Å	$\gamma = 90^\circ$
Volume	$5746.5(5)$ Å ³
Cell determination	9708 peaks with θ 2.6 to 27.1°
Empirical formula	$C_{54}H_{87}N_{12}O_2P_5Pd$
Formula weight	1197.60
Density (calculated)	1.384 g·cm ⁻³
Absorption coefficient	0.514 mm ⁻¹
F(000)	2528
Diffractometer type	Bruker D8 Quest
Wavelength	0.71073 Å
Temperature	100(2) K
Theta range for data collection	2.118 to 27.141°
Index ranges	
$-15 \leq h \leq 14, -31 \leq k \leq 26, -23 \leq l \leq 25$	
Reflections collected	75755
Independent reflections	23540 [$R(\text{int}) = 0.0460$]
Completeness to theta = 25.242°	99.9%
Observed reflections	21336 [$I > 2\sigma(I)$]
Reflections used for refinement	23540
Absorption correction	Semi-empirical from equivalents
Max. and min. transmission	0.7455 and 0.6574
Flack parameter (absolute struct.)	-0.017(8)
Largest diff. peak and hole	0.507 and -0.474 e·Å ⁻³
Solution	dual/difmap
Refinement	Full-matrix least-squares on F ²
Treatment of hydrogen atoms	geom/constr
Data / restraints / parameters	23540 / 229 / 1408
Goodness-of-fit on F ²	1.021
R index (all data)	$R_1 = 0.0417$ $wR_2 = 0.0661$
R index conventional [$I > 2\sigma(I)$]	$R_1 = 0.0328$ $wR_2 = 0.0634$

Refinement special details

The asymmetric unit contains two independent molecules. No Flack check done due to low Friedel pair coverage (85%). Three pyrrolidine rings were refined in 2-component disorder using SIMU and RIGU restraints. One reflection was omitted from the least-squares refinement using OMIT. Water accessible void of 46 Å³ was addressed by SQUEEZE routine.

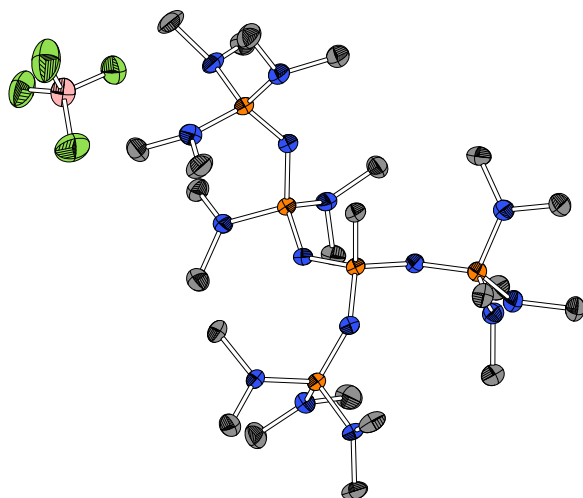
(μ -Chlorido)(chlorido)[8-{[tris(dimethylamino)phosphazeny]lphosphonio}cyclooct-4-en-1-yl]-platinum(II) dimer hexafluoridophosphate ([27a]₂PF₆)

Crystal growth	Sebastian Ullrich
Solution and refinement	Sebastian Ullrich
Identification code	SU060PtPF6
Habitus, colour	plate, clear colourless
Crystal size	0.490 x 0.156 x 0.150 mm ³
Crystal system	Monoclinic
Space group	$C2/c$ $Z = 8$
Unit cell dimensions	
$a = 19.6637(17)$ Å	$\alpha = 90^\circ$
$b = 12.0100(10)$ Å	$\beta = 101.050(2)^\circ$
$c = 38.338(3)$ Å	$\gamma = 90^\circ$
Volume	$8886.1(13)$ Å ³
Cell determination	9002 peaks with θ 2.4 to 25.4°
Empirical formula	$C_{54}H_{136}Cl_7F_6N_{24}P_9Pt_2$
Formula weight	2152.92
Density (calculated)	1.609 g·cm ⁻³
Absorption coefficient	3.580 mm ⁻¹
F(000)	4368
Diffractometer type	Bruker D8 Quest
Wavelength	0.71073 Å
Temperature	100(2) K
Theta range for data collection	2.165 to 25.461°
Index ranges	
$-23 \leq h \leq 23, -14 \leq k \leq 14, -45 \leq l \leq 46$	
Reflections collected	51325
Independent reflections	8176 [$R(\text{int}) = 0.0607$]
Completeness to theta = 25.000°	99.9%
Observed reflections	7359 [$I > 2\sigma(I)$]
Reflections used for refinement	8176
Absorption correction	Semi-empirical from equivalents
Max. and min. transmission	0.7452 and 0.5860
Largest diff. peak and hole	3.042 and -9.378 e·Å ⁻³
Solution	dual/difmap
Refinement	Full-matrix least-squares on F ²
Treatment of hydrogen atoms	geom/constr
Data / restraints / parameters	8176 / 738 / 743
Goodness-of-fit on F ²	1.394
R index (all data)	$R_1 = 0.1174$ $wR_2 = 0.2450$
R index conventional [$I > 2\sigma(I)$]	$R_1 = 0.1090$ $wR_2 = 0.2418$

Refinement special details

Poor data due to twinning/disorder does not allow detailed structure analysis. The asymmetric unit contains a half of a molecule completed by a twofold axis and one dichloromethane molecule. The phosphazeny phosphane was refined in 2-component disorder using RIGU, SIMU, ISOR and SAME.

Methyl[pentakis(dimethylamino)diphosphazeny]-bis[tris(dimethylamino)phosphazeny]phosphonium tetrafluoridoborate/iodide (30·0.78 HBF₄/ 0.22 HI)

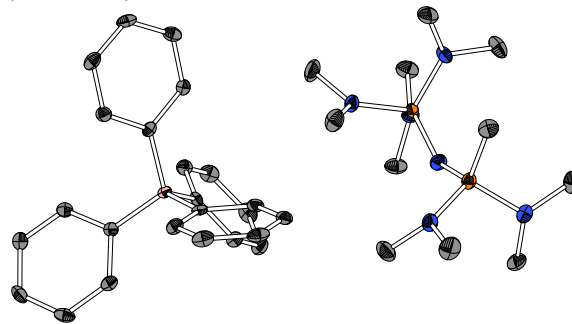


Crystal growth	Sebastian Ullrich
Solution and refinement	Sebastian Ullrich
Identification code	P5Y
Habitus, colour	prism, colourless
Crystal size	0.235 x 0.192 x 0.139 mm ³
Crystal system	Triclinic
Space group	$P\bar{1}$
Unit cell dimensions	$Z = 4$
$a = 8.5623(2)$ Å	$\alpha = 81.1190(10)^\circ$
$b = 18.8848(4)$ Å	$\beta = 83.1870(10)^\circ$
$c = 26.1839(5)$ Å	$\gamma = 81.6430(10)^\circ$
Volume	4118.60(15) Å ³
Cell determination	41685 peaks with θ 2.4 to 76.5°
Empirical formula	C ₂₃ H ₆₉ B _{0.78} F _{3.12} I _{0.22} N ₁₅ P ₅
Formula weight	806.38
Density (calculated)	1.300 g·cm ⁻³
Absorption coefficient	3.789 mm ⁻¹
F(000)	1723
Diffractometer type	Stoe Stadivari
Wavelength	1.54178 Å
Temperature	100(2) K
Theta range for data collection	2.388 to 75.898°
Index ranges	
$-10 \leq h \leq 10, -22 \leq k \leq 10, -32 \leq l \leq 32$	
Reflections collected	78955
Independent reflections	16837 [$R(\text{int}) = 0.0649$]
Completeness to theta = 70.000°	99.2 %
Observed reflections	12501 [$I > 2\sigma(I)$]
Reflections used for refinement	16837
Absorption correction	Semi-empirical from equivalents
Max. and min. transmission	1.0000 and 0.3447
Largest diff. peak and hole	1.144 and -0.879 e·Å ⁻³
Solution	dual/difmap
Refinement	Full-matrix least-squares on F ²
Treatment of hydrogen atoms	geom/constr
Data / restraints / parameters	16837 / 32 / 942
Goodness-of-fit on F ²	1.012
R index (all data)	$R_1 = 0.0936$
	$wR_2 = 0.2233$
R index conventional [$I > 2\sigma(I)$]	$R_1 = 0.0747$
	$wR_2 = 0.2066$

Refinement special details

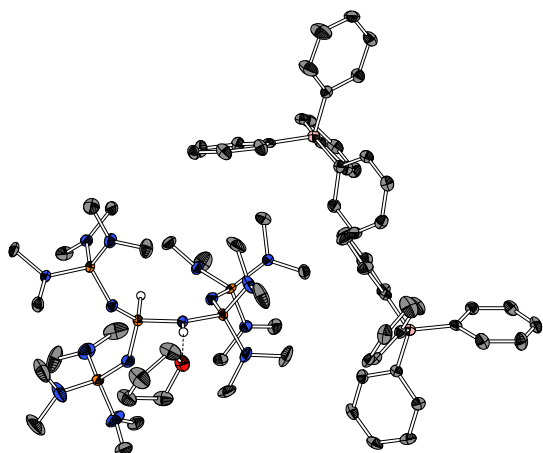
The asymmetric unit contains two independent molecules. Anion positions were refined as 2-component disorder of BF₄⁻ and I⁻ in a 0.78/0.22 ratio. BF₄⁻-Anions were refined using RIGU and SIMU restraints. One dimethylamino group was refined in 2-component disorder. One reflections was omitted from the least-squares refinement using OMIT.

Methyl[tris(dimethylamino)phosphazeny]bis-(dimethylamino)phosphonium tetraphenylborate (32·HBPh₄)



Crystal growth	Sebastian Ullrich
Solution and refinement	Sebastian Ullrich
Identification code	SU012BPh4
Habitus, colour	plate, clear colourless
Crystal size	0.369 x 0.254 x 0.104 mm ³
Crystal system	Monoclinic
Space group	$P2_1$
Unit cell dimensions	$Z = 2$
$a = 9.8579(7)$ Å	$\alpha = 90^\circ$
$b = 10.8096(7)$ Å	$\beta = 94.699(2)^\circ$
$c = 16.5553(12)$ Å	$\gamma = 90^\circ$
Volume	1758.2(2) Å ³
Cell determination	9818 peaks with θ 2.3 to 27.1°
Empirical formula	C ₃₅ H ₅₃ BN ₆ P ₂
Formula weight	630.58
Density (calculated)	1.191 g·m ⁻³
Absorption coefficient	0.157 mm ⁻¹
F(000)	680
Diffractometer type	Bruker D8 Quest
Wavelength	0.71073 Å
Temperature	100(2) K
Theta range for data collection	2.252 to 27.152°
Index ranges	
$-12 \leq h \leq 12, -13 \leq k \leq 13, -21 \leq l \leq 21$	
Reflections collected	51905
Independent reflections	7789 [$R(\text{int}) = 0.0671$]
Completeness to theta = 25.242°	99.9%
Observed reflections	7051 [$I > 2\sigma(I)$]
Reflections used for refinement	7789
Absorption correction	Semi-empirical from equivalents
Max. and min. transmission	0.7455 and 0.7035
Flack parameter (absolute struct.)	0.17(8)
Largest diff. peak and hole	0.866 and -0.449 e·Å ⁻³
Solution	dual/difmap
Refinement	Full-matrix least-squares on F ²
Treatment of hydrogen atoms	geom/constr
Data / restraints / parameters	7789 / 1 / 409
Goodness-of-fit on F ²	1.027
R index (all data)	$R_1 = 0.0403$
	$wR_2 = 0.0843$
R index conventional [$I > 2\sigma(I)$]	$R_1 = 0.0338$
	$wR_2 = 0.0818$
Refinement special details	
Refined as 2-component inversion twin.	

**[Pentakis(dimethylamino)diphosphazeny]bis-
[tris(dimethylamino)phosphazeny]phosphonium
bis(tetraphenylborate) (dma)P₄P·2HBPh₄·THF**

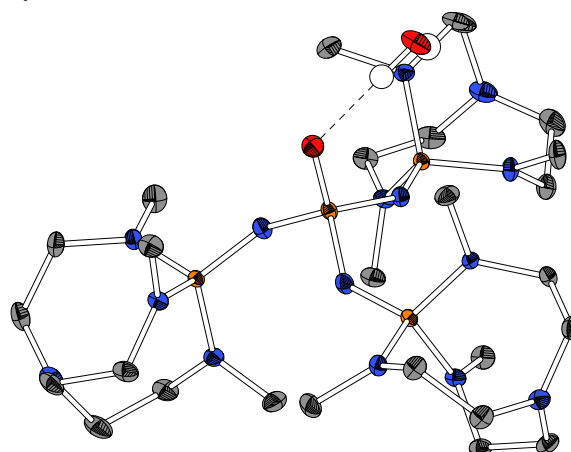


Crystal growth	Sebastian Ullrich
Solution and refinement	Sebastian Ullrich
Identification code	SU021BPh4
Habitus, colour	block, clear colourless
Crystal size	0.464 x 0.351 x 0.327 mm ³
Crystal system	Monoclinic
Space group	<i>P</i> 2 ₁ / <i>c</i> <i>Z</i> = 4
Unit cell dimensions	
<i>a</i> = 14.3325(7) Å	<i>a</i> = 90°
<i>b</i> = 25.8670(12) Å	<i>b</i> = 94.021(2)°
<i>c</i> = 21.0009(10) Å	<i>c</i> = 90°
Volume	7766.7(6) Å ³
Cell determination	9507 peaks with θ 2.3 to 25.3°
Empirical formula	C ₇₄ H ₁₁₆ B ₂ N ₁₅ OP ₅
Formula weight	1408.28
Density (calculated)	1.204 g·cm ⁻³
Absorption coefficient	0.171 mm ⁻¹
F(000)	3032
Diffractometer type	Bruker D8 Quest
Wavelength	0.71073 Å
Temperature	100(2) K
Theta range for data collection	2.293 to 25.415°
Index ranges	
	-17 ≤ <i>h</i> ≤ 17, -31 ≤ <i>k</i> ≤ 31, -25 ≤ <i>l</i> ≤ 25
Reflections collected	187824
Independent reflections	14275 [<i>R</i> (int) = 0.0625]
Completeness to theta = 25.000°	99.9%
Observed reflections	12016 [<i>I</i> > 2σ(<i>I</i>)]
Reflections used for refinement	14275
Absorption correction	Semi-empirical from equivalents
Max. and min. transmission	0.7452 and 0.7087
Largest diff. peak and hole	0.517 and -0.417 e·Å ⁻³
Solution	dual/difmap
Refinement	Full-matrix least-squares on F ²
Treatment of hydrogen atoms	mixed/mixed
Data / restraints / parameters	14275 / 222 / 1074
Goodness-of-fit on F ²	1.056
<i>R</i> index (all data)	<i>R</i> ₁ = 0.0555 <i>wR</i> ₂ = 0.1046
<i>R</i> index conventional [<i>I</i> > 2σ(<i>I</i>)]	<i>R</i> ₁ = 0.0432 <i>wR</i> ₂ = 0.0988

Refinement special details

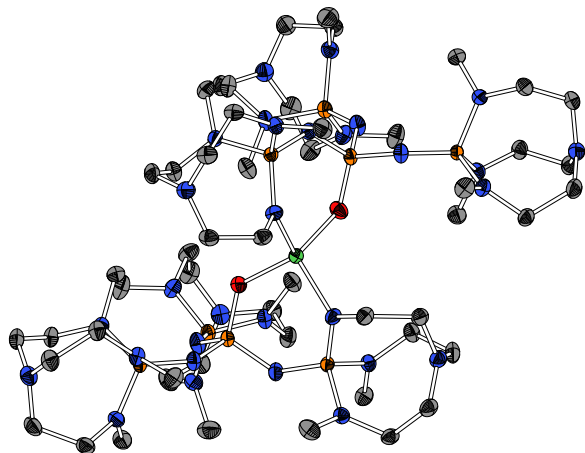
One phosphazeny group was refined in 2-component disorder using SIMU RIGU, ISOR and SAME restraints, three additional dimethylamino groups were refined in 2-component disorder using RIGU and SIMU restraints. Heteroatom bonded protons were refined with isotropic temperature factors at 1.5 times that of the carrier atom. Three reflections were omitted from the least-squares refinement using OMIT.

**Tris[1-imino-2,8,9-trimethyl-2,5,8,9-tetraaza-1-
phospha-bicyclo[3.3.3]undecane]phosphane oxide
hydrate**



Crystal growth	Jens Braczek
Solution and refinement	Sebastian Ullrich
Identification code	JBBA1001
Habitus, colour	block, clear colourless
Crystal size	0.258 x 0.130 x 0.116 mm ³
Crystal system	Triclinic
Space group	<i>P</i> $\bar{1}$ <i>Z</i> = 2
Unit cell dimensions	
<i>a</i> = 12.8045(6) Å	<i>a</i> = 82.355(2)°
<i>b</i> = 13.0880(6) Å	<i>b</i> = 69.3100(10)°
<i>c</i> = 13.6860(6) Å	<i>c</i> = 62.3810(10)°
Volume	1899.84(15) Å ³
Cell determination	9356 peaks with θ 2.3 to 27.1°
Empirical formula	C ₂₇ H ₄₅ N ₁₅ O ₂ P ₄
Formula weight	755.82
Density (calculated)	1.321 g·cm ⁻³
Absorption coefficient	0.247 mm ⁻¹
F(000)	816
Diffractometer type	Bruker D8 Quest
Wavelength	0.71073 Å
Temperature	100(2) K
Theta range for data collection	2.327 to 27.170°
Index ranges	
	-16 ≤ <i>h</i> ≤ 16, -16 ≤ <i>k</i> ≤ 16, -17 ≤ <i>l</i> ≤ 17
Reflections collected	72697
Independent reflections	8417 [<i>R</i> (int) = 0.0723]
Completeness to theta = 25.000°	99.9%
Observed reflections	6668 [<i>I</i> > 2σ(<i>I</i>)]
Reflections used for refinement	8417
Absorption correction	Semi-empirical from equivalents
Max. and min. transmission	0.7451 and 0.7296
Largest diff. peak and hole	0.314 and -0.441 e·Å ⁻³
Solution	dual/ difmap
Refinement	Full-matrix least-squares on F ²
Treatment of hydrogen atoms	mixed/hetero
Data / restraints / parameters	8417 / 0 / 450
Goodness-of-fit on F ²	1.035
<i>R</i> index (all data)	<i>R</i> ₁ = 0.0600 <i>wR</i> ₂ = 0.0897
<i>R</i> index conventional [<i>I</i> > 2σ(<i>I</i>)]	<i>R</i> ₁ = 0.0396 <i>wR</i> ₂ = 0.0828

Bis{ κ^2 -[1-imino-2,8-dimethyl-2,5,8,9-tetraaza-1-phospha-bicyclo[3.3.3]undecane]bis[1-imino-2,8,9-trimethyl-2,5,8,9-tetraaza-1-phospha-bicyclo[3.3.3]undecane]phosphane oxide}nickel(0)

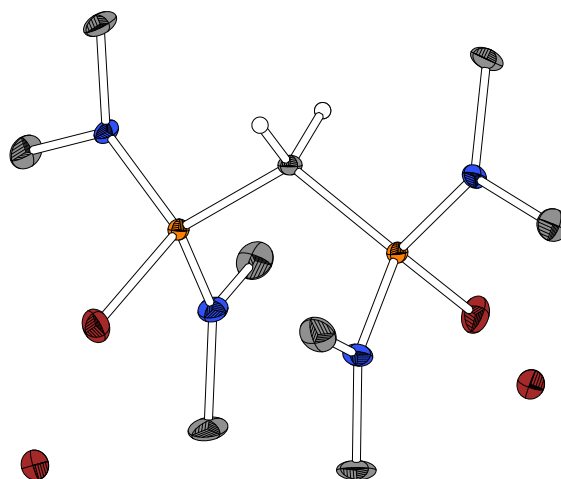


Crystal growth	Jens Braczek
Solution and refinement	Sebastian Ullrich
Identification code	JBBANiX
Habitus, colour	prism, purple
Crystal size	0.428 x 0.329 x 0.138 mm ³
Crystal system	Monoclinic
Space group	<i>C2/c</i> <i>Z</i> = 4
Unit cell dimensions	
<i>a</i> = 24.2376(6) Å	<i>α</i> = 90°
<i>b</i> = 12.7182(2) Å	<i>β</i> = 111.021(2)°
<i>c</i> = 24.9927(8) Å	<i>γ</i> = 90°
Volume	7191.5(3) Å ³
Cell determination	72317 peaks with <i>θ</i> 2.3 to 34.8°
Empirical formula	C ₅₂ H ₁₂₀ N ₃₀ NiO ₂ P ₈
Formula weight	1504.23
Density (calculated)	1.389 g·cm ⁻³
Absorption coefficient	0.510 mm ⁻¹
F(000)	3224
Diffractometer type	Stoe Stadivari
Wavelength	0.71073 Å
Temperature	100(2) K
Theta range for data collection	2.301 to 34.693°
Index ranges	
-38 ≤ <i>h</i> ≤ 28, -18 ≤ <i>k</i> ≤ 19, -38 ≤ <i>l</i> ≤ 39	
Reflections collected	53670
Independent reflections	14402 [<i>R</i> (int) = 0.0368]
Completeness to <i>θ</i> = 25.000°	99.6%
Observed reflections	11489 [<i>I</i> > 2σ(<i>I</i>)]
Reflections used for refinement	14402
Absorption correction	Semi-empirical from equivalents
Max. and min. transmission	1.0000 and 0.3621
Largest diff. peak and hole	0.712 and -0.671 e·Å ⁻³
Solution	dual/ difmap
Refinement	Full-matrix least-squares on F ²
Treatment of hydrogen atoms	geom/constr
Data / restraints / parameters	14402 / 0 / 428
Goodness-of-fit on F ²	1.029
<i>R</i> index (all data)	<i>R</i> ₁ = 0.0584
	<i>wR</i> ₂ = 0.1224
<i>R</i> index conventional [<i>I</i> > 2σ(<i>I</i>)]	<i>R</i> ₁ = 0.0426
	<i>wR</i> ₂ = 0.1120

Refinement special details

The asymmetric unit contains a half molecule completed by a twofold axis.

Methylenebis[bromobis(dimethylamino)-phosphonium] bromide



Crystal growth	Björn Koch
Solution and refinement	Sebastian Ullrich
Identification code	SU06210
Habitus, colour	block, clear colourless
Crystal size	0.430 x 0.285 x 0.226 mm ³
Crystal system	Monoclinic
Space group	<i>C2/c</i> <i>Z</i> = 4
Unit cell dimensions	
<i>a</i> = 14.4552(8) Å	<i>α</i> = 90°
<i>b</i> = 12.1542(6) Å	<i>β</i> = 112.134(2)°
<i>c</i> = 13.8218(7) Å	<i>γ</i> = 90°
Volume	2249.4(2) Å ³
Cell determination	9907 peaks with <i>θ</i> 2.3 to 27.1°
Empirical formula	C ₁₀ H ₂₈ Br ₄ Cl ₂ N ₄ P ₂
Formula weight	656.84
Density (calculated)	1.940 g·cm ⁻³
Absorption coefficient	7.537 mm ⁻¹
F(000)	1280
Diffractometer type	Bruker D8 Quest
Wavelength	0.71073 Å
Temperature	100(2) K
Theta range for data collection	2.263 to 27.145°
Index ranges	
-18 ≤ <i>h</i> ≤ 18, -15 ≤ <i>k</i> ≤ 15, -14 ≤ <i>l</i> ≤ 17	
Reflections collected	11738
Independent reflections	2472 [<i>R</i> (int) = 0.0290]
Completeness to <i>θ</i> = 25.000°	99.2 %
Observed reflections	2353 [<i>I</i> > 2σ(<i>I</i>)]
Reflections used for refinement	2472
Extinction coefficient	<i>X</i> = 0.00190(17)
Absorption correction	Semi-empirical from equivalents
Max. and min. transmission	0.7455 and 0.4181
Largest diff. peak and hole	1.712 and -0.854 e·Å ⁻³
Solution	dual/difmap
Refinement	Full-matrix least-squares on F ²
Treatment of hydrogen atoms	geom/constr
Data / restraints / parameters	2472 / 0 / 106
Goodness-of-fit on F ²	1.085
<i>R</i> index (all data)	<i>R</i> ₁ = 0.0277
	<i>wR</i> ₂ = 0.0663
<i>R</i> index conventional [<i>I</i> > 2σ(<i>I</i>)]	<i>R</i> ₁ = 0.0260
	<i>wR</i> ₂ = 0.0654

Refinement special details

The asymmetric unit contains a half molecule and a half dichloromethane molecule, both completed by a twofold axis.

9 Literaturverzeichnis

- [1] A. F. Holleman, E. Wiberg, N. Wiberg, *Lehrbuch der anorganischen Chemie*, 102. Aufl., de Gruyter, Berlin, New York, **2007**.
- [2] J. Clayden, N. Greeves, S. G. Warren, *Organic chemistry*, 2. Aufl., Oxford University Press, Oxford, New York, **2012**.
- [3] P. W. Atkins, J. de Paula, *Physikalische Chemie*, 4. Aufl., Wiley-VCH, Weinheim, **2006**.
- [4] T. Ishikawa, *Superbases for organic synthesis. Guanidines, amidines and phosphazenes and related organocatalysts*, Wiley, Chichester, West Sussex, U.K., **2009**.
- [5] S. Arrhenius, *Z. Phys. Chem.* **1887**, *1U*, 631.
- [6] J. N. Brønsted, *Recl. Trav. Chim. Pays-Bas* **1923**, *42*, 718.
- [7] T. M. Lowry, *J. Chem. Technol. Biotechnol.* **1923**, *42*, 43.
- [8] J. F. Bunnett, R. A. Y. Jones, *Pure Appl. Chem.* **1988**, *60*, 1115.
- [9] G. N. Lewis, *Valence and the Structure of Atoms and Molecules*, Chemical Catalog Company, Incorporated, New York, **1923**.
- [10] R. G. Pearson, *J. Am. Chem. Soc.* **1963**, *85*, 3533.
- [11] M. Usanovich, *J. Gen. Chem. USSR* **1939**, *9*, 182.
- [12] a) H. Lux, *Z. Elektrochem.* **1939**, *45*, 303; b) H. Flood, T. Förland, L. G. Sillén, A. Linnasalmi, P. Laukkanen, *Acta Chem. Scand.* **1947**, *1*, 592.
- [13] D.H. Ripin, D.A. Evans, "pKa Table", zu finden unter http://evans.rc.fas.harvard.edu/pdf/evans_pKa_table.pdf.
- [14] J. Saame, T. Rodima, S. Tshepelevitsh, A. Kütt, I. Kaljurand, T. Haljasorg, I. A. Koppel, I. Leito, *J. Org. Chem.* **2016**, *81*, 7349.
- [15] J. F. Kögel, X. Xie, E. Baal, D. Gesevičius, B. Oelkers, B. Kovačević, J. Sundermeyer, *Chem. Eur. J.* **2014**, *20*, 7670.
- [16] E. D. Nacsa, T. H. Lambert, *J. Am. Chem. Soc.* **2015**, *137*, 10246.
- [17] P. B. Kisanga, J. G. Verkade, R. Schwesinger, *J. Org. Chem.* **2000**, *65*, 5431.
- [18] G. Garrido, E. Koort, C. Ràfols, E. Bosch, T. Rodima, I. Leito, M. Rosés, *J. Org. Chem.* **2006**, *71*, 9062.
- [19] R. Schwesinger, H. Schlemper, C. Hasenfratz, J. Willaredt, T. Dambacher, T. Breuer, C. Ottaway, M. Fletschinger, J. Boele, H. Fritz et al., *Liebigs Ann./Recl.* **1996**, *1996*, 1055.
- [20] a) X. M. Zhang, F. G. Bordwell, *J. Am. Chem. Soc.* **1994**, *116*, 968; b) X.-M. Zhang, A. J. Fry, F. G. Bordwell, *J. Org. Chem.* **1996**, *61*, 4101.
- [21] I. Kaljurand, T. Rodima, I. Leito, I. A. Koppel, R. Schwesinger, *J. Org. Chem.* **2000**, *65*, 6202.
- [22] I. Kaljurand, A. Kütt, L. Sooväli, T. Rodima, V. Mäemets, I. Leito, I. A. Koppel, *J. Org. Chem.* **2005**, *70*, 1019.
- [23] A. Kütt, I. Leito, I. Kaljurand, L. Sooväli, V. M. Vlasov, L. M. Yagupolskii, I. A. Koppel, *J. Org. Chem.* **2006**, *71*, 2829.

- [24] I. Kaljurand, J. Saame, T. Rodima, I. Koppel, I. A. Koppel, J. F. Kögel, J. Sundermeyer, U. Köhn, M. P. Coles, I. Leito, *J. Phys. Chem. A* **2016**, *120*, 2591.
- [25] E. Paenurk, K. Kaupmees, D. Himmel, A. Kütt, I. Kaljurand, I. A. Koppel, I. Krossing, I. Leito, *Chem. Sci.* **2017**, *8*, 6964.
- [26] F. G. Bordwell, *Acc. Chem. Res.* **1988**, *21*, 456.
- [27] T. Rodima, I. Kaljurand, A. Pihl, V. Mäemets, I. Leito, I. A. Koppel, *J. Org. Chem.* **2002**, *67*, 1873.
- [28] I. Kaljurand, T. Rodima, A. Pihl, V. Mäemets, I. Leito, I. A. Koppel, M. Mishima, *J. Org. Chem.* **2003**, *68*, 9988.
- [29] A. A. Kolomeitsev, I. A. Koppel, T. Rodima, J. Barten, E. Lork, G.-V. Rösenthaller, I. Kaljurand, A. Kütt, I. Koppel, V. Mäemets et al., *J. Am. Chem. Soc.* **2005**, *127*, 17656.
- [30] A. Kütt, S. Selberg, I. Kaljurand, S. Tshepelevitsh, A. Heering, A. Darnell, K. Kaupmees, M. Piirsalu, I. Leito, *Tetrahedron Lett.* **2018**, *59*, 3738.
- [31] D. Himmel, S. K. Goll, I. Leito, I. Krossing, *Angew. Chem. Int. Ed.* **2010**, *49*, 6885; *Angew. Chem.* **2010**, *122*, 7037.
- [32] M. Nič, J. Jirát, B. Košata, A. Jenkins, A. McNaught, *IUPAC Compendium of Chemical Terminology*, IUPAC, Research Triangle Park, NC, **2009**.
- [33] Z. B. Maksić, B. Kovačević, R. Vianello, *Chem. Rev.* **2012**, *112*, 5240.
- [34] a) Z. Glasovac, M. Eckert-Maksić, I. Kaljurand, J. Saame, I. Leito, *Int. J. Mass Spectrom.* **2019**, *435*, 61; b) I. Kaljurand, I. A. Koppel, A. Kütt, E.-I. Rõõm, T. Rodima, I. Koppel, M. Mishima, I. Leito, *J. Phys. Chem. A* **2007**, *111*, 1245.
- [35] a) R. J. Gillespie, *Acc. Chem. Res.* **1968**, *1*, 202; b) R. J. Gillespie, T. E. Peel, E. A. Robinson, *J. Am. Chem. Soc.* **1971**, *93*, 5083; c) G. A. Olah, G. K. Prakash, J. Sommer, *Science* **1979**, *206*, 13.
- [36] R. Schwesinger, *Nachr. Chem. Tech. Lab.* **1990**, *38*, 1214.
- [37] E. D. Raczyńska, P.-C. Maria, J.-F. Gal, M. Decouzon, *J. Phys. Org. Chem.* **1994**, *7*, 725.
- [38] J. Sundermeyer, V. Raab, E. Gauchenova, U. Garrelts, N. Abacilar, K. Harms in *Activating unreactive substrates. The role of secondary interactions* (Hrsg.: C. Bolm, F. E. Hahn), Wiley-VCH, Weinheim, **2009**, S. 17–37.
- [39] P. Caubere, *Chem. Rev.* **1993**, *93*, 2317.
- [40] a) M. Schlosser, S. Strunk, *Tetrahedron Lett.* **1984**, *25*, 741; b) M. Schlosser, *Pure Appl. Chem.* **1988**, *60*, 1627.
- [41] E. D. Raczyńska, J.-F. Gal, P.-C. Maria, *Chem. Rev.* **2016**, *116*, 13454.
- [42] a) B. Kovačević, Z. B. Maksić, *Org. Lett.* **2001**, *3*, 1523; b) E. D. Raczyńska, M. K. Cyrański, M. Gutowski, J. Rak, J.-F. Gal, P.-C. Maria, M. Darowska, K. Duczmal, *J. Phys. Org. Chem.* **2003**, *16*, 91.
- [43] R. A. Kunetskiy, S. M. Polyakova, J. Vavřík, I. Císařová, J. Saame, E. R. Nerut, I. Koppel, I. A. Koppel, A. Kütt, I. Leito et al., *Chem. Eur. J.* **2012**, *18*, 3621.
- [44] H. Bruns, M. Patil, J. Carreras, A. Vázquez, W. Thiel, R. Goddard, M. Alcarazo, *Angew. Chem. Int. Ed.* **2010**, *49*, 3680; *Angew. Chem.* **2010**, *122*, 3762.

- [45] J. S. Bandar, T. H. Lambert, *J. Am. Chem. Soc.* **2012**, *134*, 5552.
- [46] J. S. Bandar, T. H. Lambert, *J. Am. Chem. Soc.* **2013**, *135*, 11799.
- [47] J. S. Bandar, A. Barthelme, A. Y. Mazori, T. H. Lambert, *Chem. Sci.* **2015**, *6*, 1537.
- [48] Z. B. Maksić, B. Kovačević, *J. Phys. Chem. A* **1999**, *103*, 6678.
- [49] a) K. Vazdar, R. Kunetskiy, J. Saame, K. Kaupmees, I. Leito, U. Jahn, *Angew. Chem. Int. Ed.* **2014**, *53*, 1435; *Angew. Chem.* **2014**, *126*, 1459; b) B. Kovačević, Z. B. Maksić, R. Vianello, *J. Chem. Soc., Perkin Trans. 2* **2001**, 886.
- [50] R. Schwesinger, J. Willaredt, H. Schlemper, M. Keller, D. Schmitt, H. Fritz, *Chem. Ber.* **1994**, *127*, 2435.
- [51] R. Schwesinger, H. Schlemper, *Angew. Chem. Int. Ed. Engl.* **1987**, *26*, 1167; *Angew. Chem.* **1987**, *99*, 1212.
- [52] R. Schwesinger, C. Hasenfratz, H. Schlemper, L. Walz, E.-M. Peters, K. Peters, H. G. von Schnering, *Angew. Chem. Int. Ed. Engl.* **1993**, *32*, 1361; *Angew. Chem.* **1993**, *105*, 1420.
- [53] R. Hoffmann, J. M. Howell, E. L. Muetterties, *J. Am. Chem. Soc.* **1972**, *94*, 3047.
- [54] D. G. Gilheany, *Chem. Rev.* **1994**, *94*, 1339.
- [55] A. Vogler, H. Kunkely, *Coord. Chem. Rev.* **2002**, *230*, 243.
- [56] M. Alcarazo, *Chem. Eur. J.* **2014**, *20*, 7868.
- [57] W. Kutzelnigg, *Angew. Chem. Int. Ed. Engl.* **1984**, *23*, 272; *Angew. Chem.* **1984**, *96*, 262.
- [58] F. Hartmann, D. Mootz, R. Schwesinger, *Z. Naturforsch. B* **1996**, *51*, 1375.
- [59] S. Ullrich, *CCDC 1903848: Experimental Crystal Structure Determination*, Cambridge Crystallographic Data Centre.
- [60] a) M. L. Clarke, D. J. Cole-Hamilton, A. M. Z. Slawin, J. D. Woollins, *Chem. Commun.* **2000**, 2065; b) M. L. Clarke, G. L. Holliday, A. M. Z. Slawin, J. D. Woollins, *J. Chem. Soc., Dalton Trans.* **2002**, 1093.
- [61] a) U. Köhn, M. Schulz, A. Schramm, W. Günther, H. Görls, S. Schenk, E. Anders, *Eur. J. Org. Chem.* **2006**, *2006*, 4128; b) H. Krawczyk, M. Dziegielewski, D. Deredas, A. Albrecht, Ł. Albrecht, *Chem. Eur. J.* **2015**, *21*, 10268; c) B. Teng, W. Lim, C.-H. Tan, *Synlett* **2017**, *28*, 1272.
- [62] A. J. M. Farley, P. Jakubec, A. M. Goldys, D. J. Dixon, *Tetrahedron* **2018**, *74*, 5206.
- [63] D. Uraguchi, S. Sakaki, T. Ooi, *J. Am. Chem. Soc.* **2007**, *129*, 12392.
- [64] K. J. Kolonko, H. J. Reich, *J. Am. Chem. Soc.* **2008**, *130*, 9668.
- [65] T. Imahori, C. Hori, Y. Kondo, *Adv. Synth. Catal.* **2004**, *346*, 1090.
- [66] M. Shigeno, K. Hayashi, K. Nozawa-Kumada, Y. Kondo, *Chem. Eur. J.* **2019**.
- [67] M. G. Núñez, A. J. M. Farley, D. J. Dixon, *J. Am. Chem. Soc.* **2013**, *135*, 16348.
- [68] C. Luo, J. S. Bandar, *J. Am. Chem. Soc.* **2018**, *140*, 3547.
- [69] H. Kawai, Z. Yuan, E. Tokunaga, N. Shibata, *Org. Biomol. Chem.* **2013**, *11*, 1446.

- [70] a) M. Ueno, C. Hori, K. Suzawa, M. Ebisawa, Y. Kondo, *Eur. J. Org. Chem.* **2005**, 2005, 1965; b) G.-F. Du, Y. Wang, C.-Z. Gu, B. Dai, L. He, *RSC Adv* **2015**, 5, 35421.
- [71] L. Lei, M. Tanishima, A. Goto, H. Kaji, *Polymers* **2014**, 6, 860.
- [72] S. Boileau, N. Illy, *Prog. Polym. Sci.* **2011**, 36, 1132.
- [73] T. Pietzonka, D. Seebach, *Angew. Chem. Int. Ed. Engl.* **1993**, 32, 716; *Angew. Chem.* **1993**, 105, 741.
- [74] a) S. Liu, C. Ren, N. Zhao, Y. Shen, Z. Li, *Macromol. Rapid Commun.* **2018**, 39, e1800485; b) N. Zhao, C. Ren, H. Li, Y. Li, S. Liu, Z. Li, *Angew. Chem. Int. Ed.* **2017**, 56, 12987; *Angew. Chem.* **2017**, 129, 13167; c) L. Zhang, F. Nederberg, R. C. Pratt, R. M. Waymouth, J. L. Hedrick, C. G. Wade, *Macromolecules* **2007**, 40, 4154.
- [75] W. Memeger, G. C. Campbell, F. Davidson, *Macromolecules* **1996**, 29, 6475.
- [76] a) J. Shi, N. Zhao, S. Xia, S. Liu, Z. Li, *Polym. Chem.* **2019**, 83, 383; b) P. C. Hupfield, R. G. Taylor, *J. Inorg. Organomet. Polym.* **1999**, 9, 17.
- [77] a) D. Zhang, S. K. Boopathi, N. Hadjichristidis, Y. Gnanou, X. Feng, *J. Am. Chem. Soc.* **2016**, 138, 11117; b) S. Hu, G. Dai, J. Zhao, G. Zhang, *Macromolecules* **2016**, 49, 4462.
- [78] R. W. Alder, P. S. Bowman, W. R. S. Steele, D. R. Winterman, *Chem. Commun.* **1968**, 723.
- [79] A. V. Degtyarev, O. V. Ryabtsova, A. F. Pozharskii, V. A. Ozeryanskii, Z. A. Starikova, L. Sobczyk, A. Filarowski, *Tetrahedron* **2008**, 64, 6209.
- [80] V. Raab, J. Kipke, R. M. Gschwind, J. Sundermeyer, *Chem. Eur. J.* **2002**, 8, 1682.
- [81] B. Kovačević, Z. B. Maksić, R. Vianello, M. Primorac, *New J. Chem.* **2002**, 26, 1329.
- [82] V. Raab, E. Gauchenova, A. Merkoulov, K. Harms, J. Sundermeyer, B. Kovačević, Z. B. Maksić, *J. Am. Chem. Soc.* **2005**, 127, 15738.
- [83] J. F. Kögel, B. Oelkers, B. Kovačević, J. Sundermeyer, *J. Am. Chem. Soc.* **2013**, 135, 17768.
- [84] L. Belding, T. Dudding, *Chem. Eur. J.* **2014**, 20, 1032.
- [85] a) L. Belding, P. Stoyanov, T. Dudding, *J. Org. Chem.* **2016**, 81, 6; b) D. Barić, B. Kovačević, *J. Phys. Org. Chem.* **2016**, 29, 750.
- [86] J. F. Kögel, B. Kovačević, S. Ullrich, X. Xie, J. Sundermeyer, *Chem. Eur. J.* **2017**, 23, 2591.
- [87] J. F. Kögel, N.-J. Kneusels, J. Sundermeyer, *Chem. Commun.* **2014**, 50, 4319.
- [88] A. F. Pozharskii, O. V. Ryabtsova, V. A. Ozeryanskii, A. V. Degtyarev, O. N. Kazheva, G. G. Alexandrov, O. A. Dyachenko, *J. Org. Chem.* **2003**, 68, 10109.
- [89] H. A. Staab, T. Saupe, C. Krieger, *Angew. Chem. Int. Ed. Engl.* **1983**, 22, 731; *Angew. Chem.* **1983**, 95, 748.
- [90] T. Saupe, C. Krieger, H. A. Staab, *Angew. Chem. Int. Ed. Engl.* **1986**, 25, 451; *Angew. Chem.* **1986**, 98, 460.
- [91] R. Schwesinger, M. Mißfeldt, K. Peters, H. G. von Schnering, *Angew. Chem. Int. Ed. Engl.* **1987**, 26, 1165; *Angew. Chem.* **1987**, 99, 1210.

- [92] M. A. Zirnstein, H. A. Staab, *Angew. Chem. Int. Ed. Engl.* **1987**, *26*, 460; M. A. Zirnstein, H. A. Staab, *Angew. Chem.* **1987**, *99*, 460.
- [93] A. F. Pozharskii, V. A. Ozeryanskii, V. Y. Mikshiev, A. S. Antonov, A. V. Chernyshev, A. V. Metelitsa, G. S. Borodkin, N. S. Fedik, O. V. Dyablo, *J. Org. Chem.* **2016**, *81*, 5574.
- [94] R. J. Schwamm, R. Vianello, A. Marsavelski, M. A. Garcia, R. M. Claramunt, I. Alkorta, J. Saame, I. Leito, C. M. Fitchett, A. J. Edwards et al., *J. Org. Chem.* **2016**, *81*, 7612.
- [95] Z. B. Maksić, Z. Glasovac, I. Despotovi, *J. Phys. Org. Chem.* **2002**, *15*, 499.
- [96] a) B. Kovačević, Z. Glasovac, Z. B. Maksić, *J. Phys. Org. Chem.* **2002**, *15*, 765; b) Z. Gattin, B. Kovačević, Z. B. Maksić, *Eur. J. Org. Chem.* **2005**, *2005*, 3206; c) D. Barić, I. Dragičević, B. Kovačević, *J. Org. Chem.* **2013**, *78*, 4075; d) D. Barić, I. Dragičević, B. Kovačević, *Tetrahedron* **2014**, *70*, 8571; e) S. M. Bachrach, *J. Org. Chem.* **2019**, *84*, 3467; f) S. M. Bachrach, *J. Org. Chem.* **2013**, *78*, 10909; g) S. M. Bachrach, *Org. Lett.* **2012**, *14*, 5598; h) S. M. Bachrach, C. C. Wilbanks, *J. Org. Chem.* **2010**, *75*, 2651; i) Z. Tian, A. Fattahi, L. Lis, S. R. Kass, *Croat. Chem. Acta* **2009**, *82*, 41.
- [97] Z. Glasovac, B. Kovačević, E. Meštrović, M. Eckert-Maksić, *Tetrahedron Lett.* **2005**, *46*, 8733.
- [98] M. Eckert-Maksić, Z. Glasovac, P. Trošelj, A. Kütt, T. Rodima, I. Koppel, I. A. Koppel, *Eur. J. Org. Chem.* **2008**, *2008*, 5176.
- [99] S. Goumri-Magnet, O. Guerret, H. Gornitzka, J. B. Cazaux, D. Bigg, F. Palacios, G. Bertrand, *J. Org. Chem.* **1999**, *64*, 3741.
- [100] I. A. Koppel, R. Schwesinger, T. Breuer, P. Burk, K. Herodes, I. Koppel, I. Leito, M. Mishima, *J. Phys. Chem. A* **2001**, *105*, 9575.
- [101] E. Fluck, R. Braun, *Synth. React. Inorg. Met.-Org. Chem.* **1988**, *18*, 727.
- [102] H. Schmidbaur, *Nachr. Chem. Tech. Lab.* **1979**, *27*, 620.
- [103] R. Tonner, G. Heydenrych, G. Frenking, *Chem. Phys. Chem.* **2008**, *9*, 1474.
- [104] J. F. Kögel, D. Margetić, X. Xie, L. H. Finger, J. Sundermeyer, *Angew. Chem. Int. Ed.* **2017**, *56*, 3090; *Angew. Chem.* **2017**, *129*, 3136.
- [105] a) A. J. Arduengo, R. L. Harlow, M. Kline, *J. Am. Chem. Soc.* **1991**, *113*, 361; b) W. A. Herrmann, *Angew. Chem. Int. Ed.* **2002**, *41*, 1290; *Angew. Chem.* **2002**, *114*, 1342; c) M. N. Hopkinson, C. Richter, M. Schedler, F. Glorius, *Nature* **2014**, *510*, 485; d) V. Nesterov, D. Reiter, P. Bag, P. Frisch, R. Holzner, A. Porzelt, S. Inoue, *Chem. Rev.* **2018**, *118*, 9678; e) A. Doddi, M. Peters, M. Tamm, *Chem. Rev.* **2019**, *119*, 6994.
- [106] a) V. Lavallo, Y. Canac, C. Präsang, B. Donnadieu, G. Bertrand, *Angew. Chem. Int. Ed.* **2005**, *44*, 5705; *Angew. Chem.* **2005**, *117*, 5851; b) M. Soleilhavoup, G. Bertrand, *Acc. Chem. Res.* **2015**, *48*, 256; c) Z. R. Turner, *Chem. Eur. J.* **2016**, *22*, 11461; d) M. Melaimi, R. Jazzar, M. Soleilhavoup, G. Bertrand, *Angew. Chem. Int. Ed.* **2017**, *56*, 10046; *Angew. Chem.* **2017**, *129*, 10180; e) C. M. Weinstein, G. P. Junor, D. R. Tolentino, R. Jazzar, M. Melaimi, G. Bertrand, *J. Am. Chem. Soc.* **2018**, *140*, 9255.
- [107] a) C. A. Dyker, V. Lavallo, B. Donnadieu, G. Bertrand, *Angew. Chem. Int. Ed.* **2008**, *47*, 3206; *Angew. Chem.* **2008**, *120*, 3250; b) A. Fürstner, M. Alcarazo, R. Goddard, C. W. Lehmann, *Angew. Chem. Int. Ed.* **2008**, *47*, 3210; *Angew. Chem.* **2008**, *120*, 3254; c) O. Kaufhold, F. E. Hahn, *Angew. Chem. Int. Ed.* **2008**, *47*, 4057; *Angew. Chem.* **2008**, *120*, 4122; d) C. Prankevicius, L. Liu, G. Bertrand, D. W. Stephan, *Angew. Chem. Int. Ed.*

- 2016**, 55, 5536; *Angew. Chem.* **2016**, 128, 5626; e) W.-C. Chen, W.-C. Shih, T. Jurca, L. Zhao, D. M. Andrada, C.-J. Peng, C.-C. Chang, S.-K. Liu, Y.-P. Wang, Y.-S. Wen et al., *J. Am. Chem. Soc.* **2017**, 139, 12830; f) S.-C. Chan, P. Gupta, X. Engelmann, Z. Z. Ang, R. Ganguly, E. Bill, K. Ray, S. Ye, J. England, *Angew. Chem. Int. Ed.* **2018**, 57, 15717; *Angew. Chem.* **2018**, 130, 15943.
- [108] a) R. Tonner, G. Frenking, *Chem. Eur. J.* **2008**, 14, 3273; b) M. Alcarazo, C. W. Lehmann, A. Anoop, W. Thiel, A. Fürstner, *Nat. Chem.* **2009**, 1, 295; c) W. Petz, G. Frenking in *Transition Metal Complexes of Neutral eta1-Carbon Ligands* (Hrsg.: R. Chauvin, Y. Canac), Springer Berlin Heidelberg, Berlin, Heidelberg, **2010**, S. 49–92; d) W. Petz, *Coord. Chem. Rev.* **2015**, 291, 1; e) J. E. Münzer, N.-J. H. Kneusels, B. Weinert, B. Neumüller, I. Kuzu, *Dalton Trans.* **2019**, 48, 11076.
- [109] a) R. W. Alder, P. R. Allen, S. J. Williams, *Chem. Commun.* **1995**, 1267; b) R. W. Alder, M. E. Blake, J. M. Oliva, *J. Phys. Chem. A* **1999**, 103, 11200; c) Y.-J. Kim, A. Streitwieser, *J. Am. Chem. Soc.* **2002**, 124, 5757; d) N. Wang, J. Xu, J. K. Lee, *Org. Biomol. Chem.* **2018**, 16, 8230.
- [110] a) R. Tonner, G. Frenking, *Angew. Chem. Int. Ed.* **2007**, 46, 8695; *Angew. Chem.* **2007**, 119, 8850; b) A. A. Tukov, A. T. Normand, M. S. Nechaev, *Dalton Trans.* **2009**, 7015.
- [111] I. Leito, I. A. Koppel, I. Koppel, K. Kaupmees, S. Tshepelevitsh, J. Saame, *Angew. Chem. Int. Ed.* **2015**, 54, 9262; *Angew. Chem.* **2015**, 127, 9394.
- [112] F. Ramirez, N. B. Desai, B. Hansen, N. McKelvie, *J. Am. Chem. Soc.* **1961**, 83, 3539.
- [113] O. Gasser, H. Schmidbaur, *J. Am. Chem. Soc.* **1975**, 97, 6281.
- [114] R. Appel, U. Baumeister, F. Knoch, *Chem. Ber.* **1983**, 116, 2275.
- [115] H. Schmidbaur, O. Gasser, M. S. Hussain, *Chem. Ber.* **1977**, 110, 3501.
- [116] R. Appel, K. Waid, *Z. Naturforsch. B* **1981**, 36.
- [117] A. P. Marchenko, G. N. Koidan, V. A. Oleinik, I. S. Zal'tsman, A. M. Pinchuk, *J. Gen. Chem. USSR* **1988**, 58, 1485.
- [118] a) R. Appel, F. Knoll, W. Michel, W. Morbach, H.-D. Wihler, H. Veltmann, *Chem. Ber.* **1976**, 109, 58; b) R. Appel, F. Knoll, H. Schöler, H.-D. Wihler, *Angew. Chem. Int. Ed. Engl.* **1976**, 15, 702; *Angew. Chem.* **1976**, 88, 769; c) R. Appel, H. Veltmann, *Tetrahedron Lett.* **1977**, 18, 399; e) R. Appel, W. Morbach, *Synthesis* **1977**, 1977, 699.
- [119] F. Ramirez, N. McKelvie, *J. Am. Chem. Soc.* **1957**, 79, 5829.
- [120] C. Reitsamer, S. Stallinger, W. Schuh, H. Kopacka, K. Wurst, D. Obendorf, P. Peringer, *Dalton Trans.* **2012**, 41, 3503.
- [121] a) E. A. V. Ebsworth, T. E. Fraser, Rankin, David W. H., O. Gasser, H. Schmidbaur, *Chem. Ber.* **1977**, 110, 3508; b) G. E. Hardy, J. I. Zink, W. C. Kaska, J. C. Baldwin, *J. Am. Chem. Soc.* **1978**, 100, 8001; c) H. Schmidbaur, G. Hasslberger, U. Deschler, U. Schubert, C. Kappenstein, A. Frank, *Angew. Chem. Int. Ed. Engl.* **1979**, 18, 408; *Angew. Chem.* **1979**, 91, 437; d) U. Schubert, C. Kappenstein, B. Milewski-Mahrla, H. Schmidbaur, *Chem. Ber.* **1981**, 114, 3070.
- [122] A. T. Vincent, P. J. Wheatley, *J. Chem. Soc., Dalton Trans.* **1972**, 617.
- [123] P. J. Quinlivan, G. Parkin, *Inorg. Chem.* **2017**, 56, 5493.

- [124] R. Tonner, F. Öxler, B. Neumüller, W. Petz, G. Frenking, *Angew. Chem. Int. Ed.* **2006**, *45*, 8038; *Angew. Chem.* **2006**, *118*, 8206.
- [125] R. Tonner, G. Frenking, *Chem. Eur. J.* **2008**, *14*, 3260.
- [126] a) W. C. Kaska, D. K. Mitchell, R. F. Reichelderfer, *J. Organomet. Chem.* **1973**, *47*, 391; b) G. Frenking, B. Neumüller, W. Petz, R. Tonner, F. Öxler, *Angew. Chem. Int. Ed.* **2007**, *46*, 2986; *Angew. Chem.* **2007**, *119*, 3044; c) G. Frenking, *Angew. Chem. Int. Ed.* **2014**, *53*, 6040; *Angew. Chem.* **2014**, *126*, 6152.
- [127] a) H. Schmidbaur, *Angew. Chem. Int. Ed.* **2007**, *46*, 2984-5; *Angew. Chem.* **2007**, *119*, 3042; b) D. Himmel, I. Krossing, A. Schnepf, *Angew. Chem. Int. Ed.* **2014**, *53*, 370; *Angew. Chem.* **2014**, *126*, 378; c) D. Himmel, I. Krossing, A. Schnepf, *Angew. Chem. Int. Ed.* **2014**, *53*, 6047; *Angew. Chem.* **2014**, *126*, 6159.
- [128] Z. L. Niemeyer, A. Milo, D. P. Hickey, M. S. Sigman, *Nat. Chem.* **2016**, *8*, 610.
- [129] L. Chen, P. Ren, B. P. Carrow, *J. Am. Chem. Soc.* **2016**, *138*, 6392.
- [130] G. Ung, G. Bertrand, *Chem. Eur. J.* **2011**, *17*, 8269.
- [131] C. A. Tolman, *Chem. Rev.* **1977**, *77*, 313.
- [132] a) W. McFarlane, D. S. Rycroft, *J. Chem. Soc., Dalton Trans.* **1973**, 2162; b) R. D. Kroshefsky, R. Weiss, J. G. Verkade, *Inorg. Chem.* **1979**, *18*, 469; c) D. W. Allen, B. F. Taylor, *J. Chem. Soc., Dalton Trans.* **1982**, 51.
- [133] H. A. Bent, *Chem. Rev.* **1961**, *61*, 275.
- [134] A. Poater, B. Cosenza, A. Correa, S. Giudice, F. Ragone, V. Scarano, L. Cavallo, *Eur. J. Inorg. Chem.* **2009**, *2009*, 1759.
- [135] L. Falivene, R. Credendino, A. Poater, A. Petta, L. Serra, R. Oliva, V. Scarano, L. Cavallo, *Organometallics* **2016**, *35*, 2286.
- [136] a) C. Lensink, S. K. Xi, L. M. Daniels, J. G. Verkade, *J. Am. Chem. Soc.* **1989**, *111*, 3478; b) H. Schmidt, C. Lensink, S. K. Xi, J. G. Verkade, *Z. Anorg. Allg. Chem.* **1989**, *578*, 75; c) M. A. H. Laramay, J. G. Verkade, *Z. Anorg. Allg. Chem.* **1991**, *605*, 163.
- [137] B. Kovačević, Z. B. Maksić, *Chem. Commun.* **2006**, 1524.
- [138] a) J. Münchenberg, H. Thönnessen, P. G. Jones, R. Schmutzler, *Phosphorus, Sulfur, Silicon Relat. Elem.* **1997**, *123*, 57; b) M. Freytag, V. Plack, P. G. Jones, R. Schmutzler, *Z. Naturforsch. B* **2004**, *59*, 499.
- [139] P. Mehlmann, C. Mück-Lichtenfeld, T. T. Y. Tan, F. Dielmann, *Chem. Eur. J.* **2017**, *23*, 5929.
- [140] A. P. Marchenko, G. N. Koidan, A. M. Pinchuk, A. V. Kirsanov, *J. Gen. Chem. USSR* **1984**, *54*, 1581.
- [141] K. Issleib, M. Lischewski, *J. Prakt. Chem.* **1970**, *312*, 135.
- [142] T. Scherpf, C. Schwarz, L. T. Scharf, J.-A. Zur, A. Helbig, V. H. Gessner, *Angew. Chem. Int. Ed.* **2018**, *57*, 12859; *Angew. Chem.* **2018**, *130*, 13041.
- [143] T. Witteler, H. Darmandeh, P. Mehlmann, F. Dielmann, *Organometallics* **2018**, *37*, 3064.
- [144] J. V. Kingston, J. G. Verkade, *J. Org. Chem.* **2007**, *72*, 2816.

- [145] C. V. Reddy, J. V. Kingston, J. G. Verkade, *J. Org. Chem.* **2008**, *73*, 3047.
- [146] M. A. Wünsche, P. Mehlmann, T. Witteler, F. Buß, P. Rathmann, F. Dielmann, *Angew. Chem. Int. Ed.* **2015**, *54*, 11857; *Angew. Chem.* **2015**, *127*, 12024.
- [147] P. Weber, T. Scherpf, I. Rodstein, D. Lichte, L. T. Scharf, L. J. Gooßen, V. H. Gessner, *Angew. Chem. Int. Ed.* **2019**, *58*, 3203; *Angew. Chem.* **2019**, *131*, 3235.
- [148] J.-S. Tang, J. G. Verkade, *Angew. Chem. Int. Ed. Engl.* **1993**, *32*, 896; *Angew. Chem.* **1993**, *105*, 934.
- [149] B. A. D'Sa, J. G. Verkade, *J. Org. Chem.* **1996**, *61*, 2963.
- [150] S. Arumugam, J. G. Verkade, *J. Org. Chem.* **1997**, *62*, 4827.
- [151] P. B. Kisanga, J. G. Verkade, *J. Org. Chem.* **1999**, *64*, 4298.
- [152] J. Yang, B. Chatelet, F. Ziarelli, V. Dufaud, D. Hérault, A. Martinez, *Eur. J. Org. Chem.* **2018**, *2018*, 6328.
- [153] P. B. Kisanga, P. Ilankumaran, B. M. Fetterly, J. G. Verkade, *J. Org. Chem.* **2002**, *67*, 3555.
- [154] a) P. Ilankumaran, J. G. Verkade, *J. Org. Chem.* **1999**, *64*, 3086; b) G. Liu, D. A. Cogan, T. d. Owens, T. P. Tang, J. A. Ellman, *J. Org. Chem.* **1999**, *64*, 1278.
- [155] a) B. A. D'Sa, J. G. Verkade, *J. Am. Chem. Soc.* **1996**, *118*, 12832; b) B. A. D'Sa, D. McLeod, J. G. Verkade, *J. Org. Chem.* **1997**, *62*, 5057; c) Z. Wang, B. Fetterly, J. G. Verkade, *J. Organomet. Chem.* **2002**, *646*, 161.
- [156] Hayashi Takaomi, Hara Isao, Inoue Yoshihisa, WO 2008075601, **2006**.
- [157] Y. Kondo, H. Naka, Shimo Tetsuya, JP2010030941, **2008**.
- [158] F. Buß, P. Mehlmann, C. Mück-Lichtenfeld, K. Bergander, F. Dielmann, *J. Am. Chem. Soc.* **2016**, *138*, 1840.
- [159] F. Buß, P. Roterling, C. Mück-Lichtenfeld, F. Dielmann, *Dalton Trans.* **2018**, *47*, 10420.
- [160] F. Buß, C. Mück-Lichtenfeld, P. Mehlmann, F. Dielmann, *Angew. Chem. Int. Ed.* **2018**, *57*, 4951; *Angew. Chem.* **2018**, *130*, 5045.
- [161] H. Clavier, S. P. Nolan, *Chem. Commun.* **2010**, *46*, 841.
- [162] K. Haav, J. Saame, A. Kütt, I. Leito, *Eur. J. Org. Chem.* **2012**, *2012*, 2167.
- [163] Z. Thammavongsy, I. M. Kha, J. W. Ziller, J. Y. Yang, *Dalton Trans.* **2016**, *45*, 9853.
- [164] M. A. H. Laramay, J. G. Verkade, *J. Am. Chem. Soc.* **1990**, *112*, 9421.
- [165] R. Dorta, E. D. Stevens, N. M. Scott, C. Costabile, L. Cavallo, C. D. Hoff, S. P. Nolan, *J. Am. Chem. Soc.* **2005**, *127*, 2485.
- [166] W. Petz, F. Weller, J. Uddin, G. Frenking, *Organometallics* **1999**, *18*, 619.
- [167] R. D. Jackson, S. James, A.G. Orpen, P. G. Pringle, *J. Organomet. Chem.* **1993**, *458*, C3-C4.
- [168] A. Karaçar, M. Freytag, H. Thönnessen, P. G. Jones, R. Bartsch, R. Schmutzler, *J. Organomet. Chem.* **2002**, *643-644*, 68.

- [169] A. Karaçar, M. Freytag, P. G. Jones, R. Bartsch, R. Schmutzler, *Z. Anorg. Allg. Chem.* **2001**, 627, 1571.
- [170] A. Bondi, *J. Phys. Chem.* **1964**, 68, 441.
- [171] S. A. Reiter, S. D. Nogai, K. Karaghiosoff, H. Schmidbaur, *J. Am. Chem. Soc.* **2004**, 126, 15833.
- [172] T. Costa, H. Schmidbaur, *Chem. Ber.* **1982**, 115, 1374.
- [173] P. Kilian, A. M. Z. Slawin, J. D. Woollins, *Dalton Trans.* **2006**, 2175.
- [174] B. Kovačević, *Group for Computational Life Sciences, Division of Physical Chemistry, Rudjer Bošković Institute, Bijenička 54, 10000 Zagreb, Croatia.*
- [175] S. Ullrich, *Masterarbeit*, Philipps-Universität, Marburg, **2015**.
- [176] B. Koch, *Bachelorarbeit*, Philipps-Universität, Marburg, **2018**.
- [177] Z. S. Novikova, A. A. Prishchenko, I. F. Lutsenko, *J. Gen. Chem. USSR* **1977**, 47, 707.
- [178] a) X. Liu, N. Thirupathi, I. A. Guzei, J. G. Verkade, *Inorg. Chem.* **2004**, 43, 7431; b) O. Alhomaidan, C. Beddie, G. Bai, D. W. Stephan, *Dalton Trans.* **2009**, 1991.
- [179] K. R. Dunbar, S. C. Haefner, *Polyhedron* **1994**, 13, 727.
- [180] J.-S. Tang, J. G. Verkade, *Tetrahedron* **1993**, 34, 2903.
- [181] S. Asghar, S. B. Taylor, D. Elorriaga, R. B. Bedford, *Angew. Chem. Int. Ed.* **2017**, 56, 16367; *Angew. Chem.* **2017**, 129, 16585.
- [182] T. M. Trnka, R. H. Grubbs, *Acc. Chem. Res.* **2001**, 34, 18.
- [183] a) A. P. Marchenko, I. S. Zal'tsman, A. M. Pinchuk, *J. Gen. Chem. USSR* **1986**, 56, 1687; b) A. P. Marchenko, G. N. Koidan, V. A. Oleinik, A. A. Kudryavtsev, A. M. Pinchuk, *J. Gen. Chem. USSR* **1987**, 57, 1916; c) V. A. Oleinik, A. P. Marchenko, G. N. Koidan, A. M. Pinchuk, *J. Gen. Chem. USSR* **1988**, 58, 625; d) G. N. Koidan, A. P. Marchenko, V. A. Oleinik, A. M. Pinchuk, *J. Gen. Chem. USSR* **1988**, 58, 1304.
- [184] W. L. F. Armarego, D. D. Perrin, *Purification of laboratory chemicals*, 4. Aufl., Butterworth Heinemann, Oxford, Boston, **1996**.
- [185] J. Åhman, P. Somfai, *Synthetic Commun.* **1995**, 25, 2301.
- [186] U. Berens, U. Englert, S. Geysler, J. Runsink, A. Salzer, *Eur. J. Org. Chem.* **2006**, 2006, 2100.
- [187] W. A. Herrmann, G. Brauer (Hrsg.) *Synthetic methods of organometallic and inorganic chemistry, / (Herrmann/Brauer). Ed. by Wolfgang A. Herrmann ; Vol. 1*, Thieme, Stuttgart, **1996**.
- [188] G. R. Fulmer, Miller, Alexander J. M., N. H. Sherden, H. E. Gottlieb, A. Nudelman, B. M. Stoltz, J. E. Bercaw, K. I. Goldberg, *Organometallics* **2010**, 29, 2176.
- [189] a) *Apex3*, Bruker AXS Inc., Madison, Wisconsin, USA, **2016**; b) *SAINT*, Bruker AXS Inc., Madison, Wisconsin, USA, **2015**; c) *SADABS. Bruker AXS area detector scaling and absorption correction*, Bruker AXS Inc., Madison, Wisconsin, USA, **2016**.
- [190] a) *X-Area Pilatus3_SV*, STOE & Cie GmbH, Darmstadt, Germany, **2016**; b) *X-Area Recipe*, STOE & Cie GmbH, Darmstadt, Germany, **2015**; c) *X-Area Integrate*, STOE &

- Cie GmbH, Darmstadt, Germany, **2016**; d) *X-Area LANA*, STOE & Cie GmbH, Darmstadt, Germany, **2016**.
- [191] G. M. Sheldrick, *Acta Cryst.* **2015**, *A71*, 3.
- [192] G. M. Sheldrick, *Acta Cryst.* **2015**, *C71*, 3.
- [193] L. J. Farrugia, *J. Appl. Crystallogr.* **2012**, *45*, 849.
- [194] C. B. Hübschle, G. M. Sheldrick, B. Dittrich, *J. Appl. Crystallogr.* **2011**, *44*, 1281.
- [195] K. Brandenburg, H. Putz, *Diamond - Crystal and Molecular Structure Visualization v4*, Crystal Impact GbR, Bonn, Germany, **2014**.
- [196] "Jmol colors", zu finden unter <http://jmol.sourceforge.net/jscolors/>.